frontiers | Research Topics

The role of bile acid (ba) and related metabolites and hormone abnormalities in metabolic diseases

Edited by
Yanli Pang, Changtao Jiang, Frank Gonzalez and Fang Zhongze

Published in
Frontiers in Endocrinology

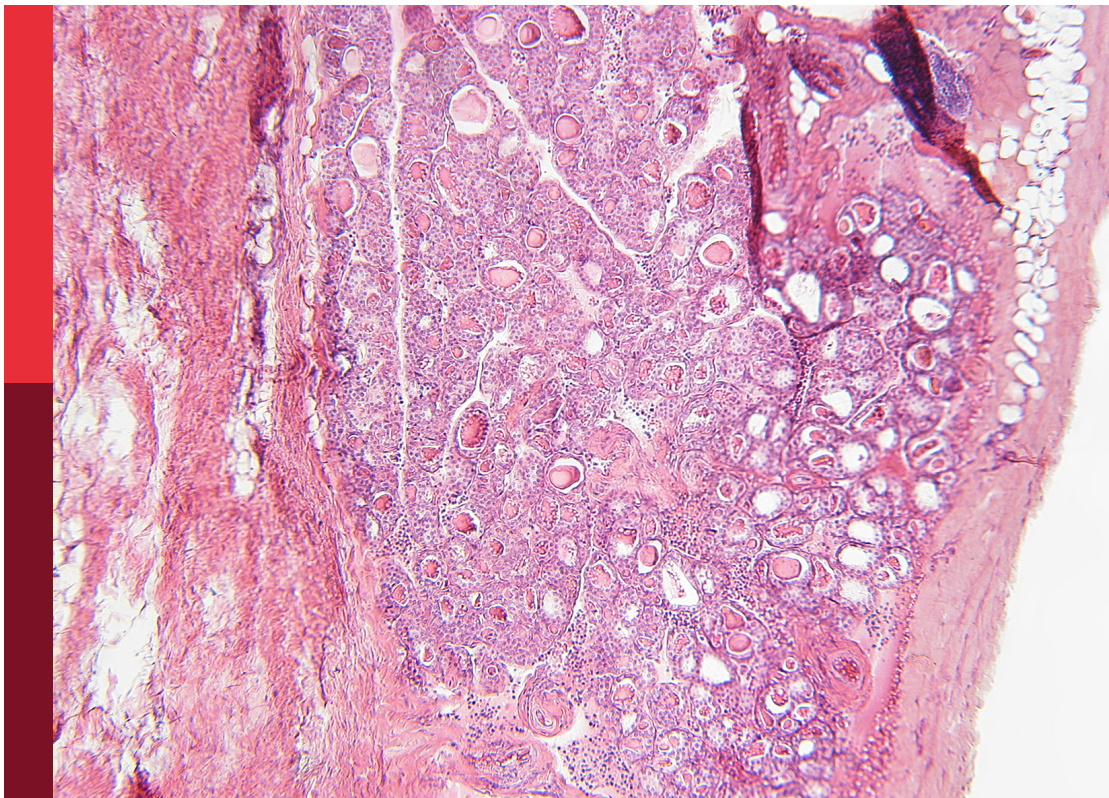

ISSN 1664-8714
ISBN 978-2-83251-570-9
DOI 10.3389/978-2-83251-570-9

About Frontiers

Frontiers is more than just an open access publisher of scholarly articles: it is a pioneering approach to the world of academia, radically improving the way scholarly research is managed. The grand vision of Frontiers is a world where all people have an equal opportunity to seek, share and generate knowledge. Frontiers provides immediate and permanent online open access to all its publications, but this alone is not enough to realize our grand goals.

Frontiers journal series

The Frontiers journal series is a multi-tier and interdisciplinary set of open-access, online journals, promising a paradigm shift from the current review, selection and dissemination processes in academic publishing. All Frontiers journals are driven by researchers for researchers; therefore, they constitute a service to the scholarly community. At the same time, the *Frontiers journal series* operates on a revolutionary invention, the tiered publishing system, initially addressing specific communities of scholars, and gradually climbing up to broader public understanding, thus serving the interests of the lay society, too.

Dedication to quality

Each Frontiers article is a landmark of the highest quality, thanks to genuinely collaborative interactions between authors and review editors, who include some of the world's best academicians. Research must be certified by peers before entering a stream of knowledge that may eventually reach the public - and shape society; therefore, Frontiers only applies the most rigorous and unbiased reviews. Frontiers revolutionizes research publishing by freely delivering the most outstanding research, evaluated with no bias from both the academic and social point of view. By applying the most advanced information technologies, Frontiers is catapulting scholarly publishing into a new generation.

What are Frontiers Research Topics?

Frontiers Research Topics are very popular trademarks of the *Frontiers journals series*: they are collections of at least ten articles, all centered on a particular subject. With their unique mix of varied contributions from Original Research to Review Articles, Frontiers Research Topics unify the most influential researchers, the latest key findings and historical advances in a hot research area.

Find out more on how to host your own Frontiers Research Topic or contribute to one as an author by contacting the Frontiers editorial office: frontiersin.org/about/contact

The role of bile acid (ba) and related metabolites and hormone abnormalities in metabolic diseases

Topic editors

Yanli Pang — Peking University Third Hospital, China
Changtao Jiang — Peking University, China
Frank Gonzalez — National Cancer Institute (NIH), United States
Fang Zhongze — Tianjin Medical University, China

Citation

Pang, Y., Jiang, C., Gonzalez, F., Zhongze, F., eds. (2023). *The role of bile acid (ba) and related metabolites and hormone abnormalities in metabolic diseases*. Lausanne: Frontiers Media SA. doi: 10.3389/978-2-83251-570-9

Table of contents

05 Acetylcarnitine Is Associated With Cardiovascular Disease Risk in Type 2 Diabetes Mellitus
Shuo Zhao, Ming-Li Liu, Bing Huang, Fu-Rong Zhao, Ying Li, Xue-Ting Cui and Rong Lin

14 Psychiatric Comorbidities and Liver Injury Are Associated With Unbalanced Plasma Bile Acid Profile During Methamphetamine Withdrawal
Yuru Ma, Hongjin Wu, Huawei Wang, Fengrong Chen, Zhenrong Xie, Zunyue Zhang, Qingyan Peng, Jiqing Yang, Yong Zhou, Cheng Chen, Minghui Chen, Yongjin Zhang, Juehua Yu and Kunhua Wang

25 The Environmental Pollutant Bromophenols Interfere With Sulfotransferase That Mediates Endocrine Hormones
Zhihong Dai, Furong Zhao, Ying Li, Jing Xu and Zhiyu Liu

32 Effects of Androgen Excess-Related Metabolic Disturbances on Granulosa Cell Function and Follicular Development
Baoying Liao, Xinyu Qi, Chuyu Yun, Jie Qiao and Yanli Pang

46 Progress in the Study of Colorectal Cancer Caused by Altered Gut Microbiota After Cholecystectomy
Yanpeng Ma, Ruize Qu, Yi Zhang, Changtao Jiang, Zhipeng Zhang and Wei Fu

57 The Mechanism Underlying the Influence of Indole-3-Propionic Acid: A Relevance to Metabolic Disorders
Binbin Zhang, Minjie Jiang, Jianan Zhao, Yu Song, Weidong Du and Junping Shi

71 Integration of Metabolomics and Proteomics in Exploring the Endothelial Dysfunction Mechanism Induced by Serum Exosomes From Diabetic Retinopathy and Diabetic Nephropathy Patients
Jing Yang, Dongwei Liu and Zhangsuo Liu

89 Inhibition of Human Sulfotransferases by Phthalate Monoesters
Hui Huang, Bei-Di Lan, Yu-Jing Zhang, Xiao-Juan Fan, Min-Cui Hu, Guo-Qiang Qin, Fei-Ge Wang, Yue Wu, Tao Zheng and Jun-Hui Liu

98 Abnormal Activation of Tryptophan-Kynurenine Pathway in Women With Polycystic Ovary Syndrome
Siyu Wang, Liangshan Mu, Chunmei Zhang, Xiaoyu Long, Yurong Zhang, Rong Li, Yue Zhao and Jie Qiao

108 Present and Future: Crosstalks Between Polycystic Ovary Syndrome and Gut Metabolites Relating to Gut Microbiota
Mingmin Zhang, Runan Hu, Yanjing Huang, Fanru Zhou, Fan Li, Zhuo Liu, Yuli Geng, Haoxu Dong, Wenwen Ma, Kunkun Song and Yufan Song

119 Gut microbiota: A new target for T2DM prevention and treatment
Lulu Liu, Jiheng Zhang, Yi Cheng, Meng Zhu, Zhifeng Xiao, Guangcong Ruan and Yanling Wei

138 Bile acids, gut microbiota and metabolic surgery
Jui Tu, Yangmeng Wang, Lihua Jin and Wendong Huang

frontiers in Endocrinology

ORIGINAL RESEARCH
published: 14 December 2021
doi: 10.3389/fendo.2021.806819

Acetylcarnitine Is Associated With Cardiovascular Disease Risk in Type 2 Diabetes Mellitus

*Shuo Zhao[1,2], Ming-Li Liu[3], Bing Huang[3], Fu-Rong Zhao[3], Ying Li[3], Xue-Ting Cui[3] and Rong Lin[1]**

[1] Department of Pharmacology, School of Basic Medical Sciences, Xi'an Jiaotong University Health Science Center, Xi'an, China, [2] Human Resources Department, The First Affiliated Hospital of Jinzhou Medical University, Jinzhou, China, [3] Department of Sceintific Research, Dalian Runsheng Kangtai Medical Lab Co. Ltd., Dalian, China

Objective: This study aimed to identify the association between specific short-chain acylcarnitines and cardiovascular disease (CVD) in type 2 diabetes mellitus (T2DM).

Method: We retrieved 1,032 consecutive patients with T2DM who meet the inclusion and exclusion criteria from the same tertiary care center and extracted clinical information from electronic medical records from May 2015 to August 2016. A total of 356 T2DM patients with CVD and 676 T2DM patients without CVD were recruited. Venous blood samples were collected by finger puncture after 8 h fasting and stored as dried blood spots. Restricted cubic spline (RCS) analysis nested in binary logistic regression was used to identify possible cutoff points and obtain the odds ratios (ORs) and 95% confidence intervals (CIs) of short-chain acylcarnitines for CVD risk in T2DM. The Ryan–Holm step-down Bonferroni procedure was performed to adjust *p*-values. Stepwise forward selection was performed to estimate the effects of acylcarnitines on CVD risk.

Result: The levels of C2, C4, and C6 were elevated and C5-OH was decreased in T2DM patients with CVD. Notably, only elevated C2 was still associated with increased CVD inT2DM after adjusting for potential confounders in the multivariable model (OR = 1.558, 95%CI = 1.124–2.159, p = 0.008). Furthermore, the association was independent of previous adjusted demographic and clinical factors after stepwise forward selection (OR = 1.562, 95%CI = 1.132–2.154, p = 0.007).

Conclusions: Elevated C2 was associated with increased CVD risk in T2DM.

Keywords: type 2 diabetes mellitus, cardiovascular disease, acylcarnitine, metabolism, relationship

OPEN ACCESS

Edited by:
Fang Zhongze,
Tianjin Medical University, China

Reviewed by:
Lihong Ye,
Nankai University, China
Yong Liu,
Dalian University of Technology, China

***Correspondence:**
Rong Lin
linrong63@aliyun.com

Specialty section:
This article was submitted to Gut Endocrinology, a section of the journal Frontiers in Endocrinology

Received: *01 November 2021*
Accepted: *17 November 2021*
Published: *14 December 2021*

Citation:
Zhao S, Liu M-L, Huang B, Zhao F-R, Li Y, Cui X-T and Lin R (2021) Acetylcarnitine Is Associated With Cardiovascular Disease Risk in Type 2 Diabetes Mellitus. Front. Endocrinol. 12:806819. doi: 10.3389/fendo.2021.806819

INTRODUCTION

Type 2 diabetes mellitus (T2DM) is a major risk factor for cardiovascular disease (CVD) alongside other risk factors such as smoking and lipid disorders; in turn, CVD is the most prevalent cause of mortality among people with T2DM (1, 2). Individuals with diabetes have two to three times higher risk of developing CVD and two to four times increased risk of dying from heart diseases compared to their counterparts without diabetes (3–5).

Generally, obesity is a common risk factor for diabetes and its cardiovascular complications and has adverse effects on blood pressure and blood lipid (6). However, the body mass index (BMI) does not fully explain the increased risk of CVD in diabetics. Compared with the value of BMI, the metabolism and distribution characteristics of lipids will also have different effects on diabetes and CVD. For example, unlike fat that accumulates in the viscera, subcutaneous fat is negatively correlated with triglycerides (TGs), blood pressure, and atherosclerosis and has a protective effect on atherosclerosis (7). Besides, there is also a large variability of CVD risk for given fat mass. A review indicated that some lean people and obese people have similar risk of cardiovascular complications due to differences in fat distribution (8). Therefore, the risk of CVD in T2DM with diabetes cannot simply be measured by BMI. Interestingly, the heart energy of diabetic patients is mainly supplied by the oxidation of fatty acids (FAs) (9). As a small metabolic molecule, acylcarnitine is a product of FAs involved in heart energy supply (10). Acylcarnitine is essential for the transport of FAs into the mitochondria, which are free carnitines combined with coenzyme A (CoA) produced by FA β-oxidation (11–13). Meanwhile, acylcarnitine is also involved in the metabolism of triglycerides, cholesterol, and other lipids, as well as in the process of gluconeogenesis, which can comprehensively reflect the changes of glucose and lipid metabolism in diabetic patients.

A previous study found that the elevation of blood contents of short- and medium-chain acylcarnitines was related to the risk of CVD in T2DM (14). Animal experiments have also shown that the plasma levels of acetylcarnitine and hydroxybutyrylcarnitine in T2DM rats were increased. Further correlation analysis indicated that T2DM-related dyslipidemia was associated with the increased level of acetylcarnitine, and hydroxybutyrylcarnitine showed higher positive correlations with homeostasis model assessment of insulin resistance (HOMA-IR) ($R > 0.64$) (15). Similarly, a Russian study found that the levels of short-chain acylcarnitines, such as acetylcarnitine and isovalerylcarnitine, were higher in patients with CVD than those in non-CVD patients (16). These studies were consistent with our previous study to a certain extent, that some short-chain acylcarnitines might play an essential role in diabetic patients developing CVD. But only a few studies have investigated the association of these short-chain acylcarnitines and the risk of T2DM patients developing CVD.

Abbreviations: CVD (cardiovascular disease) was defined as having a history of coronary artery disease, heart failure or stroke. Short-chain acylcarnitines: acetylcarnitine (C2); propionylcarnitine (C3); butyrylcarnitine (C4); hydroxylbutyrylcarnitine (C4-OH); succinylcarnitine (C4DC); isovalerylcarnitine (C5); 3-hydroxyisovalerylcarnitine (C5-OH); glutarylcarnitine (C5DC); tiglylcarnitine (C5:1); hexanoylcarnitine (C6); Demographic information T2DM, type2 diabetes mellitus; BMI, body mass index; FA, fatty acid; TG, triglyceride; COA, coenzyme A; hexanoylcarnitine; SBP, systolic blood pressure; DBP, diastolic blood pressure, HbA1c, glycated hemoglobin; LDL-C, low density lipoprotein cholesterol; HDL-C, high density lipoprotein cholesterol; OR, odds ratio; CI, confidence interval; CAD, coronary artery disease; SD, standard deviation; CPT1, carnitine palmitoyl transferase 1; CPT2, carnitine palmitoyltransferase2; CRAT, carnitine acetyltransferase; CHD, coronary heart disease.

Therefore, we carried out a cross-sectional study based on hospital patients with T2DM to explore the effects of short-chain acylcarnitines on CVD in T2DM patients.

METHODS AND RESULTS

Research Design and Population

Electronic medical records were compiled to collect the demographic and disease information of patients in May 2015. By August 2016, we recruited 2554 T2DM patients from the First Affiliated Hospital of Liaoning Medical University. T2DM was diagnosed according to the 1999 criteria of the World Health Organization (17). We excluded the following patients: 1) aged <18 years, 2) with missing demographic information, 3) had disorders of consciousness, and 4) short-chain acylcarnitine metabolites were not determined, including C2, C3, C4, C4-OH, C4DC, C5, C5-OH, C5DC, C5:1, and C6. According to the standard, a total of 1,032 patients were enrolled in this study. The Ethics Committee for Clinical Research of the First Affiliated Hospital of Liaoning Medical University granted ethical approval for the study. Informed consent was waived due to the retrospective nature of the study, which is consistent with the Declaration of Helsinki.

Data Collection and Definitions

Demographic information including age, gender, BMI, and duration of diabetes and drug use data such as of antidiabetic drugs, antihypertensive drugs, and lipid-lowering drugs were retrieved from electronic medical records. Trained doctors examined clinical data on systolic blood pressure (SBP), diastolic blood pressure (DBP), glycated hemoglobin (HbA1c), TGs, low-density lipoprotein cholesterol (LDL-C), and high-density lipoprotein cholesterol (HDL-C) in the laboratory of the hospital.

BMI was calculated as the weight at the last hospital visit (in kilograms) divided by the squared body height (in meters). Based on a previous research (18), BMI was divided into the following groups: underweight, <18.5 kg/m^2; normal weight, 18.5–24 kg/m^2; overweight, 24–28 kg/m^2; obese, ≥28.0 kg/m^2. Blood pressure was the average of two measurements using standard mercury sphygmomanometers after at least a 10-min rest in a sitting position. HbA1c ≥ 7% was defined as hyperglycemia. Dyslipidemia was diagnosed if TG ≥ 1.7 mmol/L, LDL-C ≥ 2.6 mmol/L, or HDL-C ≤ 1 mmol/L in males and HDL-C ≤ 1.3 mmol/L in females.

CVD was defined as having a medical history of coronary artery disease (CAD), heart failure, or stroke. Short-chain acylcarnitines include acetylcarnitine (C2), propionylcarnitine (C3), butyrylcarnitine (C4), hydroxylbutyrylcarnitine (C4-OH), succinylcarnitine (C4DC), isovalerylcarnitine (C5), 3-hydroxyisovalerylcarnitine (C5-OH), glutarylcarnitine (C5DC), tiglylcarnitine (C5:1), and hexanoylcarnitine (C6).

Acylcarnitine Assays

Venous blood samples were collected by finger puncture after 8 h fasting and stored as dried blood spots. Experimental determination was taken at room temperature. Acylcarnitine was extracted from blood samples using the Millipore MultiScreen HV 96-well plate

(Millipore, Billerica, MA, USA). Filtrate after extraction and quality control solutions were dried by pure nitrogen gas at 50°CC. Acylcarnitine quality control standards were purchased from Chromsystems (Grafelfing, Germany). Dried samples were dissolved by acetonitrile aqueous solution for final acylcarnitine assays. The assays were performed using an AB Sciex 4000 QTrap system (AB Sciex, Framingham, MA, USA). Acylcarnitine was scanned under positive mode. Analyst v1.6.0 software was applied for the system control and acylcarnitine data collection. Further data preprocessing is carried out through ChemoView 2.0.2 (AB Sciex).

Statistical Analysis

All statistical results were conducted using Statistical Analysis System 9.4 version (SAS Institute Inc., Cary, NC, USA). Normality of continuous variables was tested by checking the quantile–quantile (Q–Q) plot. Continuous variables with normal distribution were expressed as the mean ± standard deviation (SD) and compared using Student's *t*-test. Continuous variables with skewed distribution were expressed as medians (interquartile range) and compared using the Wilcoxon rank-sum test. Categorical variables were presented as quantity (percentage), and their differences between the CVD and non-CVD groups were compared using the chi-squared test or Fisher's exact test. Binary logistic regression was performed to assess the odds ratios (ORs) and 95% confidence intervals (CIs) of the levels of acylcarnitine for the risk of CVD in T2DM. Restricted cubic spline (RCS) analysis embedded in logistic regression was used to examine the full-range associations between acylcarnitine levels and the risk of CVD in T2DM due to possible non-linearity. As usual, three knots were adopted in the study according to a previous study and the suggestion by Harrell (19–21). The ORs of acylcarnitines will change rapidly at some cutoff points if the relationship between acylcarnitines and CVD in T2DM is nonlinear. These cutoff points were used to stratify acylcarnitines into categorical variables by carefully observing the shape of the OR curves of acylcarnitine for CVD in T2DM. A two-step adjustment scheme was performed to control potential confounders. Firstly, we preliminarily created a univariable logistic model to explore the relation between acylcarnitines and CVD in T2DM. Secondly, we further adjusted the aforementioned factors consisting of age, gender, BMI, duration of diabetes, antidiabetic drugs, antidiabetic drugs, and lipid-lowering drugs, SBP, DBP, HbA1c, TG, LDL-C, and HDL-C. In addition, a stepwise forward selection was performed to identify acylcarnitines that had effects on CVD risk in TDM independent of these factors. Mean imputation and multiple imputation were performed to control for the impact of missing data in the multivariable model. Finally, *p*-values less than 0.05 were considered as statistically significant for all these analyses. The Bonferroni test was applied to adjust *p*-values for multiple comparisons.

RESULTS

Demographic and Clinic Characteristics of Participants

Among all the study subjects, there were 356 T2DM patients suffering from CVD. Strokes were the most common (only diagnosed strokes: 193, 39.04%), followed by CAD (only diagnosed CAD: 111, 31.18%), and the least number of people suffered from heart failure (HF) (only diagnosed HF: 6, 1.69%). In both groups, there were more male than female patients. The age, duration of diabetes, SBP, and the proportions of intake of hypoglycemic drugs and lipid-lowering drugs in the CVD group were all greater than those in the non-CVD group. It was worth noting that, compared with the non-CVD group, the CVD group had more frequent HbA1c deletions, while the missing values of HDL-C, LDL-C, and TG were fewer. However, there were no statistically significant differences in the gender distribution, BMI, diastolic blood pressure, and intake of antidiabetic drugs between the two groups (**Table 1**).

Levels of Short-Chain Acylcarnitines Between the CVD and Non-CVD Groups

The levels of C2, C4, and C6 in the CVD group were higher than those in T2DM patients without CVD, whereas the concentration of C5-OH was lower. No significant differences in the levels of C3, C4-OH, C4DC, C5, C5DC, and C5:1 were found in both groups (**Table 2**).

Associations of Short-Chain Acylcarnitine and Risk of CVD in T2DM

Except for C4, the relationships between C2, C5-OH, and C6 and CVD in T2DM were nonlinear by observing the OR curves (**Figure 1**). C2 and C4 were positively associated with the risk of CVD in T2DM in the univariable model (model 1). The ORs (95%CI) were as follows: C2 = 1.576 (1.203–2.064) and C4 = 3.551 (1.409–8.946). The relationship between C5-OH and CVD was a U-shaped curve. In the univariable analysis, C5-OH less than 0.22 μmol/L was negatively associated with CVD in T2DM, utilizing 0.22–0.30 μmol/L as the reference [OR (95% CI) of C5-OH for <0.22 *vs*. 0. 22–0.30 μmol/L: 1.638 (1.181–2.270)]. Only the association of C2 with CVD in T2DM was still statistically significant after adjusting for other potential confounders in the multivariable model (model 2) (C2: OR = 1.558, 95%CI = 1.124–2.159, $p = 0.0078$, Bonferroni-adjusted $p = 0.0125$). The OR of C2 for CVD in T2DM only had a slight change, which was independent of traditional risks in the stepwise selection procedure (C2: OR = 1.562, 95%CI = 1.132–2.154) (**Table 3**). Moreover, this relationship also did not change statistically after filling in the missing values (**Supplementary Table S1**).

DISCUSSION

Our study found that the levels of C2, C4, and C6 in short-chain acylcarnitine increased in T2DM patients with CVD, while the level of C5-OH was decreased. Additionally, an elevated C2 level was associated with an increased risk of CVD in T2DM after considering demographic and clinical factors.

TABLE 1 | Demographic and clinical characteristics of diabetes according to occurrence of CVD.

	CVD (*n* = 356)	Non-CVD (*n* = 676)	*p*-value
Age (years)	65.00 (57.00–72.00)	54.00 (45.00–62.50)	<0.0001*
Gender, male	192 (53.93%)	357 (52.81%)	0.7313**
Duration of diabetes (years)	7.75 (2.00–12.00)	3.00 (0.00–10.00)	<0.0001*
BMI (kg/m^2)	24.87 (22.87–7.34)	25.24 (22.65–7.68)	0.3671*
BMI categories			0.1441**
<18.5 (underweight)	10 (2.81%)	17 (2.51)	
18.5–24 (normal weight)	119 (33.43%)	235 (34.76%)	
24–28 (overweight)	163 (45.79%)	267 (39.50%)	
≥28 (obese)	64 (17.98%)	157 (23.22%)	
SBP (mmHg)	143.00 (130.00–161.00)	135.00 (122.00–150.00)	<0.0001*
DBP (mmHg)	80.00 (74.00–92.00)	82.00 (74.00–90.00)	0.5446*
HbA1c (%)	8.40 (7.50–10.60)	9.75 (7.90–11.10)	<0.0001*
HbA1c ≥ 7	180 (50.56%)	374 (55.33%)	0.0227**
HbA1c < 7	37 (10.39%)	40 (5.92%)	
Missing value	139 (39.05%)	262 (38.76%)	
HDL-C (mmol/L)	1.03 (0.85–1.26)	1.00 (0.84–1.24)	0.5748*
<1 in males or <1.3 in females	189 (53.09%)	305 (45.12%)	<0.0001**
≥1 in males or ≥1.3 in females	99 (27.81%)	148 (21.89%)	
Missing value	68 (19.10%)	223 (32.99%)	
LDL-C (mmol/L)	2.69 (2.09–3.26)	2.78 (2.25–3.44)	0.0097*
LDL-C ≥ 2.6	156 (43.54%)	279 (41.27%)	<0.0001**
LDL-C < 2.6	133 (37.36%)	174 (25.74%)	
Missing value	68 (19.10%)	223 (32.99%)	
TG (mmol/L)	1.62 (1.09–2.22)	1.69 (1.12–2.55)	0.0391*
TG ≥ 1.7	132 (37.08%)	229 (33.88%)	<0.0001**
TG < 1.7	156 (43.82%)	227 (33.58%)	
Missing value	68 (19.10%)	220 (32.54%)	
Antidiabetic drugs	292 (82.02%)	575 (85.06%)	0.2058**
Antihypertensive drugs	214 (60.11%)	199 (29.44%)	<0.0001**
Lipid-lowering drugs	189 (53.09%)	199 (29.44%)	<0.0001**
Only CAD	111 (31.18%)		
Only HF	6 (1.69%)		
Only stroke	139 (39.04%)		
CAD and stroke	59 (16.57%)		
CAD and HF	59 (16.57%)		
HF and stroke	20 (5.62%)		
CAD and stroke and HF	19 (5.34%)		

Data are represented as n (%), means ± standard deviation, or median (interquartile range).

CVD, cardiovascular disease; BMI, body mass index; SBP, systolic blood pressure; DBP, diastolic blood pressure; HbA1c, glycated hemoglobin; TG, triglyceride; LDL-C, low-density lipoprotein cholesterol; HDL-C, high-density lipoprotein cholesterol; CAD, coronary artery disease; HF, heart failure.

**P-values for comparisons between groups derived using Wilcoxon rank-sum test. **P-values for comparisons between groups derived using chi-squared test.*

TABLE 2 | Short-chain acylcarnitine levels betweenT2DM patients with CVD and T2DM patients without CVD.

	CVD	Non-CVD	*p*-value
C2 (μmol/L)	12.540 (9.118–16.275)	11.320 (8.670–14.902)	0.0035
C3 (μmol/L)	1.355 (0.943–1.827)	1.373 (0.961–1.977)	0.2272
C4 (μmol/L)	0.212 (0.160–0.290)	0.199 (0.150–0.267)	0.0035
C4-OH (μmol/L)	0.101 (0.080–0.152)	0.108 (0.078–0.158)	0.5514
C4-DC (μmol/L)	0.660 (0.518–0.860)	0.638 (0.470–0.840)	0.1236
C5 (μmol/L)	0.146 (0.110–0.199)	0.150 (0.110–0.195)	0.9172
C5-OH (μmol/L)	0.248 (0.188–0.353)	0.270 (0.208–0.350)	0.0081
C5DC (μmol/L)	0.083 (0.060–0.126)	0.080 (0.050–0.118)	0.1178
C5:1 (μmol/L)	0.060 (0.047–0.082)	0.060 (0.048–0.080)	0.4233
C6 (μmol/L)	0.057 (0.040–0.070)	0.0480 (0.033–0.063)	<0.0001

P-values for comparisons between groups were derived using the Wilcoxon rank-sum test.

CVD, cardiovascular disease; T2DM, type 2 diabetes mellitus; C2, acetylcarnitine; C3, propionylcarnitine; C4, butyrylcarnitine; C4-OH, hydroxylbutyrylcarnitine; C4DC, succinylcarnitine; C5, isovalerylcarnitine; C5-OH, 3-hydroxyisovalerylcarnitine; C5DC, glutarylcarnitine; C5:1, tiglylcarnitine; C6, hexanoylcarnitine.

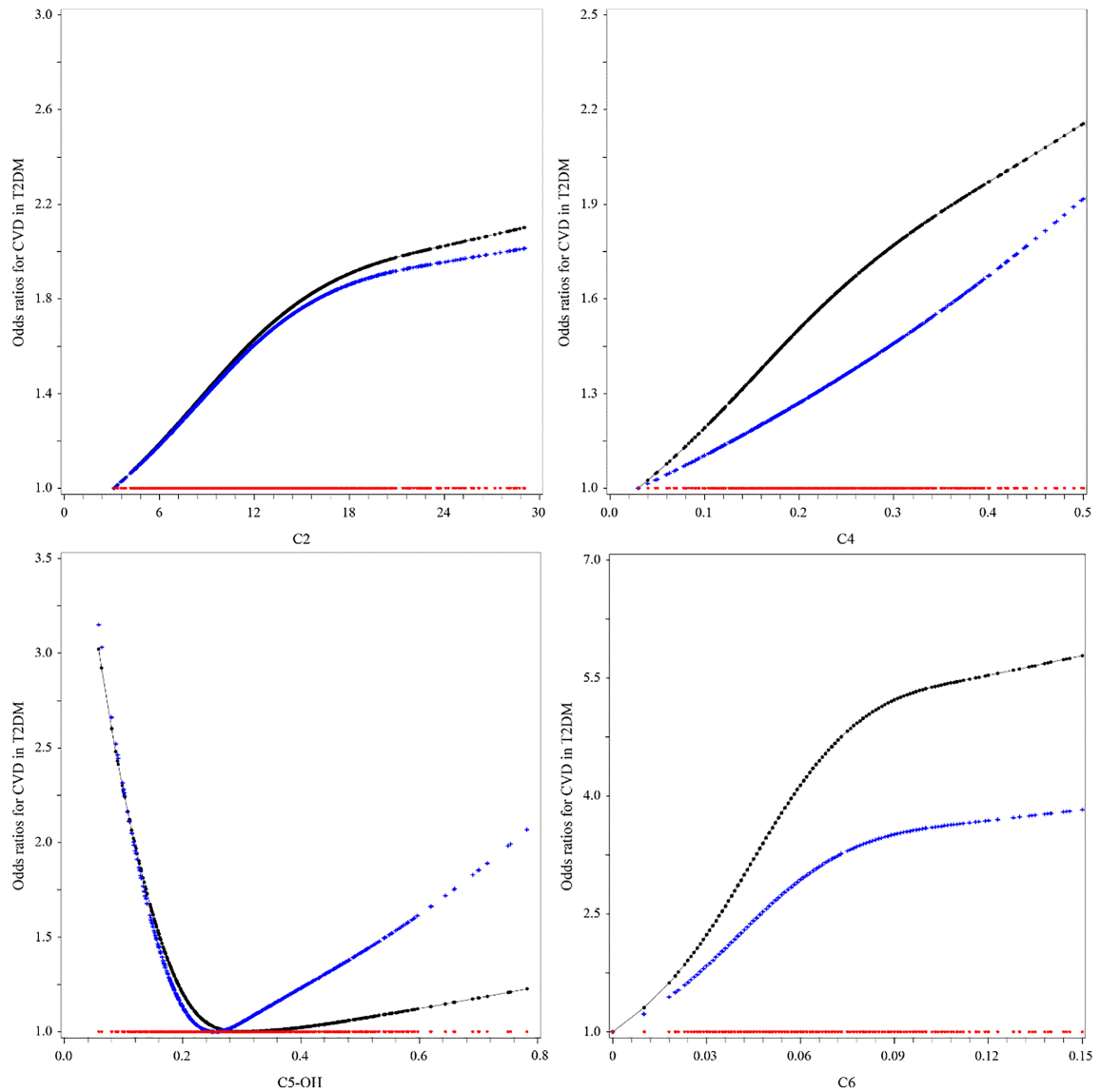

FIGURE 1 | Associations between short-chain acylcarnitine and the risk of cardiovascular disease (CVD) in type 2 diabetes mellitus (T2DM). The black lines were derived from univariable model 1, the blue lines from multivariable analyses (see **Table 3**, multivariable model 2, for the list of adjusted variables), and the red lines were the reference lines at OR = 1.

C2 is a small metabolic molecule in the body that plays a vital role in cellular respiration. It removes acetyl groups from cells and participates in energy transfer. C2 serves as a transmission tool for FAs to enter the mitochondria for the production of ATP during cellular respiration (22).

Specifically, free FAs are activated in the cytoplasm to form acyl-CoA. Acyl-CoA enters the mitochondria by carnitine shuttle through carnitine palmitoyl transferase 1 (CPT1) and carnitine palmitoyltransferase2 (CPT2) on the mitochondrial membrane (23). After entering the mitochondrial matrix, acyl-CoA is dehydrogenated, added water, dehydrogenated again, and sulfated under the catalysis of the FA oxidase system (24). Finally, acyl-CoA is broken to form one molecule of acetyl-CoA and one molecule of two-carbon chain shortened acyl-CoA (25). The shortened acyl-CoA repeats the above process to generate acetyl-CoA or combine with free carnitine to form acyl-carnitine. Acetyl-CoA is further involved in the synthesis pathway of the following substances (26): 1) acetyl-CoA and free carnitine are converted into acetylcarnitine by carnitine acetyltransferase (CRAT); 2) acetyl-CoA participates in the tricarboxylic acid (TCA) cycle to provide ATP; 3) acetyl-CoA as a direct raw material to synthesize cholesterol; 4) acetyl-CoA is converted into a ketone body.

It was worth noting that a US study indicated that CPT-I α-subtype mRNA abundance was increased in the heart of

TABLE 3 | Odds ratios of short-chain acylcarnitine for CVD risk in T2DM.

	OR	95%CI	*p*-value
Model 1			
C2 ≥ *vs*. <14 μmol/L	1.576	1.203–2.064	0.0009
C4 (μmol/L)	3.551	1.409–8.946	0.0072
C5-OH (μmol/L)			
<0.22	1.638	1.181–2.270	0.0031
≥0.22 to ≤0.30	Reference		
>0.30	1.023	0.738–1.419	0.8906
C6 ≥ *vs*. <0.08 μmol/L	0.893	0.404–1.970	0.7785
Model 2			
C2 ≥ *vs*. <14 μmol/L	1.558	1.124–2.159	0.0078
C4 (μmol/L)	3.727	1.220–11.388	0.0210
C5-OH (μmol/L)			
<0.22	1.614	1.091–2.387	0.0165
≥0.22 to ≤0.32	Reference		
>0.32	1.295	0.876–1.916	0.1952
C6 ≥ *vs*. <0.08 μmol/L	0.487	0.196–1.209	0.1208
Stepwise regression			
C2 ≥ *vs*. <14 μmol/L	1.562	1.132–2.154	0.0067

Model 1 is the univariable model. Model 2 is the multivariable model, further adjusted for age, sex, body mass index, duration of diabetes, glycated hemoglobin, systolic blood pressure, diastolic blood pressure, triglyceride, low-density lipoprotein cholesterol, high-density lipoprotein, antidiabetic drugs, lipid-lowering drugs, and antihypertensive drugs. Values in bold are p-values less than 0.0125 (Bonferroni = 0.05/4) for the association of acylcarnitine with CVD in T2DM.

CVD, cardiovascular disease; T2DM, type 2 diabetes mellitus; C2, acetylcarnitine; C4, butyrylcarnitine; C5-OH, 3-hydroxyisovalerylcarnitine; C6, hexanoylcarnitine.

diabetic or fasted rats (27). Meanwhile, increased FA uptake associated with reduced glucose oxidation has been observed in the heart of both diabetic mice (*Ob*/*ob* and *db*/*db* mice) and in patients with type 2 diabetes (28–30). The characteristic of a diabetic heart is that the supply of substrates exceeds the need for TCA cycle (31). A study found that the genes involved in glucose transport and utilization were inhibited and that significant heart failure occurred at 4 weeks of age in a lipid-toxic mouse (the FA uptake rate exceeded the utilization rate), which was constructed using transgenic technology (32). Furthermore, an increase in the acetyl-CoA/CoA ratio was discovered in the heart of patients with diabetic cardiomyopathy (33).

Therefore, we suspect that the accumulation of acetyl-CoA is caused by the FA uptake rate exceeding the need of the TCA cycle rate. Besides, a cohort study found that a higher transcriptional level of CRAT and elevated C2 were observed in impaired glucose tolerance (IGT) and T2DM patients, which presented during follow-up (34). The higher CRAT transcription level may explain the increase of acetylcarnitine due to a part of accumulation of acetyl-CoA (35). Moreover, the glycolysis pathway from pyruvate to acetyl-CoA will be further inhibited by negative feedback when excess acetyl-CoA exceeds the conversion capacity of the TCA cycle, thus exacerbating insulin resistance (36). Normal insulin signaling in the vascular endothelium can protect against atherosclerosis (37). Insulin resistance is associated with reduced production and release of nitric oxide in vascular endothelial cells (38), leading to impaired cellular function and, thus, an increased risk of atherosclerosis (39). In addition, as a direct precursor, the accumulation of acetyl-CoA may lead to increased cholesterol production in the liver, which may exceed the body's metabolic capacity, deposit in the blood vessels, leading to atherosclerosis (**Figure 2**). A study involving 1,185 hospitalized patients with suspected coronary heart disease (CHD) found that elevated C2 worsened coronary stenosis after coronary angiography (OR = 1.778, 95%CI = 1.106–2.857) (40). Other population studies have demonstrated that C2 is associated with higher severity of CHD and adverse cardiovascular outcomes (41–44).

There were several shortcomings and limitations in our study. Firstly, it was difficult to determine the causal relationship between acylcarnitine and CVD in T2DM due to the cross-sectional nature of the study. Secondly, the levels of short-chain acylcarnitine are influenced by dietary habits. Since we retrospectively retrieved the data from the hospital's electronic medical records, information regarding diet was not available for further investigation. In order to avoid the bias caused by diet as much as possible, we used fasting samples and adjusted the BMI, LDL-C, HDL-C, and TG. Thirdly, further enzyme analysis was needed to assay the levels of C2-related enzymes to support the conjecture involving related enzymes. Last but not least, the presence of missing values in our lipid index might affect the stability of the results. We reduced this effect by converting missing variables into categorical variables in the analysis. Also, the relationship between C2 and CVD in T2DM did not change significantly after mean and multiple imputations.

There are public health significance and clinical implications in our research. In combination with previous studies, we determined that C2, as a novel target for CVD in T2DM, may reflect the state of acetyl CoA accumulation in T2DM patients with CVD. C2 reflected acetyl-CoA, and its downstream metabolites are helpful in further exploring the pathogenesis of cardiovascular diseases.

In summary, an elevated level of C2 is associated with an increased risk of CVD in T2DM. Prospective studies are needed

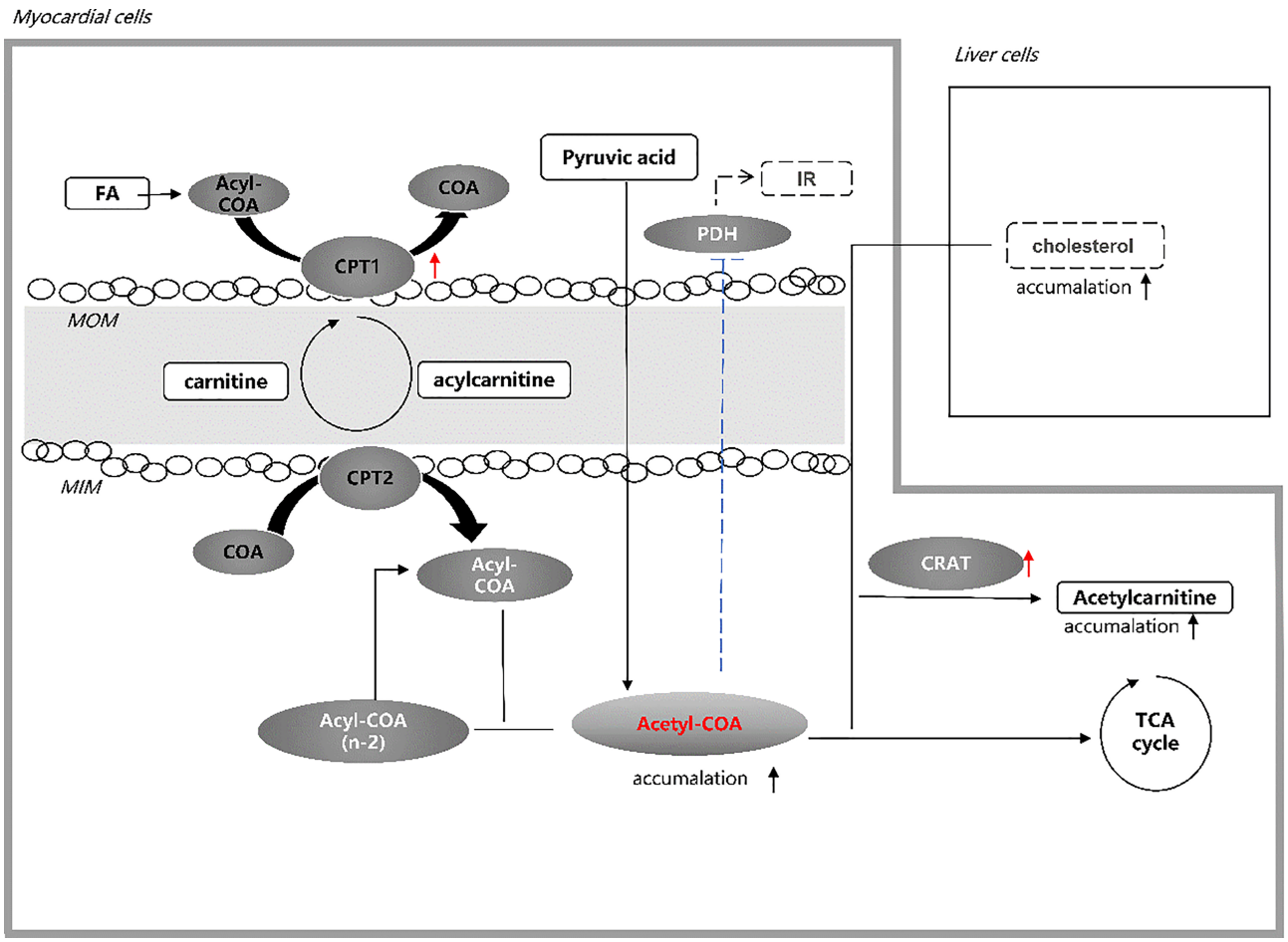

FIGURE 2 | Hypothesis of acetylcarnitine association with CVD in T2DM. Elevated acetylcarnitine due to the higher activity of CPT1 and CRAT in patients with CVD in T2DM may reflect the state of accumulation of acetyl-CoA exceeding the capacity of the TCA cycle. Increased level of acetyl-CoA in the heart of T2DM patients leads to intensified insulin resistance by inhibiting PDH and increased cholesterol production in liver cells. Both pathways may account for the high CVD risk in T2DM. *FA*, fatty acid; *CoA*, co-enzyme A; *CPT 1*, carnitine palmitoyl transferase 1; *MOM*, mitochondrial outer membrane; *MIN*, mitochondrial inner membrane; *CPT 2*, carnitine palmitoyl transferase 2; *IR*, insulin resistance; *PDH*, pyruvate dehydrogenase; *CRAT*, carnitine acetyltransferase; *TCA*, tricarboxylic acid.

to further validate this finding and explore the pathological mechanism of CVD in T2DM.

DATA AVAILABILITY STATEMENT

The raw data supporting the conclusions of this article will be made available by the authors, without undue reservation.

ETHICS STATEMENT

The studies involving human participants were reviewed and approved by the First Affiliated Hospital of Liaoning Medical University. The patients/participants provided written informed consent to participate in this study. Written informed consent was obtained from the individual(s) for the publication of any potentially identifiable images or data included in this article.

AUTHOR CONTRIBUTIONS

RL, M-LL, BH, and X-TC designed the study. SZ and M-LL analyzed the data and wrote the draft. RL, BH, F-RZ, YL, X-TC, and SZ gave critical comments and contributed to the writing of this manuscript. All authors contributed to the article and approved the submitted version.

FUNDING

This research was financially supported by the Development and Application of Clinical Mass Spectrometry Detection Technology for Important Small Molecule Metabolites (2020JH2/10300116) and the Key R&D Program of Liaoning Province: platform name: Dalian Laboratory Medicine Mass Spectrometry Technology Innovation Center.

ACKNOWLEDGMENTS

The authors thank all doctors, nurses, and research staff at the First Affiliated Hospital of Liaoning Medical University, for their participation in this study.

SUPPLEMENTARY MATERIAL

The Supplementary Material for this article can be found online at: https://www.frontiersin.org/articles/10.3389/fendo.2021.806819/full#supplementary-material

REFERENCES

1. International Diabetes Federation. *IDF Diabetes Atlas* (2019). International Diabetes Federation. Available at: https://diabetesatlas.org/en/ (Accessed September 10, 2020).
2. Forbes JM, Cooper ME. Mechanisms of Diabetic Complications. *Physiol Rev* (2013) 93:137–88. doi: 10.1152/physrev.00045.2011
3. International Diabetes Federation. *Diabetes and Cardiovascular Disease*. Available at: https://www.idf.org/our-activities/care-prevention/cardiovascular-disease.html (Accessed September 10, 2020).
4. International Diabetes Federation. *IDF Advocacy Toolkit CVD in Diabetes*. Available at: https://www.idf.org/component/attachments/?task=download&id=1606:IDF-CVD-in-Diabetes-FINAL (Accessed September 10, 2020).
5. Danaei G, Lawes CM, Vander Hoorn S, Murray CJ, Ezzati M. Global and Regional Mortality From Ischaemic Heart Disease and Stroke Attributable to Higher-Than-Optimum Blood Glucose Concentration: Comparative Risk Assessment. *Lancet (London England)* (2006) 368:1651–9. doi: 10.1016/s0140-6736(06)69700-6
6. Appel LJ, Clark JM, Yeh HC, Wang NY, Coughlin JW, Daumit G, et al. Comparative Effectiveness of Weight-Loss Interventions in Clinical Practice. *New Engl J Med* (2011) 365:1959–68. doi: 10.1056/NEJMoa1108660
7. Tankó LB, Bagger YZ, Alexandersen P, Larsen PJ, Christiansen C. Central and Peripheral Fat Mass Have Contrasting Effect on the Progression of Aortic Calcification in Postmenopausal Women. *Eur Heart J* (2003) 24:1531–7. doi: 10.1016/s0195-668x(03)00319-1
8. Stefan N. Causes, Consequences, and Treatment of Metabolically Unhealthy Fat Distribution. *Lancet Diabetes Endocrinol* (2020) 8:616–27. doi: 10.1016/s2213-8587(20)30110-8
9. Bayeva M, Sawicki KT, Ardehali H. Taking Diabetes to Heart–Deregulation of Myocardial Lipid Metabolism in Diabetic Cardiomyopathy. *J Am Heart Assoc* (2013) 2:e000433. doi: 10.1161/jaha.113.000433
10. Johnson CH, Ivanisevic J, Siuzdak G. Metabolomics: Beyond Biomarkers and Towards Mechanisms. *Nat Rev Mol Cell Biol* (2016) 17:451–9. doi: 10.1038/nrm.2016.25
11. Wedekind R, Kiss A, Keski-Rahkonen P, Viallon V, Rothwell JA, Cross AJ, et al. A Metabolomic Study of Red and Processed Meat Intake and Acylcarnitine Concentrations in Human Urine and Blood. *Am J Clin Nutr* (2020) 112:381–88. doi: 10.1093/ajcn/nqaa140
12. Sun L, Xie C, Wang G, Wu Y, Wu Q, Wang X, et al. Gut Microbiota and Intestinal FXR Mediate the Clinical Benefits of Metformin. *Nat Med* (2018) 24:1919–29. doi: 10.1038/s41591-018-0222-4
13. Qi X, Yun C, Sun L, Xia J, Wu Q, Wang Y, et al. Gut Microbiota-Bile Acid-Interleukin-22 Axis Orchestrates Polycystic Ovary Syndrome. *Nat Med* (2019) 25:1225–33. doi: 10.1038/s41591-019-0509-0
14. Zhao S, Feng XF, Huang T, Luo HH, Chen JX, Zeng J, et al. The Association Between Acylcarnitine Metabolites and Cardiovascular Disease in Chinese Patients With Type 2 Diabetes Mellitus. *Front Endocrinol* (2020) 11:212. doi: 10.3389/fendo.2020.00212
15. Nie Q, Xing M, Chen H, Hu J, Nie S. Metabolomics and Lipidomics Profiling Reveals Hypocholesterolemic and Hypolipidemic Effects of Arabinoxylan on Type 2 Diabetic Rats. *J Agric Food Chem* (2019) 67:10614–23. doi: 10.1021/acs.jafc.9b03430
16. Kukharenko A, Brito A, Kozhevnikova MV, Moskaleva N, Markin PA, Bochkareva N, et al. Relationship Between the Plasma Acylcarnitine Profile and Cardiometabolic Risk Factors in Adults Diagnosed With Cardiovascular Diseases. *Clin Chim Acta Int J Clin Chem* (2020) 507:250–56. doi: 10.1016/j.cca.2020.04.035
17. Alberti KG, Zimmet PZ. Definition, Diagnosis and Classification of Diabetes Mellitus and Its Complications. Part 1: Diagnosis and Classification of Diabetes Mellitus Provisional Report of a WHO Consultation. *Diabetic Med: J Br Diabetic Assoc* (1998) 15:539–53. doi: 10.1002/(sici)1096-9136(199807)15:7<539::Aid-dia668>3.0.Co;2-s
18. Hou Q, Guan Y, Yu W, Liu X, Wu L, Xiao M, et al. Associations Between Obesity and Cognitive Impairment in the Chinese Elderly: An Observational Study. *Clin Interventions Aging* (2019) 14:367–73. doi: 10.2147/cia.S192050
19. Andersen PK. *Regression Modeling Strategies With Applications to Linear Models, Logistic Regression and Survival Analysis* Vol. 22. FE Harrell, editor. New York: Springer-Verlag (2003) p. 2531–32. Available at: https://doi.org/10.1002/sim.1497. No. of pages: 568.
20. Huo X, Li J, Cao YF, Li SN, Shao P, Leng J, et al. Trimethylamine N-Oxide Metabolites in Early Pregnancy and Risk of Gestational Diabetes: A Nested Case-Control Study. *J Clin Endocrinol Metab* (2019) 104:5529–39. doi: 10.1210/jc.2019-00710
21. Liu J, Li J, Li S, Leng J, Li W, Yang W, et al. Circulating Lysophosphatidylcholines in Early Pregnancy and Risk of Gestational Diabetes in Chinese Women. *J Clin Endocrinol Metab* (2020) 105:e982–83. doi: 10.1210/clinem/dgaa058
22. Vivoli E, Di Cesare Mannelli L, Salvicchi A, Bartolini A, Koverech A, Nicolai R, et al. Acetyl-L-Carnitine Increases Artemin Level and Prevents Neurotrophic Factor Alterations During Neuropathy. *Neuroscience* (2010) 167:1168–74. doi: 10.1016/j.neuroscience.2010.03.017
23. Jones LL, McDonald DA, Borum PR. Acylcarnitines: Role in Brain. *Prog Lipid Res* (2010) 49:61–75. doi: 10.1016/j.plipres.2009.08.004
24. Houten SM, Wanders RJ. A General Introduction to the Biochemistry of Mitochondrial Fatty Acid β-Oxidation. *J Inherited Metab Dis* (2010) 33:469–77. doi: 10.1007/s10545-010-9061-2
25. Knottnerus SJG, Bleeker JC, Wüst RCI, Ferdinandusse S, IJ L, FA W, et al. Disorders of Mitochondrial Long-Chain Fatty Acid Oxidation and the Carnitine Shuttle. *Rev Endocrine Metab Disord* (2018) 19:93–106. doi: 10.1007/s11154-018-9448-1
26. Pietrocola F, Galluzzi L, Bravo-San Pedro JM, Madeo F, Kroemer G. Acetyl Coenzyme A: A Central Metabolite and Second Messenger. *Cell Metab* (2015) 21:805–21. doi: 10.1016/j.cmet.2015.05.014
27. Cook GA, Edwards TL, Jansen MS, Bahouth SW, Wilcox HG, Park EA. Differential Regulation of Carnitine Palmitoyltransferase-I Gene Isoforms (CPT-I Alpha and CPT-I Beta) in the Rat Heart. *J Mol Cell Cardiol* (2001) 33:317–29. doi: 10.1006/jmcc.2000.1304
28. Belke DD, Larsen TS, Gibbs EM, Severson DL. Altered Metabolism Causes Cardiac Dysfunction in Perfused Hearts From Diabetic (Db/Db) Mice. *Am J Physiol Endocrinol Metab* (2000) 279:E1104–13. doi: 10.1152/ajpendo.2000.279.5.E1104
29. Buchanan J, Mazumder PK, Hu P, Chakrabarti G, Roberts MW, Yun UJ, et al. Reduced Cardiac Efficiency and Altered Substrate Metabolism Precedes the Onset of Hyperglycemia and Contractile Dysfunction in Two Mouse Models of Insulin Resistance and Obesity. *Endocrinology* (2005) 146:5341–9. doi: 10.1210/en.2005-0938
30. Rijzewijk LJ, van der Meer RW, Lamb HJ, de Jong HW, Lubberink M, Romijn JA, et al. Altered Myocardial Substrate Metabolism and Decreased Diastolic Function in Nonischemic Human Diabetic Cardiomyopathy: Studies With Cardiac Positron Emission Tomography and Magnetic Resonance Imaging. *J Am Coll Cardiol* (2009) 54:1524–32. doi: 10.1016/j.jacc.2009.04.074
31. Kolwicz SCJr., Purohit S, Tian R. Cardiac Metabolism and its Interactions With Contraction, Growth, and Survival of Cardiomyocytes. *Circ Res* (2013) 113:603–16. doi: 10.1161/circresaha.113.302095
32. Chiu HC, Kovacs A, Ford DA, Hsu FF, Garcia R, Herrero P, et al. A Novel Mouse Model of Lipotoxic Cardiomyopathy. *J Clin Invest* (2001) 107:813–22. doi: 10.1172/jci10947

33. Berthiaume JM, Kurdys JG, Muntean DM, Rosca MG. Mitochondrial NAD (+)/NADH Redox State and Diabetic Cardiomyopathy. *Antioxid Redox Signaling* (2019) 30:375–98. doi: 10.1089/ars.2017.7415
34. Wang-Sattler R, Yu Z, Herder C, Messias AC, Floegel A, He Y, et al. Novel Biomarkers for Pre-Diabetes Identified by Metabolomics. *Mol Syst Biol* (2012) 8:615. doi: 10.1038/msb.2012.43
35. Adeva-Andany MM, Calvo-Castro I, Fernández-Fernández C, Donapetry-García C, Pedre-Piñeiro AM. Significance of L-Carnitine for Human Health. *IUBMB Life* (2017) 69:578–94. doi: 10.1002/iub.1646
36. Miyamoto Y, Miyazaki T, Honda A, Shimohata H, Hirayama K, Kobayashi M. Retention of Acetylcarnitine in Chronic Kidney Disease Causes Insulin Resistance in Skeletal Muscle. *J Clin Biochem Nutr* (2016) 59:199–206. doi: 10.3164/jcbn.15-146
37. Laakso M, Kuusisto J. Insulin Resistance and Hyperglycaemia in Cardiovascular Disease Development. *Nat Rev Endocrinol* (2014) 10:293–302. doi: 10.1038/nrendo.2014.29
38. Steinberg HO, Brechtel G, Johnson A, Fineberg N, Baron AD. Insulin-Mediated Skeletal Muscle Vasodilation Is Nitric Oxide Dependent. A Novel Action of Insulin to Increase Nitric Oxide Release. *J Clin Invest* (1994) 94:1172–9. doi: 10.1172/jci117433
39. Steinberg HO, Chaker H, Leaming R, Johnson A, Brechtel G, Baron AD. Obesity/Insulin Resistance Is Associated With Endothelial Dysfunction. Implications for the Syndrome of Insulin Resistance. *J Clin Invest* (1996) 97:2601–10. doi: 10.1172/jci118709
40. Teren A, Vogel A, Beutner F, Gielen S, Burkhardt R, Scholz M, et al. Relationship Between Fermented Dairy Consumption, Circulating Short-Chain Acylcarnitines and Angiographic Severity of Coronary Artery Disease. *Nutrition Metabol Cardiovasc Dis: NMCD* (2020) 30:1662–72. doi: 10.1016/j.numecd.2020.05.031
41. Shah AA, Craig DM, Sebek JK, Haynes C, Stevens RC, Muehlbauer MJ, et al. Metabolic Profiles Predict Adverse Events After Coronary Artery Bypass Grafting. *J Thorac Cardiovasc Surg* (2012) 143:873–8. doi: 10.1016/j.jtcvs.2011.09.070
42. Shah SH, Bain JR, Muehlbauer MJ, Stevens RD, Crosslin DR, Haynes C, et al. Association of a Peripheral Blood Metabolic Profile With Coronary Artery Disease and Risk of Subsequent Cardiovascular Events. *Circulation Cardiovasc Genet* (2010) 3:207–14. doi: 10.1161/circgenetics.109.852814
43. Wu Q, Liang X, Wang K, Lin J, Wang X, Wang P, et al. Intestinal Hypoxia-Inducible Factor 2α Regulates Lactate Levels to Shape the Gut Microbiome and Alter Thermogenesis. *Cell Metab* (2021) 33:1988–2003.e7. doi: 10.1016/j.cmet.2021.07.007
44. Zhang X, Zhang Y, Wang P, Zhang SY, Dong Y, Zeng G, et al. Adipocyte Hypoxia-Inducible Factor 2α Suppresses Atherosclerosis by Promoting Adipose Ceramide Catabolism. *Cell Metab* (2019) 30:937–51.e5. doi: 10.1016/j.cmet.2019.09.016

Conflict of Interest: Authors BH, X-TC, M-LL, F-RZ, and YL were employed by the company Dalian Runsheng Kangtai Medical Lab Co. Ltd.

The remaining authors declare that the research was conducted in the absence of any commercial or financial relationships that could be construed as a potential conflict of interest.

Publisher's Note: All claims expressed in this article are solely those of the authors and do not necessarily represent those of their affiliated organizations, or those of the publisher, the editors and the reviewers. Any product that may be evaluated in this article, or claim that may be made by its manufacturer, is not guaranteed or endorsed by the publisher.

frontiers in Endocrinology

ORIGINAL RESEARCH
published: 03 January 2022
doi: 10.3389/fendo.2021.801686

Psychiatric Comorbidities and Liver Injury Are Associated With Unbalanced Plasma Bile Acid Profile During Methamphetamine Withdrawal

Yuru Ma[1,2†], Hongjin Wu[1,2†], Huawei Wang[1,2], Fengrong Chen[1,3], Zhenrong Xie[1,2], Zunyue Zhang[1,4], Qingyan Peng[1,2], Jiqing Yang[1,3], Yong Zhou[1,2], Cheng Chen[1,2], Minghui Chen[1,2], Yongjin Zhang[1,2], Juehua Yu[1,2] and Kunhua Wang[1,2*]*

[1] National Health Commission (NHC) Key Laboratory of Drug Addiction Medicine (Kunming Medical University), First Affiliated Hospital of Kunming Medical University, Kunming,China, [2] Centre for Experimental Studies and Research, First Affiliated Hospital of Kunming Medical University, Kunming, China, [3] Medical School, Kunming University of Science and Technology, Kunming, China, [4] Yunnan University, Kunming, China

OPEN ACCESS

Edited by:
Yanli Pang,
Peking University Third Hospital, China

Reviewed by:
Tongzhi Wu,
University of Adelaide, Australia
Lili Ding,
Shanghai University of Traditional Chinese Medicine, China

***Correspondence:**
Juehua Yu
juehuayu@gmail.com
Kunhua Wang
kunhuawang1@163.com

[†]These authors have contributed equally to this work

Specialty section:
This article was submitted to Gut Endocrinology, a section of the journal Frontiers in Endocrinology

Received: 25 October 2021
Accepted: 06 December 2021
Published: 03 January 2022

Citation:
Ma Y, Wu H, Wang H, Chen F, Xie Z, Zhang Z, Peng Q, Yang J, Zhou Y, Chen C, Chen M, Zhang Y, Yu J and Wang K (2022) Psychiatric Comorbidities and Liver Injury Are Associated With Unbalanced Plasma Bile Acid Profile During Methamphetamine Withdrawal. Front. Endocrinol. 12:801686. doi: 10.3389/fendo.2021.801686

Background: The pathogenesis of methamphetamine usedisorders (MUDs) remains largely unknown; however, bile acids may play arole as potential mediators of liver injury and psychiatric comorbidities.The aim of this study was to characterize bile acid (BA) profiles in plasmaof patients with MUDs undergoing withdrawal.

Methods: Liver functions and psychiatric symptoms wereevaluated in a retrospective cohort (30 MUDs versus 30 control subjects) andan exploratory cohort (30 MUDs including 10 subjects each at the 7-day,3-month, and 12-month withdrawal stages versus 10 control subjects). BAcompositions in plasma samples from MUD patients in the exploratory cohortwere determined by gas-liquid chromatography.

Results: Both psychiatric comorbidities andmethamphetamine-induced liver injury were observed in patients in both MUDcohorts. The plasma concentrations of the total BA, cholic acid (CA), andchenodeoxycholic acid (CDCA) were lower in MUD patients relative tocontrols. The maximum decline was observed at the 3-month stage, withgradual recovery at the 12-month stage. Notably, the ratios of deoxycholicacid (DCA)/CA and lithocholic acid (LCA)/CDCA were statistically significantat the 3-month stage comparing with controls. Significant correlations werefound between the LCA/CDCA and taurolithocholic acid (TLCA)/CDCA ratios andthe levels of alanine transaminase and aspartate aminotransferase, andbetween the LCA/CDCA ratio and the HAM-A score.

Conclusion: BA profile during METH withdrawal weremarkedly altered, with these unbalanced BAs being associated with liverinjury. The associations between BA profiles and psychiatric symptomssuggest an association between specific BAs and disease progression,possibly through the liver-brain axis.

Keywords: methamphetamine withdrawal, bile acid, psychiatric comorbidities, liver injury, crosstalk

INTRODUCTION

Methamphetamine (METH), a potent addictive psychostimulant, wasinitially developed from its parent drug amphetamine, but the prevalence of METH abuse has been significantly increasing (1).According to the 2019 State Council of China report, approximately 56.1% ofregistered drug abusers suffered from some form of METH dependence (The State Council China, 2018 China Drug Situation Report, 2019).

Anxiety and depression, the most common psychiatric symptoms ofpatients with methamphetamine use disorders (MUDs), may persist for 6 months orlonger during its withdrawal (2), and may evenrecur and persist throughout life (1, 3). Our previous cross-sectional study revealedimportant associations between the key neurotransmitters GABA, serotonin andcholine, and the severities of anxiety and depression symptoms in MUDs (4, 5). Despite studies showing that METH is neurotoxic, pharmacologic interventions focusedon modulating monoaminergic pathways have largely failed and no medications to datehave been approved by the U.S. Food and Drug Administration (FDA) for treating METHdependence (6).

In addition to the stimulating and psychotropic effects to the brain(7), METH damages multiple peripheralorgans (8), including the liver, intestines,kidneys, and muscles, of which the liver is the most vulnerable organ (9, 10). For instance, patients with MUDs have shown serological evidence of METH-inducedacute liver injury and chronic liver diseases, and animal models of MUDs have shownhistological evidence of acute hepatotoxicity and oxidative stress (10, 11). Furthermore, associations among METH-induced liver injury, increased peripheral andbrain ammonia, and long-term depletions of dopamine and serotonin have been observedin METH-treated rat models (12–14), suggesting that liver injury may beassociated with the process of neurological impairment in patients with MUDs (11, 15). Thus, these systematic impairments including acute or chronic liver injury mayinterfere with pharmacologic interventions targeting brain dysfunction, leading topoor outcome. To date, however, the underlying molecular mechanisms involving theseassociations among peripheral organs and the CNS have not been extensively investigated.

Bile acids (BAs) are a large group of structurally related moleculesderived from cholesterol and synthesized exclusively in the liver (16). Although BAs were thought to primarilyfunction to expedite the digestion and absorption of dietary lipids and lipophilicvitamins by forming micelles in the small intestine (17), they could function to signal through receptors on various celltypes throughout the body, including the CNS and other organ systems (18). Abnormal circulating bile acid metabolitelevels in the patients with Alzheimer's disease predicted worse outcomes(19). Alterations in cholesterol and BAmetabolism have been shown to contribute to the development of neurodegenerative andneurological diseases, such as Alzheimer's disease, Parkinson's disease,and multiple sclerosis (20–22). Recent reports of gut-based bariatricsurgery suggest that chronically elevate systemic BA concentrations and attenuatecocaine-induced cumulative dopamine increase, and this surgery reducesreward-related behavior and psychomotor sensitization to cocaine in a mouse model (23). Moreover, fecal BA excretion levelhas been shown to correlate with alcohol abuse and abstinence (24). Thus, we hypothesized that peripheral BA profiles mayserve as a potential diagnostic biomarker or therapeutic target for substance usedisorders (SUDs). However, the direct role of BAs in the context of METH dependenceand withdrawal remains unclear.

The present study was designed to investigate thedynamic pattern of BAs in patients with MUDs currently undergoing METH withdrawaland to analyze the correlations among anxiety and depression scales,neurotransmitters, laboratory parameters associated with liver and kidney function, glycolipid metabolism, and BAs. These findings might uncover the crosstalk betweenthe liver and the central nervous system (CNS) and provide clues toward a betterunderstanding of the role of BAs in MUDs.

MATERIALS AND METHODS

Participant Cohorts

The present study recruited two independent cohorts from a jointprogram of drug detoxification and rehabilitation in the First AffiliatedHospital of Kunming Medical University and the Kunming Drug RehabilitationCenter between July 2017 and October 2019. The retrospective cohort consisted of30 male MUDs undergoing withdrawal and 30 male healthy control subjects (HCs).The exploratory cohort consisted of 30 male MUDs undergoing withdrawal, 10 eachat the 7-day, 3-month, and 12-month withdrawal stages, and 10 age-matched HCs.Subjects were excluded if they had any other Diagnostic and Statistical Manualof Mental Disorders-5 (DSM-5) axis I or II disorders, other than amphetaminedependence; were positive for anti-HIV or anti-HCV antibodies; had anyneurological disorders or serious medical conditions; or were multi-substanceabusers including abuse of an opioid containing acetaminophen, which can causeliver damage.

All protocols and recruitment procedures wereapproved by the Research Ethics Committee of the First Affiliated Hospital ofKunming Medical University (2018-L-42), and all participants provided writteninformed consent before enrollment.

Scale Administration

Interviews with a professionally trainedinterviewer were conducted simultaneously with the collection of biologicalsamples. The HAM-A scale consists of 14 questions, seven elements examining psychological stress and seven examining physical stresses (25). Total scores of < 17, 18~24,25~30, and >30, indicated mild, mild to moderate, moderate to severe, andsevere grades of stress severity, respectively. The HAM-D scale consists of a24-item questionnaire that measures the severity of depressive symptoms, withtotal scores > 20 considered indicative of major depression (26).

Blood Tests

Fasting blood specimens were collected from studyparticipants into 10 mL EDTA-2Na vacuum tubes, and the blood samples werecentrifuged at 1,500 g for 15 min. The plasma was transferred to a new tube andcentrifuged at 20,000 g at 4°C for

15 min. Thesupernatants were aliquoted and stored at -80°C until analysis. Biochemicalparameters were measured using the Beckman Coulter Synchron DxC800 ChemistryAnalyzer (Beckman, USA). Concentrations of neurotransmitters were measured byultra-performance liquid chromatography coupled to tandem mass spectrometry(UPLC-MS/MS; ACQUITY UPLC-Xevo TQ-S, Waters Corp., Milford, MA, USA).

Targeted Metabolomics Analysis of BAs

Samples were prepared and BA concentrations measured as described (27). Briefly, an internal standardsolution containing six internal standards was added to each plasma sample orstandard solution and centrifuged. The internal standard solution contained 100nM concentrations of d4-glycocholic acid (GCA), d4-taurocholic acid (TCA),d4-cholic acid (CA), d4-glycodeoxycholic acid (GDCA), and d4-deoxycholic acid(DCA) and a 200 nM concentration of d4-lithocholic acid (LCA).

BAs were analyzed using a Waters ACQUITY ultraperformance LC system coupled with a Waters XEVO TQ-S mass spectrometer with anESI source controlled by MassLynx 4.1 software. Chromatographic separations wereperformed on an ACQUITY BEH C18 column (1.7 μM, 100 mm × 2.1 mminternal dimensions) (Waters). Raw UPLC-MS data obtained in negative mode wereanalyzed using Target Lynx applications manager version 4.1 (Waters) to obtaincalibration equations and determine the concentrations of each BA in these samples (28).

Statistical Analysis

Demographic, clinical, and biochemical parameterswere compared using SPSS Statistics version 23.0 software (IBM Corp., Armonk,NY, USA). Categorical variables using Chi-squared tests. If each group ofcontinuous variables satisfied both the normality test (Shapiro-Wilk normalitytest) and the homogeneity of variance test (Levene's test), t-tests wereused to conduct variance analysis between two groups whereas one-way ANOVA wereused to conduct variance analysis among three groups; Else if any group ofcontinuous variables could not satisfy the Shapiro-Wilk normality test or theLevene's test, Wilcoxon rank-sum Test were used to conduct varianceanalysis between two groups whereas Kruskal-Wallis test were used to conductvariance analysis among three groups. All p values were corrected by Bonferronimethod, an adjusted-p value <0.05 was considered statistically significant.Box plots and correlations analyses were performed and visualized the usingpheatmap, ggplot2 and ggpubr packages in R (v 3.6.3).

RESULTS

Characteristics of the Study Participants

The clinical characteristics of the retrospective cohort(Research cohort 1) are shown in **Table 1**. Sixty men, 30 MUDs and 30 HCs, aged25–50 years were enrolled. The duration of METH use in the 30 MUDs rangedfrom 61 to 107 months. The major routes of METH administration were smoking andnasal insufflation. There were no significant differences in age, body massindex (BMI), level of education, and self-reported annual income between thesetwo groups (**Table 1**).

To determine the dynamic alterations inpsychiatric symptoms and liver damage during METH withdrawal, a second,prospective cohort (Research cohort 2) was recruited. The demographiccharacteristics of this cohort have been previously described (4, 5) and are shown in **Table S1**. There were no significant differences in age, BMI,METH-use history, and education level among the three MUD subgroups and betweenthe MUD and HC groups. Although self-reported annual income was not wellbalanced, this was corrected in the subsequent statistical analyses.

Co-Existence of Liver Injury and Psychiatric Symptoms in MUDs

Questionnaires assessing the HAM-A and HAM-D rating scales, whichwere developed to quantify the severity of anxiety and depression, respectively,were administered by experienced interviewers. Compared with the HCs, the MUDsin Research cohort 1 had significantly higher scores on both the HAM-A ($p = 2.47\times10^{-4}$) and HAM-D ($p = 4.91\times10^{-3}$)scales. In addition, measurements of liver injury-related blood parameters (**Table 1**) showedthat plasma concentrations of alanine transaminase (ALT, $p = 3.78\times10^{-5}$) and aspartate aminotransferase (AST, $p = 2.85\times10^{-4}$) were significantly higher in the MUD than in theHC group. These findings indicate that the MUDs in Research cohort 1 had obviouspsychiatric comorbidities and METH-induced liver damage.

The psychiatric symptoms and blood concentrationsof peripheral neurotransmitters in Research cohort 2 have been reported (5). Blood parameters associated with glucoseand lipid metabolism, as well as liver and kidney function, were also assessed.Both ALT and AST levels were significantly higher in the MUDs than in the HCs (**Table S1**), consistent with the findings in Research cohort 1.Interestingly, most of the parameters differing in these two groups, includingAST, ALT, and triglyceride (TG) concentrations, as well as scores on the HAM-Aand HAM-D scales, showed greatest significance in the 10 MUD patients at the3-month withdrawal stage. HAM-A scores correlated significantly with theconcentrations of ALT ($p < 0.001$, $r = 0.73$), AST ($p = 0.006$, $r = 0.49$), TG ($p < 0.001$, $r = 0.58$) and LDL-cholesterol ($p = 0.01$, $r = 0.47$), whereas HAM-Dscores correlated significantly with the concentrations of AST ($p < 0.001$, $r = 0.78$), TG ($p = 0.004$, $r = 0.51$) and HDL-cholesterol ($p = 0.004$, $r = -0.52$),and the AST/ALT ratio ($p = 0.002$, $r = 0.54$). Taken together, these findingsshowed that liver and psychiatric symptoms were altered and correlated with eachother in patients undergoing their first year of METH withdrawal (**Figure 1** and **Figure S1**).

Dynamics of Plasma BA Concentrations During METH Withdrawal

BA has been reported to play critical roles in neurodegenerativeand neurological diseases (5, 29). To determine the dynamic changes in BAconcentrations at various stages of withdrawal, 42 BAs were simultaneously evaluated in

TABLE 1 | Characteristics of study participants from the retrospective cohort.

	MUDs	HCs	p_{adj}
NO.	30	30	NA
Age,years	37.17 ± 4.32	35.28 ± 6.54	0.67
BMI,kg/m2	22.16 ± 1.28	23.47 ± 0.98	0.36
METH abuse history, months	68.79 ± 21.23	NA	NA
Education	13/10/6/1	11/10/7/2	0.21
Income	3/12/6/9/0	3/12/6/6/3	0.14
HAM-A	11.47 ± 2.71	8.30 ± 2.71	2.47×10^{-4}
HAM-D	11.83 ± 3.93	8.60 ± 3.93	4.91×10^{-3}
Total serum protein	87.27 ± 5.16	82.89 ± 4.69	1.09×10^{-3}
ALB, g/L	55.71 ± 3.85	53.33 ± 2.63	7.03×10^{-3}
GLB, g/L	37.2 ± 3.28	33.42 ± 3.81	1.23×10^{-4}
ALB/GLB	2.25 ± 0.61	1.97 ± 0.53	0.06
ALT, IU/L	33.31 ± 7.70	24.73 ± 7.18	3.78×10^{-5}
AST, IU/L	33.97 ± 5.52	25.32 ± 10.94	2.85×10^{-4}
AST/ALT	1.20 ± 0.39	1.00 ± 0.21	0.01
TBIL, umol/L	11.60 ± 3.04	10.22 ± 1.32	0.03
PAB, g/L	318.37 ± 55.86	293.60 ± 47.40	0.07
Urea, mmol/L	4.10 ± 1.12	4.75 ± 1.12	0.03
Cr, umol/L	84.65 ± 6.61	84.90 ± 5.67	0.88
UA, umol/L	369.88 ± 46.74	369.88 ± 39.13	1.00
CHOL, mmol/L	6.18 ± 1.16	6.12 ± 0.73	0.81
TG, mmol/L	2.20 ± 1.06	1.63 ± 0.88	0.03
HDL, mmol/L	3.26 ± 1.23	2.33 ± 1.03	2.48×10^{-3}
LDL, mmol/L	1.99 ± 0.91	2.61 ± 0.88	0.01

Data are mean ± SD. P values were adjusted with Bonferroni method. Education levels: illiteracy/primary school/middleschool/college; Income levels: monthly0~1000¥/1000~3000¥/3000~5000¥/5000~10000¥/10000+¥.HAM-A, Hamilton Rating Scale for Anxiety; HAM-D, Hamilton Depression Rating Scale; ALB, Albumin; GLB, Globulin; ALT, Alaninetransaminase; AST, Aspartate aminotransferase; TBIL, Serum totalbilirubin; PAB, Prealbumin; Cr, Creatinine; UA, Uric Acid; CHOL, cholesterol; TG, triacylglycerol; HDL, high-density lipoprotein; LDL, low-density lipoprotein; NA, not available.

both MUDs and HCs from Research cohort 2 (**Table S2**).Intergroup differential analysis showed significant alterations in plasma BAs ofall three MUD subgroups, with similar trends for BA profile and blood parametersassociated with liver and psychiatric symptoms. These variations were greater atthe 3-month withdrawal stage than at the 7-day and 12- month stages. Forexample, the total BA concentration in plasma was significantly lower in all 30MUDs than in the HCs ($p = 8.66\times10^{-3}$). The maximum reductionoccurred at the 3-month stage ($p = 5.21\times10^{-3}$), with theseconcentrations gradually recovering at the 12-month stage ($p = 0.59$). Theprimary BAs, including CA and CDCA, were significantly lower in all three MUDsubgroups than in the HCs ($p_{CA} = 7.44\times10^{-5}$ &$p_{CDCA} = 9.79\times10^{-3}$), with the greatest reductionsoccurring at 3-months ($p_{CA} = 1.08\times10^{-5}$ &$p_{CDCA} = 4.27\times10^{-3}$). The concentrations ofsecondary BAs, including HCA and UDCA, were significantly lower in all MUDs thanin the HCs ($p_{HCA} = 0.01$ & $p_{UDCA} = 0.02$), with only besignificantly lower at the 3-month stage in the three MUD subgroups($p_{HCA} = 3.05\times10^{-3}$ & $p_{UDCA} = 4.13\times10^{-3}$). The concentrations of conjugated BAs such asGCDCA, TCDCA and GCA, were not changed in all MUDs relative to the HCs, while the significance was only observed at the 3-month stage ($p_{GCDCA} = 0.03$, $p_{TCDCA} = 0.04$, $p_{GCA} = 0.04$).

Assessments showed that 11 BAs, including four secondary BAs(hyocholic acid (HCA), a-muricholic acid (aMCA), 23-norcholic acid (NorCA), andursodeoxycholic acid (UDCA)), and seven conjugated BAs (THCA,taurochenodeoxycholic acid (TCDCA), ursocholic acid (UCA), glycohyocholic acid(GHCA), glycocholic acid (GCA), glycochenodeoxycholic acid (GCDCA), andGLCA-3S), were significantly altered only in MUD patients at the 3-monthwithdrawal stage (**Table S2** and **Figure 2**), suggestingthat alterations in key BAs in MUDs during withdrawal were stage specific.

In addition, the ratios of selected BAs were calculated toinvestigate the enzymatic activities involved in BA metabolism. The CA/CDCAratio was used to determine the shifts in BA synthesis from the primary to thealternative pathway; the ratios of secondary to primary BAs (DCA/CA andLCA/CDCA) were used to determine the changes in enzymatic activity towardshifted production of secondary BAs; and the GDCA/DCA and TLCA/DCA ratios wereused to determine whether the dysregulation in secondary BAs was correlated withtaurine or glycine conjugation (19). Interestingly, the ratios of CA/CDCA and DCA/CA were differed significantly inthe MUD and HC groups, whereas the other ratios did not differ. Comparisons ofthe three MUD subgroups with the HC group showed that the DCA/CA and LCA/CDCAratios differed significantly only at the 3-month stage. These results suggest that changes in BA metabolism, particularly in the production of secondary BAs,were stage specific in patients undergoing METH withdrawal.

To further determine the associations betweenplasma BAs and liver injury in MUDs, the Spearman correlations between BAprofiles and plasma concentrations of ALT and AST were calculated and analyzed.The LCA/CDCA ratio correlated significantly correlated with both ALT ($r = 0.93$,$p = 5.03\times10^{-4}$) and AST ($r = 0.93$, $p = 1.37\times10^{-4}$) concentrations (**Figure 3**). Similarly, the TLCA/CDCA ratiocorrelated significantly with

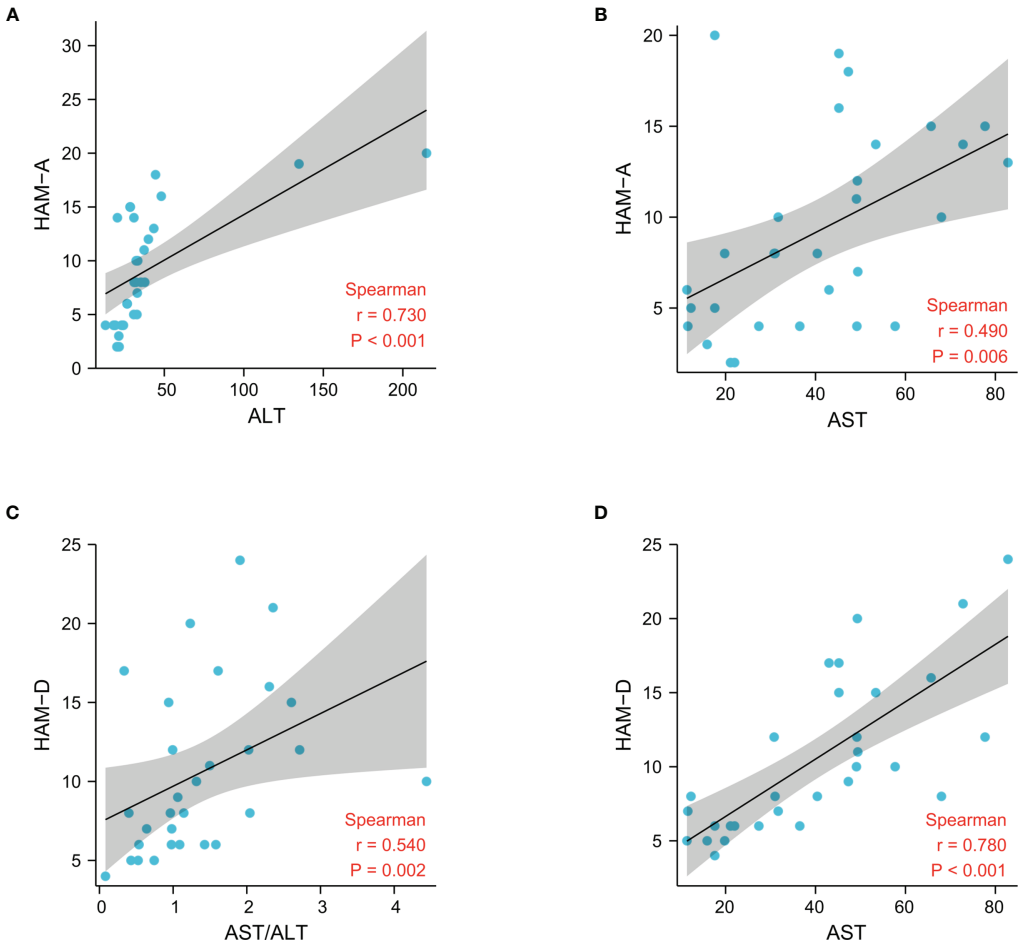

FIGURE 1 | Associations between liver damage and psychiatric comorbidities after METH withdrawal in the patient cohorts, as determined by Spearman correlation analysis.

ALT (r = 0.91, p = 2.26×10^{-4}) andAST (r = 0.90, p = 4.33×10^{-4}) concentrations. These resultsindicate that BA profiles during withdrawal are markedly altered, and that theseunbalanced BAs are associated with liver injury in patients with MUDs.

Unbalanced Plasma BAs Were Associated With Psychiatric Comorbidities and Neurotransmitters During METH Withdrawal

We also investigated the correlations among BA concentrations, psychiatric comorbidities and neurotransmitter concentrations. Theconcentrations of total BAs, bCA, CA, CDCA, UCA, THCA, GHCA, HCA, UDCA,7_ketoLCA and 3-DHCA were negatively correlated with HAM-A score in MUDs (**Figure 4**), of which theCDCA and HAM-A score showing the strongest negative correlation (r = -0.57, p =0.001). In contrast, the LCA/CDCA ratios (r = 0.46, p = 0.01) and TaMCA (r =0.42, p = 0.02) correlated positively with HAM-A scores.

In addition, CA/CDCA ratios, as well as theconcentrations of CA, GCDCA, NorCA, and THCA, were positively correlated withcholine concentrations, whereas the concentrations of total BAs, CA, CDCA,GCDCA, GHDCA, HCA, THCA, HDCA, NorCA, TCDCA, THDCA, and UCA were positively correlated with GABA concentrations (**Figure 4**). Interestingly, serotonin concentration correlated only with HCA concentration. Altogether, these results indicated that unbalanced BA profiles were associated with psychiatric symptomsand altered neurotransmitters in MUD patients during METH withdrawal.

DISCUSSION

This study recruited two cohorts of patients with MUDs andage-matched HCs and assessed the concentrations of their circulating BAs,neurotransmitters, and blood parameters related to liver and kidney function andglycolipid metabolism. To our knowledge, this study is the first to show that BAprofiles were significantly altered in patients with MUDs, and that these unbalancedBAs were associated with both liver injury and psychiatric comorbidities in patient sduring the first year of METH withdrawal.

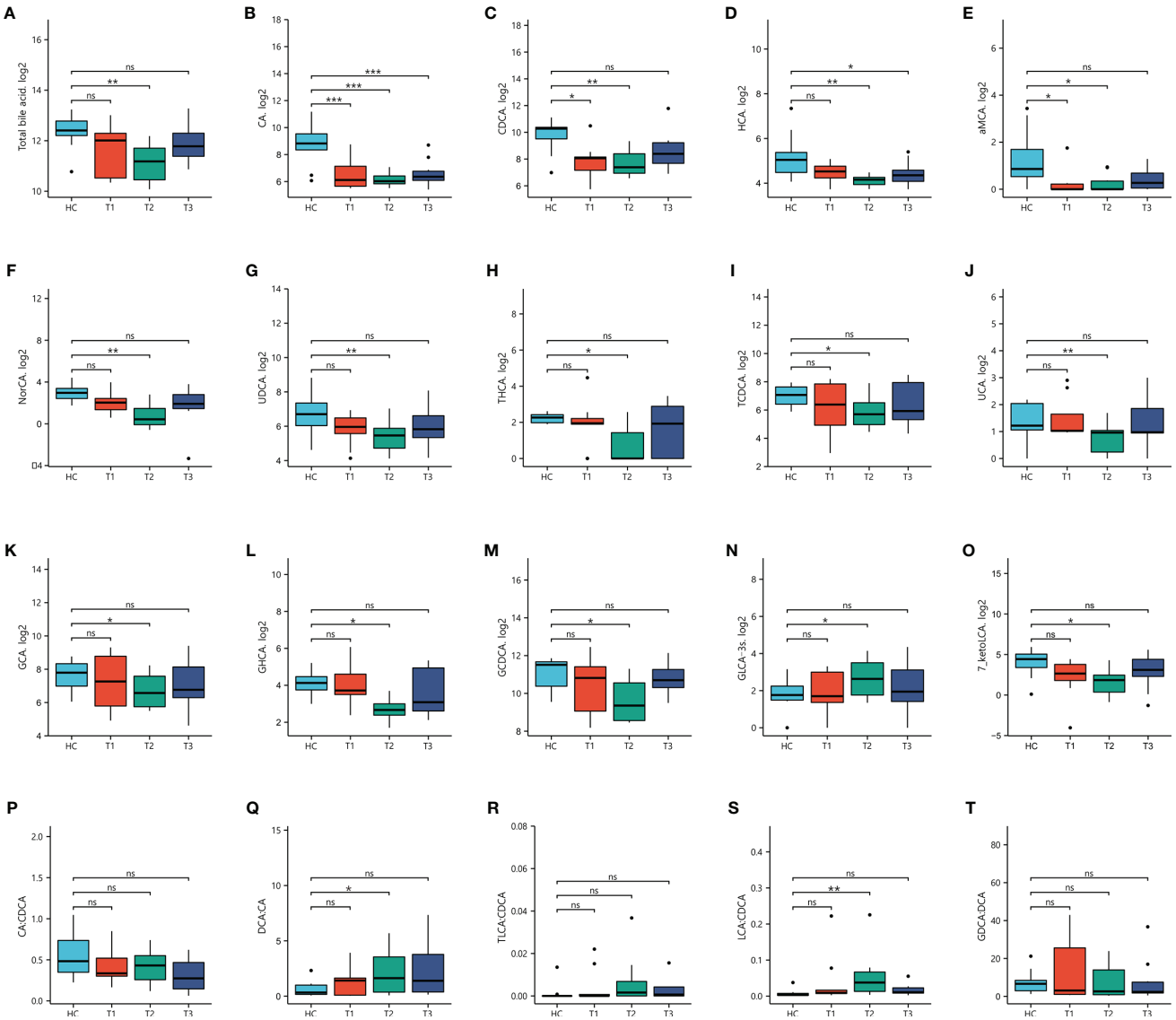

FIGURE 2 | Concentrations of bile acids in patients undergoing METH withdrawal and in healthy controls (HCs). Statistical significance were detected in three stages of METH withdrawal compared to HCs. *p < 0.05; **p < 0.01; ***p < 0.001 for between group comparisons. ns, no significance.

Mood problems (depression and anxiety) and cognitive impairments havebeen associated with liver damage, although these associations were investigatedprimarily in patients with non-alcoholic fatty liver disease (NAFLD) andnon-alcoholic steatohepatitis (NASH) (30). More recently, epidemiological studies have shown that patients with psychosis areat greater risk of presenting with damaged liver function (31), and are at increased risk of chronic liver diseases (32), even during early stages of psychosis (33). Studies using animal modelssuggested that liver dysfunction could reduce METH clearance, increase brain drugconcentrations, and therefore enhance its psychotropic effects on locomotor activityin a dose-dependent manner (34).Hyperthermia-dependent liver damage has been observed in mice after acuteadministration of METH, accompanied by increased plasma aspartate, ALT, and plasmaammonia concentrations (12). Theco-occurrence of liver injury and psychiatric comorbidities was validated in twoindependent cohorts, with ALT and AST concentrations being associated with theseverity of symptoms of anxiety and depression. Although it is unclear whether liverinjury persists along with long-lasting psychiatric comorbidities in MUDs yearsafter withdrawal, this study provides evidence supporting the critical role ofcrosstalk between dysregulation of the liver-brain axis and psychiatric symptomsduring the first year of METH withdrawal.

BAs are the end-products of cholesterol metabolism and are mainlyinvolved in liver, biliary, and intestinal diseases (35, 36). Most primary BAs areproduced in the liver, and can be modified, by conjugation with glycine or taurine,and stored in the gall

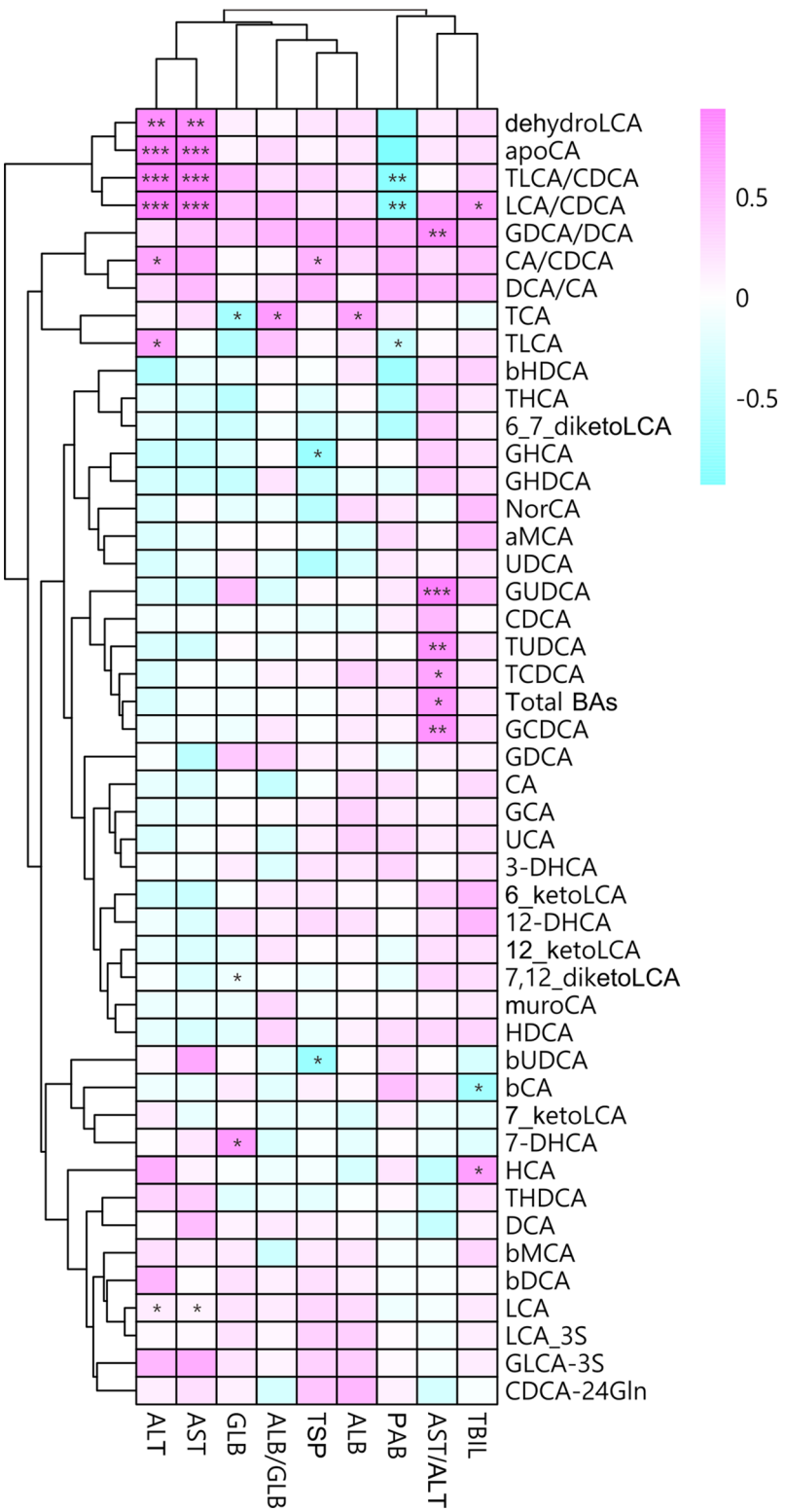

FIGURE 3 | Associations between plasma bile acid concentrations andliver damage after METH withdrawal, as determined by Spearman correlation analysis. Red indicates positive correlations and blue indicates negative correlations, with darker colors indicating stronger correlations. *p < 0.05; **p < 0.01; ***p < 0.001 for between group comparisons.

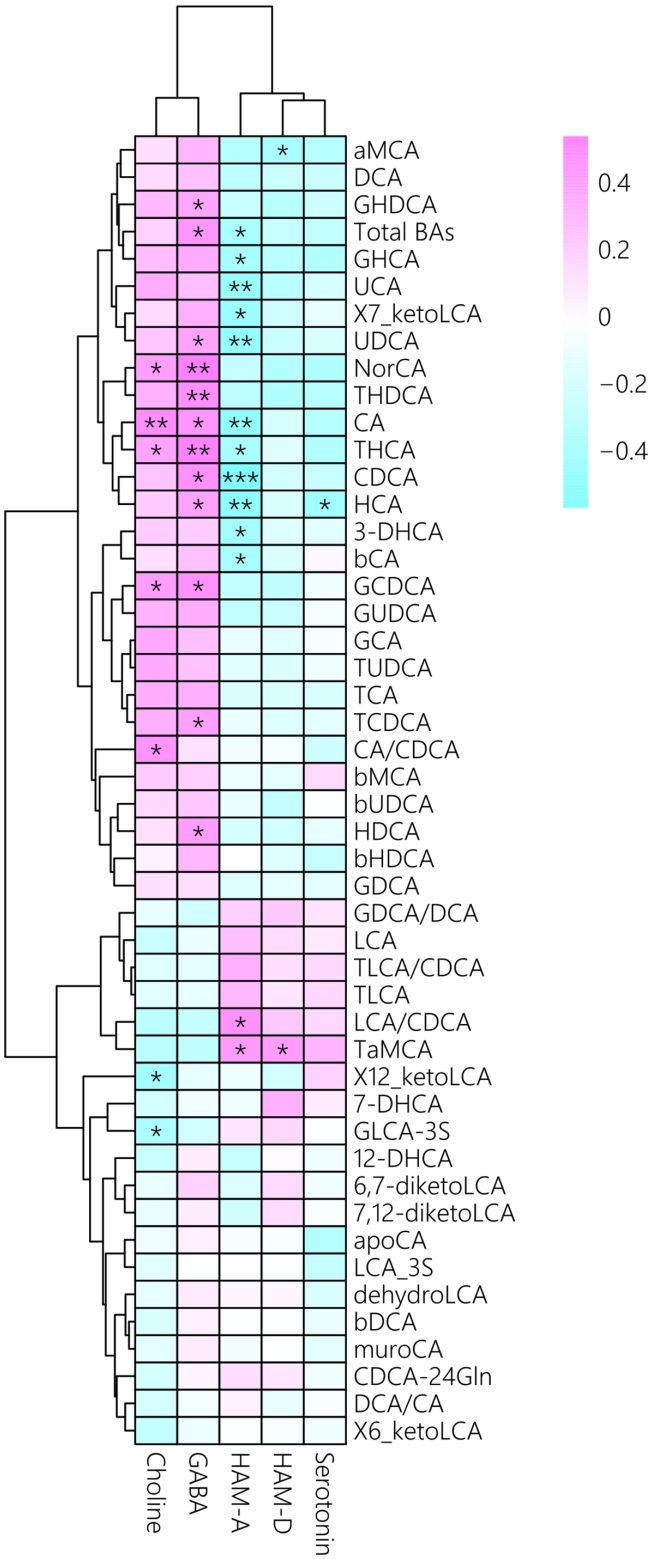

FIGURE 4 | Associations between plasma bile acid concentrations with psychiatric comorbidities and neurotransmitter concentrations after METH withdrawal, as determined by Spearman correlation analysis. Red indicates positive correlations and blue indicates negative correlations, with darker colors indicating stronger correlations.*$p < 0.05$; **$p < 0.01$; ***$p < 0.001$ for between group comparisons.

bladder until they are secreted into gut, where they arefurther modified by enzymes present in gut bacteria to produce secondary BAs (37). During this process, most BAs arereabsorbed and undergo enterohepatic recirculation through the portal venous system,with only a small fraction reaching the systemic circulation. Even though, theselection of plasma BAs could be used as diagnostic biomarkers to distinguishpatients with schizophrenia (38) or diabetes (39) from healthy controls. To elucidatethe role of BAs in the liver-brain axis in MUDs, this study profiled plasma BAs,finding that the concentrations of several key BAs were significantly lower in MUDpatients than in HCs. These BA deficiencies during METH withdrawal were consistentwith psychiatric comorbidities observed in MUDs, providing further evidence that BAshave neuroprotective functions in neurodegenerative diseases (40). The total BA concentration was found to correlatenegatively with both HAM-A and HAM-D scales, but positively correlated with theconcentrations of the neurotransmitters, choline and GABA, suggesting thatexcessively low total BA was associated with worse psychiatric comorbidities. Thistrend was observed for other differential BAs, including CA, CDCA, THCA, HCA, UCA, UDCA, NorCA and GCDCA, although these differences did not reach statisticalsignificance. These results suggest that BA deficiency is an important feature forpatients undergoing METH withdrawal and that BA deficiency may influence neuronalfunctions and enhance the risk of dementia (41). In addition, serum and fecal BA concentrations were shown todecrease in patients of irritable bowel syndrome with constipation (42). Because irritable bowel syndrome involvesinteractions between the intestines and brain and because the constipation phenotypeis very common in MUD patients and animal models of MUD (43, 44), these twoconditions may share some pathophysiological processes, with BA-mediated signalingpathways playing important roles in linking peripheral non-neuronal organ systemswith the CNS (21).

The exact mechanisms underlying the roles of BAs in the liver and CNSare not fully understood. Utilizing mass spectrometry-based targeted metabolomicstechnology and statistical analysis, we measured five selected BA ratios, findingthat the production of secondary BAs was markedly altered in patients undergoingMETH withdrawal, and that the CA/CDCA, TLCA/CDCA and LCA/CDCA ratios were associatedwith ALT and AST concentrations. Mechanistically, altered BA profiles may reflectimbalances in lipid metabolism during METH withdrawal. Hyperlipidemia, especiallyexcess TGs, has been reported to affect the development of neural cognition and mooddisorders through putative mechanisms such as brain blood barrier dysfunction or animbalance in amyloid metabolism (45–47). The present studyshowed that the plasma concentrations of TGs and LDL-cholesterol correlatedpositively with both HAM-A and HAM-D scores, whereas the plasma concentrations ofHDL-cholesterol correlated negatively with HAM-D scores. These findings suggestedthat hyperlipidemia was associated with worse psychiatric comorbidities in patientsduring METH withdrawal.

Altered production of secondary BAs in patients with MUDs mayindicate a significant change their gut microbiota. This hypothesis is supported bystudies showing that alterations in gut microbiota play key roles in the regulationof host metabolism and therefore contribute to severe withdrawal symptoms (48, 49). In addition, altered circulating BAs may affect CNS function by activating FXR inneurons and TGR5 in glial cells, thereby modulating neuroinflammatory andneuropsychiatric behaviors (50). However,this hypothesis has not been experimentally confirmed in patients with MUDs.

This study had several strengths. First, the characteristics ofpatients with MUDs in both cohorts were systematically analyzed. Second, theexploratory cohort included patients at different stages of METH withdrawal, withfindings in these subgroups showing that the critical importance of the time windowfor potential clinical intervention. Third, this study explored clues to peripheralsystems other than the CNS, which are relatively easy to obtain and to be developedas biomarkers. Finally, this study provided in-human evidence that excessively lowBA concentrations and imbalances are adverse factors for psychiatric comorbiditiesand liver injury in METH withdrawal.

This study, however, also had several limitations. First, the samplesizes were relatively small. A study with relative larger sample size shouldhypothetically obtain more accurate results. Second, this was an observational studyshowing statistical associations; therefore, causality could not be determined.Third, because the gut microbiota has been shown to affect the neuropsychiatricbehaviors associated with substance withdrawal (49, 51), future studies shouldinvestigate the association between the composition of gut microbiota and themechanisms of BA metabolism during METH withdrawal.

In conclusion, the present study evaluated the plasmaBA profile in patients with MUDs, finding that deficiencies in overall BAs and inthe production of secondary BAs were associated with psychiatric symptoms as well asMETH-induced liver injury. Additional studies are needed to determine the molecularmechanisms underlying the crosstalk between the liver and the CNS.

DATA AVAILABILITY STATEMENT

The original contributions presented in the study areincluded in the article/**Supplementary Material**. Further inquiries can be directed to the corresponding authors.

ETHICS STATEMENT

The studies involving human participants were reviewed and approved by the Research Ethics Committee of the First Affiliated Hospital of Kunming Medical University. The patients/participants provided their written informed consent to participate in this study.

AUTHOR CONTRIBUTIONS

JHY and KW designed the study and supervised the project. YM, HJW, HWW, FC, ZX, ZZ, QP, JQY, YZ, CC, MC, and YJZ

collected the data. JHY, YM, and HJW did the data analysis and interpretation. JHY took the lead in writing the manuscript. All authors reviewed the report and approved the final version.

FUNDING

This work was supported by grants from the Yunnan Fundamental Research Projects (Grant No. 202101AU070114), Science and Technology Department of Yunnan Province (Grant No. 2019FB096, 202001AV070010, 202002AA100007), and Academic leader project for health commission of Yunnan Province (Grant No. D-2017007), and Yunling Scholar (Grant No. YLXL20170002).

ACKNOWLEDGMENTS

Foremost, we would like to thank Limei Cao and YJZ for their expert technique assistance.

SUPPLEMENTARY MATERIAL

The Supplementary Material for this article can befound online at: https://www.frontiersin.org/articles/10.3389/fendo.2021.801686/full#supplementary-material

Supplementary Figure 1 | Associations of dyslipidemia parameters with psychiatric comorbidities **(A–D)** and bile acid concentrations **(E–H)** after METH withdrawal, as determined by Spearman correlation analysis.

REFERENCES

1. Paulus MP, Stewart JL. Neurobiology, Clinical Presentation, and Treatment of Methamphetamine Use Disorder: A Review. *JAMA Psychiatry* (2020)77:959–66. doi: 10.1001/jamapsychiatry.2020.0246
2. Grant KM, LeVan TD, Wells SM, Li M, Stoltenberg SF, Gendelman HE, et al. Methamphetamine-Associated Psychosis. *J Neuroimmune Pharmacol* (2012) 7:113–39. doi: 10.1007/s11481-011-9288-1
3. Lecomte T, Dumais A, Dugre JR, Potvin S. The Prevalence of Substance-Induced Psychotic Disorder in Methamphetamine Misusers: A Meta-Analysis. *Psychiatry Res* (2018) 268:189–92. doi: 10.1016/j.psychres.2018.05.033
4. Chen F, Zou L, Dai Y, Sun J, Chen C, Zhang Y, et al. Prognostic Plasma Exosomal Microrna Biomarkersin Patients With Substance Use Disorders Presenting Comorbid With Anxietyand Depression. *Sci Rep* (2021) 11:6271. doi: 10.1038/s41598-021-84501-5
5. Yu J, Chen F, Xu Y, Shi K, Zhang Z, Peng Q, et al. Dynamics of Neurotransmitter and Extracellular Vesicle-Derived Microrna Landscapes During Heroin and Methamphetamine Withdrawal. *medRxiv* (2021) 2021.04.19.21255653. doi: 10.1101/2021.04.19.21255653
6. Hay CE, Ewing LE, Hambuchen MD, Zintner SM, Small JC, Bolden CT, et al. The Development and Characterization of anScfv-Fc Fusion-Based Gene Therapy to Reduce the Psychostimulant Effects of Methamphetamine Abuse. *J Pharmacol Exp Ther* (2020) 374:16–23. doi: 10.1124/jpet.119.261180
7. Northrop NA, Yamamoto BK. Methamphetamine Effects on Blood-Brain Barrier Structure and Function. *Front Neurosci* (2015) 9:69. doi: 10.3389/fnins.2015.00069
8. Bowyer JF, Hanig JP. Amphetamine- and Methamphetamine-Induced Hyperthermia: Implications of the Effects Produced in Brain Vasculature and Peripheral Organs to Forebrain Neurotoxicity. *Temperature (Austin)* (2014) 1:172–82. doi: 10.4161/23328940.2014.982049
9. Prakash MD, Tangalakis K, Antonipillai J, Stojanovska L, Nurgali K, Apostolopoulos V. Methamphetamine: Effects on the Brain, Gut and Immune System. *Pharmacol Res* (2017) 120:60–7. doi: 10.1016/j.phrs.2017.03.009
10. Wang Q, Wei LW, Xiao HQ, Xue Y, Du SH, Liu YG, et al. Methamphetamine Induces Hepatotoxicity*via* Inhibiting Cell Division, Arresting Cell Cycle and Activating Apoptosis: *In Vivo* and *In Vitro* Studies. *Food Chem Toxicol*(2017) 105:61–72. doi: 10.1016/j.fct.2017.03.030
11. Zhao T, Zhai C, Song H, Wu Y, Ge C, Zhang Y, et al. Methamphetamine-Induced Cognitive Deficits andPsychiatric Symptoms Are Associated With Serum Markers of Liver Damage. *Neurotox Res* (2020) 37:67–76. doi: 10.1007/s12640-019-00115-w
12. Halpin LE, Yamamoto BK. Peripheral Ammonia as a Mediator of Methamphetamine Neurotoxicity. *J Neurosci* (2012) 32:13155–63. doi: 10.1523/JNEUROSCI.2530-12.2012
13. Halpin LE, Gunning WT, Yamamoto BK. Methamphetamine Causes Acute Hyperthermia-Dependent Liver Damage. *Pharmacol ResPerspect* (2013) 1: e00008. doi: 10.1002/prp2.8
14. Eskandari MR, Rahmati M, Khajeamiri AR, Kobarfard F, Noubarani M, Heidari H. A New Approach on Methamphetamine-Induced Hepatotoxicity: Involvement of Mitochondrial Dysfunction. *Xenobiotica* (2014)44:70–6. doi: 10.3109/00498254.2013.807958
15. Seo JW, Jones SM, Hostetter TA, Iliff JJ, West GA. Methamphetamine Induces the Release of Endothelin. *J Neurosci Res* (2016) 94:170–8. doi: 10.1002/jnr.23697
16. Chiang JY. Bile Acid Metabolism and Signaling. *Compr Physiol* (2013) 3:1191–212. doi: 10.1002/cphy.c120023
17. Gertzen CGW, Gohlke H, Haussinger D, Herebian D, Keitel V, Kubitz R, et al. The Many Facets of Bile Acids in the Physiologyand Pathophysiology of the Human Liver. *Biol Chem* (2021) 402:1047–62. doi: 10.1515/hsz-2021-0156
18. McMillin M, Frampton G, Quinn M, Ashfaq S, De Los Santos M3rd, Grant S, et al. Bile Acid Signaling is Involved in the Neurological Decline in a Murine Model of Acute Liver Failure. *Am J Pathol* (2016) 186:312–23. doi: 10.1016/j.ajpath.2015.10.005
19. MahmoudianDehkordi S, Arnold M, Nho K, Ahmad S, Jia W, Xie G, et al. Altered Bile Acid Profile Associates With Cognitive Impairment in Alzheimer's Disease-an Emerging Role for Gut Microbiome. *Alzheimers Dement* (2019) 15:76–92. doi: 10.1016/j.jalz.2018.07.217
20. Kiriyama Y, Nochi H. The Biosynthesis, Signaling, and Neurological Functions of Bile Acids. *Biomolecules* (2019) 9(6):232. doi: 10.3390/biom9060232
21. Mertens KL, Kalsbeek A, Soeters MR, Eggink HM. Bile Acid Signaling Pathways From the Enterohepatic Circulation to the Central Nervous System. *Front Neurosci* (2017) 11:617. doi: 10.3389/fnins.2017.00617
22. Bhargava P, Smith MD, Mische L, Harrington E, Fitzgerald KC, Martin K, et al. Bile Acid Metabolism is Altered in Multiple Sclerosis and Supplementation Ameliorates Neuroinflammation. *J Clin Invest* (2020) 130:3467–82. doi: 10.1172/JCI129401
23. Reddy IA, Smith NK, Erreger K, Ghose D, Saunders C, Foster DJ, et al. Bile Diversion, a Bariatric Surgery, and Bile Acid Signaling Reduce Central Cocaine Reward. *PloS Biol* (2018) 16:e2006682. doi: 10.1371/journal.pbio.2006682
24. Ridlon JM, Kang DJ, Hylemon PB, Bajaj JS. Gut Microbiota, Cirrhosis, and Alcohol Regulate Bile Acid Metabolism in the Gut. *Dig Dis* (2015) 33:338–45. doi: 10.1159/000371678
25. Hamilton M. The Assessment of Anxiety States by Rating. *Br J Med Psychol* (1959) 32:50–5. doi: 10.1111/j.2044-8341.1959.tb00467.x
26. Hamilton M. A Rating Scale for Depression. *J Neurol Neurosurg Psychiatry* (1960) 23:56–62. doi: 10.1136/jnnp.23.1.56
27. Xie G, Zhong W, Li H, Li Q, Qiu Y, Zheng X, et al. Alteration of Bile Acid Metabolism in the Rat Induced by Chronic Ethanol Consumption. *FASEBJ* (2013) 27:3583–93. doi: 10.1096/fj.13-231860
28. Xie G, Wang X, Huang F, Zhao A, Chen W, Yan J, et al. Dysregulated Hepatic Bile Acids Collaboratively Promote Liver Carcinogenesis. *Int J Cancer* (2016) 139:1764–75. doi: 10.1002/ijc.30219
29. Baloni P, Funk CC, Yan J, Yurkovich JT, Kueider-Paisley A, Nho K, et al. Metabolic Network Analysis Reveals Altered BileAcid Synthesis and Metabolism in Alzheimer's Disease. *Cell Rep Med* (2020) 1:100138. doi: 10.1016/j.xcrm.2020.100138

30. Colognesi M, Gabbia D, De Martin S. Depression and Cognitive Impairment-Extrahepatic Manifestations of NAFLD and NASH. *Biomedicines* (2020) 8:229–45. doi: 10.3390/biomedicines8070229
31. Baeza I, de la Serna E, Calvo-Escalona R, Merchan-Naranjo J, Rodriguez-Latorre P, Martinez-Cantarero MC, et al. One-Year Prospective Study of Liver Function Tests in Children and Adolescents on Second-Generation Antipsychotics: Is There a Link With Metabolic Syndrome? *J Child Adolesc Psychopharmacol* (2018) 28:463–73. doi: 10.1089/cap.2017.0117
32. Hsu JH, Chien IC, Lin CH, Chou YJ, Chou P. Increased Risk of Chronic Liver Disease in Patients With Schizophrenia: A Population-Based Cohort Study. *Psychosomatics* (2014) 55:163–71. doi: 10.1016/j.psym.2013.06.001
33. Erdogan A, Atasoy N, Akkurt H, Ozturk D, Karaahmet E, Yalug I, et al. Risperidone and Liver Function Tests in Children and Adolescents: A Short-Term Prospective Study. *Prog Neuropsychopharmacol Biol Psychiatry* (2008) 32:849–57. doi: 10.1016/j.pnpbp.2007.12.032
34. Hambuchen MD, Berquist MD, Simecka CM, McGill MR, Gunnell MG, Hendrickson HP, et al. Effect of Bile Duct Ligation-Induced Liver Dysfunction on Methamphetamine Pharmacokinetics and Locomotor Activity in Rats. *J Pharm Pharm Sci* (2019) 22:301–12. doi: 10.18433/jpps30471
35. Win A, Delgado A, Jadeja RN, Martin PM, Bartoli M, Thounaojam MC. Pharmacological and Metabolic Significance of Bile Acids in Retinal Diseases. *Biomolecules* (2021) 11:292. .doi: 10.3390/biom11020292
36. Marin JJ, Macias RI, Briz O, Banales JM, Monte MJ. Bile Acids in Physiology, Pathology and Pharmacology. *Curr Drug Metab* (2015) 17:4–29. doi: 10.2174/1389200216666151103115454
37. Jia W, Wei M, Rajani C, Zheng X. Targeting the Alternative Bile Acid Synthetic Pathway for Metabolic Diseases. *Protein Cell* (2021) 12:411–25. doi: 10.1007/s13238-020-00804-9
38. Tao Y, Zheng F, Cui D, Huang F, Wu X. A Combination of Three Plasma Bile Acids as a Putative Biomarker for Schizophrenia. *Acta Neuropsychiatr* (2021) 33:51–4. doi: 10.1017/neu.2020.42
39. Gu Y, Wang X, Li J, Zhang Y, Zhong H, Liu R, et al. Analyses of Gut Microbiota and Plasma Bile Acids Enable Stratification of Patients for Antidiabetic Treatment. *Nat Commun* (2017) 8:1785. doi: 10.1038/s41467-017-01682-2
40. Kaur H, Seeger D, Golovko S, Golovko M, Combs CK. Liver Bile Acid Changes in Mouse Models of Alzheimer's Disease. *Int J Mol Sci* (2021) 22:7451. doi: 10.3390/ijms22147451
41. Varma VR, Wang Y, An Y, Varma S, Bilgel M, Doshi J, et al. Bile Acid Synthesis, Modulation, and Dementia: A Metabolomic, Transcriptomic, and Pharmacoepidemiologic Study. *PloS Med* (2021) 18:e1003615. doi: 10.1371/journal.pmed.1003615
42. Vijayvargiya P, Busciglio I, Burton D, Donato L, Lueke A, Camilleri M. Bile Acid Deficiency in a Subgroup of Patients With Irritable Bowel Syndrome With Constipation Based on Biomarkers in Serumand Fecal Samples. *Clin Gastroenterol Hepatol* (2018) 16:522–7. doi: 10.1016/j.cgh.2017.06.039
43. Sun J, Chen F, Chen C, Zhang Z, Zhang Z, Tian W, et al. Intestinal Mrna Expression Profile and Bioinformatics Analysis in a Methamphetamine-Induced Mouse Model of Inflammatory Bowel Disease. *Ann Transl Med* (2020) 8:1669. doi: 10.21037/atm-20-7741
44. Shen S, Zhao J, Dai Y, Chen F, Zhang Z, Yu J, et al. Methamphetamine-Induced Alterations in Intestinal Mucosal Barrier Function Occur *via* the MicroRNA-181c/TNF-Alpha/Tight Junction Axis. *Toxicol Lett* (2020) 321:73–82. doi: 10.1016/j.toxlet.2019.12.020
45. Dimache AM, Salaru DL, Sascau R, Statescu C. The Role of High Triglycerides Level in Predicting Cognitive Impairment: A Review of Current Evidence. *Nutrients* (2021) 13:2118. doi: 10.3390/nu13062118
46. Bai YM, Su TP, Chen MH, Chen TJ, Chang WH. Risk of Developing Diabetes Mellitus and Hyperlipidemia Among Patients With Bipolar Disorder, Major Depressive Disorder, and Schizophrenia: A 10-Year Nationwide Population-Based Prospective Cohort Study. *J Affect Disord* (2013) 150:57–62. doi: 10.1016/j.jad.2013.02.019
47. Hsu JH, Chien IC, Lin CH. Increased Risk of Hyperlipidemia in Patients With Bipolar Disorder: A Population-Based Study. *Gen Hosp Psychiatry* (2015) 37:294–8. doi: 10.1016/j.genhosppsych.2015.04.003
48. Xu Y, Xie Z, Wang H, Shen Z, Guo Y, Gao Y, et al. Bacterial Diversity of Intestinal Microbiota in Patients With Substance Use Disorders Revealed by 16S Rrna Gene Deep Sequencing. *Sci Rep* (2017) 7:3628. doi: 10.1038/s41598-017-03706-9
49. Yang J, Zhang Z, Xie Z, Bai L, Xiong P, Chen F, et al. Metformin Modulates Microbiota-Derived Inosine and Ameliorates Methamphetamine-Induced Anxiety and Depression-Like Withdrawal Symptoms in Mice. *bioRxiv* (2021) 2021:9.30.462054. doi: 10.1101/2021.09.30.462054
50. Li S, Hua D, Wang Q, Yang L, Wang X, Luo A, et al. The Role of Bacteria and its Derived Metabolitesin Chronic Pain and Depression: Recent Findings and Research Progress. *Int J Neuropsychopharmacol* (2020) 23:26–41. doi: 10.1093/ijnp/pyz061
51. Yang J, Xiong P, Bai L, Zhang Z, Zhou Y, Chen C, et al. The Association of Altered Gut Microbiota and Intestinal Mucosal Barrier Integrity in Mice With Heroin Dependence. *Front Nutr* (2021) 8:765414 .doi: 10.3389/fnut.2021.765414

Conflict of Interest: The authors declare that the research was conducted in the absence of any commercial or financial relationships that could be construed as a potential conflict of interest.

Publisher's Note: All claims expressed in this article are solely those of the authors and do not necessarily represent those of their affiliated organizations, or those of the publisher, the editors and the reviewers. Any product that may be evaluated in this article, or claim that may be made by its manufacturer, is not guaranteed or endorsed by the publisher.

frontiers in Endocrinology

ORIGINAL RESEARCH
published: 07 January 2022
doi: 10.3389/fendo.2021.814373

The Environmental Pollutant Bromophenols Interfere With Sulfotransferase That Mediates Endocrine Hormones

Zhihong Dai[1], *Furong Zhao*[2,3], *Ying Li*[3], *Jing Xu*[2,3] *and Zhiyu Liu*[1]*

[1] *Department of Urology, Second Hospital of Dalian Medical University, Dalian, China,* [2] *Research Department, Dalian Innovation Center of Laboratory Medicine Mass Spectrometry Technology, Dalian, China,* [3] *Research Department, Clinical Mass Spectrometry Profession Technology Innovation Center of Liaoning Province, Jinzhou, China*

Bromophenols (BPs), known as an important environmental contaminant, can cause endocrine disruption and other chronic toxicity. The study aimed to investigate the potential inhibitory capability of BPs on four human sulfotransferase isoforms (SULT1A1, SULT1A3, SULT1B1 and SULT1E1) and interpret how to interfere with endocrine hormone metabolism. P-nitrophenol(PNP) was utilized as a nonselective probe substrate, and recombinant SULT isoforms were utilized as the enzyme resources. PNP and its metabolite PNP-sulfate were analyzed using a UPLC-UV detecting system. SULT1A1 and SULT1B1 were demonstrated to be the most vulnerable SULT isoforms towards BPs' inhibition. To determine the inhibition kinetics, 2,4,6-TBP and SULT1A3 were selected as the representative BPs and SULT isoform respectively. The competitive inhibition of 2,4,6-TBP on SULT1A3. The fitting equation was y=90.065x+1466.7, and the inhibition kinetic parameter (K_i) was 16.28 μM. *In vitro-in vivo* extrapolation (IVIVE) showed that the threshold concentration of 2,4,6-TBP to induce inhibition of SULT1A3 was 1.628 μM. *In silico* docking, the method utilized indicated that more hydrogen bonds formation contributed to the stronger inhibition of 3,5-DBP than 3-BP. In conclusion, our study gave the full description of the inhibition of BPs towards four SULT isoforms, which may provide a new perspective on the toxicity mechanism of BPs and further explain the interference of BPs on endocrine hormone metabolism.

Keywords: bromophenols (BPs), endocrine hormones, sulfotransferase (SULT), inhibition, *in vitro-in vivo* extrapolation (IVIVE)

OPEN ACCESS

Edited by:
Fang Zhongze,
Tianjin Medical University, China

Reviewed by:
Yong Liu,
Dalian University of Technology, China
Rong-Rong He,
Jinan University, China

***Correspondence:**
Zhiyu Liu
Liuzhiyudoctor@163.com

Specialty section:
This article was submitted to Gut Endocrinology, a section of the journal Frontiers in Endocrinology

Received: *13 November 2021*
Accepted: *13 December 2021*
Published: *07 January 2022*

Citation:
Dai Z, Zhao F, Li Y, Xu J and Liu Z (2022) The Environmental Pollutant Bromophenols Interfere With Sulfotransferase That Mediates Endocrine Hormones. Front. Endocrinol. 12:814373. doi: 10.3389/fendo.2021.814373

INTRODUCTION

Bromophenols (BPs), a group of brominated compounds, could come from both synthetic and natural sources. With the development of science and technology, BPs are widely used in herbicides, pesticides, wood protectants, and flame retardants, thus leading to frequent contact with such chemical products in daily life (1), and detected in multiple foods such as eggs, fish, milk, and fat. Humans are the last link in the entire chain of exposure suggesting a wide range of exposure pathways and higher concentrations due to the cumulative effect (2).

Many studies have shown that BPs can cause endocrine disruption and other chronic toxicity. For example, 3-BP, as a potential PBT (persistent, bioaccumulative, and toxic) substance, has significant thyroid hormone activity and estrogen effect. 2,4,6-TBP can disrupt the endocrine system (3) *via* interfering with the function of the Ca^{2+} channel in neuroendocrine cells, or it can inhibit the activity of thyroid hormone SULT in human hepatocytes (4). So it is necessary to study the metabolic interference of BPs on endocrine hormones.

Sulfonation as an important phase II metabolism has been known, involved in the metabolism of biomass, drugs and endogenous compounds. Compared with other Phase II enzymes, sulfotransferase (SULT) is regarded as a more vital role in protecting against xenobiotics and in regulating hormone functions during the development of fetal, neonatal, and infant (5–7). In most cases, sulfate conjugation may result in the inactivation of the substrate compounds or increase their water-solubility, thereby facilitating their removal from the body (8). SULTs can catalyze the transfer of the sulfuryl group from 3-phosphoadenosine-5-phosphosulfate (PAPS) to the many substrates such as estradiol and dehydroepiandrosterone (DHEA). 12 kinds of SULT have been found in the human body. Among them, SULT1A1, SULT1A3, SULT1B1, SULT1E1 are more abundant in the human body and metabolize many important endogenous substances (9). SULT1A1 accounts for half of the SULT protein in the liver and is responsible for the metabolism of plane phenols, thyroxine, and estrogen (10). SULT1B1 is the main sulfotransferase expressed in the small intestine, which together with SULT1A3/4 constitutes 67% of the sulfotransferase protein in this tissue (11). Due to a similar structure, its metabolic profile overlaps with that of SULT1A1. SULT1A3 exists in primates with dopamine as the prime substrate. Estrogen sulfotransferase (SULT1E1) is an enzyme that maintains hormone homeostasis and biosynthesis and metabolizes estrogen and iodine adenine.

Several xenobiotics, e.g. polychlorinated biphenyls, halogenated phenol, and dietary polyphenol, have been considered as typical environmental endocrine disruptors, which exist in persistent organic pollutants. However, there is currently no systematic and comprehensive study of BPs on endocrine hormone metabolism. In this study, the inhibitory properties of BPs on SULT were investigated through *in vitro* enzymatic reactions, which can further interpret environmental pollutants to interfere with endocrine hormone metabolism.

MATERIALS AND METHODS

Chemicals and Reagents

Eight BPs (2-BP, 3-BP, 4-BP, 2,4-DBP, 2,5-DBP, 2,6-DBP, 3,5-DBP and 2,4,6-DBP) were purchased from J&K Chemical Ltd. (Beijing, China), with purity over 98%. Recombinant human SULT isoforms were obtained from BD Gentest Corp. (Woburn, MA, USA). P-nitrophenol (PNP) and its sulfate PNP-S, Tris-HCl, and $MgCl_2$ were from Sigma-Aldrich (St. Louis, MO, USA), and so is PAPS with a purity of 60%. Acetonitrile was purchased from Tianjin Saifurui Technology Ltd. ultra-pure water was prepared by Millipore Elix 5 UV and Milli-Q Gradient Ultra-Pure Water System. The other reagents were high-performance liquid chromatography (HPLC) grade or the highest grade commercially available.

Enzyme Activity Assays and Kinetic Study

The incubation mixture (12) with a total volume of 200 μL, contained 100 mM of Tris-HCl buffer (pH=7.4), 5 mM of $MgCl_2$, 40 μM of PAPS, SULTs, and PNP. The concentrations of SULT1A1, SULT1A3, SULT1B1 and SULT1E1 were 10 μg/mL, 10 μg/mL, 10 μg/mL and 20 μg/mL, respectively. After 3-min pre-incubation, PAPS was added to initiate the metabolic reaction. The reaction temperature was set to be 37°C, and the reaction time was 30-60 min. 100 μL of ice-cold acetonitrile was added to terminate the reaction. The incubation mixture without BPs was used as a control. After centrifugation at 12,000 rpm, 10 μL of supernatants were analyzed using ultra-performance liquid chromatography (UPLC)-UV instrument. UPLC separation was achieved using a C18 column (4.6*200 mm, 5 μm, Kromasil) at a flow rate of 0.4 mL/min, and the column temperature was 25°C. The mobile phases contained phase A (H_2O containing 0.5% (v/v) formic acid) and phase B (acetonitrile). Gradient condition was used as followed: initiated at 5% B, increased to 95% over 2 minute after 6 minute, held constant for 6 minutes. The UV detection wavelength was 280 nm. In order to determine the Michaelis-constant (K_m) of PNP metabolites, incubation mixture (total volume=200 μL) contained BPs (100 μM), Tris-HCl buffer (50 mM, pH=7.4), $MgCl_2$ (5 mM), PAPS (4 mM), SULTs and PNP. The corresponding PNP concentrations for SULT1A1, SULT1A3, SULT1B1 and SULT1E1 were 1-400 μM, 0.1-7 mM, 0.1-1 mM and 0.1-1.2 mM, respectively. Incubation and analysis conditions were conducted as described above. The kinetic parameters V_{max} and K_m were determined by fitting data to the Michaelis–Menten equation or substrate inhibition equation.

Preliminary Screening of Inhibition Capability of BPs on SULTs

The incubation mixture (total volume=200 μL) contained 100 μM of BPs, 100 mM of Tris-HCl buffer (pH=7.4), 5 mM of $MgCl_2$, 40 μM of PAPS, SULTs, and PNP. The concentrations of SULT1A1, SULT1A3, SULT1B1 and SULT1E1 are 10 μg/mL, 10 μg/mL, 10 μg/mL and 20 μg/mL. The concentrations of PNP were 40, 1200, 25, 120 μM for SULT1A1, SULT1A3, SULT1B1, SULT1E1 (based on the K_m values). Incubation mixture without BPs was used as negative controls. All incubations were carried out in duplicate.

Half Inhibition Concentration (IC_{50}) and Inhibition Kinetics Determination

Half inhibition concentration (IC_{50}) was conducted by adding 0 μM to 100 μM BPs. The inhibition kinetics were determined with BPs and PNP covering the K_m (for PNP) and IC_{50} values (for BPs). Lineweaver-Burk (L-B) plot was drawn using 1/reaction velocity (v) versus 1/the concentration of PNP ([PNP]) to determine the inhibition kinetic type. In the second

plot, inhibition kinetics (K_i) were calculated by the slopes of the lines in the Lineweaver-Burk plots.

In Vitro-In Vivo Extrapolation (IVIVE)

In vitro-in vivo extrapolation (IVIVE) was employed to predict *in vivo* inhibition possibility for BPs towards SULTs by using the following equation:

$$AUC_i/AUC = 1 + [I]/K_i$$

AUC_i/AUC was the predicted ratio of *in vivo* exposure of xenobiotics or endogenous substances with or without the co-exposure of BPs. [I] was the *in vivo* exposure concentration of BPs, and the K_i value was *in vitro* inhibition constant. The AUCi/AUC cutoffs of < 1.25 were considered as an inhibition for a significant *in vivo* (13).

In Silico Docking

In silico docking was employed to understand the molecular interaction between BPs and SULTs. We constructed the structure of SULT isoforms by homology modeling method with the MODELLER9v14 program. Autodock software (version 4.2) was utilized to dock BPs into the activity cavity of SULT isoforms, respectively. The non-polar hydrogen atoms of SULTs were merged. The grid box was generated with 60 ×60×60 in X, Y, and Z coordinate to cover the entire ligand-binding site. Lamarckian Genetic Algorithm (LGA) method was utilized to study the molecular docking of active domain between BPs and SULTs. The LGA runs were set to 50 runs for each BPs. The best conformation with the lowest docked energy was analyzed for the interactions between BPs and SULTs including hydrogen bonds and hydrophobic contacts.

Data Analysis

The experimental data were presented as the mean value plus standard deviation (SD). Statistical analysis was carried out using GraphPad Prism 5.0. Comparisons between two groups were performed using a two-tailed unpaired Student's t-test. Multiple groups were compared using a one-way ANOVA.

RESULTS

Kinetic Study and Detection Result

PNP-sulfate was detected at 4.4 min by UPLC, and the substrate PNP eluted at 5.0 min. The metabolism of SULT1A1 to PNP conformed to the substrate inhibition model, and the metabolism of SULT1A3, SULT1B1, SULT1E1 to PNP conformed to the Michaelis–Menten equation (**Supplementary Figure 1**). The kinetic parameters (including K_m, K_i) of PNP catalyzed by SULTs were summarized (**Supplementary Table 1**).

Preliminary Screening of Inhibition Capability of BPs Towards SULTs

All BPs showed an inhibitory effect on the activity of four SULTs (**Figure 1**). From the preliminary screening results, we could find some structural properties of BPs for inhibiting SULTs. The introduction of 2-position bromide substituents increased the inhibitory potential of 3-BP and 4-BP towards SULT1A3 and SULT1E1. Similarly, the introduction of 5-position bromide substituents increased the inhibitory potential of 3-BP towards SULT1A3 and SULT1E1. Furthermore, BPs with 2-substituted bromine atoms exhibited severe inhibition potential towards all four tested SULTs isoforms with an inhibition rate above 80%. 3-BP and 4-BP only showed strong inhibition ability towards SULT1A1 and SULT1B1, but not SULT1A3 and SULT1E1.

Inhibition Kinetics Determination

2,4,6-TBP was selected as the representative BPs to determine the inhibition kinetics. As shown in **Figure 2**, the concentration-dependent inhibition of 2,4,6-TBP towards SULT1A1, SULT1A3, SULT1B1, and SULT1E1 was proved. The

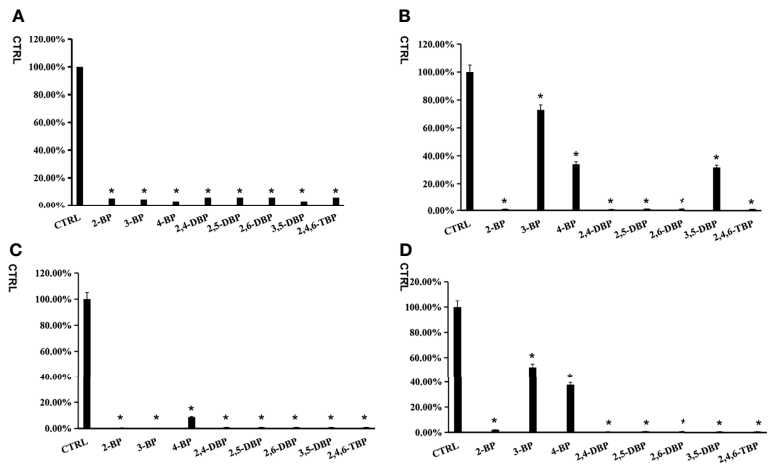

FIGURE 1 | The inhibition screening of bromophenols towards SULT1A1 **(A)**, SULT1A3 **(B)**, SULT1B1 **(C)** and SULT1E1 **(D)**. The data were given as mean value plus S.D. (n=3).*p < 0.05.

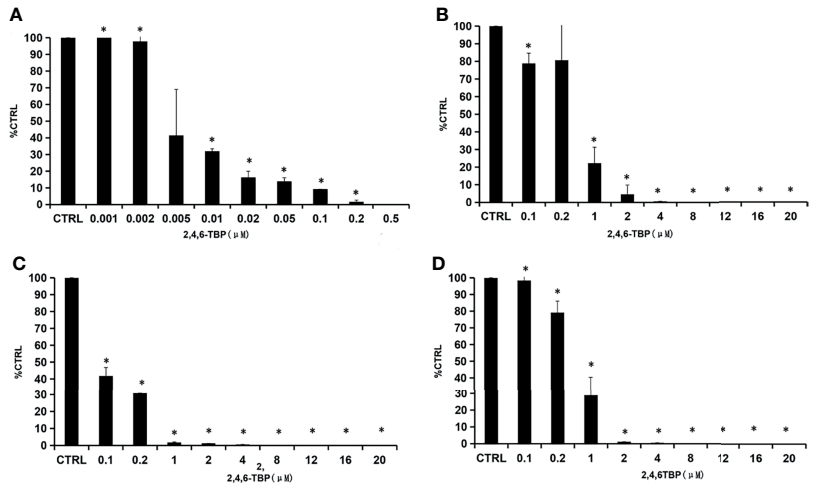

FIGURE 2 | Concentration-dependent inhibition of 2,4,6-TBP towards SULTs. **(A–D)** presents concentration-dependent inhibition of 2,4,6-TBP towards SULT1A1 **(A)**, SULT1A3 **(B)**, SULT1B1 **(C)** and SULT1E1 **(D)**.The data were given as mean value plus S.D. (n=3). *p < 0.05.

concentration-dependent inhibition of 2-BP, 2,4-DBP, 2,5-DBP, and 2,6-DBP towards SULT1A1, SULT1A3, SULT1B1, and SULT1E1 was given in **Supplementary Figures 2–5**. The calculated IC_{50} values for the inhibition of these BPs towards SULT1A1, SULT1A3, SULT1B1, and SULT1E1 were given in **Supplementary Table 2**. Furthermore, the inhibition type and kinetic parameters (K_i) were determined for SULT1A3 by 2,4,6-TBP. As shown in **Figure 3A**, the intersection point was located in the vertical axis, indicating the competitive inhibition of 2,4,6-TBP towards SULT1A3. The fitting equation of the second plot was y=90.065x+1466.7 for the inhibition of 2,4,6-TBP towards SULT1A3 (**Figure 3B**). Based on this equation, the inhibition kinetic parameter (K_i) was calculated to be 16.28 μM.

In Silico Docking to Elucidate the Inhibition Mechanism

Results of *in silico* docking showed the influence of the introduction of substituted bromine on the inhibition capability. The binding free energy of 3-BP and 3,5-DBP with SULT1A3 were -5.77 kcal/mol and -6.41kcal/mol, respectively, which is consistent with the experimental results that 3,5-DBP exerted stronger inhibition than 3-BP towards SULT1A3. 3-BP formed one hydrogen bond with SULT1A3 (**Figure 4A**), and 3,5-DBP formed three hydrogen bonds with SULT1A3 (**Figure 4B**). Similar results were found in 3-BP and 3,5-DBP towards SULT1E1 (**Figures 4C, D**). Based on these results, we get the conclusion that more hydrogen bonds formation contributed to the stronger inhibition effect of 3,5-DBP than 3-BP towards SULT1A3 and SULT1E1.

DISCUSSION

In this study, we demonstrated the inhibition characteristics of BPs towards four SULTs isoforms. All of the BPs could inhibit the

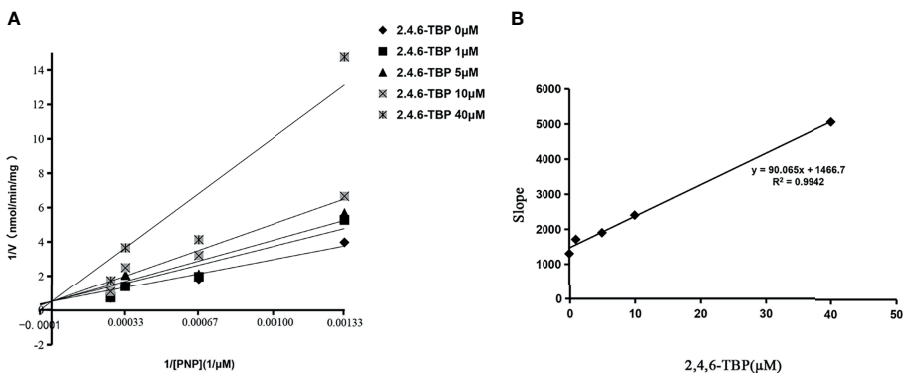

FIGURE 3 | The Lineweaver-Burk plot of 2,4,6-TBP to SULT1A3. In **(A)**, the horizontal axis represents the value of 1/[PNP]. The vertical axis represents 1/V. V is the velocity of the reaction. K_i values were calculated using the slopes of **(B)**.

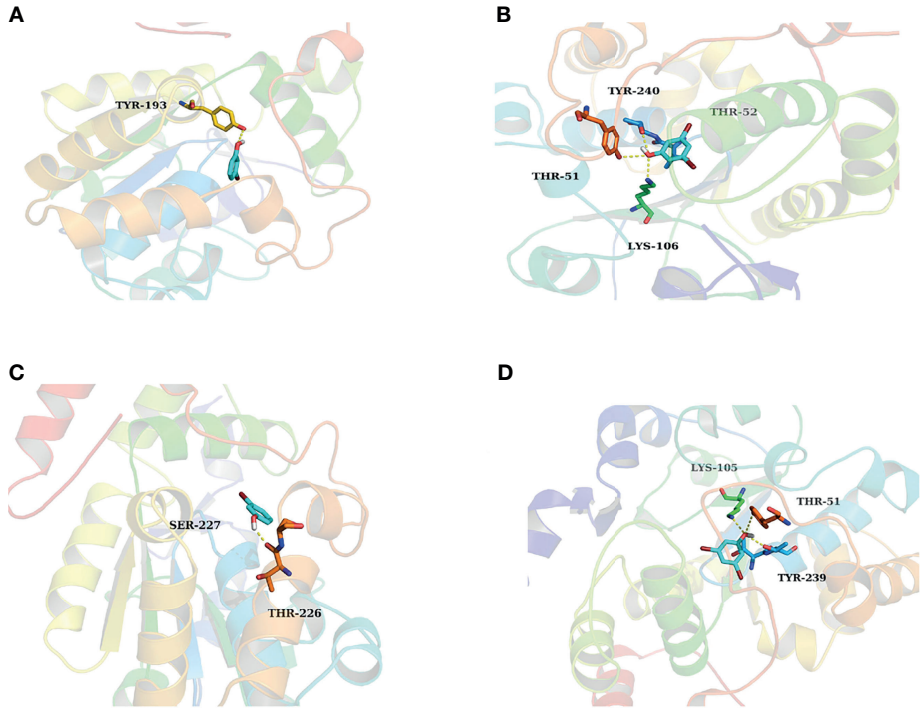

FIGURE 4 | The activity cavity of between 3-BP, 3,5-DBP and SULT1A3, SULT1E1. 3-BP formed 1 hydrogen bond with SULT1A3 **(A)** and SULT1E1 **(C)**, respectively. 3,5-DBP formed 3 hydrogen bonds with SULT1A3 **(B)** and SULT1E1 **(D)**, respectively.

metabolic activity of four SULTs isoforms. Among them, SULT1A1 and SULT1B1 were the most vulnerable isoforms. 2-substituted bromophenol exhibited severe inhibition potential towards four SULTs. 2,4,6-TBP was selected as a representative BP to determine the inhibition kinetics, including the inhibition type and kinetic parameters (K_i). Based on the IVIVE equation, the threshold value of 2,4,6-TBP was 1.628 μM. 2,4,6-TBP was regarded as the most abundant BP in the human body. The concentrations of 2,4,6-TBP ranged from 27 ng/g lipid to 81 ng/g (0.08 - 0.24 μM) lipid in serum (14) and detected and present at higher concentrations with a mean concentration of 15.4 ng/g lipid (range: 1.31-316 ng/g lipid) (0.004 - 0.95 μM) in placental tissues (15). Therefore, 2,4,6-TBP seemed to exert a low possibility to inhibit the activity of SULT1A3. However, considering the accumulation of 2,4,6-TBP and its association with other toxic substances, the possibility of 2,4,6-TBP inhibiting SULT1A3 *in vivo* might increase.

It should be noted that there are some studies to demonstrate the substrate properties of BPs for SULTs. For example, a previous study has shown that 2,4,6-TBP is a typical substrate of SULTs (16). UPLC-MS analysis of urine samples has identified the sulfate and glucuronide metabolites of 2-BP (17). Therefore, glucuronidation and sulfation are the main elimination pathways of BPs in humans.

UDP-glucuronosyltransferases (UGTs) and SULTs, the most important phase II metabolic enzymes, are the main endogenous substances that undergo the metabolism catalyzed. For example, both UGTs and SULTs are involved in the metabolic elimination of thyroid hormones (18, 19). The metabolism of estrogen needs the catalysis of SULTs and UGTs (20, 21). Oral administration to 2,4,6-TBP in adult zebrafish and found that reproductive toxicity in addition to perturbed gonadal morphology when exposed to high levels of food at 3300 μg/g dw (22). Although the *in vivo* concentrations measured in the present study are lower than the *in vivo* threshold in this study, when both of these pathways are inhibited, the metabolism of estrogen may be significantly disturbed. Therefore, due to the inhibitory effect of BPs on UGTs and SULTs, attention should be paid to the metabolic homeostasis of endocrine hormones.

CONCLUSION

This study demonstrated the inhibition of BPs towards SULT1. Our results showed that SULT1A1 and SULT1B1 were demonstrated to be the most vulnerable SULT isoforms towards BPs' inhibition. Structure-inhibition activity relationship analysis showed that 2-substituted bromophenol exhibited severe broad inhibition potential towards four SULTs, and the addition of 5-position bromide in BPs can increase the inhibition capability. *In silico* docking, we get the conclusion that more hydrogen bonds formation contributed to the stronger inhibition effect of 3,5-DBP than 3-BP towards SULT1A3 and SULT1E1. *In vitro-in vivo* extrapolation (IVIVE)

was performed to predict the threshold value of 2,4,6-TBP to induce *in vivo* inhibition of SULTs. These results may interpret BPs to interfere with endocrine hormone metabolism.

DATA AVAILABILITY STATEMENT

The original contributions presented in the study are included in the article/**Supplementary Material**. Further inquiries can be directed to the corresponding author.

AUTHOR CONTRIBUTIONS

ZL contributed to the study's conception and design. Material preparation, data collection, and analysis were performed by ZD and FZ. The first draft of the manuscript was written by ZD and YL. JX commented on previous versions of the manuscript. All authors read and approved the final manuscript.

FUNDING

This work was supported by the Educational Department of Liaoning Province (No. JYTZD2020003).

ACKNOWLEDGMENTS

The authors would like to acknowledge the support from the Department of Urology. The authors thank Dr. Liu for providing a guide.

SUPPLEMENTARY MATERIAL

The Supplementary Material for this article can be found online at: https://www.frontiersin.org/articles/10.3389/fendo.2021.814373/full#supplementary-material

REFERENCES

1. Sim WJ, Lee SH, Lee IS, Choi SD, Oh JE. Distribution and Formation of Chlorophenols and Bromophenols in Marine and Riverine Environments. *Chemosphere* (2009) 77(4):552–8. doi: 10.1016/j.chemosphere.2009.07.006
2. Yang M, Zhang X. Comparative Developmental Toxicity of New Aromatic Halogenated Dbps in a Chlorinated Saline Sewage Effluent to the Marine Polychaete Platynereis Dumerilii. *Environ Sci Technol* (2013) 47(19):10868–76. doi: 10.1021/es401841t
3. Zhao J, Franzen S. Kinetic Study of the Inhibition Mechanism of Dehaloperoxidase-Hemoglobin a by 4-Bromophenol. *J Phys Chem B* (2013) 117(28):8301–9. doi: 10.1021/jp3116353
4. Butt CM, Stapleton HM. Inhibition of Thyroid Hormone Sulfotransferase Activity by Brominated Flame Retardants and Halogenated Phenolics. *Chem Res Toxicol* (2013) 26(11):1692–702. doi: 10.1021/tx400342k
5. Pacifici GM, Franchi M, Giuliani L, Rane A. Development of the Glucuronyltransferase and Sulphotransferase Towards 2-Naphthol in Human Fetus. *Dev Pharmacol Ther* (1989) 14(2):108–14. doi: 10.1159/000480927
6. Cappiello M, Giuliani L, Rane A, Pacifici GM. Dopamine Sulphotransferase is Better Developed Than P-Nitrophenol Sulphotransferase in the Human Fetus. *Dev Pharmacol Ther* (1991) 16(2):83–8. doi: 10.1159/000480563
7. Pacifici GM, Kubrich M, Giuliani L, de Vries M, Rane A. Sulphation and Glucuronidation of Ritodrine in Human Foetal and Adult Tissues. *Eur J Clin Pharmacol* (1993) 44(3):259–64. doi: 10.1007/bf00271368
8. Suiko M, Kurogi K, Hashiguchi T, Sakakibara Y, Liu MC. Updated Perspectives on the Cytosolic Sulfotransferases (Sults) and SULT-Mediated Sulfation. *Biosci Biotechnol Biochem* (2017) 81(1):63–72. doi: 10.1080/09168451.2016.1222266
9. Coughtrie MWH. Function and Organization of the Human Cytosolic Sulfotransferase (SULT) Family. *Chem Biol Interact* (2016) 259(Pt A):2–7. doi: 10.1016/j.cbi.2016.05.005
10. Nagar S, Walther S, Blanchard RL. Sulfotransferase (SULT) 1A1 Polymorphic Variants *1, *2, and *3 Are Associated With Altered Enzymatic Activity, Cellular Phenotype, and Protein Degradation. *Mol Pharmacol* (2006) 69(6):2084–92. doi: 10.1124/mol.105.019240
11. Riches Z, Stanley EL, Bloomer JC, Coughtrie MW. Quantitative Evaluation of the Expression and Activity of Five Major Sulfotransferases (Sults) in Human Tissues: The SULT "Pie". *Drug Metab Dispos* (2009) 37(11):2255–61. doi: 10.1124/dmd.109.028399
12. Wang F, Wang S, Yang K, Liu YZ, Yang K, Chen Y, et al. Inhibition of UDP-Glucuronosyltransferases (Ugts) by Bromophenols (Bps). *Chemosphere* (2020) 238:124645. doi: 10.1016/j.chemosphere.2019.124645
13. Sudsakorn S, Bahadduri P, Fretland J, Lu C. 2020 FDA Drug-Drug Interaction Guidance: A Comparison Analysis and Action Plan by Pharmaceutical Industrial Scientists. *Curr Drug Metab* (2020) 21(6):403–26. doi: 10.2174/1389200221666200620210522
14. Gao S, Wan Y, Zheng G, Luo K, Kannan K, Giesy JP, et al. Organobromine Compound Profiling in Human Adipose: Assessment of Sources of Bromophenol. *Environ Pollution* (2015) 204:81–9. doi: 10.1016/j.envpol.2015.04.015
15. Leonetti C, Butt CM, Hoffman K, Miranda ML, Stapleton HM. Concentrations of Polybrominated Diphenyl Ethers (Pbdes) and 2,4,6-Tribromophenol in Human Placental Tissues. *Environ Int* (2016) 88:23–9. doi: 10.1016/j.envint.2015.12.002
16. Zhang Q, Liu Y, Lin Y, Kong W, Zhao X, Ruan T, et al. Multiple Metabolic Pathways of 2,4,6-Tribromophenol in Rice Plants. *Environ Sci Technol* (2019) 53(13):7473–82. doi: 10.1021/acs.est.9b01514
17. Adesina-Georgiadis KN, Gray N, Plumb RS, Thompson DF, Holmes E, Nicholson JK, et al. The Metabolic Fate and Effects of 2-Bromophenol in Male Sprague-Dawley Rats. *Xenobiotica* (2019) 49(11):1352–9. doi: 10.1080/00498254.2018.1559376
18. Martin LA, Wilson DT, Reuhl KR, Gallo MA, Klaassen CD. Polychlorinated Biphenyl Congeners That Increase the Glucuronidation and Biliary Excretion of Thyroxine are Distinct From the Congeners That Enhance the Serum Disappearance of Thyroxine. *Drug Metab Dispos* (2012) 40(3):588–95. doi: 10.1124/dmd.111.042796
19. Smythe TA, Butt CM, Stapleton HM, Pleskach K, Ratnayake G, Song CY, et al. Impacts of Unregulated Novel Brominated Flame Retardants on Human Liver Thyroid Deiodination and Sulfotransferation. *Environ Sci Technol* (2017) 51(12):7245–53. doi: 10.1021/acs.est.7b01143
20. Ambadapadi S, Wang PL, Palii SP, James MO. Celecoxib Affects Estrogen Sulfonation Catalyzed by Several Human Hepatic Sulfotransferases, But Does Not Stimulate 17-Sulfonation in Rat Liver. *J Steroid Biochem Mol Biol* (2017) 172:46–54. doi: 10.1016/j.jsbmb.2017.05.012
21. Zhou X, Zheng Z, Xu C, Wang J, Min M, Zhao Y, et al. Disturbance of Mammary UDP-Glucuronosyltransferase Represses Estrogen Metabolism and Exacerbates Experimental Breast Cancer. *J Pharm Sci* (2017) 106(8):2152–62. doi: 10.1016/j.xphs.2017.04.073
22. Haldén AN, Nyholm JR, Andersson PL, Holbech H, Norrgren L. Oral Exposure of Adult Zebrafish (Danio Rerio) to 2,4,6-Tribromophenol Affects

Reproduction. *Aquat Toxicol* (2010) 100(1):30–7. doi: 10.1016/j.aquatox.2010.07.010

Conflict of Interest: The authors declare that the research was conducted in the absence of any commercial or financial relationships that could be construed as a potential conflict of interest.

Publisher's Note: All claims expressed in this article are solely those of the authors and do not necessarily represent those of their affiliated organizations, or those of the publisher, the editors and the reviewers. Any product that may be evaluated in this article, or claim that may be made by its manufacturer, is not guaranteed or endorsed by the publisher.

frontiers in Endocrinology

ORIGINAL RESEARCH
published: 14 February 2022
doi: 10.3389/fendo.2022.815968

Effects of Androgen Excess-Related Metabolic Disturbances on Granulosa Cell Function and Follicular Development

Baoying Liao[1,2,3,4], *Xinyu Qi*[1,2,3,4], *Chuyu Yun*[5,6], *Jie Qiao*[1,2,3,4] *and Yanli Pang*[1,2,3,4]*

[1] Center for Reproductive Medicine, Department of Obstetrics and Gynecology, Peking University Third Hospital, Beijing, China, [2] National Clinical Research Center for Obstetrics and Gynecology, Peking University Third Hospital, Beijing, China, [3] Key Laboratory of Assisted Reproduction, Peking University, Ministry of Education, Beijing, China, [4] Beijing Key Laboratory of Reproductive Endocrinology and Assisted Reproductive Technology, Peking University Third Hospital, Beijing, China, [5] Department of Physiology and Pathophysiology, School of Basic Medical Sciences, Peking University, Beijing, China, [6] Key Laboratory of Molecular Cardiovascular Science, Peking University, Ministry of Education, Beijing, China

OPEN ACCESS

Edited by:
Aylin Carla Hanyaloglu, Imperial College London, United Kingdom

Reviewed by:
Lisa Owens, Imperial College London, United Kingdom
Juehua Yu, The First Affiliated Hospital of Kunming Medical University, China
YunFeng Cao, Chinese Academy of Sciences (CAS), China

***Correspondence:**
Yanli Pang
yanlipang@bjmu.edu.cn

Specialty section:
This article was submitted to Gut Endocrinology, a section of the journal Frontiers in Endocrinology

Received: *16 November 2021*
Accepted: *06 January 2022*
Published: *14 February 2022*

Citation:
Liao B, Qi X, Yun C, Qiao J and Pang Y (2022) Effects of Androgen Excess-Related Metabolic Disturbances on Granulosa Cell Function and Follicular Development. Front. Endocrinol. 13:815968. doi: 10.3389/fendo.2022.815968

Polycystic ovary syndrome (PCOS) is a common reproductive endocrine disease in women of reproductive age. Ovarian dysfunction including abnormal steroid hormone synthesis and follicular arrest play a vital role in PCOS pathogenesis. Hyperandrogenemia is one of the important characteristics of PCOS. However, the mechanism of regulation and interaction between hyperandrogenism and ovulation abnormalities are not clear. To investigate androgen-related metabolic state in granulosa cells of PCOS patients, we identified the transcriptome characteristics of PCOS granulosa cells by RNA-seq. Gene ontology (GO) and Kyoto Encyclopedia of Genes and Genomes (KEGG) analysis of differentially expressed genes (DEGs) revealed that genes enriched in lipid metabolism pathway, fatty acid biosynthetic process and ovarian steroidogenesis pathway were abnormally expressed in PCOS granulosa cells in comparison with that in control. There are close interactions among these three pathways as identified by analysis of the protein-protein interaction (PPI) network of DEGs. Furthermore, *in vitro* mouse follicle culture system was established to explore the effect of high androgen and its related metabolic dysfunction on follicular growth and ovulation. RT-qPCR results showed that follicles cultured with dehydroepiandrosterone (DHEA) exhibited decreased expression levels of cumulus expansion-related genes (*Has2*, *Ptx3*, *Tnfaip6* and *Adamts1*) and oocyte maturation-related genes (*Gdf9* and *Bmp15*), which may be caused by impaired steroid hormone synthesis and lipid metabolism, thus inhibited follicular development and ovulation. Furthermore, the inhibition effect of DHEA on follicle development and ovulation was ameliorated by flutamide, an androgen receptor (AR) antagonist, suggesting the involvement of AR signaling. In summary, our study offers new insights into understanding the role of androgen excess induced granulosa cell metabolic disorder in ovarian dysfunction of PCOS patients.

Keywords: polycystic ovary syndrome, ovarian dysfunction, metabolic disorders, *in vitro* follicle culture, follicular development

INTRODUCTION

PCOS is a common reproductive endocrine disorder in women of reproductive age. Characterized by menstrual disorder, hirsutism and acne induced by hyperandrogenism and polycystic ovarian morphology, PCOS affects 5–10% of women worldwide and is the primary cause of anovulatory infertility in women of reproductive age (1). The ovulatory disorder in women with PCOS is due to follicular development arrest, which is associated with the disorder of hypothalamic gonadotropin secretion and hyperandrogenic environment in ovaries (2). However, the precise network regulation mechanism of follicular development arrest by hyperandrogenism remains unclear.

As an important cell type in follicular formation and ovulation, the function of granulosa cells is closely related to anovulation and metabolic disorder in PCOS (3–6). Mounting of evidence supported that the disruption of follicle development and ovulation process in PCOS is associated with granulosa cell dysfunction. It is reported that the activation of endoplasmic reticulum (ER) stress in granulosa cells participated in promoting follicular atresia and anovulation in DHEA-induced PCOS like mouse model (7). Jin et al. further explored the effect of androgen exposure on the function of granulosa cells and found that testosterone significantly induced ER stress and apoptosis of ovarian granulosa cells *in vitro*, indicating the negative effect of androgen-induced ER stress on follicle development (8). In addition, Li et al. revealed a positive correlation between serum testosterone levels and the expression of autophagy-related genes, suggesting that androgen excess contributed to the activation of autophagy and apoptosis in granulosa cells, which subsequently impairs ovarian function (9, 10). Combined, these results suggested androgens promote apoptosis of granulosa cells in PCOS, while the specific role and mechanism of androgens in regulating follicular growth and ovulation remains unclear.

Metabolic disorders also play a vital role in PCOS pathogenesis. Compared to women with regular ovulation, anovulatory PCOS patients showed obvious dyslipidemia, namely, increased serum cholesterol, triglycerides, and also low-density lipoprotein (LDL) levels and decreased high-density lipoprotein (HDL) levels (11), which were closely related to testosterone levels. In addition, lipid metabolism dysfunction in granulosa cells was also found to contribute to PCOS development (12). In human granulosa cells, oxidized low-density lipoprotein induced cell death and subsequently contributed to ovulatory dysfunction, indicating that disorders of lipid metabolism in granulosa cells may be implicated in PCOS development (13). On the other hand, fatty acid levels were proposed as the predictors of *in vitro* fertilization outcomes for their bi-directional effect on granulosa cell function and oocyte competence. However, fatty acid profiles in PCOS serum and follicular fluid were both found to significantly differ from that in healthy women, suggesting the important role of granulosa cell metabolic disorders in PCOS development (14). Intriguingly, androgen excess has long been demonstrated to participate in the development of various metabolic disorders in PCOS (15). However, the mechanism of how high androgen exposure promotes metabolic disorders in PCOS granulosa cells remains elusive.

As the basic functional unit of the ovary, ovarian follicle consists of oocyte and surrounding granulosa cells. Folliculogenesis is a vital process for the production of fertilizable and developmentally-competent oocyte, which requires the regulation of various signals including, but not restricted to, hormonal regulation, paracrine signals and the bidirectional communication between oocyte and granulosa cells (4, 16, 17). To better understand the biology and regulatory mechanism of follicle development, various culture methods have been established (18–21). *In vitro* follicle culture system which uses alginate as the scaffold to preserve the structural integrity and function of ovarian follicle has been established to explore the dynamic of follicle development (22–24). Furthermore, mature oocyte and live birth were obtained from mouse follicles cultured *in vitro* (25), suggesting the superiority of this system in mimicking folliculogenesis process *in vivo*. In general, *in vitro* follicle culture system enables us to investigate the biology of folliculogenesis and oocyte maturation *in vitro*, which has great significance for fertility preservation and provides an excellent *in vitro* model to investigate the pathophysiology of ovulatory disorder in anovulatory diseases.

Here we performed RNA-seq analysis to comprehensively reveal the hyperandrogenism-induced functional disorders of PCOS granulosa cells. *In vitro* mouse follicle culture system was established to examine the effect of hyperandrogenic exposure on the function of granulosa cells and ovarian follicles, with AR antagonist supplied to figure out the action mode of androgen. Overall, this study provides insights into hyperandrogenism induced abnormal follicle development in PCOS.

METHODS AND MATERIALS

Human Subjects

The study protocol was approved by the Ethics Committee of Peking University Third Hospital according to the Council for International Organizations of Medical Sciences. According to the 2003 Rotterdam criteria, women with PCOS were diagnosed when at least two of the following clinical manifestations occurred: (1) oligo-ovulation and/or anovulation; (2) clinical and/or biochemical hyperandrogenism; and (3) polycystic ovaries. Cushing syndrome, thyroid disease, 21-hydroxylase deficiency, androgen-secreting tumors, congenital adrenal hyperplasia, and hyperprolactinemia should be excluded before the diagnosis of PCOS. Infertile individuals with only tubal occlusion or male azoospermia were recruited as the control subjects. Informed consent has been signed by all participants. The clinical characteristics of enrolled individuals are listed in **Table 1**.

Human Granulosa Cell Collection and Culture

We enrolled 6 control and 6 women with PCOS for granulosa cell collection and RNA extraction. Both individuals in control

TABLE 1 | Clinical characteristics in women with and without PCOS.

	Control (n = 6)	PCOS (n = 6)	*P*-value
Age (year)	30.3 ± 4.63	29.0 ± 4.94	0.6400
Body Mass Index	23.9 ± 1.72	22.7 ± 1.86	0.2658
FSH (mIU/ml)	6.35 ± 1.37	6.35 ± 1.21	0.9896
LH (mIU/ml)	3.09 ± 1.19	11.5 ± 5.77	0.0151
LH/FSH	0.48 ± 0.13	1.94 ± 1.36	0.0467
Estradiol (pmol/ml)	224.58 ± 146.89	219.5 ± 106.6	0.9468
Testosterone (nmol/L)	0.69 ± 0.03	1.90 ± 0.53	0.0026
Androstenedione (nmol/L)	5.37 ± 1.94	16.4 ± 2.71	1.95E-5

FSH, follicle-stimulating hormone; LH, luteinizing hormone. All data are expressed as the mean ± S.E.M. Data were analyzed by two-tailed Student's t-test.

group and women with PCOS were on the first *in vitro* fertilization cycle. Both individuals in control group and women with PCOS were on the first *in vitro* fertilization cycle. A gonadotrophin releasing hormone antagonist protocol was applied for all donors. After 36 h of human chorionic gonadotropin (hCG) administration, follicular fluid was obtained from controls and PCOS women through transvaginal ultrasound-guide follicle aspiration. As described previously (26), human granulosa cells were separated with density gradient centrifugation and culture in DMEM-F12 supplemented with 10% fetal bovine serum (FBS), and 1% penicillin–streptomycin (5,000 U/ml) for 12 h, and subsequently collected for RNA extraction.

RNA Extraction and RNA Sequencing (RNA-seq) Analysis

Total RNA was extracted from collected human granulosa cells with TRIzol reagent (15596018; Life Technologies) according to the manufacturer's protocol. Total RNA from two individuals were mixed for RNA-seq. After RNA quantification and qualification, a total amount of 1μg RNA per sample was used as input material for the RNA ample preparation. Sequencing libraries were generated using NEBNext® UltraTM RNA Library Prep Kit for Illumina® (NEB, USA) following manufacturer's recommendations and index codes were added to attribute sequences to each sample. The clustering of the index-coded samples was performed on a cBot Cluster Generation System using TruSeq PE Cluster Kit v3-cBot-HS (Illumia) according to the manufacturer's instructions. After cluster generation, the library preparations were sequenced on an Illumina Novaseq platform and 150 bp paired-end reads were generated. Before data analysis, raw data (raw reads) of fastq format were firstly processed through in-house perl scripts for quality control. In this step, clean data (clean reads) were obtained by removing reads containing adapter, reads containing ploy-N and low-quality reads from raw data. At the same time, Q20, Q30, and GC content the clean data were calculated. All the downstream analyses were based on the clean data with high quality. As to data analysis, raw data (raw reads) of fastq format were firstly processed through in-house perl scripts, at the same time, Q20, Q30, and GC content the clean data were calculated. All the downstream analyses were based on the clean data with high quality. Reference genome and gene model annotation files were downloaded from genome website directly. Index of the reference genome was built using Hisat2 v2.0.5 and paired-end clean reads were aligned to the reference genome using Hisat2 v2.0.5. Significant differentially expressed genes were defined by the criteria of FDR q <0.05 and log2(FC) ≥1. Bioinformatic analysis was performed using the OmicStudio tools at https://www.omicstudio.cn/tool. The data presented in the study are deposited in the GEO database, accession number GSE193123.

In Vitro Culture of Mouse Ovarian Follicles

Used for the mechanical separation of secondary follicles were 18 to 21-day-old C57BL/6J mice. Healthy follicles (intact and round oocyte in the central of follicles, with 2–3 layers of granulosa cells surrounded and covered with intact theca cell layer) were selected for culturing. While atretic follicles (follicles with darken granulosa cells) and damaged follicles (follicles with the extrusion of oocyte or granulosa cells) were excluded at the beginning of *in vitro* culture. Healthy follicles were incubated in maintenance media (αMEM [32571036, Sigma-Aldrich] with 1% FBS) for 1 h before encapsulation. As described previously (25, 27), each follicle was capsulated with 0.5% alginate (Sigma-Aldrich) to maintain its architecture, and then cultured with 100 μl growth media (αMEM, 3 mg/ml BSA [B2064, Sigma-Aldrich], 1 mg/ml bovine fetuin [F2379, Sigma-Aldrich], 10 mIU/ml recombinant follicular stimulating hormone, 5 μg/ml insulin, 5 μg/ml transferrin, and 5 μg/ml selenium [I3146, Sigma-Aldrich]) in 96-well plate. DHEA (10 μM; HY-14650; Med Chem Express) was supplied into growth media to mimic hyperandrogenic environment in PCOS ovaries, flutamide (10 μM; F9397; Sigma-Aldrich) was supplied into growth media to block androgen receptor. Half of the growth media was changed every 2 days and the supernatants were collected for estradiol detection after culture. Follicles were imaged by fluorescence microscope at each media change. The average length of two perpendicular measurements from basal lamina to basal lamina in ImageJ was considered as the follicle diameter.

In Vitro Maturation of Mouse Ovarian Follicles

On the 6th day of culturing, follicles were released from alginate beads using alginate lyase (A1603, Sigma-Aldrich) and incubated in maturation media (αMEM with 10% FBS, 1%PS, 1.5 IU/ml human chorionic gonadotropin, 10 ng/ml epidermal growth factor [EGF] [PHG0311, Gibco]) for 18 h. After 18 h of

incubation, ruptured follicles, ovulated COCs and oocytes were imaged, and the ovulation rate was calculated by observing the ovulation of 7 follicles. The follicular wall of ovulated follicles was ruptured, with ovulated cumulus–oocyte-complex (COC) around. Oocytes with first polar body extrusion were classified as mature oocytes. Every 3 follicles were collected for RNA extraction using RNeasy Mini Kit (74104, QIAGEN).

cDNA Synthesis and Quantitative Real-Time PCR Analysis

cDNA was synthesized from 1,000 ng RNA using the RevertAid First cDNA Synthesis Kit (K1622; Thermo Scientific) according to the manufacturer's protocols. The primers used for Real-time qPCR are listed in **Table 2**. Real-time qPCR was performed in an ABI 7500 real-time PCR system (Applied Biosystems) using SYBR Green PCR Master Mix (Invitrogen). The relative expression level of genes was normalized to those of 18S rRNA in mouse and *ACTIN* in human.

Screening of Hub Genes

The PPI network of the STRING database was applied to reveal the relationship between the DEGs. Then, the network relationship file was downloaded, and the top 10 hub genes were identified in accordance with Cytoscape 3.6.1 and its plug-in (degrees ranking of cytoHubba).

Statistical Analysis

The data are shown as Mean ± SEM. For parametric data, statistical analyses were carried out using SPSS version 23 by two-tailed Student's t-test or one-way ANOVA with Tukey's *post hoc* test and represented with GraphPad Prism version 8.0 (GraphPad Software). For nonparametric data, statistical analyses were carried out by the two-tailed Mann–Whitney U-test or the Kruskal–Wallis test followed by Dunn's *post hoc* test. *P <0.05, ** P <0.01, *** P <0.001; $^{\#}$P <0.05, $^{\#\#}$ P <0.01, $^{\#\#\#}$ P <0.001.

TABLE 2 | Primer Sequence used in quantitative real-time PCR analysis.

Target genes	Primer sequence
18S (mouse)	Forward 5'-GAAACGGCTACCACATCCAAGG-3'
	Reverse 5'-GCCCTCCAATGGATCCTCGTTA-3'
Cyp17a1 (mouse)	Forward 5'-GCCCAAGTCAAAGACACCTAAT-3'
	Reverse 5'-GTACCCAGGCGAAGAGAATAGA-3'
Cyp19a1 (mouse)	Forward 5'-ATGTTCTTGGAAATGCTGAACCC-3'
	Reverse 5'-AGGACCTGGTATTGAAGACGAG-3'
Amh (mouse)	Forward 5'-CCACACCTCTCTCCACTGGTA-3'
	Reverse 5'-GGCACAAAGGTTCAGGGGG-3'
Gdf9 (mouse)	Forward 5'-TCTTAGTAGCCTTAGCTCTCAGG-3'
	Reverse 5'-TGTCAGTCCCATCTACAGGCA-3'
Bmp15 (mouse)	Forward 5'-TCCTTGCTGACGACCCTACAT-3'
	Reverse 5'-TACCTCAGGGGATAGCCTTGG-3'
Has2 (mouse)	Forward 5'-TGTGAGAGGTTTCTATGTGTCCT-3'
	Reverse 5'-ACCGTACAGTCCAAATGAGAAGT-3'
Ptx3 (mouse)	Forward 5'-CCTGCGATCCTGCTTTGTG-3'
	Reverse 5'-GGTGGGATGAAGTCCATTGTC-3'
Adamts1 (mouse)	Forward 5'-CATAACAATGCTGCTATGTGCG-3'
	Reverse 5'-TGTCCGGCTGCAACTTCAG-3'
Tnfaip6 (mouse)	Forward 5'-GGGATTCAAGAACGGGATCTTT-3'
	Reverse 5'-TCAAATTCACATACGGCCTTGG-3'
Hmgcr (mouse)	Forward 5'-AGCTTGCCCGAATTGTATGTG-3'
	Reverse 5'-TCTGTTGTGAACCATGTGACTTC-3'
Fads2 (mouse)	Forward 5'-GATGGCTGCAACATGACTATGG-3'
	Reverse 5'-GCTGAGGCACCCTTTAAGTGG-3'
Fasn (mouse)	Forward 5'-GGAGGTGGTGATAGCCGGTAT-3'
	Reverse 5'-TGGGTAATCCATAGAGCCCAG-3'
Srebf1 (mouse)	Forward 5'-GCAGCCACCATCTAGCCTG-3'
	Reverse 5'-CAGCAGTGAGTCTGCCTTGAT-3'
Insig1 (mouse)	Forward 5'-CACGACCACGTCTGGAACTAT-3'
	Reverse 5'-TGAGAAGAGCACTAGGCTCCG-3'
Ldlr (mouse)	Forward 5'-AGTGGCCCCGAATCATTGAC-3'
	Reverse 5'-CTAACTAAACACCAGACAGAGGC-3'
Acss2 (mouse)	Forward 5'-AAACACGCTCAGGGAAAATCA-3'
	Reverse 5'-ACCGTAGATGTATCCCCCAGG-3'
Lss (mouse)	Forward 5'-TCGTGGGGGACCCTATAAAAC-3'
	Reverse 5'-CGTCCTCCGCTTGATAATAAGTC-3'
ACTB (human)	forward 5'-GAGCACAGAGCCTCGCCTTT-3'
	reverse 5'-TCATCATCCATGGTGAGCTGG-3'
HMGCR (human)	Forward 5'-TGATTGACCTTTCCAGAGCAAG-3'
	Reverse 5'-CTAAAATTGCCATTCCACGAGC-3'
FASN (human)	Forward 5'-TGATTGACCTTTCCAGAGCAAG-3'
	Reverse 5'-CTAAAATTGCCATTCCACGAGC-3'
SREBF1 (human)	Forward 5'-CGGAACCATCTTGGCAACAGT-3'
	Reverse 5'-CGCTTCTCAATGGCGTTGT-3'
SCD (human)	Forward 5'-TTCCTACCTGCAAGTTCTACACC-3'
	Reverse 5'-CCGAGCTTTGTAAGAGCGGT-3'
INSIG1 (human)	Forward 5'-GCCTACTGTACCCCTGTATCG-3'
	Reverse 5'-TGGTTAATGCCAACAAAAACTGC-3'
LDLR (human)	Forward 5'-ACGGCGTCTCTTCCTATGACA-3'
	Reverse 5'-CCCTTGGTATCCGCAACAGA-3'
LSS (human)	Forward 5'-GTACGAGCCCGGAACATTCTT-3'
	Reverse 5'-CGGCGTAGCAGTAGCTCAT-3'
SCD5 (human)	Forward 5'-TGCGACGCCAAGGAAGAAAT-3'
	Reverse 5'-CCTCCAGACGATGTTCTGCC-3'
FADS2 (human)	Forward 5'-GACCACGGCAAGAACTCAAAG-3'
	Reverse 5'-GAGGGTAGGAATCCAGCCATT-3'
ACSS2 (human)	Forward 5'-AAAGGAGCAACTACCAACATCTG-3'
	Reverse 5'-GCTGAACTGACACACTTGGAC-3'

RESULTS

Identification of the Transcriptional Landscapes of PCOS Granulosa Cells

To investigate the potential effects of hyperandrogenism on granulosa cells from PCOS patients, we performed RNA-seq analysis on granulosa cells using a PCOS cohort with significantly upregulated serum testosterone and androstenedione levels in comparison with BMI-matched individuals in control group. The raw data of RNA-seq analysis were firstly processed for quality control and downstream analyses were based on the clean data with high quality. According to the heatmap, the transcripts of PCOS granulosa cells evidently differed from that of control (**Figure 1A**). In comparison with control, a total of 1,172 genes were significantly changed in PCOS granulosa cells, of which 521 genes were upregulated and 651 genes were downregulated respectively in PCOS granulosa cells. Genes encoding inflammatory factors including interleukin-1beta (*IL1B*) and interleukin-1alpha (*IL1A*) showed remarkable upregulation in PCOS granulosa cells; besides, the expression of arachidonate 15-lipoxygenase (*ALOX15*) was also evidently upregulated. ALOX15 is a member of the lipoxygenase family, which plays an important

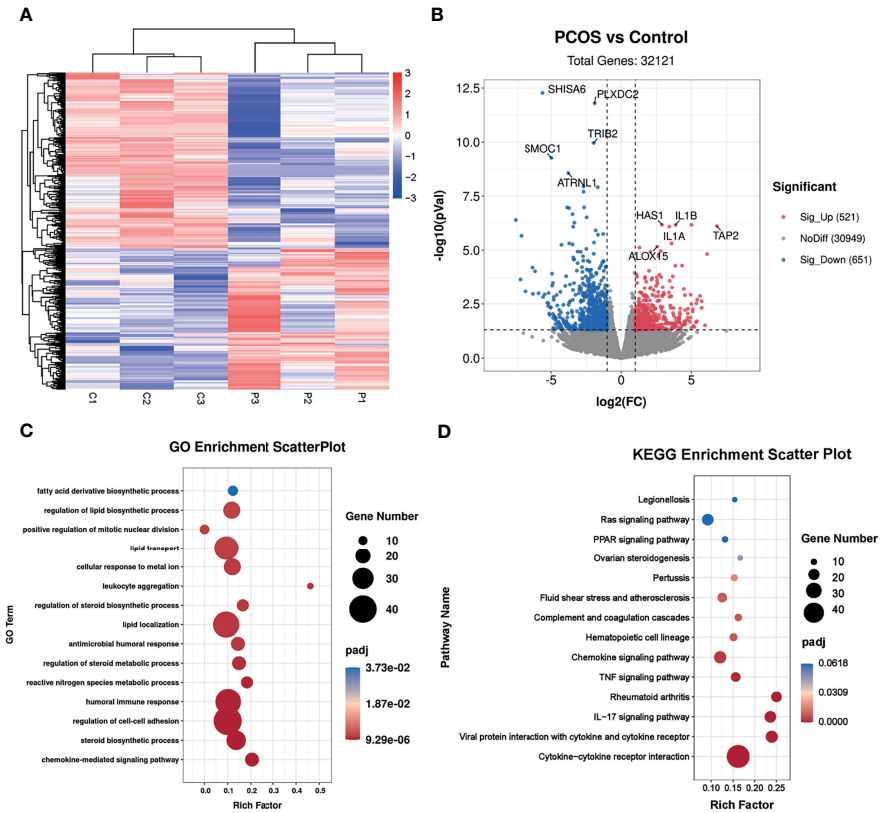

FIGURE 1 | Identification of the transcriptional landscapes of PCOS granulosa cells. **(A)** Heatmap of differential expressed genes in the control and PCOS granulosa cells. **(B)** Volcano plot showing transcriptomic landscapes in control and PCOS group. Significant differentially expressed genes (DEGs) were examined with padj (adjusted p-value) < 0.05. Meanwhile, log2 fold change >1 was set as the threshold for significant differential expression. **(C)** GO enrichment analysis showing 15 pathways from the top 50 pathways enriched in PCOS granulosa cells; **(D)** KEGG pathway analysis showing the top 15 pathways involved in PCOS pathogenesis.

role in polyunsaturated fatty acid metabolism, indicating that metabolic disorders may have occurred in PCOS granulosa cells (**Figure 1B**). To investigate the specific signaling pathway involved in PCOS pathogenesis, we performed GO enrichment analysis and KEGG analysis of all DEGs and found that DEGs were evidently enriched in immune related pathways, namely, chemokine-mediated signaling pathway and humoral immune response, indicating the possible role of immune factors in PCOS development. In addition, fatty acid biosynthetic process and lipid metabolism-related pathways were also enriched in PCOS granulosa cells (**Figure 1C**). Furthermore, more than one fifth of the top 50 pathways enriched through GO analysis were metabolic related pathways (**Table 3**), suggesting that the impairment of metabolic process, especially fatty acid biosynthetic and lipid metabolism pathways may play a vital role in promoting granulosa cells dysfunction in PCOS. Similarly, KEGG analysis of DEGs also suggested the misexpression of genes related to chemokine signaling pathway in PCOS granulosa cells. Moreover, PPAR signaling pathway were enriched in KEGG analysis, suggesting that metabolic state in PCOS granulosa cells evidently differed from that in control, and the enrichment of DEGs in ovarian steroidogenesis may further support the abnormal secretion of steroid hormones by granulosa cells in women with PCOS (**Figure 1D**). Overall, these results indicated that lipid metabolism disorders are important characteristics of granulosa cells in PCOS patients.

Interaction Between Metabolic Disorders and Ovarian Steroidogenesis in PCOS Granulosa Cells

Given the significant enrichment of DEGs in metabolic-related pathways in PCOS granulosa cells, we further analyzed the specific genes involved in these pathways. Among genes involved in the regulation of lipid biosynthetic process, *APOC1*, *APOE*, *SCAP*, *SREBF1*, and *LDLR*, which played a vital role in lipid transportation and metabolism, were significantly downregulated in PCOS patients (**Figure 2A**); some of these genes were also enriched in fatty acid biosynthetic process. *ALOX15* and *ALOX5AP*, members of lipoxygenases which promote oxygenation of poly-unsaturated fatty acids and produce pro-inflammatory agents, were upregulated in PCOS granulosa cells. Misexpression of *CYP1A1*, which encodes a member of the cytochrome P450 superfamily of enzymes, also contributed to the difference in fatty acid biosynthesis process in healthy control and women with PCOS (**Figure 2B**). DEGs involving *CYP11A1* and *CYP19A1*

TABLE 3 | GO enrichment analysis of differential expressed genes (metabolic-related pathways in the top 50 GO terms).

GOID	Description	*p*-value	padj	Gene Name
GO:0006694	steroid biosynthetic process	1.14E−07	3.30E−05	*IL1B/SCAP/NR1H4/SREBF1/HMGCR/FAXDC2/PRLR/TM7SF2/APOE/HSD11B2/ACOX2/CYP19A1/INSIG1/FASN/CYP11B1/LSS/BMP6/CYP1A1/DHCR24/SCD/CYP11A1/BMP2/FDXR/CYP27B1/SCARB1/WNT4/ABCB11*
GO:0019218	regulation of steroid metabolic process	4.22E−06	0.000985	*IL1B/SCAP/NR1H4/APOC1/SREBF1/HMGCR/TM7SF2/APOE/EPHX2/INSIG1/FASN/LSS/BMP6/LDLR/SCD/BMP2/CYP27B1/WNT4*
GO:0010876	lipid localization	7.08E−06	0.001505	*ABCA5/IL1B/NR1H4/APOC1/ZC3H12A/IL6/LCN12/ABCA10/CLU/KCNN4/C3/SERPINA5/ATP8A2/ABCA9/TNFAIP8L3/ATP8B3/APOE/EDN1/PRKN/SLC51A/MTTP/SPNS3/GULP1/CYP19A1/SLC27A6/SLCO1A2/OSBPL10/PLA2G12A/FABP6/BMP6/SPNS2/LDLR/PNLIP/SCARB1/ABCA13/ABCB11/ANO9/ACSL4*
GO:0050810	regulation of steroid biosynthetic process	7.37E−06	0.001505	*IL1B/SCAP/NR1H4/SREBF1/HMGCR/TM7SF2/APOE/INSIG1/FASN/LSS/BMP6/SCD/BMP2/CYP27B1/WNT4*
GO:0006869	lipid transport	1.23E−05	0.002105	*ABCA5/IL1B/NR1H4/APOC1/LCN12/ABCA10/CLU/KCNN4/SERPINA5/ATP8A2/ABCA9/TNFAIP8L3/ATP8B3/APOE/EDN1/PRKN/SLC51A/MTTP/SPNS3/GULP1/CYP19A1/SLC27A6/SLCO1A2/OSBPL10/PLA2G12A/FABP6/BMP6/SPNS2/LDLR/PNLIP/SCARB1/ABCA13/ABCB11/ANO9/ACSL4*
GO:0046890	regulation of lipid biosynthetic process	1.29E−05	0.002105	*IL1B/SCAP/NR1H4/APOC1/SREBF1/HMGCR/SPHK1/C3/TM7SF2/APOE/PTGS2/INSIG1/FASN/SMPD3/LSS/BMP6/LDLR/SCD/BMP2/CYP27B1/SCARB1/WNT4/PDGFB*
GO:0008202	steroid metabolic process	1.47E−05	0.002328	*IL1B/SCAP/NR1H4/APOC1/SREBF1/HMGCR/FAXDC2/DHRS9/PRLR/TM7SF2/APOE/HSD11B2/EPHX2/ACOX2/CYP19A1/INSIG1/FASN/CYP11B1/LSS/BMP6/CYP1A1/DHCR24/LDLR/SCD/CYP11A1/BMP2/WWOX/FDXR/CYP27B1/SCARB1/WNT4/ABCB11*
GO:0016125	sterol metabolic process	2.91E−05	0.003445	*SCAP/NR1H4/APOC1/SREBF1/HMGCR/FAXDC2/TM7SF2/APOE/EPHX2/CYP19A1/INSIG1/FASN/CYP11B1/LSS/DHCR24/LDLR/SCD/CYP11A1/FDXR/SCARB1*
GO:0090181	regulation of cholesterol metabolic process	3.72E−05	0.003965	*SCAP/NR1H4/SREBF1/HMGCR/TM7SF2/APOE/EPHX2/FASN/LSS/LDLR/SCD*
GO:1902652	secondary alcohol metabolic process	3.91E−05	0.004082	*SCAP/NR1H4/APOC1/SREBF1/HMGCR/TM7SF2/APOE/EPHX2/INSIG1/FASN/CYP11B1/LSS/DHCR24/LDLR/SCD/CYP11A1/FDXR/CYP27B1/SCARB1*
GO:0019216	regulation of lipid metabolic process	4.80E−05	0.004903	*IL1B/SCAP/NR1H4/APOC1/SREBF1/HMGCR/LGALS12/SPHK1/C3/TM7SF2/TNFAIP8L3/APOE/PSAPL1/PTGS2/EPHX2/CCR7/INSIG1/CCKBR/FASN/NPAS2/PLPP1/SMPD3/LSS/BMP6/CYP1A1/SOCS1/LDLR/SCD/MTMR2/BMP2/CYP27B1/ANKRD1/SCARB1/WNT4/EPHA8/PDGFB*

were significantly enriched in ovarian steroidogenesis pathway, and this may be related to abnormal steroid hormone synthesis in PCOS (**Figure 2C**). Furthermore, the PPI network of these pathways identified a close interaction between ovarian steroidogenesis, lipid biosynthetic and fatty acid biosynthetic process in PCOS granulosa cells. This network had 36 nodes and 125 interactions, indicating that abnormal ovarian steroidogenesis was evidently correlated with lipid metabolism and fatty acid biosynthetic process in PCOS granulosa cells (**Figure 2D**). Besides, 10 hub genes, including *SREBF1*, *HMGCR*, *FASN*, *SCD*, *INSIG1*, *FADS2*, *SCD5*, *ACSS2*, *LDLR*, and *LSS*, were identified by Cytohubba (**Figure 2E**), and the RT-qPCR result indicated the decreased expression of these 10 hub genes, among which *SREBF1*, *SCD*, *INSIG1*, *FADS2*, *ACSS2*, and *LDLR* were significantly decreased in granulosa cells from women with PCOS, which was consistent with the RNA-Seq result (**Figure 2F**). These results suggested that the impairment of ovarian steroidogenesis and lipid metabolism interact and may contribute to PCOS development.

DHEA Impaired Mouse Follicular Growth, Steroidogenesis and Lipid Metabolism *In Vitro*

As mentioned above, granulosa cells from women with PCOS were characterized by the disorder of ovarian steroidogenesis and lipid metabolism, whether the dysfunction of granulosa cells may be related to the impairment of follicle growth and ovulation in PCOS remains unclear. To explore the effect of high androgen exposure-induced lipid metabolism disorder on follicular development, we established an *in vitro* follicle culture system and DHEA was added to simulate the hyperandrogenic environment in PCOS patients. We observed that in the process of *in vitro* culture, separated secondary follicles in control group gradually grew, oocytes moved to one side of the follicle, thus forming antral in the other side of the follicles (**Figure 3A**). After 6 days of *in vitro* culture, follicle diameter could increase from 180 to 360 μm; while supplying DHEA significantly inhibited follicle growth, as the follicles are blocked at 300 μm in diameter (**Figure 3B**). In addition, steroidogenesis process was also

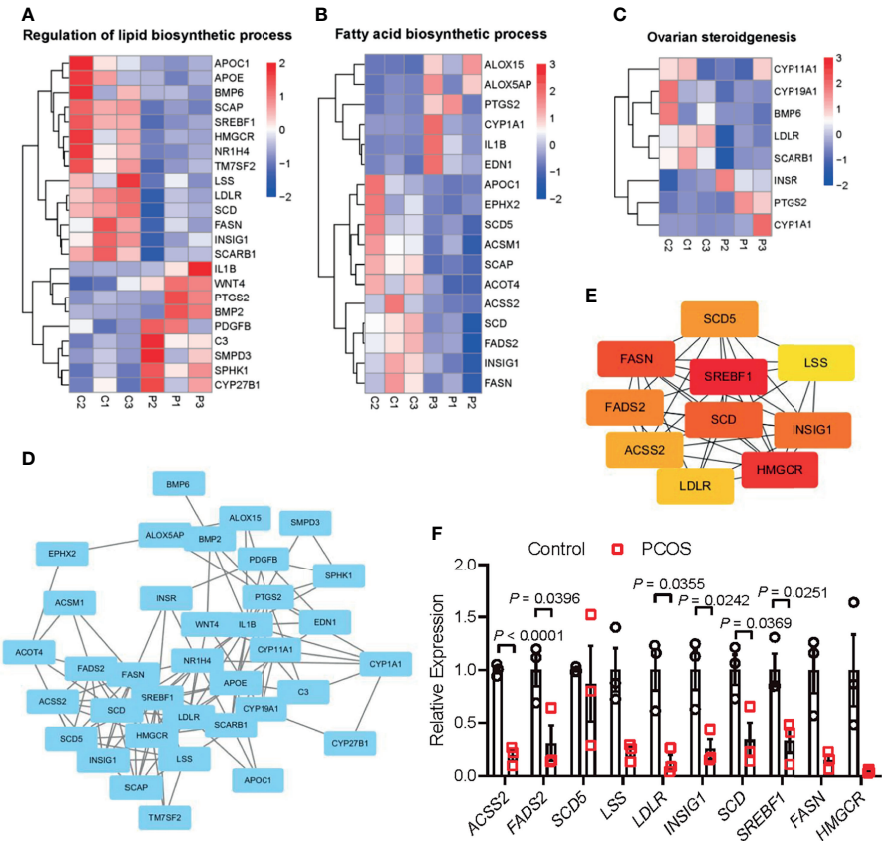

FIGURE 2 | Interaction between metabolic disorders and ovarian steroidogenesis in PCOS granulosa cells. **(A)** Heatmap of differential expressed genes involved in the fatty acid biosynthetic process, **(B)** lipid metabolism, **(C)** ovarian steroidogenesis in the PCOS group and control group. **(D)** Protein–protein interaction (PPI) network between fatty acid biosynthetic process, lipid metabolism, and ovarian steroidogenesis. **(E)** Ten hub genes (*SREBF1*, *HMGCR*, *FASN*, *SCD*, *INSIG1*, *FADS2*, *SCD5*, *ACSS2*, *LDLR*, and *LSS*) in the PPI network. **(F)** mRNA expression levels of 10 hub genes (*SREBF1*, *HMGCR*, *FASN*, *SCD*, *INSIG1*, *FADS2*, *SCD5*, *ACSS2*, *LDLR*, and LSS) in granulosa cells from control and women with PCOS, N = 3. Data were analyzed by two-tailed Student's t-test **(F)**. All data are presented as the Mean ± SEM.

impaired by DHEA as estradiol (E2) levels in the supernatant of DHEA-treated follicles was lower than that in control group during 6 days of culturing (**Figure 3C**). E2 is an important steroid hormone synthesized by granulosa cells in growing follicles. It supports the development of ovarian follicles; besides, the elevation of E2 concentrations triggers the LH surge *via* positive feedback effect system, thus inducing ovulation. The decreased E2 levels in DHEA-treated follicles may indicate the impairment of follicle development and ovulation process. We further explored the expression of gene associated with steroid hormone synthesis in follicles. RT-qPCR result showed that *Cyp17a1* and *Cyp19a1*, genes encoding enzymes responsible for the key step in the biosynthesis of androgen and estrogen respectively, were evidently decreased by DHEA (**Figure 3D**), indicating the impairment of steroidogenesis in DHEA-treated follicles. Moreover, mRNA expression levels of hub genes identified from the PPI network of lipid metabolism, fatty acid biosynthesis and ovarian steroidogenesis were investigated in DHEA-treated follicles. The RT-qPCR result indicated the evident decreased expression of *Lss*, *Insig1*and *Srebf1*, which suggested the impairment of lipid metabolism in DHEA-treated follicles and further verified that androgen excess had metabolically harmful effect on granulosa cells (**Figure 3E**). Overall, these results suggested that DHEA treatment induced failure of ovarian steroidogenesis and lipid metabolism, which may subsequently contribute to the disruption of follicle development.

Supplementation of DHEA Inhibited Ovulation *via* Obstructing Cumulus Expansion

To further investigate the effect of DHEA on ovulation, follicles were released from alginate beads on day 6 and culture with hCG for 18 h. After hCG treatment, we observed that the follicular wall was ruptured, with ovulated cumulus–oocyte-complex (COC) around the ruptured follicle; while no follicular rupture occurred in DHEA treated follicles. We also assessed maturity of follicular oocyte after hCG treatment in two groups. The first polar body extrusion was observed in oocytes denuded from ovulated COCs in control group, whereas oocyte from DHEA group was immature oocyte with germinal vesicle (**Figure 4A**),

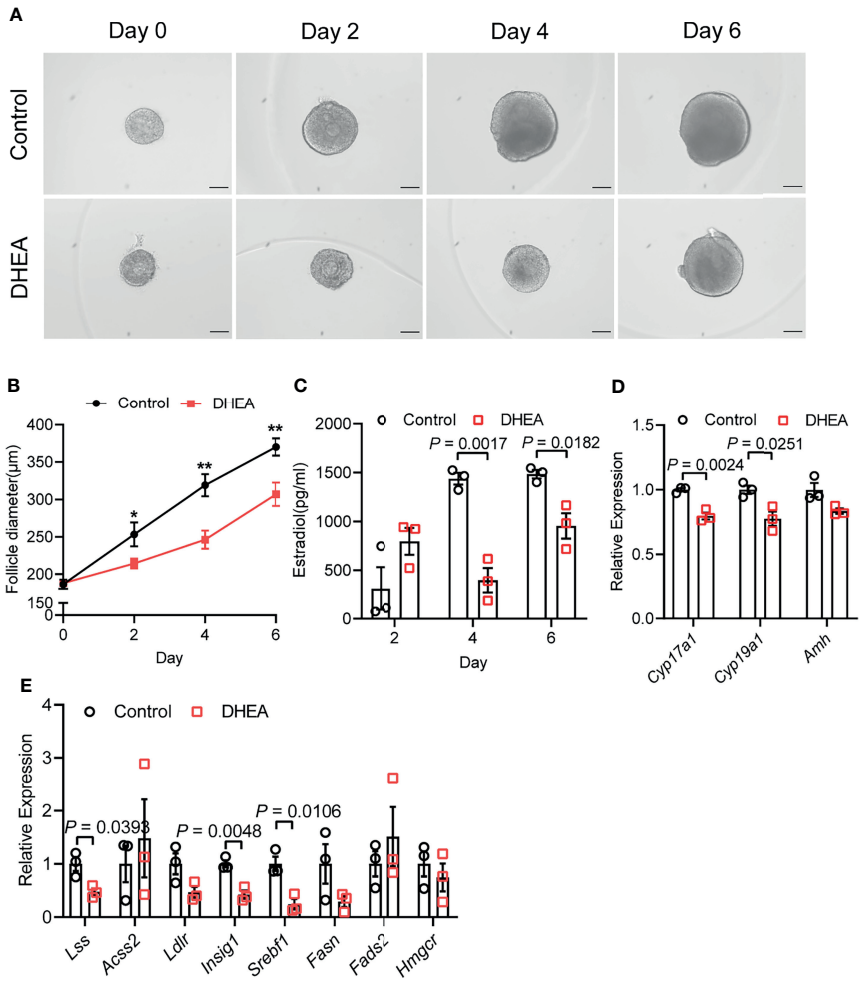

FIGURE 3 | DHEA impaired mouse follicular growth and steroidogenesis *in vitro*. **(A)** Representative micrograph of mouse follicles cultured *in vitro*. **(B)** Follicle diameters in control and DHEA group, N = 9. **(C)** Estradiol levels in the supernatant of control and DHEA-treated follicles, N = 3. **(D)** mRNA expression levels of *Cyp17a1*, *Cyp19a1*, and *Amh* in follicles cultured *in vitro*, N = 3. **(E)** mRNA expression levels of *Lss*, *Acss2*, *Ldlr*, *Insig1*, *Srebf1*, *Fasn*, *Fads2*, and *Hmgcr* in follicles cultured *in vitro*, N = 3. Scale bar: 100 μm. Data were analyzed by two-tailed Student's t-test **(B–E)**. All data are presented as the Mean ± SEM. *P < 0.05, **P < 0.01.

indicating the inhibition of DHEA on ovulation and oocyte maturation. Statistical result showed that the ovulation rate in DHEA treated follicles was significantly decreased (**Figure 4B**), which was consistent with the result of morphological observation. Ovulation is a complicated process, and the interaction between oocyte and surrounding cumulus cells is important for normal ovulation process. As oocyte secreted factors, GDF9 and BMP15 act on follicular cells adjacent to oocytes to modulate granulosa cells functions (17). GDF9 and BMP15 levels have a positively relationship with oocyte maturation (28). In the present study, *Gdf9* and *Bmp15* mRNA levels were significantly inhibited in DHEA-treated mouse follicles (**Figure 4C**). Additionally, expansion of the COC is essential to ovulation and female fertility (29), the mRNA levels of cumulus expansion related genes, namely, *Has2*, *Ptx3*, *Adamts1*, and *Tnfaip6* were all decreased in follicles treated with DHEA (**Figure 4D**), thus DHEA could inhibit ovulation by suppressing oocyte maturation and cumulus expansion.

Flutamide Reversed DHEA-Induced Impairment of Follicle Growth and Ovulation Through Blocking AR

AR is considered as key mediators of androgen actions and play an important role in the development of PCOS (30, 31). As a competitive inhibitor of AR, flutamide exhibited therapeutic effect on reproductive and metabolic disorders in PCOS (32). To demonstrate the role of AR signaling in androgen excess induced failure of follicle development and ovulation, flutamide was supplied to DHEA-treated mouse follicles which grew significantly slower than follicles in control group. Flutamide evidently improved follicle growth as the follicle diameter was significantly higher than that in DHEA-treated only group at

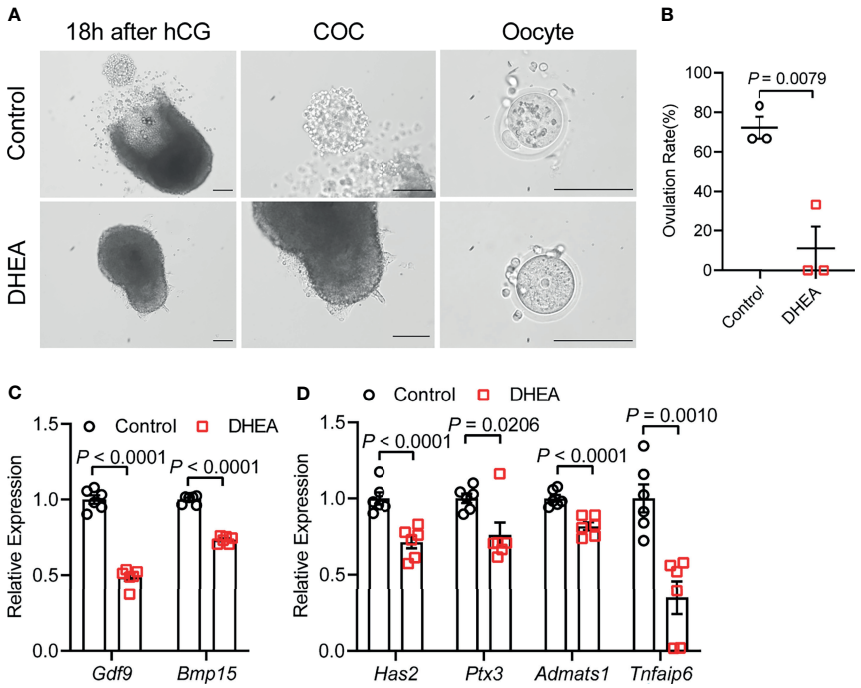

FIGURE 4 | Supplementation of DHEA inhibited ovulation *via* obstructing cumulus expansion. **(A)** The representative micrograph of follicles, ovulated COCs and oocytes after 18 h of maturation. Oocyte with first polar body extrusion was classified as mature oocyte. **(B)** Ovulation rate of *in vitro* cultured follicles, N = 3. **(C)** mRNA expression levels of *Gdf9*, *Bmp15* and **(D)** *Has2*, *Ptx3*, *Tnfaip6* and *Adamts1* in follicles cultured *in vitro*, N = 6. Scale bar: 100 μm. Data were analyzed by two-tailed Mann–Whitney U-test or the Kruskal–Wallis test followed by Dunn's *post hoc* test **(B)** and two-tailed Student's t-test **(C, D)**. All data are presented as the Mean ± SEM.

days 4 and 6 (**Figures 5A, B**). In addition, mRNA expression levels of *Gdf9* and *Bmp15* were significantly decreased in DHEA-treated follicles, while the supply of flutamide significantly reversed the inhibition of DHEA (**Figure 5C**). Furthermore, the blockage of ovulation in follicles cultured with DHEA was also ameliorated by flutamide. The expression of ovulation-related genes *Adamts1* and *Tnfaip6* in follicles was disrupted by DHEA, which was significantly improved by flutamide (**Figure 5D**), indicating the involvement of AR signaling in DHEA induced ovulation disorders. Overall, these results supported that androgen excess induced impairment of follicle growth and ovulation is AR-driven.

DISCUSSION

PCOS is a complicated reproductive and endocrine syndrome which impairs female fertility. The interaction between hyperandrogenism and metabolic disorders plays an important role in PCOS pathogenesis. In the present study, we mainly focus on the effect of androgen on metabolic dysfunction in PCOS granulosa cells. We analyzed the transcriptome characteristics of PCOS granulosa cells by RNA-seq analysis. The results of GO and KEGG pathway analysis showed that ovarian steroidogenesis, lipid metabolism, and fatty acid biosynthetic pathways were significantly enriched and closely interacted with each other in PCOS granulosa cells. To demonstrate the impact of androgen excess induced lipid metabolism and steroidogenesis disorders in granulosa cells on ovulatory disruption in PCOS, mice ovarian follicles were separated and cultured *in vitro* with DHEA supplementation. It turns out that DHEA supplementation inhibited follicle growth and steroid hormone synthesis *in vitro*; in addition, the ovulation process and oocyte maturation were also impaired by DHEA. Furthermore, the blockage of AR signalling reversed the inhibition of follicle growth and ovulation by DHEA. Combined, we have characterized the transcriptome of PCOS granulosa cells, and further identified the possible ovulation-inhibited effect of altered ovarian steroidogenesis and metabolic disorders in granulosa cells.

Reproduction is closely connected with metabolic status, as oocyte development process requires the supplementation of various nutrients. According to the analysis of the dynamic metabolome profiles in oocytes during *in vivo* maturation, lipid and fatty acid metabolism played a vital role in oocyte meiotic process (5). Additionally, the bi-directional interaction between oocyte and granulosa cells has long been proved to play a key role in oocyte growth and maturation (4, 33), indicating the possible correlation between granulosa cells metabolic status and oocyte maturation, which is less investigated in previous studies. In the present study, we compared the transcriptome of granulosa cells from healthy women and women with PCOS, and found that

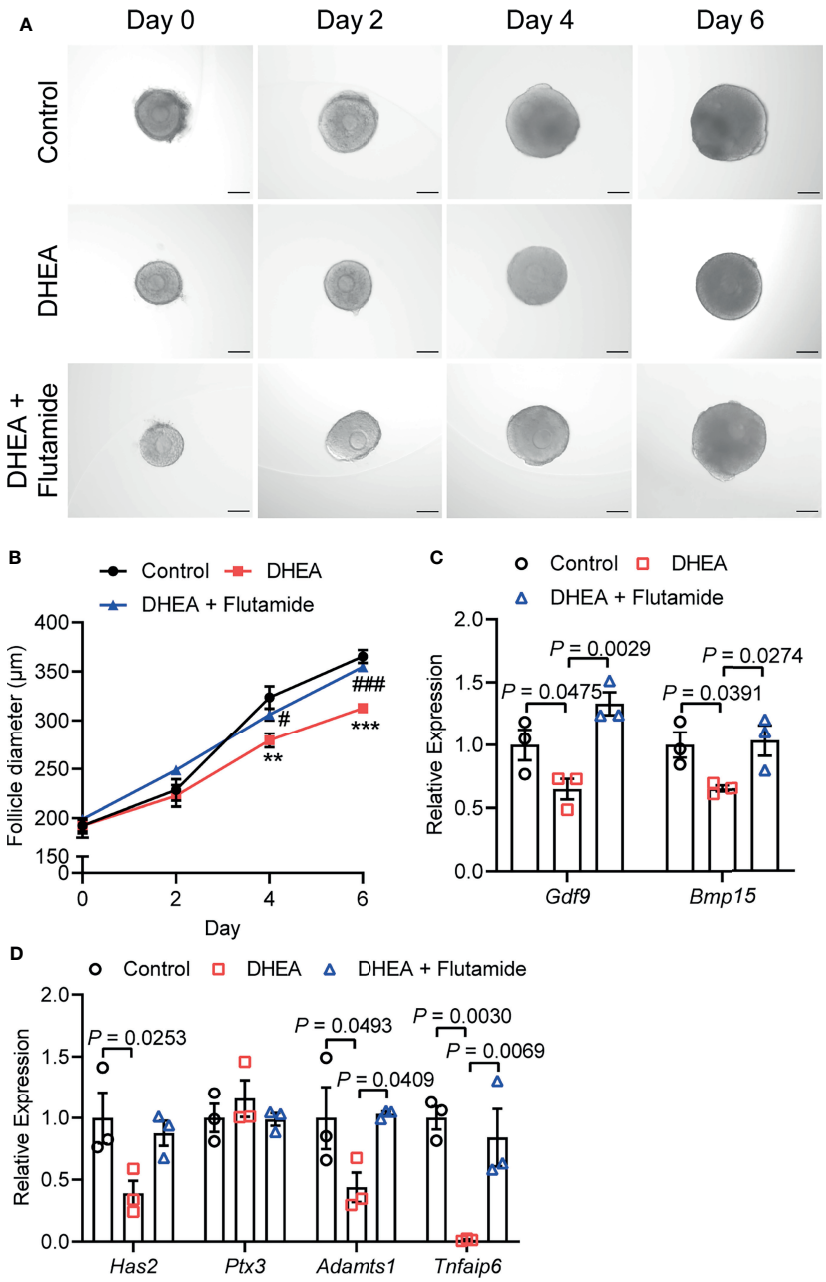

FIGURE 5 | Flutamide reversed DHEA-induced impairment of mouse follicular growth and ovulation *in vitro*. **(A)** Representative micrograph of mouse follicles cultured *in vitro*. **(B)** Follicle diameters in control, DHEA and DHEA + Flutamide group, N = 7. **P < 0.01, ***P < 0.001 versus Control; $^{\#}$P < 0.05, $^{\#\#\#}$P < 0.001 versus DHEA. **(C)** mRNA expression levels of *Gdf9*, *Bmp15* and **(D)** *Has2*, *Ptx3*, *Tnfaip6* and *Adamts1* in follicles cultured *in vitro*, N = 3. Scale bar: 100 μm. Data were analyzed by one-way ANOVA with Tukey's *post hoc* test **(B–D)**. All data are presented as the Mean ± SEM.

metabolic process and ovarian steroidogenesis were significantly impaired in PCOS granulosa cells through GO and KEGG pathway analysis. Although metabolic pathways were not ranking high, the proportion of metabolic related pathways in top 50 GO terms were relatively large. Lipid metabolism and fatty acid biosynthetic process were significantly enriched in PCOS granulosa cell. More specific roles that androgen-induced metabolic disorders played in granulosa cells dysfunction were further demonstrated in the PPI network. Among the 10 hub genes we identified through Cytoscape, the expression of 3-hydroxy-3-methylglutaryl-CoA reductase (HMGCR), a rate-limiting enzyme catalyzing cholesterol production, was decreased in human PCOS granulosa cells and prenatally hyperandrogenized animals (34), which may be caused by the feedback inhibition of elevated androgen levels in PCOS (35).

Besides, the decline of fatty acid desaturase genes 2 (*FADS2*) expression was also found in women with PCOS, which was correlated with altered androgen levels and dyslipidemia (36). Mediating the uptake of LDL by ovarian follicle cells, *LDLR* was downregulated in PCOS granulosa cells, which is consistent with previous studies (37, 38). In addition, lipid content in granulosa and cumulus cells may affect likelihood of pregnancy, loss of function of *LDLR* resulted in impaired lipid uptake and extracellular lipid accumulation, thus leading to hyperlipidemia and poor fertility in mice (39). Overall, our results showed that abnormal lipid metabolism and fatty acid synthetic pathways were closely related to the development of PCOS, while the specific mechanism underlying how these metabolic disorders contributed to ovulatory disorders in PCOS remains elusive. Actually, most of genes involved in these metabolic disorders in PCOS granulosa cells catalyzed fatty acid biosynthesis, cholesterol synthesis and ovarian steroidogenesis, besides, they were all downregulated under hyperandrogenic environment (**Figure 6**), indicating that the synthesis of fatty acid and cholesterol may be inhibited in PCOS granulosa cells, which may finally contribute to the impairment of oocyte maturation. However, there was no clue indicating changes in the degradation of fatty acid and cholesterol, the true state of fatty acid and cholesterol metabolism in PCOS still needs to be explored.

In terms of the effect of androgen on lipid metabolism, Abruzzese et al. established a prenatally hyperandrogenized rat model and clarified the effect of prenatal androgen exposure on ovarian lipid metabolism (34). Sun et al. compared the steroid and metabolic parameters between women with PCOS and healthy women and found the significantly increased serum androgen levels and upregulated lipid profiles in women with PCOS, which is consistent with previous studies; besides, the cholesterol level was also upregulated in PCOS offspring, indicating that lipid disorders, just like hyperandrogenism and insulin resistance, is a heritable clinical manifestation which may participated in the pathophysiology of PCOS from fetal stage (40). These findings suggested that abnormal lipid metabolism plays an important role in shaping the metabolic and reproductive characteristics in offspring of women with PCOS, in which androgen may participated as well. Recently, Pan et al. reported the reduction of global DNA methylation of PCOS granulosa cells in comparison with granulosa cells from healthy control, which may contributed to the abnormal expression of lipid and steroid synthesis genes for the hypomethylation of their promoters, thus providing a new insight into the possible mechanism that mediating the impact of androgen on lipid and steroid synthesis in granulosa cells (41).

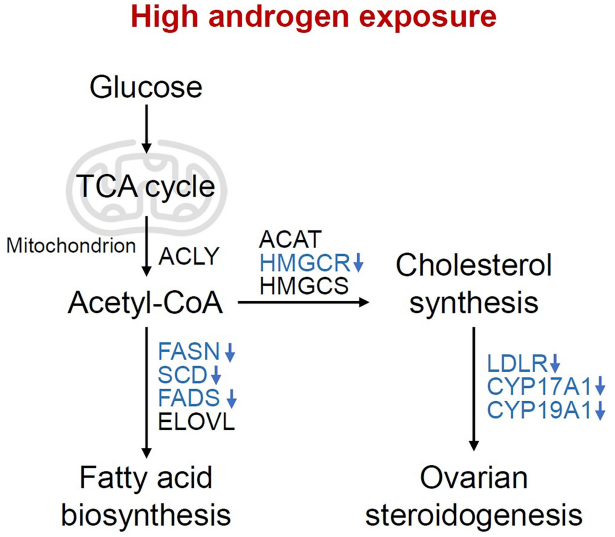

FIGURE 6 | Changes of metabolic pathways in granulosa cells under high androgen exposure. Overview of the pathways and enzymes involved in the synthesis of fatty acids, cholesterol and ovarian steroid hormone. The enzymes enriched in the present study are indicated in blue. TCA cycle, tricarboxylic acid cycle; ACLY, ATP-citrate lyase; ACAT, acetyl-CoA acetyltransferase; HMGCR, 3-hydroxy-3-methylglutaryl-CoA reductase; HMGCS, 3-hydroxy-3-methylglutaryl-CoA synthase; FASN, fatty acid synthase; SCD, stearoyl-CoA desaturase; FADS, fatty acid desaturase; ELOVL, fatty acid elongase; LDLR, Low density lipoprotein receptor; CYP17A1, Cytochrome P450 17A1; CYP19A1, Cytochrome P450 19A1.

Oocyte and surrounding granulosa cells and theca cells consist of ovarian follicle, the basic functional unit of ovary. *In vitro* follicle culture system provides an opportunity for studying the independent effect of androgen excess on follicle development and ovulation. By adding DHEA into the *in vitro* culture system of mice follicles, we found that lipid metabolism and steroid hormone synthesis in follicles was significantly inhibited by DHEA; additionally, the oocyte maturation-related gene expression was also downregulated after DHEA supplementation, and also cumulus expansion-related genes. Overall, these results indicated that lipid and fatty acid metabolic dysfunction could impair the physiological function of ovarian granulosa cells, which subsequently contribute to the disruption of oocyte maturation and ovulation. During the oocyte maturation process, beta-oxidation of fatty acid provides an important source of ATP for maturing oocyte. Besides, 7 out of 8 enzymes catalyzing fatty acid degradation were upregulated in oocyte meiosis (5), indicating that the increasing utilization of fatty acid plays an important role in promoting oocyte maturation. Furthermore, the follicular microenvironment plays a vital role in modulating oocyte maturation and competence. Fatty acid composition in follicular fluid and granulosa cells could influence oocyte quality (42, 43). In the present study, we found that genes encoding enzymes involved in fatty acid biosynthesis were downregulated in PCOS granulosa cells, which may alter the fatty acid profiles in granulosa cells, thus leading to insufficient energy supply for oocyte maturation. Overall, androgen exposure significantly influenced the metabolic status in granulosa cells from women with PCOS and impaired follicle growth and oocyte maturation, while the underlying molecular mechanism remains to be explored in the future.

AR is widely expressed throughout the body and plays an important role in the pathogenesis of PCOS (31, 44). Extra- and intra-ovarian AR actions both contribute to PCOS development. It is reported that DHT promoted the development of adipocytes hypertrophy and the decrease of adiponectin levels, which was disrupted in AR knockout mice (31). Besides, AR signaling also plays a vital role in mediating the effect of androgen in liver lipid

metabolism, as hepatic AR-knockout mice was characterized by hepatic steatosis and insulin resistance (45). In addition, AR is expressed by ovarian theca cells, granulosa cells, and oocyte (46), and granulosa cell specific AR knockout mice exhibited estrous cycle disorder and decreased fertilization rate (47). As a specific androgen antagonist, flutamide competitively inhibits androgen receptors and performs a direct blockage of androgenic effect (48). In the present study, flutamide was found to ameliorate DHEA-induced impairment of follicle development and ovulation, which further supported the direct inhibition of androgen excess on follicle development and suggested the involvement of AR signalling in androgen-induced lipid metabolism and fatty acid synthetic disorders in granulosa cell, which provides new insights into the role of AR-driven metabolic dysfunction of granulosa cells in PCOS pathogenesis.

Some limitations in our study, namely, limited number of clinical samples from both control and women with PCOS, and the functional differences between follicles cultured *in vitro* and follicles grown *in vivo* should be taken into account. Given the heterogeneity of clinical manifestations and the complexity of pathogenesis in PCOS, it is hard to fully mimic the characteristics of PCOS *in vitro*. In the current study, DHEA treatment simulate the hyperandrogenic follicular environment of PCOS ovaries *in vitro*, leading to impaired steroid hormone synthesis, anovulation, and disruption of oocyte maturation, which were partly consistent with the ovarian dysfunctions represented in PCOS patients (49). Taken together, our *in vitro* follicle culture system provided a new possibility for establishing the *in vitro* model of PCOS follicle development, and more evidences are needed to confirm this *in vitro* model.

CONCLUSION

In summary, ovarian dysfunction is the main cause for infertility in women with PCOS, and the role of hyperandrogenism in promoting ovarian dysfunction cannot be overlooked. Our study illuminates the transcript characteristics of PCOS granulosa cell and declares the interaction between ovarian steroidogenesis and lipid metabolism and fatty acid biosynthetic process in granulosa cells, which is proved to be harmful for follicle growth and ovulation *in vitro*. Furthermore, AR signalling may be the key mediator of androgen action in hyperandrogenic environment. Overall, these results provide new insights into the mechanism of ovarian dysfunction in PCOS.

DATA AVAILABILITY STATEMENT

The data presented in the study are deposited in the GEO database, accession number GSE193123.

ETHICS STATEMENT

The studies involving human participants were reviewed and approved by the Peking University Third Hospital Medical Science Research Ethics Committee. The patients/participants provided their written informed consent to participate in this study. The animal study was reviewed and approved by the Animal Care and Use Committee of Peking University.

AUTHOR CONTRIBUTIONS

BL, XQ, and CY performed experiments and analyzed data. BL and XQ prepared the figures and drafted the manuscript. JQ and YP conceived and designed the research and approved the final version of manuscript. All authors contributed to the article and approved the submitted version.

FUNDING

This work was supported by the National Key Research and Development Program of China (2018YFC1003200, 2018YFC1003900), the National Natural Science Foundation of China (82022028, 81730038, 82001506), the Key Clinical Projects of Peking University Third Hospital (BYSYZD2019020), and the CAMS Innovation Fund for Medical Sciences (2019-I2M-5-001).

REFERENCES

1. Norman RJ, Dewailly D, Legro RS, Hickey TE. Polycystic Ovary Syndrome. *Lancet* (2007) 370(9588):685–97. doi: 10.1016/S0140-6736(07)61345-2
2. Escobar-Morreale HF. Polycystic Ovary Syndrome: Definition, Aetiology, Diagnosis and Treatment. *Nat Rev Endocrinol* (2018) 14(5):270–84. doi: 10.1038/nrendo.2018.24
3. El-Hayek S, Yang Q, Abbassi L, FitzHarris G, Clarke HJ. Mammalian Oocytes Locally Remodel Follicular Architecture to Provide the Foundation for Germline-Soma Communication. *Curr Biol* (2018) 28(7):1124–31.e3. doi: 10.1016/j.cub.2018.02.039
4. Li R, Albertini DF. The Road to Maturation: Somatic Cell Interaction and Self-Organization of the Mammalian Oocyte. *Nat Rev Mol Cell Biol* (2013) 14 (3):141–52. doi: 10.1038/nrm3531
5. Li L, Zhu S, Shu W, Guo Y, Guan Y, Zeng J, et al. Characterization of Metabolic Patterns in Mouse Oocytes During Meiotic Maturation. *Mol Cell* (2020) 80(3):525–40.e9. doi: 10.1016/j.molcel.2020.09.022
6. Ding L, Gao F, Zhang M, Yan W, Tang R, Zhang C, et al. Higher PDCD4 Expression Is Associated With Obesity, Insulin Resistance, Lipid Metabolism Disorders, and Granulosa Cell Apoptosis in Polycystic Ovary Syndrome. *Fertil Steril* (2016) 105(5):1330–7.e3. doi: 10.1016/j.fertnstert.2016.01.020
7. Azhary JMK, Harada M, Kunitomi C, Kusamoto A, Takahashi N, Nose E, et al. Androgens Increase Accumulation of Advanced Glycation End Products in Granulosa Cells by Activating ER Stress in PCOS. *Endocrinology* (2020) 161(2):bqaa015. doi: 10.1210/endocr/bqaa015
8. Jin J, Ma Y, Tong X, Yang W, Dai Y, Pan Y, et al. Metformin Inhibits Testosterone-Induced Endoplasmic Reticulum Stress in Ovarian Granulosa Cells *via* Inactivation of P38 MAPK. *Hum Reprod* (2020) 35(5):1145–58. doi: 10.1093/humrep/deaa077
9. Kumariya S, Ubba V, Jha RK, Gayen JR. Autophagy in Ovary and Polycystic Ovary Syndrome: Role, Dispute and Future Perspective. *Autophagy* (2021) 17 (10):2706–33. doi: 10.1080/15548627.2021.1938914
10. Li X, Qi J, Zhu Q, He Y, Wang Y, Lu Y, et al. The Role of Androgen in Autophagy of Granulosa Cells From PCOS. *Gynecol Endocrinol* (2019) 35 (8):669–72. doi: 10.1080/09513590.2018.1540567

11. Rizzo M, Berneis K, Hersberger M, Pepe I, Di Fede G, Rini GB, et al. Milder Forms of Atherogenic Dyslipidemia in Ovulatory Versus Anovulatory Polycystic Ovary Syndrome Phenotype. *Hum Reprod* (2009) 24(9):2286–92. doi: 10.1093/humrep/dep121
12. Rice S, Christoforidis N, Gadd C, Nikolaou D, Seyani L, Donaldson A, et al. Impaired Insulin-Dependent Glucose Metabolism in Granulosa-Lutein Cells From Anovulatory Women With Polycystic Ovaries. *Hum Reprod* (2005) 20 (2):373–81. doi: 10.1093/humrep/deh609
13. Schube U, Nowicki M, Jogschies P, Blumenauer V, Bechmann I, Serke H. Resveratrol and Desferoxamine Protect Human OxLDL-Treated Granulosa Cell Subtypes From Degeneration. *J Clin Endocrinol Metab* (2014) 99(1):229–39. doi: 10.1210/jc.2013-2692
14. Niu Z, Lin N, Gu R, Sun Y, Feng Y. Associations Between Insulin Resistance, Free Fatty Acids, and Oocyte Quality in Polycystic Ovary Syndrome During *In Vitro* Fertilization. *J Clin Endocrinol Metab* (2014) 99(11):E2269–76. doi: 10.1210/jc.2013-3942
15. Sanchez-Garrido MA, Tena-Sempere M. Metabolic Dysfunction in Polycystic Ovary Syndrome: Pathogenic Role of Androgen Excess and Potential Therapeutic Strategies. *Mol Metab* (2020) 35:100937. doi: 10.1016/j.molmet.2020.01.001
16. McNeilly AS. The Ovarian Follicle and Fertility. *J Steroid Biochem Mol Biol* (1991) 40(1-3):29–33. doi: 10.1016/0960-0760(91)90164-Z
17. Gilchrist RB, Lane M, Thompson JG. Oocyte-Secreted Factors: Regulators of Cumulus Cell Function and Oocyte Quality. *Hum Reprod Update* (2008) 14 (2):159–77. doi: 10.1093/humupd/dmm040
18. Xu M, West-Farrell ER, Stouffer RL, Shea LD, Woodruff TK, Zelinski MB. Encapsulated Three-Dimensional Culture Supports Development of Nonhuman Primate Secondary Follicles. *Biol Reprod* (2009) 81(3):587–94. doi: 10.1095/biolreprod.108.074732
19. Wang TR, Yan LY, Yan J, Lu CL, Xia X, Yin TL, et al. Basic Fibroblast Growth Factor Promotes the Development of Human Ovarian Early Follicles During Growth In Vitro. *Hum Reprod* (2014) 29(3):568–76. doi: 10.1093/humrep/det465
20. Lee J, Kim EJ, Kong HS, Youm HW, Kim SK, Lee JR, et al. Comparison of the Oocyte Quality Derived From Two-Dimensional Follicle Culture Methods and Developmental Competence of *In Vitro* Grown and Matured Oocytes. *BioMed Res Int* (2018) 2018:7907092. doi: 10.1155/2018/7907092
21. Jin SY, Lei L, Shikanov A, Shea LD, Woodruff TK. A Novel Two-Step Strategy for *In Vitro* Culture of Early-Stage Ovarian Follicles in the Mouse. *Fertil Steril* (2010) 93(8):2633–9. doi: 10.1016/j.fertnstert.2009.10.027
22. Xiao S, Zhang J, Romero MM, Smith KN, Shea LD, Woodruff TK. *In Vitro* Follicle Growth Supports Human Oocyte Meiotic Maturation. *Sci Rep* (2015) 5:17323. doi: 10.1038/srep17323
23. Xiao S, Coppeta JR, Rogers HB, Isenberg BC, Zhu J, Olalekan SA, et al. A Microfluidic Culture Model of the Human Reproductive Tract and 28-Day Menstrual Cycle. *Nat Commun* (2017) 8:14584. doi: 10.1038/ncomms14584
24. Skory RM, Xu Y, Shea LD, Woodruff TK. Engineering the Ovarian Cycle Using *In Vitro* Follicle Culture. *Hum Reprod* (2015) 30(6):1386–95. doi: 10.1093/humrep/dev052
25. Xu M, Kreeger PK, Shea LD, Woodruff TK. Tissue-Engineered Follicles Produce Live, Fertile Offspring. *Tissue Eng* (2006) 12(10):2739–46. doi: 10.1089/ten.2006.12.2739
26. Qi X, Yun C, Sun L, Xia J, Wu Q, Wang Y, et al. Gut Microbiota-Bile Acid-Interleukin-22 Axis Orchestrates Polycystic Ovary Syndrome. *Nat Med* (2019) 25(8):1225–33. doi: 10.1038/s41591-019-0509-0
27. Xu M, West E, Shea LD, Woodruff TK. Identification of a Stage-Specific Permissive *In Vitro* Culture Environment for Follicle Growth and Oocyte Development. *Biol Reprod* (2006) 75(6):916–23. doi: 10.1095/biolreprod.106.054833
28. Li Y, Li RQ, Ou SB, Zhang NF, Ren L, Wei LN, et al. Increased GDF9 and BMP15 mRNA Levels in Cumulus Granulosa Cells Correlate With Oocyte Maturation, Fertilization, and Embryo Quality in Humans. *Reprod Biol Endocrinol* (2014) 12:81. doi: 10.1186/1477-7827-12-81
29. Park JY, Su YQ, Ariga M, Law E, Jin SL, Conti M. Like Growth Factors as Mediators of LH Action in the Ovulatory Follicle. *Science* (2004) 303 (5658):682–4. doi: 10.1126/science.1092463
30. Ryan GE, Malik S, Mellon PL. Antiandrogen Treatment Ameliorates Reproductive and Metabolic Phenotypes in the Letrozole-Induced Mouse Model of PCOS. *Endocrinology* (2018) 159(4):1734–47. doi: 10.1210/en.2017-03218
31. Aflatounian A, Edwards MC, Rodriguez Paris V, Bertoldo MJ, Desai R, Gilchrist RB, et al. Androgen Signaling Pathways Driving Reproductive and Metabolic Phenotypes in a PCOS Mouse Model. *J Endocrinol* (2020) 245 (3):381–95. doi: 10.1530/JOE-19-0530
32. Ibanez L, de Zegher F. Low-Dose Combination of Flutamide, Metformin and an Oral Contraceptive for Non-Obese, Young Women With Polycystic Ovary Syndrome. *Hum Reprod* (2003) 18(1):57–60. doi: 10.1093/humrep/deg056
33. Zhang Y, Wang Y, Feng X, Zhang S, Xu X, Li L, et al. Oocyte-Derived Microvilli Control Female Fertility by Optimizing Ovarian Follicle Selection in Mice. *Nat Commun* (2021) 12(1):2523. doi: 10.1038/s41467-021-22829-2
34. Abruzzese GA, Heber MF, Ferreira SR, Ferrer MJ, Motta AB. Prenatal Androgen Exposure Affects Ovarian Lipid Metabolism and Steroid Biosynthesis in Rats. *J Endocrinol* (2020) 247(3):239–50. doi: 10.1530/JOE-20-0304
35. Xu N, Taylor KD, Azziz R, Goodarzi MO. Variants in the HMG-CoA Reductase (HMGCR) Gene Influence Component Phenotypes in Polycystic Ovary Syndrome. *Fertil Steril* (2010) 94(1):255–60.e1-2. doi: 10.1016/j.fertnstert.2009.01.158
36. Tian Y, Zhang W, Zhao S, Sun Y, Bian Y, Chen T, et al. FADS1-FADS2 Gene Cluster Confers Risk to Polycystic Ovary Syndrome. *Sci Rep* (2016) 6:21195. doi: 10.1038/srep21195
37. Mondal K, Chakraborty P, Kabir SN. Hyperhomocysteinemia and Hyperandrogenemia Share PCSK9-LDLR Pathway to Disrupt Lipid Homeostasis in PCOS. *Biochem Biophys Res Commun* (2018) 503(1):8–13. doi: 10.1016/j.bbrc.2018.04.078
38. Wang M, Zhao D, Xu L, Guo W, Nie L, Lei Y, et al. Role of PCSK9 in Lipid Metabolic Disorders and Ovarian Dysfunction in Polycystic Ovary Syndrome. *Metabolism* (2019) 94:47–58. doi: 10.1016/j.metabol.2019.02.002
39. Raviv S, Hantisteanu S, Sharon SM, Atzmon Y, Michaeli M, Shalom-Paz E. Lipid Droplets in Granulosa Cells Are Correlated With Reduced Pregnancy Rates. *J Ovarian Res* (2020) 13(1):4. doi: 10.1186/s13048-019-0606-1
40. Sun M, Sun B, Qiao S, Feng X, Li Y, Zhang S, et al. Elevated Maternal Androgen Is Associated With Dysfunctional Placenta and Lipid Disorder in Newborns of Mothers With Polycystic Ovary Syndrome. *Fertil Steril* (2020) 113(6):1275–85.e2. doi: 10.1016/j.fertnstert.2020.02.005
41. Pan JX, Tan YJ, Wang FF, Hou NN, Xiang YQ, Zhang JY, et al. Aberrant Expression and DNA Methylation of Lipid Metabolism Genes in PCOS: A New Insight Into Its Pathogenesis. *Clin Epigenet* (2018) 10:6. doi: 10.1186/s13148-018-0442-y
42. Dumesic DA, Meldrum DR, Katz-Jaffe MG, Krisher RL, Schoolcraft WB. Oocyte Environment: Follicular Fluid and Cumulus Cells Are Critical for Oocyte Health. *Fertil Steril* (2015) 103(2):303–16. doi: 10.1016/j.fertnstert.2014.11.015
43. Kim JY, Kinoshita M, Ohnishi M, Fukui Y. Lipid and Fatty Acid Analysis of Fresh and Frozen-Thawed Immature and *In Vitro* Matured Bovine Oocytes. *Reproduction* (2001) 122(1):131–8. doi: 10.1530/rep.0.1220131
44. Walters KA, Rodriguez Paris V, Aflatounian A, Handelsman DJ. Androgens and Ovarian Function: Translation From Basic Discovery Research to Clinical Impact. *J Endocrinol* (2019) 242(2):R23–50. doi: 10.1530/JOE-19-0096
45. Lin HY, Yu IC, Wang RS, Chen YT, Liu NC, Altuwaijri S, et al. Increased Hepatic Steatosis and Insulin Resistance in Mice Lacking Hepatic Androgen Receptor. *Hepatology* (2008) 47(6):1924–35. doi: 10.1002/hep.22252
46. Laird M, Thomson K, Fenwick M, Mora J, Franks S, Hardy K. Androgen Stimulates Growth of Mouse Preantral Follicles *In Vitro*: Interaction With Follicle-Stimulating Hormone and With Growth Factors of the TGFbeta Superfamily. *Endocrinology* (2017) 158(4):920–35. doi: 10.1210/en.2016-1538
47. Walters KA, Middleton LJ, Joseph SR, Hazra R, Jimenez M, Simanainen U, et al. Targeted Loss of Androgen Receptor Signaling in Murine Granulosa Cells of Preantral and Antral Follicles Causes Female Subfertility. *Biol Reprod* (2012) 87(6):151. doi: 10.1095/biolreprod.112.102012
48. Diamanti-Kandarakis E, Tolis G, Duleba AJ. Androgens and Therapeutic Aspects of Antiandrogens in Women. *J Soc Gynecol Investig* (1995) 2(4):577–92. doi: 10.1177/107155769500200401

49. Azziz R, Carmina E, Chen Z, Dunaif A, Laven JS, Legro RS, et al. Polycystic Ovary Syndrome. *Nat Rev Dis Primers* (2016) 2:16057. doi: 10.1038/nrdp.2016.57

Conflict of Interest: The authors declare that the research was conducted in the absence of any commercial or financial relationships that could be construed as a potential conflict of interest.

Publisher's Note: All claims expressed in this article are solely those of the authors and do not necessarily represent those of their affiliated organizations, or those of the publisher, the editors and the reviewers. Any product that may be evaluated in this article, or claim that may be made by its manufacturer, is not guaranteed or endorsed by the publisher.

frontiers in Endocrinology

REVIEW
published: 24 February 2022
doi: 10.3389/fendo.2022.815999

Progress in the Study of Colorectal Cancer Caused by Altered Gut Microbiota After Cholecystectomy

Yanpeng Ma[1,2†], *Ruize Qu*[1,2†], *Yi Zhang*[1,2†], *Changtao Jiang*[3,4,5,6], *Zhipeng Zhang*[1,2*] *and Wei Fu*[1,2*]

[1] Department of General Surgery, Peking University Third Hospital, Beijing, China, [2] Cancer Center, Peking University Third Hospital, Beijing, China, [3] Department of Physiology and Pathophysiology, School of Basic Medical Sciences, Peking University, Beijing, China, [4] Key Laboratory of Molecular Cardiovascular Science (Peking University), Ministry of Education, Beijing, China, [5] Center of Basic Medical Research, Institute of Medical Innovation and Research, Third Hospital, Peking University, Beijing, China, [6] Center for Obesity and Metabolic Disease Research, School of Basic Medical Sciences, Peking University, Beijing, China

OPEN ACCESS

Edited by:
Ihtisham Bukhari,
Fifth Affiliated Hospital of Zhengzhou University, China

Reviewed by:
Nils Lambrecht,
VA Long Beach Healthcare System, United States
Marco Vacante,
University of Catania, Italy
Mingmei Zhou,
Shanghai University of Traditional Chinese Medicine, China

***Correspondence:**
Zhipeng Zhang
zhangzhipeng06@126.com
Wei Fu
fuwei@bjmu.edu.cn

[†]*These authors have contributed equally to this work*

Specialty section:
This article was submitted to Gut Endocrinology, a section of the journal Frontiers in Endocrinology

Received: *16 November 2021*
Accepted: *01 February 2022*
Published: *24 February 2022*

Citation:
Ma Y, Qu R, Zhang Y, Jiang C, Zhang Z and Fu W (2022) Progress in the Study of Colorectal Cancer Caused by Altered Gut Microbiota After Cholecystectomy. Front. Endocrinol. 13:815999. doi: 10.3389/fendo.2022.815999

Epidemiological studies have found an increased incidence of colorectal cancer (CRC) in people who undergo cholecystectomy compared to healthy individuals. After cholecystectomy, bile enters the duodenum directly, unregulated by the timing of meals. Disruption of the balance of bile acid metabolism and increased production of primary bile acids, which in turn affects the composition and abundance of intestinal microorganisms. The link among cholecystectomy, the gut microbiota, and the occurrence and development of CRC is becoming clearer. However, due to the complexity of the microbial community, the mechanistic connections are less well understood. In this review, we summarize the changes of gut microbiota after cholecystectomy and illuminate the potential mechanisms on CRC, such as inflammation and immune regulation, production of genotoxins, metabolism of dietary ingredients, activation of signaling pathways, and so on. By reviewing these, we aimed to unravel the interactions between the gut microbiota and its host and be better positioned to develop treatments for CRC after cholecystectomy.

Keywords: colorectal cancer, gut microbiota, bile acid, genotoxin, diet, epidemiology, cholecystectomy

INTRODUCTION

As one of the most common malignant tumors worldwide, colorectal cancer (CRC) ranks second and third in morbidity and mortality rates, respectively, and its incidence is gradually increasing in developing countries (1). It has been estimated that by 2030, the global disease burden of CRC will increase by 60%, and there will be more than 2.2 million new cases and 1.1 million deaths worldwide (2). Moreover, the morbidity and mortality rates of CRC are increasing yearly, particularly, in individuals under the age of 50 (3). Furthermore, there is continuous growth in the overall number of diagnosed cases, which contributes to the increasing disease burden of CRC (2). Therefore, research on the risk factors and pathogenesis of CRC is becoming increasingly essential.

Abbreviations: CRC, colorectal cancer; ETBF, enterotoxigenic *Bacteroides fragilis*; IBD, inflammatory bowel disease; NF-κB, nuclear factor kappa B; SCFAs, short-chain fatty acids.

CRC is associated with multiple factors, including genetic susceptibility and environmental factors, which play a greater role in its occurrence and development (4). The gut microbiota is among the various environmental factors recognized in cancer biology. There are more than 3×10^{13} bacterial cells in the human colorectum, which interact with host cells to regulate many physiological processes. Disruption of the gut microbiota affects the balance of physiological processes, contributing to the development and progression of many diseases, such as inflammatory bowel disease (IBD) and CRC (5–8).

Changes in lifestyle and eating habits are directly linked to an increase in gallbladder diseases (9). Although cholecystectomy is an acceptable standard treatment for gallbladder diseases (2016), there is evidence that it is likely to increase the incidence of CRC (10–13). However, little is known about the mechanisms responsible for this process. There are two major theories on the effects of cholecystectomy on CRC development (1): cholecystectomy may alter the concentration, composition, and excretion rhythm of bile acids, leading to an increase in the content of secondary bile acids, which can continuously stimulate intestinal cells. For example, deoxycholic acid and lithocholic acid directly induce DNA damage and activate signaling pathways, including epidermal growth factor receptor-, Wnt-β-catenin-, and protein kinase C pathways, thereby promoting the occurrence and development of CRC (14) (2). Cholecystectomy causes changes in the composition and abundance of the gut microbiota in both stool and tumor tissues. The main manifestations are a decline in the diversity of the microbiota, particularly, a decrease in beneficial bacteria and an increase in pathogenic bacteria (15–19), including carcinogenic bacteria, such as *Fusobacterium nucleatum*, enterotoxigenic *Bacteroides fragilis* (ETBF), *Clostridium difficile*, and *Escherichia coli*, which promote CRC development (20–23). A recent study showed that the gut microbiota of patients who underwent cholecystectomy was significantly different from that of healthy people, but similar to that of patients with CRC, which suggests that changes in the gut microbiota in patients undergoing cholecystectomy may activate CRC occurrence and progression (24).

In this article, we described the current knowledge on changes in the gut microbiota after cholecystectomy, the interaction between cholecystectomy and CRC, and potential mechanisms, aiming to clarify the role of gut microbiota alteration on the occurrence and development of CRC after a cholecystectomy.

EPIDEMIOLOGICAL RELATIONSHIP BETWEEN CHOLECYSTECTOMY AND CRC

In 1978, Capron was the first to report that cholecystectomy could increase the incidence of CRC (25). Subsequently, scholars worldwide conducted a series of studies on the relationship between cholecystectomy and the incidence of CRC, and two studies published in 1981 involving patients in Finland and the United States provided evidence of a significant link between cholecystectomy and CRC (10, 11).

A retrospective study in 2005 analyzed more than 8 million people on a general medicine research database in the United Kingdom and found that cholecystectomy was associated with increased risk of colon cancer, but not rectal cancer (12). Some meta-analyses have also indicated a correlation between cholecystectomy and the increasing risk of CRC. Among these, one analysis included ten cohort studies which indicated a strong correlation between the proximal colon with a history of cholecystectomy and carcinogenesis (13, 26, 27). These results indicate that a history of cholecystectomy is closely associated with the occurrence and progression of CRC.

EFFECT OF CHOLECYSTECTOMY ON GUT MICROBIOTA

Trillions of microorganisms, such as bacteria, viruses, fungi, and other life forms, live inside every person. Various organs show distinct microbial inhabitants, but the inhabitants that have drawn the most attention are those in the colorectum (28). The gut microbiota is a key player in physiological activities, including metabolism of food residues, synthesis of micronutrients (such as vitamins), metabolism of primary bile acids, synthesis of secondary bile acids, regulation of immune responses, and metabolism and production of butyric acid and other substances which provide substances for epithelial cell renewal and mucosal integrity maintenance (29). Of note, the gut microbiota is related to the development of a wide range of digestive diseases, such as IBD, irritable bowel syndrome, and CRC (30–32).

Cholecystectomy induces dramatic changes in intestinal microecology, including the composition and function of the gut microbiota. The changes in the gut microbiota after cholecystectomy are shown in **Table 1** (24, 33–37). At the phylum level, the abundance of Fusobacteria increased, whereas that of Proteobacteria decreased. Other phyla, including Bacteroidetes, Firmicutes, and Actinobacteria, showed distinct variations in different studies. Interestingly, the changes in bacterial abundance of Firmicutes and Actinobacteria were similar in all studies, in contrast to the alteration in the bacterial abundance of Bacteroidetes. Different *Bacteroides* species affect the health of the host in different ways (38–40). For example, ETBF can induce colitis and promote the occurrence of intestinal tumors, while other species, such as *Bacteroides vulgatus* and *Bacteroides fragilis*, are associated with the protection of the intestinal barrier. At the genus level, existing research has not reached a consensus. Genera reported with increasing abundance mainly include *Anaerostipes*, *Dorea*, *Clostridium*, *Mogibacterium*, *Flavonifractor*, *Shigella*, and *Escherichia*, whilst those with reduced abundance include *Paraprevotella*, *Prevotella*, *Barnesiella*, *Alistipes*, *Faecalibacterium*, *Haemophilus*, and *Desulfovibrio*. Few studies have focused on the species level; *Blautia obeum*, *Veillonella parvula*, *Bacteroides ovatus*, *Parabacteroides distasonis*, and

TABLE 1 | Comparison of gut microbiota between patients who have undergone cholecystectomy and healthy individuals.

	Country (Author & Year)	Sample size	Sequencing method	Changes of gut microbiota after cholecystectomy
1	Israel (Keren et al., 2015) (33)	20	16S rRNA	The diversity of microbiome is basically stable. **Phylum** *Bacteroides*↑ **Family** *Bacteroides*, *Parabacteraceae*↑
2	China (Wang et al., 2018) (34)	135	16S rRNA	The diversity of microbiome declined. **Phylum** *Actinomycetes*, *Firmicutes*↑ *Bacteroides*, *Proteobacteria*↓ **Genus** *Bifidobacterium*, *Dallella*, *Anaerobic*↑ *Palapuella*, *Prevotella*, *Barnesella*, *Alternaria*, *Desulfovibrio*↓
3	Korea (Yoon et al., 2019) (35)	108	16S rRNA	The diversity of microbiome declined. **Phylum** *Firmicutes*↑ *Bacteroides*↓ **Species** *Broutella ovale*, *Veillonella parvula*↑
4	China (Ren et al., 2020) (24)	104	16S rRNA	The diversity of microbiome increased. **Phylum** *Bacteroides*, *Fusobacteria*↑ *Firmicutes*, *Actinomycetes*↓ **Genus** *Prevotella*↑ *Faecalibacterium*↓ **Species** *Bacteroides ovatus*, *Parabacteroides diundi*, *Fusobacterium proteus*↑ *Eubacterium rectale, Roseburia faecis*, *Bifidobacterium adolescentis*↓
5	Germany (Frost et al., 2021) (36)	1968	16S rRNA	The diversity of microbiome declined. **Genus** *Clostridium XlVa, Flavonoids, Clostridium difficile, Escherichia, Shigella*↑ *Faecalibacterium*, *Haemophilus*↓

Fusobacterium varium were found to increase, and *Eubacterium rectale*, *Roseburia faecis*, and *Bifidobacterium adolescentis* were reported to decrease.

It was widely reported that *Escherichia* and ETBF had increased in abundance of CRC patients, promoting CRC development through damaged DNA, and produced toxins. While beneficial bacteria, including *Alistipes* and *Faecalibacterium*, which can produce active metabolites, such as butyrate and folic acid and inhibit the occurrence and development of CRC, were significantly reduced in patients with cholecystectomy history (24, 33–37). Due to differences in race, diet, and experimental conditions, changes in the gut microbiota after cholecystectomy are inconsistent. However, all the relevant studies confirm that alterations in the gut microbiota promote CRC occurrence and progression.

Transformation of the gut microbiota after cholecystectomy can be attributed to the following reasons (**Figure 1**): first, bile excretion regulation weakens or disappears after cholecystectomy; as a result, the bile flows into the intestine continuously (41). This changed pattern is conducive to the growth of bacteria that metabolize bile acid or live through bile-dependent fat decomposition but has adverse effects on the growth of other bacteria, thereby reshaping the gut microbiota. For example, experiments have shown that deoxycholic acid inhibits the growth of *Lactobacillus*, *Bifidobacterium*, and other bile-sensitive bacteria (42). Second, cholecystectomy alters bowel movements by changing the biophysical properties, fluid content, and pH of the colorectum, thereby providing favorable or harmful growth conditions for certain bacteria. For example, persistent secretion of bile, which is alkaline, after cholecystectomy, increases the pH value in the intestines, thereby inhibiting the proliferation of acidic-adapted bacteria, including *Lactobacillus* and *Bifidobacterium*. Third, changes in immune homeostasis in the intestines after cholecystectomy should be considered. For example, surfactant protein D, an important substance secreted by the gallbladder, can be transported to the intestinal lumen with the entered bile and inhibits the growth of symbiotic bacteria through direct binding. Cholecystectomy unavoidably decreases the level of surfactant protein D in the human intestines, which leads to disorders of bacterial and host-bacterial interactions and affects the natural environment of the gut microbiota (43).

ROLE OF GUT MICROBIOTA IN CRC

CRC development and progression is a multi-factor interaction, in which the role of the gut microbiota is now attracting increasing attention. A study that analyzed the Health Care Claims Database from the United States confirmed the relationship between the recurrence of CRC and disorders of the gut microbiota (44). Widespread use of antibiotics, alterations in diet, obesity, stress, and other risk factors are attributed to disorders of the gut microbiota in young people, which may partly explain their increased risk of CRC (45). A gradual increase in some bacteria and a constant decrease in some bacteria in normal, para-adenoma, adenoma, pericarcinomatous, and cancerous tissues have been found, suggesting that bacterial distribution may act as an essential factor in CRC development (46). Yu et al. conducted metagenomic sequencing of the stool samples of patients with CRC and healthy individuals and found significant differences in

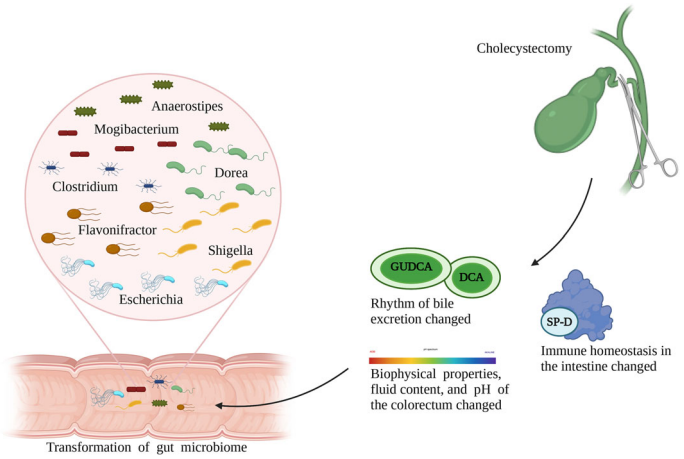

FIGURE 1 | Role of cholecystectomy in the alternation of gut microbiota.

the composition of the gut microbiota between the two groups (47). Fecal bacterial transplantation studies were conducted, and the incidence of CRC in mice inoculated with stool samples from patients with CRC increased. The gut microbiota in the stool of patients with CRC can activate the intestinal mucosal immunity of mice and induce inflammation, so as to promote the proliferation of epithelial cells and induce the development of CRC (48). A number of clinical and animal studies have clarified the relationship between the gut microbiota and CRC and identified specific bacteria as key factors that affect the occurrence and development of CRC (19, 46, 47, 49–58), as summarized in **Table 2**, including relevant studies in the past decade, reflecting the differences in the gut microbiota between patients with CRC and healthy individuals. The diversity of the gut microbiota in patients with CRC was lower than in healthy individuals, with a decrease in beneficial bacteria and an increase in pathogenic bacteria. For example, *Fusobacterium nucleatum*, *Campylobacter*, ETBF, and *Escherichia coli* that express the polyketide synthase gene (*pks*$^{+}$ *Escherichia coli*) were enriched in the intestines of patients with CRC, induced inflammation, damaged DNA, and produced toxins, thereby promoting CRC development. Beneficial bacteria, including *Bifidobacterium*, *Lachnospira*, *Alistipes*, and *Faecalibacterium*, which can produce active metabolites, such as butyrate and folic acid and inhibit the occurrence and development of CRC, were significantly reduced.

Patients who underwent cholecystectomy and those with CRC had similar gut microbial changes, an increased abundance of pathogenic bacteria, including *Escherichia*, *Clostridium*, and *Dorea*, and a decrease in beneficial bacteria, including *Prevotella*, *Alistipes*, and *Faecalibacterium* (24, 33–37). The gut microbiota can regulate the biological behavior of the host through direct cell interactions and in a metabolite-dependent manner. In addition, intestinal inflammation caused by the gut microbiota, secretion of flora-derived factors, such as genotoxins to induce DNA damage, production of metabolites, and direct activation of carcinogenic signaling pathways are major factors in CRC development. Next, we proposed to focus on the role of the gut microbiota in the process of CRC and the carcinogenic mechanism of gut microbiota alterations after cholecystectomy (**Figure 2**).

Inflammation and Immune Regulation

Inflammation is an established risk factor of CRC carcinogenesis. Patients with IBD are more susceptible to CRC than the general population (59, 60). Inflammation plays a key role in the development of colitis-associated cancer, even in CRC unrelated to IBD, and the levels of pro-inflammatory cytokines are increased (61). The gut microbiota has the potential to form an inflammatory microenvironment and, vice versa, inflammation may affect gut microbiota composition. Colon polyposis in Apc$^{min/+}$ mice is accompanied by the accumulation of microorganisms in the polyps, triggering a local inflammatory response (Dennis etal. (62). Besides, defective expression of alarmin/IL-33 renders mice highly susceptible to probiotic microbiota-promoted IL-1α-dependent colitis and colitis-associated cancer (63). Gavage with stool samples from patients with CRC caused enhanced inflammation and intestinal adenoma development in a sterile mouse model (48), indicating that specific components of the gut microbiota promote the occurrence and development of CRC through the activation of inflammation. For example, enriched *Fusobacterium nucleatum* and *Escherichia coli* in the intestines of patients with CRC can activate the nuclear factor kappa B (NF-κB) signaling pathway and drive the infiltration of myeloid cells in the tumor, producing a pro-inflammatory environment that is conducive to the progression of colorectal tumors in Apc$^{min/+}$ mice (64, 65). ETBF can trigger an inflammatory cascade involving interleukin 17, signal transducer and activator of transcription 3, and NF-κB conduction in colonic epithelial cells *via* the production of a metalloproteinase toxin, promoting the local inflammatory environment in the

TABLE 2 | Comparison of gut microbiota between patients with colorectal cancer and healthy individuals.

	Country (Author & Year)	Sample size	Sample type	Sequencing method	Changes of gut microbiota after cholecystectomy
1	China (Wang et al., 2012) (19)	102	Stool	16S rRNA	The diversity of microbiome is basically stable. **Phylum** *Firmicutes*, *Proteobacteria*, *Actinomycetes*↑ *Bacteroides*, *Fusobacteria*↓ **Genus** *Porphyromonas*, *Escherichia*, *Shigella*, *Enterococcus*, *Streptococcus*, *Peptostreptococcus*↑ *Bacteroides*, *Rossella*, *Alternaria*, *Eubacteria*, *Trichospirillum*↓
2	China (Wu et al., 2013) (50)	39	Stool	16S rRNA	The diversity of microbiome is basically stable. **Phylum** *Fusobacterium*↑ **Family** *Eubacteriaceae*, *Clostridiaceae*, *Staphylococcus*, *Enterococcus*, *Fusobacteria*, *Campylobacter*, *Porphyridaceae*↑ **Genus** *Bacteroides*, *Alternaria*, *Blautella*, *Dallella*, *Fusobacterium*, *Campylobacter*, *Escherichia*, *Shigella*, *Odorbacterium*, *Oscillatoria*, *Testa Lactobacillus*, *Rumenococcus*↑ *Rossella, Faecalibacterium*↓
3	America (Ahn et al., 2013) (49)	151	Stool	16S rRNA	The diversity of microbiome declined. **Phylum** *Bacteroides*↑ *Firmicutes*↓ **Genus** *Porphyromonas*, *Fusobacterium*, *Mirabilis*↑ *Faecococcus*, *Trichospirillum*↓
4	America (Zackular et al., 2014) (51)	60	Stool	16S rRNA	**Family** *Porphyridaceae*, *Enterobacteriaceae*↑ *Lacetospiraceae*↓ **Genus** *Porphyromonas*, *Fusobacterium*↑ *Bacteroides*↓
5	France (Zeller et al., 2014) (52)	114	Stool	Metagenomic sequencing	The diversity of microbiome is basically stable. **Phylum** *Bacteroides*, *Fusobacteria*, *Proteobacteria*↑ *Actinomycetes*, *Firmicutes*↓ **Species** *Saccharolytic Porphyromonas*, *Oral Peptostreptococcus*, *Fusobacterium nucleatum*↑
6	Australia (Feng et al., 2015) (53)	109	Stool	Metagenomic sequencing	The diversity of microbiome declined. **Genus** *Bacteroides*, *Alternaria*, *Bileophilus*, *Trichospira*, *Escherichia*, *Micromonas*, *Fusobacterium*↑ *Bifidobacterium*, *Streptococcus*, *Rumenococcus*↓
7	China (Nakatsu et al., 2015) (46)	113	Tissue	16S rRNA	**Genus** *Fusobacterium*, *Gemini*, *Peptostreptococcus*, *Micromonas*, *Streptococcus granulosus*↑ **Species** *Bacteroides fragilis*↑
8	America (Baxter et al., 2016) (54)	292	Stool	16S rRNA	**Genus** *Porphyria*, *Peptostreptococcus*, *Fusobacterium*, *Micromonas*, *Prevotella*, *Gemini*↑ **Species** *Saccharolytic Porphyromonas*, *Fusobacterium nucleatum*, *Micromonas parvum*, *Oral Peptostreptococcus*↑
9	Ireland (Flemer et al., 2017) (55)	115	Stool/ Tissue	16S rRNA	**Genus** *Bacteroides*, *Rossella*, *Rumenococcus*, *Oscillatoria*, *Porphyromonas*, *Peptostreptococcus*, *Micromonas*, *Fusobacterium*↑
10	China (Yu et al., 2017) (47)	128	Stool	Metagenomic sequencing	The diversity of microbiome declined. **Phylum** *Fusobacteria*, *Basidiomycota*↑ **Species** *Micromonas parvum*, *Oral Peptostreptococcus*, *Fusobacterium nucleatum*, *Bacteroides fragilis*, *Solobacterium moorei*↑
11	Saudi Arabia (Alomair et al., 2018) (56)	58	Tissue	Metagenomic sequencing	The diversity of microbiome is basically stable. **Genus** *Peptostreptococcus, Porphyromonas, Listeria, Atopobium, Burkholderia*, *Collins*, *Comamonas*, *Fusobacterium*↑
12	Japan (Yachida et al., 2019) (58)	616	Stool	Metagenomic sequencing	The diversity of microbiome increased. **Phylum** *Firmicutes*, *Fusobacteria*, *Bacteroides*↑ **Genus** *Bacteroides*, *Peptostreptococcus*↑ *Prevotella*, *Bifidobacterium*↓ **Species** *Fusobacterium nucleatum*, *Micromonas parvum*, *Streptococcus oralis*, *Solobacterium moorei*↑ *Phascolarctobacterium succinatutens*, *Desulfovibrio longreachensis*, *Atopobium parvulum*↓
13	Italy (Thomas et al., 2019) (57)	826	Stool	Metagenomic sequencing	The diversity of microbiome increased. **Genus** *Peptostreptococcus*, *Clostridium*, *Porphyromonas*, *Escherichia coli*↑ *Bifidobacterium*, *Trichospirillum*, *Alternative Mycobacterium*↓ **Species** *Fusobacterium nucleatum*, *Porphyromonas saccharolyticus*, *Micromonas parvum*, *Oral Peptostreptococcus*, *Escherichia coli*↑

intestines and inducing carcinogenesis (66). Cholecystectomy increases the abundance of *Escherichia coli* and decreases the abundance of *Faecalibacterium*, which can secrete small-molecule anti-inflammatory substances to inhibit intestinal inflammation (36, 50).

Intestinal homeostasis is achieved by the continuous interaction between the intestinal microbiome and the host immune system. Once this balance is disrupted, a variety of diseases, such as IBD, appear due to immune system dysfunction (67). In mice, BFT^+ *B. fragilis* colonization was able to induce Th-17-mediated colitis and distal CRC in an IL17-mediated NF-κB upregulation-dependent manner in the $APC^{min/+}$ mouse model (40), as demonstrated by Chung et al. (68) who observed repressed BFT-induced tumor formation in APC^{min}

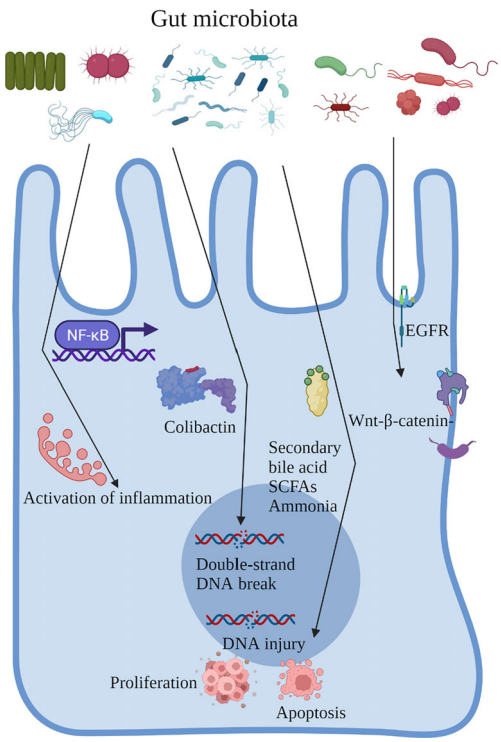

FIGURE 2 | Role of the gut microbiota in the process of CRC and the carcinogenic mechanism of gut microbiota alterations after cholecystectomy.

$^{IL17/IL17}$ mice. Furthermore, it is reported that an accumulation of regulatory T-expressing cells (Treg) cells in $APC^{min/+}$ mice after BFT colonization, which could be a trigger for IL17-mediated pro-oncogenic inflammatory responses. Certain probiotics, such as *Bifidobacterium infantis* (69) and *Bifidobacterium breve* (70), are able to activate intestinal dendritic cells (DCs) by interacting with Toll-like receptors (TLRs) and inducing retinoid metabolism, leading to the release of $Foxp3^+$ Treg and type 1 regulatory T cells (Tr1) and IL-10 (71).

Production of Genotoxins

Another carcinogenic mechanism of the gut microbiota is the production of genotoxins, which may interact with intracellular signal cascades or result in mutations by binding to particular cell surface receptors and it could also damage DNA. Colibactin is a characteristic toxin produced by *Escherichia coli*, which induces double-strand DNA breaks in intestinal cells, causing cancer through its deoxyribonuclease activity (72–74). In addition, the enriched ETBF in the intestine of patients with CRC can produce a metalloproteinase toxin, which initiates cell proliferation, activates c-Myc expression, increases polyamine metabolism, and induces DNA damage, thereby promoting the occurrence and development of CRC (75). Furthermore, *Salmonella typhi* secretes virulence protein A, which enhances the development and proliferation of colon tumors (76). Interestingly, although many genotoxins can cause tumors, recent research has indicated their potential use in cancer therapy (77). For example, *Clostridium perfringens* enterotoxin is a pore-forming toxin with selective cytotoxicity, which rapidly and effectively kills tumor cells (78). Several genotoxins have been studied as therapeutic tools for cancer, including CRC (79); however, their role as a cancer promoter is beyond doubt.

Metabolism of Dietary Ingredients

Metabolism is an essential process in the interaction between the host and the microbiome. Genes encoded by the microorganisms can metabolize several dietary nutrients, including host-indigestible carbohydrates, such as dietary fiber, and host endogenous compounds, such as bile acids. Bacteria in the intestines produce a series of metabolites, including secondary bile acids, sulfides, ammonia, nitrosamines, and short-chain fatty acids (SCFAs), which are involved in the occurrence and development of CRC.

A substantial accumulation of primary bile acids in the intestines was discovered after cholecystectomy, and the enriched *Bacteroides ovatus* and *Parabacteroides diundi* due to cholecystectomy metabolized primary bile acids into secondary ones, which participated in cell proliferation, apoptosis, DNA injury, and other processes, promoting CRC carcinogenesis (24, 80, 81). Dietary fiber is metabolized and decomposed into SCFAs, including acetate, propionate, and butyrate, in the colon. Among them, butyrate (the most widely studied SCFA) regulates cell proliferation, apoptosis, and differentiation to inhibit CRC (82, 83). Cholecystectomy drastically reduced the abundance of intestinal bacteria responsible for metabolizing butyrate, including *Faecalibacterium* and *Roseburia faecis*, thereby decreasing the expression level of butyrate and promoting the occurrence of CRC (24). *Broutella ovale* and *Veillonella parvula*, which can activate azo reductase and produce toxic ammonia substances which promote the occurrence of CRC, were observed in patients who underwent cholecystectomy (35). Additionally, the gut microbiota can also destroy the mucus barrier function by producing sulfide, thereby intensifying the stimulation of intestinal cells (84). For instance, cholecystectomy significantly decreased the abundance of *Desulfovibrio*, producing more sulfides and leading to metabolic disorders, thereby stimulating intestinal epithelial cells and promoting carcinogenesis (34).

Activation of Signaling Pathways

Multiple signaling pathways, such as the epithelial growth factor receptor (EGFR), Wnt/β-catenin, NF-κB, and transforming growth factor-beta pathways, are involved in CRC development. Notably, the gut microbiota activates host carcinogenic signaling pathways.

The EGFR signaling pathway is closely related to the proliferation, apoptosis, and survival of colonic epithelial cells. Activation of the EGFR signaling pathway by secondary bile acids is achieved mainly by disturbing the structure of the cell membrane (reduced membrane fluidity, altered membrane cholesterol distribution), binding to natural ligands (e.g., epidermal growth factor), or inducing calcium signaling-mediated non-dependent activation of ligands (85). Activation of EGFR activates downstream MAPK/RAS/RAF/MEX/

extracellular signal-regulated kinase/proto-oncogene activator protein-1, which in turn mediates cell proliferation and activates RAS/RAF1/extracellular signal-regulated kinase signaling pathway leading to upregulation of mucin 2, also activates the phosphatidylinositol 3 kinase/Akt signaling pathway, which regulates downstream target molecules such as Caspase-8, leading to apoptosis (86, 87). When it comes to practical clinical applications, using biomarkers to target anti-EGFR treatments for metastatic CRC is well established, while the anti-EGFR antibody cetuximab is only effective against a subgroup of CRC (88, 89).

Wnt/β-linked protein signaling plays a key role not only in maintaining intestinal homeostasis but also in regulating the proliferation of CRC cells. The Wnt/β-linked protein classical signaling pathway regulates the expression of Wnt/β-linked proteins through the binding of Wnt ligands to Frizzleds receptors. The Wnt/β-linked protein can transfer to the nucleus and interact with T-cell factor and lymphatic enhancer transcription factors to modulate the transcription of downstream gene targets (survivin, Cyclin D1, and c-Myc) and affect the cell cycle pathway (90). A marked accumulation of *Fusobacterium nucleatum*, which expresses FadA adhesin on its surface, was found in patients with CRC. FadA adhesin stimulates CRC cell growth by increasing the expression of inflammatory genes, oncogenes, and transcription factors by binding to E-cadherin, activating the Wnt/β-catenin signaling pathway, and promoting the transcription of oncogenes (91). *Fusobacterium nucleatum* can also directly activate toll-like receptor signaling to promote tumor development (92).

NF-κB is a key regulator associated with inflammation and cancer on multiple levels (93). The NF-κB signaling pathway regulates many genes involved in different cellular processes, such as cell differentiation, proliferation, genomic stability, and immune responses (94), and its activation is involved in the occurrence and development of CRC. *Escherichia coli*, *Fusobacterium nucleatum*, and ETBF, which are enriched in patients with CRC, are involved in the modulation of this pathway (95). Mechanistically, *Escherichia coli* activates NF-κB through increased phosphorylation of transcription factor 65 and inhibitor of NF-κB kinase alpha, inactivation of inhibitor of NF-κB alpha, and induction of the Wnt/β-catenin pathway by upregulation of β-catenin and its downstream genes (96). The hyperactivation of NF-κB was also found in CRC tissues with abundant *Fusobacterium nucleatum*. Furthermore, ETBF activates the NF-κB pathway by stimulating intracellular interleukin 17 secretion in Apc $^{min/+}$ mice (68).

However, most of the existing research on cholecystectomy is focused on clinical studies, and there is a lack of in-depth mechanistic investigation after cholecystectomy. More studies are needed in the future to elucidate the changes in signaling pathways after cholecystectomy.

CONCLUSION AND PERSPECTIVE

Epidemiological studies on CRC and cholecystectomy have proved the correlation between these two parameters and indicated that changes in the gut microbiota may be a vital intermediate link. In this review, we summarized the changes in the gut microbiota after cholecystectomy. With the variability of sequencing technologies and the complexity of bacterial populations, the conclusions were not unanimous among the studies. Despite this, the differences in the gut microbiota between patients who underwent cholecystectomy and healthy individuals have been proven, and alterations of the gut microbiota affect the development of CRC. Based on previous studies, alterations in the gut microbiota after cholecystectomy may lead to intestinal inflammation, increased metabolism of harmful substances (such as secondary bile acids), and reduction of secretion of beneficial substances (such as butyrate), resulting in the progression of CRC.

There are some potential problems with the current research on the relationship between altered gut microbiota and CRC after cholecystectomy, the results of studies on gut microbiota may vary by race, and different sequencing methods could also affect the results. In addition, alterations of gut microbiota in stool samples cannot fully reflect the tumor microenvironment. And few studies have focused on the role of beneficial bacteria in CRC. In the future, it is necessary to pay attention to the gut microbiota in cancerous and pericarcinomatous tissues and detect the changes in the local microbiome on the occurrence and development of CRC. And a decrease in abundance of beneficial bacteria should also be watched, which may be a potential therapeutic target in CRC. With the rapid development of high-throughput sequencing technology, in-depth information can be provided to understand the links between CRC, cholecystectomy, and the gut microbiota. Notably, different bacterial species of the same genus had mixed efficacy. Therefore, further studies should focus on the changes and function of the gut microbiota in patients who have undergone cholecystectomy at the species level. Hopefully, this approach will elucidate how CRC, cholecystectomy, and gut microbiota interact, allowing therapies to be targeted to individual microbiological, cancer, and lifestyle factors.

Studies on gut microbiota and CRC aim to clarify the mechanisms employed by gut microbiota in the development of CRC and further apply them to the screening, diagnosis, treatment, and prevention of CRC. For instance, Yu et al. discovered a new fecal bacterial marker ('m3' from a *Lachnoclostridium*) that can be used for the diagnosis of colorectal adenoma and CRC. This is superior to other stool-based tests such as fecal microbiota transplantation (FMT) and may be used for the early screening of CRC in the future (97). In addition, there are more clinical studies on techniques such as oral probiotics and FMT. Recent studies have found that the probiotic bacterium *Lactobacillus reuteri* and its produced antimicrobial compound, reuterin, can inhibit the development of CRC by depleting glutathione and inducing oxidative stress in CRC cells, resulting in protein oxidation and impaired ribosome activity. When CRC mice were orally administered *Lactobacillus reuteri*, remission, tumor shrinkage, and prolonged survival were observed in the mice (98). Recently, experimental studies on the efficacy of FMT have focused on animal models. A recent study reported that

FMT from wild to laboratory mice improved host adaptation and resistance to dextran sodium sulfate/azoxymethane-induced colorectal tumorigenesis, and thus a normal gut microbiome plays a protective role in the development of CRC (99). Furthermore, the effectiveness of immunotherapy seems to be strongly influenced by the composition of the gut microbiota. Oral administration of probiotics, such as *Bifidobacterium* (100) and *Akkermansia muciniphila* (101), or FMT (102) from treatment-responsive patients greatly enhanced PD1-based immunotherapy and eliminated tumor growth through enhancing dendritic cell and T-cell responses. At present, there are several ongoing international clinical trials to validate the effect of gut microbiota on CRC chemotherapy (NCT04021589, NCT04131803, NCT01579591).

Currently, cholecystectomy is still the preferred treatment option for gallbladder stones, gallbladder polyps, and cholecystitis. Cholecystectomy is a very routine procedure and more and more patients are undergoing cholecystectomy. However, the possible induction of colorectal after cholecystectomy is getting attention, and its specific mechanism has not been elucidated yet. To clarify the specific mechanism of CRC induced after cholecystectomy can interrupt the development of CRC in a targeted way. The change of gut microbiota after cholecystectomy is an important cause of CRC, and further research on specific species of bacteria and their mechanisms will provide important methods to prevent CRC in the future. As research progresses, dietary intervention with probiotics or prebiotics, or changes in diet could potentially be an effective way to prevent CRC in patients with cholecystectomy history in the future.

AUTHOR CONTRIBUTIONS

All authors listed have contributed to the article and approved its publication. YM, RQ, and YZ: designing, writing, and figure plotting. CJ, ZZ, and WF: designing, funding acquisition, and review and editing. All authors contributed to the article and approved the submitted version.

FUNDING

This research was supported in part by the National Key Research and Development Program of China (2018YFA0800700 and 2018YFC1003200), the National Natural Science Foundation of the P. R. of China (No. 91857115, 31925021, 81921001, 81972702 and 91959110), National multidisciplinary cooperative diagnosis and treatment capacity building project for major diseases: comprehensive diagnosis and treatment of gastrointestinal tumors, National Health and Family Planning Commission Foundation of China (Grant No. 2020YB57), and "Clinical Medicine + X" Foundation of Peking University (Grant No. PKU2021LCXQ001).

REFERENCES

1. Bray F, Ferlay J, Soerjomataram I, Siegel RL, Torre LA, Jemal A. Global Cancer Statistics 2018: GLOBOCAN Estimates of Incidence and Mortality Worldwide for 36 Cancers in 185 Countries. *CA: Cancer J Clin* (2018) 68 (6):394–424. doi: 10.3322/caac.21492
2. Arnold M, Sierra MS, Laversanne M, Soerjomataram I, Jemal A, Bray F. Global Patterns and Trends in Colorectal Cancer Incidence and Mortality. *Gut* (2017) 66(4):683–91. doi: 10.1136/gutjnl-2015-310912
3. Chen W, Zheng R, Baade PD, Zhang S, Zeng H, Bray F, et al. Cancer Statistics in Chin. *CA: Cancer J Clin* (2016) 66(2):115–32. doi: 10.3322/caac.21338
4. Lichtenstein P, Holm NV, Verkasalo PK, Iliadou A, Kaprio J, Koskenvuo M, et al. Environmental and Heritable Factors in the Causation of Cancer–Analyses of Cohorts of Twins From Sweden, Denmark, and Finland. *New Engl J Med* (2000) 343(2):78–85. doi: 10.1056/NEJM200007133430201
5. Turnbaugh PJ, Ley RE, Mahowald MA, Magrini V, Mardis ER, Gordon JI. An Obesity-Associated Gut Microbiome With Increased Capacity for Energy Harvest. *Nature* (2006) 444(7122):1027–31. doi: 10.1038/nature05414
6. Qin J, Li R, Raes J, Arumugam M, Burgdorf KS, Manichanh C, et al. A Human Gut Microbial Gene Catalogue Established by Metagenomic Sequencing. *Nature* (2010) 464(7285):59–65. doi: 10.1038/nature08821
7. Chung H, Pamp SJ, Hill JA, Surana NK, Edelman SM, Troy EB, et al. Gut Immune Maturation Depends on Colonization With a Host-Specific Microbiota. *Cell* (2012) 149(7):1578–93. doi: 10.1016/j.cell.2012.04.037
8. Wong SH, Yu J. Gut Microbiota in Colorectal Cancer: Mechanisms of Action and Clinical Applications. *Nat Rev Gastroenterol Hepatol* (2019) 16 (11):690–704. doi: 10.1038/s41575-019-0209-8
9. Lammert F, Gurusamy K, Ko CW, Miquel J-F, Méndez-Sánchez N, Portincasa P, et al. Gallstones. *Nat Rev Dis Primers* (2016) 2:16024. doi: 10.1038/nrdp.2016.24
10. Linos D, Beard CM, O'Fallon WM, Dockerty MB, Beart RW, Kurland LT. Cholecystectomy and Carcinoma of the Colon. *Lancet (London England)* (1981) 2(8243):379–81. doi: 10.1016/S0140-6736(81)90829-1
11. Turunen MJ, Kivilaakso EO. Increased Risk of Colorectal Cancer After Cholecystectomy. *Ann Surg* (1981) 194(5):639–41. doi: 10.1097/00000658-198111000-00014
12. Shao T, Yang Y-X. Cholecystectomy and the Risk of Colorectal Cancer. *Am J Gastroenterol* (2005) 100(8):1813–20. doi: 10.1111/j.1572-0241.2005.41610.x
13. Zhang Y, Liu H, Li L, Ai M, Gong Z, He Y, et al. Cholecystectomy can Increase the Risk of Colorectal Cancer: A Meta-Analysis of 10 Cohort Studies. *PloS One* (2017) 12(8):e0181852. doi: 10.1371/journal.pone.0181852
14. Farhana L, Nangia-Makker P, Arbit E, Shango K, Sarkar S, Mahmud H, et al. Bile Acid: A Potential Inducer of Colon Cancer Stem Cells. *Stem Cell Res Ther* (2016) 7(1):181. doi: 10.1186/s13287-016-0439-4
15. Scanlan PD, Shanahan F, Clune Y, Collins JK, O'Sullivan GC, O'Riordan M, et al. Culture-Independent Analysis of the Gut Microbiota in Colorectal Cancer and Polyposis. *Environ Microbiol* (2008) 10(3):789–98. doi: 10.1111/j.1462-2920.2007.01503.x
16. O'Keefe SJD, Ou J, Aufreiter S, O'Connor D, Sharma S, Sepulveda J, et al. Products of the Colonic Microbiota Mediate the Effects of Diet on Colon Cancer Risk. *J Nutr* (2009) 139(11):2044–8. doi: 10.3945/jn.109.104380
17. Azcárate-Peril MA, Sikes M, Bruno-Bárcena JM. The Intestinal Microbiota, Gastrointestinal Environment and Colorectal Cancer: A Putative Role for Probiotics in Prevention of Colorectal Cancer? *Am J Physiol Gastrointestinal liver Physiol* (2011) 301(3):G401–24. doi: 10.1152/ajpgi.00110.2011
18. Chen W, Liu F, Ling Z, Tong X, Xiang C. Human Intestinal Lumen and Mucosa-Associated Microbiota in Patients With Colorectal Cancer. *PloS One* (2012) 7(6):e39743. doi: 10.1371/journal.pone.0039743
19. Wang T, Cai G, Qiu Y, Fei N, Zhang M, Pang X, et al. Structural Segregation of Gut Microbiota Between Colorectal Cancer Patients and Healthy Volunteers. *ISME J* (2012) 6(2):320–9. doi: 10.1038/ismej.2011.109
20. Toprak NU, Yagci A, Gulluoglu BM, Akin ML, Demirkalem P, Celenk T, et al. A Possible Role of Bacteroides Fragilis Enterotoxin in the Aetiology of

Colorectal Cancer. *Clin Microbiol infect Off Publ Eur Soc Clin Microbiol Infect Dis* (2006) 12(8):782–6. doi: 10.1111/j.1469-0691.2006.01494.x
21. Bonnet M, Buc E, Sauvanet P, Darcha C, Dubois D, Pereira B, et al. Colonization of the Human Gut by E. Coli and Colorectal Cancer Risk. *Clin Cancer Res an Off J Am Assoc Cancer Res* (2014) 20(4):859–67. doi: 10.1158/1078-0432.CCR-13-1343
22. Abed J, Emgård JEM, Zamir G, Faroja M, Almogy G, Grenov A, et al. Fap2 Mediates Fusobacterium Nucleatum Colorectal Adenocarcinoma Enrichment by Binding to Tumor-Expressed Gal-GalNAc. *Cell Host Microbe* (2016) 20(2):215–25. doi: 10.1016/j.chom.2016.07.006
23. Jahani-Sherafat S, Azimirad M, Alebouyeh M, Ahmadi Amoli H, Hosseini P, Ghasemian-Safaei H, et al. The Rate and Importance of in Colorectal Cancer Patients. *Gastroenterol Hepatol bed to bench* (2019) 12(4):358–63.
24. Ren X, Xu J, Zhang Y, Chen G, Zhang Y, Huang Q, et al. Bacterial Alterations in Post-Cholecystectomy Patients Are Associated With Colorectal Cancer. *Front Oncol* (2020) 10:1418. doi: 10.3389/fonc.2020.01418
25. Capron JP, Delamarre J, Canarelli JP, Brousse N, Dupas JL. [Does Cholecystectomy Predispose to Colo-Rectal Cancer?]. *Gastroenterologie clin biol* (1978) 2(4):383–9.
26. Giovannucci E, Colditz GA, Stampfer MJ. A Meta-Analysis of Cholecystectomy and Risk of Colorectal Cancer. *Gastroenterology* (1993) 105(1):130–41. doi: 10.1016/0016-5085(93)90018-8
27. Schernhammer ES, Leitzmann MF, Michaud DS, Speizer FE, Giovannucci E, Colditz GA, et al. Cholecystectomy and the Risk for Developing Colorectal Cancer and Distal Colorectal Adenomas. *Br J Cancer* (2003) 88(1):79–83. doi: 10.1038/sj.bjc.6600661
28. Sender R, Fuchs S, Milo R. Revised Estimates for the Number of Human and Bacteria Cells in the Body. *PloS Biol* (2016) 14(8):e1002533. doi: 10.1371/journal.pbio.1002533
29. Almeida A, Mitchell AL, Boland M, Forster SC, Gloor GB, Tarkowska A, et al. A New Genomic Blueprint of the Human Gut Microbiota. *Nature* (2019) 568(7753):499–504. doi: 10.1038/s41586-019-0965-1
30. Shanahan F, van Sinderen D, O'Toole PW, Stanton C. Feeding the Microbiota: Transducer of Nutrient Signals for the Host. *Gut* (2017) 66(9):1709–17. doi: 10.1136/gutjnl-2017-313872
31. Vich Vila A, Imhann F, Collij V, Jankipersadsing SA, Gurry T, Mujagic Z, et al. Gut Microbiota Composition and Functional Changes in Inflammatory Bowel Disease and Irritable Bowel Syndrome. *Sci Trans Med* (2018) 10(472):eaap8914. doi: 10.1126/scitranslmed.aap8914
32. Saus E, Iraola-Guzmán S, Willis JR, Brunet-Vega A, Gabaldón T. Microbiome and Colorectal Cancer: Roles in Carcinogenesis and Clinical Potential. *Mol Aspects Med* (2019) 69:93–106. doi: 10.1016/j.mam.2019.05.001
33. Keren N, Konikoff FM, Paitan Y, Gabay G, Reshef L, Naftali T, et al. Interactions Between the Intestinal Microbiota and Bile Acids in Gallstones Patients. *Environ Microbiol Rep* (2015) 7(6):874–80. doi: 10.1111/1758-2229.12319
34. Wang W, Wang J, Li J, Yan P, Jin Y, Zhang R, et al. Cholecystectomy Damages Aging-Associated Intestinal Microbiota Construction. *Front Microbiol* (2018) 9:1402. doi: 10.3389/fmicb.2018.01402
35. Yoon WJ, Kim H-N, Park E, Ryu S, Chang Y, Shin H, et al. The Impact of Cholecystectomy on the Gut Microbiota: A Case-Control Study. *J Clin Med* (2019) 8(1):79. doi: 10.3390/jcm8010079
36. Frost F, Kacprowski T, Rühlemann M, Weiss S, Bang C, Franke A, et al. Carrying Asymptomatic Gallstones is Not Associated With Changes in Intestinal Microbiota Composition and Diversity But Cholecystectomy With Significant Dysbiosis. *Sci Rep* (2021) 11(1):6677. doi: 10.1038/s41598-021-86247-6
37. Hepner GW, Hofmann AF, Malagelada JR, Szczepanik PA, Klein PD. Increased Bacterial Degradation of Bile Acids in Cholecystectomized Patients. *Gastroenterology* (1974) 66(4):556–64. doi: 10.1016/S0016-5085(74)80044-2
38. Waidmann M, Bechtold O, Frick J-S, Lehr H-A, Schubert S, Dobrindt U, et al. Bacteroides Vulgatus Protects Against Escherichia Coli-Induced Colitis in Gnotobiotic Interleukin-2-Deficient Mice. *Gastroenterology* (2003) 125(1):162–77. doi: 10.1016/S0016-5085(03)00672-3
39. Mazmanian SK, Round JL, Kasper DL. A Microbial Symbiosis Factor Prevents Intestinal Inflammatory Disease. *Nature* (2008) 453(7195):620–5. doi: 10.1038/nature07008
40. Wu S, Rhee K-J, Albesiano E, Rabizadeh S, Wu X, Yen H-R, et al. A Human Colonic Commensal Promotes Colon Tumorigenesis *via* Activation of T Helper Type 17 T Cell Responses. *Nat Med* (2009) 15(9):1016–22. doi: 10.1038/nm.2015
41. Sauter GH, Moussavian AC, Meyer G, Steitz HO, Parhofer KG, Jüngst D. Bowel Habits and Bile Acid Malabsorption in the Months After Cholecystectomy. *Am J Gastroenterol* (2002) 97(7):1732–5. doi: 10.1111/j.1572-0241.2002.05779.x
42. Floch MH, Binder HJ, Filburn B, Gershengoren W. The Effect of Bile Acids on Intestinal Microflora. *Am J Clin Nutr* (1972) 25(12):1418–26. doi: 10.1093/ajcn/25.12.1418
43. Sarashina-Kida H, Negishi H, Nishio J, Suda W, Nakajima Y, Yasui-Kato M, et al. Gallbladder-Derived Surfactant Protein D Regulates Gut Commensal Bacteria for Maintaining Intestinal Homeostasis. *Proc Natl Acad Sci USA* (2017) 114(38):10178–83. doi: 10.1073/pnas.1712837114
44. Chen H, Zheng X, Zong X, Li Z, Li N, Hur J, et al. Metabolic Syndrome, Metabolic Comorbid Conditions and Risk of Early-Onset Colorectal Cancer. *Gut* (2021) 70(6):1147–54. doi: 10.1136/gutjnl-2020-321661
45. Hofseth LJ, Hebert JR, Chanda A, Chen H, Love BL, Pena MM, et al. Early-Onset Colorectal Cancer: Initial Clues and Current Views. *Nat Rev Gastroenterol Hepatol* (2020) 17(6):352–64. doi: 10.1038/s41575-019-0253-4
46. Nakatsu G, Li X, Zhou H, Sheng J, Wong SH, Wu WK, et al. Gut Mucosal Microbiome Across Stages of Colorectal Carcinogenesis. *Nat Commun* (2015) 6(8727):8727. doi: 10.1038/ncomms9727
47. Yu J, Feng Q, Wong SH, Zhang D, Liang QY, Qin Y, et al. Metagenomic Analysis of Faecal Microbiome as a Tool Towards Targeted non-Invasive Biomarkers for Colorectal Cancer. *Gut* (2017) 66(1):70–8. doi: 10.1136/gutjnl-2015-309800
48. Wong SH, Zhao L, Zhang X, Nakatsu G, Han J, Xu W, et al. Gavage of Fecal Samples From Patients With Colorectal Cancer Promotes Intestinal Carcinogenesis in Germ-Free and Conventional Mice. *Gastroenterology* (2017) 153(6):1621–33. doi: 10.1053/j.gastro.2017.08.022
49. Ahn J, Sinha R, Pei Z, Dominianni C, Wu J, Shi J, et al. Human Gut Microbiome and Risk for Colorectal Cancer. *J Natl Cancer Inst* (2013) 105(24):1907–11. doi: 10.1093/jnci/djt300
50. Wu N, Yang X, Zhang R, Li J, Xiao X, Hu Y, et al. Dysbiosis Signature of Fecal Microbiota in Colorectal Cancer Patients. *Microb Ecol* (2013) 66(2):462–70. doi: 10.1007/s00248-013-0245-9
51. Zackular JP, Rogers MAM, Ruffin MT, Schloss PD. The Human Gut Microbiome as a Screening Tool for Colorectal Cancer. *Cancer Prev Res (Philadelphia Pa.)* (2014) 7(11):1112–21. doi: 10.1158/1940-6207.CAPR-14-0129
52. Zeller G, Tap J, Voigt AY, Sunagawa S, Kultima JR, Costea PI, et al. Potential of Fecal Microbiota for Early-Stage Detection of Colorectal Cancer. *Mol Syst Biol* (2014) 10:766. doi: 10.15252/msb.20145645
53. Feng Q, Liang S, Jia H, Stadlmayr A, Tang L, Lan Z, et al. Gut Microbiome Development Along the Colorectal Adenoma-Carcinoma Sequence. *Nat Commun* (2015) 6:6528. doi: 10.1038/ncomms7528
54. Baxter NT, Ruffin MT, Rogers MAM, Schloss PD. Microbiota-Based Model Improves the Sensitivity of Fecal Immunochemical Test for Detecting Colonic Lesions. *Genome Med* (2016) 8(1):37. doi: 10.1186/s13073-016-0290-3
55. Flemer B, Lynch DB, Brown JMR, Jeffery IB, Ryan FJ, Claesson MJ, et al. Tumour-Associated and non-Tumour-Associated Microbiota in Colorectal Cancer. *Gut* (2017) 66(4):633–43. doi: 10.1136/gutjnl-2015-309595
56. Alomair AO, Masoodi I, Alyamani EJ, Allehibi AA, Qutub AN, Alsayari KN, et al. Colonic Mucosal Microbiota in Colorectal Cancer: A Single-Center Metagenomic Study in Saudi Arabia. *Gastroenterol Res Pract* (2018) 2018:5284754. doi: 10.1155/2018/5284754
57. Thomas AM, Manghi P, Asnicar F, Pasolli E, Armanini F, Zolfo M, et al. Metagenomic Analysis of Colorectal Cancer Datasets Identifies Cross-Cohort Microbial Diagnostic Signatures and a Link With Choline Degradation. *Nat Med* (2019) 25(4):667–78. doi: 10.1038/s41591-019-0405-7

58. Yachida S, Mizutani S, Shiroma H, Shiba S, Nakajima T, Sakamoto T, et al. Metagenomic and Metabolomic Analyses Reveal Distinct Stage-Specific Phenotypes of the Gut Microbiota in Colorectal Cancer. *Nat Med* (2019) 25(6):968–76. doi: 10.1038/s41591-019-0458-7
59. Beaugerie L, Itzkowitz SH. Cancers Complicating Inflammatory Bowel Disease. *N Engl J Med* (2015) 372(15):1441–52. doi: 10.1056/NEJMra1403718
60. Lasry A, Zinger A, Ben-Neriah Y. Inflammatory Networks Underlying Colorectal Cancer. *Nat Immunol* (2016) 17(3):230–40. doi: 10.1038/ni.3384
61. Terzić J, Grivennikov S, Karin E, Karin M. Inflammation and colon cancer. *Gastroenterology* (2010) 138(6):2101–14. doi: 10.1053/j.gastro.2010.01.058
62. Dennis KL, Wang Y, Blatner NR, Wang S, Saadalla A, Trudeau E, et al. Adenomatous Polyps are Driven by Microbe-Instigated Focal Inflammation and are Controlled by IL-10-Producing T Cells. *Cancer Res* (2013) 73 (19):5905–13. doi: 10.1158/0008-5472.CAN-13-1511
63. Malik A, Sharma D, Zhu Q, Karki R, Guy CS, Vogel P, et al. IL-33 Regulates the IgA-Microbiota Axis to Restrain IL-1α-Dependent Colitis and Tumorigenesis. *J Clin Invest* (2016) 126(12):4469–81. doi: 10.1172/JCI88625
64. Savkovic SD, Koutsouris A, Hecht G. Activation of NF-kappaB in Intestinal Epithelial Cells by Enteropathogenic Escherichia Coli. *Am J Physiol* (1997) 273(4):C1160–7. doi: 10.1152/ajpcell.1997.273.4.C1160
65. Kostic AD, Chun E, Robertson L, Glickman JN, Gallini CA, Michaud M, et al. Fusobacterium Nucleatum Potentiates Intestinal Tumorigenesis and Modulates the Tumor-Immune Microenvironment. *Cell Host Microbe* (2013) 14(2):207–15. doi: 10.1016/j.chom.2013.07.007
66. Sears CL, Geis AL, Housseau F. Bacteroides Fragilis Subverts Mucosal Biology: From Symbiont to Colon Carcinogenesis. *J Clin Invest* (2014) 124 (10):4166–72. doi: 10.1172/JCI72334
67. Gophna U, Sommerfeld K, Gophna S, Doolittle WF, Veldhuyzen van Zanten SJO. Differences Between Tissue-Associated Intestinal Microfloras of Patients With Crohn's Disease and Ulcerative Colitis. *J Clin Microbiol* (2006) 44(11):4136–41. doi: 10.1128/JCM.01004-06
68. Chung L, Thiele Orberg E, Geis AL, Chan JL, Fu K, DeStefano Shields CE, et al. Bacteroides Fragilis Toxin Coordinates a Pro-Carcinogenic Inflammatory Cascade *via* Targeting of Colonic Epithelial Cells. *Cell Host Microbe* (2018) 23(2):203–14. doi: 10.1016/j.chom.2018.01.007
69. Konieczna P, Groeger D, Ziegler M, Frei R, Ferstl R, Shanahan F, et al. Bifidobacterium Infantis 35624 Administration Induces Foxp3 T Regulatory Cells in Human Peripheral Blood: Potential Role for Myeloid and Plasmacytoid Dendritic Cells. *Gut* (2012) 61(3):354–66. doi: 10.1136/gutjnl-2011-300936
70. Jeon SG, Kayama H, Ueda Y, Takahashi T, Asahara T, Tsuji H, et al. Probiotic Bifidobacterium Breve Induces IL-10-Producing Tr1 Cells in the Colon. *PloS Pathog* (2012) 8(5):e1002714. doi: 10.1371/journal.ppat.1002714
71. Geis AL, Fan H, Wu X, Wu S, Huso DL, Wolfe JL, et al. Regulatory T-Cell Response to Enterotoxigenic Bacteroides Fragilis Colonization Triggers IL17-Dependent Colon Carcinogenesis. *Cancer Discov* (2015) 5(10):1098–109. doi: 10.1158/2159-8290.CD-15-0447
72. Nougayrède J-P, Homburg S, Taieb F, Boury M, Brzuszkiewicz E, Gottschalk G, et al. Escherichia Coli Induces DNA Double-Strand Breaks in Eukaryotic Cells. *Sci (New York NY)* (2006) 313(5788):848–51. doi: 10.1126/science.1127059
73. Cuevas-Ramos G, Petit CR, Marcq I, Boury M, Oswald E, Nougayrède J-P. Escherichia Coli Induces DNA Damage *In Vivo* and Triggers Genomic Instability in Mammalian Cells. *Proc Natl Acad Sci USA* (2010) 107 (25):11537–42. doi: 10.1073/pnas.1001261107
74. He Z, Gharaibeh RZ, Newsome RC, Pope JL, Dougherty MW, Tomkovich S, et al. Promotes Colorectal Tumorigenesis Through the Action of Cytolethal Distending Toxin. *Gut* (2019) 68(2):289–300. doi: 10.1136/gutjnl-2018-317200
75. Valguarnera E, Wardenburg JB. Good Gone Bad: One Toxin Away From Disease for Bacteroides Fragilis. *J Mol Biol* (2020) 432(4):765–85. doi: 10.1016/j.jmb.2019.12.003
76. Lu R, Wu S, Zhang YG, Xia Y, Liu X, Zheng Y, et al. Enteric Bacterial Protein AvrA Promotes Colonic Tumorigenesis and Activates Colonic Beta-Catenin Signaling Pathway. *Oncogenesis* (2014) 3:e105. doi: 10.1038/oncsis.2014.20
77. Zahaf N-I, Schmidt G. Bacterial Toxins for Cancer Therapy. *Toxins* (2017) 9 (8):236. doi: 10.3390/toxins9080236
78. Pahle J, Menzel L, Niesler N, Kobelt D, Aumann J, Rivera M, et al. Rapid Eradication of Colon Carcinoma by Clostridium Perfringens Enterotoxin Suicidal Gene Therapy. *BMC Cancer* (2017) 17(1):129. doi: 10.1186/s12885-017-3123-x
79. Karpiński TM, Adamczak A. Anticancer Activity of Bacterial Proteins and Peptides. *Pharmaceutics* (2018) 10(2):54. doi: 10.3390/pharmaceutics 10020054
80. Bernstein C, Holubec H, Bhattacharyya AK, Nguyen H, Payne CM, Zaitlin B, et al. Carcinogenicity of Deoxycholate, a Secondary Bile Acid. *Arch Toxicol* (2011) 85(8):863–71. doi: 10.1007/s00204-011-0648-7
81. Gérard P. Metabolism of Cholesterol and Bile Acids by the Gut Microbiota. *Pathog (Basel Switzerland)* (2013) 3(1):14–24. doi: 10.3390/pathogens3010014
82. Chang PV, Hao L, Offermanns S, Medzhitov R. The Microbial Metabolite Butyrate Regulates Intestinal Macrophage Function *via* Histone Deacetylase Inhibition. *Proc Natl Acad Sci USA* (2014) 111(6):2247–52. doi: 10.1073/pnas.1322269111
83. Wang G, Yu Y, Wang Y-Z, Wang J-J, Guan R, Sun Y, et al. Role of SCFAs in Gut Microbiome and Glycolysis for Colorectal Cancer Therapy. *J Cell Physiol* (2019) 234(10):17023–49. doi: 10.1002/jcp.28436
84. Ijssennagger N, Belzer C, Hooiveld GJ, Dekker J, van Mil SWC, Müller M, et al. Gut Microbiota Facilitates Dietary Heme-Induced Epithelial Hyperproliferation by Opening the Mucus Barrier in Colon. *Proc Natl Acad Sci USA* (2015) 112(32):10038–43. doi: 10.1073/pnas.1507645112
85. Centuori SM, Gomes CJ, Trujillo J, Borg J, Brownlee J, Putnam CW, et al. Deoxycholic Acid Mediates non-Canonical EGFR-MAPK Activation Through the Induction of Calcium Signaling in Colon Cancer Cells. *Biochim Biophys Acta* (2016) 1861(7):663–70. doi: 10.1016/j.bbalip.2016.04.006
86. Dong W, Liu L, Dou Y, Xu M, Liu T, Wang S, et al. Deoxycholic Acid Activates Epidermal Growth Factor Receptor and Promotes Intestinal Carcinogenesis by ADAM17-Dependent Ligand Release. *J Cell Mol Med* (2018) 22(9):4263–73. doi: 10.1111/jcmm.13709
87. Napolitano S, Matrone N, Muddassir AL, Martini G, Sorokin A, De Falco V, et al. Triple Blockade of EGFR, MEK and PD-L1 has Antitumor Activity in Colorectal Cancer Models With Constitutive Activation of MAPK Signaling and PD-L1 Overexpression. *J Exp Clin Cancer Res CR* (2019) 38(1):492. doi: 10.1186/s13046-019-1497-0
88. Bhullar DS, Barriuso J, Mullamitha S, Saunders MP, O'Dwyer ST, Aziz O. Biomarker Concordance Between Primary Colorectal Cancer and its Metastases. *EBioMedicine* (2019) 40:363–74. doi: 10.1016/j.ebiom.2019.01.050
89. Woolston A, Khan K, Spain G, Barber LJ, Griffiths B, Gonzalez-Exposito R, et al. Genomic and Transcriptomic Determinants of Therapy Resistance and Immune Landscape Evolution During Anti-EGFR Treatment in Colorectal Cancer. *Cancer Cell* (2019) 36(1):35–50. doi: 10.1016/j.ccell.2019.05.013
90. Nusse R, Clevers H. Wnt/β-Catenin Signaling, Disease, and Emerging Therapeutic Modalities. *Cell* (2017) 169(6):985–99. doi: 10.1016/j.cell.2017.05.016
91. Rubinstein MR, Wang X, Liu W, Hao Y, Cai G, Han YW. Fusobacterium Nucleatum Promotes Colorectal Carcinogenesis by Modulating E-Cadherin/β-Catenin Signaling *via* its FadA Adhesin. *Cell Host Microbe* (2013) 14 (2):195–206. doi: 10.1016/j.chom.2013.07.012
92. Yang Y, Weng W, Peng J, Hong L, Yang L, Toiyama Y, et al. Fusobacterium Nucleatum Increases Proliferation of Colorectal Cancer Cells and Tumor Development in Mice by Activating Toll-Like Receptor 4 Signaling to Nuclear Factor-κb, and Up-Regulating Expression of MicroRNA-21. *Gastroenterology* (2017) 152(4):851–66. doi: 10.1053/j.gastro.2016.11.018
93. DiDonato JA, Mercurio F, Karin M. NF-κb and the Link Between Inflammation and Cancer. *Immunol Rev* (2012) 246(1):379–400. doi: 10.1111/j.1600-065X.2012.01099.x
94. Hoesel B, Schmid JA. The Complexity of NF-κb Signaling in Inflammation and Cancer. *Mol Cancer* (2013) 12:86. doi: 10.1186/1476-4598-12-86
95. Peng C, Ouyang Y, Lu N, Li N. The NF-κb Signaling Pathway, the Microbiota, and Gastrointestinal Tumorigenesis: Recent Advances. *Front Immunol* (2020) 11:1387. doi: 10.3389/fimmu.2020.01387
96. Sahu U, Choudhury A, Parvez S, Biswas S, Kar S. Induction of Intestinal Stemness and Tumorigenicity by Aberrant Internalization of Commensal

non-Pathogenic E. Coli. *Cell Death Dis* (2017) 8(3):e2667. doi: 10.1038/cddis.2017.27
97. Liang JQ, Li T, Nakatsu G, Chen Y-X, Yau TO, Chu E, et al. A Novel Faecal Marker for the non-Invasive Diagnosis of Colorectal Adenoma and Cancer. *Gut* (2020) 69(7):1248–57. doi: 10.1136/gutjnl-2019-318532
98. Bell HN, Rebernick RJ, Goyert J, Singhal R, Kuljanin M, Kerk SA, et al. Reuterin in the Healthy Gut Microbiome Suppresses Colorectal Cancer Growth Through Altering Redox Balance. *Cancer Cell* (2021). doi: 10.1016/j.ccell.2021.12.001
99. Rosshart SP, Vassallo BG, Angeletti D, Hutchinson DS, Morgan AP, Takeda K, et al. Wild Mouse Gut Microbiota Promotes Host Fitness and Improves Disease Resistance. *Cell* (2017) 171(5):1015–28. doi: 10.1016/j.cell.2017.09.016
100. Sivan A, Corrales L, Hubert N, Williams JB, Aquino-Michaels K, Earley ZM, et al. Commensal Bifidobacterium Promotes Antitumor Immunity and Facilitates Anti-PD-L1 Efficacy. *Sci (New York NY)* (2015) 350 (6264):1084–9. doi: 10.1126/science.aac4255
101. Routy B, Le Chatelier E, Derosa L, Duong CPM, Alou MT, Daillère R, et al. Gut Microbiome Influences Efficacy of PD-1-Based Immunotherapy Against Epithelial Tumors. *Sci (New York NY)* (2018) 359(6371):91–7. doi: 10.1126/science.aan3706
102. Gopalakrishnan V, Spencer CN, Nezi L, Reuben A, Andrews MC, Karpinets TV, et al. Gut Microbiome Modulates Response to Anti-PD-1 Immunotherapy in Melanoma Patients. *Sci (New York NY)* (2018) 359 (6371):97–103. doi: 10.1126/science.aan4236

Conflict of Interest: The authors declare that the research was conducted in the absence of any commercial or financial relationships that could be construed as a potential conflict of interest.

Publisher's Note: All claims expressed in this article are solely those of the authors and do not necessarily represent those of their affiliated organizations, or those of the publisher, the editors and the reviewers. Any product that may be evaluated in this article, or claim that may be made by its manufacturer, is not guaranteed or endorsed by the publisher.

frontiers in Endocrinology

REVIEW
published: 18 March 2022
doi: 10.3389/fendo.2022.841703

The Mechanism Underlying the Influence of Indole-3-Propionic Acid: A Relevance to Metabolic Disorders

Binbin Zhang[1,2†], *Minjie Jiang*[3†], *Jianan Zhao*[4], *Yu Song*[3], *Weidong Du*[5*] *and Junping Shi*[1,6*]

[1] Department of Translational Medicine Platform, The Affiliated Hospital of Hangzhou Normal University, Hangzhou, China, [2] College of Life Sciences, Zhejiang University of Traditional Chinese Medicine, Hangzhou, China, [3] Zhejiang University of Traditional Chinese Medicine, Hangzhou, China, [4] Guanghua Clinical Medical College, Shanghai University of Traditional Chinese Medicine, Shanghai, China, [5] Zhejiang Traditional Chinese Medicine Hospital, Hangzhou, China, [6] Department of Infectious & Hepatology Diseases, Metabolic Disease Center, The Affiliated Hospital of Hangzhou Normal University, Hangzhou, China

OPEN ACCESS

Edited by:
Fang Zhongze,
Tianjin Medical University, China

Reviewed by:
Elena Rampanelli,
Amsterdam University Medical Center, Netherlands
Kang Ho Kim,
University of Texas Health Science Center at Houston, United States

***Correspondence:**
Weidong Du
hzadu@163.com
Junping Shi
20131004@hznu.edu.cn

[†]These authors have contributed equally to this work

Specialty section:
This article was submitted to Gut Endocrinology, a section of the journal Frontiers in Endocrinology

Received: 22 December 2021
Accepted: 21 February 2022
Published: 18 March 2022

Citation:
Zhang B, Jiang M, Zhao J, Song Y, Du W and Shi J (2022) The Mechanism Underlying the Influence of Indole-3-Propionic Acid: A Relevance to Metabolic Disorders. Front. Endocrinol. 13:841703. doi: 10.3389/fendo.2022.841703

The increasing prevalence of metabolic syndrome has become a serious public health problem. Certain bacteria-derived metabolites play a key role in maintaining human health by regulating the host metabolism. Recent evidence shows that indole-3-propionic acid content can be used to predict the occurrence and development of metabolic diseases. Supplementing indole-3-propionic acid can effectively improve metabolic disorders and is considered a promising metabolite. Therefore, this article systematically reviews the latest research on indole-3-propionic acid and elaborates its source of metabolism and its association with metabolic diseases. Indole-3-propionic acid can improve blood glucose and increase insulin sensitivity, inhibit liver lipid synthesis and inflammatory factors, correct intestinal microbial disorders, maintain the intestinal barrier, and suppress the intestinal immune response. The study of the mechanism of the metabolic benefits of indole-3-propionic acid is expected to be a potential compound for treating metabolic syndrome.

Keywords: metabolic syndrome, indole-3-propanoic acid, obesity, type 2 diabetes, non-alcoholic fatty liver disease, cardiovascular diseases

INTRODUCTION

Metabolic syndrome is defined as a group of interrelated comprehensive diseases characterized by visceral obesity, hypertension, hyperlipidemia, atherosclerosis, and insulin resistance. Metabolic syndrome, including overweight/obesity, type 2 diabetes (T2D) (1, 2), non-alcoholic fatty liver disease (NAFLD) (3), and cardiovascular disease (CVD) (4) has become a severe public health problem (5). Accumulating evidence has linked intestinal microbe imbalance or compositional changes with the pathogenesis of metabolic diseases (6). Intestinal microbes produce functional metabolites that regulate intestinal endocrine function and neural signals, regulate energy metabolism, and affect host immune mechanisms and homeostasis (7). Functional metabolites serve as potential markers of disease and transfer to distant organs through the intestinal barrier–peripheral circulation, affecting the metabolic phenotype of the host (8–10). Therefore, the link between functional metabolites and metabolic diseases has received increasing attention.

Indole-3-propanoic acid (IPA) is a tryptophan (Trp) metabolite produced by intestinal bacteria that is closely associated with diet. IPA has received increasing attention in recent years because of its close correlation with metabolic diseases. Recent studies have found that IPA content can predict the occurrence of obesity (11), T2D (12), NAFLD (13), and CVD (14).

In recent years, supplementation with IPA has been shown to improve blood glucose, increase insulin sensitivity (15), inhibit liver lipid synthesis and inflammatory factors (16), correct intestinal microbial disorders (17), maintain the intestinal barrier, and suppress the intestinal immune response (18). Here, we systematically reviewed the latest research on IPA, its association with metabolic diseases, and its role in metabolic disorders, and discuss its future research directions.

IPA IS THE METABOLITE OF Trp IN THE INTESTINE

IPA is a metabolite produced by the microflora of dietary Trp that accumulates in the host serum and exhibits high individual differences (19). Under physiological conditions, serum IPA concentrations range from 1 to 10 μM in humans (20, 21)

Trp is an essential amino acid from the host diet for use in protein synthesis (22). Trp is primarily metabolized through the 5-HT (23), canine uric acid (24), and intestinal microbial pathways. Indole-3-pyruvic acid (IPyA) is converted from Trp in the presence of an aromatic amino acid aminotransferase. IPyA is a precursor of indolelactic acid (ILA), and phenyllactate dehydrogenase is involved in this reduction reaction. Bacterial species containing phenyllactate dehydratase *(fldBC)* and its activator acyl-CoA ligase convert ILA to indoleacrylic acid (IA) through dehydration. IA can be further converted into IPA by acyl coenzyme A dehydrogenase, which is the final product of the reductive metabolism of Trp (**Figure 1**) (24–26). The most abundant metabolite of Trp in the intestine is indole, followed by indole-3-acetic acid and IPA (27, 28).

The metabolism of IPA in the body is affected by enzyme activity and intestinal microbes. Liquid chromatography–mass spectrometry (LC-MS) analysis was used to compare the plasma samples of sterile and conventional mice. The production of IPA was found to be entirely dependent on intestinal microbes.

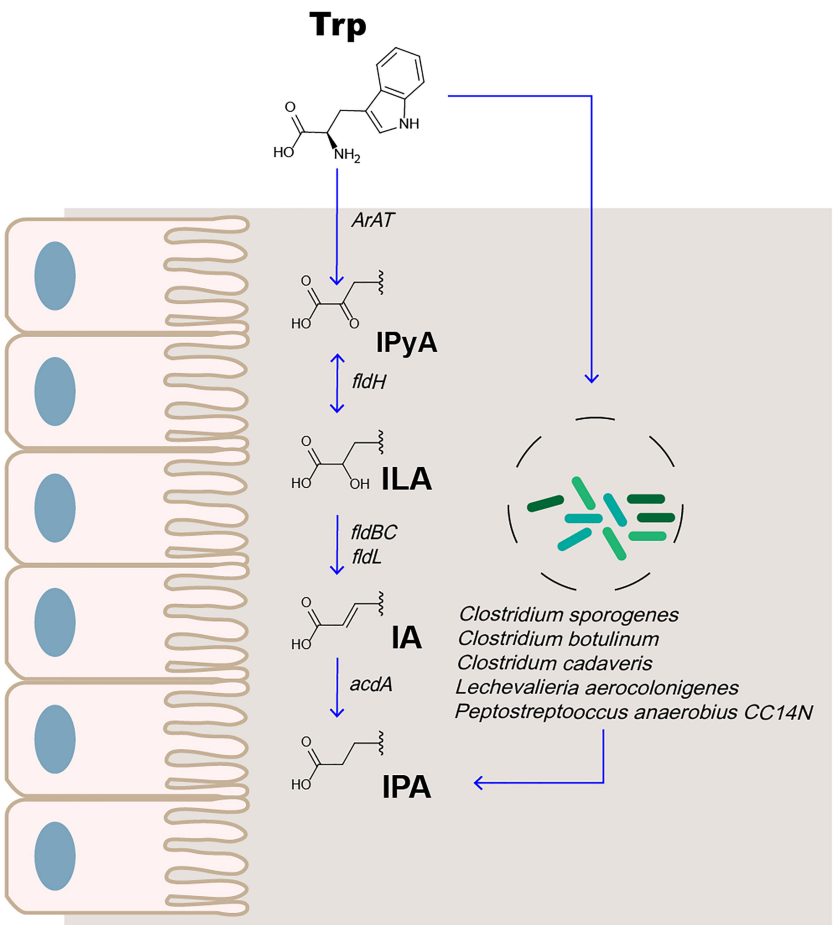

FIGURE 1 | IPA is the metabolite of Trp in the intestine.

Colonization with *Clostridium sporogenes* and *Clostridium botulinum* can promote the concentration of IPA in the plasma (29, 30). Recently, the study found that, among 36 bacterial isolates cultured in Trp-containing medium, 4 (*Peptostreptococcus anaerobius CC14N* and 3 *Clostridium cadaveris* strains) were capable of producing IPA. Simultaneously, the presence of FLDC, a homologous cluster of the *fldBC* gene cluster, was found to be a reliable marker for IPA-producing bacteria (25). Other bacteria, such as *Lechevalieria aerocolonigenes*, can synthesize IPA through Trp deamination catalyzed by amino acid oxidase (31). Therefore, IPA is an important indicator of microbial metabolism.

In a study on the metabolic benefits of Trp, the Trp diet led to a decrease in mouse body weight (32); however, the mechanism was not elucidated. In another study, it was found that a diet supplemented with neomycin and Trp led to an increase in rat body weight, which was related to the significant change in the concentration of Trp-derived bacterial metabolites in the feces and blood. Further studies showed that the change in body weight increase was most relevant to the change in the concentration of the Trp metabolite IPA. The body weight gain in rats treated with IPA alone was two times lower than that in rats treated with the vehicle, suggesting that IPA might be an effector metabolite between a Trp-rich diet and lower body weight gain (33). Therefore, for the Trp-IPA metabolic pathway, the development of related probiotics, and the promotion of the production of IPA, we need to pay attention to the study of probiotics in the treatment of metabolic syndrome in the future.

IPA CONCENTRATIONS AFFECTED BY DIETARY INTERVENTION

Diet significantly impacts NAFLD, T2D, obesity, CVD, and metabolic disorders (34, 35). Therefore, we explored the relationship between IPA and diet. IPA was the metabolite most significantly and consistently related to both total carbohydrate and fiber intake (r = 0.28, $p = 9.1 \times 10^{-5}$ and r = 0.23, s = 0.001, respectively), including whole grain wheat, rye, and whole grain rye intake (12). In another study, 117 overweight adults were randomly divided into two groups. Based on the same diet, they were supplied with fried meat or not. The study found that the participants who consumed fried meat had higher lipopolysaccharide (LPS), tumor necrosis factor-α (TNF-α), interleukin-1β (IL-1β), and IL-10 levels ($p < 0.05$). Fried meat intake lowered microbial community richness and decreased *Lachnospiraceae* and *Flavonifractor* abundances while increasing *Dialister*, *Dorea*, and *Veillonella* abundances [p false discovery rate (FDR) < 0.05], which caused a significant decrease in the fecal metabolite IPA content (36).

In a diet study, 10 healthy participants were randomly fed a Western or Mediterranean diet for 4 days, and feces were collected for 16s RNA and metabolomics after 4 days. Different diets altered the intestinal flora structure. Simultaneously, IPA content in feces was significantly increased with the Mediterranean diet but decreased in the Western diet (37). This suggests that diet can affect the composition of intestinal microorganisms within a short time (38); however, the long-term effect and stability of the microbial structure are not apparent. Promoting the increase in IPA content may be an effective way to improve the metabolic benefits of the Mediterranean diet.

In the correlation experiment between 11 types of Trp metabolism levels and T2D events in the circulation of 9,180 participants from five cohorts, it was found that intake of fiber-rich foods, rather than protein/Trp-rich foods, and peripheral IPA content were positively correlated. Further research found that higher milk and fiber intake can improve the metabolism of Trp in the circulation of patients with T2D, but only in individuals with non-persistent genetic lactase (39). This suggests that diet can interfere with host–microbe interactions and affect the metabolism of Trp-IPA in the host. The effect of the metabolic benefits of a healthy diet is partly due to the promotion of IPA production in circulation.

ROLE OF IPA IN METABOLIC DISEASES

We mainly discuss the relationship between IPA and various metabolic diseases, including obesity, T2D, NAFLD, and CVD, and focus on the potential connection between IPA and illness.

IPA as a Potential Biomarker of Obesity and its Association With Inflammation

Obesity is a complex pathophysiological disease and one of the causes of metabolic syndrome, which is characterized by chronic low-grade inflammation. In 85 obese adults (average BMI = 40.48) and 42 non-obese control individuals (average BMI = 24.03), the serum IPA content was significantly lower in obese patients and was compared with BMI, serum high-sensitivity C-reactive protein (hsCRP), and high-sensitive interleukin 6 (hsIL-6), and the hsCRP and hsIL-6 levels were negatively correlated (40). This suggests that the indole metabolic pathway of Trp is affected in obese patients, which may be related to obesity-related systemic inflammation. However, in obese patients who underwent Roux-en-Y gastric bypass surgery (RYGB) operation, the level of IPA in the blood increased substantially 3 months post-surgery compared with 1 week post-surgery (40). This suggests that IPA content can be used as a marker for obesity. In future research, it will be necessary to perform correlation analyses between IPA and obesity-related complications to provide new diagnostic methods for invasive diagnosis of diseases and to predict obesity-related complications.

IPA as a Potential Biomarker for Predicting the Risk of T2D

Current studies have found that IPA content is closely related to T2D and can predict the risk of T2D, distinguish different stages of T2D, and decrease with the improvement of T2D. IPA can be used as a biomarker of disease progression. When studying the brain–gut–microbiota characteristics of women with obesity and food addiction, a negative correlation was found between IPA in

serum and food addiction (41). Bariatric surgery, such as RYGB, can improve T2D, obesity, NAFLD, and other metabolic diseases (42). In clinical studies, IPA content in the peripheral blood of obese patients with T2D was significantly lower than that in healthy participants. The IPA content in blood samples of these patients 3 months post-RYGB surgery was significantly higher than that in blood samples 1 week post-surgery (11)."XenoScan," a metabolomics platform established by the University of California, Davis, used LC-MS to characterize a series of intestinal microflora metabolites and found that several metabolites, including IPA, could distinguish early T2D rats from rats 3 months after the onset of diabetes (43).

In a clinical trial, researchers used a non-targeted metabolomics approach to investigate whether serum metabolite profiles can predict the incidence of T2D in patients with impaired glucose tolerance. During the 15-year follow-up, patients with glucose tolerance who developed (n = 96) or did not develop (n = 104) T2D had lower and higher serum IPA levels, respectively. This suggests that higher serum IPA levels lead to a low risk of T2D (12). In a clinical study with a 7-year follow-up, it was verified that higher serum IPA levels were negatively correlated with the occurrence of T2D (OR [CI]: 0.86 [0.73–0.99], $p = 0.04$), directly correlated with insulin secretion ($\beta = 0.10$, $p = 0.06$), and negatively correlated with hsCRP when blood samples were collected ($r = -0.22$, $p = 0.0001$), and during follow-up visits ($\beta = -0.19$, $p = 0.001$). This suggests that IPA might be mediated by low-grade inflammation or enhance insulin sensitivity by protecting β-cell function to reduce the risk of T2D (21)

IPA Reduces Lipotoxicity to Inhibit the Development of NAFLD

NAFLD manifests as liver fat accumulation, and the disease progresses to non-alcoholic steatohepatitis (NASH) or even hepatocellular carcinoma (HCC). Globally, the prevalence of NAFLD-related HCC may increase with an obesity epidemic (44).

IPA in the intestinal tract is absorbed by the intestinal epithelial cells and diffuses into the blood, which enters multiple target organs such as the liver after passing through the peripheral and portal circulation (30). This suggests that the liver may be a target organ for IPA biology. In 233 patients who underwent bariatric surgery and detailed liver histological examinations, the circulating IPA in patients with liver fibrosis was lower than that in those without fibrosis. Circulating IPA levels are also associated with the liver richness in genes that regulate hepatic stellate cell activation and liver fibrosis signaling. *In vitro* experiments have verified that IPA reduces the mRNA expression of fibrosis signaling markers such as *COL1A2*, *aSMA*, and *ITGA3* in LX-2 cells (13).

Cholesterol is considered the primary lipotoxic molecule among liver lipids in NASH development (45–47). Lipotoxicity promotes the progression of NAFLD to NASH, liver cirrhosis, and even liver cancer (48, 49). Depletion of IPA was noted in both hypercholesterolemia-fed HCC mice and in sterile mouse serum transplanted with hypercholesterolemia-fed HCC mouse feces. *In vitro* experiments showed that IPA could inhibit the accumulation of triglycerides (TG) in the cholesterol-induced human normal hepatocyte line LO2 and inhibit the proliferation of NASH-HCC cell lines (HKCI-2 and HKCI10). Therefore, the partial reason for cholesterol-induced lipotoxicity is the damage to tryptophan metabolism in microorganisms and the reduced serum IPA content, thereby promoting the development of NASH-HCC (50).

IPA Improves CVD by Lowering Blood Lipid Levels

CVD is a serious cause of death due to metabolic diseases (51, 52). In a cohort study from an advanced atherosclerosis (n = 100) and gender- and age-matched control group (n = 20), the level of IPA in plasma metabolites of the advanced atherosclerosis group was significantly reduced (0.41 [0.27–0.90] μM vs. 0.22 [0.16–0.34] μM; $p < 0.01$). In a study of risk factors for atherosclerosis, IPA (OR, 0.27; 95% CI, 0.019–0.91; $p = 0.02$) was negatively correlated with advanced atherosclerosis (14). In mice experiments, oral administration of IPA significantly reduced high-fat diet (HFD)-induced body weight gain and reduced serum total cholesterol (TC), low-density lipoprotein cholesterol (LDL-c), and TG levels, showing sufficient anti-hyperlipidemic effects (16).

IPA and Other Metabolic Diseases

In a 1-year follow-up study of patients with chronic kidney disease (CKD), the estimated glomerular filtration rate (eGFR) rapidly decreased by >20% (n = 10) and the control group (n = 10), and the eGFR decreased by <5%. It was found that IPA was the only metabolite that dropped significantly in eGFR rapidly decreased group of plasma. In cross-sectional clinical studies, it can also be found that the serum IPA content of the normal group was significantly higher than that of the CKD group (49.8 ± 15.9 vs. 34.7 ± 10.8 ng/ml; $p < 0.01$) (53). Intervention with IPA can also inhibit the gene expression of fibrosis and inflammation in proximal renal tubular cells induced by indophenol sulfate (54). In previous studies, oxidative stress was found to be associated with increased kidney damage (55), and IPA as a potent antioxidant may be an important bioprotective agent for CKD.

In another study, oral IPA supplementation reduced the systemic inflammation level in radiation-exposed mice, restored hematopoietic organs, relieved bone marrow suppression, and improved gastrointestinal function and epithelial integrity after irradiation, thereby exerting therapeutic effects on radiation toxicity (56). Supplementation with mouse probiotic *Clostridia* resulted in an increase in IPA production in the intestinal lumen and increased mitochondrial transcription factor A (Tfam) expression in osteoblasts by promoting Kdm6b/Jmjd3 histone demethylase, thereby inhibiting the epigenetic methylation of H3K27me3 at the Tfam promoter from preventing pathological bone loss in obese mice induced by a HFD (57). IPA is neuroprotective as a potent hydroxyl radical scavenger (58). IPA inhibits β-amyloid fibril formation, a potent neuroprotective agent, and is a potential drug for the treatment of Alzheimer's disease (59).

IPA also exhibits protective effects against streptozotocin-induced diabetic peripheral neuropathy in rats and high-glucose-induced neurotoxicity in neural 2a cells (60).

MECHANISMS OF IPA ACTION ON METABOLIC DISEASES

As mentioned above, IPA contributes to various metabolic diseases, and its mechanism is complex. It may be involved in the physiological and pathological processes of the disease through different pathways. Therefore, we comprehensively analyzed the mechanism of IPA in terms of glucose metabolism, insulin resistance, lipid synthesis, inflammatory reactions, and the intestinal microenvironment.

IPA Can Improve Blood Glucose and Increase Insulin Sensitivity

Impaired glucose tolerance and insulin tolerance are also pathogenic factors in metabolic syndrome. Rats fed a diet rich in IPA had improved glucose metabolism and significantly reduced HOMA index of fasting blood glucose, insulin, and insulin resistance (15).

Cognitive decline is a complication of T2D, and intermittent fasting (IF) is a dietary intervention used to alleviate the symptoms of T2D. In research of its mechanism, IF was found to improve cognition through the microorganism–metabolite–brain axis. Among the metabolites affected by IF, the complementary metabolite IPA showed similar results with IF. In db/db mice, IPA was found to improve cognitive function and insulin sensitivity, enhance mitochondrial biogenesis, and protect the ultrastructure of synapses (61). This may be related to IPA as an antioxidant, preventing neuronal death induced by amylin and β-amyloids and restoring mitochondrial function (62, 63).

First, the protective effect of serum IPA in T2D may be achieved through its efficacy in regulating the secretion of incretin, particularly glucagon-like peptide (GLP)-1 release by intestinal endocrine L cells (64). GLP-1 inhibits the occurrence of T2D by reducing B-cell apoptosis and increasing cell proliferation and regeneration (65)

Second, as a strong oxidant (62), IPA can protect β cells from damage related to metabolism and oxidative stress, and possibly from the accumulation of amyloid (66). These results suggest that IPA may be a promising candidate for the treatment of insulin-resistant metabolic disorders, including T2D.

IPA Inhibits Liver Lipid Synthesis and Inflammatory Factors

IPA intervention can improve NASH model mice induced by a HFD through intestinal microenvironment homeostasis (17). In an *in vitro* experiment, supplementation with oleic acid (OA; 100 μM) resulted in significant accumulation of TG in a human hepatocarcinoma cell line of HepG2 cells, and IPA treatment significantly reduced OA-induced TG accumulation in a dose-dependent manner (10, 25, and 50 μM). Further research showed that IPA dose-dependently reduced the transcription of essential genes involved in fatty acid (*Srebp1-c* and *Fas*) and cholesterol biosynthesis (*Srebp2* and *Hmgr*) in HepG2 cells (16).

In addition to inhibiting lipid synthesis in the liver, IPA intervention could inhibit the expression levels of pro-inflammatory cytokines such as TNF-α, IL-1β, and IL-6 in the liver of NASH rats induced by a HFD. In an *in vitro* LPS-induced mouse macrophage model, IPA also inhibited nuclear factor kappa B) NF-κB signaling, p65 phosphorylation, and the expression of NF-κB downstream target genes in a dose-dependent manner (17).

Excess free Fe(3+) and was also found to cause oxidative damage, which deteriorates NAFLD to NASH. In an *in vitro* experiment, FeCl(3+) (0.2 mM) was used to induce the isolated rat liver microsomes to simulate the oxidative damage model and then incubated with IPA. It was found that co-incubated IPA (concentrations of 10, 3, 2, and 1 mM) can prevent the decrease in cell membrane fluidity caused by Fe(3+). The increase in lipid peroxidation caused by Fe(3+) was only inhibited after incubation with the highest concentration (10 mM) of IPA (67). Moreover, IPA at a concentration of 5 mM was able to inhibit lipid peroxidation damage in hamster testes caused by iron ions (68). This suggests that IPA can act as an effective free radical scavenger to prevent iron-induced oxidative damage to cell membranes. The antioxidant effect of IPA is concentration dependent, which also explains the protective effect of high concentrations of IPA on the periphery of the body.

IPA Can Correct Intestinal Microbial Disorders

IPA maintains the stability of the intestinal microenvironment. Its primary mechanism is to correct the disordered intestinal microflora, repair the intestinal barrier, and inhibit the intestinal immune response.

The intestinal microbial structure can affect the host's absorption of dietary monosaccharides and lipids, promoting the accumulation of TG in the adipose tissue and liver and causing metabolic disease (69, 70). An imbalance of intestinal microbes affects the TLR9- and TLR4-related inflammatory pathways in the liver (71). In multi-ethnic cohort studies, intestinal microbial α diversity was generally low in patients with metabolic diseases (72). In a clinical cohort study of 1,018 middle-aged women from TwinsUK, the relationship between serum IPA levels and gut microbial genes was evaluated, and a positive correlation between microbiota alpha diversity and serum IPA content was found (Shannon diversity: β [Shannon diversity: beta (95% CI) = 0.19 [0.13; 0.25], $p = 6.41 \times 10^{-10}$) (73).

In an 8-week NAFLD rat model induced by a HFD, IPA (20 mg/kg) was administered to rats for the 8-week experiment. The 16s rRNA method was used to detect rat feces, and principal coordinate and non-metric multidimensional scale analyses showed that the intestinal microbes of rats in the IPA administration group were significantly different from those in the model group. This suggests that IPA administration can improve the overall structure of the intestinal microbes in NAFLD rats. An increase and decrease in the abundance of

Firmicutes and *Bacteroidetes*, respectively, were biomarkers of obesity (74, 75). Based on this feature, the authors analyzed the intestinal microbial composition, and an HFD was found to increase the ratio of *Firmicutes* to *Bacteroidetes*, which could be reversed by IPA treatment. The abundance of the two potential pathogenic bacteria *Bacteroides* and *Streptococcus* (76) was increased by an HFD and decreased by IPA treatment. It has also been reported that the abundance of the genus *Parasutterella* (77) associated with chronic intestinal inflammation was reduced by IPA treatment. In addition, the abundance of the two genera *Oscillibacter* and *Odoribacter*, which are important for maintaining intestinal homeostasis, were reduced in the HFD-fed group (78) and restored in the IPA group (17). In addition, IPA supplementation can inhibit the growth of *Mycobacterium tuberculosis* by blocking the synthesis of Trp in *M. tuberculosis* through the catalytic step of TrpE, thereby exerting an anti-tubercular effect (79).

IPA Maintains the Intestinal Barrier

Increased intestinal permeability and abnormal intestinal tight junctions caused by ecological imbalance are frequently observed in patients with metabolic diseases (80). Intestinal ecological imbalance leads to an increase in LPS and bile acid production, which is related to whole-body low-grade inflammation (81).

Treatment of HFD-fed mice with IPA reduced intestinal permeability (decreased circulating FITC-dextran) and reduced circulating LPS levels. *In vitro*, researchers used monolayers of T84 cells incubated with the pro-inflammatory cytokines interferon-γ (IFN-γ) and TNF-α. IPA was found to reduce the permeability of monolayers through an FITC-dextran permeability experiment (82).

The ratio of villi to crypts in the ileum of HFD-fed rats was reduced (83), and the villi height was restored by IPA treatment, which also promoted the protein expressions of zonula occludens-1 (ZO-1), occludin, and tight junction proteins in the rat ileum (17). The end of the afferent neurons of the vagus nerve is located in the intestinal mucosa, and the increase in LPS changes the afferent signals of the vagus nerve and reduces the satiety induced by cholecystokinin, thus promoting appetite and leading to obesity (84). Thus, IPA can inhibit appetite by inhibiting LPS levels in the plasma.

The Caco-2/HT29 co-culture model was used to evaluate the effect of IPA on the intestinal barrier and explore its potential mechanism. Studies have shown that IPA increases transepithelial resistance and decreases paracellular permeability. Simultaneously, IPA enhances the mucus barrier by increasing the expression of mucins MUC2 and MUC4 and the goblet cell secretion products TFF3 and RELMβ. In addition, IPA reduces the expression of inflammatory factors in LPS-induced Caco-2/HT29 cells. These findings provide a new perspective for the intestinal microbial metabolite of Trp to improve the intestinal barrier (85). SLC2A5 (GLUT5-encoded) is the leading fructose absorption transporter in the kidneys, small intestine, and proximal tubules, and its overexpression causes metabolic syndrome by increasing fructose intake (86). Expression of the fructose transporter *SLC2A5* mRNA was increased in IFN-γ-induced intestinal epithelial T84 cells, and IPA intervention reversed *SLC2A5* mRNA expression (11).

IPA Suppresses Intestinal Immune Response

Impaired intestinal barrier function and increased leakage of intestinal-derived antigens may lead to visceral lipid deposition and metabolic dysfunction (87). Serum IPA was reported to be decreased by approximately 60% in patients with active inflammatory bowel disease compared with that in healthy controls. During the recovery period of inflammatory bowel disease, the level of IPA in the serum gradually recovered (27, 88).

Administration of IPA showed significant induction of IL-10 receptor protein 1 expression in cultured intestinal epithelial cells T84 (27), based on a close correlation between epithelial IL-10 receptors and the maintenance and recovery of epithelial barrier function (89), which further supported the role of IPA in the maintenance of intestinal immunity.

Recent studies have suggested that IPA is an endogenous ligand for intestinal PXR. IPA induces the transcription of PXR target genes *Mdr1*, *Cyp3a11*, and *Ugt1a1* mRNA *in vivo* (82). However, IPA alone is a weak human PXR ligand (82). Inoculated *Clostridium sporogenes* in germ-free mice accompanied with L-Trp-supplemented diets promoted the production of IPA to protect mice from dextran sulfate sodium-induced colitis through the PXR pathway (82). Studies have also confirmed that IPA improves intestinal permeability (FITC-dextran permeability) in a colitis (indomethacin-induced) mouse model with intestinal barrier defects. Intestinal *TNF-α* mRNA expression and p38-MAPK protein phosphorylation were inhibited, while in PXR-deficient ($Nr1i2^{-/-}$) mice, the benefits of IPA were inhibited, suggesting that IPA improved the intestinal barrier *via* the PXR pathway (82). Furthermore, IPA can modulate vascular function by modulating PXR activity, and IPA exposure reduces the vasodilatory responses of nitric oxide-mediated muscarinic and protease-activated receptor 2-stimulated mouse aortic tissue (90).

In another study, IPA was shown to be an agonist of the aromatic meridian receptor (Ahr) of a commensal bacterial product (91), and Ahr activation was beneficial to the maintenance of intestinal homeostasis and the regulation of immunity (92, 93). Therefore, these studies indicated that promoting IPA formation by bacteria or the direct administration of IPA is beneficial for inflammatory bowel disease.

CONCLUSION

The intestinal microflora is a diverse microbial community that encodes functional genes several orders of magnitude higher than the human genome and can regulate human health (94). With the development of metabolomics, intestinal microbial metabolites play an increasingly important role in regulating host health and disease; however, the disturbance of metabolites is related to multiple chronic diseases (95). Therefore, research on bacteria-derived metabolites offers the possibility of

personalized medicine for chronic diseases with complex pathogenesis. The study found that IPA, a metabolite produced by Trp under the action of intestinal microbes, was correlated with the occurrence and development of metabolic diseases (**Figure 2**). Metabolic diseases such as obesity, T2D, NAFLD, and CVD have been reported. The IPA content in the peripheral region was significantly consumed. After 3 months of bariatric surgery, it recovered, suggesting that IPA might be a potential biomarker for metabolic diseases. However, further studies have shown that IPA could be a potential biomarker of metabolic illnesses (**Table 1**). The intervention with IPA reduced the body weight and peripheral fat content; improved insulin resistance, liver lipid deposition, and peripheral blood lipid content; and maintained intestinal homeostasis, thereby improving metabolic syndrome (**Table 2**). The metabolic benefit mechanism of IPA may be predominantly related to its strong oxidant effect, which has an excellent antagonistic effect on chronic inflammation caused by metabolic diseases. Moreover, as a bacterial-derived metabolite (**Table 3**), IPA exerts its beneficial effects in regulating intestinal immune responses through Ahr and PXR ligand. Intestinal bacteria play an important role in the pathogenesis of metabolic diseases. In future research, we need to pay attention to the secondary metabolites produced by the interaction between IPA and the bacterial flora and its remote target organs to further study the mechanism of IPA.

However, the beneficial effects of IPA are all based on the HFD-induced NAFLD model mice, and the opposite result has been found in other models. In CCL4-induced liver fibrosis model mice, IPA aggravated CCL4-induced liver fibrosis injury through transforming growth factor-β1 (TGF-β1) and the Smad signaling pathway (98). Therefore, multiple models are required to verify the potential beneficial effects of IPA on metabolic diseases. At present, the therapeutic effects of IPA are primarily concentrated in basic animal experiments, and no clinical experiments have been performed. Therefore, an in-depth study on the toxicity and safe use of IPA is necessary to provide a sufficient theoretical basis for the development and utilization of IPA.

Furthermore, to fully exploit the potential of the intestinal microbiota in disease prevention, we need to understand in greater depth how dietary components and host genetics affect IPA production. Finally, these findings are converted into clinical practice and developed into clinical methods that can be widely used to predict the prognosis and outcome of diseases and even have diagnostic effects on some metabolic disorders. While

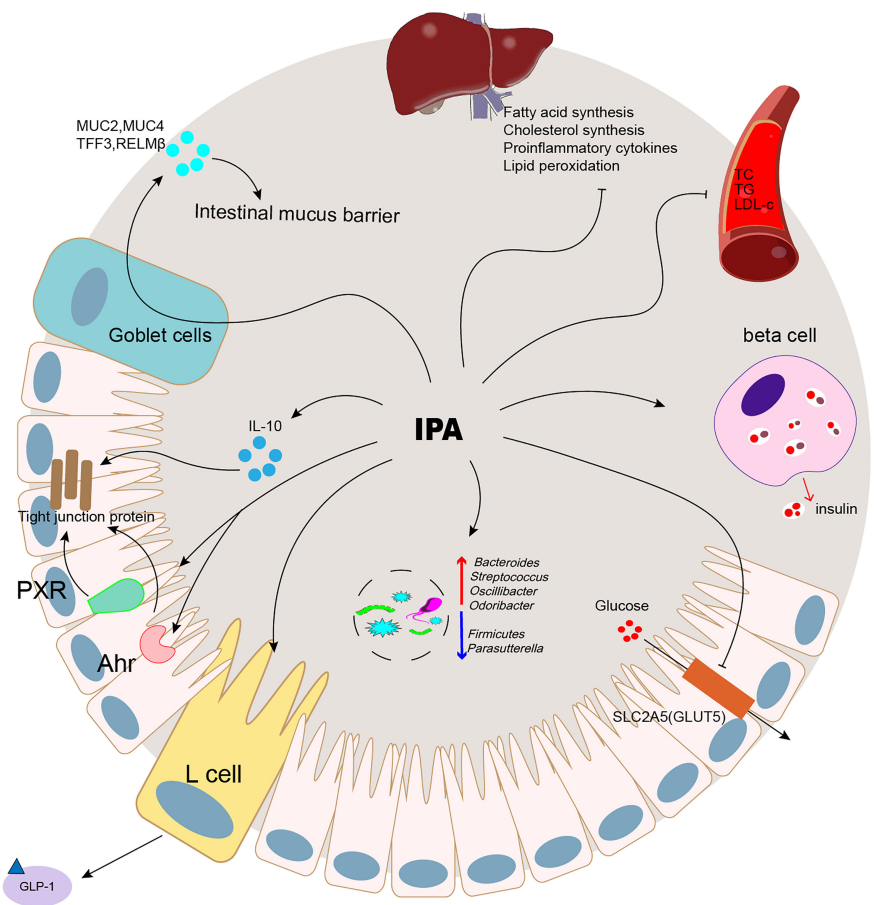

FIGURE 2 | IPA was correlated with the occurrence and development of metabolic diseases.

TABLE 1 | The relationship between IPA and metabolic diseases.

Disease	Research object	Clinical trials number	Study population nation	Sample	Detection method	Main research results	Reference
Liver fibrosis	A total of 233 patients (BMI 43.1 ± 5.4 kg/m^2) undergoing bariatric surgery with detailed liver histology were included. Normal liver (n = 79), Simple steatosis (n = 40), NASH (n = 45)	NA	Finland (Europe)	Serum	LC-MS	IPA levels were decreased in liver fibrosis compared to those without fibrosis (p = 0.039 for all participants; p = 0.013 for 153 individuals without T2D); IPA levels negatively correlated with lobular inflammation (p = 0.039) and fibrosis (p = 0.039); IPA levels negatively correlated with fibrosis signaling genes, including *ITGA3*, *ITGAV*, *LAMC3*, and *COL1A2* mRNA	(13)
T2D	Prospective analysis of 11 circulating Trp metabolites and T2D incidence; up to 9180 participants from 5 cohorts by meta-analysis	NA	Diverse racial/ethnic backgrounds (USA)	Serum	LC-MS	IPA levels positively associated with fiber-rich foods (p = 7.3×10^{-60}); IPA negatively associated with T2D incidence, (Spearman's r = –0.05 to 0.06); IPA showed a potential causal relationship with T2D (genetic causality proportion = 76%, p = 1.6×10^{-24})	(39)
T2D	Total 415 diabetes participants lifestyle (n = 209); control groups (n = 206)	NCT00518167	Finland (Europe)	Serum	HPLC-QQQ-MS/MS	IPA levels inversely associated with incidence of diabetes during the mean 7-year follow-up (odds ratio [confidence interval]: 0.86 [0.73–0.99], p = 0.04); positively correlated with insulin secretion (DI30) during the mean 7 years (β = 0.10, p = 0.06; positively correlated with dietary fiber, r = 0.24, $p = 1 \times 10^{-6}$); inversely associated with serum hsCRP levels (r = –0.22, p = 0.0001); inversely associated with BMI (p = 0.001)	(21)
T2D	Two groups of individuals who took part in the Finnish Diabetes Prevention Study Those who either early developed T2D early (n = 96) or did not develop T2D (n = 104) within the 15-year follow-up	NCT00518167	Finland, Sweden (Europe)	Serum	LC-MS	IPA levels inversely associated with T2D incidence (OR: 0.80 [0.70, 0.93], p = 0.003); positively correlated with insulin secretion (β = 0.25 [0.06–0.44], p = 0.011); inversely associated with high hsCRP levels (r = -0.23, p = 0.006); high IPA level inversely associated with the likelihood of developing T2D during the 5-year follow-up (OR: 0.31 [0.12– 0.76], p = 0.01)	(12)
Advanced atherosclerosis	Advanced atherosclerosis cohort (n = 100); the control cohort (n = 22) were age- and sex-matched participants	NA	USA	Serum	LC-MS	IPA content decreases in advanced atherosclerosis and carotid stenosis subgroups. IPA levels inversely associated with advanced atherosclerosis incidence (OR, 0.27; 95% CI, 0.019–0.91; p = 02)	(14)
Obesity	obese adults (n = 85, BMI = 40.48); non-obese controls (n = 42, BMI = 24.03)	Registration numbers 2010/36 and 2016/40 for obese and non-obese participants, respectively	France (Europe)	Serum	UHPLC-ESI-MS/MS	IPA content decreases in obesity (F[1,122] =13.89, p<0.001); IPA levels inversely associated with BMI (data not shown); inversely associated with serum levels Of hsCRP (β = –0.268 0.261, p < 0.05) hsIL-6 levels (β = –0.244, P < 0.05)	(40)

(Continued)

TABLE 1 | Continued

Disease	Research object	Clinical trials number	Study population nation	Sample	Detection method	Main research results	Reference
Obesity	A total of 117 overweight (BMI > 24 kg/m^2) adults were randomized into two groups. One group was provided fried meat four times per week (n = 59); one group of 58 participants had no fried meat intake (n = 58).	ChiCTR1900028562	China (Asia)	Fecal	UPLC-MS/MS	IPA content decreases in fried meat group (p FDR < 0.05); IPA levels inversely associated with insulin resistance index (r = 0.243); inversely associated with serum LPS levels (r = 0.243); IPA levels inversely associated with serum TNF-a levels (r = 0.436)	(36)
Obesity	Food addiction (n = 19,BMI = 35.6); No food addiction (n = 86)	IRB # 16–000187	USA	Fecal	Mass spectroscopy	IPA was inversely associated with food addiction in patients with obesity (Cohen's d = 0.74, p = 0.045); inversely associated with abundance of genus Prevotella; positively correlated with abundance of *Akkermansia muciniphila* and *Bacteroides*	(41)
Obese T2D	Lean (n = 7); obese T2D participants either before (n = 9) or after RYGB surgery (1 week post-surgery [n=9]; 3 months post-surgery [n=7])	NA	NA	Serum	LC-MS	IPA content decreased in fried meat group obese T2D; unchanged 1 week after RYGB surgery; increased 3 months after RYGB surgery	(11)
Chronic kidney disease	The estimated glomerular filtration rate (eGFR) rapid decline 20% group (n = 10) vs. control group (n = 10) was defined as having a yearly eGFR decline < 5%; the CKD group (n = 140) vs. the normal group (n = 144).	IRB no. 100-2243A3	China	Serum	NA	IPA content decreased in the CKD group; IPA content decreased in patients with rapid decline 20% group	(53)
UC	Healthy controls (n = 20); participants with active ulcerative colitis (UC; n = 15); participants with UC in remission (n = 20)	NA	NA	Serum	EC-HPLC	Serum IPA was decreased by approximately 60% in participants with active UC compared to healthy controls (p < 0.05); IPA content returned to normal in participants with UC in remission	(27)

NA, Not Available.

TABLE 2 | Benefits of IPA in metabolic diseases.

Disease	Modeling	IPA concentration	Result	Mechanism	References
Liver fibrosis	LX-2 cell co-treatment with TGF-β1	100 μM	IPA treatment with 100 μM of IPA also significantly reduced LX-2 cell migration	IPA treatment reduced activation of LX-2 cells stimulated by TGF-β1; reduced hepatic stellate cell activation gene expression of *COL1A2, aSMA, ITGA3* mRNA	(13)
T2D	Male Sprague–Dawley rats (diet not shown)	Mean intake 27.3 mg/kg/day	IPA was associated with a reduction in fasting blood glucose concentration by 0.42 mM (95% CI: 0.11–0.73; t22 = 2.78; $p = 0.01$); IPA treatment reduced plasma insulin level (t19 = 2.26; $p = 04$) and the HOMA index (t19 = 2.46; $p = 02$)	NA	(15)
T2D cognitive decline	db/db mice fed with regular chow and pure water	Mice were intraperitoneally injected with IPA (10 mg kg/day) for 14 days	IPA treatment significantly attenuated cognitive deficits in diabetic mice; improved insulin sensitivity; enhanced mitochondrial biogenesis, and protected the ultrastructure of synapses.	IPA has been reported to protect against Aβ-induced neuronal death and restore mitochondrial function	(61)
Obesity	High-fat diet (HFD)-fed mice	20 mg kg^{-1} po. for 4 days	IPA treatment did not change body weight; significantly attenuated intestinal permeability; and reduced LPS levels.	IPA treatment reduced protein expression of SLC2A5 (GLUT5, facilitated fructose transporter) and ALDOB (fructose-1,6-bisphosphate aldolase glycolytic enzyme) in T84 cells	(40)
NAFLD	Sprague–Dawley rats; rats were fed a standard chow diet or a HFD	Gavage with IPA (20 mg/kg/day) for 8 weeks	IPA treatment modulated the microbiota composition in the gut and inhibited microbial dysbiosis in rats fed a HFD.	IPA induced the expression of tight junction proteins, such as ZO-1 and occludin, and maintained intestinal epithelium homeostasis, leading to a reduction in plasma endotoxin levels. IPA inhibited NF-κB signaling and reduced the levels of proinflammatory cytokines, such as *TNFα, IL-1β*, and *IL-6*, in response to endotoxin in macrophages to repress hepatic inflammation and liver injury	(17)
NASH-HCC	Cholesterol-induced hepatocyte cell line LO2, and NASH–HCC cell lines HKCI-2 and HKCI-10	IPA (10 μM,100 μM)	IPA treatment suppressed cholesterol-induced lipid accumulation in LO2 cells, and cell proliferation in NAFLD-HCC cell lines (HKCI-2 and HKCI-10).	NA	(50)
HCC	Rat hepatic microsomal membrane incubated with FeCl(3) (0.2 mM), ADP (1.7 mM), and NADPH (0.2 mM) to induce oxidative damage	IPA (10, 3, 2, 1, 0.3, 0.1, 0.01 or 0.001 mM)	IPA may be used as a pharmacological agent to protect against iron-induced oxidative damage to membranes and, potentially, against carcinogenesis.	IPA, when used in concentrations of 10, 3, or 2 mM, increased membrane fluidity; IPA at concentrations of 10, 3, 2, or 1 mM completely prevented a decrease in membrane fluidity due to Fe(3+); the enhanced lipid peroxidation due to Fe(3+) was prevented by IPA only at the highest concentration (10 mM)	(67)
Hyperlipidemia	Male and female ICR mice	Orally administered IPA (100 mg/kg) for 60 days	IPA treatment significantly reduced the body weight gain in mice; decreased serum levels of TC, LDL-c, and TG.	IPA dose-dependently decreased the transcription of the key genes involved in fatty acid (*SREBP1c* and *FAS*) and cholesterol biosynthesis (*SREBP2* and *HMGR*)	(16)
IBD	$Nr1i2^{+/+}$ and $Nr1i2^{-/-}$ mice using an inflammation-based barrier defect (indomethacin) model	Mice were gavaged with 10, 20, and 40 mg/kg IPA for 4 days	IPA treatment significantly reduced FITC dextran permeability in $Nr1i2^{+/+}$ mice, but not in $Nr1i2^{-/-}$, mice; IPA notably decreased TNF-a mRNA expression more in the $Nr1i2^{+/+}$ mice (3.73-fold) intestinal epithelium relative to $Nr1i2^{-/-}$ mice (1.72-fold)	IPA Protects against indomethacin-induced intestinal injury *via* PXR and TLR4	(82)
IBD	C57BL/6 mice were administered 2.5% (wt/vol) dextran sodium sulfate (DSS)	IPA 0.1 mg/ml was administered to water for 9 days	Serum indole and IPA levels were significantly decreased in actively colitic animals ($p < 0.05$)	DSS colitic mice displayed significantly lower levels of IPA ($p < 0.01$); IPA-treated animals displayed significantly less reduction in colon length ($p < 0.05$); IPA-treated mice had decreased colonic tissue cytokine levels: IFN-γ ($p < 0.05$), TNF-α ($p < 0.01$), IL-1β ($p < 0.05$) mRNA	(27)

NA, Not Available.

TABLE 3 | Microorganisms that produce IPA.

Microorganisms	Relation	References
Escherichia coli	Produce	(96)
E. coli, Bacillus spp., and *Clostridium* spp.	Produce	(97)
Clostridium sporogenes(ATCC 15579)	Produce	(30)
Akkermansia and *Clostridium* XlVa	Correlation exists	(16)
Peptostreptococcus anaerobius CC14N	Produce	(25)
Clostridium cadaveris CC88A		
Clostridium cadaveris CC44 001G		
Clostridium cadaveris CC40 001C		
Clostridioides caloritolerans	Produce	(29)
Clostridioides. Botulinum		

leveraging metabolomics poses significant challenges in promoting human health, past studies have demonstrated that certain metabolites have considerable potential for the treatment of human diseases.

AUTHOR CONTRIBUTIONS

BZ and MJ: writing—original draft. These authors have contributed equally to this work. YS and JZ: writing—review and editing. WD and JS: funding acquisition. All authors contributed to the article and approved the submitted version.

FUNDING

This work was supported by the National Natural Science Foundation of China (No. 81570524); Key Medical Disciplines of Hangzhou; Zhejiang Province Basic Public Welfare Research Program Project "Relationship between cognitive impairment and gut microbial dysbiosis in patients with non-alcoholic fatty liver disease" (GF20H030035).

REFERENCES

1. Bril F, Cusi K. Nonalcoholic Fatty Liver Disease: The New Complication of Type 2 Diabetes Mellitus. *Endocrinol Metab Clinics North Am* (2016) 45 (4):765–81. doi: 10.1016/j.ecl.2016.06.005
2. Vilar-Gomez E, Calzadilla-Bertot L, Wai-Sun Wong V, Castellanos M, Aller-de la Fuente R, Metwally M, et al. Fibrosis Severity as a Determinant of Cause-Specific Mortality in Patients With Advanced Nonalcoholic Fatty Liver Disease: A Multi-National Cohort Study. *Gastroenterology* (2018) 155 (2):443–457.e17. doi: 10.1053/j.gastro.2018.04.034
3. Lim S, Kim J, Targher G. Links Between Metabolic Syndrome and Metabolic Dysfunction-Associated Fatty Liver Disease. *Trends Endocrinol Metabolism: TEM* (2021) 32(7):500–14. doi: 10.1016/j.tem.2021.04.008
4. Yoneda M, Yamamoto T, Honda Y, Imajo K, Ogawa Y, Kessoku T, et al. Risk of Cardiovascular Disease in Patients With Fatty Liver Disease as Defined From the Metabolic Dysfunction Associated Fatty Liver Disease or Nonalcoholic Fatty Liver Disease Point of View: A Retrospective Nationwide Claims Database Study in Japan. *J Gastroenterol* (2021) 56 (11):1022–32. doi: 10.1007/s00535-021-01828-6
5. Aguilar M, Bhuket T, Torres S, Liu B, Wong RJ. Prevalence of the Metabolic Syndrome in the United States, 2003-2012. *JAMA* (2015) 313(19):1973–4. doi: 10.1001/jama.2015.4260
6. Sharpton SR, Schnabl B, Knight R, Loomba R. Current Concepts, Opportunities, and Challenges of Gut Microbiome-Based Personalized Medicine in Nonalcoholic Fatty Liver Disease. *Cell Metab* (2021) 33(1):21–32. doi: 10.1016/j.cmet.2020.11.010
7. Fan Y, Pedersen O. Gut Microbiota in Human Metabolic Health and Disease. *Nat Rev Microbiol* (2021) 19(1):55–71. doi: 10.1038/s41579-020-0433-9
8. Bishai JD, Palm NW. Small Molecule Metabolites at the Host-Microbiota Interface. *J Immunol (Baltimore Md 1950)* (2021) 207(7):1725–33. doi: 10.4049/jimmunol.2100528
9. Koh A, Bäckhed F. From Association to Causality: The Role of the Gut Microbiota and Its Functional Products on Host Metabolism. *Mol Cell* (2020) 78(4):584–96. doi: 10.1016/j.molcel.2020.03.005
10. Nicholson JK, Holmes E, Kinross J, Burcelin R, Gibson G, Jia W, et al. Host-Gut Microbiota Metabolic Interactions. *Science* (2012) 336(6086):1262–7. doi: 10.1126/science.1223813
11. Jennis M, Cavanaugh CR, Leo GC, Mabus JR, Lenhard J, Hornby PJ. Microbiota-Derived Tryptophan Indoles Increase After Gastric Bypass Surgery and Reduce Intestinal Permeability *In Vitro* and In Vivo. *Neurogastroenterol Motil* (2018) 30(2):e13178. doi: 10.1111/nmo.13178
12. de Mello VD, Paananen J, Lindstrom J, Lankinen MA, Shi L, Kuusisto J, et al. Indolepropionic Acid and Novel Lipid Metabolites are Associated With a Lower Risk of Type 2 Diabetes in the Finnish Diabetes Prevention Study. *Sci Rep* (2017) 7:46337. doi: 10.1038/srep46337
13. Sehgal R, Ilha M, Vaittinen M, Kaminska D, Männistö V, Kärjä V, et al. Indole-3-Propionic Acid, a Gut-Derived Tryptophan Metabolite, Associates With Hepatic Fibrosis. *Nutrients* (2021) 13(10):3509. doi: 10.3390/nu13103509
14. Cason CA, Dolan KT, Sharma G, Tao M, Kulkarni R, Helenowski IB, et al. Plasma Microbiome-Modulated Indole- and Phenyl-Derived Metabolites Associate With Advanced Atherosclerosis and Postoperative Outcomes. *J Vasc Surg* (2018) 68(5):1552–1562.e7. doi: 10.1016/j.jvs.2017.09.029
15. Abildgaard A, Elfving B, Hokland M, Wegener G, Lund S. The Microbial Metabolite Indole-3-Propionic Acid Improves Glucose Metabolism in Rats, But Does Not Affect Behaviour. *Arch Physiol Biochem* (2018) 124(4):306–12. doi: 10.1080/13813455.2017.1398262
16. Li Y, Xu W, Zhang F, Zhong S, Sun Y, Huo J, et al. The Gut Microbiota-Produced Indole-3-Propionic Acid Confers the Antihyperlipidemic Effect of Mulberry-Derived 1-Deoxynojirimycin. *mSystems* (2020) 5(5):e00313–20. doi: 10.1128/mSystems.00313-20
17. Zhao ZH, Xin FZ, Xue Y, Hu Z, Han Y, Ma F, et al. Indole-3-Propionic Acid Inhibits Gut Dysbiosis and Endotoxin Leakage to Attenuate Steatohepatitis in Rats. *Exp Mol Med* (2019) 51(9):103. doi: 10.1038/s12276-019-0304-5
18. Hendrikx T, Schnabl B. Indoles: Metabolites Produced by Intestinal Bacteria Capable of Controlling Liver Disease Manifestation. *J Internal Med* (2019) 286 (1):32–40. doi: 10.1111/joim.12892
19. Danaceau JP, Anderson GM, McMahon WM, Crouch DJ. A Liquid Chromatographic-Tandem Mass Spectrometric Method for the Analysis of Serotonin and Related Indoles in Human Whole Blood. *J Analytical Toxicol* (2003) 27(7):440–4. doi: 10.1093/jat/27.7.440
20. Negatu DA, Gengenbacher M, Dartois V, Dick T. Indole Propionic Acid, an Unusual Antibiotic Produced by the Gut Microbiota, With Anti-Inflammatory and Antioxidant Properties. *Front Microbiol* (2020) 11:575586. doi: 10.3389/fmicb.2020.575586
21. Tuomainen M, Lindström J, Lehtonen M, Auriola S, Pihlajamäki J, Peltonen M, et al. Associations of Serum Indolepropionic Acid, a Gut Microbiota Metabolite, With Type 2 Diabetes and Low-Grade Inflammation in High-Risk Individuals. *Nutr Diabetes* (2018) 8(1):35. doi: 10.1038/s41387-018-0046-9
22. Grifka-Walk HM, Jenkins BR, Kominsky DJ. Amino Acid Trp: The Far Out Impacts of Host and Commensal Tryptophan Metabolism. *Front Immunol* (2021) 12:653208. doi: 10.3389/fimmu.2021.653208
23. Bender DA. Biochemistry of Tryptophan in Health and Disease. *Mol aspects Med* (1983) 6(2):101–97. doi: 10.1016/0098-2997(83)90005-5
24. Keszthelyi D, Troost FJ, Masclee AA. Understanding the Role of Tryptophan and Serotonin Metabolism in Gastrointestinal Function. *Neurogastroenterol Motil Off J Eur Gastrointestinal Motil Soc* (2009) 21(12):1239–49. doi: 10.1111/j.1365-2982.2009.01370.x
25. Dodd D, Spitzer MH, Van Treuren W, Merrill BD, Hryckowian AJ, Higginbottom SK, et al. A Gut Bacterial Pathway Metabolizes Aromatic

Amino Acids Into Nine Circulating Metabolites. *Nature* (2017) 551 (7682):648–52. doi: 10.1038/nature24661
26. Kim J, Park W. Indole Inhibits Bacterial Quorum Sensing Signal Transmission by Interfering With Quorum Sensing Regulator Folding. *Microbiol (Reading England)* (2013) 159(Pt 12):2616–25. doi: 10.1099/mic.0.070615-0
27. Alexeev E, Lanis J, Kao D, Campbell E, Kelly C, Battista K, et al. Microbiota-Derived Indole Metabolites Promote Human and Murine Intestinal Homeostasis Through Regulation of Interleukin-10 Receptor. *Am J Pathol* (2018) 188(5):1183–94. doi: 10.1016/j.ajpath.2018.01.011
28. Pavlova T, Vidova V, Bienertova-Vasku J, Janku P, Almasi M, Klanova J, et al. Urinary Intermediates of Tryptophan as Indicators of the Gut Microbial Metabolism. *Analytica Chimica Acta* (2017) 987:72–80. doi: 10.1016/j.aca.2017.08.022
29. Elsden SR, Hilton MG, Waller JM. The End Products of the Metabolism of Aromatic Amino Acids by Clostridia. *Arch Microbiol* (1976) 107(3):283–8. doi: 10.1007/bf00425340
30. Wikoff WR, Anfora AT, Liu J, Schultz PG, Lesley SA, Peters EC, et al. Metabolomics Analysis Reveals Large Effects of Gut Microflora on Mammalian Blood Metabolites. *Proc Natl Acad Sci USA* (2009) 106 (10):3698–703. doi: 10.1073/pnas.0812874106
31. Nishizawa T, Aldrich CC, Sherman DH. Molecular Analysis of the Rebeccamycin L-Amino Acid Oxidase From Lechevalieria Aerocolonigenes ATCC 39243. *J bacteriology* (2005) 187(6):2084–92. doi: 10.1128/jb.187.6.2084-2092.2005
32. Gartner SN, Aidney F, Klockars A, Prosser C, Carpenter EA, Isgrove K, et al. Intragastric Preloads of L-Tryptophan Reduce Ingestive Behavior *via* Oxytocinergic Neural Mechanisms in Male Mice. *Appetite* (2018) 125:278–86. doi: 10.1016/j.appet.2018.02.015
33. Konopelski P, Konop M, Gawrys-Kopczynska M, Podsadni P, Szczepanska A, Ufnal MJN. Indole-3-Propionic Acid, a Tryptophan-Derived Bacterial Metabolite, Reduces Weight Gain in Rats. *Nutrients* (2019) 11(3):591. doi: 10.3390/nu11030591
34. Panagiotakos DB, Pitsavos C, Arvaniti F, Stefanadis C. Adherence to the Mediterranean Food Pattern Predicts the Prevalence of Hypertension, Hypercholesterolemia, Diabetes and Obesity, Among Healthy Adults; the Accuracy of the MedDietScore. *Prev Med* (2007) 44(4):335–40. doi: 10.1016/j.ypmed.2006.12.009
35. Schulze MB, Hoffmann K, Manson JE, Willett WC, Meigs JB, Weikert C, et al. Dietary Pattern, Inflammation, and Incidence of Type 2 Diabetes in Women. *Am J Clin Nutr* (2005) 82(3):675–84; quiz 714-5. doi: 10.1093/ajcn.82.3.675
36. Gao J, Guo X, Wei W, Li R, Hu K, Liu X, et al. The Association of Fried Meat Consumption With the Gut Microbiota and Fecal Metabolites and Its Impact on Glucose Homoeostasis, Intestinal Endotoxin Levels, and Systemic Inflammation: A Randomized Controlled-Feeding Trial. *Diabetes Care* (2021) 44(9):1970–9. doi: 10.2337/dc21-0099
37. Zhu C, Sawrey-Kubicek L, Beals E, Rhodes CH, Houts HE, Sacchi R, et al. Human Gut Microbiome Composition and Tryptophan Metabolites Were Changed Differently by Fast Food and Mediterranean Diet in 4 Days: A Pilot Study. *Nutr Res* (2020) 77:62–72. doi: 10.1016/j.nutres.2020.03.005
38. Leeming ER, Johnson AJ, Spector TD, Le Roy CI. Effect of Diet on the Gut Microbiota: Rethinking Intervention Duration. *Nutrients* (2019) 11(12):2862. doi: 10.3390/nu11122862
39. Qi Q, Li J, Yu B, Moon JY, Chai JC, Merino J, et al. Host and Gut Microbial Tryptophan Metabolism and Type 2 Diabetes: An Integrative Analysis of Host Genetics, Diet, Gut Microbiome and Circulating Metabolites in Cohort Studies. *Gut* (2021) gutjnl-2021–324053. doi: 10.1136/gutjnl-2021-324053
40. Cussotto S, Delgado I, Anesi A, Dexpert S, Aubert A, Beau C, et al. Tryptophan Metabolic Pathways Are Altered in Obesity and Are Associated With Systemic Inflammation. *Front Immunol* (2020) 11:557. doi: 10.3389/fimmu.2020.00557
41. Dong TS, Mayer EA, Osadchiy V, Chang C, Katzka W, Lagishetty V, et al. A Distinct Brain-Gut-Microbiome Profile Exists for Females With Obesity and Food Addiction. *Obes (Silver Spring Md.)* (2020) 28(8):1477–86. doi: 10.1002/oby.22870
42. Schauer PR, Kashyap SR, Wolski K, Brethauer SA, Kirwan JP, Pothier CE, et al. Bariatric Surgery Versus Intensive Medical Therapy in Obese Patients With Diabetes. *N Engl J Med* (2012) 366(17):1567–76. doi: 10.1056/NEJMoa1200225
43. Mercer KE, Yeruva L, Pack L, Graham JL, Stanhope KL, Chintapalli SV, et al. Xenometabolite Signatures in the UC Davis Type 2 Diabetes Mellitus Rat Model Revealed Using a Metabolomics Platform Enriched With Microbe-Derived Metabolites. American Journal of Physiology. *Gastrointestinal Liver Physiol* (2020) 319(2):G157–g169. doi: 10.1152/ajpgi.00105.2020
44. Huang DQ, El-Serag HB, Loomba R. Global Epidemiology of NAFLD-Related HCC: Trends, Predictions, Risk Factors and Prevention. *Nat Rev Gastroenterol Hepatol* (2021) 18(4):223–38. doi: 10.1038/s41575-020-00381-6
45. Ioannou GN. The Role of Cholesterol in the Pathogenesis of NASH. *Trends Endocrinol Metab* (2016) 27(2):84–95. doi: 10.1016/j.tem.2015.11.008
46. McGettigan B, McMahan R, Orlicky D, Burchill M, Danhorn T, Francis P, et al. Dietary Lipids Differentially Shape Nonalcoholic Steatohepatitis Progression and the Transcriptome of Kupffer Cells and Infiltrating Macrophages. *Hepatology* (2019) 70(1):67–83. doi: 10.1002/hep.30401
47. Van Rooyen DM, Larter CZ, Haigh WG, Yeh MM, Ioannou G, Kuver R, et al. Hepatic Free Cholesterol Accumulates in Obese, Diabetic Mice and Causes Nonalcoholic Steatohepatitis. *Gastroenterology* (2011) 141(4):1393–403, 1403.e1-5. doi: 10.1053/j.gastro.2011.06.040
48. Jaeschke. Reactive oxygen H. And Mechanisms of Inflammatory Liver Injury: Present Concepts. *J Gastroenterol Hepatol* (2011) 26(Suppl 1):173–9. doi: 10.1111/j.1440-1746.2010.06592.x
49. Wong RJ, Cheung R, Ahmed A. Nonalcoholic Steatohepatitis is the Most Rapidly Growing Indication for Liver Transplantation in Patients With Hepatocellular Carcinoma in the U. *S Hepatol* (2014) 59(6):2188–95. doi: 10.1002/hep.26986
50. Zhang X, Coker OO, Chu ES, Fu K, Lau HCH, Wang YX, et al. Dietary Cholesterol Drives Fatty Liver-Associated Liver Cancer by Modulating Gut Microbiota and Metabolites. *Gut* (2021) 70(4):761–74. doi: 10.1136/gutjnl-2019-319664
51. Angulo P, Kleiner DE, Dam-Larsen S, Adams LA, Bjornsson ES, Charatcharoenwitthaya P, et al. Liver Fibrosis, But No Other Histologic Features, Is Associated With Long-Term Outcomes of Patients With Nonalcoholic Fatty Liver Disease. *Gastroenterology* (2015) 149(2):389–97.e10. doi: 10.1053/j.gastro.2015.04.043
52. Hagström H, Nasr P, Ekstedt M, Hammar U, Stål P, Hultcrantz R, et al. Fibrosis Stage But Not NASH Predicts Mortality and Time to Development of Severe Liver Disease in Biopsy-Proven NAFLD. *J Hepatol* (2017) 67(6):1265–73. doi: 10.1016/j.jhep.2017.07.027
53. Sun CY, Lin CJ, Pan HC, Lee CC, Lu SC, Hsieh YT, et al. Clinical Association Between the Metabolite of Healthy Gut Microbiota, 3-Indolepropionic Acid and Chronic Kidney Disease. *Clin Nutr (Edinburgh Scotland)* (2019) 38 (6):2945–8. doi: 10.1016/j.clnu.2018.11.029
54. Yisireyili M, Takeshita K, Saito S, Murohara T, Niwa T. Indole-3-Propionic Acid Suppresses Indoxyl Sulfate-Induced Expression of Fibrotic and Inflammatory Genes in Proximal Tubular Cells. *Nagoya J Med Sci* (2017) 79(4):477–86. doi: 10.18999/nagjms.79.4.477
55. Hosohata K, Jin D, Takai S. *In Vivo* and *In Vitro* Evaluation of Urinary Biomarkers in Ischemia/Reperfusion-Induced Kidney Injury. *Int J Mol Sci* (2021) 22(21):11448. doi: 10.3390/ijms222111448
56. Xiao HW, Cui M, Li Y, Dong JL, Zhang SQ, Zhu CC, et al. Gut Microbiota-Derived Indole 3-Propionic Acid Protects Against Radiation Toxicity *via* Retaining Acyl-CoA-Binding Protein. *Microbiome* (2020) 8(1):69. doi: 10.1186/s40168-020-00845-6
57. Behera J, Ison J, Voor MJ, Tyagi N. Probiotics Stimulate Bone Formation in Obese Mice *via* Histone Methylations. *Theranostics* (2021) 11(17):8605–23. doi: 10.7150/thno.63749
58. Poeggeler B, Pappolla MA, Hardeland R, Rassoulpour A, Hodgkins PS, Guidetti P, et al. Indole-3-Propionate: A Potent Hydroxyl Radical Scavenger in Rat Brain. *Brain Res* (1999) 815(2):382–8. doi: 10.1016/s0006-8993(98)01027-0
59. Bendheim PE, Poeggeler B, Neria E, Ziv V, Pappolla MA, Chain DG. Development of Indole-3-Propionic Acid (OXIGON) for Alzheimer's Disease. *J Mol Neurosci MN* (2002) 19(1-2):213–7. doi: 10.1007/s12031-002-0036-0
60. Gundu C, Arruri VK, Sherkhane B, Khatri DK, Singh SB. Indole-3-Propionic Acid Attenuates High Glucose Induced ER Stress Response and Augments Mitochondrial Function by Modulating PERK-IRE1-ATF4-CHOP Signalling in Experimental Diabetic Neuropathy. *Arch Physiol Biochem* (2022), 1–14. doi: 10.1080/13813455.2021.2024577
61. Liu Z, Dai X, Zhang H, Shi R, Hui Y, Jin X, et al. Gut Microbiota Mediates Intermittent-Fasting Alleviation of Diabetes-Induced Cognitive Impairment. *Nat Commun* (2020) 11(1):855. doi: 10.1038/s41467-020-14676-4

62. Chyan YJ, Poeggeler B, Omar RA, Chain DG, Frangione B, Ghiso J, et al. Potent Neuroprotective Properties Against the Alzheimer Beta-Amyloid by an Endogenous Melatonin-Related Indole Structure, Indole-3-Propionic Acid. *J Biol Chem* (1999) 274(31):21937–42. doi: 10.1074/jbc.274.31.21937
63. Dragicevic N, Copes N, O'Neal-Moffitt G, Jin J, Buzzeo R, Mamcarz M, et al. Melatonin Treatment Restores Mitochondrial Function in Alzheimer's Mice: A Mitochondrial Protective Role of Melatonin Membrane Receptor Signaling. *J pineal Res* (2011) 51(1):75–86. doi: 10.1111/j.1600-079X.2011.00864.x
64. Chimerel C, Emery E, Summers DK, Keyser U, Gribble FM, Reimann F. Bacterial Metabolite Indole Modulates Incretin Secretion From Intestinal Enteroendocrine L Cells. *Cell Rep* (2014) 9(4):1202–8. doi: 10.1016/j.celrep.2014.10.032
65. Garber AJ. Incretin Effects on β-Cell Function, Replication, and Mass: The Human Perspective. *Diabetes Care* (2011) 34 Suppl 2(Suppl 2):S258–63. doi: 10.2337/dc11-s230
66. Lutz TA, Meyer U. Amylin at the Interface Between Metabolic and Neurodegenerative Disorders. *Front Neurosci* (2015) 9:216. doi: 10.3389/fnins.2015.00216
67. Karbownik M, Reiter RJ, Garcia JJ, Cabrera J, Burkhardt S, Osuna C, et al. Indole-3-Propionic Acid, a Melatonin-Related Molecule, Protects Hepatic Microsomal Membranes From Iron-Induced Oxidative Damage: Relevance to Cancer Reduction. *J Cell Biochem* (2001) 81(3):507–13. doi: 10.1002/1097-4644(20010601)81:3<507::AID-JCB1064>3.0.CO;2-M
68. Karbownik M, Gitto E, Lewiński A, Reiter RJ. Relative Efficacies of Indole Antioxidants in Reducing Autoxidation and Iron-Induced Lipid Peroxidation in Hamster Testes. *J Cell Biochem* (2001) 81(4):693–9. doi: 10.1002/jcb.1100
69. Bäckhed F, Ding H, Wang T, Hooper LV, Koh GY, Nagy A, et al. The Gut Microbiota as an Environmental Factor That Regulates Fat Storage. *Proc Natl Acad Sci U.S.A.* (2004) 101(44):15718–23. doi: 10.1073/pnas.0407076101
70. Bäckhed F, Ley RE, Sonnenburg JL, Peterson DA, Gordon JI. Host-Bacterial Mutualism in the Human Intestine. *Science* (2005) 307(5717):1915–20. doi: 10.1126/science.1104816
71. Henao-Mejia J, Elinav E, Jin C, Hao L, Mehal WZ, Strowig T, et al. Inflammasome-Mediated Dysbiosis Regulates Progression of NAFLD and Obesity. *Nature* (2012) 482(7384):179–85. doi: 10.1038/nature10809
72. Hullar MAJ, Jenkins IC, Randolph TW, Curtis KR, Monroe KR, Ernst T, et al. Associations of the Gut Microbiome With Hepatic Adiposity in the Multiethnic Cohort Adiposity Phenotype Study. *Gut Microbes* (2021) 13(1):1965463. doi: 10.1080/19490976.2021.1965463
73. Menni C, Hernandez MM, Vital M, Mohney RP, Spector TD, Valdes AM. Circulating Levels of the Anti-Oxidant Indoleproprionic Acid are Associated With Higher Gut Microbiome Diversity. *Gut Microbes* (2019) 10(6):688–95. doi: 10.1080/19490976.2019.1586038
74. Ley RE, Bäckhed F, Turnbaugh P, Lozupone CA, Knight RD, Gordon JI. Obesity Alters Gut Microbial Ecology. *Proc Natl Acad Sci USA* (2005) 102(31):11070–5. doi: 10.1073/pnas.0504978102
75. Turnbaugh PJ, Ley RE, Mahowald MA, Magrini V, Mardis ER, Gordon JI. An Obesity-Associated Gut Microbiome With Increased Capacity for Energy Harvest. *Nature* (2006) 444(7122):1027–31. doi: 10.1038/nature05414
76. Krzyściak W, Pluskwa KK, Jurczak A, Kościelniak D. The Pathogenicity of the Streptococcus Genus. *Eur J Clin Microbiol Infect Dis Off Publ Eur Soc Clin Microbiol* (2013) 32(11):1361–76. doi: 10.1007/s10096-013-1914-9
77. Hod K, Dekel R, Aviv Cohen N, Sperber A, Ron Y, Boaz M, et al. The Effect of a Multispecies Probiotic on Microbiota Composition in a Clinical Trial of Patients With Diarrhea-Predominant Irritable Bowel Syndrome. *Neurogastroenterol Motil Off J Eur Gastrointestinal Motil Soc* (2018) 30(12):e13456. doi: 10.1111/nmo.13456
78. Li J, Sung CY, Lee N, Ni Y, Pihlajamäki J, Panagiotou G, et al. Probiotics Modulated Gut Microbiota Suppresses Hepatocellular Carcinoma Growth in Mice. *Proc Natl Acad Sci USA* (2016) 113(9):E1306–15. doi: 10.1073/pnas.1518189113
79. Negatu DA, Yamada Y, Xi Y, Go ML, Zimmerman M, Ganapathy U, et al. Gut Microbiota Metabolite Indole Propionic Acid Targets Tryptophan Biosynthesis in Mycobacterium Tuberculosis. *mBio* (2019) 10(2):e02781–18. doi: 10.1128/mBio.02781-18
80. Mao JW, Tang HY, Zhao T, Tan XY, Bi J, Wang BY, et al. Intestinal Mucosal Barrier Dysfunction Participates in the Progress of Nonalcoholic Fatty Liver Disease. *Int J Clin Exp Pathol* (2015) 8(4):3648–58.
81. Plaza-Díaz J, Solis-Urra P, Aragón-Vela J, Rodríguez-Rodríguez F, Olivares-Arancibia J, Álvarez-Mercado AI. Insights Into the Impact of Microbiota in the Treatment of NAFLD/NASH and Its Potential as a Biomarker for Prognosis and Diagnosis. *Biomedicines* (2021) 9(2). doi: 10.3390/biomedicines9020145
82. Venkatesh M, Mukherjee S, Wang H, Li H, Sun K, Benechet AP, et al. Symbiotic Bacterial Metabolites Regulate Gastrointestinal Barrier Function *via* the Xenobiotic Sensor PXR and Toll-Like Receptor 4. *Immunity* (2014) 41(2):296–310. doi: 10.1016/j.immuni.2014.06.014
83. Rahman K, Desai C, Iyer SS, Thorn NE, Kumar P, Liu Y, et al. Loss of Junctional Adhesion Molecule A Promotes Severe Steatohepatitis in Mice on a Diet High in Saturated Fat, Fructose, and Cholesterol. *Gastroenterology* (2016) 151(4):733–746.e12. doi: 10.1053/j.gastro.2016.06.022
84. de La Serre CB, de Lartigue G, Raybould HE. Chronic Exposure to Low Dose Bacterial Lipopolysaccharide Inhibits Leptin Signaling in Vagal Afferent Neurons. *Physiol Behav* (2015) 139:188–94. doi: 10.1016/j.physbeh.2014.10.032
85. Li J, Zhang L, Wu T, Li Y, Zhou X, Ruan Z. Indole-3-Propionic Acid Improved the Intestinal Barrier by Enhancing Epithelial Barrier and Mucus Barrier. *J Agric Food Chem* (2021) 69(5):1487–95. doi: 10.1021/acs.jafc.0c05205
86. Soleimani M. Dietary Fructose, Salt Absorption and Hypertension in Metabolic Syndrome: Towards a New Paradigm. *Acta physiologica (Oxford England)* (2011) 201(1):55–62. doi: 10.1111/j.1748-1716.2010.02167.x
87. Gummesson A, Carlsson LM, Storlien LH, Bäckhed F, Lundin P, Löfgren L, et al. Intestinal Permeability is Associated With Visceral Adiposity in Healthy Women. *Obes (Silver Spring Md.)* (2011) 19(11):2280–2. doi: 10.1038/oby.2011.251
88. Wlodarska M, Luo C, Kolde R, d'Hennezel E, Annand JW, Heim CE, et al. Indoleacrylic Acid Produced by Commensal Peptostreptococcus Species Suppresses Inflammation. *Cell Host Microbe* (2017) 22(1):25–37.e6. doi: 10.1016/j.chom.2017.06.007
89. Kominsky DJ, Campbell EL, Ehrentraut SF, Wilson KE, Kelly CJ, Glover LE, et al. IFN-γ-Mediated Induction of an Apical IL-10 Receptor on Polarized Intestinal Epithelia. *J Immunol (Baltimore Md 1950)* (2014) 192(3):1267–76. doi: 10.4049/jimmunol.1301757
90. Pulakazhi Venu VK, Saifeddine M, Mihara K, Tsai YC, Nieves K, Alston L, et al. The Pregnane X Receptor and its Microbiota-Derived Ligand Indole 3-Propionic Acid Regulate Endothelium-Dependent Vasodilation. *Am J Physiol Endocrinol Metab* (2019) 317(2):E350–e361. doi: 10.1152/ajpendo.00572.2018
91. Rothhammer V, Mascanfroni ID, Bunse L, Takenaka MC, Kenison JE, Mayo L, et al. Type I Interferons and Microbial Metabolites of Tryptophan Modulate Astrocyte Activity and Central Nervous System Inflammation *via* the Aryl Hydrocarbon Receptor. *Nat Med* (2016) 22(6):586–97. doi: 10.1038/nm.4106
92. Hubbard TD, Murray IA, Perdew GH. Indole and Tryptophan Metabolism: Endogenous and Dietary Routes to Ah Receptor Activation. *Drug Metab disposition: Biol fate chemicals* (2015) 43(10):1522–35. doi: 10.1124/dmd.115.064246
93. Lanis JM, Alexeev EE, Curtis VF, Kitzenberg DA, Kao DJ, Battista KD, et al. Tryptophan Metabolite Activation of the Aryl Hydrocarbon Receptor Regulates IL-10 Receptor Expression on Intestinal Epithelia. *Mucosal Immunol* (2017) 10(5):1133–44. doi: 10.1038/mi.2016.133
94. Turnbaugh PJ, Ley RE, Hamady M, Fraser-Liggett CM, Knight R, Gordon JI. The Human Microbiome Project. *Nature* (2007) 449(7164):804–10. doi: 10.1038/nature06244
95. Lynch SV, Pedersen O. The Human Intestinal Microbiome in Health and Disease. *New Engl J Med* (2016) 375(24):2369–79. doi: 10.1056/NEJMra1600266
96. Bansal T, Alaniz RC, Wood TK, Jayaraman A. The Bacterial Signal Indole Increases Epithelial-Cell Tight-Junction Resistance and Attenuates Indicators of Inflammation. *Proc Natl Acad Sci USA* (2010) 107(1):228–33. doi: 10.1073/pnas.0906112107
97. Chappell CL, Darkoh C, Shimmin L, Farhana N, Kim DK, Okhuysen PC, et al. Fecal Indole as a Biomarker of Susceptibility to Cryptosporidium Infection. *Infect Immun* (2016) 84(8):2299–306. doi: 10.1128/iai.00336-16
98. Liu F, Sun C, Chen Y, Du F, Yang Y, Wu G. Indole-3-Propionic Acid-Aggravated CCl4-Induced Liver Fibrosis *via* the TGF-β1/Smads Signaling Pathway. *J Clin Trans Hepatol* (2021) 000(000):000–0. doi: 10.14218/jcth.2021.00032

Conflict of Interest: The authors declare that the research was conducted in the absence of any commercial or financial relationships that could be construed as a potential conflict of interest.

this article, or claim that may be made by its manufacturer, is not guaranteed or endorsed by the publisher.

frontiers in Endocrinology

ORIGINAL RESEARCH
published: 25 March 2022
doi: 10.3389/fendo.2022.830466

Integration of Metabolomics and Proteomics in Exploring the Endothelial Dysfunction Mechanism Induced by Serum Exosomes From Diabetic Retinopathy and Diabetic Nephropathy Patients

Jing Yang[1,2,3,4], *Dongwei Liu*[2,3,4,5] *and Zhangsuo Liu*[2,3,4,5]*

[1] Department of Ophthalmology, The First Affiliated Hospital of Zhengzhou University, Zhengzhou, China, [2] Research Institute of Nephrology, Zhengzhou University, Zhengzhou, China, [3] Henan Province Research Center for Kidney Disease, Zhengzhou, China, [4] Key Laboratory of Precision Diagnosis and Treatment of Chronic Kidney Disease in Henan Province, Zhengzhou, China, [5] Department of Integrated Traditional and Western Nephrology, The First Affiliated Hospital of Zhengzhou University, Zhengzhou, China

OPEN ACCESS

Edited by:
Yanli Pang,
Peking University Third Hospital, China

Reviewed by:
Andrei I. Tarasov,
Ulster University, United Kingdom
Xiaohui Li,
Central South University, China

***Correspondence:**
Zhangsuo Liu
zhangsuoliu@zzu.edu.cn

Specialty section:
This article was submitted to Gut Endocrinology, a section of the journal Frontiers in Endocrinology

Received: *07 December 2021*
Accepted: *07 February 2022*
Published: *25 March 2022*

Citation:
Yang J, Liu D and Liu Z (2022) Integration of Metabolomics and Proteomics in Exploring the Endothelial Dysfunction Mechanism Induced by Serum Exosomes From Diabetic Retinopathy and Diabetic Nephropathy Patients. Front. Endocrinol. 13:830466. doi: 10.3389/fendo.2022.830466

Background: The prevalence of diabetic microvascular diseases has increased significantly worldwide, the most common of which are diabetic nephropathy (DN) and diabetic retinopathy (DR). Microvascular endothelial cells are thought to be major targets of hyperglycemic damage, while the underlying mechanism of diffuse endothelial dysfunction in multiple organs needs to be further investigated.

Aim: The aim of this study is to explore the endothelial dysfunction mechanisms of serum exosomes (SExos) extracted from DR and DN (DRDN) patients.

Methods: In this study, human glomerular endothelial cells (HGECs) were used as the cell model. Metabolomics ultraperformance liquid chromatography-tandem mass spectrometry (UPLC-MS/MS) and proteomics tandem mass tag (TMT)-based liquid chromatography-tandem mass spectrometry (LC-MS/MS) together with bioinformatics, the correlation analysis, and the joint pathway analysis were employed to discover the underlying mechanisms of endothelial dysfunction caused by patient's SExos.

Results: It can be assumed that serum exosomes extracted by DRDN patients might cause endothelial dysfunction mainly by upregulating alpha subunit of the coagulation factor fibrinogen (FIBA) and downregulating 1-methylhistidine (1-MH). Bioinformatics analysis pointed to an important role in reducing excess cysteine and methionine metabolism.

Conclusion: FIBA overexpression and 1-MH loss may be linked to the pathogenicity of diabetic endothelial dysfunction in DR/DN, implying that a cohort study is needed to further investigate the role of FIBA and 1-MH in the development of DN and DR, as well as the related pathways between the two proteins.

Keywords: metabolomics, proteomics, exosomes, diabetic nephropathy, diabetic retinopathy, endothelial dysfunction

1 INTRODUCTION

Diabetes has become much more common during the last few decades all throughout the world. Diabetes' global occurrence has risen substantially from 108 million in 1980 to 422 million in 2014, according to epidemiological data, and diabetes is anticipated to become the seventh leading cause of death by 2030 (1–4). The major lethal causes for diabetic patients are diabetic macrovascular and microvascular complications that are derived from the diabetes-induced endothelial dysfunction. Because their failure to downregulate the glucose transport rate results in intracellular hyperglycemia when glucose levels are high, microvascular endothelial cells are regarded to be the major targets of hyperglycemic damage (4, 5). High blood sugar level is considered to induce the microvascular endothelial dysfunction in which diabetic nephropathy (DN) and diabetic retinopathy (DR) are the most common disorders. According to the epidemiological type-2 diabetes surveys in Chinese major cities, DN and DR account for 39.7% and 31.5% of diabetic microangiopathy, respectively (4).

It is recognized that retinopathy and nephropathy occur simultaneously in long-term diabetes. As an important structural and overlapping determinant of disease development, the relationship between kidney disease and retinal disease has been discussed, and the term "renal-retinal syndrome" has been recognized by the public (6, 7). The polyol pathway is involved in the development of the two disorders, as are increased advanced glycation end products (AGEs) synthesis, increased expression of the AGE receptor and its activating ligands, activation of protein kinase C isoforms, overactivity of the hexosamine pathway, and other pathways (8–10). Additionally, the systemic inflammation induced by the albuminuria-impaired kidney is considered to accelerate the clinical course of microvascular complications in both the eye and the kidney (11–17). In this sense, the underlying mechanisms of hyperglycemic injury for microvascular endothelial cells require further investigation.

In type 2 diabetes (T2D) patients with reduced glomerular endothelial fenestrae, albuminuria and a drop in glomerular filtration rate (GFR) are significantly connected (18–21). Multiple causes contribute to glomerular endothelial cell (GEC) dysfunction, including increased permeability of GECs, stimulation of endothelial apoptosis, glycocalyx breakdown, and poor cross communication between endothelial cells and other renal cells (e.g., podocytes) (22–24). GEC injury is responsible for the occurrence of microalbuminuria, which is the early event of DN (22). Microalbuminuria is also a sign of endothelial dysfunction in the kidneys and throughout the body (25, 26). The retina is harmed by chronic hyperglycemia, which compromises the blood–retina barrier, resulting in extracellular fluid accumulation in the macula, as well as thickening of the capillary basement membrane and increased deposition of extracellular matrix (ECM) components (27–29). By upregulating angiogenic factors [e.g., vascular endothelial growth factor (VEGF)] over time, chronic retinal microvasculature damage induces capillary non-perfusion and retinal ischemia (14, 30–34). DR increases the risk of life-threatening systemic vascular disorders regardless of vision loss (35, 36).

Endothelial dysfunction is linked to diabetic microvascular problems due to a deficiency in angiogenesis, increased endothelial permeability, increased leukocyte adhesion, and reduced nitric oxide action (11). In the process of diabetes, the diffused endothelial dysfunction appears in multiple organs, indicating the existence of potential factors that induce endothelial cell injuries in the circulation. Exosomes are nanoscale membranous vesicles (30–100 nm) and enriched in specific proteins, lipids, nucleic acids, and glycoconjugates. There are abundant exosomes in blood, and they are involved in various cellular activities. For instance, they are responsible for remodeling the ECM and then releasing contents into recipient cells for the purpose of transmitting signals and molecules to target cells and organs. This pathway of vesicle transportation plays crucial roles in various disease developments, such as diabetes mellitus (DM) and diabetic microvascular diseases (37). DM patients had significantly larger quantities of extracellular vesicles (EVs) in their circulation than euglycemic control participants, according to a previous study (38). In addition, serum exosomes (SExos) from diabetic db/db mice severely impair the aortic endothelial cell functions from non-diabetic db/m+ mice, indicating the changes in the composition of SExos (39). We employed quantitative proteomics and metabolomics to examine the differential proteins and metabolites produced by exosomes in human glomerular endothelial cells (HGECs) to better understand the molecular mechanism of exosomes in diabetic macrovascular endothelial dysfunction.

2 MATERIALS AND METHODS

2.1 Cell Culture

ScienCell Research Laboratories (PS-4000, San Diego, CA) provided the HGECs, which were grown at 37°C and 5% CO_2 in endothelial cell medium (ECM; Sciencell Research Laboratories), which contained 10% fetal bovine serum (FBS, Gibco), 100 U/ml penicillin, and 100 mg/ml streptomycin. Cell passages ranging from 2 to 5 were used in these studies.

2.2 Patients and Samples

From January to November 2020, the enrolled patients were admitted to Zhengzhou University's First Affiliated Hospital. Serum samples for the exosome's isolations were obtained from 20 healthy volunteers and 20 patients diagnosed with DR and DN. All of the samples were frozen at -80°C. The ethics committee of Zhengzhou University's First Affiliated Hospital gave its approval to this study (2021-KY-0872-002). Prior to participation in the study, all patients signed a written informed permission form.

2.3 Exosome Experiments

2.3.1 Serum Exosome Isolation and Identification

SExos were isolated as previously reported (40). In order to eradicate cells and cellular debris, the collected serum had been centrifuged for 15 min at 3,000g for 15 min. The exosome separation was done with ExoQuick, a fast-acting exosome

precipitation solution (System Biosciences, CA, USA). The exosome suspension was dissolved in phosphate-buffered saline (PBS) and kept at -80°C for future use. The exosomes were identified using transmission electron microscopy (TEM; Tecnai G2 Spirit 120KV). The exosome particle size and concentration were assessed at VivaCell Biosciences using the nanoparticle tracking analysis (NTA) method and the related software ZetaView 8.04.02 with the ZetaView PMX 110 (Particle Metrix, Meerbusch, Germany). The isolated exosome samples were diluted in 1× PBS buffer to assess particle size and concentration (Biological Industries, Israel). At 11 different sites, the NTA measurement was obtained and analyzed. The ZetaView system was calibrated using polystyrene particles with a diameter of 110 nm. Temperatures were maintained between 24°C and 26°C.

2.3.2 Exosome Labeling

To suspend the exosomes obtained from patients' serum, a mixture of 100 L PBS and 1 ml PKH67 (Sigma, in Diluent C) was utilized. After 5 min at room temperature, exosome labeling was halted by adding 3 ml of 1% bovine serum albumin, and the colored exosomes were extracted using the ExoQuick exosome precipitation solution. Here, 10 g of exosomes were introduced to HGECs after suspension in basal media. The cells were cultured for 6, 12, and 24 h at 37°C before being washed and fixed at room temperature. The addition of 4′,6-diamidino-2-phenylindole (DAPI; Sigma) was used to stain the nuclei for 10 min. The stained cells were observed using an Olympus confocal microscope (Japan).

2.4 Western Blot

Before being lysed in radioimmunoprecipitation assay buffer (RIPA) buffer, the cells were collected and rinsed in cold PBS (Solarbio, Beijing, China). At 4°C, the whole-cell lysates were centrifuged for 15 min at 12,000 rpm. Protein concentrations were determined using the bicinchoninic acid method. Sodium dodecyl sulfate–polyacrylamide gel electrophoresis (SDS-PAGE) was used to separate the proteins, which were then transferred to a nitrocellulose membrane. In the PBS containing 5% evaporated milk and 1% Tween-20, the membranes were blocked for 1 h before being treated overnight at 4°C with primary antibodies dissolved in PBS containing 1% Tween-20. The primary antibodies were anti-CD9 (Abcam, Hong Kong, China; # ab92726), anti-CD63 (Abcam, ab216130), anti-TSG101 (Sino Biological, Beijing, China; #102286-T38), anti-CD31 (Zen-Bioscience, Chengdu, China; #383815), anti-von Willebrand factor (vWF), (Abcam, #ab154193), anti-intercellular adhesion molecule 1 (ICAM-1) (Abcam, #ab171123), anti-vascular cell adhesion protein 1 (VCAM-1) (Abcam, #ab134047), and anti-Glyceraldehyde-3-Phosphate Dehydrogenase (GAPDH) (Goodhere, Hangzhou, China; #AB-P-R 001). The blots were then treated with the appropriate secondary antibodies on the second day: horse radish peroxidase (HRP)-labeled goat anti-rabbit immunoglobulin G (IgG) (Dingguo Changsheng, Beijing, China; #IH-0011) and HRP-labeled goat anti-mouse IgG (Dingguo Changsheng, Beijing, China; #IH-0011). The Odyssey two-color infrared laser imaging system (LICOR) or HRP-based chemiluminescence analysis was used to detect the signals. Image J/Fiji and GraphPad Prism 9.0 were used to analyze the grayscale of the Western blot (WB) bands (GraphPad Software, Inc., La Jolla, CA, USA).

2.5 Immunofluorescence

The immunofluorescence (IF) assays were conducted as described before (41). The HGEC lines were seeded on collagen-coated glass and cultured in ECM medium overnight at 37°C in a humidified 5% CO_2 atmosphere. The cells were rinsed twice with PBS before being fixed with 4% formaldehyde and permeabilized with 0.2% Triton X-100. The cells were treated with fluorescein Alexa-Fluor 488-conjugated secondary antibodies for one night at 4°C after being blocked with 1% BSA for 30 min and photographed using a fluorescence microscope (Leica, Wetzlar, Germany). Tissues were treated overnight at 4°C with primary antibodies, then with secondary antibodies Goat Anti-Rabbit IgG H&L fluorescein isothiocyanate (FITC) (Abcam, #ab7086) pre-absorbed, Goat anti-Mouse IgG (H+L) cross-adsorbed, Alexa Fluor 555, and finally imaged using a confocal microscope (Olympus, Japan) and scanned using a slide scanner Pann (3DHISTECH, Hungary).

2.6 Proteomics Study

2.6.1 Protein Extraction

Enzymatic hydrolysis was performed for 300 mg of each sample. After diluting dithiothreitol (DTT) to 100 mM, the sample was heated for 5 min and then cooled to room temperature. After that, the sample was given 200 ml of ultrasound-assisted (UA) buffer (8 M urea, 150 mM Tris-HCl, pH 8.0). The mixture was evenly mixed before being transferred to a 10-kD ultrafiltration centrifuge tube and centrifuged for 15 min at 12,000g. After adding 15 ml of UA buffer to the sample, it was centrifuged for 15 min and the filtrate was discarded. The sample was then incubated at room temperature for 30 min in the dark before being centrifuged at 12,000g for 10 min after being added 100 ml of 50 mM iodoacetamide (IAA) (in UA) and shaken at 600 rpm for 1 min. Samples were centrifuged twice at 12,000g for 10 min each time after being washed twice with 100 ml UA buffer. The material was then rinsed twice with NH_4HCO_3 buffer (100 ml) and centrifuged for 10 min at 14,000g. The sample was then treated with trypsin (20 mg trypsin in 40 ml NH_4HCO_3 buffer), agitated at 600 rpm for 1 min, and incubated at 37°C for 16–18 h. The material was centrifuged at 12,000g for 10 min after the collection tube was changed. After adding the trifluoroacetic acid (TFA) solution to the filtrate to a final concentration of 0.1%, the sample was desalinated with a C18 cartridge. The samples were quantified using OD280.

2.6.2 Tandem Mass Tag (TMT)-Based Liquid Chromatography-Tandem Mass Spectrometry (LC-MS/MS)

Metware Biotechnology Co., Ltd., completed the TMT-based LC-MS/MS identification and data normalization analysis (Wuhan, China). The protein samples were diluted 6-fold and underwent enzyming and desalting. The peptide samples were diluted to 1 g/l on-board buffer in a 5-L container, and the scanning mode was set to 120 min. The peptides were scanned in the sample with a

mass-to-charge ratio of 350–1,500. After preparing mobile phase A solution [98% water, 2% acetonitrile (ACN), 0.1% formic acid (FA)], B solution (98% ACN, 2% water, 0.1% FA), pre-column (300 m0.5mm, 3 m), analytical column (3 m, 75 m150 mm; Welch Materials, Inc), and spray voltage, peptides separated by liquid phase were ionized by the nanoESI source and transferred into the tandem mass spectrometer Q-Exactive (Thermo Fisher Scientific, San Jose, CA, USA). The main parameters are set as follows: 320°C of the ion transfer tube temperature, 350–1,500 m/z of scanning range, 60,000 of primary resolution, 3e6 of C-Trap, 80 ms of inject time (IT), 15,000 of secondary resolution, 1e5 of C-Trap, 100 ms of IT, 28 of CE, 1.0e4 of threshold intensity, and dynamic exclusion for 30 s. The raw data for mass detection (.raw) were generated, and the mass spectrometer data were retrieved and analyzed using MaxQuant 1.6.15.0.

2.6.3 Protein Identification and Quantitative Analysis

The data from the mass spectrometer were collected and analyzed using MaxQuant 1.6.15.0. The following were the search parameters: TMT-10plex (Peptide Labeled) quantification type; Enzyme: Trypsin/P; Max. missed cleavages: 2; carbamidomethyl (C) is a fixed alteration. Protein quantification includes the following modifications: oxidation (M), acetyl (Protein N-term); First search MS/MS tolerance: 20 ppm; Main search MS/MS tolerance: 5 ppm; Include contaminants: TRUE; Decoy mode: revert; Peptides used for protein quantification: Razor; Protein FDR: 0.01; PSM FDR: 0.01; Include contaminants: TRUE; The sequencing was done using the UniProt Taxonomy Database (**Supplementary Material S1**). The mass spectrometry proteomics data have been deposited with the dataset number PXD030660 to the ProteomeXchange Consortium (http://proteomecentral.proteomexchange.org) *via* the iProX partner repository (42).

2.6.4 Bioinformatics Methods

To learn more about the causes of SExo-induced endothelial dysfunction in DR+DN patients, researchers used the UniProt-GOA Database (http://www.ebi.ac.uk/GOA/) for Gene Ontology (GO) functional annotation and Kyoto Encyclopedia of Genes and Genomes (KEGG) pathway enrichment analysis. FDR 0.01 was chosen as the cutoff point. The UniProt Gene Ontology Annotation (GOA) database was used to enhance the GO annotation proteome, which was supplemented by InterProScan soft. Subcellular localization was predicted using Wolf PSORT software. The KEGG database was used to annotate protein pathways. The pheatmap function in the R package was used to build the clustering heat map. The bar graph and circos graph were created using the ggplot function from the R package -ggplot2.

2.6.5 Protein Interaction Network Analysis

To use the IntAct (http://www.ebi.ac.uk/intact/main.xhtml) or STRING (https://string-db.org/) databases, first, get the gene symbol from the target protein's sequence database. STRING is used to create protein–protein interaction (PPI) networks (a search tool for finding interacting genes). A confidence score of 0:4 and a maximum number of interactors of 0 are the cutoff conditions for this study. Then, using the Cytoscape software 3.2.1 (http://www.cytoscape.org/) platform, the interaction network of differentially expressed proteins was screened using cytoHubba based on high connectedness (43).

2.6.6 Parallel Reaction Monitoring

The results of the TMT-based LC-MS/MS analysis were backed up by parallel reaction monitoring (PRM) analysis of chosen proteins. The distinctive peptides of the selected proteins were identified using TMT-based LC-MS/MS data, and only a few peptide sequences were chosen for PRM analysis. Trypsin was used to digest, reduce, alkylate, and absorb the selected proteins (100 mg). Through a C18 trap column (0.10 20 mm; 3 mm) and then a C18 column (0.15 120 mm; 1.9 mm), the collected peptide mixtures were injected into the mass spectrometer. A tabletop Orbitrap mass spectrometer (Q Exactive; Thermo Scientific) with a quadrupole mass filter was used to make the MS computation. Proteome Discoverer 1.4 was used to collect and evaluate raw data (Thermo Fisher Scientific). The false discovery rate (FDR) for proteins and peptides had been set to 0.01. Skyline 2.6 software was used for quantification and proteomic analysis. For the PRM analysis, three biological replicates were performed in each group.

2.7 Metabolomics Study

2.7.1 Ultraperformance Liquid Chromatography-Tandem Mass Spectrometry (UPLC-MS/MS) Analysis

A Ultra High Performance Liquid Chromatography (UHPLC) system was used to perform the chromatographic separation (Waters Corp., Milford, MA, USA). ACQUITYTM UPLC BEH C18 (2.1 mm 100 mm, 1.7 m) was used to analyze all of the analytes. The column was held at a constant temperature of 35°C. The mobile phase was made up of solvent A (water and 0.1% formic acid) and solvent B (water and 0.1% formic acid) (acetonitrile). The injection volume and flow rate were set at 0.4 ml/min and 2 L/min, respectively. A Waters SynaptTM QTOF/MS spectrometer (Waters Corp., Milford, MA, USA) was coupled to a UHPLC system through an ESI source in both positive and negative ionization modes.

2.7.2 Data Processing

Using the self-built target standard metware database, the qualitative analysis was performed based on the retention period of the detected chemical, the information of the precursor ion pairs, and secondary spectrum data (MWDB, containing business trade secrets). The metabolites were quantified using triple quadrupole mass spectrometry's multiple reaction monitoring (MRM) mode analysis.

The metabolite content data were standardized using the unit variance scaling (UV) method. The R program (https://www.r-project.org/) was used to compare diverse samples and perform hierarchical cluster analysis (HCA) on the accumulation manner of metabolites. Principal component analysis (PCA; R function prcomp, parameters center = TRUE, scale = TRUE), orthogonal partial least squares discriminant analysis (OPLS-DA), and partial least squares discriminant analysis (PLS-DA) were used to analyze the data. The S-plot was made to see which marker components differed significantly between the groups. By scanning Internet

databases such as KEGG, Human Metabolome Database (HMDB), and Metabolite Set Enrichment Analysis (MSEA), possible endogenous metabolites were discovered using accurate molecular masses, MS/MS fragments, and retention behavior. The R package MetaboAnalystR was used to run OPLS-DA (parameters, opls_log, "MeanCenter," "S10T0," ratio = FALSE, ratioNum = 20). Heat map was drawn by R package Heatmap [parameters na_col = 'grey,' rect_gp = gpar(col = cell.border.color, lwd = 1)]. R function cor was used to analyze Pearson's correlation coefficient [parameter method = pearson; correlation graph was used to R package corrplot, parameters add = TRUE, type = 'lower,' method = 'number,' number.cex = mycex, number.digits = 2, diag = F, tl.pos = 'n'].

2.8 Proteomics and Metabolomics Integration Analysis

The data were transformed to normalize the distributions. At least 20% of metabolites that were not presented in the samples were filtered out. Differential abundances of proteins among CON-EXO vs. DRDN-EXO individuals were calculated using the linear modeling R-package limma. Multiple testing corrections were applied using Benjamin and Hochberg FDR ($P < 0.05$ for significance). Volcano plots were plotted by R-package ggplot2. Pathway analysis was performed using the limma ROAST method. The analysis of the integrated proteomics and metabolite interaction network included the proteins related to 1-methylhistidine (1-MH) and excluded the isolated nodes.

2.9 Statistical Analysis

SPSS24.0 statistical software was used for the data analysis. The independent T test was used to compare the two groups, whereas the multivariate variance was used to compare the numerous groups. Statistical significance was defined as a P-value <0.05.

3 RESULTS

3.1 Circulating Exosomes Could Influence Renal and Retinal Endothelial Cells and Cause Endothelial Dysfunction

All of the patients in this study were separated into two groups: CON (healthy persons) and DR+DN (diagnosed as both DR and DN). **Figure 1A** shows the renal biopsy pathological and fundus images obtained from one DR+DN patient and one healthy participant, indicating that endothelial microvascular leakage of retina and kidney could occur simultaneously. In retina, the diabetic endothelial dysfunction led to several disorders such as the capillary wall dilatation (microaneurysms), the leakage (edema and hard exudates), and the rupture (hemorrhages). The dilation of the retinal capillary walls was an early physiological sign of microvascular malfunction. Diabetic endothelium damage manifested itself in the glomerulus as endothelial cell enlargement, glomerular basement membrane reduplication, mesangial expansion, and arteriolar hyalinosis. SExos from DR+DN patients were separated from the serum by ultracentrifugation and visualized by TEM after negative staining. Most of the SExos were less than 100 nm. A characteristic cup-shaped morphology was identified using TEM (**Figure 1B**). In the exosome fraction, Western blot analysis revealed strong CD9, CD63, and TSG101 (exosome markers) signals (**Figure 1C**). The Delta Nano C particle analyzer was used to characterize the characteristics of SExos in real time (ZetaView, Particle Metrix). The size of SExos was 121.8 ± 50.1 nm (mean ± SD) (**Figure 1D**). To investigate the communications between endothelial cells and SExos, we cocultured HGECs and PKH67-labeled SExos and photographed them using a confocal microscope at different time points (**Figure 1E**). The internalization of fluorescent exosomes was observed inside the endothelial cells, and it was found that exosomes had entered endothelial cells at 6 h, and the number of exosomes entering endothelial cells gradually increased over time.

In order to verify whether the serum exosomes extracted from DR+DN patients could induce injury effect on endothelial cells, we cultured HGECs with exosomes from DR+DN patients and healthy participants, respectively, and extracted cellular protein and mRNA 48 h later. Endothelial dysfunction indicators such as ICAM-1 and VCAM-1, as well as CD31 and vWF, were increased in HGECs treated with DR+DN SExos, whereas CD31 and vWF were dramatically downregulated (**Figures 2A, B**). Cellular immunofluorescence confirmed that HGECs were injured when cocultured with the DR+DN-SExos (**Figure 2C**).

3.2 Analysis of Differentially Expressed Proteins by iTRAQ-Based Quantitative Proteomics

To investigate the molecular mechanism that DR+DN-SExos induce endothelial cell dysfunction, HGECs were treated with SExos from healthy participants (CON group) and DR+DN patients (DRDN groups). The differentially expressed proteins between the CON groups and the DRDN groups were identified using iTRAQ-based proteomics (**Figure 3A**). Qualitative control analysis on the test samples was carried out (**Supplementary Figure S2**).

The FDR strategy's BH (Benjamini and Hochberg) approach was utilized to further adjust the P-value of the multiple tests and obtain the adj. P-value. Finally, the differences of protein were screened out based on the differences between the multiple and the adj. P-value. Criteria for significant differences in expression are shown as follows: when the comparison group's adj. P-value ≤0.05 and the fold change ≥1.5 (upregulation of expression) or fold change ≤0.67 (downregulation of expression), the expression is considered as a significant variety. **Figure 3B** depicted the volcano plots of proteins retrieved from healthy volunteers and DR+DN patients in HGECs treated with SExos. Results showed that after the treatment with 50 mM SExos from DR+DN patients for 48 h, a total of 185 differentially expressed proteins were identified in HGECs with 87 proteins upregulated (red dots) and 98 proteins downregulated (blue dots). The significant differences of expressed proteins between the groups were observed in the hierarchical clustering heat map as shown in **Figure 3C**. **Figure 3D** showed the proteins associated with endothelial dysfunction of the profile. Among the differentially expressed proteins, fibrinogen alpha

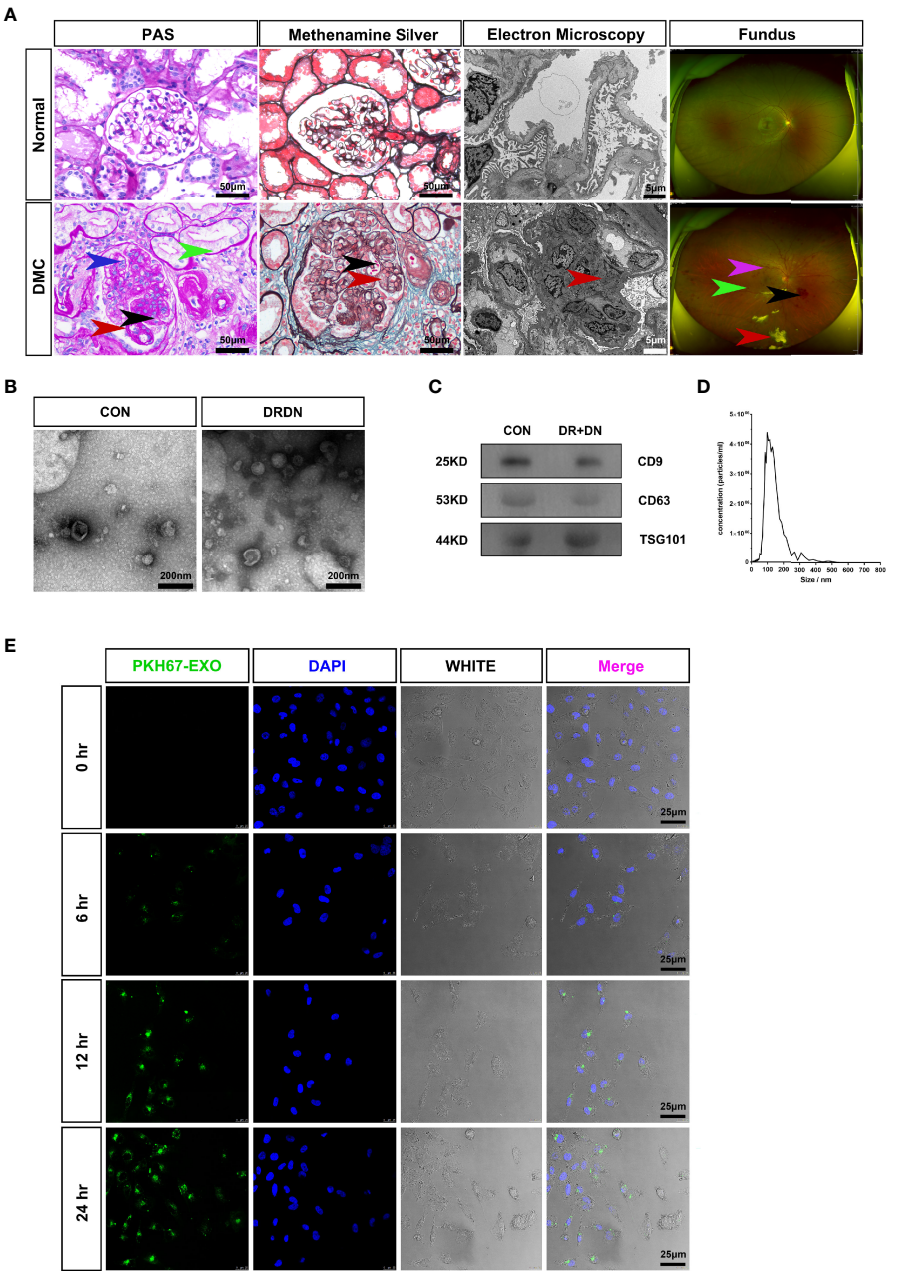

FIGURE 1 | Serum exosomes from diabetic retinopathy and nephropathy patients could induce endothelial dysfunction. **(A)** The typical pathological kidney images and fundus images obtained from healthy people and a diabetic microvascular disease patient. **PAS**: The DMC biopsy sample showed proliferation and swelling of the endothelial cell (blue arrow), reduplication (double contour appearance) of the glomerular basement membrane (red arrow), mesangial expansion (black arrow), arteriolar hyalinosis (green arrow). Scale bar: 50 μm. **Methenamine silver:** Renal biopsy samples from the DMC patient show the swelling of the endothelial cells (red arrow) and reduplication (double contour appearance) of the glomerular basement membrane (black arrow). Scale bar: 50 μm. **Electron microscopy:** The slice from the DMC patient showed mesangial expansion (red arrow). Scale bar: 5 μm. **Fundus:** The fundus from DMC showed microhemangioma (green arrow), retinal exudates (red arrow), intraretinal hemorrhage (black arrow), and intraretinal microvascular abnormalities (IRMAs; violet arrow). **(B)** Identification of serum exosomes from CON patients and DRDN patients by transmission electron microscopy (TEM). Scale bar: 200 nm. **(C)** Western blotting was used to look for the exosomal markers CD9, CD63, and TSG101 in exosome samples. **(D)** Analysis of the size distribution of exosomes from patients using the NanoSight technology; the average size of serum exosomes was 107.5 ± 55.2 nm. **(E)** Exosome tracing experiment captured by confocal microscope. Blue for DNA dyed by DAPI and green for exosomes derived from DR+DN patients dyed by PKH67. HGECs were subjected to 6, 12, and 24 h of incubation with exosomes. Scale bar: 25 μm. PAS, Periodic acid–Schiff stain; DMC, diabetic microvascular complications; CON, healthy controls; DRDN, patients diagnosed with both diabetic retinopathy and diabetic nephropathy.

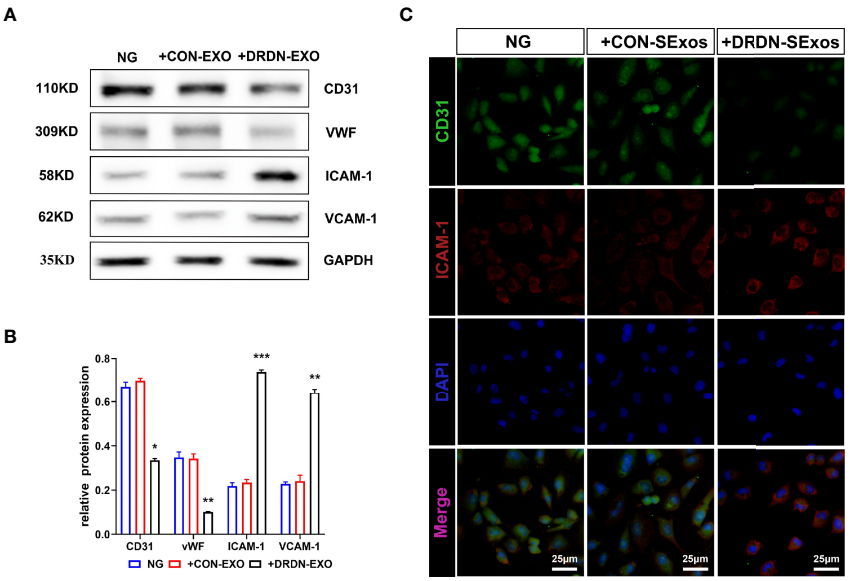

FIGURE 2 | Serum exosomes from diabetic retinopathy and nephropathy patients could induce endothelial dysfunction. **(A)** Western blot analysis of CD31, vWF, ICAM-1, and VCAM-1 in HGECs treated with serum exosomes from healthy people and DR+DN patients. **(B)** Grayscale analysis of Western blot in HGECs treated with serum exosomes from healthy people and DR+DN patients, N = 3, *P < 0.05, **P < 0.01, ***P < 0.001. **(C)** The cellular immunofluorescence of HGECs stained with CD31 (green fluorescence) and ICAM-1 (red fluorescence). Scale bar: 50 μm.

chain (FGA) was the highest elevated (fold change: 4.024). Transforming growth factors beta 1 (TGFβ1) and Collagen Type I Alpha 1 Chain (COL1A1) have been linked to the diabetic endothelial-to-mesenchymal transition and have been shown to worsen diabetic glomerulosclerosis (44, 45). Circulating ICAM-1 levels are positively connected with albuminuria in individuals with type 1 diabetes (T1D) and T2D (46, 47). ICAM-1 is an endothelial damage protein marker (46). S100A6 is an important component of the PPP5C-FKBP51 axis, which protects the endothelium barrier from calcium entry-induced disruption (48).

3.3 Function Analysis of the Differentially Expressed Proteins in Human Glomerular Endothelial Cells Affected by Serum Exosomes Extracted From DR+DN Patients

The GO is an international classification system for gene functions that provides a systematic up-to-date standard vocabulary (controlled vocabulary) to thoroughly characterize the properties of genes and gene products in organisms. The GO annotation results of the differentially expressed proteins were shown in **Figure 4A** and **Supplementary Material S3**, revealing that the majority of these proteins are involved in bacterial response, defense response, acute inflammatory response, biotic stimulus, inorganic substance response, and inflammatory response.

The metabolic pathway, the focal adhesion pathway, the arginine and proline metabolism pathway, the phagosome pathway, the tight junction pathway, and the ECM–receptor interaction pathway were among the key pathways identified by the KEGG pathway annotation analysis (**Figure 4B** and **Supplementary Material S4**). The results of GO and KEGG analysis showed that the endothelial dysfunction mechanism of the DR+DN patients' SExos was mainly affected by the metabolism processes and the multicellular communication processes and might have some correlations with the cell junction and inflammation processes.

The Cluster of Orthologous Groups of Proteins (COG) is a database that categorizes proteins into orthologous groups. The proteins constituting each type of COG are assumed to be derived from an ancestor protein and therefore are either orthologs or paralogs. The COG database was compared to the discovered proteins, and probable functions were anticipated using a functional categorization statistical analysis. **Figure 4C** and **Supplementary Material S5** showed the comparison of these statistical results with the COG database. The abscissa represents the number of proteins, and the ordinate represents the COG entry annotated. The upregulated proteins had a higher concentration of COG annotations in the categories of energy production and conversion, secondary metabolite biosynthesis transport and catabolism, amino acid transport and metabolism, and lipid transport and metabolism. The COG annotations for downregulated proteins were in the following order: posttranslational modification, protein turnover, chaperones, amino acid transport and metabolism, nucleotide transport and metabolism, and carbohydrate transport and metabolism. Other proteins were solely implicated in predicting general function and other metabolism processes. These findings suggest that SExos'

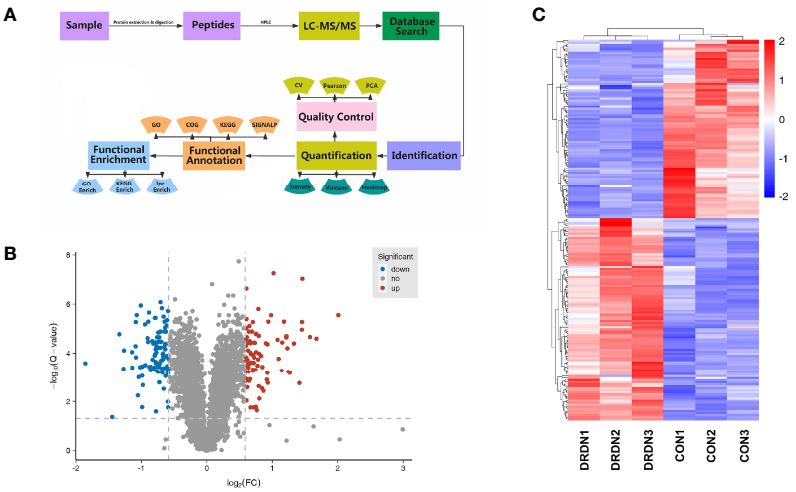

D

Endothelial function related proteins in differentially expressed protein profile

Description	Gene Symbol	UniProt Accession	Sequence Coverage [%]	pI	Unique Peptides
Fibrinogen alpha chain	FIBA	P02671	4.6	5.9	4
Transforming growth factor beta-1-induced transcript 1 protein	TGFB1I1	O43294	5.6	7	2
Collagen alpha-1(I) chain	COL1A1	P02452	3.1	5.5	5
Retinol-binding protein 4	RBP4	P02753	10	5.8	3
Peptidyl-prolyl cis-trans isomerase NIMA-interacting 4	PIN4	Q9Y237	26	10.5	6
Superoxide dismutase [Mn], mitochondrial	SOD2	P04179	42.3	8.4	10
Intercellular adhesion molecule 1	ICAM1	P05362	30.3	8.1	14
Protein S100-A6	S100A6	P06703	55.6	5.2	6
Insulin-like growth factor-binding protein 6	IGFBP6	P24592	4.2	7.9	1
Prostaglandin E synthase	PTGES	O14684	16.4	9.8	3

FIGURE 3 | Global proteomics profiles of HGECs incubated with CON- and DRDN-SExo. **(A)** Technical route flowchart of metabolic profiles. **(B)** Volcano plot showing the relative content of differently between groups and the statistical differences. To create a volcano map, use log 2 (FC) as the abscissa and negative logarithm -log10 (adj. P-value) as the ordinate. There were 12 upregulated metabolites (red dots) and 8 downregulated metabolites (blue dots) (green dots). **(C)** Hierarchical clustering heat map of significantly differentially expressed proteins in all comparison groups. **(D)** Endothelial function-related proteins in differentially expressed protein profile.

endothelial cell-damaging effects are linked to its ability to influence protein interactions and enzymatic processes.

It is only when proteins are transported to the correct position that the subcellular structures can perform different biological functions of organisms and participate in various cell activities. Therefore, it is very important to understand the protein subcellular location information for the organism activities. The subcellular location prediction was done using the Wolf PSORT website, and the statistical map of the prediction findings for differential subcellular positioning is displayed in **Figure 4D** and **Supplementary Material S6** (the abscissa represents the subcellular, and the ordinate represents the number of proteins). From the results, it can be seen that the subcellular localization is mainly concentrated in the area of the nucleus, cytoplasm, ECM, coexistence of nucleus and cytoplasm, and mitochondria. The functional analysis of proteomics profiling all pointed to the metabolic process.

3.4 Protein Interaction Network Analysis and Parallel Reaction Monitoring Validation of the Differentially Expressed Proteins in Human Glomerular Endothelial Cells Affected by Patients' Serum Exosomes

To identify putative interactions between differentially expressed proteins, we created a PPI network using the STRING database version 9.0 (**Figure 5A**). Our analysis revealed that a majority of the screened proteins interact with one another directly or indirectly. We discovered 96 proteins linked to PPI networks

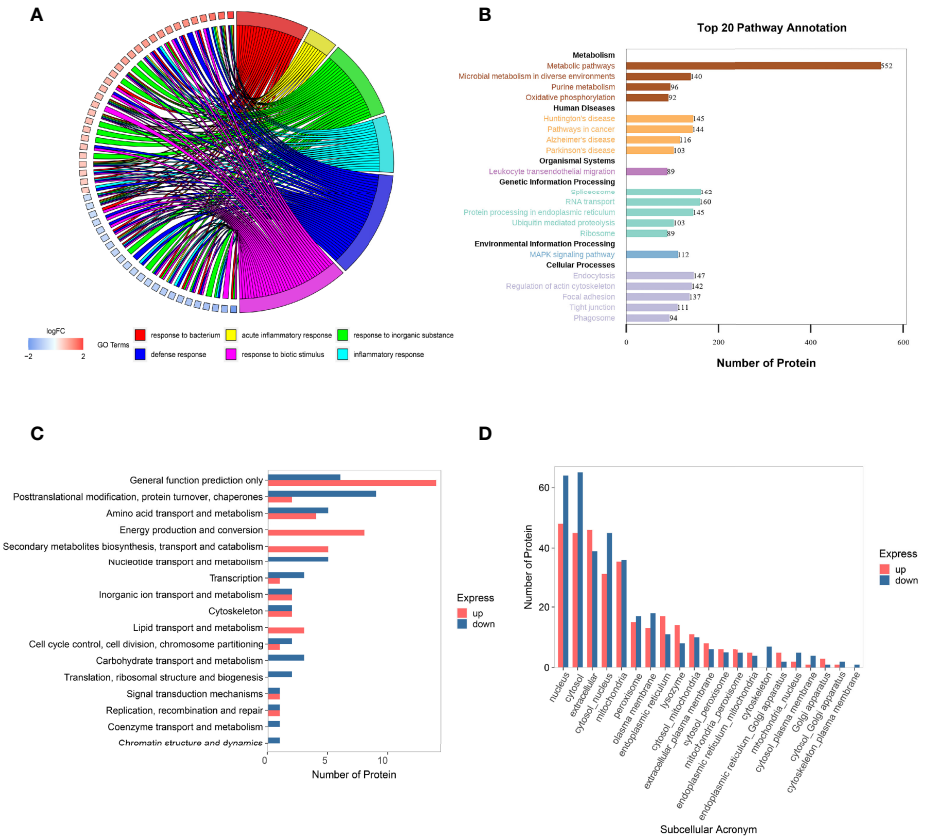

FIGURE 4 | Function analysis of the differentially expressed proteins in HGECs affected by DR+DN patients' SExos. **(A)** Circus plots of GO Classification Annotation of differential protein. **(B)** Pathway annotated result statistics chart. A histogram of the top 20 pathway names sorted by the number of annotated proteins. The abscissa represents the number of proteins, and the ordinate represents the annotated KEGG entry. **(C)** Differential protein COG classification annotation bar graph. Take differential protein as the analysis object, perform COG functional classification analysis, and compare the functional classification of upregulation and downregulation. **(D)** Statistics of subcellular localization results of differential proteins. Sub-cells are shown by the abscissa, while the number of proteins is represented by the ordinate.

in this PPI network. Fibronectin 1 (*FN1*) was the most important hub among these proteins, connecting with 19 others.

The most complicated networks contained *FN1*, COL1A1, and superoxide dismutase 2 (SOD2). As a result, these proteins should be given specific attention in follow-up investigations on DN dysfunction. SOD2 has been linked to diabetic microvascular problems such as DR and retinopathy. Among its related pathways are apoptosis and survival_anti-apoptotic action of nuclear ESR1 and ESR2 and oxidative stress. GO annotations related to this gene include identical protein binding and oxygen binding. Fibronectin, a protein involved in cell adhesion and migration, including embryogenesis, wound healing, and blood coagulation, is encoded by the *FN1* gene. *FN1* is linked to glomerulopathy with fibronectin deposits. The pathways of integrin cell surface contacts and VEGF signalling are linked. COL1A1 gives instructions for creating a part of type I collagen, the most abundant type of collagen in the human body. The VEGF signaling pathway is also linked to COL1A1.

FIBA, ICAM-1, and Peptidylprolyl Cis/Trans Isomerase, NIMA-Interacting 4 (PIN4), endothelial function proteins, were chosen and confirmed using PRM analysis to further investigate the target proteins. We explored that the levels of FIBA and ICAM-1 in SExos-induced HGECs were increased 1.37-fold and 1.21-fold, respectively, and the level of PIN4 was deceased 0.78-fold (**Table 1**). The validation results were compatible with the protein analysis data, even though the fold change values differed. **Figure 5B** showed the fragment ion peak distribution of FIBA peptides in all samples. Protein levels of FIBA were significantly upregulated in DR+DN-SExos-incubated HGECs.

3.3 Global Metabolic Changes in Human Glomerular Endothelial Cells Incubated With CON/DRDN-SExos

To further explore the metabolites and metabolic processes that DR+DN patients' SExos induce endothelial dysfunction, the UPLC-MS/MS detection platform, combined with the univariate and multivariate statistical analysis methods, was used to study the metabolome differences between groups.

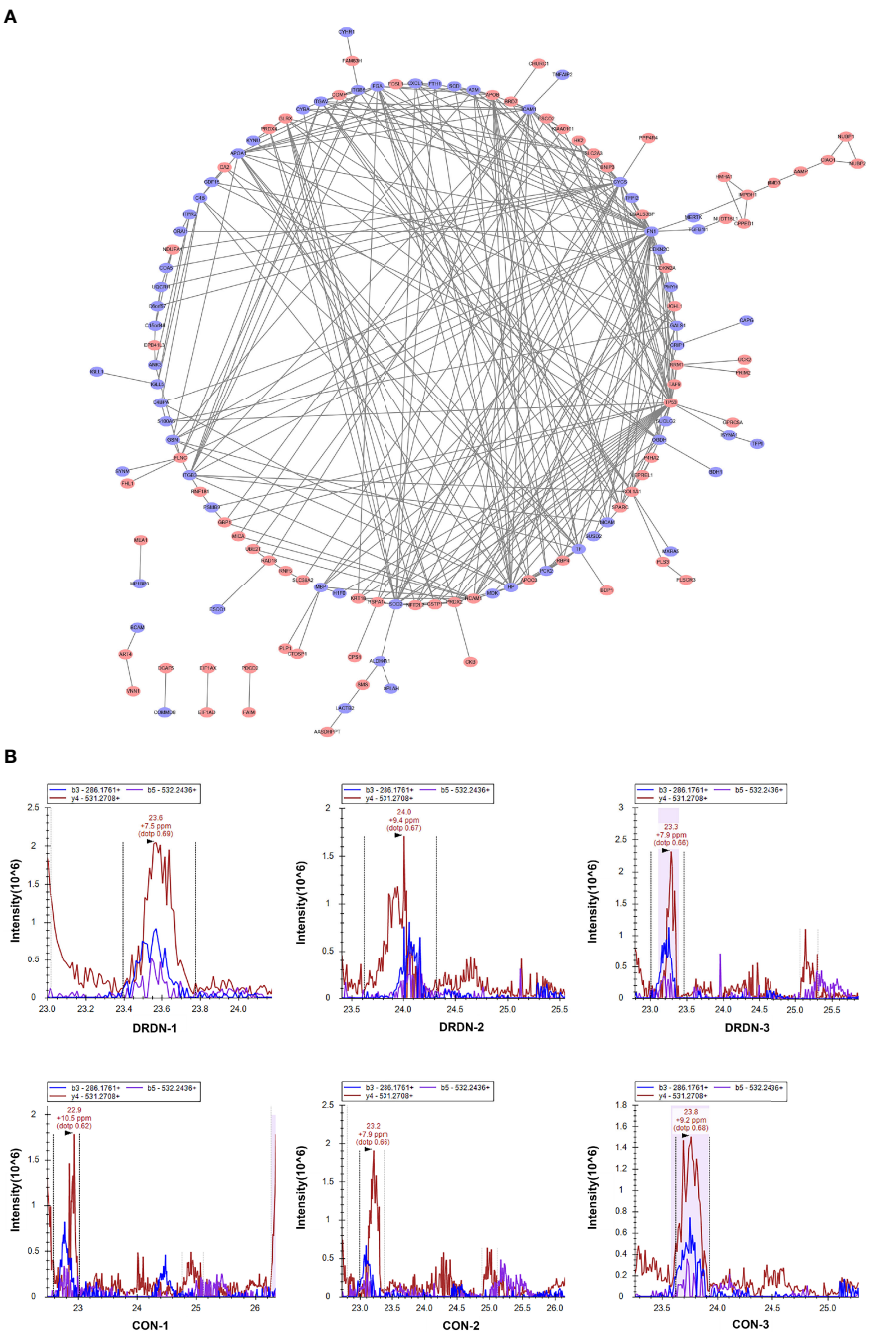

FIGURE 5 | PPI analysis and PRM validation of significantly differentially expressed proteins in HGECs incubated with CON- and DRDN-SExo. **(A)** PPI analysis of differentially expressed proteins to describe putative links between the adhesion-related proteins tested. **(B)** PRM validation of FIBA protein in CON and DRDN groups.

TABLE 1 | Confirmation of potential differentially expressed proteins related to endothelial function using PRM analysis.

Peptide	Protein	Gene Name	Fold Change (TMT)	Fold Change (PRM)
ALTDMPQMR	sp|P02671|FIBA_HUMAN	FGA	4.024	1.37
CQVEGGAPR	sp|P05362|ICAM1_HUMAN	ICAM-1	1.684	1.21
QGGDLGWMTR	sp|Q9Y237|PIN4_HUMAN	PIN4	0.666	0.78

TMT, Tandem mass tag-based liquid chromatography-tandem mass spectrometry; PRM, Parallel Reaction Monitoring; FGA,Fibrinogen alpha chain; ICAM-1, Intercellular Adhesion Molecule 1; PIN4, Peptidylprolyl Cis/Trans Isomerase, NIMA-Interacting 4.

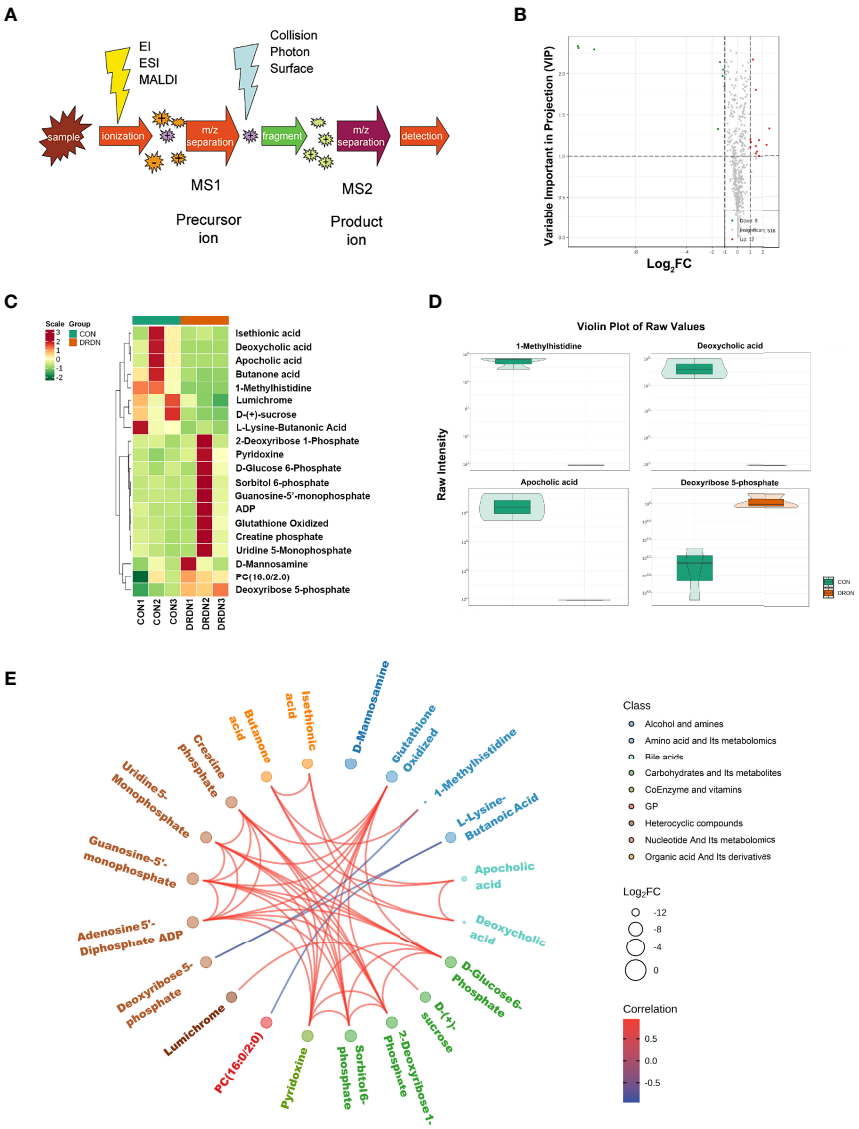

FIGURE 6 | Metabolic profiles of HGECs incubated with CON- and DRDN-SExo. **(A)** Schematic diagram of the mass spectrometry multi-reaction monitoring mode. **(B)** The overall cluster diagram of the sample. The horizontal is the sample information, and the vertical is the metabolite information. Scale represents the obtained value after the standardization of the relative content of metabolites (the redder the color, the higher the content), and Group represents the grouping. **(C)** Volcano map of differential metabolite. A metabolite is represented by each point on the volcano map, with the green point representing the differential metabolite that is downregulated, the red point representing the differential metabolite that is upregulated, and the gray point representing the metabolite that is detected but not significantly different. The ordinate shows the VIP value, while the abscissa represents the logarithmic value of the relative content difference of the metabolites in the two groups. **(D)** Differential metabolite diagram in the form of a violin. The abscissa represents the sample, while the ordinate represents the differential metabolite's relative content (original peak area). The interquartile range is shown by the middle box, the 95% confidence interval is represented by the thin black line that extends from it, the median is represented by the black horizontal line in the center, and the data distribution density is represented by the outside shape. **(E)** Differential metabolites are depicted as a chord diagram. The log2 FC value of the different metabolites is the outermost layer in the figure; the different colors represent the different classifications of the corresponding metabolites; the line represents the size of the Pearson correlation coefficient between the corresponding different metabolites, the positive correlation is represented by the pink line, and the negative correlation is demonstrated by the blue line; the line represents the size of the Pearson correlation coefficient between the corresponding different metabolites, the positive correlation is represented by the pink line, and the blue line represents negative correlation. By default, plot the differential metabolites with $|r| > 0.8$ and $P < 0.05$.

Metabolite quantification was performed by using the MRM mode analysis of triple quadrupole mass spectrometry (**Figure 6A**). **Supplementary Figure S7** showed the overlay of the total ion current (TIC) graph using mass spectrometry detection for the quality control sample. The TIC curves for metabolite detection include a lot of overlap, indicating that signal stability is better when the mass spectrometer detects the same sample multiple times.

Based on the OPLS-DA results, the resulting variable importance projection (VIP) of the OPLS-DA model can be used to filter different metabolites between groups. Simultaneously, the univariate analysis P-value and fold change were employed to select other differential metabolites. When a metabolite met the conditions of fold change ≥2/≤0.5 and VIP ≥1, it was selected as a differential metabolite. The clustering heat map for different metabolites were shown in **Figure 6B**, with the ordinate representing the main differentially selected metabolites. The volcano plot shown in **Figure 6C** presented the relative contents of different metabolites and the statistical differences between the groups. There were 12 upregulated metabolites (red dots) and 8 downregulated metabolites (green dots). The details of differential metabolites between CON and DRDN groups had been demonstrated in **Supplementary Material S8**.

In order to show the data distribution density of different metabolites between groups, a violin chart showing the 4 differential metabolites which were the most significantly expressed was drawn with the ordinate representing the relative content of the different metabolites (**Figure 6D**). It was found that 1-MH, deoxycholic acid, apocholic acid, and deoxyribose 5-phosphate were the most changed metabolites after endothelial cells were treated with DR+DN patients' SExos. The Pearson correlation analysis method (**Figure 6E**) was performed, and results showed that 1-MH, deoxycholic acid, and apocholic acid presented the positive correlations with butanone acid, while 1-MH presented the negative correlation with deoxyribose 5-phosphate.

3.4 Function Analysis of Differential Metabolites in Human Glomerular Endothelial Cells Treated With CON/DR+DN-SExos

The possible metabolic processes for different metabolites were investigated by the KEGG pathway classification analysis. **Figure 7A** and **Supplementary Material S9** show the KEGG classification of the different metabolites, with the ordinate representing the KEGG metabolic pathway and the abscissa representing the number of different metabolites annotated to the pathway and their proportion to the total number of annotated metabolites. The metabolic pathways, which include starch and sucrose metabolism, pyrimidine metabolism, and purine metabolism, had the highest value of 85.62%, as expected. It is to be noted that the taste transduction is also one of the most important pathways. Because traditional enrichment analysis focuses on metabolites that are considerably upregulated or downregulated, it is easy to overlook metabolites that are not significantly differently expressed but have major biological implications. The MSEA was carried out using the MetaboAnalyst database (http://www.metaboanalyst.ca/). **Figure 7B** and **Supplementary Material S10** show the findings of the analysis. Cysteine and methionine metabolism, pantothenate and CoA biosynthesis, vitamin B6 metabolism, drug metabolism, and phenylalanine metabolism were the most important metabolic sets. The metabolic pathway enrichment was then performed simultaneously using the HMDB (https://hmdb.ca/) (**Figure 7C**, **Supplementary Material S11**). Transaldolase deficit, ribose-5-phosphate isomerase deficiency, pentose phosphate route, and glucose-6-phosphate dehydrogenase shortage were the most important metabolic pathways.

3.5 Integration Analysis Between Metabolomics and Proteomics

According to the enrichment analysis results of differential metabolites and differential proteins, the histogram was drawn to show the degree of enrichment of pathways with differential metabolites and differential proteins at the same time (**Figure 8A**). The most noticeable pathway was the carbohydrate digestion and absorption, which was significant in the pathways with the coexistence of both differential proteins and differential metabolites. Moreover, the most significant pathway of differential protein in joint analysis was the arginine and proline metabolism that were reported to have specific associations with diabetic complications (49).

To investigate the link between metabolites and proteins, the Pearson correlation matrix was used (**Figure 8B**). Differential proteins expressed by endothelial cells treated by patient's SExos showed a strong correlation with L-lysine-butanoic acid, 1-MH, deoxycholic acid, PC (16:0/2:0), apocholic acid, deoxyribose 5-phosphate, lumichrome, D-(+)-sucrose, and butanone acid.

Then, an O2PLS model was established based on all differential proteins and differential metabolites. The load diagram was used to preliminarily select the metabolites with high correlation and weight and screen out the metabolites that have the greatest impact on the differentially expressed proteins (**Figure 8C**). Results showed that 1-MH, D-(+)-sucrose, and deoxyribose 5-phosphate presented the greatest impacts. Then, the differential proteins and differential metabolites with correlations greater than 0.8 in all analysis pathways were selected for the network diagram (**Figure 8D**, **Supplementary Material S12**). It could be seen that 1-MH and FIBA had a positive correlation, while 1-MH had a negative correlation with superoxide dismutase [Mn] (SODM), integrin beta-3 (ITB3), and 5-Oxoprolinase (OPLA). Here, 1-MH was the most significant metabolite of endothelial cells processed by DR+DN patients' SExos according to the metabolic analysis and was also the differential metabolite that was closely related to the differential proteins from the analysis above.

3.6 Overexpression of Fibrinogen Alpha Chain Exacerbated Endothelial Cell Injury in Human Glomerular Endothelial Cells

Using adenovirus-mediated expression of FGA shRNA, we were able to successfully overexpress FGA (shFGA group). FIBA levels were considerably overexpressed in HGECs compared to untransfected HGECs (CON group) and vector control cells (shCON group) (**Figure 9A**). In order to verify whether overexpression of FGA could injure endothelial cells, we cultured HGECs with shFGA and high-glucose culture medium (HG group), respectively, and extracted cellular

FIGURE 7 | Function analysis of differential metabolites in HGECs treated with CON/DR+DN-SExos. **(A)** KEGG classification of various metabolites. The ordinate is the KEGG metabolic pathway, while the abscissa is the number of differential metabolites ascribed to the route and its fraction of the overall number of annotated metabolites **(B)** MSEA enrichment analysis chart. The ordinate indicates the name of the metabolic set, which corresponds to the P-value of the labeled metabolic set; the abscissa indicates the fold enrichment; the color indicates the P-value. **(C)** HMDB enrichment map for different metabolites. The abscissa is the rich factor associated with each path, whereas the ordinate is the path's noun. The number of different metabolites enriched is represented by the size of the dot, and the color of the point denotes the P-value.

protein 48 h later. The protein expressions of endothelial dysfunction markers including ICAM-1 and VCAM-1 were upregulated in shFGA and HG groups, while CD31 and vWF were significantly downregulated (**Figure 9B**).

3.9 1-Methylhistidine Rescued Human Glomerular Endothelial Cells From Injury Induced by High Glucose

To further explore the effect of 1-MH on endothelial function, we added 1-methyl-L-histidine solution to HG-incubated HGECs (+1-MH group). The control group was HGECs incubated with HG culture medium added with the same volume of PBS (+PBS group). Compared with HG and +PBS groups, the protein expressions of ICAM-1 and VCAM-1 were significantly downregulated while CD31 and vWF were upregulated (**Figure 9C**). The increase of 1-MH could weaken the impairment effect of high glucose on HGECs. The chemical structural formula of 1-MH is shown in **Figure 9D**.

4 DISCUSSION

DN and DR are the most common diabetic microvascular complications (2, 4, 5). However, the pathogenesis is still

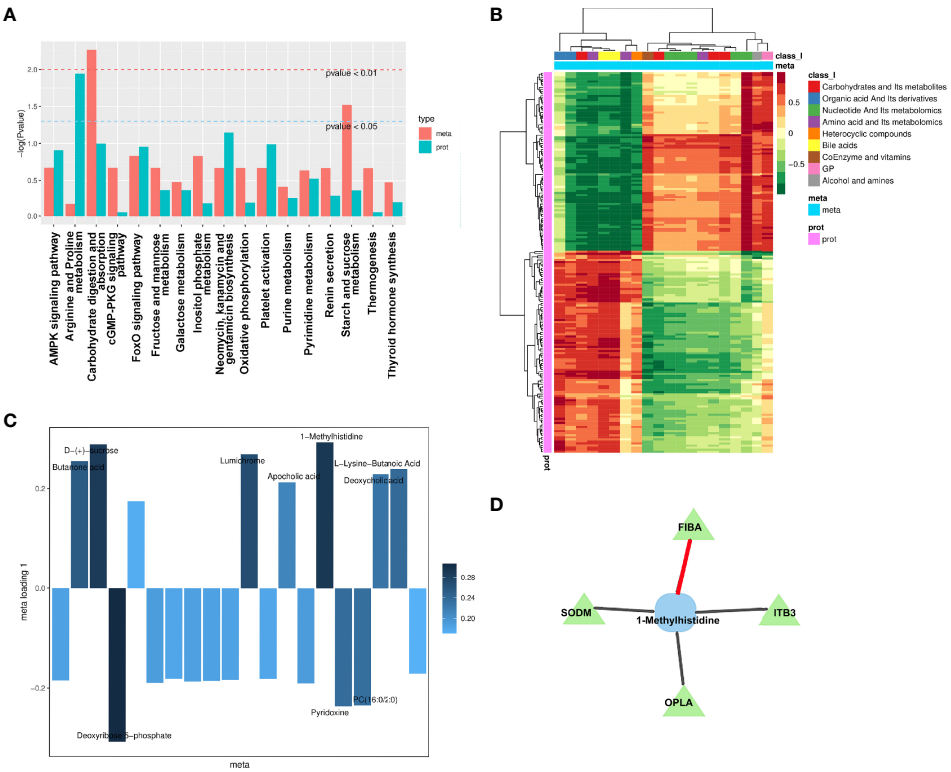

FIGURE 8 | Integration analysis between metabolomics and proteomics. **(A)** Analysis of KEGG enrichment histogram of P-values. The metabolic route is indicated by the abscissa, the enriched P-value of differential metabolites is represented by red on the ordinate, and the enriched P-value of differential proteins is represented by green on the ordinate (P-value). **(B)** Correlation coefficient clustering heat map. Each row represents a protein, and each column represents a metabolite in the diagram. A positive correlation between genes and metabolites is represented by red, whereas a negative correlation between proteins and metabolites is represented by green. **(C)** Loading diagram of metabolites. The distance from each point in the figure to the origin or the height of the bar graph represents the correlation between matter and proteomics. **(D)** Diagram of a correlation network. Proteins are represented by green triangles, while metabolites are represented by blue squares. Positive correlation is shown by the black line, while negative correlation is represented by the red line.

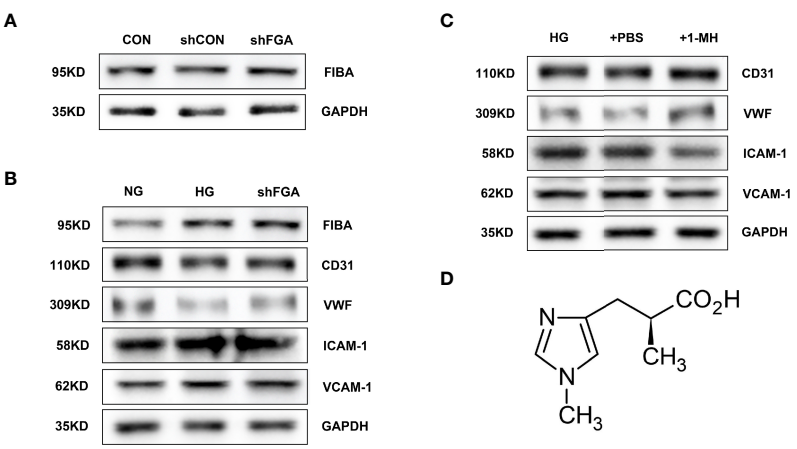

FIGURE 9 | Overexpression of FGA exacerbated endothelial cell injury in HGECs; 1-MH rescued HGEC from injury induced by high glucose. **(A)** FIBA levels were considerably elevated in HGECs transplanted with FGA overexpressed shRNA compared to untransfected HGECs (CON group) and vector control cells (shCON group) (shFGA group). **(B)** The protein expressions of ICAM-1 and VCAM-1 were upregulated in shFGA and HG groups, while CD31 and vWF were significantly downregulated. **(C)** Compared with HG and +PBS groups, the protein expressions of ICAM-1 and VCAM-1 were significantly downregulated in HGECs with the increase of 1-MH content, while CD31 and vWF were upregulated. **(D)** The chemical structural formula of 1-MH.

unclear. To date, there is rarely a proteomic profile or metabolome analysis involving diabetic SExos-induced endothelial dysfunction. We used TMT-based LC-MS/MS technology for the first time to characterize the whole proteome of HGECs incubated with SExos from DR+DN patients and UPLC-MS/MS analysis to investigate the differential metabolites. In this work, TMT technology was used to quantitatively analyze HGECs treated with SExos from healthy people or DR+DN patients, and a targeted metabolomic approach was applied to find 87 upregulated proteins and 98 downregulated proteins in HGECs treated with SExos from DR+DN patients. FGA was the most upregulated protein among the differentially expressed proteins. FGA encodes the alpha subunit of the coagulation factor fibrinogen (FIBA), which is a component of blood clot (50, 51). An important paralog of FGA is *FN1*, which is also the protein that interacts directly with most other proteins in PPI analysis. The researchers next used a broad-target metabolome study to detect 12 upregulated and 8 downregulated metabolites, with 1-MH showing the most significant changes in HGECs treated with SExos. A joint analysis of differential proteins and differential metabolites was conducted to further determine the role of target metabolites in DRDN and explore the link between differential proteins and differential metabolites. The results showed that 1-MH and FIBA may be correlated in the pathology of DR and DN. Overexpression of FGA worsened endothelial cell injury in HGECs *in vitro*, whereas 1-MH protected HGECs from injury caused by high glucose.

The coincidence of retinal and nephropathy pathology in diabetic patients is recognized, and the definition of "renal-retinal syndrome" has been proposed in the literature (52). In diabetes, endothelial dysfunction occurs in both the retina and kidney, indicating that there might exist potential factors inducing endothelial cell damage in the circulation. Exosomes carrying a variety of proteins and RNAs are vesicles actively secreted by cells (14–16). Exosomes play a role in cell communication, cell migration, tumor cell development, and angiogenesis (14–16). Exosomes abundant in serum have multiple activities, such as remodeling the ECM and releasing the contents into recipient cells to deliver signals and molecules to target cells and organs (16). Differentially expressed proteins and metabolites in HGECs incubated with SExos from DR and DN patients were discovered in this study, demonstrating that SExos can mediate changes in the expression of proteins and related metabolites in endothelial cells, affecting the function of the microvascular endothelial barrier in diabetes.

Under physiological conditions, microvascular endothelial cells mainly exert anticoagulant activity (53, 54). When microvascular endothelial cells are damaged, they lose their coagulation activity and exert procoagulant activity (53–55). Fibrinogen is a critical coagulation factor that plays a role in diabetic vascular disease, and fibrinogen synthesis is increased in T2D (56, 57). Furthermore, hyperfibrinogenemia is a marker for inflammatory alterations that result in endothelial dysfunction (56, 58, 59). According to this research, despite correcting for a range of factors in type 2 diabetes mellitus (T2DM), serum fibrinogen and DR show an independent connection, suggesting that they may play a role in the development of diabetic microvascular issues (60). There was a significant connection between retinopathy and serum fibrinogen level in DM participants after adjusting for all traditional indicators of atherosclerosis except serum creatinine (61). When serum creatinine was added to the other markers, the association was attenuated (61). In T2D individuals with higher urine albumin excretion, fibrinogen is upregulated and albuminuria is linked to increased fibrinogen and albumin production (62, 63). Plasma fibrinogen is required for the regulation of the inflammatory response, and high levels of plasma fibrinogen are linked to increased inflammation (64, 65). Plasma fibrinogen is a strong predictor of DN in T2D patients, according to earlier research. Fibrinogen is a protein that is released in the acute phase of infection or systemic inflammation (66–68). Furthermore, it is widely known that total fibrinogen levels rise during inflammation (68). Many studies have found that patients with diabetic microvascular problems had high plasma fibrinogen levels and that plasma fibrinogen levels are associated with the severity of DR (60). In this study, the proteomic profiles and PRM results showed that FIBA was significantly upregulated in HGECs cultured with DR+DN patients' SExos. WB results confirmed that FIBA was significantly increased in HGECs incubated in high glucose, consistent with the trend in previous studies.

Metabolite 1-MH is a biological derivative of the dipeptide anserine, classified as a methylamino acid, which is abundantly presented in muscles (69). 1-MH was reported to be associated with the increased rate of chronic kidney disease (CKD) (70). In a previous study, 1-MH was measured to be decreased in the plasma of DM (71). In our study, the content of 1-MH in HGECs treated with SExos from DR+DN patients was significantly reduced. The latest study indicated that the visceral adipose tissues of metabolic syndrome presented a decreased 1-MH compared with non-obese individuals (72). The level of urinary 1-MH of patients with arterial hypertension is recognized to decrease (73). High 1-MH concentration in the urine is independently associated with the lower risk of graft failure in kidney transplant recipient, (KTR) (74). In our study, 1-MH could reverse the HGEC injury induced by high glucose, demonstrating the protective effect of 1-MH on endothelial cells under a high glucose environment.

The correlation network of differentially expressed proteins and differential metabolites indicated that SODM, OPLA, and ITB3 presented positive correlations with 1-MH, while FIBA presented negative correlations with 1-MH. However, the pathway between 1-MH related to FIBA that affects the diabetic microvascular endothelial barrier still needs further verification, which we will conduct in the follow-up experiments. In our joint bioinformatics analysis results, the MSEA pathway enrichment result showed that the cysteine and methionine metabolism might play an essential role in the pathogenic process of diabetic endothelial dysfunction. It has been reported that, compared to the human donors from the age-matched non-diabetic people, the retina from DR patients

presented up to 3-fold higher homocysteine levels, and the key enzymes that are important for cysteine metabolism show 40%–60% lower levels in the retinal microvasculature from DR donors (75). By constricting vessels, modifying blood coagulant characteristics, causing oxidative harm to the vascular endothelium, and damaging the arterial walls, abnormal cysteine metabolism can induce cardiovascular disorders (76). Homocysteine levels in diabetes are thought to be a biomarker for microvascular problems such as diabetic neuropathy, retinopathy, and nephropathy (76). Elevated oxidative stress and reactive oxygen species (ROS), which produce glomerular endothelial dysfunction, result in a change in GFR, which causes renal dysfunction as seen by increased homocysteine and cysteine, according to studies (77, 78). Moreover, previous studies reported the importance of the KEGG pathway taste transduction in the pathogenic process, which addresses our attention. Hispanic individuals with lower carotid plaque have different allele frequencies for single-nucleotide polymorphism (SNPs) within the taste receptor genes compared to those of Hispanic individuals with a more significant plaque burden (79). The sweet taste receptors were reported to be involved in the activation of ROS-NLR family pyrin domain containing 3 (NLRP3) inflammasome signaling in the pathogenesis of DN, suggesting that the taste transduction pathway might be the potential pathogenic pathway in DN (80). Pulmonary microvascular barrier dysfunction could be alleviated by activating the sweet taste receptor (81).

However, some limitations must be considered when interpreting the outcomes of this study. The first is the metabolomics and proteomics analyses' sample size constraint. The second constraint is the link between 1-MH and FIBA, which necessitates the use of additional metabolomics methods to quantify and verify small-molecule metabolites. In the future, we will further explore the roles of FIBA and 1-MH in the microvascular endothelial barrier of diabetes by using transfection technology, high glucose-incubated endothelial cell model and streptozotocin (STZ)-induced rat model. To investigate the damage effect and mechanism of SExos from DR +DN patients on endothelial cells, *in vitro* studies, metabolomics, proteomics, and bioinformatics were combined. From the results, it can be confirmed that patients' SExos might cause endothelial dysfunction mainly by upregulating FIBA and downregulating 1-MH; FIBA correlating to 1-MH might be through the pathway of reducing the excessive cysteine and methionine metabolism. Taste transduction could possibly play a role.

Overall, our findings suggest that FIBA overexpression and 1-MH loss may be linked to the pathogenicity of diabetic endothelial dysfunction in DR/DN, implying that a cohort study is needed to further investigate the role of FIBA and 1-MH in the development of DN and DR, as well as the related pathways between the two proteins.

DATA AVAILABILITY STATEMENT

The original contributions presented in the study are publicly available. These data can be found here: ProteomeXchange, PXD030660.

ETHICS STATEMENT

The studies involving human participants were reviewed and approved by the Clinical Trial Management System of the First Affiliated Hospital of Zhengzhou University. The patients/participants provided their written informed consent to participate in this study. Written informed consent was obtained from the individual(s) for the publication of any potentially identifiable images or data included in this article.

AUTHOR CONTRIBUTIONS

JY implemented the study, collected the data, analyzed the data, and wrote the article. JY, DL and ZL participated in the design and interpretation of the studies, analysis of the data, and review of the article. All authors contributed to the article and approved the submitted version.

FUNDING

This work was supported by the National Natural Science Foundation of China (General Program–81970633), Natural Science Foundation of Henan Province (202300410363), National Natural Science Foundation of China (81800648), and Major Science and Technology Special Project of Henan Province (201300310600).

SUPPLEMENTARY MATERIAL

The Supplementary Material for this article can be found online at: https://www.frontiersin.org/articles/10.3389/fendo.2022.830466/full#supplementary-material

REFERENCES

1. Wild S, Roglic G, Green A, Sicree R, King H. Global Prevalence of Diabetes: Estimates for the Year 2000 and Projections for 2030. *Diabetes Care* (2004) 27:1047–53. doi: 10.2337/diacare.27.5.1047
2. Yau JWY, Rogers SL, Kawasaki R, Lamoureux EL, Kowalski JW, Bek T, et al. Global Prevalence and Major Risk Factors of Diabetic Retinopathy. *Diabetes Care* (2012) 35:556–64. doi: 10.2337/dc11-1909
3. Stitt AW, Curtis TM, Chen M, Medina RJ, McKay GJ, Jenkins A, et al. The Progress in Understanding and Treatment of Diabetic Retinopathy. *Prog Retin Eye Res* (2016) 51:156–86. doi: 10.1016/j.preteyeres.2015.08.001
4. Brownlee M. Biochemistry and Molecular Cell Biology of Diabetic Complications. *Nature* (2001) 414:813–20. doi: 10.1038/414813a
5. Kdoqi K. KDOQI Clinical Practice Guidelines and Clinical Practice Recommendations for Diabetes and Chronic Kidney Disease. *Am J Kidney Dis* (2006) 49:S12–S154. doi: 10.1053/j.ajkd.2006.12.005

6. Lu B, Gong W, Yang Z, Yang Z, Yang Y, Wen J, et al. An Evaluation of the Diabetic Kidney Disease Definition in Chinese Patients Diagnosed With Type 2 Diabetes Mellitus. *J Int Med Res* (2009) 37:1493–500. doi: 10.1177/147323000903700526
7. Nathan DM, Zinman B, Cleary PA, Backlund JY, Genuth S, Miller R, et al. Modern-Day Clinical Course of Type 1 Diabetes Mellitus After 30 Years' Duration: The Diabetes Control and Complications Trial/Epidemiology of Diabetes Interventions and Complications and Pittsburgh Epidemiology of Diabetes Complications Experience (1983-2005). *Arch Intern Med* (2009) 169:1307–16. doi: 10.1001/archinternmed.2009.193
8. Nathan DM. The Diabetes Control and Complications Trial/Epidemiology of Diabetes Interventions and Complications Study at 30 Years: Overview. *Diabetes Care* (2013) 37:9–16. doi: 10.2337/dc13-2112
9. Zhao L, Ren H, Zhang J, Cao Y, Wang Y, Meng D, et al. Diabetic Retinopathy, Classified Using the Lesion-Aware Deep Learning System, Predicts Diabetic End-Stage Renal Disease in Chinese Patients. *Endocr Pract* (2020) 26:429–43. doi: 10.4158/EP-2019-0512
10. Keenan HA, Costacou T, Sun JK, Doria A, Cavellerano J, Coney J, et al. Clinical Factors Associated With Resistance to Microvascular Complications in Diabetic Patients of Extreme Disease Duration: The 50-Year Medalist Study. *Diabetes Care* (2007) 30:1995–7. doi: 10.2337/dc06-2222
11. Stehouwer CDA, Jan L, Donker AJM, Van Hinsbergh Victor WM. Endothelial Dysfunction and Pathogenesis of Diabetic Angiopathy. *Cardiovasc Res* (1997) 34:55–68. doi: 10.1016/s0008-6363(96)00272-6
12. Tremolada G, Lattanzio R, Mazzolari G, Zerbini G. The Therapeutic Potential of VEGF Inhibition in Diabetic Microvascular Complications. *Am J Cardiovasc Drug* (2007) 7:393–8. doi: 10.2165/00129784-200707060-00002
13. Théry C. Exosomes: Secreted Vesicles and Intercellular Communications. *F1000 Biol Rep* (2011) 3:15. doi: 10.3410/B3-15
14. Kalluri R, LeBleu VS. The Biology, Function, and Biomedical Applications of Exosomes. *Science* (2020) 367:u6977. doi: 10.1126/science.aau6977
15. Wortzel I, Dror S, Kenific CM, Lyden D. Exosome-Mediated Metastasis: Communication From a Distance. *Dev Cell* (2019) 49:347–60. doi: 10.1016/j.devcel.2019.04.011
16. Kita S, Maeda N, Shimomura I. Interorgan Communication by Exosomes, Adipose Tissue, and Adiponectin in Metabolic Syndrome. *J Clin Invest* (2019) 129:4041–9. doi: 10.1172/JCI129193
17. Pardo F, Villalobos-Labra R, Sobrevia B, Toledo F, Sobrevia L. Extracellular Vesicles in Obesity and Diabetes Mellitus. *Mol Aspects Med* (2018) 60:81–91. doi: 10.1016/j.mam.2017.11.010
18. Chen L, Yang L. Regulation of Circrna Biogenesis. *RNA Biol* (2015) 12:381–8. doi: 10.1080/15476286.2015.1020271
19. Li X, Yang L, Chen L. The Biogenesis, Functions, and Challenges of Circular Rnas. *Mol Cell* (2018) 71:428–42. doi: 10.1016/j.molcel.2018.06.034
20. Li Y, Zheng Q, Bao C, Li S, Guo W, Zhao J, et al. Circular RNA Is Enriched and Stable in Exosomes: A Promising Biomarker for Cancer Diagnosis. *Cell Res* (2015) 25:981–4. doi: 10.1038/cr.2015.82
21. Baruah J, Wary KK. Exosomes in the Regulation of Vascular Endothelial Cell Regeneration. *Front Cell Dev Biol* (2020) 7:353. doi: 10.3389/fcell.2019.00353
22. Jakhotia S, Sivaprasad M, Shalini T, Reddy PY, Viswanath K, Jakhotia K, et al. Circulating Levels of Hsp27 in Microvascular Complications of Diabetes: Prospects as a Biomarker of Diabetic Nephropathy. *J Diabetes Complicat* (2018) 32:221–5. doi: 10.1016/j.jdiacomp.2017.10.004
23. Stehouwer CDA. Microvascular Dysfunction and Hyperglycemia: A Vicious Cycle With Widespread Consequences. *Diabetes* (2018) 67:1729–41. doi: 10.2337/dbi17-0044
24. Hung C, Lin HY, Hwang D, Kuo I, Chiu Y, Lim L, et al. Diabetic Retinopathy and Clinical Parameters Favoring the Presence of Diabetic Nephropathy Could Predict Renal Outcome in Patients With Diabetic Kidney Disease. *Sci Rep* (2017) 7:1236. doi: 10.1038/s41598-017-01204-6
25. Shan K, Liu C, Liu B, Chen X, Dong R, Liu X, et al. Circular Noncoding RNA HIPK3 Mediates Retinal Vascular Dysfunction in Diabetes Mellitus. *Circulation* (2017) 136:1629–42. doi: 10.1161/CIRCULATIONAHA.117.029004
26. Liu C, Yao M, Li C, Shan K, Yang H, Wang J, et al. Silencing of Circular RNA-ZNF609 Ameliorates Vascular Endothelial Dysfunction. *Theranostics* (2017) 7:2863–77. doi: 10.7150/thno.19353
27. Hammes H. Diabetic Retinopathy: Hyperglycaemia, Oxidative Stress and Beyond. *Diabetologia* (2018) 61:29–38. doi: 10.1007/s00125-017-4435-8
28. Cho A, Park HC, Lee Y, Shin YJ, Bae SH, Kim H. Progression of Diabetic Retinopathy and Declining Renal Function in Patients With Type 2 Diabetes. *J Diabetes Res* (2020) 2020:1–7. doi: 10.1155/2020/8784139
29. Sasso FC, Pafundi PC, Gelso A, Bono V, Costagliola C, Marfella R, et al. Relationship Between Albuminuric CKD and Diabetic Retinopathy in a Real-World Setting of Type 2 Diabetes: Findings From No Blind Study. *Nutr Metab Cerebrovasc Dis* (2019) 29:923–30. doi: 10.1016/j.numecd.2019.05.065
30. Zhang K, Liu X, Xu J, Yuan J, Cai W, Chen T, et al. Deep-Learning Models for the Detection and Incidence Prediction of Chronic Kidney Disease and Type 2 Diabetes From Retinal Fundus Images. *Nat BioMed Eng* (2021) 5:533–45. doi: 10.1038/s41551-021-00745-6
31. He F, Xia X, Wu XF, Yu XQ, Huang FX. Diabetic Retinopathy in Predicting Diabetic Nephropathy in Patients With Type 2 Diabetes and Renal Disease: A Meta-Analysis. *Diabetologia* (2013) 56:457–66. doi: 10.1007/s00125-012-2796-6
32. Pegtel DM, Gould SJ. Exosomes. *Annu Rev Biochem* (2019) 88:487–514. doi: 10.1146/annurev-biochem-013118-111902
33. Yu M, Liu W, Li J, Lu J, Lu H, Jia W, et al. Exosomes Derived From Atorvastatin-Pretreated MSC Accelerate Diabetic Wound Repair by Enhancing Angiogenesis *via* AKT/Enos Pathway, Stem Cell Res. *Ther* (2020) 11:1–17. doi: 10.1186/s13287-020-01824-2
34. Shi R, Jin Y, Hu W, Lian W, Cao C, Han S, et al. Exosomes Derived From Mmu_Circ_0000250-Modified Adipose-Derived Mesenchymal Stem Cells Promote Wound Healing in Diabetic Mice by Inducing Mir-128-3p/SIRT1-Mediated Autophagy. *Am J Physiol.-Cell Ph* (2020) 318:C848–56. doi: 10.1152/ajpcell.00041.2020
35. Hsieh YT, Hsieh MC. Time-Sequential Correlations Between Diabetic Kidney Disease and Diabetic Retinopathy in Type 2 Diabetes-an 8-Year Prospective Cohort Study. *Acta Ophthalmol* (2021) 99:e1–6. doi: 10.1111/aos.14487
36. Yahalom C, Volovelsky O, Macarov M, Altalbishi A, Alsweiti Y, Schneider N, et al. Senior–Løken Syndrome. *Retina* (2021) 41:2179–87. doi: 10.1097/IAE.0000000000003138
37. Freeman DW, Noren Hooten N, Eitan E, Green J, Mode NA, Bodogai M, et al. Altered Extracellular Vesicle Concentration, Cargo, and Function in Diabetes. *Diabetes* (2018) 67:2377–88. doi: 10.2337/db17-1308
38. Akbar N, Azzimato V, Choudhury RP, Aouadi M. Extracellular Vesicles in Metabolic Disease. *Diabetologia* (2019) 62:2179–87. doi: 10.1007/s00125-019-05014-5
39. Zhang H, Liu J, Qu D, Wang L, Wong CM, Lau C, et al. Serum Exosomes Mediate Delivery of Arginase 1 as a Novel Mechanism for Endothelial Dysfunction in Diabetes. *Proc Natl Acad Sci* (2018) 115:E6927–36. doi: 10.1073/pnas.1721521115
40. Chen W, Quan Y, Fan S, Wang H, Liang J, Huang L, et al. Exosome-Transmitted Circular RNA Hsa_Circ_0051443 Suppresses Hepatocellular Carcinoma Progression. *Cancer Lett* (2020) 475:119–28. doi: 10.1016/j.canlet.2020.01.022
41. Yang R, Xing L, Zheng X, Sun Y, Wang X, Chen J. The Circrna Circagfg1 Acts as a Sponge of Mir-195-5p to Promote Triple-Negative Breast Cancer Progression Through Regulating CCNE1 Expression. *Mol Cancer* (2019) 18:4. doi: 10.1186/s12943-018-0933-7
42. Ma J, Chen T, Wu SF, Yang CY, Bai MZ, Shu KX. Iprox: An Integrated Proteome Resource. *Nucleic Acids Res* (2019) 47:D1211–7. doi: 10.1093/nar/gky869
43. Szklarczyk D, Franceschini A, WyderK. Forslund S. STRING V10: Protein–Protein Interaction Networks, Integrated Over the Tree of Life. *Nucleic Acids Res* (2015) 43:D447–52. doi: 10.1093/nar/gku1003
44. Hammoutene A, Biquard L, Lasselin J, Kheloufi M, Tanguy M, Vion A, et al. A Defect in Endothelial Autophagy Occurs in Patients With Non-Alcoholic Steatohepatitis and Promotes Inflammation and Fibrosis. *J Hepatol* (2020) 72(3):528–38. doi: 10.1016/j.jhep.2019.10.028
45. Takahashi N, Yoshida H, Kimura H, Kamiyama K, Kurose T, Sugimoto H, et al. Chronic Hypoxia Exacerbates Diabetic Glomerulosclerosis Through Mesangiolysis and Podocyte Injury in Db/Db Mice. *Nephrol Dialysis Transplant* (2020) 35(10):1678–88. doi: 10.1093/ndt/gfaa074
46. Zhang X, Seman NA, Falhammar H, Brismar K, Gu HF. Genetic and Biological Effects of ICAM-1 E469K Polymorphism in Diabetic Kidney Disease. *J Diabetes Res* (2020) 8305460:1–7. doi: 10.1155/2020/8305460

47. Lang PP, Bai J, Zhang YL, Yang XL, Xia YL, Lin QY, et al. Blockade of Intercellular Adhesion Molecule-1 Prevents Angiotensin II-Induced Hypertension and Vascular Dysfunction. *Lab Invest* (2020) 100(3):378–86. doi: 10.1038/s41374-019-0320-z
48. Haldar B, Hamilton CL, Solodushko V, Abney K, Alexeyev M, Honkanen R, et al. S100A6 Is a Positive Regulator of PPP5C-FKBP51-Dependent Regulation of Endothelial Calcium Signaling. *FASEB J* (2020) 34(2):3179–96. doi: 10.1096/fj.201901777R
49. Mangoni AA, Rodionov RN, McEvoy M, Zinellu A, Carru C, Sotgia S. New Horizons in Arginine Metabolism, Ageing and Chronic Disease States. *Age Ageing* (2019) 48:776–82. doi: 10.1093/ageing/afz083
50. Lowe GDO, Rumley A. Fibrinogen and Its Degradation Products as Thrombotic Risk Factors. *Ann NY Acad Sci* (2010) 936:560–5. doi: 10.1111/j.1749-6632.2001.tb03544.x
51. de Vries JJ, Snoek CJ, Rijken DC, de Maat MP. Effects of Post-Translational Modifications of Fibrinogen on Clot Formation, Clot Structure, and Fibrinolysis: A Systematic Review. *Arteriosclerosis thrombosis Vasc Biol* (2020) 40:554–69. doi: 10.1161/ATVBAHA.119.313626
52. Wong CW, Wong TY, Cheng CY, Sabanayagam C. Kidney and Eye Diseases: Common Risk Factors, Etiological Mechanisms, and Pathways. *Kidney Int* (2014) 85:1290–302. doi: 10.1038/ki.2013.491
53. Knapp M, Tu X, Wu R. Vascular Endothelial Dysfunction, a Major Mediator in Diabetic Cardiomyopathy. *Acta Pharmacol Sin* (2019) 40:1–8. doi: 10.1038/s41401-018-0042-6
54. Duque P, Mora L, Levy JH, H, Schö chl. Pathophysiological Response to Trauma-Induced Coagulopathy: A Comprehensive Review. *Anesthesia \& Analgesia* (2020) 130:654–64. doi: 10.1213/ANE.0000000000004478
55. Zheng N, Shi X, Chen X, Lv W. Associations Between Inflammatory Markers, Hemostatic Markers, and Microvascular Complications in 182 Chinese Patients With Type 2 Diabetes Mellitus. *Labmedicine* (2015) 46:214–20. doi: 10.1309/LMF8R2KSTOW3FLKD
56. Goldberg RB. Cytokine and Cytokine-Like Inflammation Markers, Endothelial Dysfunction, and Imbalanced Coagulation in Development of Diabetes and Its Complications. *J Clin Endocrinol Metab* (2009) 94:3171–82. doi: 10.1210/jc.2008-2534
57. Mosesson MW. Fibrinogen and Fibrin Structure and Functions. *J Thromb Haemost* (2005) 3:1894–904. doi: 10.1111/j.1538-7836.2005.01365.x
58. Vilar R, Fish RJ, CasiniM. Neerman-Arbez A. Fibrin (Ogen) in Human Disease: Both Friend and Foe. *Haematologica* (2020) 105:284. doi: 10.3324/haematol.2019.236901
59. Zhang X, Long Q. Elevated Serum Plasma Fibrinogen Is Associated With Advanced Tumor Stage and Poor Survival in Hepatocellular Carcinoma Patients. *Medicine* (2017) 96:e6694. doi: 10.1097/MD.0000000000006694
60. Azad N, Agrawal L, EmanueleR. Klein NV. Association of PAI-1 and Fibrinogen With Diabetic Retinopathy in the Veterans Affairs Diabetes Trial (VADT). *Diabetes Care* (2014) 37:501–6. doi: 10.2337/dc13-1193
61. Huang Q, Wu H, WoJ. Ma M. Clinical and Predictive Significance of Plasma Fibrinogen Concentrations Combined Monocyte-Lymphocyte Ratio in Patients With Diabetic Retinopathy. *Int J Med Sci* (2021) 18:1390. doi: 10.7150/ijms.51533
62. Tessari P, Kiwanuka E, BarazzoniM. Vettore R. Diabetic Nephropathy Is Associated With Increased Albumin and Fibrinogen Production in Patients With Type 2 Diabetes. *Diabetologia* (2006) 49:1955–61. doi: 10.1007/s00125-006-0288-2
63. Klein RL, Hunter SJ, JenkinsD. Zheng AJ. Fibrinogen Is a Marker for Nephropathy and Peripheral Vascular Disease in Type 1 Diabetes: Studies of Plasma Fibrinogen and Fibrinogen Gene Polymorphism in the DCCT/EDIC Cohort. *Diabetes Care* (2013) 26(2):1439–48. doi: 10.2337/diacare.26.5.1439
64. Kattula S, Byrnes JR, Wolberg AS. Fibrinogen and Fibrin in Hemostasis and Thrombosis. *Arteriosclerosis Thrombosis Vasc Biol* (2017) 37:e13–21. doi: 10.1161/ATVBAHA.117.308564
65. GauleR TG, Ajjan A. Fibrin (Ogen) as a Therapeutic Target: Opportunities and Challenges. *Int J Mol Sci* (2021) 22:6916. doi: 10.3390/ijms22136916
66. Alexander KS, MaddenD TE, Farrell H. Association Between γ′ Fibrinogen Levels and Inflammation. *Thromb Haemostasis* (2010) 105:605–9. doi: 10.1160/TH10-09-0626
67. WeiselR JW, Litvinov I. Fibrin Formation, Structure and Properties. *Fibrous Proteins: Structures Mech* (2017) 82:405–56. doi: 10.1007/978-3-319-49674-0_13
68. Luyendyk JP, SchoeneckerM JG, Flick J. The Multifaceted Role of Fibrinogen in Tissue Injury and Inflammation. *Blood J Am Soc Hematol* (2019) 133:511–20. doi: 10.1182/blood-2018-07-818211
69. Holeček M. Histidine in Health and Disease: Metabolism, Physiological Importance, and Use as a Supplement. *Nutrients* (2020) 12:848. doi: 10.3390/nu12030848
70. Yamaguchi Y, Zampino M, Moaddel R, Chen TK, Tian Q, Ferrucci L, et al. Plasma Metabolites Associated With Chronic Kidney Disease and Renal Function in Adults From the Baltimore Longitudinal Study of Aging. *Metabolomics* (2021) 17:1–11. doi: 10.1007/s11306-020-01762-3
71. Zhou Y, Qiu L, Xiao Q, Wang Y, Meng X, Xu R, et al. Obesity and Diabetes Related Plasma Amino Acid Alterations. *Clin Biochem* (2013) 46:1447–52. doi: 10.1016/j.clinbiochem.2013.05.045
72. Piro MC, Tesauro M, Lena AM, Gentileschi P, Sica G, Rodia G, et al. Free-Amino Acid Metabolic Profiling of Visceral Adipose Tissue From Obese Subjects. *Amino Acids* (2020) 52:1125–37. doi: 10.1007/s00726-020-02877-6
73. Chachaj A, Matkowski R, Gröbner G, Szuba A, Dudka I. Metabolomics of Interstitial Fluid, Plasma and Urine in Patients With Arterial Hypertension: New Insights Into the Underlying Mechanisms. *Diagnostics* (2020) 10:936. doi: 10.3390/diagnostics10110936
74. Said MY, Rodriguez-Niño A, Post A, Schutten JC, Kieneker LM, Gomes-Neto AW, et al. Meat Intake and Risk of Mortality and Graft Failure in Kidney Transplant Recipients. *Am J Clin Nutr* (2021) 114:1505–17. doi: 10.1093/ajcn/nqab185
75. Kowluru RA, Mohammad G, Sahajpal N. Faulty Homocysteine Recycling in Diabetic Retinopathy. *Eye Vis* (2020) 7:1–11. doi: 10.1186/s40662-019-0167-9
76. Rehman T, Shabbir MA, Inam Ur Raheem M, Manzoor MF, Ahmad N, Liu ZW, et al. Cysteine and Homocysteine as Biomarker of Various Diseases. *Food Sci Nutr* (2020) 8:4696–707. doi: 10.1002/fsn3.1818
77. Barroso M, Handy DE, Castro R. The Link Between Hyperhomocysteinemia and Hypomethylation. *J Inb Err Metab Scr* (2017) 5:216785237. doi: 10.1177/2326409817698994
78. Bhargava S. Homocysteine in Occlusive Vascular Disease. *Clin Appl Homocysteine Springer Singapore* (2018) pp:414–20. doi: 10.1007/978-981-10-7632-9_3
79. Dueker ND, Doliner B, Gardener H, Dong C, Beecham A, Della-Morte D, et al. Extreme Phenotype Approach Suggests Taste Transduction Pathway for Carotid Plaque in a Multi-Ethnic Cohort. *Stroke* (2020) 51:2761–9. doi: 10.1161/STROKEAHA.120.028979
80. Zhou L, Huang W, Xu Y, Gao C, Zhang T, Guo M, et al. Sweet Taste Receptors Mediated ROS-NLRP3 Inflammasome Signaling Activation: Implications for Diabetic Nephropathy. *J Diabetes Res* (2018) 2018:1–15. doi: 10.1155/2018/7078214
81. Harrington EO, Vang A, Braza J, Shil A, Chichger H. Activation of the Sweet Taste Receptor, T1R3, by the Artificial Sweetener Sucralose Regulates the Pulmonary Endothelium. *Am J Physiol.-Lung C* (2018) 314:L165–76. doi: 10.1152/ajplung.00490.2016

Conflict of Interest: The authors declare that the research was conducted in the absence of any commercial or financial relationships that could be construed as a potential conflict of interest.

Publisher's Note: All claims expressed in this article are solely those of the authors and do not necessarily represent those of their affiliated organizations, or those of the publisher, the editors and the reviewers. Any product that may be evaluated in this article, or claim that may be made by its manufacturer, is not guaranteed or endorsed by the publisher.

frontiers | Frontiers in Immunology

ORIGINAL RESEARCH
published: 22 April 2022
doi: 10.3389/fendo.2022.868105

Inhibition of Human Sulfotransferases by Phthalate Monoesters

Hui Huang[1†], Bei-Di Lan[2†], Yu-Jing Zhang[1], Xiao-Juan Fan[2], Min-Cui Hu[3], Guo-Qiang Qin[4], Fei-Ge Wang[4], Yue Wu[2], Tao Zheng[2] and Jun-Hui Liu[2,5*]*

[1] Department of Cardiology, General Hospital of Ningxia Medical University, Yinchuan, China, [2] Department of CardioMetabolic Center, The First Affiliated Hospital of Xi'an Jiaotong University, Xi'an, China, [3] Tianjin Life Science Research Center, Department of Microbiology, School of Basic Medical Sciences, Tianjin Medical University, Tianjin, China, [4] Human Resources Department, The First Affiliated Hospital of Jinzhou Medical University, Jinzhou, China, [5] Department of Clinical Laboratory, The First Affiliated Hospital of Xi'an Jiaotong University, Xi'an, China

OPEN ACCESS

Edited by:
Fang Zhongze,
Tianjin Medical University, China

Reviewed by:
Kun Zhou,
Shenyang University of Chemical Technology, China
Liangliang Zhu,
Anqing Normal University, China

***Correspondence:**
Tao Zheng
zhengtao900305@163.com
Jun-Hui Liu
liu1109@xjtu.edu.cn

[†]These authors have contributed equally to this work

Specialty section:
This article was submitted to Gut Endocrinology, a section of the journal Frontiers in Endocrinology

Received: *02 February 2022*
Accepted: *14 March 2022*
Published: *22 April 2022*

Citation:
Huang H, Lan B-D, Zhang Y-J, Fan X-J, Hu M-C, Qin G-Q, Wang F-G, Wu Y, Zheng T and Liu J-H (2022) Inhibition of Human Sulfotransferases by Phthalate Monoesters. Front. Endocrinol. 13:868105. doi: 10.3389/fendo.2022.868105

Objective: This study aimed to investigate the inhibition of human important phase II metabolic enzyme sulfotransferases (SULTs) by phthalate monoesters, which are important metabolites of phthalate esters (PAEs).

Method: Recombinant SULT-catalyzed metabolism of p-nitrophenol (PNP) was employed as the probe reactions of SULTs to investigate the inhibition of 8 kinds of phthalate monoesters towards SULT isoforms. An *in vitro* incubation system was utilized for preliminary screening, and 100 μM of phthalate monoesters was used. Inhibition kinetics were carried out to determine the inhibition of SULTs by phthalate monoesters.

Result: Multiple phthalate monoesters have been demonstrated to exert strong inhibition potential towards SULT1A1, SULT1B1, and SULT1E1, and no significant inhibition of phthalate monoesters towards SULT1A3 was found. The activity of SULT1A1 was strongly inhibited by mono-hexyl phthalate (MHP), mono-octyl phthalate (MOP), mono-benzyl phthalate (MBZP), and mono-ethylhexyl phthalate (MEHP). Monobutyl phthalate (MBP), MHP, MOP, mono-cyclohexyl phthalate (MCHP), and MEHP significantly inhibited the activity of SULT1B1. MHP, MOP, and MEHP significantly inhibited the activity of SULT1E1. MOP was chosen as the representative phthalate monoester to determine the inhibition kinetic parameters (K_i) towards SULT1B1 and SULT1E1. The inhibition kinetic parameters (K_i) were calculated to be 2.23 μM for MOP-SULT1B1 and 5.54 μM for MOP-SULT1E1. *In silico* docking method was utilized to understand the inhibition mechanism of SULT1B1 by phthalate monoesters.

Conclusions: All these information will be beneficial for understanding the risk of phthalate monoester exposure from a new perspective.

Keywords: phthalate esters (PAEs), sulfotransferases (SULTs), enzyme inhibition, *in silico* docking, *in vitro–in vivo* extrapolation

INTRODUCTION

Phthalate esters (PAEs) are softening chemicals that are widely used in homes and industries as plasticizers (1). PAEs are commonly used and can easily cause harm to human body. Humans are exposed to PAEs mainly through respiratory inhalation, skin absorption, and dietary intake (2). PAEs have been found to affect the reproductive system in animals, and epidemiological studies have shown that high doses of PAEs affect the endocrine and reproductive systems in humans (3, 4). PAEs are eliminated through a two-step metabolic process in the body, and the metabolic processes contain phase I and phase II (conjugation) metabolism (5). PAEs are metabolized into phthalate monoesters in the human body through the phase I biotransformation (6). PAEs with low molecular weight are excreted in urine and feces mainly as monoesters; in contrast, phthalates with high molecular weight can be further metabolized by hydroxylation or oxidation after conversion to monoesters to produce a large number of oxidative metabolites (7). In recent years, more and more attention has been paid to the effect of phthalates on human health. Some studies have shown that phthalate monoesters have higher biological activity and toxicity than the parent compound (8).

Sulfotransferases (SULTs) are an enzyme that catalyzes the sulfuration of various endogenous and exogenous substrates. Sulfuryl transfer reaction has important basic biological significance (9). SULT catalyzes the transfer of a sulfuryl group provided by 3′-phosphoadenosine-5′-phosphosulfate (PAPS) to a receptor substrate, a process originally referred to as sulfate (10). Sulfation is an important conjugation pathway responsible for detoxification and elimination of a series of exogenous and endogenous small molecules in the body (11), and is an important mechanism for regulating the biological activity of various hormones and neurotransmitters (12). For example, SULT1C4 has been shown to sulfonate estrogen compounds, and sulfation is also an important pathway for thyroid hormone metabolism (13, 14). As a phase II metabolic enzyme, human SULTs show complex patterns of broad, differential, and overlapping substrate selectivity (15, 16). Although substrates of each subtype of SULTs have certain intersections, there are corresponding specific substrates. Thirteen expressed SULT genes are included in the human genome, and they encode 13 known SULT enzymes, although each gene does not produce a single protein (9). Many endogenous and exogenous chemicals are metabolized primarily in the liver; human SULTs include 4 families in which SULT1 and SULT2 enzymes are expressed in human liver (17).

The purpose of this study was to investigate the inhibitory effect of phthalate monoesters on the activities of human SULTs. Eight phthalate monoesters commonly used in industry were selected as inhibitors, and four SULT isoforms (SULT1A1, 1A3, 1B1, and 1E1) were selected for the experiments. In addition, preliminary inhibition screening, inhibition kinetic type, and parameters were determined, and *in silico* docking and *in vitro–in vivo* extrapolation (*IVIVE*) were carried out.

MATERIALS AND METHODS

Chemicals and Reagents

Eight phthalate monoesters (the structures of phthalate monoesters are given in **Figure 1**) were purchased from J&K Chemical (Beijing, China). Human SULT isoforms (SULT1A1, 1A3, 1B1, and 1E1) were obtained from BD Gentest Corp (Woburn, MA, USA). 4-Nitrophenol (PNP) and its sulfate PNP-S,3′-phosphoadenosine-5′-phosphosulfate (PAPS), Tris-HCl, and $MgCl_2$ were purchased from Sigma-Aldrich (St. Louis, MO, USA). Ultra-performance liquid chromatography (UPLC) grade acetonitrile was purchased from Tianjin Saifurui Technology Ltd. Millipore Elix 5 UV and Milli-Q Gradient

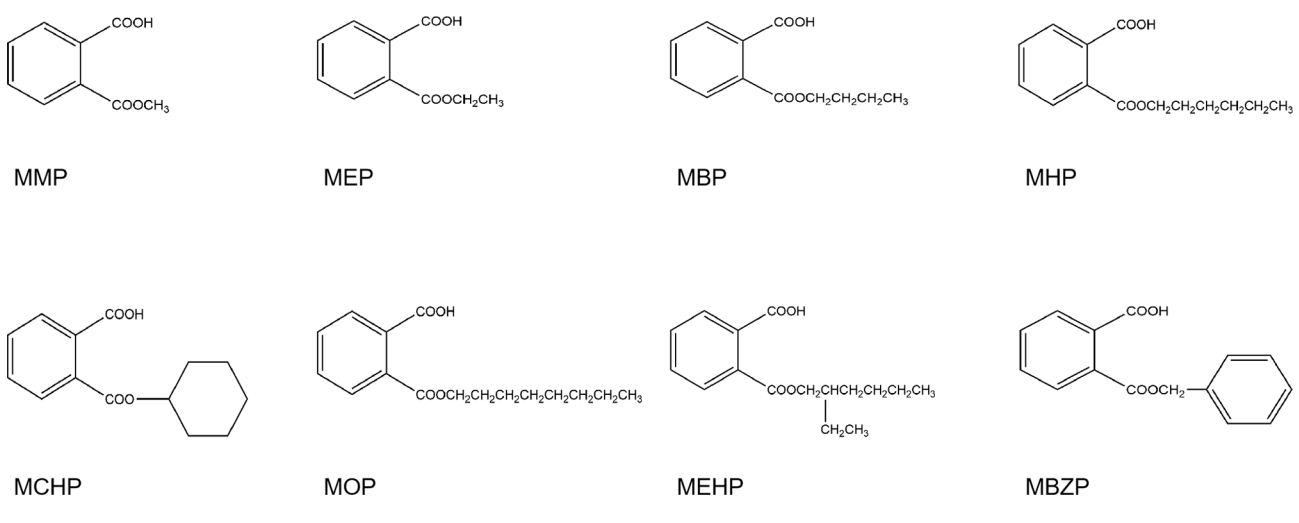

FIGURE 1 | The structure of eight phthalate monoesters.

Ultra-Pure Water System were used for the preparation of ultra-pure water. Other reagents were of ultra-performance liquid chromatography (UPLC) grade or of the highest grade commercially available.

Enzyme Activity Assays and Kinetic Study

The incubation system (total volume = 200 μl) containing 100 mM of Tris-HCl buffer (pH 7.4), 5 mM of $MgCl_2$, 40 μM of PAPS, SULTs, and PNP. The concentrations of SULT 1A1, SULT1A3, SULT1B1, and SULT1E1 were 10 μg/ml, 10 μg/ml, 20 μg/ml, and 10 μg/ml, respectively. In the incubation process, a 3-minute pre-incubation was performed, and then PAPS was added to initiate the metabolic reaction. The reaction temperature was 37°C and the reaction time was 30–60 min. At the end of the reaction, 200 μl of ice-cold acetonitrile was added for termination. An incubation solution without phthalate monoesters was used as a control. Then, after centrifugation at 12,000 rpm, 10 μl of supernatant was taken for analysis with liquid chromatography (UPLC)-UV instrument. The column used for UPLC separation is a C18 column (4.6*200 mm, 5 μm, Kromasil) with a flow rate of 0.4 ml/min and a column temperature of 25°C. The mobile phase is 0.5% formic acid aqueous solution for phase A and acetonitrile for phase B. The gradient condition was used as follows: 0–6 min, 5% B; 6–8 min, 95% B; 8–14 min, 95% B; 14–17 min, 5% B. The detection wavelength was 280 nm. The incubation system (total volume = 200 μl) containing 100 μM of phthalate monoesters, Tris-HCl buffer (50 mM, pH 7.4), $MgCl_2$ (5 mM), PAPS (40 μM), SULTs, and PNP was used to determine the Michaelis constant (K_m) of PNP metabolites. The used concentration range was 1–400 μM for SULT1A1, 0.1–7 mM for SULT1A3, 0.1–1 mM for SULT1B1, and 0.1–1.2 mM for SULT1E1. The kinetic parameters (V_{max} and K_m) were determined through fitting the data to the Michaelis–Menten equation or the substrate inhibition equation using Prism 4 software.

Preliminary Investigation of the Inhibition of Phthalate Monoesters on SULTs

4-Nitrophenol was employed as a nonselective probe substrate for human SULT isoforms to investigate the inhibition of phthalate monoesters on SULT isoforms. The incubation system (total volume = 200 μl) containing 100 μM of phthalate monoesters,100 mM of Tris-HCl buffer (pH 7.4), 5 mM of $MgCl_2$, and 40 μM of PAPS, and the concentrations of 4-nitrophenol and SULTs are different. The concentrations of 4-nitrophenol were 40, 1,200, 40, and 120 μM for SULT1A1, SULT1A3, SULT1B1, and SULT1E1, respectively. In addition, the concentrations of SULT isoforms were 10, 10, 20, and 10 μg/ml for SULT1A1, SULT1A3, SULT1B1, and SULT1E1, respectively. The absence of phthalate monoesters was set as the negative control. After pre-incubation at 37°C for 3 min, 40 μM PAPS were added for the reaction. The metabolic reaction is terminated by the addition of acetonitrile of the same volume and ensures that the incubation time can reach 30–60 min according to different SULTs. The optimized microsome protein concentration and incubation time were used to ensure linear velocity (v). The final mixture was centrifuged at 12,000 rpm for 10 min, and the supernatant of 10 μl was then used for ultra-performance liquid chromatography (UPLC)-UV instrument. All experiments were repeated in two independent experiments. Screening of phthalate monoesters was carried out with a SULT inhibition rate greater than 80% for subsequent experiments.

Determination of Half Inhibition Concentration and Evaluation of Inhibition Kinetics

The concentration-dependent inhibition effect of phthalate monoesters on SULTs was investigated using different concentrations of phthalate monoesters (ranging from 0 μM to 100 μM), and the half inhibition concentration (IC_{50}) was calculated. Based on different SULT isoforms, multiple concentrations of 4-Nitrophenol (covering the K_m value) and phthalate monoesters (covering the IC_{50} values) were used to determine the inhibition kinetics. Lineweaver–Burk plots are used to determine the type of inhibition kinetics. The second plot was used to calculate the inhibition kinetic parameters (K_i), using the linear slope of the Lineweaver–Burk double reciprocal plot and the concentration of the inhibitor phthalate monoesters.

In Vitro–In Vivo Extrapolation

In vivo inhibition magnitude of SULTs was determined through *IVIVE*. The following equation was used:

$$AUC_{i/}AUC = 1 + [I]/K_i$$

The terms are defined as follows: AUC_i/AUC was the predicted ratio of *in vivo* exposure of xenobiotics or endogenous substances with or without the co-exposure of phthalate monoesters. [I] was the *in vivo* exposure concentration of phthalate monoesters, and the K_i was the *in vitro* inhibition constant. The standard used was as follows: $[I]/K_i < 0.1$, low possibility; $0.1 < [I]/K_i < 1$, medium possibility; $[I]/K_i > 1$, high possibility.

In Silico Docking

In order to better clarify the molecular interaction between phthalate monoesters and SULTs, an *in silico* docking method was used to dock the chemical structure of phthalate monoesters into the activity cavity of SULTs. Three-dimensional (3D) structure of SULT isoforms was established using a homology modeling method. Autodock Version 4.2 was employed to dock the flexible small molecule of phthalate monoesters into the rigid protein of SULTs. The non-polar hydrogen atoms of SULT enzymes were merged. The gridbox was generated with 60 × 60 × 60 in X, Y, and Z coordinates, covering the entire ligand-binding site. Lamarckian Genetic Algorithm (LGA) method was selected to possess molecular docking study for the binding of phthalate monoesters towards SULTs. The interactions between phthalate monoesters and SULTs were analyzed, including hydrogen bonds and hydrophobic contacts.

Statistical Analysis

Experimental data were expressed as the mean value plus standard deviation (S.D.). Statistical analysis between two groups using a two-tailed unpaired Student's t-test. Multiple

groups were compared using the one-way ANOVA, and $p < 0.05$ was considered to be significant.

RESULTS

Preliminary Inhibition Screening of Phthalate Monoesters Towards SULT Isoforms

The inhibition of phthalate monoesters on SULT1A1, SULT1B1, and SULT1E1 is shown in **Figure 2**, and multiple phthalate monoesters have strong inhibition towards SULT1A1, SULT1B1, and SULT1E1. MHP, MOP, MBZP, and MEHP significantly inhibited the activity of SULT1A1. MBP, MHP, MOP, MCHP, and MEHP significantly inhibited the activity of SULT1B1. MHP, MOP, and MEHP significantly inhibited the activity of SULT1E1. As shown in **Figure 2B**, relatively more phthalate monoesters exhibited strong inhibition towards SULT1B1, with more than 80% activity inhibited by 100 μM of phthalate monoesters. All phthalate monoesters have no significant inhibition on the activity of SULT1A3 (**Supplementary Figure 1**). According to the preliminary screening results, we can find some structure–activity relationship for the inhibition of SULTs by phthalate monoesters. Phthalate monoesters with long chains inhibit the activity of SULTs relatively strongly, while phthalate monoesters with short chains (e.g., MMP, MEP, etc.) showed no significant inhibition towards all SULTs isoforms.

Inhibition Kinetic Analysis

Some phthalate monoesters significantly inhibited SULT1A1, SULT1B1, and SULT1E1, and IC_{50} was further determined. The concentration-dependent inhibition of MHP and MOP towards SULT1A1, SULT1B1, and SULT1E1 was exhibited (**Figure 3**). The concentration-dependent inhibition curve for other phthalate monoesters towards other SULTs isoforms are given in **Supplementary Figure 2**. The IC_{50} values for the inhibition of MHP, MOP, MBZP, and MEHP towards SULT1A1 were calculated to be 17.1, 5.6, 0.3, and 2.3 μM, respectively; IC_{50} values for the inhibition of MBP, MHP, MOP, MCHP, and MEHP towards SULT1B1 were calculated to be 8.5, 11.6, 2.7, 12.8, and 13.9 μM, respectively; IC_{50} values for the inhibition of MHP, MOP, and MEHP towards SULT1E1 were calculated to be 4.5, 1.8, and 1.7 μM, respectively (**Table 1**). In addition, inhibition kinetics were further determined, including kinetic types and parameters (K_i). As shown in **Figures 4A, B**, the intersection point was located in the vertical axis in the Lineweaver–Burk plot for the inhibition of SULT1B1 and

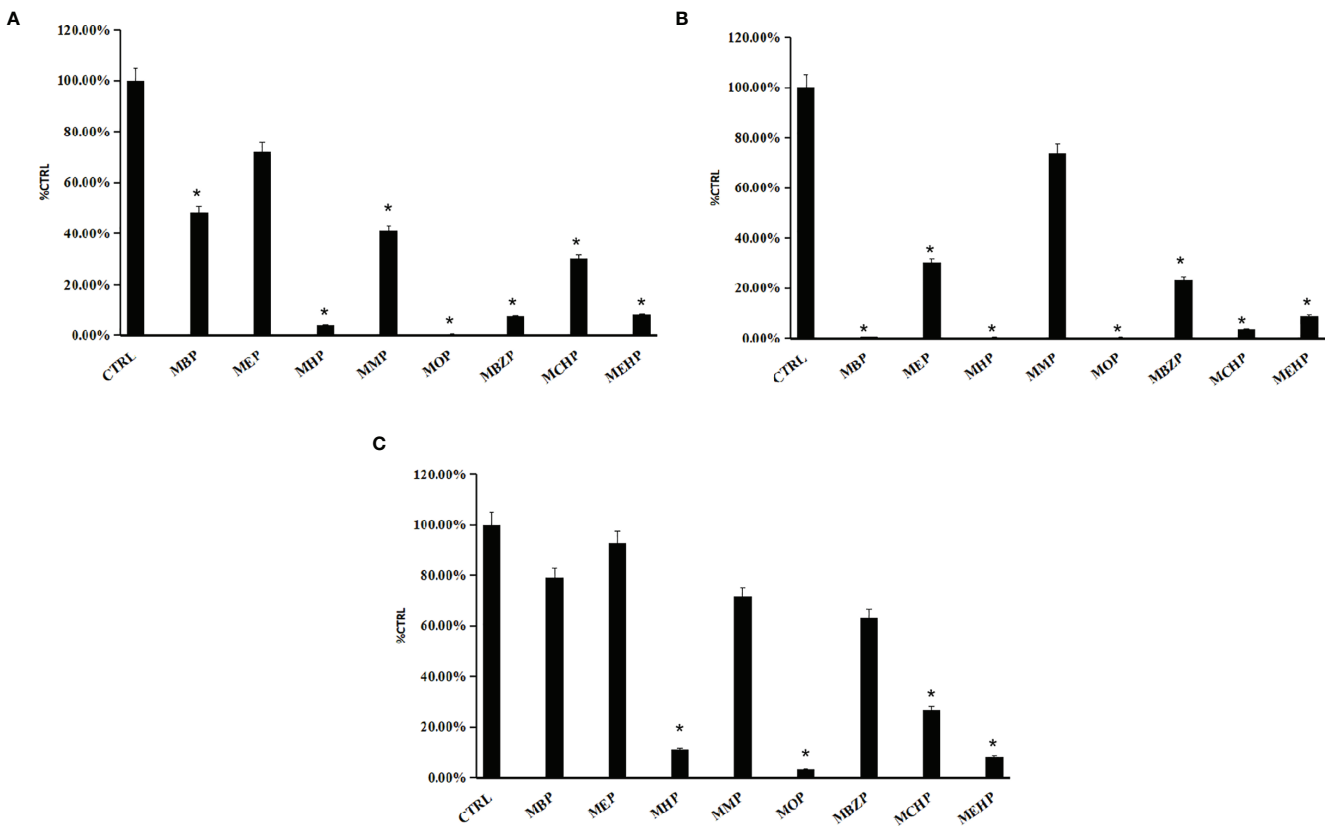

FIGURE 2 | The preliminary inhibition screening of phthalate monoesters towards SULT1A1 **(A)**, SULT1B1 **(B)**, and SULT1E1 **(C)**. The data were given as mean value plus SD; *$p < 0.05$.

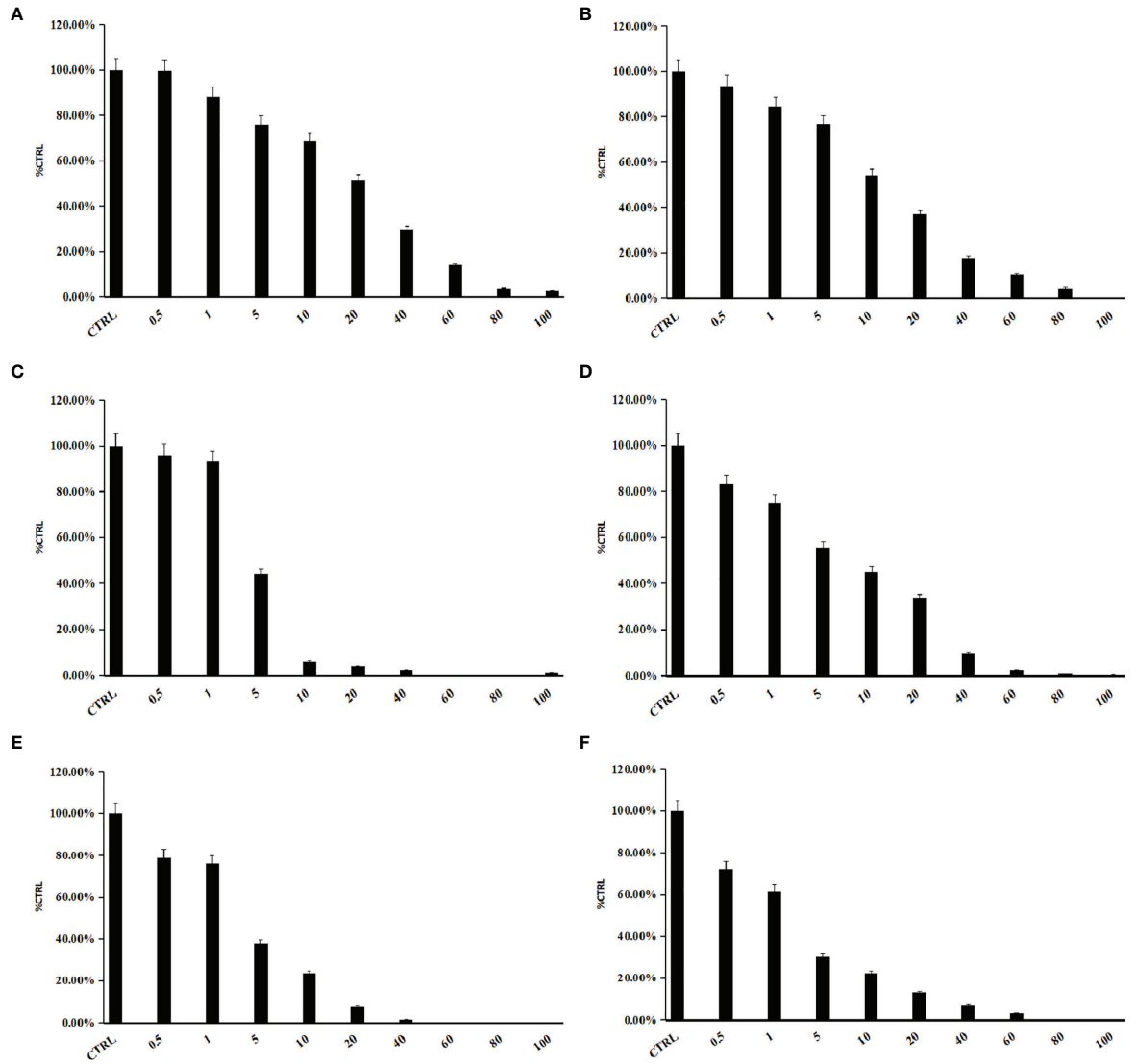

FIGURE 3 | **(A)** to **(C)** present concentration-dependent inhibition of MHP towards SULT1A1 **(A)**, SULT1B1 **(B)**, and SULT1E1 **(C)**. **(D)** to **(F)** present concentration-dependent inhibition of MOP towards SULT1A1 **(D)**, SULT1B1 **(E)**, and SULT1E1 **(F)**. IC50 was determined by different concentrations of phthalate monoesters. Parallel samples were made, and the average values were used to draw the graph. Data were presented as the mean value plus SD.

SULT1E1 by MOP, indicating the competitive inhibition of MOP towards SULT1B1 and SULT1E1. The slopes of the lines in the Lineweaver–Burk plot were calculated and drawn versus the concentrations of MOP. The second plot was used to calculate the inhibition kinetic parameters (K_i). According to **Figures 4C, D**, the inhibition kinetic parameters (K_i) were calculated to be 2.2 μM and 5.5 μM for the inhibition of MOP on SULT1B1 and SULT1E1, respectively.

In Silico Docking to Elucidate the Inhibition Mechanism

Since phthalate monoesters showed broad inhibition on SULT1B1, SULT1B1 was selected as the representative SULT isoform. We used the *in silico* docking method to analyze the mechanism of its inhibition of SULT1B1. The *in silico* docking method was used to dock the chemical structure of phthalate monoesters into the activity cavities of SULT1B1, and the representative docking results of MHP and MOP were given. The active site where SULT1B1 binds to MHP consists of amino acid residues ARG-131, SER-49, TRP-53, GLY-50, THR-52, THR-51, PHE-256, LYS-48, PRO-255, SER-139, ARG-258, HIS-142, and PHE-143, as shown in **Figure 5A**. The active site where SULT1B1 binds to MOP consists of amino acid residues MET-233, THR-52, MET-257, PHE-256, TRP-53, SER-139, LYS-48, SER-49, GLY-50, PHE-230, GLY-260, LYS-259, TYR-194, ARG-258, and ARG-131, as shown in **Figure 5B**. In the binding pocket of SULT1B1, MHP formed eight hydrogen bonds to SER-139, ARG-131, LYS-48, SER-49, GLY-50, and THR-51 (**Figure 6A**), and 4 hydrophobic contacts

TABLE 1 | Half inhibition concentrations (IC50) of phthalate monoesters towards SULTs isoforms.

	SULT1A1	SULT1A3	SULT1B1	SULT1E1
MBP	—	—	8.49	—
MEP	—	—	—	—
MHP	17.12	—	11.57	4.54
MMP	—	—	—	—
MOP	5.61	—	2.73	1.77
MBZP	0.25	—	—	—
MCHP	—	—	12.80	—
MEHP	2.32	—	13.90	1.73

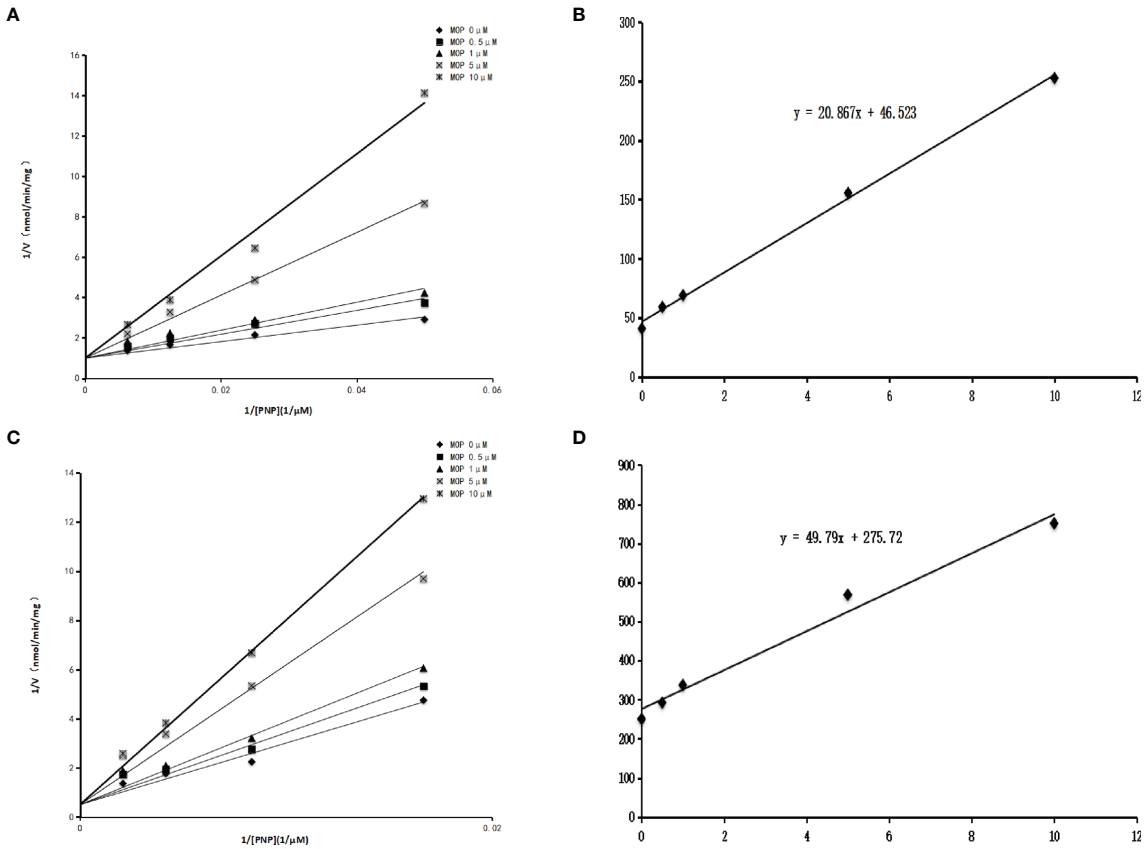

FIGURE 4 | Inhibition kinetics of MOP on SULT1B1 and SULT1E1. Lineweaver–Burk plot of the inhibition of MOP on the activity of SULT1B1 **(A)** and SULT1E1 **(B)**. Each data point represents the mean value of duplicate experiments. Determination of inhibition kinetic parameter (K_i) of MOP on the activity of SULT1B1 **(C)** and SULT1E1 **(D)** using the second plots. The vertical axis represents the slopes of the lines from Lineweaver–Burk plots, and the horizontal axis represents the concentrations of MOP.

were formed between MHP and the active cavity of SULT1B1 (**Figure 7A**). MOP formed three hydrogen bonds to SER-139, ARG-131, and LYS-48 (**Figure 6B**), and 4 hydrophobic contacts were formed between MOP and the active cavity of SULT1B1 (**Figure 7B**). The binding free energy of MBP, MHP, MOP, MCHP, and MEHP towards SULT1B1 were −7.66, −8.05, −8.23, −8.92, and −8.43 kcal/mol, respectively. The other phthalate monoester docking results are given in **Supplementary Figures 3A–C, 4A–C, and 5A–C**.

DISCUSSION

In this study, an *in vitro* determination system was used to investigate the inhibition behavior of phthalate monoesters on the activity of various isoforms of SULTs. The results showed that SULT1A1, SULT1B1, and SULT1E1 were strongly inhibited by some kinds of phthalate monoesters, but no significant inhibition on SULT1A3. In addition, the results also showed that short-chain phthalate monoesters, such as MMP and MEP,

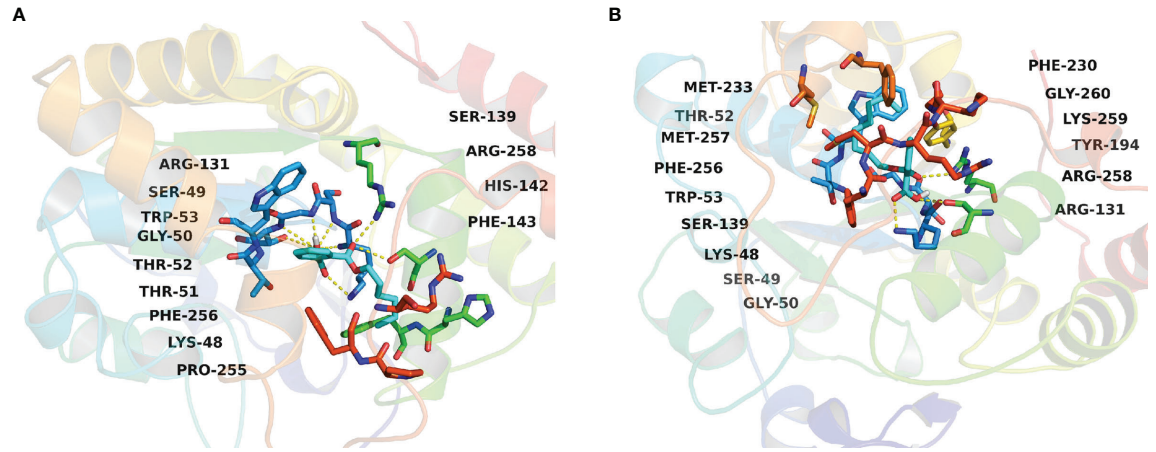

FIGURE 5 | Active pocket of SULT1B1 binding with MHP **(A)** and MOP **(B)**.

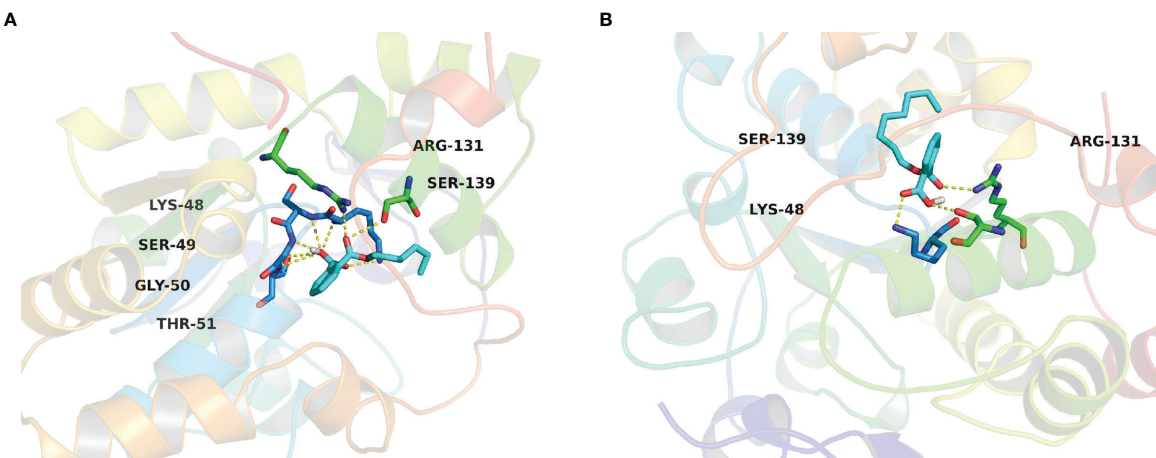

FIGURE 6 | Hydrogen bonds interaction between MHP **(A)** and MOP **(B)** with the active cavity of SULT1B1.

had no significant inhibition on all SULTs isomers, while SULT1B1 was relatively significantly inhibited.

The *IVIVE* was used to calculate the *in vivo* potential inhibition of SULTs isoforms by phthalate monoesters. MOP was chosen as the representative phthalate monoesters, and the determined K_i values were 2.23 μM and 5.54 μM for SULT1B1 and SULT1E1, respectively. According to the $[I]/K_i$ ratio ($[I]/K_i > 0.1$) evaluation standard, the threshold values were calculated to be 0.223 and 0.554μM for the inhibition of MOP towards SULT1B1 and SULT1E1, respectively. Therefore, when the *in vivo* exposure concentration of MOP is greater than 0.223μM, the metabolism of endogenous substances mediated by SULT1B1 may be inhibited. When the *in vivo* exposure concentration of MOP is greater than 0.554μM, the metabolism of endogenous substances mediated by SULT1E1 may be inhibited. SULT1A1 and SULT1B1 are generally considered to be the main enzymes involved in the detoxification of exogenous drugs in the human body (18, 19), which means that phthalate monoesters may reduce the body's detoxification of exogenous substances by inhibiting enzyme activity. SULT1E1 (estrogen sulfotransferase) is an important enzyme in hormone homeostasis regulation and biosynthesis, showing a high affinity for beta-estradiol (E2) (20), and estrogen is associated with the growth and development of human breast cancer cells (21). SULT1E1 was related to the metabolism of estrogen, so phthalate monoesters may cause certain cancer by disturbing the metabolism of estrogen. As an important phase II metabolic enzymes in human body, UDP-glucuronosyltransferases (UGTs) and SULTs play an important role in the metabolism of most endogenous substances. Previous studies have shown that UGTs can also be inhibited by phthalate monoesters (22). Therefore, because phthalate monoesters inhibit both SULTs and UGTs, it may cause greater harm to the human body.

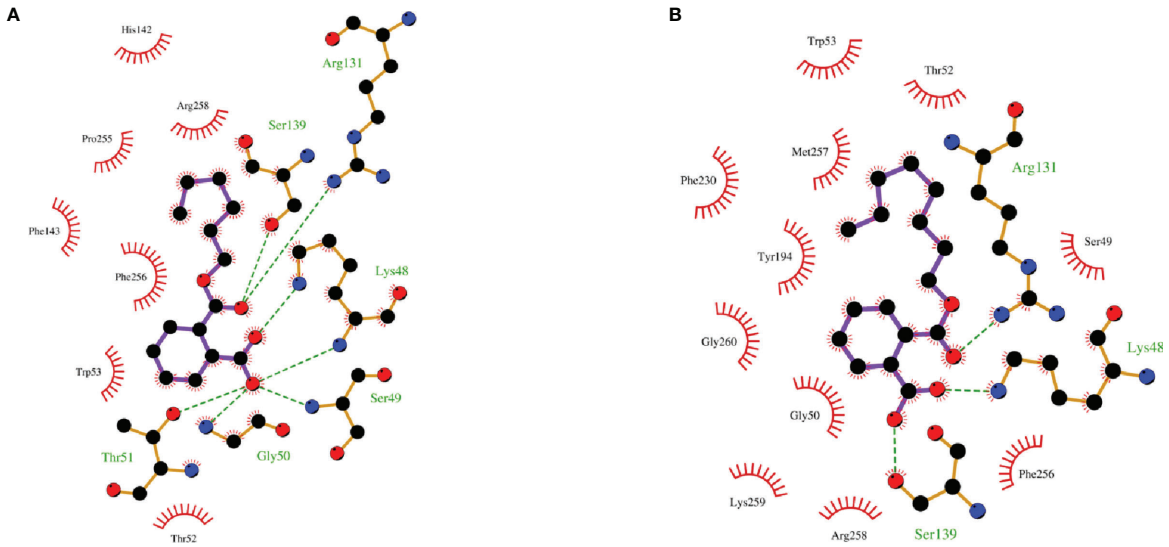

FIGURE 7 | Hydrophobic interaction between MHP **(A)** and MOP **(B)** and the active cavity of SULT1B1.

It should be noted that phthalates undergo the first phase I biotransformation after entering the body to produce monoesters. For phthalate monoesters of different molecular weights, the way they are excreted from the body and the reactions that occur in the body may be different (7). For the excretion of phthalate monoesters, the phase II metabolic enzymes play an important role. Phthalate monoesters have stronger biological activity and toxicity, so it is of great significance to select 8 phthalate monoesters in this study to explore the inhibition of SULTs.

In conclusion, our study fully described the inhibition of phthalate monoesters towards SULT isoforms. These results will provide a new perspective for the toxicity study of phthalate monoesters.

DATA AVAILABILITY STATEMENT

The raw data supporting the conclusions of this article will be made available by the authors, without undue reservation.

AUTHOR CONTRIBUTIONS

J-HL and TZ designed this study. HH and B-DL performed the experiment, analyzed the data, and wrote the draft. Y-JZ, X-JF, M-CH, and G-QQ performed the instrument analysis. F-GW and YW gave critical comments and contributed to the writing of this manuscript. All authors contributed to the article and approved the submitted version.

FUNDING

This research was funded by the National Key R&D Program of China (2019YFA0802300 and 2021YFA1301200), the National Natural Science Foundation of China (81970351 and 81822005), the Key Research and Development Program of Shaanxi (No. 2020SF-253), the Central University Basic Science Foundation of China (119132971000056), and the Clinical Research Award of the First Affiliated Hospital of Xi'an Jiaotong University, China (No. XJTU1AF-CRF-2017-006).

SUPPLEMENTARY MATERIAL

The Supplementary Material for this article can be found online at: https://www.frontiersin.org/articles/10.3389/fendo.2022.868105/full#supplementary-material

REFERENCES

1. Feng YX, Feng NX, Zeng LJ, Chen X, Xiang L, Li YW, et al. Occurrence and Human Health Risks of Phthalates in Indoor Air of Laboratories. *Sci Total Environ* (2020) 707:135609. doi: 10.1016/j.scitotenv.2019.135609
2. Gong M, Zhang Y, Weschler CJ. Measurement of Phthalates in Skin Wipes: Estimating Exposure From Dermal Absorption. *Environ Sci Technol* (2014) 48(13):7428–35. doi: 10.1021/es501700u
3. Shi YQ, Fu GQ, Zhao J, Cheng SZ, Li Y, Yi LN, et al. Di(2-Ethylhexyl) Phthalate Induces Reproductive Toxicity *via* JAZF1/TR4 Pathway and Oxidative Stress in Pubertal Male Rats. *Toxicol Ind Health* (2019) 35 (3):228–38. doi: 10.1177/0748233718824911
4. Weuve J, Hauser R, Calafat AM, Missmer SA, Wise LA. Association of Exposure to Phthalates With Endometriosis and Uterine Leiomyomata: Findings From NHANES, 1999-2004. *Environ Health Perspect* (2010) 118 (6):825–32. doi: 10.1289/ehp.0901543

5. Praveena SM, Teh SW, Rajendran RK, Kannan N, Lin CC, Abdullah R, et al. Recent Updates on Phthalate Exposure and Human Health: A Special Focus on Liver Toxicity and Stem Cell Regeneration. *Environ Sci Pollut Res Int* (2018) 25(12):11333–42. doi: 10.1007/s11356-018-1652-8
6. Silva MJ, Barr DB, Reidy JA, Kato K, Malek NA, Hodge CC, et al. Glucuronidation Patterns of Common Urinary and Serum Monoester Phthalate Metabolites. *Arch Toxicol* (2003) 77(10):561–7. doi: 10.1007/s00204-003-0486-3
7. Kim SH, Park MJ. Phthalate Exposure and Childhood Obesity. *Ann Pediatr Endocrinol Metab* (2014) 19(2):69–75. doi: 10.6065/apem.2014.19.2.69
8. Ito R, Seshimo F, Miura N, Kawaguchi M, Saito K, Nakazawa H. Effect of Sterilization Process on the Formation of Mono(2-Ethylhexyl)Phthalate From Di(2-Ethylhexyl)Phthalate. *J Pharm BioMed Anal* (2006) 41(2):455–60. doi: 10.1016/j.jpba.2005.12.021
9. Coughtrie MWH. Function and Organization of the Human Cytosolic Sulfotransferase (SULT) Family. *Chem Biol Interact* (2016) 259:2–7. doi: 10.1016/j.cbi.2016.05.005
10. Wang LQ, James MO. Inhibition of Sulfotransferases by Xenobiotics. *Curr Drug Metab* (2006) 7(1):83–104. doi: 10.2174/138920006774832596
11. Falany CN. Molecular Enzymology of Human Liver Cytosolic Sulfotransferases. *Trends Pharmacol Sci* (1991) 12(7):255–9. doi: 10.1016/0165-6147(91)90566-B
12. Richard K, Hume R, Kaptein E, Stanley EL, Visser TJ, Coughtrie MW. Sulfation of Thyroid Hormone and Dopamine During Human Development: Ontogeny of Phenol Sulfotransferases and Arylsulfatase in Liver, Lung, and Brain. *J Clin Endocrinol Metab* (2001) 86(6):2734–42. doi: 10.1210/jc.86.6.2734
13. Guidry AL, Tibbs ZE, Runge-Morris M, Falany CN. Expression, Purification and Characterization of Human Cytosolic Sulfotransferase (SULT) 1c4. *Horm Mol Biol Clin Investig* (2017) 29(1):27–36. doi: 10.1515/hmbci-2016-0053
14. Ebmeier CC, Anderson RJ. Human Thyroid Phenol Sulfotransferase Enzymes 1A1 and 1A3: Activities in Normal and Diseased Thyroid Glands, and Inhibition by Thyroid Hormones and Phytoestrogens. *J Clin Endocrinol Metab* (2004) 89(11):5597–605. doi: 10.1210/jc.2003-031939
15. Zhu J, Qi R, Liu Y, Zhao L, Han W. Mechanistic Insights Into the Effect of Ligands on Structural Stability and Selectivity of Sulfotransferase 2A1 (SULT2A1). *ACS Omega* (2019) 4(26):22021–34. doi: 10.1021/acsomega.9b03136
16. Dong D, Ako R, Wu B. Crystal Structures of Human Sulfotransferases: Insights Into the Mechanisms of Action and Substrate Selectivity. *Expert Opin Drug Metab Toxicol* (2012) 8(6):635–46. doi: 10.1517/17425255.2012.677027
17. Dubaisi S, Caruso JA, Gaedigk R, Vyhlidal CA, Smith PC, Hines RN, et al. Developmental Expression of the Cytosolic Sulfotransferases in Human Liver. *Drug Metab Dispos* (2019) 47(6):592–600. doi: 10.1124/dmd.119.086363
18. Riches Z, Stanley EL, Bloomer JC, Coughtrie MWH. Quantitative Evaluation of the Expression and Activity of Five Major Sulfotransferases (SULTs) in Human Tissues: The SULT "Pie". *Drug Metab Dispos* (2009) 37(11):2255–61. doi: 10.1124/dmd.109.028399
19. Gamage N, Barnett A, Hempel N, Duggleby RG, Windmill KF, Martin JL, et al. Human Sulfotransferases and Their Role in Chemical Metabolism. *Toxicol Sci* (2006) 90(1):5–22. doi: 10.1093/toxsci/kfj061
20. Zhang H, Varlamova O, Vargas FM, Falany CN, Leyh TS. Sulfuryl Transfer: The Catalytic Mechanism of Human Estrogen Sulfotransferase. *J Biol Chem* (1998) 273(18):10888–92. doi: 10.1074/jbc.273.18.10888
21. Falany JL, Macrina N, Falany CN. Regulation of MCF-7 Breast Cancer Cell Growth by Beta-Estradiol Sulfation. *Breast Cancer Res Treat* (2002) 74(2):167–76. doi: 10.1023/A:1016147004188
22. Du Z, Cao YF, Li SN, Hu CM, Fu ZW, Huang CT, et al. Inhibition of UDP-Glucuronosyltransferases (UGTs) by Phthalate Monoesters. *Chemosphere* (2018) 197:7–13. doi: 10.1016/j.chemosphere.2018.01.010

Conflict of Interest: The authors declare that the research was conducted in the absence of any commercial or financial relationships that could be construed as a potential conflict of interest.

The handling editor [FZ] declared a shared affiliation with the author [CH] at the time of review.

frontiers | Frontiers in Endocrinology

ORIGINAL RESEARCH
published: 01 June 2022
doi: 10.3389/fendo.2022.877807

Abnormal Activation of Tryptophan-Kynurenine Pathway in Women With Polycystic Ovary Syndrome

Siyu Wang[1,2,3†], *Liangshan Mu*[1,4†], *Chunmei Zhang*[1,4], *Xiaoyu Long*[1,4], *Yurong Zhang*[1,2,3], *Rong Li*[1,2,3,4], *Yue Zhao*[1,2,3,4,5*] and *Jie Qiao*[1,2,3,4,5]

[1] Center for Reproductive Medicine, Department of Obstetrics and Gynecology, Peking University Third Hospital, Beijing, China, [2] Key Laboratory of Assisted Reproduction, Ministry of Education, Beijing, China, [3] Beijing Key Laboratory of Reproductive Endocrinology and Assisted Reproductive Technology, Beijing, China, [4] National Clinical Research Center for Obstetrics and Gynecology (Peking University Third Hospital), Beijing, China, [5] Research Units of Comprehensive Diagnosis and Treatment of Oocyte Maturation Arrest, Chinese Academy of Medical Sciences, Beijing, China

OPEN ACCESS

Edited by:
Fang Zhongze,
Tianjin Medical University, China

Reviewed by:
Guimin Hao,
The Second Hospital of Hebei Medical University, China
Ze Wu,
The First People's Hospital of Yunnan Province, China
Yanmin Ma,
Capital Medical University, China

***Correspondence:**
Yue Zhao
zhaoyue0630@163.com

[†]These authors have contributed equally to this work

Specialty section:
This article was submitted to Gut Endocrinology, a section of the journal Frontiers in Endocrinology

Received: 17 February 2022
Accepted: 19 April 2022
Published: 01 June 2022

Citation:
Wang S, Mu L, Zhang C, Long X, Zhang Y, Li R, Zhao Y and Qiao J (2022) Abnormal Activation of Tryptophan-Kynurenine Pathway in Women With Polycystic Ovary Syndrome. Front. Endocrinol. 13:877807. doi: 10.3389/fendo.2022.877807

Background: Women with polycystic ovary syndrome (PCOS) suffer from dysfunctional metabolism and studies have reported increased levels of tryptophan in patients with PCOS. However, the changes of downstream metabolites in tryptophan catabolism pathways remain unclear.

Methods: This is a cross-sectional study that included 200 PCOS patients and 200 control women who were recruited from the Reproductive Medicine Center of Peking University Third Hospital from October 2017 to June 2019. The PCOS patients and the control group were further divided into subtypes of normal weight and overweight/obesity. Fasting blood samples from all subjects were collected on days 2~3 of a natural menstrual cycle or when amenorrhea for over 40 days with follicle diameter not exceeding 10 mm. The plasma levels of tryptophan metabolites were quantitatively determined by the liquid chromatograph mass spectrometer, including tryptophan, serotonin, kynurenine, kynurenic acid, 3-hydroxykynurenine, and quinolinic acid.

Results: The tryptophan-kynurenine pathway was dysregulated in women with PCOS, along with significantly elevated levels of tryptophan, serotonin, kynurenine, kynurenic acid, and quinolinic acid. Moreover, levels of tryptophan, kynurenine, and kynurenic acid were positively correlated with luteinizing hormone, anti-Müllerian hormone, fasting insulin, HOMA-IR. tryptophan, and kynurenine and quinolinic acid had an obvious association with C-reactive protein levels. Furthermore, logistic regression showed that tryptophan, serotonin, kynurenine, kynurenic acid and quinolinic acid were all associated significantly with the increased risk of PCOS with the adjustment for potential confounding factors. Additionally, tryptophan, kynurenine, and kynurenic acid had good diagnostic performances for PCOS, and their combination exhibited higher sensitivity and specificity to diagnostic efficiency, with the area under the ROC curve of 0.824 (95% CI 0.777-0.871), which was comparable to the endocrine indicators.

Conclusion (s): The tryptophan-kynurenine pathway was abnormally activated in PCOS patients.

Keywords: polycystic ovary syndrome, tryptophan metabolism, kynurenine, kynurenic acid, obesity

INTRODUCTION

Polycystic ovary syndrome (PCOS) is the most complicated reproductive endocrine disease in women of childbearing age, which is also recognized as the most common cause of anovulatory infertility (1). Worldwide, the prevalence of PCOS is 4–21% (2, 3), and can reach 5.6% in Chinese women (4). Typical clinical presentations of PCOS include hyperandrogenemia, oligo- or anovulation and polycystic ovaries (5, 6). In addition to reproductive disorders, PCOS patients often suffer from dysfunctional metabolism, such as obesity, insulin resistance, dyslipidemia and metabolic syndrome (7). Furthermore, the elevations of inflammatory cytokines, such as interleukins and chemokines, exacerbate metabolic disturbance in PCOS patients (8). These complications will greatly increase the long-term risk of type 2 diabetes and cardiovascular disease, with an earlier onset age (9, 10). Clinical studies have indicated that rectifying metabolic disorders could improve endocrine and reproductive disorders of PCOS patients (11). Therefore, the exploration of metabolic abnormality and the potential mechanism is the key to detect potential prediction markers and control the incidence of PCOS and complications.

Some metabolomic studies have indicated the imbalance of amino acid metabolism in PCOS, especially the significantly increased levels of aromatic amino acids (tryptophan, phenylalanine, and tyrosine) (12, 13). Tryptophan is one of the essential amino acids necessary for protein synthesis and it is metabolized mainly through kynurenine pathway and serotonin pathway. Under physiological conditions, more than 95% of tryptophan is metabolized by kynurenine (14), with the remainder converted to serotonin through the enterochromaffin cells (15). Tryptophan is firstly catalyzed by the rate-limiting enzyme, indoleamine 2,3-dioxygenase (IDO) or tryptophan 2,3-dioxygenase (TDO), to generate kynurenine. TDO is mainly expressed in the liver and drives tryptophan metabolism under physiological conditions (16); while IDO is widely distributed in whole body tissues outside the liver and its expression is up-regulated under the activation of stress, psychological pressure, and inflammation cytokines (17–20). Kynurenine generates 3-hydroxykynurenine *via* kynurenine monooxygenase and 3-hydroxykynurenine is transformed into 3-hydroxyanthranilic acid and then quinolinic acid through kynureninase and oxidase, respectively (21). In another branch of the kynurenine pathway, kynurenine can be converted into kynurenic acid *via* kynurenine aminotransferases (KAT I-IV).

In existing studies, abnormal activation of the tryptophan-kynurenine pathway is involved in the pathophysiological process of many complex diseases, including tumors, schizophrenia, and metabolic diseases, such as obesity, diabetes, and cardiovascular disease (18, 22–28). In obese adults, serum concentration of kynurenine was positively correlated with BMI and the expression of IDO1 enzymes in adipose tissue increased (29). In a cohort study of diabetic patients, it was found that tryptophan, kynurenine, quinolinic acid, and the ratio of kynurenine to tryptophan (indirect reaction of IDO/TDO enzyme activity) had predictive significance for insulin resistance and the risk of disease after a one-year follow-up (30). Moreover, in the plaque of patients with atherosclerosis, the expression of IDO enzyme in macrophages was up-regulated (31). In view of the multiple metabolic disorders in PCOS, the present study aimed to investigate the changes of the tryptophan-kynurenine pathway in PCOS patients, as well as for the detection of potential metabolic biomarkers for PCOS risk prediction.

MATERIALS AND METHODS

Ethical Approval

This study was approved by the Reproductive Medicine Ethics Committee of Peking University Third Hospital and informed consent of all participants was obtained prior to inclusion in the study.

Study Population

This is a cross-sectional study included 200 PCOS patients and 200 control women who were recruited from the Reproductive Medicine Center of Peking University Third Hospital from October 2017 to June 2019. PCOS was diagnosed according to the 2003 Rotterdam criteria (6) and met at least two of the following three characteristics: clinical and/or biochemical signs of hyperandrogenemia, oligo-ovaulation or anovulation, and polycystic ovarian ultrasound changes, after exclusion of other causes (such as hypothyroidism, Cushing's syndrome, congenital adrenal hyperplasia, and hyperprolactinemia). The control group was included from women attending the clinic due to tubal infertility or male factors. All of the control women had normal menstrual cycles, normal ovarian morphology, and did not have clinical or biochemical hyperandrogenemia. All subjects did not take medications known to affect metabolic function or reproductive function within 3 months before enrollment.

Definition of Metabolic Subtypes

Obesity was defined as body mass index (BMI) ≥ 24kg/m^2 (32). The index of homeostasis model assessment of insulin resistance (HOMA-IR) was calculated according to the formula: HOMA-IR=fasting insulin (μU/ml) × fasting glucose (mmol/L)/22.5, and insulin resistance was defined as HOMA-IR ≥ 2.69 (33). The diagnostic standard for metabolic syndrome (MetS) is based on the National Cholesterol Education Program Adult Treatment Panel III (NCEP ATP III), which requires at least three of the following features (34): (1) waist circumference (WC) ≥80cm, (2) fasting blood glucose (FPG) ≥ 5.6 mmol/L, (3) systolic blood pressure (SBP) ≥130 mmHg and/or diastolic blood pressure (DBP) ≥85 mmHg, (4) fasting triglycerides (TG) ≥ 1.70 mmol/L, (5) fasting high-density lipoprotein cholesterol (HDL-C) <1.30 mmol/L.

Sample Collection and Biochemical Measurement

The peripheral blood samples on days 2–3 of a natural menstrual cycle or when amenorrhea for over 40 days with follicle diameter

not exceeding 10 mm were collected in the morning after 8 hours of overnight fasting. The serum levels of FPG and fasting serum insulin (FINS) were determined by chemiluminescence method using Immulite 1000 system (DPC, USA). Total cholesterol (T-CHO), TG, low-density lipoprotein cholesterol (LDL-C) and HDL-C were measured by a dry slide enzymatic colorimetric assay. Measurements of serum follicle stimulating hormone (FSH), luteinizing hormone (LH), estradiol, total testosterone (T), androstenedione (AND), and progesterone were performed using a Siemens Immulite 2000 immunoassay system (Siemens Healthcare Diagnostics, USA). Ultrasensitive two-site enzyme-linked immunosorbent assay (Ansh Labs, USA) was used to measure anti-Müllerian hormone (AMH). The plasma samples were centrifuged for the quantitative analyses of metabolites in tryptophan-kynurenine pathway.

Measurement of Metabolites in Tryptophan-Kynurenine Pathway

Plasma concentrations of tryptophan, serotonin, kynurenine, kynurenic acid, 3-hydroxykynurenine, and quinolinic acid were determined by the liquid Chromatograph (Ultimate3000, Dionex, USA) Mass Spectrometer (API 3200 Q TRAP, AB, USA) (LC-MS) and 50ul of plasma sample was mixed with 150ul of pre-cooled acetonitrile and vortexed for 4 minutes at room temperature. After standing at -20°C for 10 minutes to completely precipitate the protein, the sample was centrifuged at 15000 g for 4 minutes at 4°C and 100ul of the supernatant was taken into the sample bottle of the autosampler to be tested. Tryptophan, serotonin, kynurenine, 3-hydroxykynurenine, and kynurenic acid were tested by +electrospray ionization (ESI) electrospray ion source in multiple reaction monitoring (MRM) scanning mode. The MRM ion pairs of the above metabolites were 205.1/188.1, 177.1/160.0, 209.1/146.1, 225.1/110.1 and 190.0/144.0. The spray voltage was +5500V, the collision gas CAD was Medium, and the atomization temperature was 500°C. The atomization gas was 55PSI, the auxiliary gas was 60PSI, the curtain gas was 20PSI, and the injection voltage was 10V. Chromatographic separation adopted Sapphire C18 chromatographic column (100*4.6mm 5um 100A), and its temperature was 50°C, flow rate was 1ml/min, mobile water phase was distilled water containing 0.1% formic acid, and organic phase was chromatographically pure acetonitrile containing 0.1%. Quinolinic acid adopted -ESI electrospray ion source in MRM multi-reaction monitoring scanning mode. The MRM ion pair of quinolinic acid was 166.1/122.0, and the MRM ion pair of internal standard chloramphenicol was 321.15/152.15. The spray voltage was -4200V, the collision gas CAD was Medium, and the atomization temperature was 500°C. The atomization gas was 55PSI, the auxiliary gas was 60PSI, the curtain gas was 20PSI, and the injection voltage was -10V. The chromatographic separation used a Sapphire C18 column (100*4.6mm 5um 100A), and its temperature was 50°C, the flow rate was 1ml/min, the mobile water phase was distilled water containing 5mM amine acetate, and the organic phase was pure acetonitrile. The chromatographic separation adopted a gradient elution method. Analyst Software version 1.61 was used for mass spectrometry data processing.

Statistical Analysis

The data were analyzed in SPSS Statistics (version 23.0; IBM, USA). The Kolmogorov-Smirnov test was used to determine whether the continuous variable is normally distributed. Comparisons between PCOS and control groups were performed using an independent sample *t* test and the Mann-Whitney *U* test for normally and non-normally distributed variables, respectively. The data were represented by the median (interquartile range). Spearman's rank correlation was used to evaluate the correlation between metabolites and baseline endocrine and metabolic indicators. Binary logistic regression was performed to evaluate the correlation between metabolites and the presence of PCOS, before and after adjustment for baseline variables including age, BMI, LH, AND, and AMH. The concentrations of metabolites were further scaled to standard deviation (SD) units for easy comparison of metabolites with large differences in their concentration distributions. Receiver operating characteristic (ROC) curves were prepared for comparison of the diagnostic performance of metabolites in tryptophan-kynurenine pathway and clinical parameters, individually or in combination. All reported confidence interval (CI) values were calculated at the 95% level. $P < 0.05$ was considered statistically significant.

RESULTS

Baseline Characteristics of Subjects

The baseline information, endocrine and metabolic indicators between PCOS, and control groups are shown in **Table 1**. Compared with the control group, PCOS patients had significantly increased levels of LH, total testosterone, androstenedione, AMH, fasting insulin, TG, T-CHO and LDL-C, which were in accordance with the typical abnormal characteristics of endocrine and metabolic disorders in PCOS. Also, the levels of uric acid, high sensitivity C-reactive protein (hsCRP) and HOMA-IR, were elevated in PCOS group, indicating the hyperuricemia and inflammatory state in PCOS patients.

Abnormal Activation of Tryptophan-Kynurenine Pathway in PCOS

The alterations of the metabolite levels and the ratio of the upstream and downstream metabolites in tryptophan-kynurenine pathway are shown in **Figure 1A**. The plasma levels of tryptophan and its metabolites, including serotonin, kynurenine, kynurenic acid, and quinolinic acid, were all elevated in the PCOS group which suggests abnormal activation of the tryptophan catabolism pathway. Also, the ratio of tryptophan to kynurenine (TRP/KYN) was decreased, while the ratio of tryptophan to serotonin (TRP/5-HT) was increased in PCOS group, indicating that the downstream metabolism of tryptophan was more inclined to the direction of the kynurenine pathway. Since the ratio of the up and downstream metabolites could indirectly indicate the enzyme activity involved in the conversion, the increased ratio of

TABLE 1 | The clinical information of polycystic ovary syndrome (PCOS) and control subjects.

	Control	PCOS	*P* value
Number	200	200	
Age (year)	30.00 (28.00-33.00)	30.00 (28.00-32.00)	0.228
BMI (kg/m2)	23.40 (21.06-25.40)	23.95 (20.84-28.28)	0.064
SBP (mmHg)	120.00 (112.00-127.75)	122.00 (113.50-132.00)	0.101
DBP (mmHg)	76.50 (70.00-81.00)	78.00 (70.50-84.00)	0.173
Prolactin (ng/mL)	10.80 (7.99-14.30)	11.00 (7.76-14.80)	0.876
FSH (mIU/ml)	5.97 (4.71-7.30)	5.69 (4.64-6.74)	0.111
LH (mIU/ml)	3.29 (2.22-4.83)	6.38 (3.73-9.89)	<0.001
LH/FSH	0.55 (0.40-0.79)	1.05 (0.69-1.99)	<0.001
Estradiol (pmol/L)	161.00 (124.50-202.00)	170.00 (141.00-217.00)	0.086
T (nmol/l)	0.69 (0.69-0.70)	0.78 (0.69-1.40)	<0.001
AND (nmol/l)	4.94 (3.47-7.21)	8.77 (5.88-12.60)	<0.001
Progesterone (nmol/L)	0.98 (0.67-1.40)	0.94 (0.68-1.20)	0.577
AMH (ng/ml)	2.88 (1.78-4.28)	7.40 (4.80-11.65)	<0.001
AFC	11.00 (9.00-14.00)	24.00 (18.00-24.00)	<0.001
FPG (mmol/L)	5.10 (4.80-5.30)	5.00 (4.70-5.40)	0.415
FSI (mU/L)	6.72 (4.77-9.84)	11.20 (7.06-17.26)	<0.001
HOMA-IR	1.57 (1.02-2.42)	2.44 (1.51-4.04)	<0.001
T-CHO (mmol/L)	4.26 (3.79-4.81)	4.52 (4.01-5.21)	<0.001
TG (mmol/L)	1.00 (0.73-1.48)	1.24 (0.87-1.83)	0.001
HDL-C (mmol/L)	1.27 (1.11-1.48)	1.26 (1.09-1.48)	0.913
LDL-C (mmol/L)	2.69 (2.29-3.14)	2.95 (2.42-3.59)	0.001
Uric acid (mmol/L)	274.00 (242.00-316.00)	302.00 (254.00-357.00)	<0.001
hsCRP (ng/ml)	0.16 (0.13-0.27)	0.64 (0.24-1.94)	<0.001

BMI, body mass index; SBP, systolic blood pressure; DBP, diastolic blood pressure; FSH, follicle stimulating hormone; LH, luteinizing hormone; T, total testosterone; AND, androstenedione; AMH, anti-Müllerian hormone; AFC, antral follicle counting; FPG, fasting plasma glucose; FSI, fasting serum insulin; HOMA-IR, homeostasis model assessment of insulin resistance; T-CHO, total cholesterol; TG, triglycerides; LDL-C, low-density lipoprotein cholesterol; HDL-C, high-density lipoprotein cholesterol; hsCRP, high sensitivity C-reactive protein. The data were represented by the median (interquartile range). Independent sample t test and the Mann-Whitney U test were used for normally and non-normally distributed variables, respectively.

kynurenine to tryptophan demonstrated the enhanced activity of IDO/TDO enzyme in PCOS patients (**Figure 1B**). Similarly, a significant decrease in the ratio of kynurenine to kynurenic acid (KYN/KYNA) indirectly indicated an activation of KATs enzyme in the PCOS group (**Figure 1B**).

Previous studies have shown that obesity interacted with the pathophysiological mechanism of PCOS and kynurenine concentration was positively correlated with BMI (35, 36). Although there was no statistically significant difference in BMI between the PCOS and control groups, we further compared the subgroups of normal-weight or overweight/obese population in order to determine whether obesity had an effect on the levels of tryptophan metabolites. The levels of tryptophan, serotonin, kynurenine, kynurenic acid, and quinolinic acid were still significantly increased in PCOS group compared with controls in both normal-weight and overweight/obese population, respectively (**Supplementary Table 1**), indicating that excluding the influence of obesity factors, there was still an interaction between the pathophysiological mechanism of PCOS and abnormal tryptophan metabolism.

Additionally, the abnormal activation of the tryptophan-kynurenine pathway was closely associated with the endocrine and metabolic indicators of PCOS. As **Figure 1C** shows, the levels of tryptophan, kynurenine, and kynurenic acid are positively correlated with LH, AMH, fast insulin levels and HOMA-IR in all subjects and the concentrations of kynurenine and quinolinic acid were positively correlated to BMI. Tryptophan, kynurenic acid, and quinolinic acid had a positive association with TG and negative relation to HDL-C. Interestingly, tryptophan, kynurenine, and quinolinic acid were obviously associated with uric acid and CRP levels. Hence, abnormal activation of the tryptophan-kynurenine pathway might have an impact on the neuroendocrine feedback, insulin sensitivity, and inflammatory state in PCOS patients.

Identification of Metabolites in Tryptophan-Kynurenine Pathway Associated With PCOS

Moreover, we evaluated the potential influence of metabolites in the tryptophan-kynurenine pathway on the occurrence of PCOS and found per SD elevation of the plasma levels of tryptophan metabolites (tryptophan, serotonin, kynurenine, kynurenic acid, and quinolinic acid) and per SD decrease of KYN/KYNA, all were significantly associated with the increased risk of PCOS (**Figure 2A**; **Supplementary Table 2**). With adjustment for baseline age, BMI, and endocrine confounding factors, the correlations between these metabolites and PCOS were still statistically significant and the odds ratios (95% CI) were 3.113 (1.953-4.963), 2.379 (1.406-4.026), 3.658 (2.294-5.833), 3.198 (1.615-6.333) and 1.786 (1.185-2.690), respectively (**Figure 2B**; **Supplementary Table 2**).

Besides, the prevalence of PCOS was dramatically raised with the quartiles of tryptophan, kynurenine, kynurenic acid, and quinolinic acid levels, while notably reduced with the quartiles of KYN/KYNA before and after adjustment for age, BMI, LH, androstenedione, and AMH (**Figures 2C, D**; **Supplementary**

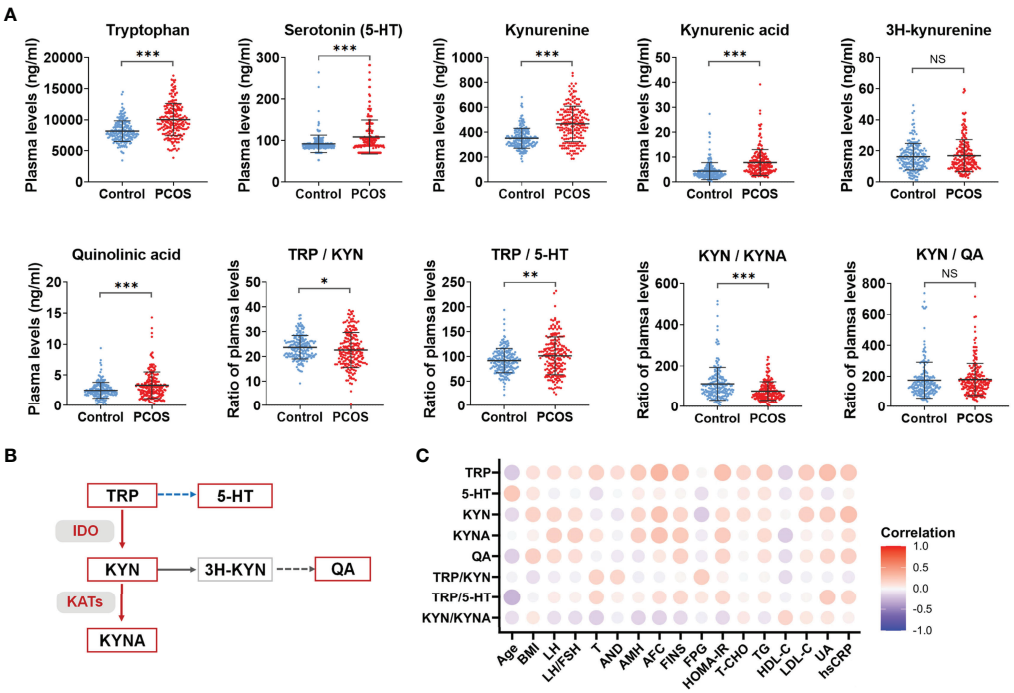

FIGURE 1 | Abnormal activation of tryptophan-kynurenine pathway in PCOS. **(A)** The plasma level changes of metabolites in tryptophan-kynurenine pathway in PCOS patients compared with control groups, ***$p < 0.001$; **$p < 0.01$; *$p < 0.05$; NS, not significant. **(B)** The sketch Map of changes of metabolites and key enzymes in tryptophan-kynurenine pathway in PCOS patients. The red color indicates increased metabolism and activated enzymes, the blue color indicates decreased metabolism, and the grey color indicates that the change trend of this pathway was not yet clear. **(C)** Correlation analysis of differential metabolites levels with the endocrine and metabolic parameters in all subjects. TRP, tryptophan; 5-HT, serotonin; KYN, kynurenine; KYNA, kynurenic acid; QA, quinolinic acid.

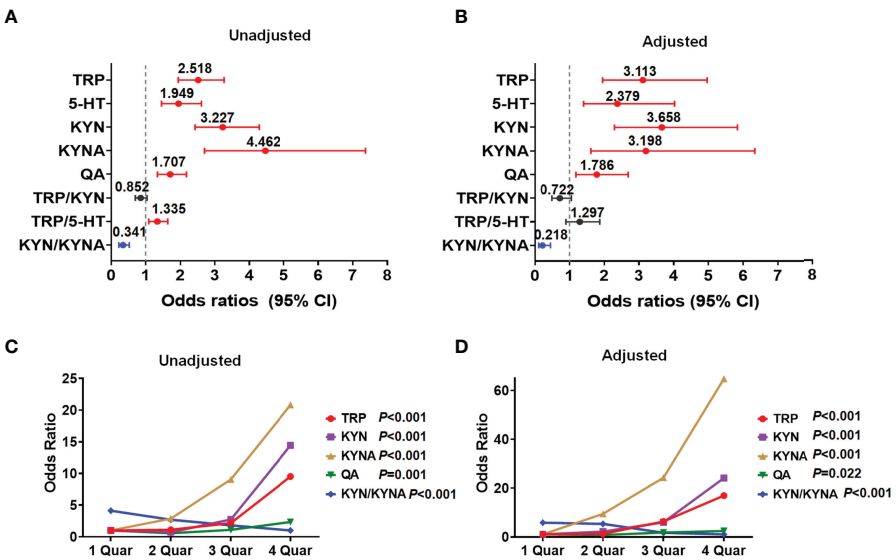

FIGURE 2 | Identification of metabolites in tryptophan-kynurenine pathway associated with PCOS. **(A)** Unadjusted odds ratios (95% CIs) of PCOS per 1 SD change in plasma abundance of each metabolite. **(B)** The odds ratios (95% CIs) of PCOS per 1 SD increase in plasma abundance of each metabolite adjusted for baseline age, BMI, LH, androstenedione, and AMH. **(C, D)** Concentration-effect relationship of metabolites in tryptophan-kynurenine pathway associated with PCOS. The prevalence of PCOS was dramatically raised with the quartiles of TRP, tryptophan; KYN, kynurenine; KYNA,kynurenic acid and QA, quinolinic acid while decreased with quartiles of KYN/KYNA, before **(C)** and after **(D)** adjusting for baseline age, BMI, LH, androstenedione and AMH.

Table 3), demonstrating that the abnormal activation of the tryptophan-kynurenine pathway and obviously altered metabolites levels, indeed, profoundly affect the occurrence and development of PCOS.

Plasma Metabolite Levels of Tryptophan-Kynurenine Pathway Showed Comparable Diagnostic Effect to Endocrine Indicators for PCOS

Since the plasma levels of tryptophan, kynurenine, and kynurenic acid were notably enhanced and most correlated with the odds of PCOS, we further compared the ability of these metabolites to distinguish PCOS. Kynurenine exhibited an area under the ROC curve (AUC) of 0.744 (95%CI, 0.658-0.774) and a highest specificity of 87.3%. Kynurenic acid had an AUC of 0.805 (95%CI, 0.756-0.854) with a sensitivity of 76.5% and a specificity of 74.7%, which was better than the diagnostic abilities of LH and androgen and close to that of AMH (**Figure 3A**). Moreover, the combination of tryptophan, kynurenine, and kynurenic acid performed relatively well and distinguished women with PCOS from the controls, and the AUC was 0.824 (95%CI, 0.777-0.871), with well-balanced sensitivity of 77.8% and specificity of 76.0% (**Figure 3B**). Furthermore, the combination of three metabolites and AMH could achieve an AUC of 0.910 (95% CI, 0.875-0.940) with the highest sensitivity of 87.6% and specificity of 80%. These results suggest that the diagnostic performances of metabolites in the tryptophan-kynurenine pathway for PCOS were comparable to the clinical endocrine indicators and could be used as the potential predictive markers of PCOS.

Determination of Metabolites in Tryptophan-Kynurenine Pathway Associated With the Different Metabolic Disorders in Women With PCOS

To determine whether the tryptophan catabolites were associated with the risk of metabolic disorders in PCOS, we further analyzed the alterations of metabolites in the tryptophan-kynurenine pathway in the different subgroups of PCOS patients. The concentrations of kynurenic acid and quinolinic acid were clearly increased in the plasma of overweight/obese PCOS women compared with the subgroup of normal weight PCOS women (**Figures 4A, B**), whereas other metabolites in the tryptophan-kynurenine pathway had no marked alteration (**Supplementary Table 1**). In addition, kynurenic acid and quinolinic acid were found to be associated with the increased odds of obesity in PCOS before and after adjusted for baseline age, LH, androstenedione, and AMH (**Figure 4C**; **Supplementary Table S4**). Conversely, there were no significant alterations in metabolites of the tryptophan-kynurenine pathway between normal weight and obese control subjects (**Supplementary Table 1**), which suggests the alterations of kynurenic acid and quinolinic acid could be specifically used as the predictors of obesity risk in PCOS women but not in non-PCOS women. Unexpectedly, there were no significant changes of metabolites in the tryptophan-kynurenine pathway in the subgroup of PCOS with insulin resistance in comparison to

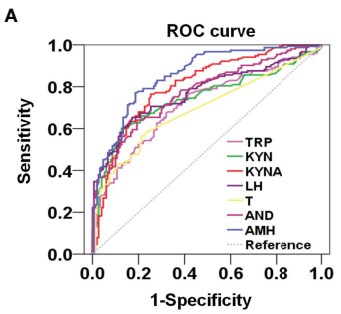

Variables	AUC	95%CI	*P*	Cut-off	Sensitivity	Specificity
TRP	0.716	0.658-0.774	<0.001	8853.37	68.0%	67.3%
KYN	0.744	0.687-0.801	<0.001	436.20	60.1%	87.3%
KYNA	0.805	0.756-0.854	<0.001	4.79	76.5%	74.7%
LH	0.772	0.718-0.825	<0.001	5.48	65.4%	82.7%
T	0.693	0.633-0.753	<0.001	0.72	56.2%	78.7%
AND	0.774	0.722-0.826	<0.001	7.58	64.1%	80.7%
AMH	0.855	0.813-0.897	<0.001	4.50	77.1%	81.3%

Variables	AUC	95%CI	*P*	Cut-off	Sensitivity	Specificity
TRP+KYN+KYNA	0.824	0.777-0.871	<0.001	0.46	77.8%	76.0%
TRP+KYN+KYNA+AND	0.908	0.875-0.940	<0.001	0.47	83.7%	85.3%
TRP+KYN+KYNA+AMH	0.910	0.878-0.942	<0.001	0.39	87.6%	80.0%

FIGURE 3 | Developing a diagnostic signature of PCOS based on the metabolites in tryptophan-kynurenine pathway. **(A)** Diagnostic potential of TRP, tryptophan; KYN, kynurenine; KYNA,kynurenic acid and the endocrine indicators by ROC analysis to distinguish PCOS from control in all participants. **(B)** Diagnostic potential of the combination of TRP, tryptophan; KYN, kynurenine; KYNA,kynurenic acid with or without the endocrine indicators by ROC analysis to distinguish PCOS from control in all participants. T, total testosterone; AND, androstenedione.

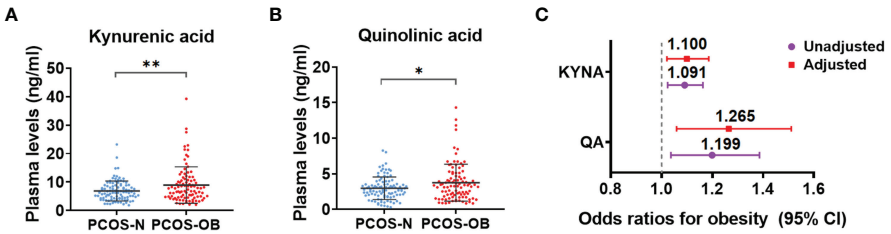

FIGURE 4 | Determination of metabolites in tryptophan-kynurenine pathway associated with the obesity risk in women with PCOS. **(A, B)** The plasma level changes of kynurenic acid **(A)** and quinolinic acid **(B)** in overweight/obese PCOS patients compared with normal weight PCOS women. $^{**}p < 0.01$; $^{*}p < 0.05$. **(C)** The odds ratios (95% CIs) of obesity in women with PCOS per 1 SD increase in plasma abundance of KYNA, kynurenic acid and QA, quinolinic acid before and after adjusting for baseline age, LH, androstenedione and AMH.

patients with normal insulin sensitivity (**Supplementary Table 5**), as well as in the subgroups of PCOS with and without metabolic syndrome (**Supplementary Table 6**). Thus, the activated tryptophan-kynurenine pathway and dramatically changed metabolites were most affected by the metabolic risk of obesity in PCOS.

DISCUSSION

Tryptophan is one of the essential mammalian amino acids and the kynurenine pathway is the major metabolic route of tryptophan degradation, which is known to play an important role in the nervous, endocrine, and immune systems (20, 23, 37). In the present study, we detected the plasma levels of tryptophan and its catabolites (serotonin, kynurenine, kynurenic acid, and quinolinic acid) in PCOS patients were significantly increased compared with the control group, as well as the enhanced activities of IDO/TDO and KATs enzymes. Remarkably, elevated metabolites were closely related to increased risk of PCOS and a combination of tryptophan, kynurenine, and kynurenic acid could be used as potential marker to predict the risk of PCOS. In addition, the plasma alterations of kynurenic acid and quinolinic acid most affected the obesity risk in PCOS.

Previous studies have reported the significant change of tryptophan metabolism in several metabolic diseases. The activation of tryptophan metabolism was found in obese adults, meanwhile the ratio of kynurenine to tryptophan was positively correlated with BMI, accompanied by elevated inflammatory cytokines in the plasma (38). Moreover, the elevated level of kynurenine led to the abnormal glucose and lipid metabolism *via* aryl hydrocarbon receptor (AhR) (39, 40). Kynurenic acid, another endogenous ligand of AhR, promoted the occurrence of atherosclerosis by activating the receptor, and thereby could be used as a risk biomarker for the prognosis of atherosclerosis and plaque stability (41). Furthermore, quinolinic acid was involved in the underlying mechanism of diabetes and dyslipidemia by destroying the function of pancreatic cells and adipocytes (29, 42). At present, it is recognized that PCOS is a chronic metabolic disease. Our findings demonstrate the positive association between levels of metabolites in the tryptophan-kynurenine pathway and some metabolic indicators, such as BMI, TG, fast insulin level, and HOMA-IR (**Figure 1C**), indicating the abnormal activation of the kynurenine pathway disturbed the metabolic profile in PCOS. Our study also detected that kynurenic acid and quinolinic acid could aggravate the obesity risk of PCOS patients (**Figure 4**).

Conversely, our results show a positive correlation between the levels of tryptophan, kynurenine, and kynurenic acid and PCOS-related endocrine indexes, LH and AMH, which implies these metabolites had a crucial impact on hypothalamic-pituitary-gonadal (HPG) axis. In previous research on neurological diseases, the initial rate-limiting enzyme IDO was activated, under stress and anxiety, to promote the abnormal metabolism of tryptophan (43). It has been found that tryptophan, kynurenine, and 3-hydroxykynurenine could cross the blood-brain barrier (BBB) and kynurenic acid and quinolinic acid were produced, respectively, in astrocytes and microglia (44, 45). Kynurenic acid had function on neuroprotection and anti-inflammation, and maintained synaptic plasticity (46); quinolinic acid exerted neurotoxicity by inhibiting the reuptake of glutamate, promoting the production of reactive oxygen species, and destroying the BBB (47). Although the mechanism by which its homeostasis was broken is not yet clear, abnormally enhanced levels of kynurenine and its metabolites could induce neuroinflammation (48). In our analysis, the increased plasma concentrations of tryptophan and kynurenine were all notably correlated to the CRP level. Since plasma concentrations of tryptophan and kynurenine could indirectly reflect their contents in brain tissue, the elevation of these two metabolites might lead to the inflammatory reaction of central nervous system and influence the neuroendocrine function in women with PCOS.

In the tryptophan-kynurenine pathway, the initial rate-limiting enzyme is IDO or TDO. In most studies, the plasma ratio of kynurenine to tryptophan was measured as the activity of IDO and TDO. Compared to TDO, IDO is widely distributed as the immunobiologically relevant enzyme that catalyzes the conversion of tryptophan to kynurenine. Clinically, IDO activity was increased in obese adults and positively correlated with BMI (49). The inhibition of IDO activity could improve insulin sensitivity, maintain the intestinal mucosal barrier, reduce endotoxemia and chronic inflammation, and regulate lipid metabolism in both liver and adipose tissues (50). In the current study, the elevation of ratio of kynurenine to tryptophan (**Figure 1A**) intimated IDO and/or TDO might be activated in PCOS patients, which needs further

exploration. In addition, because there was no obvious change of ratio of quinolinic acid to kynurenine in PCOS group compared with controls, the increased ratio of kynurenic acid to kynurenine suggests kynurenine metabolism was promoted and shunted to the kynurenic acid pathway in PCOS patients.

Our study also has several limitations. First, due to lack of 40 FINS values, there were 160 patients included in the risk analysis of IR in PCOS (**Supplementary Table 5**). Meanwhile, due to the lack of waist circumference values, it could not be accurately determined if some patients belonged to the MetS group, therefore, 165 were patients included in the risk analysis of MetS in PCOS (**Supplementary Table 6**). Second, it would be ideal to further validate the performance of selected metabolic marker for diagnosing PCOS and predicting the metabolic risks in an independent cohort. Third, it remains unclear whether the abnormal metabolites in the tryptophan-kynurenine pathway contribute directly to the pathogenesis of PCOS or are only a biomarker in the development of disease.

CONCLUSIONS

We investigated systematically the tryptophan catabolism profiles in PCOS and found the abnormal activation of the tryptophan-kynurenine pathway. Our study showed the obvious enhancement of tryptophan, kynurenine, and kynurenic acid in the circulation system; and that they may be considered as biomarkers of PCOS and become potential metabolic intervention targets. Intervention on this pathway, for instance, inhibiting the activities of key enzymes and competitively binding to related receptors, could provide a new strategy for improving metabolic and endocrine disorders in women with PCOS.

DATA AVAILABILITY STATEMENT

The original contributions presented in the study are included in the article/**Supplementary Material**. Further inquiries can be directed to the corresponding author.

ETHICS STATEMENT

The studies involving human participants were reviewed and approved by Reproductive Medicine Ethics Committee of Peking University Third Hospital. The patients/participants provided their written informed consent to participate in this study.

AUTHOR CONTRIBUTIONS

JQ, RL, and YZ conceived and designed this study. SW analyzed the data and wrote the manuscript. LM collected the samples. CZ and XL completed the clinical information. YRZ participated in the sample preparation. All authors took part in the final approval of this study.

FUNDING

This study was supported by the National Key Research and Development Project of China (2021YFC2700402), the National Natural Science Foundation of China (82071608, 82001503), the CAMS Innovation Fund for Medical Sciences (2019-I2M-5-001), the China Postdoctoral Science Foundation (2021T140600, 2020M671760), and the Beijing-Tianjin-Hebei Basic Research Cooperation Project (19JCZDJC65000).

ACKNOWLEDGMENTS

The authors would like to thank all the sample donors and the clinicians of the Reproduction Centre of Peking University Third Hospital for their valuable assistance.

SUPPLEMENTARY MATERIAL

The Supplementary Material for this article can be found online at: https://www.frontiersin.org/articles/10.3389/fendo.2022.877807/full#supplementary-material

REFERENCES

1. Escobar-Morreale HF. Polycystic Ovary Syndrome: Definition, Aetiology, Diagnosis and Treatment. *Nat Rev Endocrinol* (2018) 14(5):270–84. doi: 10.1038/nrendo.2018.24
2. Helvaci N, Yildiz BO. Polycystic Ovary Syndrome and Aging: Health Implications After Menopause. *Maturitas* (2020) 139:12–9. doi: 10.1016/j.maturitas.2020.05.013
3. Lizneva D, Suturina L, Walker W, Brakta S, Gavrilova-Jordan L, Azziz R. Criteria, Prevalence, and Phenotypes of Polycystic Ovary Syndrome. *Fertil Steril* (2016) 106(1):6–15. doi: 10.1016/j.fertnstert.2016.05.003
4. Li R, Yu G, Yang D, Li S, Lu S, Wu X, et al. Prevalence and Predictors of Metabolic Abnormalities in Chinese Women With PCOS: A Cross- Sectional Study. *BMC Endocr Disord* (2014) 14:76. doi: 10.1186/1472-6823-14-76
5. Nader S. Hyperandrogenism During Puberty in the Development of Polycystic Ovary Syndrome. *Fertil Steril* (2013) 100(1):39–42. doi: 10.1016/j.fertnstert.2013.03.013
6. Azziz R. Controversy in Clinical Endocrinology: Diagnosis of Polycystic Ovarian Syndrome: The Rotterdam Criteria are Premature. *J Clin Endocrinol Metab* (2006) 91(3):781–5. doi: 10.1210/jc.2005-2153
7. Moran LJ, Norman RJ, Teede HJ. Metabolic Risk in PCOS: Phenotype and Adiposity Impact. *Trends Endocrinol Metab* (2015) 26(3):136–43. doi: 10.1016/j.tem.2014.12.003
8. Shorakae S, Ranasinha S, Abell S, Lambert G, Lambert E, de Courten B, et al. Inter-Related Effects of Insulin Resistance, Hyperandrogenism, Sympathetic Dysfunction and Chronic Inflammation in PCOS. *Clin Endocrinol (Oxf)* (2018) 89(5):628–33. doi: 10.1111/cen.13808
9. Anagnostis P, Tarlatzis BC, Kauffman RP. Polycystic Ovarian Syndrome (PCOS): Long-Term Metabolic Consequences. *Metabolism* (2018) 86:33–43. doi: 10.1016/j.metabol.2017.09.016
10. Velez LM, Motta AB. Association Between Polycystic Ovary Syndrome and Metabolic Syndrome. *Curr Med Chem* (2014) 21(35):3999–4012. doi: 10.2174/0929867321666140915141030

11. Naderpoor N, Shorakae S, de Courten B, Misso ML, Moran LJ, Teede HJ. Metformin and Lifestyle Modification in Polycystic Ovary Syndrome: Systematic Review and Meta-Analysis. *Hum Reprod Update* (2015) 21 (5):560–74. doi: 10.1093/humupd/dmv025
12. Zhao Y, Fu L, Li R, Wang LN, Yang Y, Liu NN, et al. Metabolic Profiles Characterizing Different Phenotypes of Polycystic Ovary Syndrome: Plasma Metabolomics Analysis. *BMC Med* (2012) 10:153. doi: 10.1186/1741-7015-10-153
13. Buszewska-Forajta M, Rachon D, Stefaniak A, Wawrzyniak R, Konieczna A, Kowalewska A, et al. Identification of the Metabolic Fingerprints in Women With Polycystic Ovary Syndrome Using the Multiplatform Metabolomics Technique. *J Steroid Biochem Mol Biol* (2019) 186:176–84. doi: 10.1016/j.jsbmb.2018.10.012
14. Savitz J. The Kynurenine Pathway: A Finger in Every Pie. *Mol Psychiatry* (2020) 25(1):131–47. doi: 10.1038/s41380-019-0414-4
15. Bar KJ, Kohler S, Cruz F, Schumann A, Zepf FD, Wagner G. Functional Consequences of Acute Tryptophan Depletion on Raphe Nuclei Connectivity and Network Organization in Healthy Women. *Neuroimage* (2020) 207:116362. doi: 10.1016/j.neuroimage.2019.116362
16. Sas K, Szabo E, Vecsei L. Mitochondria, Oxidative Stress and the Kynurenine System, With a Focus on Ageing and Neuroprotection. *Molecules* (2018) 23 (1):191. doi: 10.3390/molecules23010191
17. Oxenkrug GF. Metabolic Syndrome, Age-Associated Neuroendocrine Disorders, and Dysregulation of Tryptophan-Kynurenine Metabolism. *Ann N Y Acad Sci* (2010) 1199:1–14. doi: 10.1111/j.1749-6632.2009.05356.x
18. Chaves Filho AJM, Lima CNC, Vasconcelos SMM, de Lucena DF, Maes M, Macedo D. IDO Chronic Immune Activation and Tryptophan Metabolic Pathway: A Potential Pathophysiological Link Between Depression and Obesity. *Prog Neuropsychopharmacol Biol Psychiatry* (2018) 80(Pt C):234–49. doi: 10.1016/j.pnpbp.2017.04.035
19. Zang X, Zheng X, Hou Y, Hu M, Wang H, Bao X, et al. Regulation of Proinflammatory Monocyte Activation by the Kynurenine-AhR Axis Underlies Immunometabolic Control of Depressive Behavior in Mice. *FASEB J* (2018) 32(4):1944–56. doi: 10.1096/fj.201700853R
20. Metghalchi S, Ponnuswamy P, Simon T, Haddad Y, Laurans L, Clément M, et al. Indoleamine 2,3-Dioxygenase Fine-Tunes Immune Homeostasis in Atherosclerosis and Colitis Through Repression of Interleukin-10 Production. *Cell Metab* (2015) 22(3):460–71. doi: 10.1016/j.cmet.2015.07.004
21. Cervenka I, Agudelo LZ, Ruas JL. Kynurenines: Tryptophan's Metabolites in Exercise, Inflammation, and Mental Health. *Science* (2017) 357(6349): eaaf9794. doi: 10.1126/science.aaf9794
22. Kindler J, Lim CK, Weickert CS, Boerrigter D, Galletly C, Liu D, et al. Dysregulation of Kynurenine Metabolism is Related to Proinflammatory Cytokines, Attention, and Prefrontal Cortex Volume in Schizophrenia. *Mol Psychiatry* (2020) 25(11):2860–72. doi: 10.1038/s41380-019-0401-9
23. Kadriu B, Farmer CA, Yuan P, Park LT, Deng ZD, Moaddel R, et al. The Kynurenine Pathway and Bipolar Disorder: Intersection of the Monoaminergic and Glutamatergic Systems and Immune Response. *Mol Psychiatry* (2019) 26(8):4085–95. doi: 10.1038/s41380-019-0589-8
24. Audrito V, Manago A, Gaudino F, Sorci L, Messana VG, Raffaelli N, et al. NAD-Biosynthetic and Consuming Enzymes as Central Players of Metabolic Regulation of Innate and Adaptive Immune Responses in Cancer. *Front Immunol* (2019) 10:1720. doi: 10.3389/fimmu.2019.01720
25. Bishnupuri KS, Alvarado DM, Khouri AN, Shabsovich M, Chen B, Dieckgraefe BK, et al. IDO1 and Kynurenine Pathway Metabolites Activate PI3K-Akt Signaling in the Neoplastic Colon Epithelium to Promote Cancer Cell Proliferation and Inhibit Apoptosis. *Cancer Res* (2019) 79(6):1138–50. doi: 10.1158/0008-5472.CAN-18-0668
26. Haroon E, Welle JR, Woolwine BJ, Goldsmith DR, Baer W, Patel T, et al. Associations Among Peripheral and Central Kynurenine Pathway Metabolites and Inflammation in Depression. *Neuropsychopharmacology* (2020) 45 (6):998–1007. doi: 10.1038/s41386-020-0607-1
27. Oxenkrug GF. Increased Plasma Levels of Xanthurenic and Kynurenic Acids in Type 2 Diabetes. *Mol Neurobiol* (2015) 52(2):805–10. doi: 10.1007/s12035-015-9232-0
28. Agudelo LZ, Ferreira DMS, Cervenka I, Bryzgalova G, Dadvar S, Jannig PR, et al. Kynurenic Acid and Gpr35 Regulate Adipose Tissue Energy Homeostasis and Inflammation. *Cell Metab* (2018) 27(2):378–92 e5. doi: 10.1016/j.cmet.2018.01.004
29. Favennec M, Hennart B, Caiazzo R, Leloire A, Yengo L, Verbanck M, et al. The Kynurenine Pathway is Activated in Human Obesity and Shifted Toward Kynurenine Monooxygenase Activation. *Obes (Silver Spring)* (2015) 23 (10):2066–74. doi: 10.1002/oby.21199
30. Yu E, Papandreou C, Ruiz-Canela M, Guasch-Ferre M, Clish CB, Dennis C, et al. Association of Tryptophan Metabolites With Incident Type 2 Diabetes in the PREDIMED Trial: A Case-Cohort Study. *Clin Chem* (2018) 64(8):1211–20. doi: 10.1373/clinchem.2018.288720
31. Niinisalo P, Oksala N, Levula M, Pelto-Huikko M, Jarvinen O, Salenius JP, et al. Activation of Indoleamine 2,3-Dioxygenase-Induced Tryptophan Degradation in Advanced Atherosclerotic Plaques: Tampere Vascular Study. *Ann Med* (2010) 42(1):55–63. doi: 10.3109/07853890903321559
32. Consultation WHOE. Appropriate Body-Mass Index for Asian Populations and its Implications for Policy and Intervention Strategies. *Lancet* (2004) 363 (9403):157–63. doi: 10.1016/S0140-6736(03)15268-3
33. Xing X-y, Yang W-y, Yang Z-j. The Diagnostic Significance of Homeostasis Model Assessment of Insulin Resistance in Metabolic Syndrome Among Subjects With Different Glucose Tolerance. *Chin J Diabetes* (2004) 12 (3):182–6.
34. Expert Panel on Detection E and Treatment of High Blood Cholesterol in A. Executive Summary of The Third Report of The National Cholesterol Education Program (NCEP) Expert Panel on Detection, Evaluation, And Treatment of High Blood Cholesterol In Adults (Adult Treatment Panel III). *JAMA* (2001) 285(19):2486–97. doi: 10.1001/jama.285.19.2486
35. Silvestris E, de Pergola G, Rosania R, Loverro G. Obesity as Disruptor of the Female Fertility. *Reprod Biol Endocrinol* (2018) 16(1):22. doi: 10.1186/s12958-018-0336-z
36. Behboudi-Gandevani S, Ramezani Tehrani F, Bidhendi Yarandi R, Noroozzadeh M, Hedayati M, Azizi F. The Association Between Polycystic Ovary Syndrome, Obesity, and the Serum Concentration of Adipokines. *J Endocrinol Invest* (2017) 40(8):859–66. doi: 10.1007/s40618-017-0650-x
37. Kim H, Chen L, Lim G, Sung B, Wang S, McCabe MF, et al. Brain Indoleamine 2,3-Dioxygenase Contributes to the Comorbidity of Pain and Depression. *J Clin Invest* (2012) 122(8):2940–54. doi: 10.1172/JCI61884
38. Cussotto S, Delgado I, Anesi A, Dexpert S, Aubert A, Beau C, et al. Tryptophan Metabolic Pathways Are Altered in Obesity and Are Associated With Systemic Inflammation. *Front Immunol* (2020) 11:557. doi: 10.3389/fimmu.2020.00557
39. Rojas IY, Moyer BJ, Ringelberg CS, Wilkins OM, Pooler DB, Ness DB, et al. Kynurenine-Induced Aryl Hydrocarbon Receptor Signaling in Mice Causes Body Mass Gain, Liver Steatosis, and Hyperglycemia. *Obes (Silver Spring)* (2021) 29(2):337–49. doi: 10.1002/oby.23065
40. Moyer BJ, Rojas IY, Kerley-Hamilton JS, Hazlett HF, Nemani KV, Trask HW, et al. Inhibition of the Aryl Hydrocarbon Receptor Prevents Western Diet-Induced Obesity. Model for AHR Activation by Kynurenine *via* Oxidized-LDL, TLR2/4, TGFbeta, and IDO1. *Toxicol Appl Pharmacol* (2016) 300:13–24. doi: 10.1016/j.taap.2016.03.011
41. Baumgartner R, Berg M, Matic L, Polyzos KP, Forteza MJ, Hjorth SA, et al. Evidence That a Deviation in the Kynurenine Pathway Aggravates Atherosclerotic Disease in Humans. *J Intern Med* (2021) 289(1):53–68. doi: 10.1111/joim.13142
42. Hu P, Hunt NH, Arfuso F, Shaw LC, Uddin MN, Zhu M, et al. Increased Indoleamine 2,3-Dioxygenase and Quinolinic Acid Expression in Microglia and Muller Cells of Diabetic Human and Rodent Retina. *Invest Ophthalmol Vis Sci* (2017) 58(12):5043–55. doi: 10.1167/iovs.17-21654
43. Heisler JM, O'Connor JC. Indoleamine 2,3-Dioxygenase-Dependent Neurotoxic Kynurenine Metabolism Mediates Inflammation-Induced Deficit in Recognition Memory. *Brain Behavior Immunity* (2015) 50:115–24. doi: 10.1016/j.bbi.2015.06.022
44. Owe-Young R, Webster NL, Mukhtar M, Pomerantz RJ, Smythe G, Walker D, et al. Kynurenine Pathway Metabolism in Human Blood-Brain-Barrier Cells: Implications for Immune Tolerance and Neurotoxicity. *J Neurochem* (2008) 105(4):1346–57. doi: 10.1111/j.1471-4159.2008.05241.x
45. Platten M, Nollen EAA, Rohrig UF, Fallarino F, Opitz CA. Tryptophan Metabolism as a Common Therapeutic Target in Cancer, Neurodegeneration

and Beyond. *Nat Rev Drug Discovery* (2019) 18(5):379–401. doi: 10.1038/s41573-019-0016-5
46. Potter MC, Elmer GI, Bergeron R, Albuquerque EX, Guidetti P, Wu HQ, et al. Reduction of Endogenous Kynurenic Acid Formation Enhances Extracellular Glutamate, Hippocampal Plasticity, and Cognitive Behavior. *Neuropsychopharmacology* (2010) 35(8):1734–42. doi: 10.1038/npp.2010.39
47. Ferreira FS, Schmitz F, Marques EP, Siebert C, Wyse ATS. Intrastriatal Quinolinic Acid Administration Impairs Redox Homeostasis and Induces Inflammatory Changes: Prevention by Kynurenic Acid. *Neurotox Res* (2020) 38(1):50–8. doi: 10.1007/s12640-020-00192-2
48. Heyes MP, Saito K, Crowley JS, Davis LE, Demitrack MA, Der M, et al. Quinolinic Acid and Kynurenine Pathway Metabolism in Inflammatory and non-Inflammatory Neurological Disease. *Brain* (1992) 115(5):1249–73. doi: 10.1093/brain/115.5.1249
49. Oxenkrug G. Insulin Resistance and Dysregulation of Tryptophan-Kynurenine and Kynurenine-Nicotinamide Adenine Dinucleotide Metabolic Pathways. *Mol Neurobiol* (2013) 48(2):294–301. doi: 10.1007/s12035-013-8497-4
50. Laurans L, Venteclef N, Haddad Y, Chajadine M, Alzaid F, Metghalchi S, et al. Genetic Deficiency of Indoleamine 2,3-Dioxygenase Promotes Gut Microbiota-Mediated Metabolic Health. *Nat Med* (2018) 24(8):1113–20. doi: 10.1038/s41591-018-0060-4

Conflict of Interest: The authors declare that the research was conducted in the absence of any commercial or financial relationships that could be construed as a potential conflict of interest.

Publisher's Note: All claims expressed in this article are solely those of the authors and do not necessarily represent those of their affiliated organizations, or those of the publisher, the editors and the reviewers. Any product that may be evaluated in this article, or claim that may be made by its manufacturer, is not guaranteed or endorsed by the publisher.

frontiers | Frontiers in Endocrinology

REVIEW
published: 19 July 2022
doi: 10.3389/fendo.2022.933110

Present and Future: Crosstalks Between Polycystic Ovary Syndrome and Gut Metabolites Relating to Gut Microbiota

Mingmin Zhang[1†], Runan Hu[2†], Yanjing Huang[2], Fanru Zhou[2], Fan Li[2], Zhuo Liu[2], Yuli Geng[2], Haoxu Dong[1], Wenwen Ma[1], Kunkun Song[1] and Yufan Song[1,2]*

[1] Department of Integrated Traditional Chinese and Western Medicine, Tongji Hospital, Tongji Medical College, Huazhong University of Science and Technology, Wuhan, China, [2] Institute of Integrated Traditional Chinese and Western Medicine, Tongji Hospital, Tongji Medical College, Huazhong University of Science and Technology, Wuhan, China

Polycystic ovary syndrome (PCOS) is a common disease, affecting 8%–13% of the females of reproductive age, thereby compromising their fertility and long-term health. However, the pathogenesis of PCOS is still unclear. It is not only a reproductive endocrine disease, dominated by hyperandrogenemia, but also is accompanied by different degrees of metabolic abnormalities and insulin resistance. With a deeper understanding of its pathogenesis, more small metabolic molecules, such as bile acids, amino acids, and short-chain fatty acids, have been reported to be involved in the pathological process of PCOS. Recently, the critical role of gut microbiota in metabolism has been focused on. The gut microbiota-related metabolic pathways can significantly affect inflammation levels, insulin signaling, glucose metabolism, lipid metabolism, and hormonal secretions. Although the abnormalities in gut microbiota and metabolites might not be the initial factors of PCOS, they may have a significant role in the pathological process of PCOS. The dysbiosis of gut microbiota and disturbance of gut metabolites can affect the progression of PCOS. Meanwhile, PCOS itself can adversely affect the function of gut, thereby contributing to the aggravation of the disease. Inhibiting this vicious cycle might alleviate the symptoms of PCOS. However, the role of gut microbiota in PCOS has not been fully explored yet. This review aims to summarize the potential effects and modulative mechanisms of the gut metabolites on PCOS and suggests its potential intervention targets, thus providing more possible treatment options for PCOS in the future.

Keywords: polycystic ovary syndrome, gut metabolites, crosstalk, bile acids, short chain fatty acids, amino acids

OPEN ACCESS

Edited by:
Yanli Pang,
Peking University Third Hospital, China

Reviewed by:
Rong Li,
Peking University Third Hospital, China
Agnieszka Pazderska,
St. James's Hospital, Ireland

***Correspondence:**
Yufan Song
songyufan23@163.com

[†]These authors have contributed equally to this work and share first authorship

Specialty section:
This article was submitted to Gut Endocrinology, a section of the journal Frontiers in Endocrinology

Received: *30 April 2022*
Accepted: *20 June 2022*
Published: *19 July 2022*

Citation:
Zhang M, Hu R, Huang Y, Zhou F, Li F, Liu Z, Geng Y, Dong H, Ma W, Song K and Song Y (2022) Present and Future: Crosstalks Between Polycystic Ovary Syndrome and Gut Metabolites Relating to Gut Microbiota. Front. Endocrinol. 13:933110. doi: 10.3389/fendo.2022.933110

1 INTRODUCTION

Polycystic ovary syndrome (PCOS), characterized by oligo-ovulation or anovulation, hyperandrogenemia, and polycystic ovarian morphology, is a common disorder of the reproductive endocrine system, affecting 8%–13% of the women of reproductive age as well as impairing their fertility and long-term health (1, 2). Women with PCOS have a higher risk of

infertility and pregnancy complications, accompanied by subsequent complications, such as obesity, type 2 diabetes, non-alcoholic fatty liver disease (NAFLD) (3), cardiovascular disease (4), endometrial cancer, and osteoporosis (5). All these complications have a far-reaching impact on the physical and mental health of women (6).

Until now, the specific etiology and pathophysiology of PCOS remain unclear. PCOS might be a polygenic heritable condition, which is affected by a variety of acquired variables (7). Hyperandrogenemia is generally regarded as the core part of PCOS, causing reproductive disorders, insulin resistance (IR), and metabolic imbalances, such as glucose and lipid metabolic imbalance (8). In particular, the IR and compensatory hyperinsulinemia might cause abnormality in the sex hormone levels, chronic inflammation, and metabolic disorders, thereby contributing to follicular dysplasia (9). These pathological factors create a vicious cycle, which increases the obstacles to PCOS treatment.

With a deeper understanding of gut biology, the potential role of the gut in PCOS has become the center of attention. Gut microbiota, also known as the "second genome" of the host, can affect the metabolism and immune response of the host by interacting with the external environment (8). Alpha-diversity (α-diversity) is regarded as an indicator of ecosystem health, representing the number of species present in the given community, whereas beta-diversity (β-diversity) denotes the similarity of a community or individual sample with another community or individual sample, respectively (10). As compared to the normal group, the dysbiosis of gut microbiota in the PCOS women showed lower α- and β-diversities, decreased relative abundance of *Bifidobcterium*, and increased relative abundances of *Bacteroides*, *Parabacteroides*, and *Clostridium* (11–13). Furthermore, the dehydroepiandrosterone (DHEA)–induced PCOS rats showed the dysbiosis of gut microbiota, and transferring this microbiota to healthy rats could induce the PCOS-like metabolic and endocrinal dysfunctions, indicating that the gut might be a novel therapeutic target for the treatment of PCOS (14).

Recently, studies on gut metabolites have emphasized the importance of the gut in maintaining general homeostasis. The gut metabolites, such as bile acids (BAs), amino acids, and short-chain fatty acids (SCFAs), are greatly involved in modulating the integrity of the gut barrier, thereby maintaining the internal environment and homeostasis. A disturbance in gut metabolites might increase the gut permeability, leading to the leakage of lipopolysaccharides (LPSs) and endotoxemia, which might disturb the endocrine system, immune system, insulin signaling, glucose metabolism, lipid metabolism (8), and gut microbiota (15). Furthermore, the SCFAs, BAs, and branched-chain amino acids (BCAAs) can directly regulate the secretion and sensitivity of pancreatic insulin in the target organs through endocrine signaling. While circulating through the portal venous system, these metabolites reach the liver to regulate lipid metabolism and oxidation. Moreover, these metabolites also take part in neuronal homeostasis by modulating the integrity of the blood–brain barrier (16). The gut–brain peptides, which can be affected by gut metabolites, might communicate with the brain, thereby influencing appetite and energy maintenance as well as increasing the secretion of luteinizing hormone (LH) (17).

Interestingly, the activity and contents of gut metabolites can be regulated by the gut microbiota (18, 19). The correlations between gut metabolites and gut microbiota have been demonstrated in numerous metabolic diseases, such as obesity, type 2 diabetes, NAFLD, and cardiovascular diseases (20, 21). Qiao and colleagues also demonstrated that an increase in the relative abundance of *Bacteroides* in patients with PCOS was related to the disturbance in gut metabolites, which might have a potential pathological role in PCOS (13, 22).

These studies indicate that, in PCOS, the gut microbiota and related metabolites might be affected. They both are closely linked to the insulin signaling pathway, steroid hormone levels, glucose metabolism, lipid metabolism, and immunological homeostasis, all of which are greatly involved in the pathogenesis of PCOS (16, 17). However, understanding the mechanism of interactions between gut metabolites and PCOS is still unclear. This review aims to summarize the existing studies and demonstrates the interaction between PCOS and gut microbiota-related metabolites, which might help in developing novel treatments for PCOS.

2 BAS

2.1 Biosynthesis and Metabolism of BAs

BAs are the key metabolites, which include primary BAs and secondary BAs. In humans, cholic acid (CA) and chenodeoxycholic acid (CDCA) are the most common primary BAs. Under normal physiological conditions, these primary BAs are synthesized from cholesterol in the pericentral hepatocytes through "classical" (neutral) and "alternative" (acidic) pathways (23, 24). The classical pathway favors the biosynthesis of CA and CDCA (25), whereas the alternative pathway only favors the biosynthesis of CDCA. After the primary BAs are modified and transported by various enzymes and transporters, they are conjugated with taurine or glycine and secreted into the bile, which are then released into the small intestine and aid in lipid digestion (26). In the ileocecum, the gut microbiota and bile salt hydrolase (BSH) convert the conjugated BAs to free BAs. Following the modifications, such as the removal, oxidation, or epimerization of the nuclear hydroxyl by the host or gut microbiota, the free primary BAs are converted into secondary BAs (25, 27). The secondary BAs play a critical role in regulating glucose metabolism, insulin signaling, lipid metabolism, and inflammation. In the distal ileum, most of the secreted molecules (95%) are reabsorbed through apical sodium-dependent BA transporter (ASBT) and are ultimately transported into the liver through the portal vein system. This phenomenon is known as enterohepatic circulation. Meanwhile, the remaining secreted molecules are excreted in feces (15, 25). In the ileum, BAs facilitate the secretion of fibroblast growth factor 19 (FGF19) in humans or FGF15 in mice by activating the

farnesoid X receptor (FXR). FGF19 further represses the BA synthesis as negative feedback when circulated to the liver (26).

The above process relies heavily on gut microbiota. The gut microbiota can affect the production of BAs by regulating the liver enzymes, such as 7a hydroxylase and sterol-27-hydroxylase, especially CDCA in humans (28). BSH has been widely detected in rodent and human gut microbiota, such as *Clostridium* spp (29).. The diversity of secondary BAs is greatly affected by the species differences in gut microbiota (23). The mouse models in the absence of gut microbiota demonstrate that almost all the BAs were primary BAs, indicating the importance of gut microbiota in the production of free BAs (15, 30). The gut microbiota could affect the ileum mucosa and ASBT to regulate the reabsorption of BA in rodents (28). Moreover, the gut microbiota partially inhibits the BA biosynthesis through the FXR-dependent mechanism (31–33). The BAs shape the structure of gut microbiota and exert antibacterial effects by selectively promoting the growth of BA-synthesizing bacteria, thereby showing a bidirectional communication between the gut microbiota and BAs (15, 33).

2.2 Role of BAs in Metabolism, Endocrine, and Inflammation

One of the most important functions of BAs is their participation in lipid emulsification and solubilization. They convert fat into fat droplets, which can be digested by trypsin and absorbed by gut mucosa, thereby assisting the absorption of dietary fat, which is critically important for lipid metabolism (34). Certain essential vitamins, such as vitamins A and D, are non-polar lipids, which can only be absorbed if bound to micelles in the presence of BAs (25, 35). Whenever the concentration of cholate is lower, cholesterol absorption is inhibited (25).

The BAs modulate metabolic homeostasis by stimulating the receptors, such as G protein receptor 5 (TGR5) and FXR. TGR5 is widely distributed in a variety of animal tissues, such as fat, central nervous system, liver, and gut and participates in regulating insulin signaling, glucose metabolism, and energy expenditure in brown adipose tissue and muscle (36). The intestinal hormone glucagon-like peptide 1 (GLP-1) and peptide YY (PYY) are simulated by TGR5 (37). In the murine brain, BAs could activate TGR5, causing the central anorexigenic actions to control the appetite (38). FXR is another BAs receptor, which is found in white adipose tissue, liver, gut, immune cells, and other tissues (39). The BAs, in combination with FXR, can induce FGF15 and/or FGF19, which might regulate glucose tolerance and normal glycemia by reducing hepatic gluconeogenesis. A reduction in the number of activated FXR might reduce the secretion of FGF15 and/or FGF19. This might result in the increase of hepatic gluconeogenesis, deposition of hepatic lipid, and disruption of glucose homeostasis in adipocytes and the decrease of insulin production in pancreatic cells (26, 32). Moreover, in the cardiac and visceral fat cells, tauroursodeoxycholic acid (TUDCA) could reduce endoplasmic reticulum stress, thereby preventing obesity and inflammation (40). Therefore, reduction in the TUDCA might result in the diminished suppression of abdominal and visceral fat inflammation, aggravating the IR and metabolic disorders (8, 40).

However, the current studies on the link between BAs and metabolic syndrome include a few individuals in the BAs pool. The levels of fasting circulating total BAs were higher among the populations with mild IR and obesity (25). However, the changes in the levels of fasting circulating BAs in disease states as well as the role of each BA in metabolic diseases are needed to be investigated.

3 SCFAS

3.1 Biosynthesis and Metabolism of SCFAs

Recently, the crosstalk between SCFAs and gut has been focused on. The SCFAs originated from the microbiota-accessible carbohydrates (MACs) in the colon (41), which are fermented from the dietary fibers and resistant starch ferment. They mainly consist of acetic, propionic, butyric, valeric, and caproic acids, which are biosynthesized in various pathways, such as the Wood–Ljungdahl pathway, aided by the different classes of gut microbes (42). The exact contents and relative proportion of each type of SCFA might differ based on the diet, composition of the microbiota, and gut transit time (43, 44). When the BCAAs, including valine, isoleucine, and leucine, escape digestion in the upper gut, they might be fermented into branched-chain fatty acids (43, 44). Furthermore, the SCFAs are taken up by colonocytes *via* passive diffusion or active transport (42). A part of the unmetabolized SCFAs are transported into the liver through the portal system and serve as substrates for the energy metabolism and anabolic processes, thereby playing a prominent role in the inhibition of glycolysis, stimulation of lipogenesis and gluconeogenesis, and regulation of mitochondrial energy production (45).

3.2 Role of SCFAs in Metabolism, Endocrine, and Inflammation

SCFAs are important for balancing metabolism and energy. They are taken up by colon cells after binding to G protein–coupled receptors (GPCRs), which are also known as free fatty acid receptors (FFARs) and are present on the enteroendocrine cells of the gastrointestinal mucosa (46), thereby stimulating the secretion of intestinal hormones, such as GLP-1, PYY, gamma-aminobutyric acid (GABA), and serotonin (5-HT) (46). The intestinal hormones aid in reducing the production of hepatic glucose, enhancing the absorption of peripheral glucose, and suppressing the appetite (47). Moreover, the SCFAs can also stimulate leptin secretion in adipocytes and insulin secretion in the pancreatic cells (48). The circulating SCFAs can activate the burning of brown adipose tissue, thereby increasing energy consumption and preventing weight gain (43, 49). In addition, the SCFAs also improve insulin sensitivity in the muscle and liver tissues (47).

In contrast to hepatic gluconeogenesis, intestinal gluconeogenesis (IGN) is beneficial for controlling the glucose level by reducing food intake and hepatic glucose output (47, 49).

In a study based on mouse models, butyrate could directly promote the IGN expression in enterocytes in a Cyclic Adenosine Monophosphate (cAMP)-dependent manner, whereas propionate could increase the IGN expression by binding to FFAR3 in the portal nerve, thereby initiating the portal-hypothalamic crosstalk, improving the insulin sensitivity and glucose tolerance, and lowering the fat mass (47).

Recently, studies have demonstrated that SCFAs could affect the host's immune system. SCFAs could affect the hematopoietic progenitors in the murine bone marrow, implying that they were important for the development of innate and adaptive immune systems (50). Moreover, they exerted a systematic anti-inflammatory effect in mice by affecting the peripheral DCs and T cells (51). In particular, the SCFAs increased the number of T-regulatory (Treg) cells, induced the differentiation of Treg cells, and regulated the production of interleukin, thereby minimizing the oxidative stress and protecting pancreatic cells (52–54). In a murine model of gout, SCFAs could bind to the GPCR43 in the central nervous system and act on microglia to regulate host immunity (55). Furthermore, they strengthened the integrity of the blood–brain barrier and regulated the levels of neuronal factors and neurogenesis to relieve the neural and central inflammation (52).

Moreover, SCFAs can also increase the expression of intestinal epithelial tight junction protein and decrease the death of intestinal epithelial cells (IEC), thereby promoting gut mucosal immunity and barrier integrity (56, 57). Once the intestinal mucosal barrier is disrupted, LPS enters the blood circulation, resulting in a persistent inflammation, which is correlated with IR (51).

The SCFAs, when reaching the brain, can alter the integrity of the blood–brain barrier by increasing the expression of tight junction proteins in the blood–brain barrier and regulating the state of neural and central inflammation (41, 52). SCFAs also affect the function of glial cells and neurogenesis in order to maintain neuronal homeostasis (41).

4 AMINO ACIDS

4.1 Anabolism and Catabolism of Amino Acids

Amino acids, consisting of essential and non-essential amino acids, are life-supporting molecules, which provide raw materials for protein synthesis. The food amino acids are primarily absorbed in the small intestine *via* the concentrative amino acid transporters. A small number of amino acids are also absorbed by the large intestine, whereas the remaining are excreted in the feces (58, 59). Then, the amino acids are released primarily through passive efflux across the basolateral membrane, which is mediated by a group of transporters (59, 60). When released into the bloodstream, they are transported into the cells *via* the corresponding secondary active transporters, which are also called functional transporters (61). Simultaneously, an increase in the cytoplasmic amino acid pool activates the amino acid metabolism, forcing the excess amino acids to be catabolized *via* oxidation, hydroxylation, and other processes (62). The majority of amino acids are metabolized and restored in the liver (58). However, they may also be stored in extrahepatic tissues, such as muscle, brown fat, kidneys, liver, and heart tissues (62); this storage in extrahepatic tissues is regulated by the insulin-mediated signaling in the hypothalamus (63).

4.2 Role of Amino Acids in Metabolism, Endocrine, and Inflammation

In addition to synthesizing proteins, amino acids are also involved in glycolysis and mitochondrial metabolism through the tricarboxylic acid (TCA) cycle and oxidative phosphorylation and modulate the cellular activities, such as lipid and glucose metabolism (64). By acting on the IR substrates (IRSs), the amino acids can affect insulin signaling (65). Furthermore, recent studies have demonstrated that amino acids are the potential precursors of the brain neurotransmitter, impacting habits (66). Furthermore, amino acids participate in ATP generation, nucleotide synthesis, and redox balance, which support the growth, proliferation, and effector function of immune cells (64, 67).

5 CROSSTALK BETWEEN PCOS AND GUT METABOLITES

5.1 Effect of PCOS on Gut Metabolites

To date, significant differences have been reported between the gut microbiota and metabolites in patients with PCOS as compared to the control group. PCOS, as a multi-system endocrine disease, has a negative impact on the function and composition of gut microbiota and metabolites.

5.1.1 Impact of Sex Hormones on Gut Microbiota and Related Metabolites

According to studies, sex hormones have a substantial impact on the composition of the gut microbiota. They affect the composition of gut microbiota in a sex-specific manner after puberty (10, 68). As a result, the gut microbiota in females has higher α-diversity but significantly lower abundances of *Bacteroides* species, including *Prevotella* and *Bacteroides thetaiotomicron*, as compared to that of males. The studies of rodents and other species have also shown similar results, but the outcomes vary across the studies (68, 69). Meanwhile, the dysbiosis of gut microbiota in the PCOS women was characterized by the lower α-diversity, decreased relative abundance of *Bifidobacterium*, increased relative abundance of *Bacteroides*, and changes in the β-diversity as compared to the control group (11–13). This showed that the gut microbiota of the PCOS women altered when compared to that of the men. Although different conclusions have been presented, the accumulating data confess that hyperandrogenism might affect the gut microbiota of patients with PCOS by affecting the gut function and regulating the activity of β-glucuronidase and its substrate levels, such as bilirubin, neurotransmitters, and

hormones, which are present in the liver (10, 11, 70). Because the gut metabolites are closely related to the gut microbiota, the changes in gut microbiota in response to hormones might also change the gut metabolites. For example, Sherman et al. revealed that the prenatal androgens were linked to the changes in the abundance of gut microbiota involved in the production of SCFAs in the rat (71). In a nutshell, the disruption of sex hormones in PCOS affects the composition of gut metabolites and microbiota.

5.1.2 Impact of Obese on Gut Microbiota and Related Metabolites

The dysbiosis of gut microbiota is correlated with the phenotype of PCOS. There are differences in the gut microbiota of non-obese and obese individuals with PCOS (17). The abundance of clostridium cluster XVII increased in the non-obese patients with PCOS, whereas that of *Clostridium sensustricto* and *Roseburia* decreased (72). Liu et al. reported that the relative abundances of gut microbiota, including *Bacteroides*, *Escherichia/Shigella*, and *Streptococcus* increased, whereas those of *Akkermansia* and *Ruminococcaceae* decreased in the patients with PCOS, which were correlated with body mass index (BMI) (17). It has also been reported that obese women with PCOS tend to have lower α-diversity and biodiversity of the gut microbiota as compared to the women with normal BMI (69). Furthermore, according to Li and colleagues, obesity was associated with the altered BA metabolism caused by the dysbiosis of gut microbiota (21). Because adiposity is a source of sex steroids, it might affect the composition of gut microbiota and gut metabolites by affecting the production of sex hormones (73). In addition, obesity might contribute to the development of a chronic inflammatory state, which might alter the gut permeability and microbiota, thereby affecting the function and composition of gut metabolites (21, 74).

5.1.3 Impact of IR on Gut Microbiota and Related Metabolites

Among the women with IR, the relative abundance of *Bacteroidaceae* increased, whereas that of *Prevotellaceae* decreased as compared to the PCOS women without IR (71). The IR-induced gut dysbiosis could result in the accumulation of BCAAs (13, 36, 75, 76). On the other hand, the TCA cycle was significantly inhibited by IR, resulting in decreased BCAA clearance (77). Furthermore, IR and compensatory hyperinsulinism contributed to hyperandrogenism, thereby disrupting the gut dysbiosis and metabolites (8, 10).

5.1.4 Impact of Habits on Gut Microbiota and Related Metabolites

Numerous patients with PCOS have bad habits, such as an adoration of sweets, a love of fat, an absence of dietary fiber, and little exercise, which affects gut health (18, 78). A high-fat diet (HFD) was linked to an increase in the pro-inflammatory microbiota, such as *Clostridiales*, *Bacteroides*, and *Enterobacteriales*, and a decrease in the anti-inflammatory microbiota, such as *Lactobacillus*, in the rat (75). The high levels of glucose, fructose, and sucrose could increase the relative abundance of *Bifidobacteria* while suppressing that of *Bacteroides* (75). The lack of dietary fiber might result in a decrease in the production of SCFAs. All these could affect the biosynthesis of gut metabolites.

Exercise can enhance gut health by increasing the diversity of gut microbiota and balancing the beneficial and pathogenic bacterial communities (79). Specifically, exercise increases the ratio of butyrate-producing bacteria, such as *Roseburia hominis*, thereby increasing the concentration of butyrate (80, 81). Moreover, exercise can reduce the contact time between feces and the gastrointestinal mucus layer by enhancing gastrointestinal motility to benefit gut health (79, 80). It also boosts the production of key antioxidant enzymes and anti-inflammatory cytokines in the intestinal lymphocytes, thereby reducing intestinal inflammation (76, 77). A reduction in exercise might disrupt the gut metabolites (43, 44, 79).

In a nutshell, the dysbiosis of gut microbiota is caused by unhealthy habits, hyperandrogenism, obesity, hyperinsulinism, and disturbances in the glucose and lipid metabolism in PCOS, leading to increased gut permeability, exaggerated dysbiosis, and altered gut metabolites (82, 83).

5.2 Effect of Gut Metabolites on PCOS

5.2.1 Effect of BAs on PCOS

The BA metabolism is a key metabolic pathway affected by the changes in gut microbiota in patients with PCOS. Zhang and colleagues demonstrated that an increase in the circulating conjugated primary BAs was positively correlated with hyperandrogenism in women with PCOS (84). In both the stool and serum, the levels of secondary BAs, such as glycodeoxycholic acid (GDCA) and TUDCA, were lower in the PCOS group as compared to those in the control group and were correlated with the disturbance of gut microbiota (13).

The findings from PCOS rats revealed that UDCA administration could improve ovarian morphology and decrease the total testosterone and insulin levels. However, the lipid parameters, E1, E2, glucose, and homeostatic model assessment for IR were comparable between the groups (85).

Moreover, BAs could also regulate the performance of gut immune cells. Both the protein and mRNA levels of Interleukin-22 (IL-22) in the cultured group 3 innate lymphoid cells (ILCs) were greatly stimulated in the presence of TUDCA or GDCA, which was also confirmed in mouse models, showing that TUDCA or GDCA therapy could enhance the mRNA levels of gut IL-22 and alleviate the disease symptoms (13). These beneficial effects of BAs on IR and ovarian function in PCOS mice were reversed by knocking out the *IL-22 receptor* gene (13). The IL-22 levels in serum and follicle fluid of patients with PCOS decreased, whereas the IL-22 administration could improve IR, ovarian dysfunction, dysbiosis of gut microbiota, and prenatal Müllerian hormone in the DHEA-induced PCOS mice (86). Therefore, it could be proposed that the regulatory effects of BAs on PCOS were at least partially mediated by IL-22 (13).

IL-22 has diverse benefits, such as improving insulin sensitivity and regulating the lipid metabolism in the liver and

adipose tissues. IL-22 can promote the proliferation of IEC and the production of antimicrobial peptides and mucins in IEC (13, 51). Therefore, a reduction in the IL-22 level might further disrupt the integrity of the gut barrier and microbiome hemostasis, thereby aggravating the endotoxemia, chronic inflammation state, and particularly the IR (13, 87, 88). Recently, Qi et al. reported that IL-22 could reverse the disturbed menstrual cycle in PCOS mice by relieving the inflammatory state in ovarian granulosa cells, further indicating the possible role of IL-22 in the PCOS intervention (86).

5.2.2 Effect of SCFAs on PCOS

SCFAs are essential elements in maintaining the homeostasis of gut microbiota and regulating the intestinal mucosal barrier as an important energy source for the gut microbiota and IEC (51, 89). For instance, butyrate regulates the utilization of intestinal oxygen, thereby regulating the proportion of aerobic and anaerobic gut microbiota. Therefore, a reduction in the SCFA levels might cause gut dysbiosis in PCOS (90) and disrupt the intestinal mucosal barrier to exacerbate the chronic inflammatory state (51).

In addition to affecting the gut health and microbiota, the SCFAs also exert various physiological effects through IL-22. SCFAs could promote the IL-22 production in $CD4^+$ T cells and ILCs by binding to the histone deacetylase inhibitors and GPCRs (89). The IL-22 could maintain metabolic homeostasis, which was disturbed by SCFAs reduction (89), thereby producing a synergistic effect with BA–IL-22. In addition, studies reported that the secretion of gastrointestinal hormones in patients with PCOS was disturbed, such as a decrease in the GLP-1 level (91). SCFAs could stimulate the secretion of gastrointestinal hormones, such as GLP-1, PYY, GABA, and 5-HT, thereby reversing their decreased levels in the patients with PCOS, maintaining insulin homeostasis, and suppressing the appetite (46).

In addition to their effects on the gut, SCFAs also exert peripheral effects. SCFAs could promote the *IGN* gene expression in enterocytes through the portal-hypothalamic circuit, thereby maintaining food intake and hepatic glucose output in mice (49). The decrease in the SCFA levels can boost insulin secretion from the pancreatic cells *via* GPCRs, improve insulin sensitivity, increase the energy expenditure in brown adipose tissue, and upregulate the antilipolytic activity of glucose transporter type 4, thereby further aggravating the PCOS (41, 45, 47).

Moreover, Lin et al. discovered that the absorption of SCFAs decreased in the PCOS rats. They demonstrated that the fecal SCFA concentrations increased and were positively correlated with the tumor necrosis factor and IL-6 levels (92). Enhancing the SCFA absorption could improve the integrity of the intestinal mucosal barrier and inhibit intestinal and parenteral inflammation (92).

Therefore, SCFAs are critically important for maintaining glucose and insulin homeostasis and ameliorating chronic inflammation throughout the body. The supplementation of SCFAs or enhancing their beneficial effects, such as activating the relevant receptors, might be helpful in the PCOS treatment.

5.2.3 Effect of Amino Acids on PCOS

Recently, the correlations between BCAAs and metabolic dysbiosis have been focused on. The human body cannot synthesize BCAAs, which are essential amino acids; therefore, they must be absorbed from the digestion of food (65). By phosphorylating the IRS-1 and IRS-2 at serine or damaging the mitochondrial function in the β-pancreatic cells, excessive BCAAs could aggravate IR in rodents with PCOS (65, 88, 93). Furthermore, BCAAs might induce the expression of proinflammatory genes to deteriorate chronic inflammation, thereby developing IR (65).

As compared to the SCFAs and BAs, the current studies on intestinal amino acids are limited. Moreover, the conclusions are not completely consistent due to the inter- and intra-species differences and experimental conditions. The correlations between amino acids and PCOS are still unclear. However, it could be concluded that downregulating the excessive BCAAs or blocking their associated binding sites might further ameliorate IR in PCOS. Whether and how BCAAs can be applied for the prediction and treatment of PCOS are worth exploring.

6 PROSPECTS AND IMPLICATIONS

Currently, the primary goal of PCOS treatment is to alleviate its symptoms, such as hyperandrogenism, IR, oligo- or anovulation, and infertility. For example, letrozole aids in developing the dominant follicles, whereas metformin is typically for the treatment of metabolic symptoms and IR, possibly restoring their ovulation (94). These treatment strategies can only provide temporary relief from the symptoms or achieve a short-term goal. Therefore, the fundamental and permanent treatment of the pathological processes in PCOS is worth exploring.

As stated above, the PCOS-related hyperandrogenism, IR, obesity, metabolic disturbance, unhealthy diet, and other factors could disrupt the gut microbiota and metabolites, which, in turn, deteriorated the pathological process of PCOS, forming a vicious cycle (95) (**Figure 1**).

Interestingly, the changes in gut metabolites could predict PCOS (23, 96) and might even be associated with the different clinical phenotypes (17). The gut metabolites could be more precise predictors than the gut microbiota due to the susceptibility of gut microbiota to a variety of factors, such as environmental contamination and abrupt changes in diet.

The therapies, targeting the gut homeostasis to break the vicious circle between hyperandrogenism and metabolic abnormalities, can be the tipping point for the treatment of PCOS. For example, adopting a healthier lifestyle; supplementing the specific BAs (TDUCA and GDCA), SCFAs, and IL-22; regulating the metabolism of amino acids; and blocking the BCAA targets could be beneficial for the treatment of PCOS (89, 95). It has been reported that the IL-22 levels in patients with PCOS were significantly lower than those in the normal group

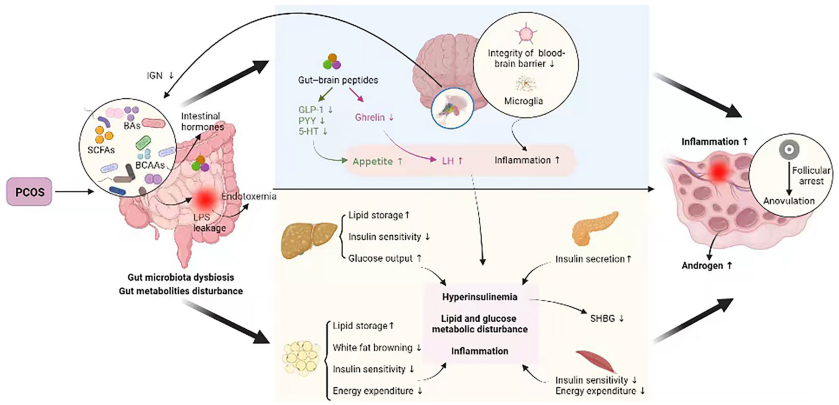

FIGURE 1 | Crosstalk between PCOS and gut metabolites. PCOS, polycystic ovary syndrome; BAs, bile acids; SCFAs, short-chain fatty acids; BCAAs, branched-chain amino acids; IGN, intestinal gluconeogenesis; LPS, lipopolysaccharide; GLP-1, glucagon-like peptide 1; PYY, peptide YY; 5-HT, 5-hydroxytryptamine; LH, luteinizing hormone; SHBG, sex hormone–binding globulin. PCOS disturbs intestinal microbial homeostasis and metabolites, which may be linked to the insulin signaling pathway, steroid hormone levels, glucose metabolism, lipid metabolism, and immunological homeostasis etc., all of which are involved in PCOS pathogenesis, thus forming a vicious cycle.

(22). Therefore, the IL-22 supplementation could be an effective treatment option for PCOS. Studies on the PCOS mice confirmed that the intraperitoneal injection of IL-22 could improve endocrine and metabolic disorders (13). However, there were certain side effects, such as liposarcoma (97). On the other hand, there is limited clinical evidence, supporting the efficiency and safety of IL-22 in humans. Thus, safer therapies are needed to be developed as soon as possible.

The probiotics (or synbiotics) supplementation and fecal microbiota transplantation (FMT) might have a significant impact in this regard. Studies indicated that the administration of probiotics (or synbiotics) for 8–12 weeks could lower serum levels of glucose, insulin, triglycerides (TGs), very low–density lipoprotein, and cholesterol while improving the IR, lipid metabolic disturbance, and inflammatory state. It could also effectively lower the body weight and BMI of patients with PCOS (98–100). Nevertheless, a meta-analysis showed that the effects of probiotics (or synbiotics) supplementation on LDL, weight, BMI, and IR were not significant (101). However, probiotics had certain effects on regulating the metabolisms of glucose, insulin, and lipids, which could lower the serum levels of glucose, insulin, and TG while increasing HDL (101). Another study indicated that the supplementation of probiotics (or synbiotics) improved androgen metabolism without having any other therapeutic effect (102). The administration of different probiotic species and doses to the patients with varied PCOS phenotypes might explain the differences in these outcomes. In rodents, FMT could treat PCOS by restoring the composition of gut microbiota and improving the sex hormone balance and ovarian function (103). However, currently, there are limited applications of FMT in the treatment of PCOS. Therefore, the use of FMT in humans is yet to be determined.

The results showed that the supplementation of insulin-enriched synbiotic yogurt to the PCOS mice could decrease the body weight gain, improve estrus cycles and ovary morphology, and reduce the levels of LH while increasing those of follicle-stimulating hormone and IL-22 in serum. At the genus level, the synbiotic yogurt increased the relative abundances of *Lactobacillus*, *Bifidobacterium*, and *Akkermansia* (104).

Traditional Chinese medicines (TCMs) are vast treasure, which need to be explored. The TCMs, including flavonoids, polysaccharides, saponins, and other compounds, might possess tremendous prospects for stimulating the growth of a particular gut microbial species, increasing the production of beneficial SCFAs and BAs, and suppressing the growth of pathogenic bacteria and BCAA products (94, 105, 106). Berberine, a powerful natural product, which is used for the treatment of metabolic syndrome, could lower the abundance of BCAA-producing bacteria and aberrant blood BCAA levels in the HFD-induced rodents, thereby improving the glucose metabolism, lipid metabolism, and IR in the PCOS rodents (107, 108). Studies on the rodents demonstrated that baicalin could boost the SCFA generation and alter the BA metabolism by modifying the immunology and gut microbiota, as well as affecting the liver–gut axis by regulating the BA-FXR/TGR5 signaling pathway (109). Ginseng polysaccharides and ginsenosides could also boost the growth of *Lactobacillus* spp. and *Bacteroides* spp. in the rat. These two were the most significantly boosted probiotics, restoring the balance of gut microbiota and thereby regulating intestinal metabolism (110). Thus, the TCM and natural products might affect the gut immunity, barrier, and gut microbiota to modulate the local metabolisms. Although studies have revealed that some TCM products have low bioavailability, it is remarkable that gut microbes can transform them into components, which can be absorbed more easily, thereby improving their efficiency and indicating the positive interaction between TCM and gut microbiota (94, 111–113).

Adopting a healthier lifestyle might also improve PCOS, especially the exercise and diet, which act as the modulators of gut microbiota. As mentioned before, bad habits such as an adoration of sweets, a love of fat, an absence of dietary fiber, and

little exercise, might disrupt gut health. As compared to the Western diet (enriched in animal protein and fat and low in fiber), gluten-free diet, vegetarian diets (high in fermentable plant-based foods), etc., the Mediterranean diet is more recommended for the patients with PCOS (114). Numerous human or rodent studies have demonstrated that the Western diet could significantly decrease the abundance of total and beneficial bacteria species, including *Bifidobacterium* and *Eubacterium* (115). The beneficial bacterial populations, such as *Bifidobacterium* and *Lactobacillus*, decreased, whereas those of potentially harmful bacteria increased in the human who consumed a gluten-free diet (116). The results of various studies on vegetarian diets are contradictory. In general, the Mediterranean diet is characterized as a healthy and balanced diet, which can improve obesity, lipid profile, and inflammation (114, 117). Specifically, the assorted fruits, vegetables, nuts, legumes, and cereals are recommended, whereas the intake of red meat, processed meat, and sweets should be limited (114). Exercise can enhance gut health by increasing the diversity of gut microbiota and balancing the beneficial and pathogenic bacterial communities, and a minimum of 150-min exercise of moderate intensity per week is necessary for patients with PCOS (1).

The studies on gut health and PCOS are still in the initial stages, which limit the scope of this review. On one hand, this review mainly focused on the interactions of PCOS with the SCFAs, BAs, and amino acids. Nevertheless, there might be additional metabolic loops closely associated with the PCOS, such as carnitine metabolism (118). The amino acids, other than BCAAs, are also needed to be thoroughly investigated in the future. On the other hand, there might be some changes in the synthesis and transit of gastrointestinal metabolites between species. Therefore, the findings from animal studies remain to be validated in humans.

AUTHOR CONTRIBUTIONS

MZ and YS contributed to the conception of this review. RH wrote the manuscript. RH, MZ, and YS revised the manuscript. RH and YH designed and illustrated the figures. YH, FZ, FL, ZL, and YG performed the literature search and interpretation. MZ, RH, YH, FZ, FL, ZL, YG, HD, WM, KS, and YS reviewed the manuscript. All authors approved the submission.

ACKNOWLEDGMENTS

Thanks to BioRender. The figure is created with BioRender.com.

REFERENCES

1. Teede HJ, Misso ML, Costello MF, Dokras A, Laven J, Moran L, et al. Recommendations From the International Evidence-Based Guideline for the Assessment and Management of Polycystic Ovary Syndrome. *Fertil Steril* (2018) 110(3):364–79. doi: 10.1016/j.fertnstert.2018.05.004
2. Liao B, Qiao J, Pang Y. Central Regulation of Pcos: Abnormal Neuronal-Reproductive-Metabolic Circuits in Pcos Pathophysiology. *Front Endocrinol (Lausanne)* (2021) 12:667422. doi: 10.3389/fendo.2021.667422
3. Azziz R, Carmina E, Chen Z, Dunaif A, Laven JS, Legro RS, et al. Polycystic Ovary Syndrome. *Nat Rev Dis Primers* (2016) 2:16057. doi: 10.1038/nrdp.2016.57
4. Lizneva D, Suturina L, Walker W, Brakta S, Gavrilova-Jordan L, Azziz R. Criteria, Prevalence, and Phenotypes of Polycystic Ovary Syndrome. *Fertil Steril* (2016) 106(1):6–15. doi: 10.1016/j.fertnstert.2016.05.003
5. Rosenfield RL. The Diagnosis of Polycystic Ovary Syndrome in Adolescents. *Pediatrics* (2015) 136(6):1154–65. doi: 10.1542/peds.2015-1430
6. Han Q, Wang J, Li W, Chen ZJ, Du Y. Androgen-Induced Gut Dysbiosis Disrupts Glucolipid Metabolism and Endocrinal Functions in Polycystic Ovary Syndrome. *Microbiome* (2021) 9(1):101. doi: 10.1186/s40168-021-01046-5
7. De Leo V, Musacchio MC, Cappelli V, Massaro MG, Morgante G, Petraglia F. Genetic, Hormonal and Metabolic Aspects of Pcos: An Update. *Reprod Biol Endocrinol* (2016) 14(1):38. doi: 10.1186/s12958-016-0173-x
8. Giampaolino P, Foreste V, Di Filippo C, Gallo A, Mercorio A, Serafino P, et al. Microbiome and Pcos: State-Of-Art and Future Aspects. *Int J Mol Sci* (2021) 22(4):2048. doi: 10.3390/ijms22042048
9. Rajska A, Buszewska-Forajta M, Rachoń D, Markuszewski MJ. Metabolomic Insight Into Polycystic Ovary Syndrome-An Overview. *Int J Mol Sci* (2020) 21(14):4835. doi: 10.3390/ijms21144853
10. Thackray VG. Sex, Microbes, and Polycystic Ovary Syndrome. *Trends Endocrinol Metab* (2019) 30(1):54–65. doi: 10.1016/j.tem.2018.11.001
11. Insenser M, Murri M, Del Campo R, Martínez-García M, Fernández-Durán E, Escobar-Morreale HF. Gut Microbiota and the Polycystic Ovary Syndrome: Influence of Sex, Sex Hormones, and Obesity. *J Clin Endocrinol Metab* (2018) 103(7):2552–62. doi: 10.1210/jc.2017-02799
12. Zhang J, Sun Z, Jiang S, Bai X, Ma C, Peng Q, et al. Probiotic Bifidobacterium Lactis V9 Regulates the Secretion of Sex Hormones in Polycystic Ovary Syndrome Patients Through the Gut-Brain Axis. *mSystems* (2019) 4(2):e00017-19. doi: 10.1128/mSystems.00017-19
13. Qi X, Yun C, Sun L, Xia J, Wu Q, Wang Y, et al. Gut Microbiota-Bile Acid-Interleukin-22 Axis Orchestrates Polycystic Ovary Syndrome. *Nat Med* (2019) 25(8):1225–33. doi: 10.1038/s41591-019-0509-0
14. Garcha D, Walker SP, MacDonald TM, Hyett J, Jellins J, Myers J, et al. Circulating Syndecan-1 Is Reduced in Pregnancies With Poor Fetal Growth and Its Secretion Regulated by Matrix Metalloproteinases and the Mitochondria. *Sci Rep* (2021) 11(1):16595. doi: 10.1038/s41598-021-96077-1
15. Wahlström A, Sayin SI, Marschall HU, Bäckhed F. Intestinal Crosstalk Between Bile Acids and Microbiota and Its Impact on Host Metabolism. *Cell Metab* (2016) 24(1):41–50. doi: 10.1016/j.cmet.2016.05.005
16. Wang L, Zhou J, Gober HJ, Leung WT, Huang Z, Pan X, et al. Alterations in the Intestinal Microbiome Associated With Pcos Affect the Clinical Phenotype. *BioMed Pharmacother* (2021) 133:110958. doi: 10.1016/j.biopha.2020.110958
17. Liu R, Zhang C, Shi Y, Zhang F, Li L, Wang X, et al. Dysbiosis of Gut Microbiota Associated With Clinical Parameters in Polycystic Ovary Syndrome. *Front Microbiol* (2017) 8:324. doi: 10.3389/fmicb.2017.00324
18. Zheng YH, Xu Y, Ma HX, Liang CJ, Yang T. Effect of High-Fat Diet on the Intestinal Flora in Letrozole-Induced Polycystic Ovary Syndrome Rats. *Evid Based Complement Alternat Med* (2021) 2021:6674965. doi: 10.1155/2021/6674965
19. Wang T, Sha L, Li Y, Zhu L, Wang Z, Li K, et al. Dietary α-Linolenic Acid-Rich Flaxseed Oil Exerts Beneficial Effects on Polycystic Ovary Syndrome Through Sex Steroid Hormones-Microbiota-Inflammation Axis in Rats. *Front Endocrinol (Lausanne)* (2020) 11:284. doi: 10.3389/fendo.2020.00284
20. Zhang C, Fang R, Lu X, Zhang Y, Yang M, Su Y, et al. Lactobacillus Reuteri J1 Prevents Obesity by Altering the Gut Microbiota and Regulating Bile Acid Metabolism in Obese Mice. *Food Funct* (2022) 13(12):6688–6701. doi: 10.1039/d1fo04387k
21. Li R, Andreu-Sánchez S, Kuipers F, Fu J. Gut Microbiome and Bile Acids in Obesity-Related Diseases. *Best Pract Res Clin Endocrinol Metab* (2021) 35(3):101493. doi: 10.1016/j.beem.2021.101493

22. Qi X, Nie Q, Pang Y, Qiao J. IL-22 and Its Interaction With Amino Acid and Glycolipid Metabolite in Polycystic Ovary Syndrome (Pcos) Patients. *Chin Med J* (2021). doi: 10.1097/cm9.0000000000001915
23. Li J, Dawson PA. Animal Models to Study Bile Acid Metabolism. *Biochim Biophys Acta Mol Basis Dis* (2019) 1865(5):895–911. doi: 10.1016/j.bbadis.2018.05.011
24. Russell DW. The Enzymes, Regulation, and Genetics of Bile Acid Synthesis. *Annu Rev Biochem* (2003) 72:137–74. doi: 10.1146/annurev.biochem.72.121801.161712
25. McGlone ER, Bloom SR. Bile Acids and the Metabolic Syndrome. *Ann Clin Biochem* (2019) 56(3):326–37. doi: 10.1177/0004563218817798
26. Liu H, Hu C, Zhang X, Jia W. Role of Gut Microbiota, Bile Acids and Their Cross-Talk in the Effects of Bariatric Surgery on Obesity and Type 2 Diabetes. *J Diabetes Investig* (2018) 9(1):13–20. doi: 10.1111/jdi.12687
27. Ridlon JM, Harris SC, Bhowmik S, Kang DJ, Hylemon PB. Consequences of Bile Salt Biotransformations by Intestinal Bacteria. *Gut Microbes* (2016) 7 (1):22–39. doi: 10.1080/19490976.2015.1127483
28. Sayin SI, Wahlström A, Felin J, Jäntti S, Marschall HU, Bamberg K, et al. Gut Microbiota Regulates Bile Acid Metabolism by Reducing the Levels of Tauro-Beta-Muricholic Acid, a Naturally Occurring Fxr Antagonist. *Cell Metab* (2013) 17(2):225–35. doi: 10.1016/j.cmet.2013.01.003
29. Dawson PA, Karpen SJ. Intestinal Transport and Metabolism of Bile Acids. *J Lipid Res* (2015) 56(6):1085–99. doi: 10.1194/jlr.R054114
30. Selwyn FP, Csanaky IL, Zhang Y, Klaassen CD. Importance of Large Intestine in Regulating Bile Acids and Glucagon-Like Peptide-1 in Germ-Free Mice. *Drug Metab Dispos* (2015) 43(10):1544–56. doi: 10.1124/dmd.115.065276
31. Schmitt J, Kong B, Stieger B, Tschopp O, Schultze SM, Rau M, et al. Protective Effects of Farnesoid X Receptor (Fxr) on Hepatic Lipid Accumulation Are Mediated by Hepatic Fxr and Independent of Intestinal Fgf15 Signal. *Liver Int* (2015) 35(4):1133–44. doi: 10.1111/liv.12456
32. Jiang C, Xie C, Li F, Zhang L, Nichols RG, Krausz KW, et al. Intestinal Farnesoid X Receptor Signaling Promotes Nonalcoholic Fatty Liver Disease. *J Clin Invest* (2015) 125(1):386–402. doi: 10.1172/jci76738
33. Parséus A, Sommer N, Sommer F, Caesar R, Molinaro A, Ståhlman M, et al. Microbiota-Induced Obesity Requires Farnesoid X Receptor. *Gut* (2017) 66 (3):429–37. doi: 10.1136/gutjnl-2015-310283
34. Saeed A, Hoekstra M, Hoeke MO, Heegsma J, Faber KN. The Interrelationship Between Bile Acid and Vitamin a Homeostasis. *Biochim Biophys Acta Mol Cell Biol Lipids* (2017) 1862(5):496–512. doi: 10.1016/j.bbalip.2017.01.007
35. Charach G, Argov O, Geiger K, Charach L, Rogowski O, Grosskopf I. Diminished Bile Acids Excretion is a Risk Factor for Coronary Artery Disease: 20-Year Follow Up and Long-Term Outcome. *Ther Adv Gastroenterol* (2018) 11:1756283x17743420. doi: 10.1177/1756283x17743420
36. Qi X, Yun C, Pang Y, Qiao J. The Impact of the Gut Microbiota on the Reproductive and Metabolic Endocrine System. *Gut Microbes* (2021) 13 (1):1–21. doi: 10.1080/19490976.2021.1894070
37. Kuhre RE, Wewer Albrechtsen NJ, Larsen O, Jepsen SL, Balk-Møller E, Andersen DB, et al. Bile Acids are Important Direct and Indirect Regulators of the Secretion of Appetite- and Metabolism-Regulating Hormones From the Gut and Pancreas. *Mol Metab* (2018) 11:84–95. doi: 10.1016/j.molmet.2018.03.007
38. Perino A, Velazquez-Villegas LA, Bresciani N, Sun Y, Huang Q, Fenelon VS, et al. Central Anorexigenic Actions of Bile Acids Are Mediated by Tgr5. *Nat Metab* (2021) 3(5):595–603. doi: 10.1038/s42255-021-00398-4
39. Alemi F, Kwon E, Poole DP, Lieu T, Lyo V, Cattaruzza F, et al. The Tgr5 Receptor Mediates Bile Acid-Induced Itch and Analgesia. *J Clin Invest* (2013) 123(4):1513–30. doi: 10.1172/jci64551
40. Xie Y, He Y, Cai Z, Cai J, Xi M, Zhang Y, et al. Tauroursodeoxycholic Acid Inhibits Endoplasmic Reticulum Stress, Blocks Mitochondrial Permeability Transition Pore Opening, and Suppresses Reperfusion Injury Through Gsk-3ß in Cardiac H9c2 Cells. *Am J Transl Res* (2016) 8(11):4586–97.
41. Silva YP, Bernardi A, Frozza RL. The Role of Short-Chain Fatty Acids From Gut Microbiota in Gut-Brain Communication. *Front Endocrinol (Lausanne)* (2020) 11:25. doi: 10.3389/fendo.2020.00025
42. Koh A, De Vadder F, Kovatcheva-Datchary P, Bäckhed F. From Dietary Fiber to Host Physiology: Short-Chain Fatty Acids as Key Bacterial Metabolites. *Cell* (2016) 165(6):1332–45. doi: 10.1016/j.cell.2016.05.041
43. Hernández MAG, Canfora EE, Jocken JWE, Blaak EE. The Short-Chain Fatty Acid Acetate in Body Weight Control and Insulin Sensitivity. *Nutrients* (2019) 11(8):1943. doi: 10.3390/nu11081943
44. Portincasa P, Bonfrate L, Vacca M, De Angelis M, Farella I, Lanza E, et al. Gut Microbiota and Short Chain Fatty Acids: Implications in Glucose Homeostasis. *Int J Mol Sci* (2022) 23(3):1105. doi: 10.3390/ijms23031105
45. Schönfeld P, Wojtczak L. Short- and Medium-Chain Fatty Acids in Energy Metabolism: The Cellular Perspective. *J Lipid Res* (2016) 57(6):943–54. doi: 10.1194/jlr.R067629
46. Bolognini D, Tobin AB, Milligan G, Moss CE. The Pharmacology and Function of Receptors for Short-Chain Fatty Acids. *Mol Pharmacol* (2016) 89(3):388–98. doi: 10.1124/mol.115.102301
47. Kim YA, Keogh JB, Clifton PM. Probiotics, Prebiotics, Synbiotics and Insulin Sensitivity. *Nutr Res Rev* (2018) 31(1):35–51. doi: 10.1017/S095442241700018X
48. Puddu A, Sanguineti R, Montecucco F, Viviani GL. Evidence for the Gut Microbiota Short-Chain Fatty Acids as Key Pathophysiological Molecules Improving Diabetes. *Mediators Inflamm* (2014) 2014:162021. doi: 10.1155/2014/162021
49. De Vadder F, Kovatcheva-Datchary P, Goncalves D, Vinera J, Zitoun C, Duchampt A, et al. Microbiota-Generated Metabolites Promote Metabolic Benefits *via* Gut-Brain Neural Circuits. *Cell* (2014) 156(1-2):84–96. doi: 10.1016/j.cell.2013.12.016
50. Dang AT, Marsland BJ. Microbes, Metabolites, and the Gut-Lung Axis. *Mucosal Immunol* (2019) 12(4):843–50. doi: 10.1038/s41385-019-0160-6
51. Rooks MG, Garrett WS. Gut Microbiota, Metabolites and Host Immunity. *Nat Rev Immunol* (2016) 16(6):341–52. doi: 10.1038/nri.2016.42
52. Kim CH, Park J, Kim M. Gut Microbiota-Derived Short-Chain Fatty Acids, T Cells, and Inflammation. *Immune Netw* (2014) 14(6):277–88. doi: 10.4110/in.2014.14.6.277
53. Nowarski R, Jackson R, Gagliani N, de Zoete MR, Palm NW, Bailis W, et al. Epithelial Il-18 Equilibrium Controls Barrier Function in Colitis. *Cell* (2015) 163(6):1444–56. doi: 10.1016/j.cell.2015.10.072
54. Smith PM, Howitt MR, Panikov N, Michaud M, Gallini CA, Bohlooly YM, et al. The Microbial Metabolites, Short-Chain Fatty Acids, Regulate Colonic Treg Cell Homeostasis. *Science* (2013) 341(6145):569–73. doi: 10.1126/science.1241165
55. Vieira AT, Macia L, Galvão I, Martins FS, Canesso MC, Amaral FA, et al. A Role for Gut Microbiota and the Metabolite-Sensing Receptor Gpr43 in a Murine Model of Gout. *Arthritis Rheumatol* (2015) 67(6):1646–56. doi: 10.1002/art.39107
56. Mathewson ND, Jenq R, Mathew AV, Koenigsknecht M, Hanash A, Toubai T, et al. Gut Microbiome-Derived Metabolites Modulate Intestinal Epithelial Cell Damage and Mitigate Graft-Versus-Host Disease. *Nat Immunol* (2016) 17(5):505–13. doi: 10.1038/ni.3400
57. Stilling RM, van de Wouw M, Clarke G, Stanton C, Dinan TG, Cryan JF. The Neuropharmacology of Butyrate: The Bread and Butter of the Microbiota-Gut-Brain Axis? *Neurochem Int* (2016) 99:110–32. doi: 10.1016/j.neuint.2016.06.011
58. Bröer S, Gauthier-Coles G. Amino Acid Homeostasis in Mammalian Cells With a Focus on Amino Acid Transport. *J Nutr* (2022) 152(1):16–28. doi: 10.1093/jn/nxab342
59. Bröer S, Fairweather SJ. Amino Acid Transport Across the Mammalian Intestine. *Compr Physiol* (2018) 9(1):343–73. doi: 10.1002/cphy.c170041
60. Yan R, Zhao X, Lei J, Zhou Q. Structure of the Human Lat1-4f2hc Heteromeric Amino Acid Transporter Complex. *Nature* (2019) 568 (7750):127–30. doi: 10.1038/s41586-019-1011-z
61. Gauthier-Coles G, Vennitti J, Zhang Z, Comb WC, Xing S, Javed K, et al. Quantitative Modelling of Amino Acid Transport and Homeostasis in Mammalian Cells. *Nat Commun* (2021) 12(1):5282. doi: 10.1038/s41467-021-25563-x
62. Neinast MD, Jang C, Hui S, Murashige DS, Chu Q, Morscher RJ, et al. Quantitative Analysis of the Whole-Body Metabolic Fate of Branched-Chain Amino Acids. *Cell Metab* (2019) 29(2):417–29.e4. doi: 10.1016/j.cmet.2018.10.013
63. Shin AC, Fasshauer M, Filatova N, Grundell LA, Zielinski E, Zhou JY, et al. Brain Insulin Lowers Circulating Bcaa Levels by Inducing Hepatic Bcaa Catabolism. *Cell Metab* (2014) 20(5):898–909. doi: 10.1016/j.cmet.2014.09.003

64. Kelly B, Pearce EL. Amino Assets: How Amino Acids Support Immunity. *Cell Metab* (2020) 32(2):154–75. doi: 10.1016/j.cmet.2020.06.010
65. Chen W, Pang Y. Metabolic Syndrome and Pcos: Pathogenesis and the Role of Metabolites. *Metabolites* (2021) 11(12):869. doi: 10.3390/metabo11120869
66. Usuda K, Kawase T, Shigeno Y, Fukuzawa S, Fujii K, Zhang H, et al. Hippocampal Metabolism of Amino Acids by L-Amino Acid Oxidase is Involved in Fear Learning and Memory. *Sci Rep* (2018) 8(1):11073. doi: 10.1038/s41598-018-28885-x
67. Miyajima M. Amino Acids: Key Sources for Immunometabolites and Immunotransmitters. *Int Immunol* (2020) 32(7):435–46. doi: 10.1093/intimm/dxaa019
68. Markle JG, Frank DN, Mortin-Toth S, Robertson CE, Feazel LM, Rolle-Kampczyk U, et al. Sex Differences in the Gut Microbiome Drive Hormone-Dependent Regulation of Autoimmunity. *Science* (2013) 339(6123):1084–8. doi: 10.1126/science.1233521
69. Dominianni C, Sinha R, Goedert JJ, Pei Z, Yang L, Hayes RB, et al. Sex, Body Mass Index, and Dietary Fiber Intake Influence the Human Gut Microbiome. *PloS One* (2015) 10(4):e0124599. doi: 10.1371/journal.pone.0124599
70. Torres PJ, Siakowska M, Banaszewska B, Pawelczyk L, Duleba AJ, Kelley ST, et al. Gut Microbial Diversity in Women With Polycystic Ovary Syndrome Correlates With Hyperandrogenism. *J Clin Endocrinol Metab* (2018) 103(4):1502–11. doi: 10.1210/jc.2017-02153
71. Sherman SB, Sarsour N, Salehi M, Schroering A, Mell B, Joe B, et al. Prenatal Androgen Exposure Causes Hypertension and Gut Microbiota Dysbiosis. *Gut Microbes* (2018) 9(5):400–21. doi: 10.1080/19490976.2018.1441664
72. Mammadova G, Ozkul C, Yilmaz Isikhan S, Acikgoz A, Yildiz BO. Characterization of Gut Microbiota in Polycystic Ovary Syndrome: Findings From a Lean Population. *Eur J Clin Invest* (2021) 51(4):e13417. doi: 10.1111/eci.13417
73. Bulun SE, Chen D, Moy I, Brooks DC, Zhao H. Aromatase, Breast Cancer and Obesity: A Complex Interaction. *Trends Endocrinol Metab* (2012) 23(2):83–9. doi: 10.1016/j.tem.2011.10.003
74. Cani PD, Bibiloni R, Knauf C, Waget A, Neyrinck AM, Delzenne NM, et al. Changes in Gut Microbiota Control Metabolic Endotoxemia-Induced Inflammation in High-Fat Diet-Induced Obesity and Diabetes in Mice. *Diabetes* (2008) 57(6):1470–81. doi: 10.2337/db07-1403
75. Zheng Y, Yu J, Liang C, Li S, Wen X, Li Y. Characterization on Gut Microbiome of Pcos Rats and Its Further Design by Shifts in High-Fat Diet and Dihydrotestosterone Induction in Pcos Rats. *Bioprocess Biosyst Eng* (2021) 44(5):953–64. doi: 10.1007/s00449-020-02320-w
76. Pedersen HK, Gudmundsdottir V, Nielsen HB, Hyotylainen T, Nielsen T, Jensen BA, et al. Human Gut Microbes Impact Host Serum Metabolome and Insulin Sensitivity. *Nature* (2016) 535(7612):376–81. doi: 10.1038/nature18646
77. Sun Z, Chang HM, Wang A, Song J, Zhang X, Guo J, et al. Identification of Potential Metabolic Biomarkers of Polycystic Ovary Syndrome in Follicular Fluid by Swath Mass Spectrometry. *Reprod Biol Endocrinol* (2019) 17(1):45. doi: 10.1186/s12958-019-0490-y
78. Halama A, Aye MM, Dargham SR, Kulinski M, Suhre K, Atkin SL. Metabolomics of Dynamic Changes in Insulin Resistance Before and After Exercise in Pcos. *Front Endocrinol (Lausanne)* (2019) 10:116. doi: 10.3389/fendo.2019.00116
79. Gubert C, Kong G, Renoir T, Hannan AJ. Exercise, Diet and Stress as Modulators of Gut Microbiota: Implications for Neurodegenerative Diseases. *Neurobiol Dis* (2020) 134:104621. doi: 10.1016/j.nbd.2019.104621
80. Allen JM, Mailing LJ, Cohrs J, Salmonson C, Fryer JD, Nehra V, et al. Exercise Training-Induced Modification of the Gut Microbiota Persists After Microbiota Colonization and Attenuates the Response to Chemically-Induced Colitis in Gnotobiotic Mice. *Gut Microbes* (2018) 9(2):115–30. doi: 10.1080/19490976.2017.1372077
81. Allen JM, Mailing LJ, Niemiro GM, Moore R, Cook MD, White BA, et al. Exercise Alters Gut Microbiota Composition and Function in Lean and Obese Humans. *Med Sci Sports Exerc* (2018) 50(4):747–57. doi: 10.1249/mss.0000000000001495
82. Nakajima M, Arimatsu K, Kato T, Matsuda Y, Minagawa T, Takahashi N, et al. Oral Administration of P. Gingivalis Induces Dysbiosis of Gut Microbiota and Impaired Barrier Function Leading to Dissemination of Enterobacteria to the Liver. *PloS One* (2015) 10(7):e0134234. doi: 10.1371/journal.pone.0134234
83. Muccioli GG, Naslain D, Bäckhed F, Reigstad CS, Lambert DM, Delzenne NM, et al. The Endocannabinoid System Links Gut Microbiota to Adipogenesis. *Mol Syst Biol* (2010) 6:392. doi: 10.1038/msb.2010.46
84. Zhang B, Shen S, Gu T, Hong T, Liu J, Sun J, et al. Increased Circulating Conjugated Primary Bile Acids Are Associated With Hyperandrogenism in Women With Polycystic Ovary Syndrome. *J Steroid Biochem Mol Biol* (2019) 189:171–5. doi: 10.1016/j.jsbmb.2019.03.005
85. Gozukara I, Dokuyucu R, Özgür T, Özcan O, Pınar N, Kurt RK, et al. Histopathologic and Metabolic Effect of Ursodeoxycholic Acid Treatment on Pcos Rat Model. *Gynecol Endocrinol* (2016) 32(6):492–7. doi: 10.3109/09513590.2015.1134478
86. Qi X, Yun C, Liao B, Qiao J, Pang Y. The Therapeutic Effect of Interleukin-22 in High Androgen-Induced Polycystic Ovary Syndrome. *J Endocrinol* (2020) 245(2):281–9. doi: 10.1530/joe-19-0589
87. Bartelt A, Heeren J. Adipose Tissue Browning and Metabolic Health. *Nat Rev Endocrinol* (2014) 10(1):24–36. doi: 10.1038/nrendo.2013.204
88. Lynch CJ, Adams SH. Branched-Chain Amino Acids in Metabolic Signalling and Insulin Resistance. *Nat Rev Endocrinol* (2014) 10(12):723–36. doi: 10.1038/nrendo.2014.171
89. Yang W, Yu T, Huang X, Bilotta AJ, Xu L, Lu Y, et al. Intestinal Microbiota-Derived Short-Chain Fatty Acids Regulation of Immune Cell Il-22 Production and Gut Immunity. *Nat Commun* (2020) 11(1):4457. doi: 10.1038/s41467-020-18262-6
90. Litvak Y, Byndloss MX, Bäumler AJ. Colonocyte Metabolism Shapes the Gut Microbiota. *Science* (2018) 362(6418):eaat9076. doi: 10.1126/science.aat9076
91. Aydin K, Arusoglu G, Koksal G, Cinar N, Aksoy DY, Yildiz BO. Fasting and Post-Prandial Glucagon Like Peptide 1 and Oral Contraception in Polycystic Ovary Syndrome. *Clin Endocrinol (Oxf)* (2014) 81(4):588–92. doi: 10.1111/cen.12468
92. Lin W, Wen L, Wen J, Xiang G. Effects of Sleeve Gastrectomy on Fecal Gut Microbiota and Short-Chain Fatty Acid Content in a Rat Model of Polycystic Ovary Syndrome. *Front Endocrinol (Lausanne)* (2021) 12:747888. doi: 10.3389/fendo.2021.747888
93. Newgard CB. Interplay Between Lipids and Branched-Chain Amino Acids in Development of Insulin Resistance. *Cell Metab* (2012) 15(5):606–14. doi: 10.1016/j.cmet.2012.01.024
94. Feng W, Ao H, Peng C, Yan D. Gut Microbiota, a New Frontier to Understand Traditional Chinese Medicines. *Pharmacol Res* (2019) 142:176–91. doi: 10.1016/j.phrs.2019.02.024
95. Agus A, Clement K, Sokol H. Gut Microbiota-Derived Metabolites as Central Regulators in Metabolic Disorders. *Gut* (2021) 70(6):1174–82. doi: 10.1136/gutjnl-2020-323071
96. Ye Z, Zhang C, Wang S, Zhang Y, Li R, Zhao Y, et al. Amino Acid Signatures in Relation to Polycystic Ovary Syndrome and Increased Risk of Different Metabolic Disturbances. *Reprod BioMed Online* (2021) 44(4):737–746. doi: 10.1016/j.rbmo.2021.11.012
97. Wang Z, Yang L, Jiang Y, Ling ZQ, Li Z, Cheng Y, et al. High Fat Diet Induces Formation of Spontaneous Liposarcoma in Mouse Adipose Tissue With Overexpression of Interleukin 22. *PloS One* (2011) 6(8):e23737. doi: 10.1371/journal.pone.0023737
98. Ahmadi S, Jamilian M, Karamali M, Tajabadi-Ebrahimi M, Jafari P, Taghizadeh M, et al. Probiotic Supplementation and the Effects on Weight Loss, Glycaemia and Lipid Profiles in Women With Polycystic Ovary Syndrome: A Randomized, Double-Blind, Placebo-Controlled Trial. *Hum Fertil (Camb)* (2017) 20(4):254–61. doi: 10.1080/14647273.2017.1283446
99. Shoaei T, Heidari-Beni M, Tehrani HG, Feizi A, Esmaillzadeh A, Askari G. Effects of Probiotic Supplementation on Pancreatic β-Cell Function and C-Reactive Protein in Women With Polycystic Ovary Syndrome: A Randomized Double-Blind Placebo-Controlled Clinical Trial. *Int J Prev Med* (2015) 6:27. doi: 10.4103/2008-7802.153866
100. Jamilian M, Mansury S, Bahmani F, Heidar Z, Amirani E, Asemi Z. The Effects of Probiotic and Selenium Co-Supplementation on Parameters of Mental Health, Hormonal Profiles, and Biomarkers of Inflammation and Oxidative Stress in Women With Polycystic Ovary Syndrome. *J Ovarian Res* (2018) 11(1):80. doi: 10.1186/s13048-018-0457-1
101. Heshmati J, Farsi F, Yosaee S, Razavi M, Rezaeinejad M, Karimie E, et al. The Effects of Probiotics or Synbiotics Supplementation in Women With

Polycystic Ovarian Syndrome: A Systematic Review and Meta-Analysis of Randomized Clinical Trials. *Probiotics Antimicrob Proteins* (2019) 11 (4):1236–47. doi: 10.1007/s12602-018-9493-9
102. Shamasbi SG, Ghanbari-Homayi S, Mirghafourvand M. The Effect of Probiotics, Prebiotics, and Synbiotics on Hormonal and Inflammatory Indices in Women With Polycystic Ovary Syndrome: A Systematic Review and Meta-Analysis. *Eur J Nutr* (2020) 59(2):433–50. doi: 10.1007/s00394-019-02033-1
103. Guo Y, Qi Y, Yang X, Zhao L, Wen S, Liu Y, et al. Association Between Polycystic Ovary Syndrome and Gut Microbiota. *PloS One* (2016) 11(4): e0153196. doi: 10.1371/journal.pone.0153196
104. Li T, Zhang Y, Song J, Chen L, Du M, Mao X. Yogurt Enriched With Inulin Ameliorated Reproductive Functions and Regulated Gut Microbiota in Dehydroepiandrosterone-Induced Polycystic Ovary Syndrome Mice. *Nutrients* (2022) 14(2):279. doi: 10.3390/nu14020279
105. Wang HY, Qi LW, Wang CZ, Li P. Bioactivity Enhancement of Herbal Supplements by Intestinal Microbiota Focusing on Ginsenosides. *Am J Chin Med* (2011) 39(6):1103–15. doi: 10.1142/s0192415x11009433
106. Chang CJ, Lin CS, Lu CC, Martel J, Ko YF, Ojcius DM, et al. Ganoderma Lucidum Reduces Obesity in Mice by Modulating the Composition of the Gut Microbiota. *Nat Commun* (2015) 6:7489. doi: 10.1038/ncomms8489
107. Shen HR, Xu X, Ye D, Li XL. Berberine Improves the Symptoms of Dhea-Induced Pcos Rats by Regulating Gut Microbiotas and Metabolites. *Gynecol Obstet Invest* (2021) 86(4):388–97. doi: 10.1159/000518040
108. Yue SJ, Liu J, Wang AT, Meng XT, Yang ZR, Peng C, et al. Berberine Alleviates Insulin Resistance by Reducing Peripheral Branched-Chain Amino Acids. *Am J Physiol Endocrinol Metab* (2019) 316(1):E73–e85. doi: 10.1152/ajpendo.00256.2018
109. Hu Q, Zhang W, Wu Z, Tian X, Xiang J, Li L, et al. Baicalin and the Liver-Gut System: Pharmacological Bases Explaining Its Therapeutic Effects. *Pharmacol Res* (2021) 165:105444. doi: 10.1016/j.phrs.2021.105444
110. Zhou SS, Xu J, Zhu H, Wu J, Xu JD, Yan R, et al. Gut Microbiota-Involved Mechanisms in Enhancing Systemic Exposure of Ginsenosides by Coexisting Polysaccharides in Ginseng Decoction. *Sci Rep* (2016) 6:22474. doi: 10.1038/srep22474
111. Zheng HR, Chu Y, Zhou DZ, Ju AC, Li W, Li X, et al. Integrated Pharmacokinetics of Ginsenosides After Intravenous Administration of Yiqifumai Powder Injection in Rats With Chronic Heart Failure by Uflc-Ms/Ms. *J Chromatogr B Analyt Technol BioMed Life Sci* (2018) 1072:282–9. doi: 10.1016/j.jchromb.2017.10.056
112. Chen F, Wen Q, Jiang J, Li HL, Tan YF, Li YH, et al. Could the Gut Microbiota Reconcile the Oral Bioavailability Conundrum of Traditional Herbs? *J Ethnopharmacol* (2016) 179:253–64. doi: 10.1016/j.jep.2015.12.031
113. Feng R, Shou JW, Zhao ZX, He CY, Ma C, Huang M, et al. Transforming Berberine Into Its Intestine-Absorbable Form by the Gut Microbiota. *Sci Rep* (2015) 5:12155. doi: 10.1038/srep12155
114. Singh RK, Chang HW, Yan D, Lee KM, Ucmak D, Wong K, et al. Influence of Diet on the Gut Microbiome and Implications for Human Health. *J Transl Med* (2017) 15(1):73. doi: 10.1186/s12967-017-1175-y
115. Wu GD, Chen J, Hoffmann C, Bittinger K, Chen YY, Keilbaugh SA, et al. Linking Long-Term Dietary Patterns With Gut Microbial Enterotypes. *Science* (2011) 334(6052):105–8. doi: 10.1126/science.1208344
116. Sanz Y. Effects of a Gluten-Free Diet on Gut Microbiota and Immune Function in Healthy Adult Humans. *Gut Microbes* (2010) 1(3):135–7. doi: 10.4161/gmic.1.3.11868
117. Koloverou E, Panagiotakos DB, Pitsavos C, Chrysohoou C, Georgousopoulou EN, Grekas A, et al. Adherence to Mediterranean Diet and 10-Year Incidence (2002-2012) of Diabetes: Correlations With Inflammatory and Oxidative Stress Biomarkers in the Attica Cohort Study. *Diabetes Metab Res Rev* (2016) 32(1):73–81. doi: 10.1002/dmrr.2672
118. Jia C, Xu H, Xu Y, Xu Y, Shi Q. Serum Metabolomics Analysis of Patients With Polycystic Ovary Syndrome by Mass Spectrometry. *Mol Reprod Dev* (2019) 86(3):292–7. doi: 10.1002/mrd.23104

Conflict of Interest: The authors declare that the research was conducted in the absence of any commercial or financial relationships that could be construed as a potential conflict of interest.

Publisher's Note: All claims expressed in this article are solely those of the authors and do not necessarily represent those of their affiliated organizations, or those of the publisher, the editors and the reviewers. Any product that may be evaluated in this article, or claim that may be made by its manufacturer, is not guaranteed or endorsed by the publisher.

frontiers | Frontiers in Endocrinology

TYPE Review
PUBLISHED 11 August 2022
DOI 10.3389/fendo.2022.958218

OPEN ACCESS

EDITED BY
Yanli Pang,
Peking University Third Hospital, China

REVIEWED BY
Tingtao Chen,
Nanchang University, China
Qiyi Chen,
Tongji University, China

*CORRESPONDENCE
Yanling Wei
lingzi016@126.com
Guangcong Ruan
ruanguangcong@163.com

†These authors have contributed equally to this work

SPECIALTY SECTION
This article was submitted to Gut Endocrinology, a section of the journal Frontiers in Endocrinology

RECEIVED 31 May 2022
ACCEPTED 22 July 2022
PUBLISHED 11 August 2022

CITATION
Liu L, Zhang J, Cheng Y, Zhu M, Xiao Z, Ruan G and Wei Y (2022) Gut microbiota: A new target for T2DM prevention and treatment. *Front. Endocrinol.* 13:958218. doi: 10.3389/fendo.2022.958218

Gut microbiota: A new target for T2DM prevention and treatment

Lulu Liu[1,2†], Jiheng Zhang[2†], Yi Cheng[1], Meng Zhu[2], Zhifeng Xiao[1], Guangcong Ruan[1*] and Yanling Wei[1*]

[1]Department of Gastroenterology, Chongqing Key Laboratory of Digestive Malignancies, Daping Hospital, Army Medical University (Third Military Medical University), Chongqing, China, [2]Department of Plastic and Cosmetic Surgery, Daping Hospital, Army Medical University (Third Military Medical University), Chongqing, China

Type 2 diabetes mellitus (T2DM), one of the fastest growing metabolic diseases, has been characterized by metabolic disorders including hyperglycemia, hyperlipidemia and insulin resistance (IR). In recent years, T2DM has become the fastest growing metabolic disease in the world. Studies have indicated that patients with T2DM are often associated with intestinal flora disorders and dysfunction involving multiple organs. Metabolites of the intestinal flora, such as bile acids (BAs), short-chain fatty acids (SCFAs) and amino acids (AAs)may influence to some extent the decreased insulin sensitivity associated with T2DM dysfunction and regulate metabolic as well as immune homeostasis. In this paper, we review the changes in the gut flora in T2DM and the mechanisms by which the gut microbiota modulates metabolites affecting T2DM, which may provide a basis for the early identification of T2DM-susceptible individuals and guide targeted interventions. Finally, we also highlight gut microecological therapeutic strategies focused on shaping the gut flora to inform the improvement of T2DM progression.

KEYWORDS

gut microbiota, type 2 diabetes mellitus, bile acids, short-chain fatty acids, amino acids, fecal microbiota transplantation, probiotics, herbal medicines

1 Introduction

T2DM is the most common metabolic disease and is mainly characterized by metabolic disorders, such as hyperglycemia, hyperlipidemia and IR. Diabetes can lead to various serious complications, such as coronary artery disease, lower extremity arteriopathy, retinopathy and diabetic nephropathy, which affect the life quality of a large populations worldwide (1, 2). The rapid growth of diabetes poses an alarming burden on global social and economic development (3). Recent data by the International Diabetes Federation (IDF) in 2021 have demonstrated that the global prevalence of

diabetes in 20- to 79-year-olds was estimated at 10.5% (approximately 537 million people) and predicted to increase to 12.2% (783.2 million people) in 2045. The diabetes prevalence is projected to be higher in middle-income countries (21.1%) than in low-income countries (11.9%) and high-income countries (12.2%) between 2021 and 2045 (4, 5). The prevalence of T2DM is greater than 25% in older patients over 65 years of age; treatment of older patients is more difficult because complications are more likely to occur (6, 7). Today, the main treatment strategies for T2DM include surgery, pharmacotherapy, exercise therapy, diet, nutrition and multifactorial therapy (8, 9). The core of the treatment of T2DM is to solve the problem of hyperglycemia. The use of medication based on lifestyle modification is the cornerstone of the treatment of T2DM. If blood glucose remains uncontrolled, additional treatment with insulin and other injectable drugs will eventually be needed (10). Insulin injection therapy is the most effective way to control blood glucose (11). However, with increased IR, the risk of hypoglycemia is increased if insulin injections are increased, thus escalating the risk of cardiovascular-related complications. Therefore, the underlying mechanisms of T2DM need to be identified for early diagnosis and treatment.

Recognized risk factors for diabetes include obesity, poor dietary habits, positive family history and genetics (12, 13). A variety of factors play a critical part in the development of diabetes. Recently, plenty of studies have proposed a link of the intestinal microbiome and its metabolites with the metabolic health of the human body (14, 15). Genome-wide association reports show significant associations between specific gut microbes, bacterial genes and metabolic pathway variants in T2DM (16). The possible mechanisms of T2DM induced by the gut microbiota may be linked to IR, BA metabolism, disturbances of lipid metabolism and endotoxemia (17). Furthermore, many researches have shown that the relationship between BAs and microbiome plays a key role in the pathogenesis of metabolic disorders including T2DM (18, 19). The study showed that the imbalance in the interplay between BAs and the intestinal flora led to composition changes of the BA pool, as well as alterations in the intestinal flora structure and endocrine signaling pathways, which they suggest will influence the development of T2DM (20, 21). In addition, increased production of trimethylamine N-oxide (TMAO) and branched-chain amino acids (BCAAs) as well as changes in BA and SCFA metabolism may lead to changes in fat levels, thereby affecting insulin signaling (22–24).

Disorders of energy balance due to gut microbial dysbiosis have an integral role in the progression of T2DM (25). However, the mechanisms of intestinal flora in T2DM are not fully understood. Thus, the purpose of this review is to discuss the altered intestinal microbiota in T2DM and the role of metabolites in T2DM relative to a healthy human host. We provide a summary of microbiota-based therapeutic approaches to improve T2DM.

2 Association between intestinal flora and T2DM

The impact of societal advances and changes in people's lifestyles, which have led to a greater intake of high-energy foods and a lack of physical activity, has left individuals in a suboptimal state of metabolic health with a high incidence of metabolic diseases, such as obesity, T2DM, nonalcoholic liver disease and cardiometabolic disease (CMD) (26, 27). The two main pathogenic mechanisms of diabetes are the relative lack of insulin secretion and IR, with IR being the main cause of T2DM. Diabetes biomarkers, such as venous glucose levels and glycated hemoglobin (HbA1c), have limitations as predictive biomarkers, especially in elderly or hyperlipidemic patients. Therefore, the identification of other early predictors is needed.

The collection of all gut microbial genes in an individual (i.e., the microbiome) represents a gene pool that is an order of magnitude higher than the human genome (28). Therefore, the intestinal microbiome is considered an " organ" with important roles in enhancing host immunity, facilitating the digestion of food, regulating intestinal endocrine function, regulating neural signaling, modifying drug action, modifying metabolism and eliminating toxins. This symbiotic relationship with the host ensures proper development of the human metabolic system. Gut microbial metabolites absorbed by the host act on receptors in organs such as the liver, gut, brown adipose tissue (BAT), white adipose tissue (WAT) and the central nervous system (CNS), and they are involved in micronutrient synthesis, intestinal motility, mineral absorption and electrolyte absorption (29, 30). A growing number of studies have demonstrated a strong link between the intestinal flora and human disease, particularly its role in obesity and T2DM (17, 31–35). Improvement of insulin sensitivity by altering the composition of the intestinal microbiota has gained attention from many researchers, and gut flora therapy has become a new treatment modality.

3 Changes of intestinal flora in patients with T2DM and obesity

Approximately 86% of patients with T2DM are overweight or obese, and obesity is considered the greatest risk factor for T2DM (36), which is commonly used as an early warning marker for T2DM. Compared to healthy adults, obese and T2DM populations show significant changes in gut microbes and their metabolites (Table 1). Studies have shown that modern

TABLE 1 Changes in intestinal flora and metabolites in T2DM and obesity.

Status	Gut bacteria (↑)	Gut bacteria (↓)	Changes in metabolites	Functional changes	Reference
T2DM	——	*Roseburia* *Subdoligranulum*	Degradation of Catalase and ribose, glycine and tryptophan amino acid ↑	Peroxide stress ↑ Inflammation↑ Insulin resistance	(37–40)
	——	*Akkermansia*	Butyrate and propionate production↓	Insulin resistance Insulin sensitivity↓ Appetite and body weight↑	(41, 42)
	Proteobacteria *Bacteroidetes* *R. gnavus*	*Anareotruncus colihominis, Butyrivibrio crossotus, Faecalibacterium*	Butyrate ↓ Mucus degradation ↑	Insulin resistance Inflammation↑	(39, 43–45)
	Escherichia/ *Shigella*		BCAA↑	Insulin resistance	(46)
	Prevotella copri	——	SCFAs↓	——	(47)
	——	*Roseburia* *Ruminococcus* *Eubacterium*	SCFAs↓	——	(48)
	——	*Ruminococcus* *Bifidobacterium, Bacteroides, Clostridium, Eubacterium, Listeria,*	Secondary bile acids↓	Insulin ↓ Glucose sensitivity↓	(49, 50)
	Prevotella copri *Bacteroides vulgatus* *Streptococcus*	——	BCAAs↑	Insulin resistance	(17, 51, 52)
	——	*Lactobacillus* *Akkermansia*	SCFAs↓	Inflammation↑ Glucose and energy disorders	(39, 40)
	Dorea	*Akkermansia* *Parabacteroides* *Streptococcus* *Bifidobacterium*	Tyrosine and butyrate production↓	Insulin resistance Damage to the intestinal mucosal barrier	(53)
	——	*Bacteroidetes*	Sulphate reduction↑ Butyrate↓	Oxidative stress↑	(38)
	Prevotella copri *Bacteroides vulgatus*	*Butyrivibrio crossotus* *Eubacterium siraeum*	Increased plasma BCAA concentrations	Insulin resistance ↑ Aggravated glucose intolerance	(17, 54)
	Streptococcus mutans *Eggerthella lenta*	——	Imidazole ↑	Impair insulin signalling	(55)
	Desulfovibrio spp.	——	Promote interleukin6 (IL-6) and IL-8 secretion	Inflammatory response↑	(56)
	——	*A. muciniphila*		Glycolipid levels↑	(57)
Obesity		*Akkermansia*	SCFA↓	Insulin sensitivity ↓ Inflammation↑	(58, 59)
	Firmicutes	*Bacteroidetes*	——	Insulin resistance	(38, 60)
	Bacteroidetes *Firmicutes* *Betaproteobacteria*	——	BCAA↑	Insulin-resistant	(61, 62)
	Bacteroides *Parabacteroides*	*Turicibacteraceae* *Moryella* *Lachnospiraceae* *Akkermansia*	SCFA↓	Glucose and energy disorders	(63)
	——	*Ruminococcaceae* *Lachnospiraceae*	SCFAs	Fat accumulation	(64)
	——	*Ruminococcaceae* *Clostridia* *Christensenellaceae* *Dehalobacteriaceae* *SHA-98*	Acetate and butyrate↓	Affect energy metabolism Insulin sensitivity	(34, 65–68)

(Continued)

TABLE 1 Continued

Status	Gut bacteria (↑)	Gut bacteria (↓)	Changes in metabolites	Functional changes	Reference
		MethanobacteriaceaeRF39 *Oscillospira*			
	——	*Eubacterium ventriosum* *Roseburia intestinalis*	SCFA↓	Insulin resistance Inflammation↑	(69)
	Ruminococcus champaneliensis *Prevotella copri*	*Bacteroides*	——	Fat accumulation	(70)
	——	*Firmicutes species* *Proteobacteria species*	LPS Amino acids Short-chain fatty acids↓	Insulin resistance	(71)

Meaning of symbols in the table. ↑, increase; ↓, decrease.

lifestyle changes and the use of antimicrobial drugs, among other factors, have led to a decrease in gut microbial diversity in many developed populations (72).

Studies have shown that individuals with low abundance of intestinal flora are predisposed to obesity, IR and dyslipidemia (43). A study of gut microbial diversity in patients with low gene count (LGC) and high gene count (HGC) has shown that *Lactobacillus*, *Prevotella*, *Bacteroides*, *Desulfovibrio* and *Oxalobacter* spp. in the intestinal microbiota are decreasing in abundance; this decrease in diversity may promote the development of metabolic disorders. Functional changes in the microbiota of individuals with LGC mainly include a reduction in butyrate-producing bacteria and an elevation in the ratio of *Akkermansia* to *R. torque/gnavus*, leading to enhanced mucus degradation, decreased hydrogen production potential, decreased methane production potential, increased *Campylobacter/Shigella* abundance and increased peroxidase activity (43). This metabolic disturbance caused by an imbalance between pro- and anti-inflammatory bacterial species in LGC individuals puts them at an increased risk for metabolic diseases, such as prediabetes and T2DM (73).

A previous study has shown that feces from obese twins transplanted into germ-free mice results in weight gain (61). Additionally, fecal transplantation studies have shown that obese subjects with metabolic syndrome have increased insulin sensitivity after the transfer of gut microbiota from a lean donor (37, 74, 75). These studies provide a theoretical basis for linking intestinal flora and whole-body energy metabolism, and they also highlight the important role of the intestinal flora in host metabolism (76, 77). Recent studies have suggested that the human intestinal microbiota is altered in obese individuals relative to lean individuals, probably primarily by an elevation in the obesity-associated *phylum Ligustrum* and a reduction in *Bacteroidetes (*78, 79). A study of 416 twin pairs has shown that *Dehalobacteriaceae*, *Christensenellaceae* and SHA-98 were found to be significantly lower in the intestinal flora of obese individuals compared to those of lighter weight. The *Christensenellaceae* family is known to be producer of SCFAs (80). In addition, it has been demonstrated that *Christensenella minuta* amended and transplanted into recipient mice results in a tendency to lose weight. *Oscillospira* also produces SCFAs by degrading host blood glucose. In recent studies, we observed that *Oscillospira* and the methanogenic archaeon *Methanobrevibacter smithii* are abundant in healthy weight subjects and may promote leanness (65, 66, 81). Lean individuals also exist in T2DM (82). A study on the intestinal flora of lean diabetic patients has demonstrated that lean T2DM patients show a reduced *Akkermansia muciniphila* abundance, which is positively associated with a decrease in their insulin secretion (37). Studies have shown that *Ruminococcus*, *Clostridium*, *Bifidobacterium*, *Bacteroides*, *Eubacterium*, *Listeria* and others are the main intestinal microorganisms that affect the formation of secondary bile acids (49, 50). It has been shown that BAs modulate the metabolism and energy homeostasis of host by activating FXR receptors and TGR5, thereby shaping the intestinal flora (19).

Microorganisms including *Blastocystis* spp. and *Prevotella copri* have been found to be indicators of favorable postprandial glucose metabolism. And studies have shown that *Prevotella copri* supplementation improves glucose metabolism in mice (83). However, a study has demonstrated that *Prevotella copri* was associated with the production of BCAA, which is correlated with IR and glucose intolerance (17). It has been suggested that the elevated richness of *Bacteroides vulgatus* and *Prevotella copri* in IR individuals relative to the normal group may lead to an increased potential for BCAA synthesis; however, *Butyrivibrio crossotus* and *Eubacterium siraeum* abundance decreases, leading to reduced BCAA catabolism (17). Increased concentrations of BCAAs in circulation (including leucine, isoleucine and valine) may be biomarkers of IR and increased risk of T2DM (54).

Patients with T2DM are often treated with multiple drugs for glycemic control and prevention of cardiovascular complications. Thus, drug therapy usually affects the gut microbiota of patients, and the role of the gut microbiota may be confounded by the effects of various drugs (84). Therefore,

many recent studies on T2DM flora have focused on the early stages of T2DM (not yet taking drugs). Although plasma glucose concentrations have not yet reached the diabetic range in the early stages of diabetes, individuals are at escalated risk of developing significant T2DM and cardiovascular disease (85). Alterations in the intestinal microbiota of unmedicated prediabetic patients have been reported to be dominated by butyrate-producing bacteria, *Akkermansia muciniphila*, and some bacteria with pro-inflammatory potential (86).

A previous study on the effect of metformin treatment on intestinal microbes in individuals with T2DM has reported a reduction in *Roseburia*, *Subdoligranulum* and a cluster of butyrate-producing *Clostridium* spp. in metformin-naïve T2DM patients, consistent with previous indications (37, 38). Metformin treatment modifies the intestinal microbiota in individuals with diabetes as indicated by enrichments in mucin-degrading *Akkermansia muciniphila* and SCFA-producing bacteria such as *Bifidobacterium bifidum* and *Butyrivibrio* (87). An independent amplicon-based T2DM cohort analysis has similarly validated an elevation in *Escherichia coli* and a reduction in *Enterobacteriaceae* abundance in metformin-treated patients with several gut microbial genera more similar in abundance to normal control levels, particularly *Subdoligranulum* and *Akkermansia*. Therefore, we hypothesized that metformin may alleviate T2DM by affecting the microbiota and its microbial production of SCFAs. It has been shown that probiotic therapy based on flora modulation increases the richness of SCFAs while achieves a reduction in IR, and this therapy has been reported to have a similar effect under metformin treatment (41, 42, 88). Some studies have shown that probiotics act as adjuvants to metformin by increasing the production of butyrate, thus allowing enhanced glucose management (89).

All of these findings provide strong evidence that the gut microbiome can be used to improve the prediction of metabolic diseases, such as T2DM, and to discover new targets for diabetes treatment. In this review, we focus on how the intestinal microbiota and its metabolites affect the pathogenesis of T2DM. We summarize examples of microbiota-targeted interventions for T2DM and highlight the great promise of this therapeutic approach in the field of T2DM research.

4 Relationship between gut microbial metabolites and T2DM

4.1 BAs

In the liver, BAs are synthesized from cholesterol and act as promoters for emulsification, absorption and transportation of dietary lipids as well as fat-soluble vitamins in the intestinal lumen. BAs are mainly metabolized by the actions of intestinal bacteria, which play a critical role in glucose regulation. BAs also act as regulators of intestinal microbiota as well as signaling molecules that modulate metabolic homeostasis (Figure 1). Interactions of BAs and intestinal flora have a profound impact on IR and the progression of T2DM.

4.1.1 Synthesis of BAs

Cholesterol 7α-hydroxylase (CYP7A1) predominantly regulates the classic pathway (namely, the neutral pathway) of BA synthesis, while the alternative pathway (namely, the acidic pathway) depends mainly on CYP27A1. CYP8A1 and CYP7B1 also play distinct roles in the process (49). Glucose and insulin act as the main postprandial factors inducing CYP7A1 gene expression as well as BA synthesis (90). Mechanistically, glucose induces CYP7A1 gene transcription by increasing ATP to reduce the AMP/ATP ratio, which inhibits AMP-activated protein kinase (AMPK) activity, or by epigenetically modifying the acetylation state of the CYP7A1 chromatin structure (91). Cold exposure may also trigger hepatic conversion of cholesterol to BAs through the alternative pathway by induction of CYP7B1, leading to increased plasma levels and fecal excretion of BAs accompanied by alterations in intestinal microbiota that are characterized by higher abundance of *Deferribacteraceae* and *Lachnospiraceae* as well as lower abundance of *Porphyromonadaceae* and *Clostridiales*. Increased energy expenditure is also related to hepatic CYP7B1 induction, which is reduced in individuals with T2DM, suggesting that the alternative pathway plays a role in metabolic homeostasis (92). Another regulator of BA composition, CYP8B1 (an 12α-hydroxylase) has been reported to contribute to metabolic anomalies in T2DM as greater 12α-hydroxy/non12α-hydroxy BA ratios are correlated with decreased insulin sensitivity (93).

4.1.2 BSHs and HSDHs in gut flora

Hepatocytes conjugate bile acids with taurine or glycine to increase their solubility before secretion (18). In the distal ileum, roughly 95% of conjugated bile acids (CBAs) are reuptaken *via* the apical sodium-dependent BA transporter (IBAT or ASBT) in conjugated form, while a small portion are deconjugated by the gut microbiota prior to resorption or converted into secondary bile acids (DCA from CA and LCA from CDCA, respectively), which are either absorbed through passive diffusion or excreted in the feces (94). BAs absorbed recirculate through the portal vein to the liver, where they are conveyed into hepatocytes to be reconjugated and then resecreted with newly synthesized BAs (95).

Microbial deconjugation refers to enzymatic hydrolysis by bile salt hydrolases (BSHs), namely, the removal of taurine or glycine conjugates, and it impedes active reabsorption of BAs *via* ASBT in the small intestine. In the human intestinal

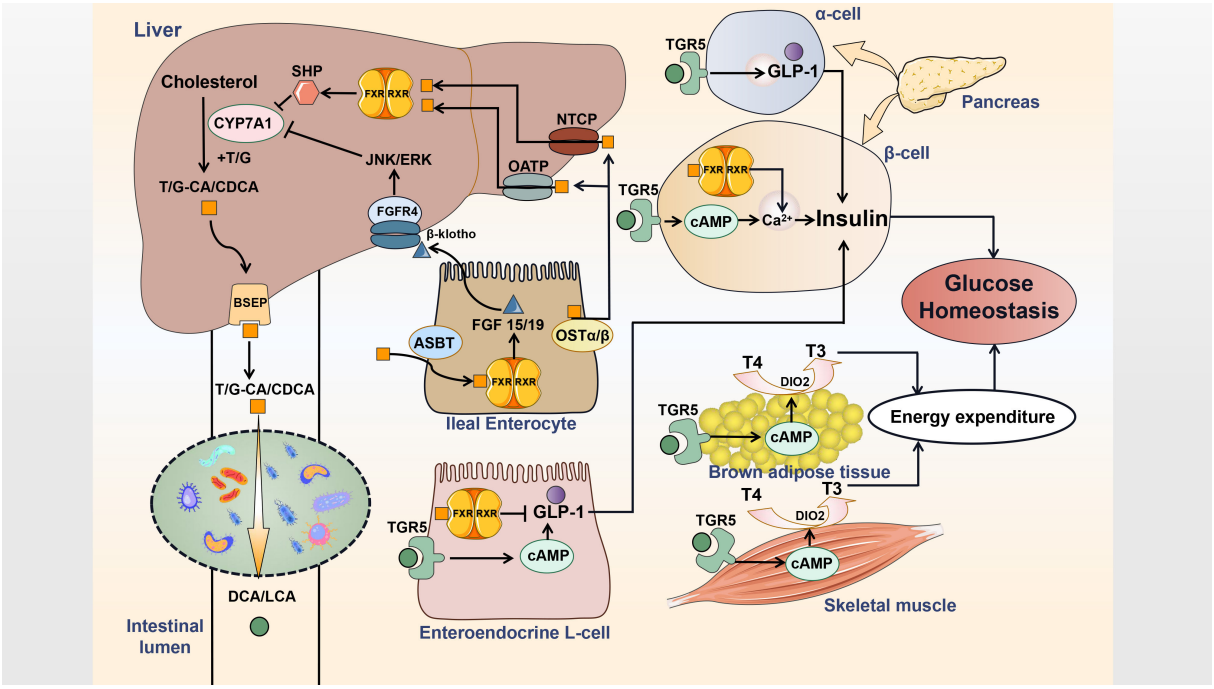

FIGURE 1
Interactions of BAs and gut microbe influence host metabolism. Primary bile acids are synthesized and then conjugated with taurine or glycine in hepatocytes. Conjugated bile acids are transported into the bile duct by BSEP. Most conjugated bile acids are reabsorbed *via* ASBT and circulate to the liver by OSTα/β, OATP and NTCP, while a small part is converted into secondary bile acids by deconjugation and dehydroxylation of gut flora. Bile acids acts as the endogenous ligands for FXR and TGR5 to generate distinct effects on metabolism regulation. T, taurine; G, glycine; CA, cholic acid; CDCA, chenodeoxycholic acid; DCA, deoxycholic acid; LCA, lithocholic acid; BSEP, bile salt export protein; FGF, fibroblast growth factor; FGFR, FGF receptor; RXR, retinoid X receptor; SHP, small heterodimer partner; JNK, c-Jun N-terminal kinase; ERK, extracellular signal-regulated kinase; OST, organic solute transporter; OATP, organic anion-transporting polypeptide; NTCP, sodium taurocholate cotransporting polypeptide; ASBT, apical sodium-dependent bile acid transporter; DIO2, type 2 iodothyronine deiodinase; T4, thyroxine; T3, thyroid hormone.

microbiome, BSHs are distributed among various microbial species and were identified early in several microbial genera, such as *Lactobacillus* (96–99), *Clostridium* (100), *Bifidobacterium* (101–103), *Listeria* (104, 105), *Enterococcus* (106) and *Bacteroides* (107). BSH activity exerts beneficial effects on bacteria by strengthening resistance to CBAs, assisting surviving in the gastrointestinal environment without causing bacterial overgrowth or damage to the host. This may facilitate colonization and development of the gut microbiota (108). High levels of BSH have also been reported to decrease body weight gain and plasma cholesterol in conventionally raised mice (109). However, some controversial results have suggested that deconjugated bile acids (DBAs) with higher binding affinity to farnesoid X receptor (FXR) may suppress the transcription of CYP7A1 and reduce BA synthesis from cholesterol (110). Moreover, some studies have deviated from previous concepts, indicating that the intrinsic chemical features and enzymatic preferences of various BSHs change the *Lactobacillus* transcriptome in a BA-dependent manner and contribute to the toxicity during *Lactobacillus* growth (111). Therefore, the importance of BSHs classification is highlighted as distinct BSHs in the identical *Bacteroides* strain differ in deconjugation ability. Generally, BSHs benefit metabolism, but the higher relative abundance (RA) of BSH phylotype with high activity may exert detrimental effects. To explore the relationship between the RA of BSHs and disease, it is important to first assess activity to identify particular BSHs rather than use an estimated RA of total BSHs (112).

BAs are C-24 steroids hydroxylated at the C-3, C-7 position, and also the C-12 position in the case of CA (113). 7α/β-dehydroxylating bacteria play an important role in transformations of BAs as the pool of secondary bile acids mainly consists of 7α/β-dehydroxylated BAs (e.g., LCA and DCA) (114). Different from deconjugation, BA 7α/β-dehydroxylation is confined to a limited number of gut bacteria, which lead to the salvage of BAs that evade active reuptake in the distal ileum, as deconjugation and 7α/β-dehydroxylation increase Pka and hydrophobicity of BAs to further permit passive absorption across the colonic epithelium (115). Because 7α/β-dehydroxylation is restricted to free bile acids, deconjugation is a prerequisite. 7α/β-Hydroxysteroid dehydrogenases (7α/β-HSDHs) have been identified in gut

bacteria such as *Clostridium* (116–118), *Bacteroides* (119–121), *Escherichia* (122–124) and *Eubacterium* (125–127). While 7α-dehydroxylation functions as the most quantitatively vital bacterial biotransformation of BAs, 7β-dehydroxylation appears to be not essential in the human colon (128).

In diabetic patients, the BA pool composition and the associated pathways of biosynthesis are altered, which may involve a higher conversion of primary bile acids to secondary bile acids by the gut microbiota (129). Cirrhotics show lower abundance of *Ruminococcaceae*, *Lachonospiraceae* and *Blautia* (7α-dehydroxylating bacteria) while increased *Enterobacteriaceae* (potentially pathogenic), resulting in decreased conversion of primary to secondary fecal BAs (130). *Clostridium scindens* with 7α-HSDHs activity strengthens resistance to *Clostridium difficile* infection in a secondary bile acid-dependent manner upon administration (131). In addition to 7α/β-dehydroxylation, 3β-HSDH is identified in *Odoribacteraceae* strains to produce isoalloLCA, which exerts antibacterial effects against Gram-positive pathogens including *Enterococcus faecium* and *Clostridioides difficile* to maintain the intestinal homeostasis (132). 12α-dehydrogenation is involved in synthetic process from CA to ursodeoxycholic acid (UDCA), which functions in the therapy of certain gastrointestinal tract diseases, and contributes to counter the effects of LCA and DCA (133). *Clostridium scindens*, *Clostridium hylemonae* and *Peptacetobacter hiranonis* are identified as 12α-HSDH expressing strains (134). A new fecal isolate, Eggerthella lenta strain C592, is found to be a critical microbe in BA metabolism and express 3α-, 3β-, 7α-, and 12α-HSDHs (135, 136). 12β-HSDH interconverts the 12-oxo bile acids to the 12β-configuration to completes the epimerization, forming less toxic and more hydrophilic bile acids. 12β-HSDH activity is proved in *Clostridium paraputrificum* (137).

The effects of acarbose are based on the gut microbiota-plasma BA axis as acarbose elevates the RA of *Bifidobacterium and Lactobacillus* while depleting *Bacteroides*, leading to altered RA of microbial genes that are responsible for BA metabolism. The results of acarbose treatment depend on microbiota compositions in the gut before treatment, and diverse abilities of the gut flora to metabolize BAs result in distinguishing therapeutic effects (138). Antibiotics modify the intestinal microbiota to change high-fat diet (HFD)-driven inflammatory signaling and BA composition, resulting in improved glucose metabolism and IR. These effects depend on interactions with the host's systemic inflammatory response and genetic background (139).Patients undergoing bariatric surgery (especially gastric bypass procedures) show improvements in insulin sensitivity, which are correlated with increased BA concentrations in circulation and alterations in intestinal microbiome, indicating that elevations in circulating BAs and the interaction of BAs and gut flora following bariatric surgery as well as calorie restriction and body mass loss lead to T2DM remission (140).

4.1.3 Targets of BAs

FXR, which is mainly activated by the primary BA CDCA, plays a critical role in modulating glucose homeostasis as well as insulin sensitivity (141, 142). In ileal enterocytes, activation of FXR promotes transcription of FGF19 (FGF15 in mouse), which circulates through the portal vein to the liver and further activates JNK/ERK signaling by binding to FGFR4/β-klotho heterodimer complex to inhibit expression of CYP7A1 in hepatocytes (143). In the liver, FXR activation not only induces small heterodimer partner (SHP) expression to inhibit CYP7A1, but also negatively interferes with glycolysis by inhibiting the carbohydrate response element binding protein (ChREBP), which is responsible for the expression of hepatic glycolytic genes (144–146). In intestinal L cells, FXR interacts with ChREBP to inhibit proglucagon mRNA levels induced by glucose. The effects of FXR on ChREBP also decrease intracellular ATP levels by inhibiting the transcription of glycolytic enzymes, resulting in a reduction in ATP-dependent Glucagon-like peptide-1 (GLP-1) secretion (147). In pancreatic β cells, FXR activation has been suggested to inhibit the K_{ATP} current and increase the cytosolic Ca^{2+} concentration, eventually resulting in increased insulin secretion (148, 149). These observations highlight the importance of the FXR-dependent control of BAs and glucose homeostasis.

In T2DM individuals, metformin decreases the abundance and BSH activity of *Bacteroides fragilis* to increase intestinal levels of glycoursodeoxycholic acid (GUDCA), which has been identified as a novel endogenous FXR antagonist in the gut. This finding demonstrates that metformin improves glucose metabolic dysfunction *via* a *Bacteroides fragilis*-GUDCA-intestinal FXR axis (150). In NAFLD patients with T2DM, obeticholic acid (OCA, an FXR agonist) activates FXR to mediate an increase in FGF19, resulting in weight loss and improved insulin sensitivity, accompanied by decreased endogenous BA production and 7a-hydroxy-4-cholesten-3-one (C4, a biomarker for BA synthesis) levels (151). Although serum levels of BA and C4 vary significantly among individuals, C4 plasma levels are considerably elevated in patients with T2DM and metabolic syndrome (MetS) (152). Studies in FXR-deficient mice fed a HFD have demonstrated that intestinal flora takes part in the development of IR and obesity by modulating BA and FXR signaling, and conversely, FXR may contribute to adiposity increase by changing the composition of gut microbiome, which is characterized by elevation in *Bacteroidetes* and reduction in *Firmicutes* (153).

TGR5, a transmembrane G protein-coupled receptor, is activated mainly by the secondary bile acids, DCA and LCA (154). Previous studies have shown that TGR5 activation results in increased intracellular cyclic AMP (cAMP), leading to the maintenance of glucose homeostasis, preservation of pancreatic function and insulin sensitivity as a consequence of increased GLP-1 secretion and energy expenditure induced by enhanced

mitochondrial function (155). In enteroendocrine L cells, activation triggers an increase in the synthesis and release of GLP-1. In systemic circulation, BAs escaping hepatic clearance activate TGR5 in BAT and muscle to activate type 2 iodothyronine deiodinase (DIO2), which converts inactive thyroxine (T4) into active thyroid hormone (T3) to promote energy expenditure (156). In addition, TGR5 positively regulates insulin secretion *via* a cAMP/$Ca2^+$ pathway in pancreatic β cells, while it reprograms pancreatic α cells to produce GLP-1 to mediate the proliferation and mass of β cells (157, 158).

The FXR agonist, fexaramine (FEX), activates FXR to shape the gut flora inducing *Bacteroides* and *Acetatifactor*, which convert CDCA and UDCA to LCA. LCA not only activates TGR5 and further stimulates L cells to secrete GLP-1, resulting in improved insulin sensitivity, but also induces WAT browning by activating TGR5/cAMP signaling to improve energy metabolism and ultimately reduce weight (159). Wu et al. demonstrated that ablation of intestinal HIF-2a leads to an elevation in *Ruminococcus torques* abundance and a decrease in *Bacteroides vulgatus* by reducing lactate synthesis, resulting in elevated levels of taurine-conjugated cholic acid (TCA) and DCA. These changes activate adipose TGR5 to upregulate WAT thermogenesis, ultimately improving obesity and IR (160). Cholic acid-7-sulfate (CA7S), an endogenous BA sulfated metabolite, has been identified as a potent gut-restricted TGR5 agonist that induces the secretion of GLP1 from enteroendocrine L cells. CA7S is increased in the gastrointestinal tract after sleeve gastrectomy (SG), exhibiting anti-diabetic effects by enhancing glucose tolerance and reducing blood glucose levels (161). LCA has been identified to mediate the synthesis of CA7S in hepatocytes to influence host metabolism. Changes in the gut flora post-SG, particularly a decline in *Clostridia*, lead to a reduction in the production of LCA, resulting in increased production of CA7S (162). As CA7S is generated through microbiome-dependent signaling, its stability may differ among individual gut microbiomes (163).

GLP-1 is a proteolytic product of the proglucagon gene and regulates glucose homeostasis in the body. GLP-1 reduces appetite and slows gastric emptying in response to ingestion, and it acts on the pancreas to reduce glucagon secretion. GLP-1 also promotes glucose uptake and storage in muscle and adipose tissues while inhibiting glucose production in the liver (164, 165). Moreover, GLP-1 activates the GLP-1 receptor (GLP-1R) to promote proliferation and inhibit apoptosis of islet β cells to increase insulin biosynthesis and secretion (166). In T2DM patients, postprandial BA concentration is higher, and BA metabolism is upregulated, which may be due to the advantage of glucose-induced BA stimulation over other inhibiting factors to maintain GLP-1 levels as a compensation. Thus, the requirement of higher BA levels to stimulate enteroendocrine L cells to release GLP-1 as resistance to BA in L cells is suggested (167). Recently, studies have found that *Akkermansia muciniphila* secretes P9, a novel protein identified to induce the secretion of GLP-1 (168, 169).

4.2 SCFAs

The fermentation of undigested dietary components (e.g. fibre and resistant starch) in the large intestine mainly produces three SCFAs including acetate, propionate as well as butyrate, and various biochemical pathways are involved in the process (170). Thus far, as the most well studied metabolites of gut flora, SCFAs control immunomodulatory functions, promote the integrity of intestinal epithelium, as well as regulate insulin secretion and the proliferation of pancreatic β cell, playing a variety of roles in IR and T2DM (171). Most enteric bacteria are identified as acetate producers such as *Akkermansia muciniphila*, *Blautia hydrogenotrophica*, *Clostridium* spp., *Ruminococcus* spp., *Prevotella* spp., *Bifidobacterium* spp., *Bacteroides* spp., *Streptococcus* spp. Propionate producers include *Roseburia inulinivorans*, *Phascolarctobacterium succinatutens*, *Megasphaera elsdenii*, *Coprococcus catus*, *Ruminococcus obeum*, *Bacteroides* spp., *Dialister* spp., *Veillonella* spp., while *Roseburia* spp., *Anaerostipes* spp., *Faecalibacterium prausnitzii*, *Coprococcus catus*, *Coprococcus eutactus*, *Coprococcus comes*, *Eubacterium hallii*, *Eubacterium rectale* are proved to be burytate producers (170, 172, 173).

SCFAs exert benefits by activating G-protein coupled receptors (GPCRs) such as GPR41, GPR43 and GPR109A (174). Acetate, as well as propionate promotes GPR43 and GPR41 to release peptide YY (PYY) and GLP-1 to influence satiety and intestinal transit (175). Butyrate has also been proved to induce GLP-1 and PYY to increase insulin secretion and maintain glucose homeostasis (176, 177). In addition, butyrate not only activates GPR109A and inhibits histone deacetylases (HDACs) to exert anti-inflammatory effects, but also produces antimicrobial peptides to promote epithelial barrier function (178). Another study has shown that butyrate induces satiety to reduce food intake and activate BAT to promote fat oxidation by influencing the gut-brain neural circuit (179). A study suggested that butyrate produced in the gut mainly improves dynamic insulin response to food ingestion, instead of maintaining glucose homeostasis in the fasted state, and increased butyrate production driven by a genetically influenced change in the gut microbiome is beneficial for pancreatic β-cell function (180). Furthermore, butyrate was reported to maintain the gut microecological balance by limiting the bioavailability of respiratory electron acceptors of *Enterobacteriaceae* in the colonic lumen and thus preventing a dysbiotic proliferation of opportunistic pathogenic *Salmonella* and *Escherichia* (181). *Dysosmobacter welbionis* $J115^T$, a new butyrate-producing bacterium belonging to the *Ruminococcaceae* family and isolated from human feces, is identified to be negatively

correlated with fasting plasma glucose, HbA1c and BMI in overweight or obese individuals with metabolic syndrome, and influences host metabolism in beneficial and direct way (182). However, another study highlighted the importance of functional dysbiosis of gut flora in association with T2DM pathophysiology, rather than a specific microbial species. They found only a mild degree dysbiosis of gut flora in T2DM patients, while a decrease in butyrate-producing bacteria, which seemed to be metabolically beneficial (38). In T2DM patients, reduced SCFA levels caused by decreased abundance of SCFA-producing bacteria may contribute to the progression of IR and T2DM (31). Yet animal and clinical researches have demonstrated that the levels of fecal SCFA are positively correlated with IR and body weight (183), controversies over the role of SCFAs in T2DM and IR still remain, and further investigations are required.

4.3 AAs

Research has shown that elevated concentrations of AAs, particularly BCAAs, are correlated with increased IR and risks of T2DM (184). BCAAs also promote the development of IR associated with obesity in a setting of a HFD (185). The intestinal microbiota acts as an independent factor of increased serum BCAA levels in individuals with IR. *Prevotella copri* and *Bacteroides vulgatus* have been identified as the major gut microbes correlated with the biosynthesis of BCAAs and IR (17). Among BCAAs, a previous study has further identified a critical role of isoleucine in metabolic health as a diet with low isoleucine activates the FGF21-UCP1 axis to reprogram the metabolism of adipose tissue and liver, improving energy expenditure and hepatic insulin sensitivity. Reducing dietary valine induces similar but milder metabolic effects, whereas low leucine does not show these effects, thus suggesting that decreasing dietary isoleucine is important to prevent and treat diabetes (186). Of note, IR may induce the protein degradation normally suppressed by insulin and impair the oxidative metabolism of BCAA to result in aminoacidemia, suggesting that increased BCAA may be a marker of insulin action loss instead of a causation (187).

Similar to BCAAs, aromatic amino acids (AAAs) also take part in the pathogenesis of hyperglycemia as the metabolisms of BCAAs and AAAs change prior to alteration of glucose homeostasis (188). BCAAs and AAAs both act as markers of IR development in young adults with normoglycemia, suggesting that their correlation with diabetes risk partly depends on IR (189). *Clostridium sporogenes* has been identified to metabolize all three AAAs in the human gut (190). Ka et al. demonstrated that excessive consumption of monosodium glutamate (MSG) positively correlates with overweight and BMI among healthy Chinese adults, suggesting a correlation between glutamate and obesity (191). In obese individuals, Liu et al. observed a decrease in *Bacteroides thetaiotaomicron* abundance, which is negatively correlated with serum levels of glutamate. These microbial and metabolic changes are partly reversed by bariatric surgery, and the reduced glutamate levels in circulation contribute to the improvement of IR and hyperglycemia (81).

4.4 Others

Gut flora convert choline in diet to trimethylamine (TMA), the precursor of TMAO. A high-fat diet elevates choline catabolism of *Escherichia coli* by changing the physiology of colonic epithelium, thus increases TMAO levels in circulation (192). Intestinal microbiota (predominantly *Enterobacteriaceae*) also reduces TMAO to TMA, which is untaken by the host and circulated to the liver to be further converted into TMAO by hepatic enzymes. Conversely, TMAO influences the metabolism and growth of intestinal microbiota in a taxon and source-dependent manner (193). Urocanate produced by histidine metabolism is converted to imidazole propionate by microbiota expressing urocanate reductase. T2DM patients show higher concentrations of imidazole propionate in peripheral and portal blood than healthy individuals, indicating that imidazole propionate may impair insulin signaling. *Eggerthella lenta* and *Streptococcus mutans* were identified to produce imidazole propionate, which was proved to aggravate glucose intolerance in mice (55). In addition, elevated serum levels of imidazole propionate are correlated with decreased abundance of intestinal flora (194). Gut flora-produced indolepropionic acid, a promising biomarker for T2DM progression, is suggested to be positively correlated with insulin secretion and negatively associated with low-grade inflammation as it preserves function of islet β cells (195).

5 Therapeutic options for targeting the gut microbiota in T2DM and obesity

In summary, the intestinal microbiota and its metabolites are involved in the occurrence and progression of T2DM, and the process can be reversed to some extent by regulating the intestinal microbiota and its metabolites, providing a new idea for clinical treatment (196) (Figure 2).

5.1 Probiotics

When applied in appropriate amounts, probiotics, which are described as the living microbes, provide the host with health benefits (197). Studies have shown that the administration of

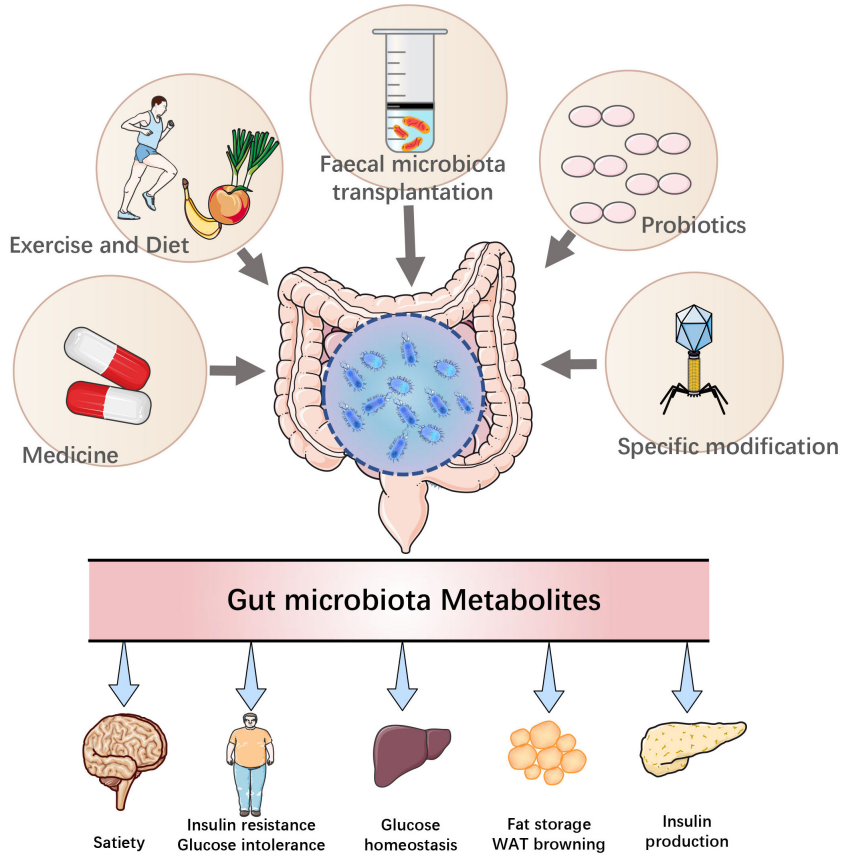

FIGURE 2
Modulation of T2DM by therapeutic approaches targeting the gut microbiota.

probiotics regulates intestinal flora, suppresses inflammatory responses, improves intestinal barrier function, antagonizes each other with pathogens and produces beneficial microbial metabolites, including SCFAs and BAs (198). Studies on the molecular mechanisms of probiotic intervention in T2DM have shown that probiotics have ameliorative effects on IR and hyperglycemia (199).

Studies have shown that *Akkermansia muciniphila* treatment improves liver function, reduces oxidative stress and inhibits inflammation in diabetic mice. *Akkermansia muciniphila* supplementation reduces chronic low-grade inflammation and increases anti-inflammatory factors, such as α-tocopherol and β-sitosterol (200). Glucose tolerance and insulin sensitivity in diabetic mice were also ameliorated by supplementation with *Lactobacillus mucilaginosa*. In addition, it has been shown that supplementation with *Lactobacillus acidophilus* improves intestinal barrier function, and a reduced inflammatory response in the liver and colon has been observed in animal models of diabetes. Studies have shown that *Akkermansia muciniphila* strains are not even required to colonize the intestine to exert beneficial metabolic health effects (201, 202). In addition, 14 probiotics were isolated from fermented camel milk, and the effects of these 14 probiotics encompassed an increase in SCFA, an improvement in function of intestinal barrier, an upregulation of GLP-1 secretion, all of which showed significant improvements in blood glucose in db/db mice (203). A randomized, double-blinded, placebo-controlled study has reported that the administration of probiotic improves glucose metabolism in T2DM individuals, while the consumption of fermented milk results in other metabolic alterations including an elevation in acetic acid and a reduction in inflammatory cytokines (TNF-α and resistin) (204).The role of probiotics in T2DM deserves recognition, but the FDA and EFSA do not yet have any approval statements for probiotics (205–207). To verify the effectiveness of probiotics, more clinical trials are required.

5.2 Fecal microbiota transplantation (FMT)

Microbiologists have isolated many probiotic bacteria in the last century, and although studies have demonstrated their efficacy in standard animal models, single microorganisms are weak in preventing and treating human diseases (208, 209).

Consequently, their clinical benefits are limited (210). Therefore, it is necessary for multiple microbes to work together to remodel the intestinal microbiota. In recent years, FMT has received increasing attention in the field of biomedical and clinical medicine (211). FMT refers to the transfer of fecal microbiota from a healthy donor to an unhealthy recipient *via* capsules with freeze-dried stool (or other ways), it may correct dysbiosis by increasing microbial diversity and restoring microbial function (212).

Official guidelines have ratified FMT as a standard treatment for recurrent *Clostridium difficile* infection (CDI) (213). According to data available on clinicaltrials.gov, ongoing trials on FMT are focused on indications other than CDI, and many clinical trials have shown that it also has strong potential in the treatment of refractory ulcerative colitis, Crohn's disease, irritable bowel syndrome and other intestinal diseases as well as many extraintestinal diseases, including diabetes, cancer, cirrhosis, entero-brain disease and other metabolic diseases (214–217).

Early studies have shown that germ-free mice receiving samples from obese donors gained more weight than those from lean suppliers (78). After transplantation of Kazaks normal glucose tolerance (KNGT) fecal bacteria to db/db mice, the richness of *Clostridium coccoides* and *Desulfovibrio* in the intestine markedly declined, while the fecal abundance of *Akkermansia muciniphila* are increased. Moreover, the levels of fasting blood glucose and postprandial glucose are significantly downregulated in db/db mice, while the levels of HDL-cholesterol are upregulated, suggesting that fecal bacteria from KNGT may be a promising source for treating T2DM individuals with FMT (218, 219).

Previous studies have demonstrated that BA concentrations are changed in T2DM patients (147, 220). In addition, a study on the functional identification of bacterial and viral genes before and after FMT has shown that metabolic pathways such as the degradation of fluorobenzoate and the biosynthesis of secondary bile acids were significantly altered. A recent study has shown that the composition of the intestinal flora affects metabolism of BAs (211). The formation of BAs, SCFAs, and intestinal transit time of the organism are altered after FMT treatment. A previous study showed that allogenic FMT using feces from post-Roux-en-Y gastric bypass donor (rYgB-D) exerted short-term effects on metabolism of glucose, adipose tissue inflammation and intestinal transit time in obese and treatment-naive male individuals with IR, compared with feces from a metabolic syndrome donor (MetS-D) (74, 212).

Some studies have shown high interindividual variability in strain-level outcomes following FMT (221). Changes in plasma metabolites are also reported. The improvement in glucose metabolism, and the regulation of gut microbiota and plasma metabolites by FMT from lean donors are dependent on the reduction in fecal microbial diversity at baseline. Thus, pretreatment fecal microbiota characteristics may differ in response to bacterial species of lean donors, and thus pretreatment status may be correlated with the treatment effects (44, 58, 74).

However, some contradictory results have been reported. A 12-week double-blinded randomized placebo-controlled pilot trial of oral FMT capsules has shown that weekly treatment of FMT capsules to obese adults led to intestinal microbiota transplantation in most recipients for at least 12 weeks. Despite the successful implantation of the colonies, obviously clinical metabolic effects were not observed during the study period (222). Because researchers tend to publish studies with positive data, it makes it more difficult to determine the actual results. Studies have shown that performing FMT is also risky, and that harmful microorganisms may be transferred to the recipient *via* FMT. A previous study showed that an individual receiving feces from an overweight but healthy donor had developed new-onset obesity. Therefore, it is essential to publish studies with negative data so that we can have an unbiased understanding of the intestinal microbiota and its role in diseases (223).

To explore the potential of FMT in metabolic diseases (T2DM), further detailed work is needed, such as determining the indications for recipients, optimal donor microbiome profile and appropriate dose frequency. Modulation of the gut microbiota by techniques including FMT may become a potential therapeutic option for T2DM management.

5.3 Herbal medicines

There is growing evidence that many herbs or their herbal compounds may have a therapeutic effect on T2DM by modulating the intestinal microbiota. Radix scutellariae can eliminate heat and dampness, cure jaundice and quench thirst. A modern pharmacological study has shown that scutellaria achieves hypoglycemic and lipid-regulating effects by reducing intrahepatic cholestasis or increasing BA excretion in the feces (224). Studies have shown that baicalin improves diabetes by modulating the interplay between BAs and intestinal flora, an effect that may be mediated by FXR (225).

A study has shown that licorice extract improves IR, endotoxemia-related colonic inflammation and serum lipids in diabetic mice. In addition, licorice extract reshapes the intestinal flora by reducing *Lachnospiraceae_NK4A136_group*, while increasing *Akkermansia* and *Bacteroides*.These results indicate that the modulation of intestinal microbiota and colonic TLR4/NF-κB signaling pathway in diabetic mice may be the main reason for the anti-diabetic effect of licorice extracts (226). Studies have shown that the antidiabetic effect of Scutellaria-coptis herb couple (SC), one of the famous herbal compounds in traditional herbal combinations for diabetes treatment, is attributed to its modulation of gut microbiota and anti-inflammatory effects involving TLR4 signaling pathway (227).

A rich-polyphenols extract of *Dendrobium loddigesii* (DJP) has been used to treat diabetic db/db mice, possibly due to the effects of DJP-induced reduction of inflammation and oxidative stress and improved intestinal flora balance, resulting in improved diabetic symptoms and complications in mice (228). Gegen Qinlian Decoction (GQD), a traditional Chinese medicine formula, has already been applied to treat common metabolic diseases such as T2DM. The mechanism of GQD for T2DM is mainly through altering the structure of the entire intestinal microbiota, enriching it with many butyrate-producing bacteria, thereby reducing intestinal inflammation and lowering blood glucose (229). Berberine, a hypothetical key active pharmaceutical ingredient of GQD, is also isolated from rhizoma coptidis and acts as an active alkaloid to achieve pharmacological effects by regulating the intestinal microbiota (230). In animal models of T2DM, berberine has been shown to increase the number of beneficial bacteria, reduce potentially pathogenic bacteria, and protect the islets and protect insulin target organs by reducing the invasion of inflammatory cells and inhibiting the development of a systemic inflammatory response (231). In a mouse model with T2DM, ginsenosides have been shown to modulate the intestinal flora, thereby reducing gut mucosal damage and a range of inflammatory responses (232, 233). Purified citrus polymethoxyflavone-rich extract (PMFE) significantly increases the abundance of *Bacteroides ovatus*, *Bacteroides uniformis* and *Bacteroides thetaiotaomicron*. The enrichment of *Bacteroides ovatus* by PMFE contributes to lower BCAA levels, weight loss and MetS relief (234). Ginsenoside Rb1 (Rb1) significantly changes the composition of the intestinal microbiota as it significantly increases the abundance of the bacterium *Akkermansia* spp. to which circulating alanine levels are related. Modulation of alanine may be correlated with *Akkermansia* spp., which is elevated in abundance by Rb1 to gain glucose homeostasis (235).

The role of herbal medicines in improving the intestinal microbiota in the treatment of T2DM deserves recognition. However, from the perspective of modern science, the underlying mechanism requires more explorations. Most of the effects of herbal medicines on microbiota are associated with intestinal flora structure modulation, increased richness of beneficial bacteria and butyrate concentration in gut, inhibition of opportunistic pathogens. Most of the findings are based on animal experiments, thus indicating the need of further evidence from human studies, and the underlying principles remain to be explored.

5.4 Diet and exercise

Studies have shown that weight loss of approximately 15 kg achieved through calorie restriction resulted in T2DM remission in 80% of obese and T2DM individuals. In addition, this remission is proportional to the amount of weight loss (236). Therefore, optimizing carbohydrate intake and increasing dietary fiber supplementation is particularly important for patients with T2DM. Fiber has already been recognized to play a critical role in regulating metabolism and preventing chronic gastroenterological diseases (237). The lower fiber content in the Western diet (especially in industrialized countries) is closely related to the elevated prevalence of metabolic disease states. Thus, alteration of the microbiota through dietary fiber interventions can improve health. Associations have been found between plant-based diets and taxa, such as *Roseburia*, *Faecalibacterium prausnitzii* and *Eubacterium rectale*, as well as an elevation in total SCFAs (238). SCFAs are produced by microbial fermentation of dietary fiber, which have cholesterol-lowering and glucose-control effects (239). Dietary fiber has been identified to markedly increase the RA of *Bifidobacterium* and total SCFAs while reducing glycated hemoglobin (240). Another study has reported that *Bifidobacterium pseudocatenulatum*, an acetate producer, is one of the most significantly promoted SCFA-produced microbiota by dietary fibers, and inoculation with this strain results in improved IR and postprandial glycemic response (31). A previous study has also shown that an almond-based low carbohydrate diet may improve glucose metabolism in patients with T2DM by increasing SCFA-producing bacteria, including *Roseburia*, *Ruminococcus* and *Eubacterium*, to elevate SCFA production and activate GPR43 to sustain GLP-1 secretion (48). Consistently, another study has suggested that almond-based diets may promote SCFA-producing bacteria while decreasing hemoglobin and body mass index (BMI) in T2DM individuals (241). The Green-Mediterranean diet with a gradual increase in plant components induces specific alterations in the intestinal flora and BCAA metabolism, including an elevation in *Prevotella* abundance and BCAA degradation as well as a decrease in *Bifidobacterium* abundance and BCAA biosynthesis, leading to increased insulin sensitivity (242).

Similarly, increasing physical activity and fitness is another important factor in alleviating T2DM. Physical activity is essential for reducing blood glucose and improving insulin sensitivity (243). A previous study has shown that exercise increases the abundance of *Akkermansia muciniphila* in the intestinal flora of athletes and increases the diversity of the intestinal microbiota (244). Regular exercise has also been reported to influence the composition of intestinal flora, elevate the production of SCFAs and plasma SCFA concentrations to ameliorate IR in skeletal muscle (245). Furthermore, exercise-induced elevation of SCFA-producing bacteria and improvement of intestinal barrier integrity play critical roles in T2DM improvement (246). Studies have shown that taxa producing SCFAs are positively correlated with changes in locomotion and mass, indicating that SCFAs may be involved in improving locomotor performance (247, 248).

6 Conclusion and future perspective

The recognized risk factors for the development of diabetes include the interaction among different elements such as genetic susceptibility, diet, physical activity, smoking, and stress. The interplay of diet and gut microbiota determines the formation and absorption of different metabolites. It has been found that T2DM individuals can be divided into different clusters depending on characteristics of patients and risk of developing complications. Differences in pathophysiology of various groups in the pathogenesis were also found in individuals with prediabetes (249). Different patient subgroups may respond to the same treatment in very different ways. Thus, early identification of patients with diverse traits of T2DM has allowed us to predict the disease progression and response of individuals to the corresponding treatment regimen (250).

Only recently has the importance of the gut microbiota been more widely recognized. Bacteria that live in symbiosis with humans play a critical part in health and disease, and this makes microbiology one of the most active frontiers in biomedicine today. The microbial "organ" of the intestinal flora has involved in the regulation of human health and metabolism (251).Numerous animal studies and clinical trials have strongly supported the role of intestinal flora in obesity, IR and T2DM, as well as the proposition that the gut microbiome may influence a range of host systems and metabolic pathways through the production of metabolites (39, 40, 77, 252, 253). As mentioned before, *Bacteroidetes*, *Firmicutes*, *Ruminococcus torques*, and other species regulate changes in BAs. *Akkermansia muciniphila*, *Roseburia* spp., *Prevotella* spp., and others play important roles in the production of SCAAs. *Prevotella copri* and *Bacteroides vulgatus* are closely related to the biosynthesis of BCAAs. The metabolites of these microorganisms are highly associated with the evolution of obesity and T2DM in humans. However, changes in other microbial metabolites, such as imidazole propionate, indole, and TMAO, also play an important role in T2DM, but the corresponding clinical evidences are not sufficient.

Microbially directed interventions for diabetes can be divided into nontargeted and targeted therapies. Nontargeted interventions include exercise, personalized nutrition, Probiotics and FMT, which act on the overall improvement of flora composition and function. Targeted interventions include engineered microorganisms and drugs that target the metabolism of specific microorganisms, which act on specific changes in the metabolism-related flora. Numerous animal experiments and clinical trials have shown that groups with distinct base states respond very differently to therapeutic measures targeting the gut microbiota (45, 46). This discrepancy may be closely related to the composition of the microbial flora present in the organism itself. Therefore, an important prerequisite for the application of microbial therapies is the clarification of the pathogenic mechanism and the baseline microbial level of the organism. It is also the basis for successfully colonizing the transplanted microorganisms in an individualized manner. Overall, by analyzing the causal relationship between T2DM and gut flora, we conclude that gut flora can be used not only as a diagnostic biomarker but also as a promising therapeutic target for T2DM. The utilization of gut microbiota may contribute to a more precise and personalized treatment of T2DM patients.

Author contributions

Conceptualization: YW, GR. Investigation: LL, JZ, GR, YC, MZ, and ZX. Writing—original draft preparation: LL, JZ, and YW. Writing—review and editing: LL, JZ, GR, YC, and MZ. Supervision: YW, GR. All authors contributed to the article and approved the submitted version.

Funding

This work was funded by grants from the National Natural Science Foundation of China (NSFC 82070571), Chongqing Science and Health Joint Project (2022MSXM052), and Army Medical Center Military Medical Frontier Innovation Capability Program (CX2019JS222).

Acknowledgments

We thank Servier Medical Art (http://smart.servier.com/) for the reference of Figures in this review, licensed under a Creative Common Attribution 3.0 Generic License (https://creativecommons.org/licenses/by/3.0/).

Conflict of interest

The authors declare that the research was conducted in the absence of any commercial or financial relationships that could be construed as a potential conflict of interest.

Publisher's note

References

1. American Diabetes A. Diagnosis and classification of diabetes mellitus. *Diabetes Care* (2014) 37 Suppl 1:S81–90. doi: 10.2337/dc14-S081

2. Sung KC, Lee MY, Kim YH, Huh JH, Kim JY, Wild SH, et al. Obesity and incidence of diabetes: Effect of absence of metabolic syndrome, insulin resistance, inflammation and fatty liver. *Atherosclerosis* (2018) 275:50–7. doi: 10.1016/j.atherosclerosis.2018.05.042

3. Jaacks LM, Siegel KR, Gujral UP, Narayan KM. Type 2 diabetes: A 21st century epidemic. *Best Pract Res Clin Endocrinol Metab* (2016) 30:331–43. doi: 10.1016/j.beem.2016.05.003

4. Sun H, Saeedi P, Karuranga S, Pinkepank M, Ogurtsova K, Duncan BB, et al. IDF diabetes atlas: Global, regional and country-level diabetes prevalence estimates for 2021 and projections for 2045. *Diabetes Res Clin Pract* (2022) 183:109119. doi: 10.1016/j.diabres.2021.109119

5. Ayadurai S, Hattingh HL, Tee LB, Md Said SN. A narrative review of diabetes intervention studies to explore diabetes care opportunities for pharmacists. *J Diabetes Res* (2016) 2016:5897452. doi: 10.1155/2016/5897452

6. Umpierrez GE, Pasquel FJ. Management of inpatient hyperglycemia and diabetes in older adults. *Diabetes Care* (2017) 40:509–17. doi: 10.2337/dc16-0989

7. Munshi MN. Cognitive dysfunction in older adults with diabetes: What a clinician needs to know. *Diabetes Care* (2017) 40:461–7. doi: 10.2337/dc16-1229

8. Durrer Schutz D, Busetto L, Dicker D, Farpour-Lambert N, Pryke R, Toplak H, et al. European Practical and patient-centred guidelines for adult obesity management in primary care. *Obes Facts* (2019) 12:40–66. doi: 10.1159/000496183

9. Koch TR, Shope TR. Laparoscopic vertical sleeve gastrectomy as a treatment option for adults with diabetes mellitus. *Adv Exp Med Biol* (2021) 1307:299–320. doi: 10.1007/5584_2020_487

10. Silver B, Ramaiya K, Andrew SB, Fredrick O, Bajaj S, Kalra S, et al. EADSG guidelines: Insulin therapy in diabetes. *Diabetes Ther* (2018) 9:449–92. doi: 10.1007/s13300-018-0384-6

11. Home P, Riddle M, Cefalu WT, Bailey CJ, Bretzel RG, Del Prato S, et al. Insulin therapy in people with type 2 diabetes: opportunities and challenges? *Diabetes Care* (2014) 37:1499–508. doi: 10.2337/dc13-2743

12. DeFronzo RA. Pathogenesis of type 2 diabetes mellitus. *Med Clin North Am* (2004) 88:787–835. doi: 10.1016/j.mcna.2004.04.013

13. Forbes JM, Cooper ME. Mechanisms of diabetic complications. *Physiol Rev* (2013) 93:137–88. doi: 10.1152/physrev.00045.2011

14. Zhou W, Sailani MR, Contrepois K, Zhou Y, Ahadi S, Leopold SR, et al. Longitudinal multi-omics of host-microbe dynamics in prediabetes. *Nature* (2019) 569:663–71. doi: 10.1038/s41586-019-1236-x

15. Yu F, Han W, Zhan G, Li S, Jiang X, Wang L, et al. Abnormal gut microbiota composition contributes to the development of type 2 diabetes mellitus in db/db mice. *Aging (Albany NY)* (2019) 11:10454–67. doi: 10.18632/aging.102469

16. Vallianou NG, Stratigou T, Tsagarakis S. Microbiome and diabetes: Where are we now? *Diabetes Res Clin Pract* (2018) 146:111–8. doi: 10.1016/j.diabres.2018.10.008

17. Pedersen HK, Gudmundsdottir V, Nielsen HB, Hyotylainen T, Nielsen T, Jensen BA, et al. Human gut microbes impact host serum metabolome and insulin sensitivity. *Nature* (2016) 535:376–81. doi: 10.1038/nature18646

18. Thomas C, Pellicciari R, Pruzanski M, Auwerx J, Schoonjans K. Targeting bile-acid signalling for metabolic diseases. *Nat Rev Drug Discov* (2008) 7:678–93. doi: 10.1038/nrd2619

19. Wahlstrom A, Sayin SI, Marschall HU, Backhed F. Intestinal crosstalk between bile acids and microbiota and its impact on host metabolism. *Cell Metab* (2016) 24:41–50. doi: 10.1016/j.cmet.2016.05.005

20. Zhao L, Lou H, Peng Y, Chen S, Zhang Y, Li X. Comprehensive relationships between gut microbiome and faecal metabolome in individuals with type 2 diabetes and its complications. *Endocrine* (2019) 66:526–37. doi: 10.1007/s12020-019-02103-8

21. Zhao L, Lou H, Peng Y, Chen S, Fan L, Li X. Elevated levels of circulating short-chain fatty acids and bile acids in type 2 diabetes are linked to gut barrier disruption and disordered gut microbiota. *Diabetes Res Clin Pract* (2020) 169:108418. doi: 10.1016/j.diabres.2020.108418

22. Munoz-Garach A, Diaz-Perdigones C, Tinahones FJ. Gut microbiota and type 2 diabetes mellitus. *Endocrinol Nutr* (2016) 63:560–8. doi: 10.1016/j.endonu.2016.07.008

23. Heianza Y, Sun D, Li X, DiDonato JA, Bray GA, Sacks FM, et al. Gut microbiota metabolites, amino acid metabolites and improvements in insulin sensitivity and glucose metabolism: the POUNDS lost trial. *Gut* (2019) 68:263–70. doi: 10.1136/gutjnl-2018-316155

24. Gurung M, Li Z, You H, Rodrigues R, Jump DB, Morgun A, et al. Role of gut microbiota in type 2 diabetes pathophysiology. *EBioMedicine* (2020) 51:102590. doi: 10.1016/j.ebiom.2019.11.051

25. Patterson E, Ryan PM, Cryan JF, Dinan TG, Ross RP, Fitzgerald GF, et al. Gut microbiota, obesity and diabetes. *Postgrad Med J* (2016) 92:286–300. doi: 10.1136/postgradmedj-2015-133285

26. Jaacks LM, Vandevijvere S, Pan A, McGowan CJ, Wallace C, Imamura F, et al. The obesity transition: Stages of the global epidemic. *Lancet Diabetes Endocrinol* (2019) 7:231–40. doi: 10.1016/S2213-8587(19)30026-9

27. Younossi ZM, Koenig AB, Abdelatif D, Fazel Y, Henry L, Wymer M. Global epidemiology of nonalcoholic fatty liver disease-meta-analytic assessment of prevalence, incidence, and outcomes. *Hepatology* (2016) 64:73–84. doi: 10.1002/hep.28431

28. Lynch SV, Pedersen O. The human intestinal microbiome in health and disease. *N Engl J Med* (2016) 375:2369–79. doi: 10.1056/NEJMra1600266

29. Olofsson LE, Backhed F. The metabolic role and therapeutic potential of the microbiome. *Endocr Rev* (2022). doi: 10.1210/endrev/bnac004

30. Gill SR, Pop M, Deboy RT, Eckburg PB, Turnbaugh PJ, Samuel BS, et al. Metagenomic analysis of the human distal gut microbiome. *Science* (2006) 312:1355–9. doi: 10.1126/science.1124234

31. Zhao L, Zhang F, Ding X, Wu G, Lam YY, Wang X, et al. Gut bacteria selectively promoted by dietary fibers alleviate type 2 diabetes. *Science* (2018) 359:1151–6. doi: 10.1126/science.aao5774

32. Boulange CL, Neves AL, Chilloux J, Nicholson JK, Dumas ME. Impact of the gut microbiota on inflammation, obesity, and metabolic disease. *Genome Med* (2016) 8:42. doi: 10.1186/s13073-016-0303-2

33. Chobot A, Gorowska-Kowolik K, Sokolowska M, Jarosz-Chobot P. Obesity and diabetes-not only a simple link between two epidemics. *Diabetes Metab Res Rev* (2018) 34:e3042. doi: 10.1002/dmrr.3042

34. Peters BA, Shapiro JA, Church TR, Miller G, Trinh-Shevrin C, Yuen E, et al. A taxonomic signature of obesity in a large study of American adults. *Sci Rep* (2018) 8:9749. doi: 10.1038/s41598-018-28126-1

35. Cani PD. Human gut microbiome: hopes, threats and promises. *Gut* (2018) 67:1716–25. doi: 10.1136/gutjnl-2018-316723

36. Singer-Englar T, Barlow G, Mathur R. Obesity, diabetes, and the gut microbiome: An updated review. *Expert Rev Gastroenterol Hepatol* (2019) 13:3–15. doi: 10.1080/17474124.2019.1543023

37. Karlsson FH, Tremaroli V, Nookaew I, Bergstrom G, Behre CJ, Fagerberg B, et al. Gut metagenome in European women with normal, impaired and diabetic glucose control. *Nature* (2013) 498:99–103. doi: 10.1038/nature12198

38. Qin J, Li Y, Cai Z, Li S, Zhu J, Zhang F, et al. A metagenome-wide association study of gut microbiota in type 2 diabetes. *Nature* (2012) 490:55–60. doi: 10.1038/nature11450

39. Forslund K, Hildebrand F, Nielsen T, Falony G, Le Chatelier E, Sunagawa S, et al. Disentangling type 2 diabetes and metformin treatment signatures in the human gut microbiota. *Nature* (2015) 528:262–6. doi: 10.1038/nature15766

40. Wu H, Tremaroli V, Schmidt C, Lundqvist A, Olsson LM, Kramer M, et al. The gut microbiota in prediabetes and diabetes: A population-based cross-sectional study. *Cell Metab* (2020) 32:379–390.e3. doi: 10.1016/j.cmet.2020.06.011

41. Shin NR, Lee JC, Lee HY, Kim MS, Whon TW, Lee MS, et al. An increase in the akkermansia spp. population induced by metformin treatment improves glucose homeostasis in diet-induced obese mice. *Gut* (2014) 63:727–35. doi: 10.1136/gutjnl-2012-303839

42. Lee H, Ko G. Effect of metformin on metabolic improvement and gut microbiota. *Appl Environ Microbiol* (2014) 80:5935–43. doi: 10.1128/AEM.01357-14

43. Le Chatelier E, Nielsen T, Qin J, Prifti E, Hildebrand F, Falony G, et al. Richness of human gut microbiome correlates with metabolic markers. *Nature* (2013) 500:541–6. doi: 10.1038/nature12506

44. Cotillard A, Kennedy SP, Kong LC, Prifti E, Pons N, Le Chatelier E, et al. Dietary intervention impact on gut microbial gene richness. *Nature* (2013) 500:585–8. doi: 10.1038/nature12480

45. De Vadder F, Kovatcheva-Datchary P, Goncalves D, Vinera J, Zitoun C, Duchampt A, et al. Microbiota-generated metabolites promote metabolic benefits *via* gut-brain neural circuits. *Cell* (2014) 156:84–96. doi: 10.1016/j.cell.2013.12.016

46. Volzke H, Alte D, Schmidt CO, Radke D, Lorbeer R, Friedrich N, et al. Cohort profile: The study of health in pomerania. *Int J Epidemiol* (2011) 40:294–307. doi: 10.1093/ije/dyp394

47. Maldonado-Contreras A, Noel SE, Ward DV, Velez M, Mangano KM. Associations between diet, the gut microbiome, and short-chain fatty acid production among older Caribbean Latino adults. *J Acad Nutr Diet* (2020) 120:2047–60.e6. doi: 10.1016/j.jand.2020.04.018

48. Ren M, Zhang H, Qi J, Hu A, Jiang Q, Hou Y, et al. An almond-based low carbohydrate diet improves depression and glycometabolism in patients with type 2 diabetes through modulating gut microbiota and GLP-1: A randomized controlled trial. *Nutrients* (2020) 12:3036. doi: 10.3390/nu12103036

49. Jia W, Xie G, Jia W. Bile acid-microbiota crosstalk in gastrointestinal inflammation and carcinogenesis. *Nat Rev Gastroenterol Hepatol* (2018) 15:111–28. doi: 10.1038/nrgastro.2017.119

50. Chiang JYL, Ferrell JM. Bile acids as metabolic regulators and nutrient sensors. *Annu Rev Nutr* (2019) 39:175–200. doi: 10.1146/annurev-nutr-082018-124344

51. Yue SJ, Liu J, Wang AT, Meng XT, Yang ZR, Peng C, et al. Berberine alleviates insulin resistance by reducing peripheral branched-chain amino acids. *Am J Physiol Endocrinol Metab* (2019) 316:E73–85. doi: 10.1152/ajpendo.00256.2018

52. Tett A, Huang KD, Asnicar F, Fehlner-Peach H, Pasolli E, Karcher N, et al. The prevotella copri complex comprises four distinct clades underrepresented in westernized populations. *Cell Host Microbe* (2019) 26:666–679.e7. doi: 10.1016/j.chom.2019.08.018

53. Li Q, Chang Y, Zhang K, Chen H, Tao S, Zhang Z. Implication of the gut microbiome composition of type 2 diabetic patients from Northern China. *Sci Rep* (2020) 10:5450. doi: 10.1038/s41598-020-62224-3

54. Wang TJ, Larson MG, Vasan RS, Cheng S, Rhee EP, McCabe E, et al. Metabolite profiles and the risk of developing diabetes. *Nat Med* (2011) 17:448–53. doi: 10.1038/nm.2307

55. Koh A, Molinaro A, Stahlman M, Khan MT, Schmidt C, Manneras-Holm L, et al. Microbially produced imidazole propionate impairs insulin signaling through mTORC1. *Cell* (2018) 175:947–961.e17. doi: 10.1016/j.cell.2018.09.055

56. Zhang C, Zhang M, Wang S, Han R, Cao Y, Hua W, et al. Interactions between gut microbiota, host genetics and diet relevant to development of metabolic syndromes in mice. *ISME J* (2010) 4:232–41. doi: 10.1038/ismej.2009.112

57. Hong S, Zhou W, Fang B, Lu W, Loro E, Damle M, et al. Dissociation of muscle insulin sensitivity from exercise endurance in mice by HDAC3 depletion. *Nat Med* (2017) 23:223–34. doi: 10.1038/nm.4245

58. Dao MC, Everard A, Aron-Wisnewsky J, Sokolovska N, Prifti E, Verger EO, et al. Akkermansia muciniphila and improved metabolic health during a dietary intervention in obesity: Relationship with gut microbiome richness and ecology. *Gut* (2016) 65:426–36. doi: 10.1136/gutjnl-2014-308778

59. Lukovac S, Belzer C, Pellis L, Keijser BJ, de Vos WM, Montijn RC, et al. Differential modulation by akkermansia muciniphila and faecalibacterium prausnitzii of host peripheral lipid metabolism and histone acetylation in mouse gut organoids. *mBio* (2014) 5:e01438-14. doi: 10.1128/mBio.01438-14

60. Schwiertz A, Taras D, Schafer K, Beijer S, Bos NA, Donus C, et al. Microbiota and SCFA in lean and overweight healthy subjects. *Obes (Silver Spring)* (2010) 18:190–5. doi: 10.1038/oby.2009.167

61. Ridaura VK, Faith JJ, Rey FE, Cheng J, Duncan AE, Kau AL, et al. Gut microbiota from twins discordant for obesity modulate metabolism in mice. *Science* (2013) 341:1241214. doi: 10.1126/science.1241214

62. Larsen N, Vogensen FK, van den Berg FW, Nielsen DS, Andreasen AS, Pedersen BK, et al. Gut microbiota in human adults with type 2 diabetes differs from non-diabetic adults. *PLoS One* (2010) 5:e9085. doi: 10.1371/journal.pone.0009085

63. Sung MM, Kim TT, Denou E, Soltys CM, Hamza SM, Byrne NJ, et al. Improved glucose homeostasis in obese mice treated with resveratrol is associated with alterations in the gut microbiome. *Diabetes* (2017) 66:418–25. doi: 10.2337/db16-0680

64. Vital M, Howe AC, Tiedje JM. Revealing the bacterial butyrate synthesis pathways by analyzing (meta)genomic data. *mBio* (2014) 5:e00889. doi: 10.1128/mBio.00889-14

65. Beaumont M, Goodrich JK, Jackson MA, Yet I, Davenport ER, Vieira-Silva S, et al. Heritable components of the human fecal microbiome are associated with visceral fat. *Genome Biol* (2016) 17:189. doi: 10.1186/s13059-016-1052-7

66. Konikoff T, Gophna U. Oscillospira: a central, enigmatic component of the human gut microbiota. *Trends Microbiol* (2016) 24:523–4. doi: 10.1016/j.tim.2016.02.015

67. Goodrich JK, Waters JL, Poole AC, Sutter JL, Koren O, Blekhman R, et al. Human genetics shape the gut microbiome. *Cell* (2014) 159:789–99. doi: 10.1016/j.cell.2014.09.053

68. Le Roy CI, Beaumont M, Jackson MA, Steves CJ, Spector TD, Bell JT. Heritable components of the human fecal microbiome are associated with visceral fat. *Gut Microbes* (2018) 9:61–7. doi: 10.1080/19490976.2017.1356556

69. Tims S, Derom C, Jonkers DM, Vlietinck R, Saris WH, Kleerebezem M, et al. Microbiota conservation and BMI signatures in adult monozygotic twins. *ISME J* (2013) 7:707–17. doi: 10.1038/ismej.2012.146

70. Newman TM, Shively CA, Register TC, Appt SE, Yadav H, Colwell RR, et al. Diet, obesity, and the gut microbiome as determinants modulating metabolic outcomes in a non-human primate model. *Microbiome* (2021) 9:100. doi: 10.1186/s40168-021-01069-y

71. Orsso CE, Peng Y, Deehan EC, Tan Q, Field CJ, Madsen KL, et al. Composition and functions of the gut microbiome in pediatric obesity: Relationships with markers of insulin resistance. *Microorganisms* (2021) 9:1490. doi: 10.3390/microorganisms9071490

72. Clemente JC, Pehrsson EC, Blaser MJ, Sandhu K, Gao Z, Wang B, et al. The microbiome of uncontacted amerindians. *Sci Adv* (2015) 1:e1500183. doi: 10.1126/sciadv.1500183

73. Ouchi N, Parker JL, Lugus JJ, Walsh K. Adipokines in inflammation and metabolic disease. *Nat Rev Immunol* (2011) 11:85–97. doi: 10.1038/nri2921

74. Kootte RS, Levin E, Salojarvi J, Smits LP, Hartstra AV, Udayappan SD, et al. Improvement of insulin sensitivity after lean donor feces in metabolic syndrome is driven by baseline intestinal microbiota composition. *Cell Metab* (2017) 26:611–619.e6. doi: 10.1016/j.cmet.2017.09.008

75. Zhang X, Shen D, Fang Z, Jie Z, Qiu X, Zhang C, et al. Human gut microbiota changes reveal the progression of glucose intolerance. *PLoS One* (2013) 8:e71108. doi: 10.1371/journal.pone.0071108

76. Turnbaugh PJ, Backhed F, Fulton L, Gordon JI. Diet-induced obesity is linked to marked but reversible alterations in the mouse distal gut microbiome. *Cell Host Microbe* (2008) 3:213–23. doi: 10.1016/j.chom.2008.02.015

77. Turnbaugh PJ, Ley RE, Mahowald MA, Magrini V, Mardis ER, Gordon JI. An obesity-associated gut microbiome with increased capacity for energy harvest. *Nature* (2006) 444:1027–31. doi: 10.1038/nature05414

78. Ley RE, Turnbaugh PJ, Klein S, Gordon JI. Microbial ecology: human gut microbes associated with obesity. *Nature* (2006) 444:1022–3. doi: 10.1038/4441022a

79. Furet JP, Kong LC, Tap J, Poitou C, Basdevant A, Bouillot JL, et al. Differential adaptation of human gut microbiota to bariatric surgery-induced weight loss: links with metabolic and low-grade inflammation markers. *Diabetes* (2010) 59:3049–57. doi: 10.2337/db10-0253

80. Morotomi M, Nagai F, Watanabe Y. Description of christensenella minuta gen. nov., sp. nov., isolated from human faeces, which forms a distinct branch in the order clostridiales, and proposal of christensenellaceae fam. nov. *Int J Syst Evol Microbiol* (2012) 62:144–9. doi: 10.1099/ijs.0.026989-0

81. Liu R, Hong J, Xu X, Feng Q, Zhang D, Gu Y, et al. Gut microbiome and serum metabolome alterations in obesity and after weight-loss intervention. *Nat Med* (2017) 23:859–68. doi: 10.1038/nm.4358

82. Daousi C, Casson IF, Gill GV, MacFarlane IA, Wilding JP, Pinkney JH. Prevalence of obesity in type 2 diabetes in secondary care: Association with cardiovascular risk factors. *Postgrad Med J* (2006) 82:280–4. doi: 10.1136/pmj.2005.039032

83. Kovatcheva-Datchary P, Nilsson A, Akrami R, Lee YS, De Vadder F, Arora T, et al. Dietary fiber-induced improvement in glucose metabolism is associated with increased abundance of prevotella. *Cell Metab* (2015) 22:971–82. doi: 10.1016/j.cmet.2015.10.001

84. Vich Vila A, Collij V, Sanna S, Sinha T, Imhann F, Bourgonje AR, et al. Impact of commonly used drugs on the composition and metabolic function of the gut microbiota. *Nat Commun* (2020) 11:362. doi: 10.1038/s41467-019-14177-z

85. Allin KH, Tremaroli V, Caesar R, Jensen BAH, Damgaard MTF, Bahl MI, et al. Aberrant intestinal microbiota in individuals with prediabetes. *Diabetologia* (2018) 61:810–20. doi: 10.1007/s00125-018-4550-1

86. Zhong H, Ren H, Lu Y, Fang C, Hou G, Yang Z, et al. Distinct gut metagenomics and metaproteomics signatures in prediabetics and treatment-naive type 2 diabetics. *EBioMedicine* (2019) 47:373–83. doi: 10.1016/j.ebiom.2019.08.048

87. de la Cuesta-Zuluaga J, Mueller NT, Corrales-Agudelo V, Velasquez-Mejia EP, Carmona JA, Abad JM, et al. Metformin is associated with higher relative abundance of mucin-degrading akkermansia muciniphila and several short-chain fatty acid-producing microbiota in the gut. *Diabetes Care* (2017) 40:54–62. doi: 10.2337/dc16-1324

88. Everard A, Belzer C, Geurts L, Ouwerkerk JP, Druart C, Bindels LB, et al. Cross-talk between akkermansia muciniphila and intestinal epithelium controls diet-induced obesity. *Proc Natl Acad Sci USA* (2013) 110:9066–71. doi: 10.1073/pnas.1219451110

89. Palacios T, Vitetta L, Coulson S, Madigan CD, Lam YY, Manuel R, et al. Targeting the intestinal microbiota to prevent type 2 diabetes and enhance the effect of metformin on glycaemia: A randomised controlled pilot study. *Nutrients* (2020) 12:2041. doi: 10.3390/nu12072041

90. Li T, Francl JM, Boehme S, Ochoa A, Zhang Y, Klaassen CD, et al. Glucose and insulin induction of bile acid synthesis: Mechanisms and implication in diabetes and obesity. *J Biol Chem* (2012) 287:1861–73. doi: 10.1074/jbc.M111.305789

91. Li T, Chanda D, Zhang Y, Choi HS, Chiang JY. Glucose stimulates cholesterol 7alpha-hydroxylase gene transcription in human hepatocytes. *J Lipid Res* (2010) 51:832–42. doi: 10.1194/jlr.M002782

92. Worthmann A, John C, Ruhlemann MC, Baguhl M, Heinsen FA, Schaltenberg N, et al. Cold-induced conversion of cholesterol to bile acids in mice shapes the gut microbiome and promotes adaptive thermogenesis. *Nat Med* (2017) 23:839–49. doi: 10.1038/nm.4357

93. Haeusler RA, Astiarraga B, Camastra S, Accili D, Ferrannini E. Human insulin resistance is associated with increased plasma levels of 12alpha-hydroxylated bile acids. *Diabetes* (2013) 62:4184–91. doi: 10.2337/db13-0639

94. de Aguiar Vallim TQ, Tarling EJ, Edwards PA. Pleiotropic roles of bile acids in metabolism. *Cell Metab* (2013) 17:657–69. doi: 10.1016/j.cmet.2013.03.013

95. Chavez-Talavera O, Tailleux A, Lefebvre P, Staels B. Bile acid control of metabolism and inflammation in obesity, type 2 diabetes, dyslipidemia, and nonalcoholic fatty liver disease. *Gastroenterology* (2017) 152:1679–94.e3. doi: 10.1053/j.gastro.2017.01.055

96. Christiaens H, Leer RJ, Pouwels PH, Verstraete W. Cloning and expression of a conjugated bile acid hydrolase gene from lactobacillus plantarum by using a direct plate assay. *Appl Environ Microbiol* (1992) 58:3792–8. doi: 10.1128/aem.58.12.3792-3798.1992

97. Corzo G, Gilliland SE. Bile salt hydrolase activity of three strains of lactobacillus acidophilus. *J Dairy Sci* (1999) 82:472–80. doi: 10.3168/jds.S0022-0302(99)75256-2

98. Wang Z, Zeng X, Mo Y, Smith K, Guo Y, Lin J. Identification and characterization of a bile salt hydrolase from lactobacillus salivarius for development of novel alternatives to antibiotic growth promoters. *Appl Environ Microbiol* (2012) 78:8795–802. doi: 10.1128/AEM.02519-12

99. Chae JP, Valeriano VD, Kim GB, Kang DK. Molecular cloning, characterization and comparison of bile salt hydrolases from lactobacillus johnsonii PF01. *J Appl Microbiol* (2013) 114:121–33. doi: 10.1111/jam.12027

100. Coleman JP, Hudson LL. Cloning and characterization of a conjugated bile acid hydrolase gene from clostridium perfringens. *Appl Environ Microbiol* (1995) 61:2514–20. doi: 10.1128/aem.61.7.2514-2520.1995

101. Tanaka H, Hashiba H, Kok J, Mierau I. Bile salt hydrolase of bifidobacterium longum-biochemical and genetic characterization. *Appl Environ Microbiol* (2000) 66:2502–12. doi: 10.1128/AEM.66.6.2502-2512.2000

102. Kim GB, Miyamoto CM, Meighen EA, Lee BH. Cloning and characterization of the bile salt hydrolase genes (bsh) from bifidobacterium bifidum strains. *Appl Environ Microbiol* (2004) 70:5603–12. doi: 10.1128/AEM.70.9.5603-5612.2004

103. Kim GB, Brochet M, Lee BH. Cloning and characterization of a bile salt hydrolase (bsh) from bifidobacterium adolescentis. *Biotechnol Lett* (2005) 27:817–22. doi: 10.1007/s10529-005-6717-3

104. Glaser P, Frangeul L, Buchrieser C, Rusniok C, Amend A, Baquero F, et al. Comparative genomics of listeria species. *Science* (2001) 294:849–52. doi: 10.1126/science.1063447

105. Dussurget O, Cabanes D, Dehoux P, Lecuit M, Buchrieser C, Glaser P, et al. Listeria monocytogenes bile salt hydrolase is a PrfA-regulated virulence factor involved in the intestinal and hepatic phases of listeriosis. *Mol Microbiol* (2002) 45:1095–106. doi: 10.1046/j.1365-2958.2002.03080.x

106. Wijaya A, Hermann A, Abriouel H, Specht I, Yousif NM, Holzapfel WH, et al. Cloning of the bile salt hydrolase (bsh) gene from enterococcus faecium FAIR-e 345 and chromosomal location of bsh genes in food enterococci. *J Food Prot* (2004) 67:2772–8. doi: 10.4315/0362-028x-67.12.2772

107. Stellwag EJ, Hylemon PB. Purification and characterization of bile salt hydrolase from bacteroides fragilis subsp. fragilis. *Biochim Biophys Acta* (1976) 452:165–76. doi: 10.1016/0005-2744(76)90068-1

108. Jones BV, Begley M, Hill C, Gahan CG, Marchesi JR. Functional and comparative metagenomic analysis of bile salt hydrolase activity in the human gut microbiome. *Proc Natl Acad Sci USA* (2008) 105:13580–5. doi: 10.1073/pnas.0804437105

109. Joyce SA, MacSharry J, Casey PG, Kinsella M, Murphy EF, Shanahan F, et al. Regulation of host weight gain and lipid metabolism by bacterial bile acid modification in the gut. *Proc Natl Acad Sci USA* (2014) 111:7421–6. doi: 10.1073/pnas.1323599111

110. Choi SB, Lew LC, Yeo SK, Nair Parvathy S, Liong MT. Probiotics and the BSH-related cholesterol lowering mechanism: a Jekyll and Hyde scenario. *Crit Rev Biotechnol* (2015) 35:392–401. doi: 10.3109/07388551.2014.889077

111. Foley MH, O'Flaherty S, Allen G, Rivera AJ, Stewart AK, Barrangou R, et al. Lactobacillus bile salt hydrolase substrate specificity governs bacterial fitness and host colonization. *Proc Natl Acad Sci USA* (2021) 118:e2017709118. doi: 10.1073/pnas.2017709118

112. Song Z, Cai Y, Lao X, Wang X, Lin X, Cui Y, et al. Taxonomic profiling and populational patterns of bacterial bile salt hydrolase (BSH) genes based on worldwide human gut microbiome. *Microbiome* (2019) 7:9. doi: 10.1186/s40168-019-0628-3

113. Hofmann AF, Hagey LR. Key discoveries in bile acid chemistry and biology and their clinical applications: history of the last eight decades. *J Lipid Res* (2014) 55:1553–95. doi: 10.1194/jlr.R049437

114. Marion S, Studer N, Desharnais L, Menin L, Escrig S, Meibom A, et al. *In vitro* and *in vivo* characterization of clostridium scindens bile acid transformations. *Gut Microbes* (2019) 10:481–503. doi: 10.1080/19490976.2018.1549420

115. Lee JY, Arai H, Nakamura Y, Fukiya S, Wada M, Yokota A. Contribution of the 7beta-hydroxysteroid dehydrogenase from ruminococcus gnavus N53 to ursodeoxycholic acid formation in the human colon. *J Lipid Res* (2013) 54:3062–9. doi: 10.1194/jlr.M039834

116. Coleman JP, Hudson LL, Adams MJ. Characterization and regulation of the NADP-linked 7 alpha-hydroxysteroid dehydrogenase gene from clostridium sordellii. *J Bacteriol* (1994) 176:4865–74. doi: 10.1128/jb.176.16.4865-4874.1994

117. Bakonyi D, Hummel W. Cloning, expression, and biochemical characterization of a novel NADP(+)-dependent 7alpha-hydroxysteroid dehydrogenase from clostridium difficile and its application for the oxidation of bile acids. *Enzyme Microb Technol* (2017) 99:16–24. doi: 10.1016/j.enzmictec.2016.12.006

118. Lou D, Wang Y, Tan J, Zhu L, Ji S, Wang B. Functional contribution of coenzyme specificity-determining sites of 7alpha-hydroxysteroid dehydrogenase from clostridium absonum. *Comput Biol Chem* (2017) 70:89–95. doi: 10.1016/j.compbiolchem.2017.08.004

119. Hirano S, Masuda N. Enhancement of the 7 alpha-dehydroxylase activity of a gram-positive intestinal anaerobe by bacteroides and its significance in the 7-dehydroxylation of ursodeoxycholic acid. *J Lipid Res* (1982) 23:1152–8.

120. Bennett MJ, McKnight SL, Coleman JP. Cloning and characterization of the NAD-dependent 7alpha-hydroxysteroid dehydrogenase from bacteroides fragilis. *Curr Microbiol* (2003) 47:475–84. doi: 10.1007/s00284-003-4079-4

121. Fukiya S, Arata M, Kawashima H, Yoshida D, Kaneko M, Minamida K, et al. Conversion of cholic acid and chenodeoxycholic acid into their 7-oxo derivatives by bacteroides intestinalis AM-1 isolated from human feces. *FEMS Microbiol Lett* (2009) 293:263–70. doi: 10.1111/j.1574-6968.2009.01531.x

122. Zhang X, Fan D, Hua X, Zhang T. Large-Scale production of ursodeoxycholic acid from chenodeoxycholic acid by engineering 7alpha- and 7beta-hydroxysteroid dehydrogenase. *Bioprocess Biosyst Eng* (2019) 42:1537–45. doi: 10.1007/s00449-019-02151-4

123. Kim KH, Lee CW, Pardhe BD, Hwang J, Do H, Lee YM, et al. Crystal structure of an apo 7alpha-hydroxysteroid dehydrogenase reveals key structural changes induced by substrate and co-factor binding. *J Steroid Biochem Mol Biol* (2021) 212:105945. doi: 10.1016/j.jsbmb.2021.105945

124. Li D, Liu R, Wang M, Peng R, Fu S, Fu A, et al. 3beta-hydroxysteroid dehydrogenase expressed by gut microbes degrades testosterone and is linked to depression in males. *Cell Host Microbe* (2022) 30:329–339.e5. doi: 10.1016/j.chom.2022.01.001

125. Baron SF, Franklund CV, Hylemon PB. Cloning, sequencing, and expression of the gene coding for bile acid 7 alpha-hydroxysteroid dehydrogenase from eubacterium sp. strain VPI 12708. *J Bacteriol* (1991) 173:4558–69. doi: 10.1128/jb.173.15.4558-4569.1991

126. de Prada P, Setchell KD, Hylemon PB. Purification and characterization of a novel 17 alpha-hydroxysteroid dehydrogenase from an intestinal eubacterium sp. VPI 12708. *J Lipid Res* (1994) 35:922–9.

127. Mallonee DH, Lijewski MA, Hylemon PB. Expression in escherichia coli and characterization of a bile acid-inducible 3 alpha-hydroxysteroid dehydrogenase from eubacterium sp. strain VPI 12708. *Curr Microbiol* (1995) 30:259–63. doi: 10.1007/BF00295498

128. Ridlon JM, Kang DJ, Hylemon PB. Bile salt biotransformations by human intestinal bacteria. *J Lipid Res* (2006) 47:241–59. doi: 10.1194/jlr.R500013-JLR200

129. Suhre K, Meisinger C, Doring A, Altmaier E, Belcredi P, Gieger C, et al. Metabolic footprint of diabetes: A multiplatform metabolomics study in an epidemiological setting. *PLoS One* (2010) 5:e13953. doi: 10.1371/journal.pone.0013953

130. Kakiyama G, Pandak WM, Gillevet PM, Hylemon PB, Heuman DM, Daita K, et al. Modulation of the fecal bile acid profile by gut microbiota in cirrhosis. *J Hepatol* (2013) 58:949–55. doi: 10.1016/j.jhep.2013.01.003

131. Buffie CG, Bucci V, Stein RR, McKenney PT, Ling L, Gobourne A, et al. Precision microbiome reconstitution restores bile acid mediated resistance to clostridium difficile. *Nature* (2015) 517:205–8. doi: 10.1038/nature13828

132. Sato Y, Atarashi K, Plichta DR, Arai Y, Sasajima S, Kearney SM, et al. Novel bile acid biosynthetic pathways are enriched in the microbiome of centenarians. *Nature* (2021) 599:458–64. doi: 10.1038/s41586-021-03832-5

133. Sutherland JD, Macdonald IA, Forrest TP. The enzymic and chemical synthesis of ursodeoxycholic and chenodeoxycholic acid from cholic acid. *Prep Biochem* (1982) 12:307–21. doi: 10.1080/00327488208065679

134. Doden H, Sallam LA, Devendran S, Ly L, Doden G, Daniel SL, et al. Metabolism of oxo-bile acids and characterization of recombinant 12alpha-hydroxysteroid dehydrogenases from bile acid 7alpha-dehydroxylating human gut bacteria. *Appl Environ Microbiol* (2018) 84:e00235-18. doi: 10.1128/AEM.00235-18

135. Mythen SM, Devendran S, Mendez-Garcia C, Cann I, Ridlon JM. Targeted synthesis and characterization of a gene cluster encoding NAD(P)H-dependent 3alpha-, 3beta-, and 12alpha-hydroxysteroid dehydrogenases from eggerthella CAG:298, a gut metagenomic sequence. *Appl Environ Microbiol* (2018) 84: e02475-17. doi: 10.1128/AEM.02475-17

136. Harris SC, Devendran S, Mendez-Garcia C, Mythen SM, Wright CL, Fields CJ, et al. Bile acid oxidation by eggerthella lenta strains C592 and DSM 2243(T). *Gut Microbes* (2018) 9:523–39. doi: 10.1080/19490976.2018.1458180

137. Doden HL, Wolf PG, Gaskins HR, Anantharaman K, Alves JMP, Ridlon JM. Completion of the gut microbial epi-bile acid pathway. *Gut Microbes* (2021) 13:1–20. doi: 10.1080/19490976.2021.1907271

138. Gu Y, Wang X, Li J, Zhang Y, Zhong H, Liu R, et al. Analyses of gut microbiota and plasma bile acids enable stratification of patients for antidiabetic treatment. *Nat Commun* (2017) 8:1785. doi: 10.1038/s41467-017-01682-2

139. Fujisaka S, Ussar S, Clish C, Devkota S, Dreyfuss JM, Sakaguchi M, et al. Antibiotic effects on gut microbiota and metabolism are host dependent. *J Clin Invest* (2016) 126:4430–43. doi: 10.1172/JCI86674

140. Kaska L, Sledzinski T, Chomiczewska A, Dettlaff-Pokora A, Swierczynski J. Improved glucose metabolism following bariatric surgery is associated with increased circulating bile acid concentrations and remodeling of the gut microbiome. *World J Gastroenterol* (2016) 22:8698–719. doi: 10.3748/wjg.v22.i39.8698

141. Ma K, Saha PK, Chan L, Moore DD. Farnesoid X receptor is essential for normal glucose homeostasis. *J Clin Invest* (2006) 116:1102–9. doi: 10.1172/JCI25604

142. Prawitt J, Abdelkarim M, Stroeve JH, Popescu I, Duez H, Velagapudi VR, et al. Farnesoid X receptor deficiency improves glucose homeostasis in mouse models of obesity. *Diabetes* (2011) 60:1861–71. doi: 10.2337/db11-0030

143. Potthoff MJ, Kliewer SA, Mangelsdorf DJ. Endocrine fibroblast growth factors 15/19 and 21: From feast to famine. *Genes Dev* (2012) 26:312–24. doi: 10.1101/gad.184788.111

144. Lu TT, Makishima M, Repa JJ, Schoonjans K, Kerr TA, Auwerx J, et al. Molecular basis for feedback regulation of bile acid synthesis by nuclear receptors. *Mol Cell* (2000) 6:507–15. doi: 10.1016/s1097-2765(00)00050-2

145. Duran-Sandoval D, Mautino G, Martin G, Percevault F, Barbier O, Fruchart JC, et al. Glucose regulates the expression of the farnesoid X receptor in liver. *Diabetes* (2004) 53:890–8. doi: 10.2337/diabetes.53.4.890

146. Caron S, Huaman Samanez C, Dehondt H, Ploton M, Briand O, Lien F, et al. Farnesoid X receptor inhibits the transcriptional activity of carbohydrate response element binding protein in human hepatocytes. *Mol Cell Biol* (2013) 33:2202–11. doi: 10.1128/MCB.01004-12

147. Trabelsi MS, Daoudi M, Prawitt J, Ducastel S, Touche V, Sayin SI, et al. Farnesoid X receptor inhibits glucagon-like peptide-1 production by enteroendocrine l cells. *Nat Commun* (2015) 6:7629. doi: 10.1038/ncomms8629

148. Popescu IR, Helleboid-Chapman A, Lucas A, Vandewalle B, Dumont J, Bouchaert E, et al. The nuclear receptor FXR is expressed in pancreatic beta-cells and protects human islets from lipotoxicity. *FEBS Lett* (2010) 584:2845–51. doi: 10.1016/j.febslet.2010.04.068

149. Dufer M, Horth K, Wagner R, Schittenhelm B, Prowald S, Wagner TF, et al. Bile acids acutely stimulate insulin secretion of mouse beta-cells *via* farnesoid X receptor activation and K(ATP) channel inhibition. *Diabetes* (2012) 61:1479–89. doi: 10.2337/db11-0815

150. Sun L, Xie C, Wang G, Wu Y, Wu Q, Wang X, et al. Gut microbiota and intestinal FXR mediate the clinical benefits of metformin. *Nat Med* (2018) 24:1919–29. doi: 10.1038/s41591-018-0222-4

151. Mudaliar S, Henry RR, Sanyal AJ, Morrow L, Marschall HU, Kipnes M, et al. Efficacy and safety of the farnesoid X receptor agonist obeticholic acid in patients with type 2 diabetes and nonalcoholic fatty liver disease. *Gastroenterology* (2013) 145:574–82.e1. doi: 10.1053/j.gastro.2013.05.042

152. Steiner C, Othman A, Saely CH, Rein P, Drexel H, von Eckardstein A, et al. Bile acid metabolites in serum: intraindividual variation and associations with coronary heart disease, metabolic syndrome and diabetes mellitus. *PLoS One* (2011) 6:e25006. doi: 10.1371/journal.pone.0025006

153. Parseus A, Sommer N, Sommer F, Caesar R, Molinaro A, Stahlman M, et al. Microbiota-induced obesity requires farnesoid X receptor. *Gut* (2017) 66:429–37. doi: 10.1136/gutjnl-2015-310283

154. Chen X, Lou G, Meng Z, Huang W. TGR5: A novel target for weight maintenance and glucose metabolism. *Exp Diabetes Res* (2011) 2011:853501. doi: 10.1155/2011/853501

155. Thomas C, Gioiello A, Noriega L, Strehle A, Oury J, Rizzo G, et al. TGR5-mediated bile acid sensing controls glucose homeostasis. *Cell Metab* (2009) 10:167–77. doi: 10.1016/j.cmet.2009.08.001

156. Watanabe M, Houten SM, Mataki C, Christoffolete MA, Kim BW, Sato H, et al. Bile acids induce energy expenditure by promoting intracellular thyroid hormone activation. *Nature* (2006) 439:484–9. doi: 10.1038/nature04330

157. Kumar DP, Rajagopal S, Mahavadi S, Mirshahi F, Grider JR, Murthy KS, et al. Activation of transmembrane bile acid receptor TGR5 stimulates insulin secretion in pancreatic beta cells. *Biochem Biophys Res Commun* (2012) 427:600–5. doi: 10.1016/j.bbrc.2012.09.104

158. Kumar DP, Asgharpour A, Mirshahi F, Park SH, Liu S, Imai Y, et al. Activation of transmembrane bile acid receptor TGR5 modulates pancreatic islet alpha cells to promote glucose homeostasis. *J Biol Chem* (2016) 291:6626–40. doi: 10.1074/jbc.M115.699504

159. Pathak P, Xie C, Nichols RG, Ferrell JM, Boehme S, Krausz KW, et al. Intestine farnesoid X receptor agonist and the gut microbiota activate G-protein bile acid receptor-1 signaling to improve metabolism. *Hepatology* (2018) 68:1574–88. doi: 10.1002/hep.29857

160. Wu Q, Liang X, Wang K, Lin J, Wang X, Wang P, et al. Intestinal hypoxia-inducible factor 2alpha regulates lactate levels to shape the gut microbiome and alter thermogenesis. *Cell Metab* (2021) 33:1988–2003.e7. doi: 10.1016/j.cmet.2021.07.007

161. Chaudhari SN, Harris DA, Aliakbarian H, Luo JN, Henke MT, Subramaniam R, et al. Bariatric surgery reveals a gut-restricted TGR5 agonist with anti-diabetic effects. *Nat Chem Biol* (2021) 17:20–9. doi: 10.1038/s41589-020-0604-z

162. Chaudhari SN, Luo JN, Harris DA, Aliakbarian H, Yao L, Paik D, et al. A microbial metabolite remodels the gut-liver axis following bariatric surgery. *Cell Host Microbe* (2021) 29:408–424.e7. doi: 10.1016/j.chom.2020.12.004

163. Ridlon JM. Bariatric surgery stirs symbionts to counteract diabesity by CA (7)Sting a liver-generated bile acid into the mix. *Cell Host Microbe* (2021) 29:320–2. doi: 10.1016/j.chom.2021.02.011

164. Baggio LL, Drucker DJ. Biology of incretins: GLP-1 and GIP. *Gastroenterology* (2007) 132:2131–57. doi: 10.1053/j.gastro.2007.03.054

165. Junker AE, Gluud LL, van Hall G, Holst JJ, Knop FK, Vilsboll T. Effects of glucagon-like peptide-1 on glucagon secretion in patients with non-alcoholic fatty liver disease. *J Hepatol* (2016) 64:908–15. doi: 10.1016/j.jhep.2015.11.014

166. Drucker DJ. Mechanisms of action and therapeutic application of glucagon-like peptide-1. *Cell Metab* (2018) 27:740–56. doi: 10.1016/j.cmet.2018.03.001

167. Vincent RP, Omar S, Ghozlan S, Taylor DR, Cross G, Sherwood RA, et al. Higher circulating bile acid concentrations in obese patients with type 2 diabetes. *Ann Clin Biochem* (2013) 50:360–4. doi: 10.1177/0004563212473450

168. Yoon HS, Cho CH, Yun MS, Jang SJ, You HJ, Kim JH, et al. Akkermansia muciniphila secretes a glucagon-like peptide-1-inducing protein that improves glucose homeostasis and ameliorates metabolic disease in mice. *Nat Microbiol* (2021) 6:563–73. doi: 10.1038/s41564-021-00880-5

169. Cani PD, Knauf C. A newly identified protein from akkermansia muciniphila stimulates GLP-1 secretion. *Cell Metab* (2021) 33:1073–5. doi: 10.1016/j.cmet.2021.05.004

170. Louis P, Hold GL, Flint HJ. The gut microbiota, bacterial metabolites and colorectal cancer. *Nat Rev Microbiol* (2014) 12:661–72. doi: 10.1038/nrmicro3344

171. Morrison DJ, Preston T. Formation of short chain fatty acids by the gut microbiota and their impact on human metabolism. *Gut Microbes* (2016) 7:189–200. doi: 10.1080/19490976.2015.1134082

172. Scott KP, Martin JC, Campbell G, Mayer CD, Flint HJ. Whole-genome transcription profiling reveals genes up-regulated by growth on fucose in the human gut bacterium "Roseburia inulinivorans". *J Bacteriol* (2006) 188:4340–9. doi: 10.1128/JB.00137-06

173. Rey FE, Faith JJ, Bain J, Muehlbauer MJ, Stevens RD, Newgard CB, et al. Dissecting the *in vivo* metabolic potential of two human gut acetogens. *J Biol Chem* (2010) 285:22082–90. doi: 10.1074/jbc.M110.117713

174. Bolognini D, Dedeo D, Milligan G. Metabolic and inflammatory functions of short-chain fatty acid receptors. *Curr Opin Endocr Metab Res* (2021) 16:1–9. doi: 10.1016/j.coemr.2020.06.005

175. Koh A, De Vadder F, Kovatcheva-Datchary P, Backhed F. From dietary fiber to host physiology: Short-chain fatty acids as key bacterial metabolites. *Cell* (2016) 165:1332–45. doi: 10.1016/j.cell.2016.05.041

176. Bindels LB, Dewulf EM, Delzenne NM. GPR43/FFA2: physiopathological relevance and therapeutic prospects. *Trends Pharmacol Sci* (2013) 34:226–32. doi: 10.1016/j.tips.2013.02.002

177. Everard A, Cani PD. Gut microbiota and GLP-1. *Rev Endocr Metab Disord* (2014) 15:189–96. doi: 10.1007/s11154-014-9288-6

178. Parada Venegas D, de la Fuente MK, Landskron G, Gonzalez MJ, Quera R, Dijkstra G, et al. Short chain fatty acids (SCFAs)-mediated gut epithelial and immune regulation and its relevance for inflammatory bowel diseases. *Front Immunol* (2019) 10:277. doi: 10.3389/fimmu.2019.00277

179. Li Z, Yi CX, Katiraei S, Kooijman S, Zhou E, Chung CK, et al. Butyrate reduces appetite and activates brown adipose tissue *via* the gut-brain neural circuit. *Gut* (2018) 67:1269–79. doi: 10.1136/gutjnl-2017-314050

180. Sanna S, van Zuydam NR, Mahajan A, Kurilshikov A, Vich Vila A, Vosa U, et al. Causal relationships among the gut microbiome, short-chain fatty acids and metabolic diseases. *Nat Genet* (2019) 51:600–5. doi: 10.1038/s41588-019-0350-x

181. Byndloss MX, Olsan EE, Rivera-Chavez F, Tiffany CR, Cevallos SA, Lokken KL, et al. Microbiota-activated PPAR-gamma signaling inhibits dysbiotic enterobacteriaceae expansion. *Science* (2017) 357:570–5. doi: 10.1126/science.aam9949

182. Le Roy T, Moens de Hase E, Van Hul M, Paquot A, Pelicaen R, Regnier M, et al. Dysosmobacter welbionis is a newly isolated human commensal bacterium preventing diet-induced obesity and metabolic disorders in mice. *Gut* (2022) 71:534–43. doi: 10.1136/gutjnl-2020-323778

183. Teixeira TF, Grzeskowiak L, Franceschini SC, Bressan J, Ferreira CL, Peluzio MC. Higher level of faecal SCFA in women correlates with metabolic syndrome risk factors. *Br J Nutr* (2013) 109:914–9. doi: 10.1017/S0007114512002723

184. Gaggini M, Carli F, Rosso C, Buzzigoli E, Marietti M, Della Latta V, et al. Altered amino acid concentrations in NAFLD: Impact of obesity and insulin resistance. *Hepatology* (2018) 67:145–58. doi: 10.1002/hep.29465

185. Newgard CB, An J, Bain JR, Muehlbauer MJ, Stevens RD, Lien LF, et al. A branched-chain amino acid-related metabolic signature that differentiates obese and lean humans and contributes to insulin resistance. *Cell Metab* (2009) 9:311–26. doi: 10.1016/j.cmet.2009.02.002

186. Yu D, Richardson NE, Green CL, Spicer AB, Murphy ME, Flores V, et al. The adverse metabolic effects of branched-chain amino acids are mediated by isoleucine and valine. *Cell Metab* (2021) 33:905–922.e6. doi: 10.1016/j.cmet.2021.03.025

187. Lynch CJ, Adams SH. Branched-chain amino acids in metabolic signalling and insulin resistance. *Nat Rev Endocrinol* (2014) 10:723–36. doi: 10.1038/nrendo.2014.171

188. Wurtz P, Tiainen M, Makinen VP, Kangas AJ, Soininen P, Saltevo J, et al. Circulating metabolite predictors of glycemia in middle-aged men and women. *Diabetes Care* (2012) 35:1749–56. doi: 10.2337/dc11-1838

189. Wurtz P, Soininen P, Kangas AJ, Ronnemaa T, Lehtimaki T, Kahonen M, et al. Branched-chain and aromatic amino acids are predictors of insulin resistance in young adults. *Diabetes Care* (2013) 36:648–55. doi: 10.2337/dc12-0895

190. Dodd D, Spitzer MH, Van Treuren W, Merrill BD, Hryckowian AJ, Higginbottom SK, et al. A gut bacterial pathway metabolizes aromatic amino acids into nine circulating metabolites. *Nature* (2017) 551:648–52. doi: 10.1038/nature24661

191. He K, Du S, Xun P, Sharma S, Wang H, Zhai F, et al. Consumption of monosodium glutamate in relation to incidence of overweight in Chinese adults: China health and nutrition survey (CHNS). *Am J Clin Nutr* (2011) 93:1328–36. doi: 10.3945/ajcn.110.008870

192. Yoo W, Zieba JK, Foegeding NJ, Torres TP, Shelton CD, Shealy NG, et al. High-fat diet-induced colonocyte dysfunction escalates microbiota-derived trimethylamine n-oxide. *Science* (2021) 373:813–8. doi: 10.1126/science.aba3683

193. Hoyles L, Jimenez-Pranteda ML, Chilloux J, Brial F, Myridakis A, Aranias T, et al. Metabolic retroconversion of trimethylamine n-oxide and the gut microbiota. *Microbiome* (2018) 6:73. doi: 10.1186/s40168-018-0461-0

194. Molinaro A, Bel Lassen P, Henricsson M, Wu H, Adriouch S, Belda E, et al. Imidazole propionate is increased in diabetes and associated with dietary patterns and altered microbial ecology. *Nat Commun* (2020) 11:5881. doi: 10.1038/s41467-020-19589-w

195. de Mello VD, Paananen J, Lindstrom J, Lankinen MA, Shi L, Kuusisto J, et al. Indolepropionic acid and novel lipid metabolites are associated with a lower risk of type 2 diabetes in the Finnish diabetes prevention study. *Sci Rep* (2017) 7:46337. doi: 10.1038/srep46337

196. Valdes AM, Walter J, Segal E, Spector TD. Role of the gut microbiota in nutrition and health. *BMJ* (2018) 361:k2179. doi: 10.1136/bmj.k2179

197. Hill C, Guarner F, Reid G, Gibson GR, Merenstein DJ, Pot B, et al. Expert consensus document. The international scientific association for probiotics and prebiotics consensus statement on the scope and appropriate use of the term probiotic. *Nat Rev Gastroenterol Hepatol* (2014) 11:506–14. doi: 10.1038/nrgastro.2014.66

198. Sanders ME, Merenstein DJ, Reid G, Gibson GR, Rastall RA. Probiotics and prebiotics in intestinal health and disease: from biology to the clinic. *Nat Rev Gastroenterol Hepatol* (2019) 16:605–16. doi: 10.1038/s41575-019-0173-3

199. Won G, Choi SI, Kang CH, Kim GH. Lactiplantibacillus plantarum MG4296 and Lacticaseibacillus paracasei MG5012 Ameliorates Insulin Resistance in Palmitic Acid-Induced HepG2 Cells and High Fat Diet-Induced Mice. *Microorganisms* (2021) 9:1139. doi: 10.3390/microorganisms9061139

200. Zhao S, Liu W, Wang J, Shi J, Sun Y, Wang W, et al. Akkermansia muciniphila improves metabolic profiles by reducing inflammation in chow diet-fed mice. *J Mol Endocrinol* (2017) 58:1–14. doi: 10.1530/JME-16-0054

201. Zmora N, Zilberman-Schapira G, Suez J, Mor U, Dori-Bachash M, Bashiardes S, et al. Personalized gut mucosal colonization resistance to empiric probiotics is associated with unique host and microbiome features. *Cell* (2018) 174:1388–405.e21. doi: 10.1016/j.cell.2018.08.041

202. Suez J, Zmora N, Zilberman-Schapira G, Mor U, Dori-Bachash M, Bashiardes S, et al. Post-antibiotic gut mucosal microbiome reconstitution is impaired by probiotics and improved by autologous FMT. *Cell* (2018) 174:1406–23.e16. doi: 10.1016/j.cell.2018.08.047

203. Wang Y, Dilidaxi D, Wu Y, Sailike J, Sun X, Nabi XH. Composite probiotics alleviate type 2 diabetes by regulating intestinal microbiota and inducing GLP-1 secretion in db/db mice. *BioMed Pharmacother* (2020) 125:109914. doi: 10.1016/j.biopha.2020.109914

204. Tonucci LB, Olbrich Dos Santos KM, Licursi de Oliveira L, Rocha Ribeiro SM, Duarte Martino HS. Clinical application of probiotics in type 2 diabetes mellitus: A randomized, double-blind, placebo-controlled study. *Clin Nutr* (2017) 36:85–92. doi: 10.1016/j.clnu.2015.11.011

205. Rittiphairoj T, Pongpirul K, Janchot K, Mueller NT, Li T. Probiotics contribute to glycemic control in patients with type 2 diabetes mellitus: A systematic review and meta-analysis. *Adv Nutr* (2021) 12:722–34. doi: 10.1093/advances/nmaa133

206. Tao YW, Gu YL, Mao XQ, Zhang L, Pei YF. Effects of probiotics on type II diabetes mellitus: a meta-analysis. *J Transl Med* (2020) 18:30. doi: 10.1186/s12967-020-02213-2

207. Kocsis T, Molnar B, Nemeth D, Hegyi P, Szakacs Z, Balint A, et al. Probiotics have beneficial metabolic effects in patients with type 2 diabetes mellitus: a meta-analysis of randomized clinical trials. *Sci Rep* (2020) 10:11787. doi: 10.1038/s41598-020-68440-1

208. Gibson GR, Hutkins R, Sanders ME, Prescott SL, Reimer RA, Salminen SJ, et al. Expert consensus document: The international scientific association for probiotics and prebiotics (ISAPP) consensus statement on the definition and scope of prebiotics. *Nat Rev Gastroenterol Hepatol* (2017) 14:491–502. doi: 10.1038/nrgastro.2017.75

209. Brodmann T, Endo A, Gueimonde M, Vinderola G, Kneifel W, de Vos WM, et al. Safety of novel microbes for human consumption: Practical examples of assessment in the European union. *Front Microbiol* (2017) 8:1725. doi: 10.3389/fmicb.2017.01725

210. Miller LE, Zimmermann AK, Ouwehand AC. Contemporary meta-analysis of short-term probiotic consumption on gastrointestinal transit. *World J Gastroenterol* (2016) 22:5122–31. doi: 10.3748/wjg.v22.i21.5122

211. Zhang F, Cui B, He X, Nie Y, Wu K, Fan D, et al. Microbiota transplantation: Concept, methodology and strategy for its modernization. *Protein Cell* (2018) 9:462–73. doi: 10.1007/s13238-018-0541-8

212. Allegretti JR, Kassam Z, Osman M, Budree S, Fischer M, Kelly CR. The 5D framework: a clinical primer for fecal microbiota transplantation to treat clostridium difficile infection. *Gastrointest Endosc* (2018) 87:18–29. doi: 10.1016/j.gie.2017.05.036

213. van Nood E, Vrieze A, Nieuwdorp M, Fuentes S, Zoetendal EG, de Vos WM, et al. Duodenal infusion of donor feces for recurrent clostridium difficile. *N Engl J Med* (2013) 368:407–15. doi: 10.1056/NEJMoa1205037

214. Cui B, Li P, Xu L, Zhao Y, Wang H, Peng Z, et al. Step-up fecal microbiota transplantation strategy: A pilot study for steroid-dependent ulcerative colitis. *J Transl Med* (2015) 13:298. doi: 10.1186/s12967-015-0646-2

215. Bak SH, Choi HH, Lee J, Kim MH, Lee YH, Kim JS, et al. Fecal microbiota transplantation for refractory crohn's disease. *Intest Res* (2017) 15:244–8. doi: 10.5217/ir.2017.15.2.244

216. Johnsen PH, Hilpusch F, Cavanagh JP, Leikanger IS, Kolstad C, Valle PC, et al. Faecal microbiota transplantation versus placebo for moderate-to-severe irritable bowel syndrome: A double-blind, randomised, placebo-controlled, parallel-group, single-centre trial. *Lancet Gastroenterol Hepatol* (2018) 3:17–24. doi: 10.1016/S2468-1253(17)30338-2

217. He Z, Cui BT, Zhang T, Li P, Long CY, Ji GZ, et al. Fecal microbiota transplantation cured epilepsy in a case with crohn's disease: The first report. *World J Gastroenterol* (2017) 23:3565–8. doi: 10.3748/wjg.v23.i19.3565

218. Tao Y, Mao X, Xie Z, Ran X, Liu X, Wang Y, et al. The prevalence of type 2 diabetes and hypertension in uygur and kazak populations. *Cardiovasc Toxicol* (2008) 8:155–9. doi: 10.1007/s12012-008-9024-0

219. Zhang PP, Li LL, Han X, Li QW, Zhang XH, Liu JJ, et al. Fecal microbiota transplantation improves metabolism and gut microbiome composition in db/db mice. *Acta Pharmacol Sin* (2020) 41:678–85. doi: 10.1038/s41401-019-0330-9

220. Sonne DP, van Nierop FS, Kulik W, Soeters MR, Vilsboll T, Knop FK. Postprandial plasma concentrations of individual bile acids and FGF-19 in patients with type 2 diabetes. *J Clin Endocrinol Metab* (2016) 101:3002–9. doi: 10.1210/jc.2016-1607

221. Khanna S, Kraft CS. Fecal microbiota transplantation: Tales of caution. *Clin Infect Dis* (2021) 72:e881–2. doi: 10.1093/cid/ciaa1492

222. Yu EW, Gao L, Stastka P, Cheney MC, Mahabamunuge J, Torres Soto M, et al. Fecal microbiota transplantation for the improvement of metabolism in obesity: The FMT-TRIM double-blind placebo-controlled pilot trial. *PLoS Med* (2020) 17:e1003051. doi: 10.1371/journal.pmed.1003051

223. Alang N, Kelly CR. Weight gain after fecal microbiota transplantation. *Open Forum Infect Dis* (2015) 2:ofv004. doi: 10.1093/ofid/ofv004

224. Waisundara VY, Siu SY, Hsu A, Huang D, Tan BK. Baicalin upregulates the genetic expression of antioxidant enzymes in type-2 diabetic goto-kakizaki rats. *Life Sci* (2011) 88:1016–25. doi: 10.1016/j.lfs.2011.03.009

225. Zhao L, Ma P, Peng Y, Wang M, Peng C, Zhang Y, et al. Amelioration of hyperglycaemia and hyperlipidaemia by adjusting the interplay between gut microbiota and bile acid metabolism: Radix scutellariae as a case. *Phytomedicine* (2021) 83:153477. doi: 10.1016/j.phymed.2021.153477

226. Zhang Y, Xu Y, Zhang L, Chen Y, Wu T, Liu R, et al. Licorice extract ameliorates hyperglycemia through reshaping gut microbiota structure and inhibiting TLR4/NF-kappaB signaling pathway in type 2 diabetic mice. *Food Res Int* (2022) 153:110945. doi: 10.1016/j.foodres.2022.110945

227. Zhang CH, Sheng JQ, Sarsaiya S, Shu FX, Liu TT, Tu XY, et al. The anti-diabetic activities, gut microbiota composition, the anti-inflammatory effects of scutellaria-coptis herb couple against insulin resistance-model of diabetes involving the toll-like receptor 4 signaling pathway. *J Ethnopharmacol* (2019) 237:202–14. doi: 10.1016/j.jep.2019.02.040

228. Li XW, Chen HP, He YY, Chen WL, Chen JW, Gao L, et al. Effects of rich-polyphenols extract of dendrobium loddigesii on anti-diabetic, anti-inflammatory, anti-oxidant, and gut microbiota modulation in db/db mice. *Molecules* (2018) 23:3254. doi: 10.3390/molecules23123245

229. Xu X, Gao Z, Yang F, Yang Y, Chen L, Han L, et al. Antidiabetic effects of gegen qinlian decoction *via* the gut microbiota are attributable to its key ingredient berberine. *Genomics Proteomics Bioinf* (2020) 18:721–36. doi: 10.1016/j.gpb.2019.09.007

230. Habtemariam S. Berberine pharmacology and the gut microbiota: A hidden therapeutic link. *Pharmacol Res* (2020) 155:104722. doi: 10.1016/j.phrs.2020.104722

231. Huang J, Guan B, Lin L, Wang Y. Improvement of intestinal barrier function, gut microbiota, and metabolic endotoxemia in type 2 diabetes rats by curcumin. *Bioengineered* (2021) 12:11947–58. doi: 10.1080/21655979.2021.2009322

232. Gao Y, Li J, Wang J, Li X, Li J, Chu S, et al. Ginsenoside Rg1 prevent and treat inflammatory diseases: A review. *Int Immunopharmacol* (2020) 87:106805. doi: 10.1016/j.intimp.2020.106805

233. Wei Y, Yang H, Zhu C, Deng J, Fan D. Hypoglycemic effect of ginsenoside Rg5 mediated partly by modulating gut microbiota dysbiosis in diabetic db/db mice. *J Agric Food Chem* (2020) 68:5107–17. doi: 10.1021/acs.jafc.0c00605

234. Zeng SL, Li SZ, Xiao PT, Cai YY, Chu C, Chen BZ, et al. Citrus polymethoxyflavones attenuate metabolic syndrome by regulating gut microbiome and amino acid metabolism. *Sci Adv* (2020) 6:eaax6208. doi: 10.1126/sciadv.aax6208

235. Yang X, Dong B, An L, Zhang Q, Chen Y, Wang H, et al. Ginsenoside Rb1 ameliorates glycemic disorder in mice with high fat diet-induced obesity *via* regulating gut microbiota and amino acid metabolism. *Front Pharmacol* (2021) 12:756491. doi: 10.3389/fphar.2021.756491

236. Magkos F, Hjorth MF, Astrup A. Diet and exercise in the prevention and treatment of type 2 diabetes mellitus. *Nat Rev Endocrinol* (2020) 16:545–55. doi: 10.1038/s41574-020-0381-5

237. O'Keefe SJ. The association between dietary fibre deficiency and high-income lifestyle-associated diseases: Burkitt's hypothesis revisited. *Lancet Gastroenterol Hepatol* (2019) 4:984–96. doi: 10.1016/S2468-1253(19)30257-2

238. David LA, Maurice CF, Carmody RN, Gootenberg DB, Button JE, Wolfe BE, et al. Diet rapidly and reproducibly alters the human gut microbiome. *Nature* (2014) 505:559–63. doi: 10.1038/nature12820

239. O'Grady J, O'Connor EM, Shanahan F. Review article: dietary fibre in the era of microbiome science. *Aliment Pharmacol Ther* (2019) 49:506–15. doi: 10.1111/apt.15129

240. Ojo O, Feng QQ, Ojo OO, Wang XH. The role of dietary fibre in modulating gut microbiota dysbiosis in patients with type 2 diabetes: A systematic review and meta-analysis of randomised controlled trials. *Nutrients* (2020) 12:3239. doi: 10.3390/nu12113239

241. Ojo O, Wang XH, Ojo OO, Adegboye ARA. The effects of almonds on gut microbiota, glycometabolism, and inflammatory markers in patients with type 2 diabetes: A systematic review and meta-analysis of randomised controlled trials. *Nutrients* (2021) 13:3377. doi: 10.3390/nu13103377

242. Rinott E, Meir AY, Tsaban G, Zelicha H, Kaplan A, Knights D, et al. The effects of the green-Mediterranean diet on cardiometabolic health are linked to gut microbiome modifications: A randomized controlled trial. *Genome Med* (2022) 14:29. doi: 10.1186/s13073-022-01015-z

243. Zaharieva DP, McGaugh S, Davis EA, Riddell MC. Advances in exercise, physical activity, and diabetes. *Diabetes Technol Ther* (2020) 22:S109–18. doi: 10.1089/dia.2020.2508

244. Clarke SF, Murphy EF, O'Sullivan O, Lucey AJ, Humphreys M, Hogan A, et al. Exercise and associated dietary extremes impact on gut microbial diversity. *Gut* (2014) 63:1913–20. doi: 10.1136/gutjnl-2013-306541

245. Yang L, Lin H, Lin W, Xu X. Exercise ameliorates insulin resistance of type 2 diabetes through motivating short-chain fatty acid-mediated skeletal muscle cell autophagy. *Biol (Basel)* (2020) 9:203. doi: 10.3390/biology9080203

246. Valder S, Brinkmann C. Exercise for the diabetic gut-potential health effects and underlying mechanisms. *Nutrients* (2022) 14:203. doi: 10.3390/nu14040813

247. Allen JM, Mailing LJ, Niemiro GM, Moore R, Cook MD, White BA, et al. Exercise alters gut microbiota composition and function in lean and obese humans. *Med Sci Sports Exerc* (2018) 50:747–57. doi: 10.1249/MSS.0000000000001495

248. O'Sullivan O, Cronin O, Clarke SF, Murphy EF, Molloy MG, Shanahan F, et al. Exercise and the microbiota. *Gut Microbes* (2015) 6:131–6. doi: 10.1080/19490976.2015.1011875

249. Tremaroli V, Backhed F. Functional interactions between the gut microbiota and host metabolism. *Nature* (2012) 489:242–9. doi: 10.1038/nature11552

250. Musso G, Gambino R, Cassader M. Interactions between gut microbiota and host metabolism predisposing to obesity and diabetes. *Annu Rev Med* (2011) 62:361–80. doi: 10.1146/annurev-med-012510-175505

251. de Groot PF, Belzer C, Aydin O, Levin E, Levels JH, Aalvink S, et al. Distinct fecal and oral microbiota composition in human type 1 diabetes, an observational study. *PLoS One* (2017) 12:e0188475. doi: 10.1371/journal.pone.0188475

252. Tolhurst G, Heffron H, Lam YS, Parker HE, Habib AM, Diakogiannaki E, et al. Short-chain fatty acids stimulate glucagon-like peptide-1 secretion *via* the G-protein-coupled receptor FFAR2. *Diabetes* (2012) 61:364–71. doi: 10.2337/db11-1019

253. Canfora EE, Jocken JW, Blaak EE. Short-chain fatty acids in control of body weight and insulin sensitivity. *Nat Rev Endocrinol* (2015) 11:577–91. doi: 10.1038/nrendo.2015.128

frontiers | Frontiers in Endocrinology

TYPE Mini Review
PUBLISHED 22 August 2022
DOI 10.3389/fendo.2022.929530

OPEN ACCESS

EDITED BY
Hannelouise Kissow,
University of Copenhagen, Denmark

REVIEWED BY
Francesca Abbatini,
Azienda Sanitaria Locale Roma 6, Italy

*CORRESPONDENCE
Wendong Huang
whuang@coh.org

SPECIALTY SECTION
This article was submitted to Gut Endocrinology, a section of the journal Frontiers in Endocrinology

RECEIVED 27 April 2022
ACCEPTED 02 August 2022
PUBLISHED 22 August 2022

CITATION
Tu J, Wang Y, Jin L and Huang W (2022) Bile acids, gut microbiota and metabolic surgery. *Front. Endocrinol.* 13:929530. doi: 10.3389/fendo.2022.929530

Bile acids, gut microbiota and metabolic surgery

Jui Tu[1,2], Yangmeng Wang[1], Lihua Jin[1] and Wendong Huang[1,2]*

[1]Department of Diabetes Complications and Metabolism, Arthur Riggs Diabetes and Metabolism Research Institute, Beckman Research Institute, City of Hope National Medical Center, Duarte, CA, United States, [2]Irell & Manella Graduate School of Biomedical Science, City of Hope National Medical Center, Duarte, CA, United States

Metabolic surgery, or bariatric surgery, is currently the most effective approach for treating obesity and its complications. Vertical sleeve gastrectomy (VSG) and Roux-en-Y gastric bypass (RYGB) are the top two types of commonly performed metabolic surgery now. The precise mechanisms of how the surgeries work are still unclear, therefore much research has been conducted in this area. Gut hormones such as GLP-1 and PYY have been studied extensively in the context of metabolic surgery because they both participate in satiety and glucose homeostasis. Bile acids, whose functions cover intestinal lipid absorption and various aspects of metabolic regulation *via* the action of FXR, TGR5, and other bile acid receptors, have also been actively investigated as potential mediators of metabolic surgery. Additionally, gut microbiota and their metabolites have also been studied because they can affect metabolic health. The current review summarizes and compares the recent scientific progress made on identifying the mechanisms of RYGB and VSG. One of the long-term goals of metabolic/bariatric surgery research is to develop new pharmacotherapeutic options for the treatment of obesity and diabetes. Because obesity is a growing health concern worldwide, there is a dire need in developing novel non-invasive treatment options.

KEYWORDS

bile acid, gut microbiota, metabolic surgery, obesity, diabetes, bariatric surgery

Introduction

Obesity imposes significant healthcare burden worldwide. The World Health Organization reports that the current number of individuals who have obesity has increased by three-fold since 1975. In 2016, 39% of the adults worldwide were overweight (1). In the United States alone, 20% of the adults had obesity in 2019 (2). These numbers are alarming; according to one report, people who have class III obesity (body mass index, or BMI, ≥40 kg/m^2) could lose up to almost 14 years in life expectancy (3). There are several comorbidities associated with obesity, such as hypertension, dyslipidemia,

cardiovascular diseases, and type 2 diabetes mellitus (T2D) (4, 5). T2D affects many people in the US. The "National Diabetes Statistics Report, 2020" published by the Center for Disease Control and Prevention reports that approximately 34.1 million of adults have diabetes, and T2D accounts for 90-95% of those cases (6).

Treatments of T2D include lifestyle intervention, pharmacotherapies, and bariatric surgery (7). The term "bariatric surgery" is gradually being replaced by "metabolic surgery" because the surgery is not only recommended for the treatment of obesity, but also other metabolic diseases (8). There are several kinds of metabolic surgery: gastric banding, sleeve gastrectomy (SG; or vertical sleeve gastrectomy, VSG) Roux-en-Y gastric bypass (RYGB), and several others. Right now, VSG and RYGB are the most frequently performed metabolic surgical procedures globally, and the number of VSG performed has been steadily increasing in the US (9). RYGB is the more technically complicated surgery of the two. In brief, the stomach is first divided into two portions: the smaller, proximal pouch, and the larger, distal pouch. Then, the jejunum is cut, and the distal end is anastomosed with the small gastric pouch. The proximal end of the cut jejunum is anastomosed to the rest of the jejunum, distal to the jejunal limb that is anastomosed to the small gastric pouch (Figure 1A) (10). The VSG surgery is simpler: approximately 75-80% of the stomach is removed along the greater curvature, leaving a sleeve-like gastric pouch (10, 11). VSG is also often referred to as LSG (laparoscopic sleeve gastrectomy) or simply SG (sleeve gastrectomy). For the sake of consistency, "VSG" will be used throughout the rest of the text, even when referencing publications that originally use a different terminology.

Generally, metabolic surgery is recommended to patients with BMI ≥40 kg/m^2 (BMI ≥ 37.5 kg/m^2 for Asian Americans), and who have not successfully achieved adequate weight loss and management of comorbidities (7). While metabolic surgeries are effective, they are not without risks and complications. Intra-operative complications such as bleeding and leakage, and post-operative complications such as hair loss, bone loss, and nutrient deficiency, could all burden patients (11–14). Therefore, there is a clear medical need to identify the underlying mechanisms of action of metabolic surgery, so that new pharmacotherapy options can be developed for treating obesity, T2D, and other metabolic diseases. This review will summarize in the following sections the recent progress made in metabolic surgery research that is related to gut hormones, bile acids and their receptors, and gut microbiota.

Gut hormones

The feedback loop of hunger, eating, feeling of satiety, and the inhibition of eating behavior is intricately regulated by hormones and peptides (15). Therefore, studying changes in these hormones and peptides after metabolic surgery may provide clues for how the surgery works. Glucagon-like peptide-1 (GLP-1) and peptide tyrosine tyrosine (PYY) are two gastrointestinal hormones that are frequently investigated in metabolic surgery research. GLP-1 is produced by the brainstem and the L cells in the small intestine, and then released upon ingestion of a meal. The release of GLP-1 leads to insulin secretion, reduced hepatic glucose production, reduced food intake, and slowed gastric emptying (16, 17). PYY is also released by the L-cells at the distal small intestine and colon after a meal. Similar to GLP-1, PYY release leads to decreased gastric emptying and suppressed pancreatic secretion (16). In most VSG and RYGB studies, GLP-1 and PYY levels are found to be elevated after the surgeries. In studies done in rats and mice, GLP-1 level was elevated after VSG and RYGB (18, 19). Numerous studies done in humans show similar findings. GLP-1 and PYY are increased after both VSG and RYGB in

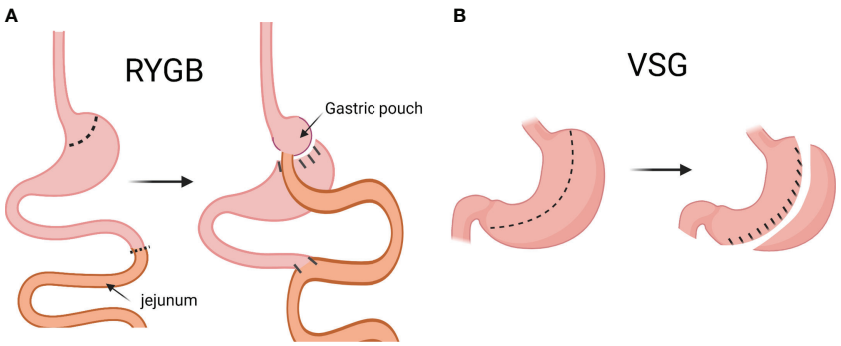

FIGURE 1
Graphical description of Roux-en-Y gastric bypass (RYGB) and vertical sleeve gastrectomy (VSG). In RYGB, the jejunum is cut, and the distal end is anastomosed to the small gastric pouch, and the proximal end is anastomosed to the rest of the jejunum **(A)**. In VSG, approximately 75-80% of the stomach is removed along the greater curvature to create a sleeve-like gastric pouch **(B)**. (Created with BioRender.com).

human patients (20–22), and a systemic review reports that GLP-1 and PYY increased in VSG patients about one year after the surgery (23). A prospective study by Arakawa et al. in human patients also reported that there was a temporal relationship between gut hormone changes and metabolic surgery (24). The authors reported that postprandial GLP-1 level increased in both VSG and RYGB patients at 26 weeks after the surgery. For RYGB patients, their postprandial GLP-1 level was still elevated at 26 weeks after the surgery, and the elevation persisted at 52 weeks after the surgery (24).

Current evidence seems to suggest that gut hormones play important roles in the mechanisms behind metabolic surgery. How VSG and RYGB lead to increase in GLP-1 is believed to be through the alteration in anatomy. GLP-1 production is higher in the distal intestinal tract, and its release is stimulated by carbohydrates, fats, and protein (25). Larraufie et al. found that VSG shortened gastrointestinal transit time of nutrients in mice, and the finding was correlated with an increase in GLP-1 release (26). Further investigation into the roles that gut hormones play in metabolic surgery is needed for finding out how to exploit their therapeutic potential for the treatment of obesity and its comorbidities.

Bile acids and their receptors

Bile acids are fascinating molecules because they participate in many biological functions. The synthesis of bile acids takes place in the liver, starting with cholesterol. Cholesterol is hydroxylated and modified by several sterol hydroxylases that act on different positions of the cholesterol's carbon structure. The result is a large variety of bile acid molecules with different degrees of hydrophobicity (27, 28). Traditionally, bile acids are known for their roles in dietary lipid absorption. Upon ingestion of a meal, bile acids are released into the duodenum to begin the process of lipid absorption by emulsifying the lipids (29). When bile acids reach the ileum, they are re-absorbed and circulated back to the liver *via* enterohepatic circulation. The reabsorption of bile acids is very efficient; about 95% of the total bile acid pool is reabsorbed daily, and the rest is excreted in feces and urine (28, 30). Besides lipid absorption, bile acids also function as signaling molecules. Farnesoid X receptor (FXR) and Tekeda-G-protein receptor 5 (TGR5) are two major receptors of bile acids, and their functions will be discussed in a later section (28, 31). Bile acids also interact with gut microbiota; the bi-directional relationship between bile acids and gut microbiota allows them to influence each other's composition (32). Therefore, bile acids have received substantial interest from the medical and research communities for their therapeutic potential in metabolic diseases.

The roles that bile acids play in metabolic surgery will be discussed in two sections below: Bile Acids, and the Receptors of Bile Acids.

Bile acids

The composition and kinetics of bile acids have been studied in the context of metabolic surgery in both rodent models and humans. Many studies report that metabolic surgery and its metabolic improvements are associated with the elevation of bile acids in the circulation. Nakatani et al. studied adult obese patients who underwent one of the following metabolic surgeries laparoscopically: RYGB, VSG with duodenal jejunal bypass, VSG, and adjustable gastric banding. The authors found that serum bile acids increased after surgery (33). However, Nakatani et al. did not analyze the surgery types separately. In a later study, Patti et al. focused their study scope on RYGB only, and they also found that total bile acids was significantly higher in individuals who had RYGB than those who were overweight or severely obese (34). The findings in VSG are a bit more varied. A study done in rodents reported that total serum bile acids increased after VSG (35), but a meta-analysis showed that total serum bile acids did not increase in human subjects after VSG (36). In another study by Chen *et al*, the authors reported that after human patients received RYGB and VSG, total bile acids in the blood was increased at both three days and three months after surgery (37).

To better understand the relationship between bile acids and metabolic surgery, it is important to not only look at total serum bile acids level, but also at the alteration of the bile acid composition after metabolic surgery. Ding et al. found that while the total serum bile acids did not change significantly in mice after VSG, the composition of bile acids did: the concentration of taurine-conjugated bile acids increased in the serum after VSG (38). A study done by Wu et al. in a diabetic rat model also reports that besides elevation in total serum bile acids, taurine-conjugated bile acids were elevated after VSG as well (39). One pattern of post-metabolic surgery alteration in bile acid composition that has recently received some attention is the change in the ratio between 12-alpha-hydroxylated (12-α-OH) bile acids and non-12-α-OH bile acids. 12-α-OH and non-12-α-OH bile acids are two major classes of bile acids. In humans, cholic acid (CA), one of the two primary bile acids, is a 12-α-OH BA. The other primary bile acid, chenodeoxycholic acid (CDCA), is a non-12-α-OH bile acids (32). In mice, most members of the non-12-α-OH bile acids are in the form of muricholic acids (MCA) and its associated forms. The ratio between the two classes is determined by the activity of a bile acid synthesis enzyme named sterol-12α-hydroxylase (CYP8B1) because CYP8B1 catalyzes the production of CA (28). High 12-α-OH: non-12-α-OH ratio has been shown to be associated with insulin resistance and obesity in both humans and rodents (40, 41). Rats fed with a Western-style diet were found to produce more 12-α-OH bile acids (42), and mice that were deficient in CYP8B1 were found to be resistant to obesity induced by high-fat diet-feeding due to decreased lipid absorption (43). A recent

study performed on a large cohort of VSG patients demonstrated that after the surgery, serum level of CA decreased (a 12-α-OH bile acid), and serum level of taurine-conjugated lithocholic acid (LCA; a non-12-α-OH bile acid) increased (44). Another study reports similar findings: the levels of non-12-α-OH bile acids increased in both RYGB and VSG patients one year after surgery, and the increase was greater in RYGB patients (45). On the contrary, a meta-analysis published by Zhang et al. revealed that after RYGB, the ratio of 12-α-OH: non-12-α-OH bile acids increased instead of decreased in human subjects (36).

Although it is not yet clear why there are differing reports on the post-surgery bile acids composition between RYGB and VSG, what is clear is that the currently available evidence supports the notion that total serum bile acids level and bile acids composition are linked to metabolic surgery. Further research is needed to define how specific bile acids species mediate the health benefits of metabolic surgery. The following section on the functions of bile acids will further underscore the reason for their importance in metabolic surgery research.

Receptors of bile acids

Bile acids interact with several receptors to regulate physiologic pathways. Different species of bile acids possess different affinity for the receptors. For example, primary bile acids CDCA and CA are potent ligands for FXR, and secondary bile acids like LCA and DCA are potent ligands for TGR5 (46). Therefore, it is crucial to include the receptors in the discussion of how metabolic surgeries work through bile acids.

FXR is a nuclear receptor highly expressed in the liver and the intestine, where bile acids can bind to it directly (47). FXR regulates many genes that are involved in various aspects of metabolism, such as bile acids synthesis and transport, gluconeogenesis, lipogenesis, and fatty acid oxidation, *etc.* (47). Therefore, FXR has been studied extensively in metabolic surgery research. Rodent models are extremely valuable here because they allow genetic modifications to be made, and the collection of tissues for gene and protein expression analysis. Some studies suggest that FXR is required for the success of the surgery. Ryan et al. found that while VSG was successful in bringing significant weight loss to obese WT mice, it failed to do the same in mice deficient of FXR (48). Another group investigated the role of FXR in RYGB surgery: Kong et al. performed RYGB on spontaneous diabetic Goto-Kakizaki rats, and found that CDCA, a potent agonist of FXR, was increased in serum significantly after RYGB (49). The capacity of pancreatic β-cells to secrete insulin also increased after RYGB. However, when RYGB was performed in FXR-deficient mice, their pancreatic β-cells did not improve in insulin secretion (49). On the other hand, some publications report that FXR is not required for metabolic surgery to bring forth metabolic improvement. Li et al. showed that RYGB induced loss of body weight in both WT and FXR-deficient mice (50), even though FXR-deficient mice did not improve in glycemic control following RYGB the same way that WT mice did. By using mice that were deficient in FXR specifically in the liver and the intestine, Ding et al. reported that VSG was still able to improve metabolic parameters in mice (51). The study also shows that perhaps instead of FXR, the decreased intestinal bile acid level and subsequently decreased lipid absorption are part of the underlying mechanism of metabolic surgery.

The variability in the reports of how FXR plays a role in metabolic surgery is not surprising, considering the wide range of its tissue expression and physiologic processes that it mediates. Therefore, analysis of FXR's downstream targets may be a good direction for finding the underlying mechanisms of metabolic surgery (52). One such target is the gut-derived hormone fibroblast growth factor (FGF) 15 or 19 (FGF15 in mice, and FGF19 in humans). FGF15/19 is produced by the enterocytes in the ileum, and it is released after FXR activation. Once released, FGF15/19 then enters the circulation to reach the liver, where it can bind to its receptor FGFR4. Finally, FGF15/19 completes the negative feedback loop of bile acids synthesis by suppressing the rate-limiting enzyme of bile acids synthesis in the liver, CYP7A1 (28, 46, 52). The significance of FGF15/19 in metabolic surgery has been investigated in both animal and human studies. In FGF15-deficient mice, VSG caused significant weight loss but did not improve glucose tolerance (35). In human patients that received VSG or RYGB, Chen et al. found that FGF19 levels increased at three days following both surgeries. However, by three months after the surgeries, the levels were no longer different between the groups (37). In another study that followed up with patients one year after VSG and RYGB, Nemati et al. reported that FGF19 increased after both VSG and RYGB, and the level of increase was similar between the two groups (45). Additionally, the increase of FGF19 was found to be correlated with T2D improvement. Available evidence suggests that it is worthwhile to investigate FGF15/19 further as a potential player behind metabolic surgery.

Besides FXR, another receptor that bile acids interact with is TGR5. Unlike FXR, TGR5 is a membrane-bound G protein-coupled receptor. Activation of TGR5 leads to the stimulation of adenylate cyclase, production of cAMP, then finally activation of protein kinase A. These processes lead to the modulation of various inflammation and metabolism functions, such as bile acids homeostasis, GLP-1 production, insulin sensitivity, and energy expenditure (47). In contrast to FXR, TGR5 has stronger affinity for secondary bile acids (LCA more than DCA) than primary bile acids. Taurine-conjugated bile acids also produce higher potency at TGR5 than unconjugated and glycine-conjugated bile acids (46). TGR5 mediates the outcome of metabolic surgery in the aspects of glucose regulation and bile acid composition. Mice that were deficient in TGR5 showed dampened response to VSG in their metabolic improvements compared to the WT control mice (38).

Moreover, McGavigan et al. found that the shift in bile acids composition that is usually observed after VSG surgery, namely, the decrease in 12-α-OH/non-12-α-OH bile acids ratio in serum, was not observed in TGR5-deficient mice after VSG surgery (53). On the contrary, a study conducted in mice reported that TGR5 is not necessary for the health benefits of RYGB (54).

The evidence mentioned in this section not only reinforces the notion that bile acids composition is an important mediator of the beneficial changes that metabolic surgery brings, but also provides insights into how bile acids and associated molecular targets may be part of the equation of how metabolic surgery works.

Gut microbiota

The microbial communities that reside in an individual person or animal are numerous and diverse. The estimated number of microbes that inhabits the colon of an adult human is 3.2 x 10^{11} cells per gram of content (55). Growing evidence shows that the gut microbiota is involved in a large variety of physiologic and pathologic processes. Many factors can affect the composition of gut microbiota, such as diet, medication, and external environment (Figure 2) (56). "Normal" or "healthy" composition of gut microbiota contributes to physiologic processes such as nutrient extraction and the development of immune system (57). Disruption of the normal composition could lead to alteration in the health status of organ systems such as the brain, the heart, and the lung (56, 58, 59). Specifically, mental health status (60), inflammatory responses (61, 62), and even pain perception (63, 64), can all be affected by the gut microbiota.

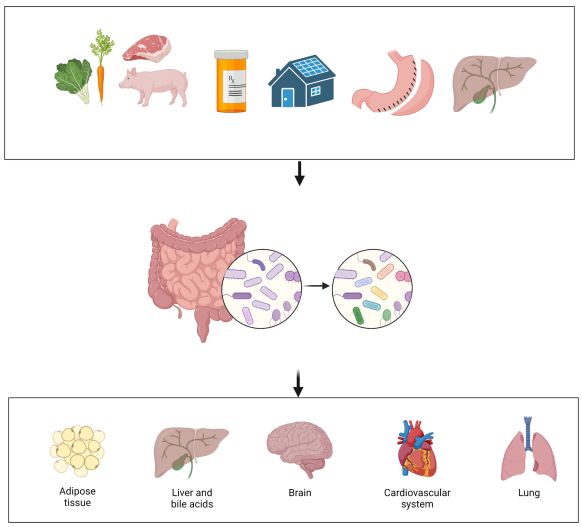

FIGURE 2
Interaction among environment, gut microbiota and host. Many factors can affect the gut microbiota, such as diet, medication, environment, bariatric surgery, and bile acids. Alteration in the gut microbiota can then affect the health status of multiple organ systems. (Created with BioRender.com).

Gene sequencing technologies such as 16s rRNA sequencing and shotgun metagenomic sequencing, combined with powerful analytic tools, allow for the extraction of genetic and functional information from samples (65). Most of the gut bacteria in humans and laboratory rodents belongs to two major phyla: Firmicutes and Bacteroidetes (57, 66). Studies found that the relative abundance of the two phyla is associated with obesity. In both mice and humans, obesity is reported to be associated with higher ratio of Firmicutes: Bacteroidetes (66–68). However, some studies found either opposite or lack of association between obesity status and Firmicutes: Bacteroidetes ratio (69, 70). This conflict could be the result of technical differences between studies, or due to the complex nature of obesity and microbiota (70).

As the field of gut microbiota research progresses, more and more studies report gut microbiota data that are beyond the phylum level. Studies conducted in mice show that some species are associated with metabolic disturbance. For example, several species of *Lactobacillus* have been reported to have the ability to prevent weight gain and blood glucose disorder in mice that were fed high-fat diet (71). The results from a clinical trial supported the beneficial effect of *Lactobacillus* spp, showing that overweight subjects who consumed yogurt containing heat-killed *Lactobacillus plantarum* OLL1712 displayed significantly less abdominal fat accumulation and lower fasting plasma glucose (72). Similarly, *Akkermansia muciniphila* and *Parabacteroides distasonis* have both been deemed beneficial to metabolic health (73–75).

Gut microbiota has also been investigated as part of the underlying mechanism of metabolic surgery. The close interaction between gut microbiota and bile acids makes studying the gut microbiota in this context particularly interesting. The following sections will introduce the roles that gut microbiota may play in metabolic surgery. First, the interaction between the gut microbiota and bile acids will be introduced. Then, the way that the gut microbiota is influenced by metabolic surgery will be discussed, and the discussion will also include changes in adipose tissues after metabolic surgery. Finally, the discussion of gut microbiota will be concluded with how certain metabolites of gut microbiota could be exploited as therapeutic options for obesity, T2D, and other metabolic diseases.

Gut microbiota and bile acids

The gut microbiota possesses the ability to modulate the composition of bile acids. The production of secondary bile acids relies on the hydroxylation and dehydroxylation carried out by the gut microbiota at the distal small intestine and the

colon (32, 76). Bile acids are conjugated mostly with glycine in humans, and with taurine in rodents, which increases their solubility (32, 77). The gut bacterial species that have bile salt hydrolase can deconjugate bile acids from taurine and glycine; then, further modification by other mechanisms of the gut bacteria results in the production of secondary and tertiary bile acids (77). The gut microbiota can also influence the activity of FXR and TGR5 through altering the composition of bile acid pool (32). The impressive impact that gut microbiota has on bile acid composition and the genes that regulate bile acid synthesis is perhaps best demonstrated in germ-free mice (GF). Compared to conventionally-raised mice, GF mice showed a lack of secondary bile acids, decreased overall bile acid pool size, and altered composition of bile acids at various segments of the intestines (78). Additionally, the expression levels of bile acid synthesis enzymes CYP7A1, CYP7B1, CYP8B1, and CYP27A1 have also been found to be different between GF and conventionally-raised mice (78, 79). These findings further support the notion that gut microbiota can impact bile acid composition.

Bile acids can influence the composition of gut microbiota as well. Bile acids have long been known to have antimicrobial property. An *in vitro* study showcased the antimicrobial activity of bile acids against *Staphylococcus aureus* (80) by demonstrating that CA and DCA decreased the viability of *S. aureus* in a concentration-dependent manner. In mice, feeding of ursodeoxycholic acid (UDCA) altered both the microbiota and bile acid compositions (81). In rats, feeding of CA for 10 days increased the proportion of the Firmicutes phylum in the gut microbiota (82).

The relationship between bile acids and gut microbiota is bi-directional. It should be no surprise, then, that the gut microbiota has received much attention in the realm of metabolic surgery research.

Gut microbiota and metabolic surgery

The implication of gut microbiota in how metabolic surgery works has been acknowledged for some time now. Many studies have reported on the shifts in gut microbiota in rodents and humans after metabolic surgery. Taken into consideration of the bi-directional relationship between bile acid and gut microbiota, how metabolic surgery influences the gut microbiota (or vice versa) could hold the key to uncovering the underlying mechanisms of metabolic surgery.

The early investigation of the role of gut microbiota in metabolic surgery was focused on finding trends or patterns of how gut microbiota changed after metabolic surgery. In a small study of nine human subjects, changes in fecal microbiota were detected between individuals that were lean, morbidly obese, and after RYGB (83). Phylogenic analysis revealed that the microbiota communities tended to cluster together in individuals within the same cohort, with pronounced distinction between lean and obese individuals. A later study investigated the alteration in fecal microbiota after dietary intervention aimed at treating obesity, and after VSG (84). The authors found that although similar degree of weight loss was achieved by both groups, the ways that the microbiota compositions altered were not the same. After dietary intervention, the proportion of Bacteroidetes phylum decreased, and the proportion of Firmicutes phylum increased; but the opposite changes were observed after VSG. Similarly, a recent study that also analyzed the gut microbiota of individuals who received dietary interventions or VSG reported no common pattern of microbiota changes between the groups (85). These reports showed that although gut microbiota can be influenced by the metabolic health status of an individual, it can also be influenced by the type of intervention the individual receives. In other words, it is possible that metabolic surgery places a unique signature on the gut microbiota.

Several studies also compare how different types of metabolic surgery could alter the gut microbiota. Gastric banding surgery does not require drastic anatomic alteration like VSG and RYGB do, so it is not surprising that the gut microbiota was not significantly affected in human subjects after gastric banding surgery (86). However, the same study also found that the gut microbiota of the human subjects who received RYGB was significantly different from subjects who did not receive the surgery. A more recent study compared VSG and RYGB surgeries in human subjects, and the authors reported that VSG imposed more prominent effect on gut microbiota than RYGB (87). The authors found that after VSG, 23 bacterial genera increased in abundance and 10 genera decreased; after RYGB, 19 genera increased in abundance and one decreased. It is important to note that among the differences, there are also similarities; of the affected genera, VSG and RYGB shared 10 of the increased genera, and one of the decreased genera.

The reason why dietary intervention and different types of metabolic surgeries alter the gut microbiota differently is still being investigated. If the gut microbiota contains the ability to influence metabolism, then fecal microbiota transplantation (FMT) experiments may help answer some questions. Liou et al. performed FMT experiment in which feces from mice that received RYGB or sham surgery were transplanted to GF mice. The results showed that the body weight and adiposity of the recipients of RYGB feces were lower than the recipients of sham feces (88). Later, Groot et al. conducted a FMT study with human subjects: fecal microbiota from human subjects who had metabolic syndrome and who received RYGB surgery were transferred to nonsurgical subjects with metabolic syndrome (89). The results showed that while recipients of gut microbiota from donors with metabolic syndrome had worsened insulin sensitivity, recipients of gut microbiota from RYGB donors showed trends of improvement in insulin sensitivity, although

the improvement was statistically insignificant. There is clearly much more to discover and investigate in the role that gut microbiota plays in the beneficial effects of metabolic surgery.

Efforts have been made to identify bacterial species that can mediate the health benefits of metabolic surgery. One candidate is *Akkermancia muciniphila.* Abundance of *A. muciniphila* was found to be lower in leptin-deficient obese mice and high-fat-diet-fed mice than in lean mice (90). When the bacterium was administered to the mice, body weight and body composition improved. Similar findings have been reported in humans. A proof-of-concept study published by Depommier et al. shows that *A. muciniphila* could be safely administered to human volunteers. Although the changes were not significant, the authors found that *A. muciniphila* treatment had beneficial metabolic effects such as improvement in insulin sensitivity, reduction of insulinemia, and loss of body weight (75). However, there are conflicting reports. A recent study looked at the abundance of *A. muciniphila* in patients after gastric banding and RYGB surgeries (91). *A. muciniphila* was not increased in gastric banding patients, but it was increased in RYGB patients. The authors also reported that the abundance of the bacterium at baseline was not correlated with clinical outcome after RYGB, and after RYGB the increase in the abundance of *A. muciniphila* was not correlated with glucose homeostasis and other clinical variables. The question of whether or not *A. muciniphila* or any one bacterium has the ability to effectively treat obesity is still being studied. Instead of focusing on the bacteria themselves, some groups have turned their attention to the metabolites of the bacteria. In the next section, how the metabolites and functions of the gut microbiota can be exploited for metabolic health benefits will be discussed.

Metabolites and functions of gut microbiota, and their therapeutic values

Metabolomics is another area of focus in metabolic surgery research. Metabolomic studies may enhance the efforts of mining gut microbiota for mechanistic clues by narrowing down the physiologic pathways that are impacted after metabolic surgery. Then, the alteration in gut microbiota composition can be taken into account while studying the impacted pathways. Because identifying specific bacterial species or groups thar bear therapeutic potentials for obesity is challenging, redirecting our attention to the physiologic pathways and metabolites over which the surgery-associated gut microbiota profile has influence may be a more practical strategy.

A tryptophan-derived metabolite named indole-3-acetic acid (IAA) has been studied for its association in metabolic health. IAA levels in the serum was lower in HFD-fed mice, and correspondingly, the abundance of the gut bacteria that metabolize tryptophan to produce IAA also was found to be decreased (92). One of the consequences of obesity is non-alcoholic fatty liver disease (NAFLD) (93), and Yu et al. explored the role of IAA in improving NAFLD after VSG (94). The authors found that in human patients, NAFLD was improved after VSG, and serum IAA level was increased at both one and three months after the surgery. By using mice, the authors established the link between IAA and NAFLD by administering IAA to HFD-fed mice. As expected, administration of IAA improved NAFLD and increased the number of anti-inflammatory macrophages in the livers of HFD-fed mice. Some studies looked at bacterial functional pathways at various time points after metabolic surgery. Shen *et al.* reported that 15 bacterial functional pathways were enriched in post-RYGB patients compared to before surgery (95). Examples of these pathways are metabolism of amino acids, carbohydrates, lipids, and vitamins, etc. However, 12 of these pathways regressed to pre-surgery levels at 12 months after RYGB, despite sustained weight loss. Analysis of the alteration in gut microbiota at pre-surgery and 12 months after surgery revealed similar regression. The question of how much gut microbiota can influence metabolic surgery outcome is still up for debate. Shen *et al's* results show that it is possible for the surgery to overpower the influence of gut microbiota.

Metabolites and the effects of metabolic surgery on adipose tissues

Metabolic surgeries efficiently reduce body mass and adiposity. Adipose tissues are remodeled after VSG with smaller fat pad and adipocyte size. Growing evidence showed that VSG induced microbiota and metabolites alteration have key effects on reduced fat mass. As an endocrine organ, gut microbiota produced metabolites like bile acids, SCFA (short chain fatty acids) and BCAA (Branched-Chain Amino Acids) have been reported to regulate lipid metabolisms in adipose tissue. These metabolites have potential regulatory roles in metabolic surgery induced fat loss.

Bile acids

The level and composition of bile acids are known to be altered by metabolic surgery. Our previous study showed that after VSG surgery, remodeled bile acids activate TGR5-cAMP signaling pathway in brown adipose tissue (BAT) and promote BAT thermogenesis. $TGR5^{-/-}$ mice failed to maintain VSG-induced body weight loss, BAT activity and energy expenditure (38). It has also been reported that bile acid–TGR5 axis promotes white fat browning and lipolysis (96). VSG induced elevation of conjugated bile acids have more potency to activate TGR5 than un-conjugated bile acids (97). Bile acid-TGR5 signaling plays a key role in reduced adiposity after VSG (38). Interestingly, compared with bariatric surgery, microbiota and bile acids alteration after caloric restriction (CR)

TABLE 1 List of potential mechanisms underlying metabolic surgery, and how they are affected by the surgery.

Mechanism	Surgery type	Study subject	Effect	Reference
GLP-1	RYGB and VSG VSG with transit bipartition	Animal (Rat)	Increased	(18)
	VSG	Animal (Mouse)	Increased	(19)
	VSG and RYGB	Human	Increased	(24)
GLP-1 and PYY	VSG and RYGB	Human	Increased	(20, 21)
	VSG	Human	Increased	(23)
		Animal (Mouse)	Increased	(26)
PYY	VSG and RYGB	Human	Increased	(22)
Bile acids	VSG, VSG with duodenal-jejunal bypass, RYGB, and adjustable gastric banding	Human	Increased: total serum bile acids.	(33)
	VSG and duodenal-jejunal bypass	Animal (Rat)	Increased: total serum bile acids. Increased: Taurine-conjugated bile acids.	(39)
	VSG and RYGB	Human	Increased: serum secondary and conjugated bile acids.	(37)
			Increased: non- 12α-OH bile acids.	(45)
	RYGB	Human	Increased: 12α-OH bile acids.	(36)
			Increased: total serum bile acids.	(34)
	VSG	Animal (Mouse)	Increased: total serum bile acids.	(35)
			No significant difference: total serum bile acids. Increased: serum concentration of unconjugated and taurine-conjugated bile acids.	(38)
		Human	Increased: LCA in the serum. Decreased: conjugated and unconjugated CA in the serum.	(44)
FXR	RYGB	Animal (Rat)	CDCA, a potent ligand for FXR, was elevated after RYGB. Pancreatic β-cells from FXR-deficient mice did not improve in insulin secretion after RYGB.	(49)
		Animal (Mouse)	FXR was not required for RYGB to induce metabolic changes in mice.	(50)
	VSG	Animal (Mouse)	FXR-deficient mice did not benefit from VSG	(48)
			Liver- and intestine-FXR tissue specific knockout mice still responded to VSG.	(51)
FGF15	VSG	Animal (Mouse)	FGF15-deficient mice lost weight but did not improve glucose tolerance after VSG	(35)
FGF19	VSG and RYGB	Human	Increased at 3 days after surgeries, but decreased back to baseline at 3 months after surgeries	(37)
			Increased at 1 year after VSG and RYGB.	(45)
TGR5	RYGB	Animal (Mouse)	Mice deficient in TGR5 still benefited from RYGB.	(54)
	VSG	Animal (Mouse)	Increased; mice deficient in TGR5 showed dampened response to VSG.	(38)
			Mice deficient in TGR5 showed dampened response to VSG. Mice deficient in TGR5 did not show decrease in the ratio of 12-α-OH and non-12-α-OH bile acids after VSG.	(53)
TGR5 and bile acids	VSG	Animal (Mouse)	Mice had increased amount of CA7S (sulfated CA) after VSG, and CA7S acted on TGR5 to induce anti-diabetic effects.	(108)
Gut microbiota	RYGB	Human	Firmicutes phylum decreased after RYGB.	(83)
	VSG and dietary intervention	Human	After VSG, patients had increased abundance of Bacteroidetes and decreased abundance of Firmicutes. After dietary intervention, patients had decreased abundance of Bacteroidetes and increased abundance of Firmicutes.	(84)
			Gut microbiota pattern is more associated with the particular type of weight loss intervention than weight loss alone.	(85)
	Gastric banding and RYGB	Human	RYGB altered gut microbiota to a greater degree than gastric banding did.	(86)
				(91)

(Continued)

TABLE 1 Continued

Mechanism	Surgery type	Study subject	Effect	Reference
			The abundance of *A. muciniphila* was not increased in patients after gastric banding, but it increased after RYGB. The increase in *A. muciniphila* was not correlated with clinical variables of metabolic health.	
	VSG and RYGB	Human	VSG imposed greater alteration on gut microbiota than RYGB did.	(87)
	RYGB	Animal (Mouse)	FMT: after receiving feces from post-RYGB mice, recipient mice showed reduced body weight and adiposity.	(88)
		Human	FMT: feces from RYGB patients were giving to non-surgical obese recipients, and the recipients showed improved insulin sensitivity (though statistically insignificant).	(89)
Gut microbiota		Human	Bacterial functional pathways were modified after RYGB, and most modifications regressed at 12 months after surgery.	(95)
Gut microbiota metabolites	VSG	Human and animal (Mouse)	IAA was increased in the serum of patients after VSG. IAA administration to mice improved NAFLD.	(94)

are responsible for rebound weight gain in mice. CR caused dramatically increased proportion of non-12α-OH bile acids, ursodeoxycholic acid and lithocholic acid. These alterations lead to decreased UCP1 expression in brown adipose tissue of weight rebounded mice (98). The difference of bile acids level and composition between bariatric surgery and CR explains why bariatric surgeries are more effective in maintenance of lower body weight than CR.

BCAA

BCAAs, including leucine, isoleucine, and valine are essential amino acids which can be synthesized or degraded by gut bacteria. Obesity increases, while bariatric surgery decreases the circulating levels of BCAAs. Mice fed with BCAA deficient diets exhibit reduced body weight and adiposity, accompanied with reduced lipogenesis and increased lipolysis in white adipose tissue. (99–101). But another publication showed that decreased circulating BCAAs is not required for VSG induced weight loss (102). When mice fed with HFD supplemented with BCAAs were subjected to VSG surgery, sustained weight loss and improved glucose tolerance were identical to mice fed with regular HFD. Impaired BCAA catabolism by depletion of Pp2cm didn't affect VSG induced weight loss. This study suggests that although circulating BCAAs level is reduced after VSG, it's not the driver of VSG induced weight loss.

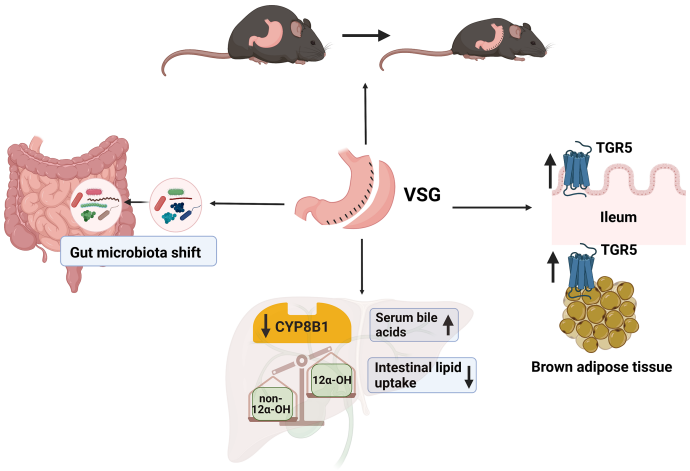

FIGURE 3
A summary of what we know about VSG, bile acids, and gut microbiota. After VSG in mice, bile acid receptor TGR5 in the ileum and brown adipose tissue is activated, and subsequently leads to increased energy expenditure and decrease in body weight (109). Total serum bile acids is increased after VSG, and intestinal lipid uptake is decreased. The downregulation of CYP8B1 after VSG leads to a decrease the ratio of 12α-OH and non-12α-OH bile acids. Finally, the gut microbiota profile is shifted after VSG; but the precise relationship between VSG and gut microbiota needs further investigation. (Created with BioRender.com).

SCFA

SCFA produced by anaerobic intestinal microbiota has been known to be involved in the regulation of immune response and glucose and lipid metabolism. A previous study showed SCFA acetate plays an important role in regulating human adipose tissue lipolysis. Acetate can reduce phosphor-HSL level and lipolysis in human white adipocyte (103). After metabolic surgery, total level of fecal SCFAs was reduced. Among the SCFAs, acetate, propionate, and butyrate were reduced, while the branched SCFAs isobutyrate, isovalerate and isocaproic acid were increased (104). However, the effects of SCFAs on metabolic surgery induced fat mass loss still need to be elucidated.

Many other bacterial metabolites have been investigated, such as lipopolysaccharides, aromatic amino acids, and methylamines (105). More research is needed to discover the connection between bacterial metabolites and metabolic surgery. The complexity of the subject highlights the need for unbiased reporting of both positive and negative results, so that the scientific community can take advantage of all the available knowledge and take the next steps towards developing new therapies for obesity and metabolic diseases.

Adipocyte-derived exosomal miRNA

Exosomes are nanosized extracellular lipid bilayer vesicles secreted from cells which contain nucleic acids, proteins and lipids. By transferring the biological information to other cells or tissues, exosomes play key roles in intracellular communication and biological activities. Exosomes derived from adipose tissue have been linked to insulin resistance in obese individuals (106). Growing evidence indicates that adipocyte-derived exosomal miRNAs target adipose tissue and distal organs, primarily liver, to regulate metabolic gene expressions (107). Recent studies showed that after bariatric surgery, circulating exosomal miRNA derived from adipocyte significantly changed which correlated to improvements in insulin sensitivity (106). Alteration of adipocyte-derived exosomal miRNA after bariatric surgery provides a novel way to understand the underlying mechanism of the metabolic improvements caused by bariatric surgeries.

Perspective

Identifying the underlying mechanisms of metabolic surgery is an enormous endeavor. There are likely multiple mechanisms, all of them interconnected in some ways. There is still much to learn about the physiological changes after metabolic surgery. knowledge gained from studying the post-surgery changes could provide clues to how the surgery works. Gut hormones, bile acids, and gut microbiota are just some of players that are investigated. The gut microbiota influences many aspects of metabolism, but the extent to which it can influence the outcome of metabolic surgery is still being investigated. The metabolites of gut microbiota have been receiving more attention, and they may be harboring important clues for developing new therapeutics for treating obesity.

Readers may refer to Table 1 for a summary of the key references mentioned in this text, and their main findings. Figure 3 is a graphical summary of what is known about VSG, bile acids and the gut microbiota.

Author contributions

WH and JT prepared the manuscript. YW and LJ helped edit and provide related information. All authors contributed to the article and approved the submitted version.

Funding

This study was supported by grants from the George & Irina Schaeffer Foundation, the John Hench Foundation, and the National Institutes of Health (R01DK124627) to WH. WH was also supported by the National Institutes of Health (R01CA139158).

Conflict of interest

The authors declare that the research was conducted in the absence of any commercial or financial relationships that could be construed as a potential conflict of interest.

Publisher's note

References

1. WHO. *Obesity and overweight*. (2020) https://www.who.int/news-room/fact-sheets/detail/obesity-and-overweight

2. CDC. *Adult obesity prevalence maps*. (2020) https://www.cdc.gov/obesity/data/prevalence-maps.html#overall.

3. Kitahara CM, Flint AJ, Berrington de Gonzalez A, Bernstein L, Brotzman M, MacInnis RJ, et al. Singh PN et al: Association between class III obesity (BMI of 40-59 kg/m2) and mortality: a pooled analysis of 20 prospective studies. *PLoS Med* (2014) 11(7):e1001673. doi: 10.1371/journal.pmed.1001673

4. Nguyen NT, Magno CP, Lane KT, Hinojosa MW, Lane JS. Association of hypertension, diabetes, dyslipidemia, and metabolic syndrome with obesity: findings from the national health and nutrition examination survey, 1999 to 2004. *J Am Coll Surgeons* (2008) 207(6):928–34. doi: 10.1016/j.jamcollsurg.2008.08.022

5. Wilson PW, D'Agostino RB, Sullivan L, Parise H, Kannel WB. Overweight and obesity as determinants of cardiovascular risk: the framingham experience. *Arch Internal Med* (2002) 162(16):1867–72. doi: 10.1001/archinte.162.16.1867

6. CDC. *National diabetes statistics report*. (2020) https://www.cdc.gov/diabetes/pdfs/data/statistics/national-diabetes-statistics-report.pdf.

7. American Diabetes Association. Obesity management for the treatment of type 2 diabetes: Standards of medical care in diabetes-2020. *Diabetes Care* (2020) 43(Suppl 1):S89–s97. doi: 10.2337/dc20-S008

8. Cummings DE, Cohen RV. Beyond BMI: the need for new guidelines governing the use of bariatric and metabolic surgery. *Lancet Diabetes Endocrinol* (2014) 2(2):175–81. doi: 10.1016/S2213-8587(13)70198-0

9. Almino Ramos LK, Brown W, Welbourn R, Dixon J, Kinsman R, Walton P. *The IFSO global registry*. (2019) Dendrite Clinical Systems Ltd, Fifth Floor, Reading Bridge House, George Street Reading RG1 8LS United Kingdom. https://www.ifso.com/pdf/5th-ifso-global-registry-report-september-2019.pdf

10. Gandhi D, Boregowda U, Sharma P, Ahuja K, Jain N, Khanna K, et al. A review of commonly performed bariatric surgeries: Imaging features and its complications. *Clin Imaging* (2021) 72:122–35. doi: 10.1016/j.clinimag.2020.11.020

11. Kheirvari M, Dadkhah Nikroo N, Jaafarinejad H, Farsimadan M, Eshghjoo S, Hosseini S, et al. The advantages and disadvantages of sleeve gastrectomy; clinical laboratory to bedside review. *Heliyon* (2020) 6(2):e03496. doi: 10.1016/j.heliyon.2020.e03496

12. Zhang W, Fan M, Wang C, Mahawar K, Parmar C, Chen W, et al. Hair loss after metabolic and bariatric surgery: a systematic review and meta-analysis. *Obes Surg* (2021) 31:2649–59. doi: 10.1007/s11695-021-05311-2

13. Paccou J, Caiazzo R, Lespessailles E, Cortet B. Bariatric surgery and osteoporosis. *Calcified Tissue Int* (2021) 110:576–91. doi: 10.1007/s00223-020-00798-w

14. Miras AD, le Roux CW. Can medical therapy mimic the clinical efficacy or physiological effects of bariatric surgery? *Int J Obes* (20052014) 38(3):325–33. doi: 10.1038/ijo.2013.205

15. Steinert RE, Feinle-Bisset C, Asarian L, Horowitz M, Beglinger C, Geary N. Ghrelin, CCK, GLP-1, and PYY(3-36): Secretory controls and physiological roles in eating and glycemia in health, obesity, and after RYGB. *Physiol Rev* (2017) 97(1):411–63. doi: 10.1152/physrev.00031.2014

16. Alhabeeb H, AlFaiz A, Kutbi E, AlShahrani D, Alsuhail A, AlRajhi S, et al. Gut hormones in health and obesity: The upcoming role of short chain fatty acids. *Nutrients* (2021) 13(2):481. doi: 10.3390/nu13020481

17. Gribble FM, Reimann F. Metabolic messengers: glucagon-like peptide 1. *Nat Metab* (2021) 3(2):142–8. doi: 10.1038/s42255-020-00327-x

18. Liu P, Widjaja J, Dolo PR, Yao L, Hong J, Shao Y, et al. Comparing the anti-diabetic effect of sleeve gastrectomy with transit bipartition against sleeve gastrectomy and roux-en-Y gastric bypass using a diabetic rodent model. *Obes Surg* (2021) 31:2203–10. doi: 10.1007/s11695-021-05256-6

19. Douros JD, Niu J, Sdao S, Gregg T, Merrins MJ, Campbell J, et al. Temporal plasticity of insulin and incretin secretion and insulin sensitivity following sleeve gastrectomy contribute to sustained improvements in glucose control. *Mol Metab* (2019) 28:144–50. doi: 10.1016/j.molmet.2019.07.003

20. Gudbrandsen OA, Dankel SN, Skumsnes L, Flølo TN, Folkestad OH, Nielsen HJ, et al. Sagen JV et al: Short-term effects of vertical sleeve gastrectomy and roux-en-Y gastric bypass on glucose homeostasis. *Sci Rep* (2019) 9(1):14817. doi: 10.1038/s41598-019-51347-x

21. Perakakis N, Kokkinos A, Peradze N, Tentolouris N, Ghaly W, Pilitsi E, et al. Circulating levels of gastrointestinal hormones in response to the most common types of bariatric surgery and predictive value for weight loss over one year: Evidence from two independent trials. *Metabolism* (2019) 101:153997. doi: 10.1016/j.metabol.2019.153997

22. Guida C, Stephen SD, Watson M, Dempster N, Larraufie P, Marjot T, et al. Tomlinson J et al: PYY plays a key role in the resolution of diabetes following bariatric surgery in humans. *EBioMedicine* (2019) 40:67–76. doi: 10.1016/j.ebiom.2018.12.040

23. McCarty TR, Jirapinyo P, Thompson CC. Effect of sleeve gastrectomy on ghrelin, GLP-1, PYY, and GIP gut hormones: A systematic review and meta-analysis. *Ann Surg* (2020) 272(1):72–80. doi: 10.1097/SLA.0000000000003614

24. Arakawa R, Febres G, Cheng B, Krikhely A, Bessler M, Korner J. Prospective study of gut hormone and metabolic changes after laparoscopic sleeve gastrectomy and roux-en-Y gastric bypass. *PLoS One* (2020) 15(7):e0236133–e0236133. doi: 10.1371/journal.pone.0236133

25. Roberts GP, Larraufie P, Richards P, Kay RG, Galvin SG, Miedzybrodzka EL, et al. Ma MKL et al: Comparison of human and murine enteroendocrine cells by transcriptomic and peptidomic profiling. *Diabetes* (2019) 68(5):1062–72. doi: 10.2337/db18-0883

26. Larraufie P, Roberts GP, McGavigan AK, Kay RG, Li J, Leiter A, et al. Davy K Et al: Important role of the GLP-1 axis for glucose homeostasis after bariatric surgery. *Cell Rep* (2019) 26(6):1399–408.e1396. doi: 10.1016/j.celrep.2019.01.047

27. di Gregorio MC, Cautela J, Galantini L. Physiology and physical chemistry of bile acids. *Int J Mol Sci* (2021) 22(4):1780. doi: 10.3390/ijms22041780

28. Chiang JY. Bile acids: regulation of synthesis. *J Lipid Res* (2009) 50(10):1955–66. doi: 10.1194/jlr.R900010-JLR200

29. Xie C, Huang W, Young RL, Jones KL, Horowitz M, Rayner CK, et al. Role of bile acids in the regulation of food intake, and their dysregulation in metabolic disease. *Nutrients* (2021) 13(4):1104. doi: 10.3390/nu13041104

30. Baiocchi L, Zhou T, Liangpunsakul S, Lenci I, Santopaolo F, Meng F, et al. Dual role of bile acids on the biliary epithelium: Friend or foe? *Int J Mol Sci* (2019) 20(8):1869. doi: 10.3390/ijms20081869

31. Chiang JYL, Pathak P, Liu H, Donepudi A, Ferrell J, Boehme S. Intestinal farnesoid X receptor and takeda G protein couple receptor 5 signaling in metabolic regulation. *Digestive Dis* (2017) 35(3):241–5. doi: 10.1159/000450981

32. Wahlström A, Sayin SI, Marschall HU, Bäckhed F. Intestinal crosstalk between bile acids and microbiota and its impact on host metabolism. *Cell Metab* (2016) 24(1):41–50. doi: 10.1016/j.cmet.2016.05.005

33. Nakatani H, Kasama K, Oshiro T, Watanabe M, Hirose H, Itoh H. Serum bile acid along with plasma incretins and serum high-molecular weight adiponectin levels are increased after bariatric surgery. *Metabolism* (2009) 58(10):1400–7. doi: 10.1016/j.metabol.2009.05.006

34. Patti ME, Houten SM, Bianco AC, Bernier R, Larsen PR, Holst JJ, et al. Pihlajamaki J et al: Serum bile acids are higher in humans with prior gastric bypass: potential contribution to improved glucose and lipid metabolism. *Obesity* (2009) 17(9):1671–7. doi: 10.1038/oby.2009.102

35. Myronovych A, Bhattacharjee J, Salazar-Gonzalez RM, Tan B, Mowery S, Ferguson D, et al. Oehrle m et al: Assessment of the role of FGF15 in mediating the metabolic outcomes of murine vertical sleeve gastrectomy (VSG). *Am J Physiol Gastrointestinal liver Physiol* (2020) 319(6):G669–684. doi: 10.1152/ajpgi.00175.2020

36. Zhang C, Zhang J, Zhou Z. Changes in fasting bile acid profiles after roux-en-Y gastric bypass and sleeve gastrectomy. *Med (Baltimore)* (2021) 100(3):e23939–9. doi: 10.1097/MD.0000000000023939

37. Chen Y, Lu J, Nemati R, Plank LD, Murphy R. Acute changes of bile acids and FGF19 after sleeve gastrectomy and roux-en-Y gastric bypass. *Obes Surg* (2019) 29(11):3605–21. doi: 10.1007/s11695-019-04040-x

38. Ding L, Sousa KM, Jin L, Dong B, Kim BW, Ramirez R, et al. Vertical sleeve gastrectomy activates GPBAR-1/TGR5 to sustain weight loss, improve fatty liver, and remit insulin resistance in mice. *Hepatology* (2016) 64(3):760–73. doi: 10.1002/hep.28689

39. Wu Q, Zhang X, Zhong M, Han H, Liu S, Liu T, et al. Hu s et al: Effects of bariatric surgery on serum bile acid composition and conjugation in a diabetic rat model. *Obes Surg* (2016) 26(10):2384–92. doi: 10.1007/s11695-016-2087-2

40. Haeusler RA, Astiarraga B, Camastra S, Accili D, Ferrannini E. Human insulin resistance is associated with increased plasma levels of 12α-hydroxylated bile acids. *Diabetes* (2013) 62(12):4184–91. doi: 10.2337/db13-0639

41. Haeusler RA, Camastra S, Nannipieri M, Astiarraga B, Castro-Perez J, Xie D, et al. Increased bile acid synthesis and impaired bile acid transport in human obesity. *J Clin Endocrinol Metab* (2016) 101(5):1935–44. doi: 10.1210/jc.2015-2583

42. Hori S, Abe T, Lee DG, Fukiya S, Yokota A, Aso N, et al. Association between 12α-hydroxylated bile acids and hepatic steatosis in rats fed a high-fat diet. *J Nutr Biochem* (2020) 83:108412. doi: 10.1016/j.jnutbio.2020.108412

43. Bertaggia E, Jensen KK, Castro-Perez J, Xu Y, Di Paolo G, Chan RB, et al. Cyp8b1 ablation prevents Western diet-induced weight gain and hepatic steatosis

because of impaired fat absorption. *Am J Physiol Endocrinol Metab* (2017) 313(2): E121–e133. doi: 10.1152/ajpendo.00409.2016

44. De Vuono S, Ricci MA, Nulli Migliola E, Monti MC, Morretta E, Boni M, et al. Distrutti e et al: Serum bile acid levels before and after sleeve gastrectomy and their correlation with obesity-related comorbidities. *Obes Surg* (2019) 29(8):2517–26. doi: 10.1007/s11695-019-03877-6

45. Nemati R, Lu J, Dokpuang D, Booth M, Plank LD, Murphy R. Increased bile acids and FGF19 after sleeve gastrectomy and roux-en-Y gastric bypass correlate with improvement in type 2 diabetes in a randomized trial. *Obes Surg* (2018) 28 (9):2672–86. doi: 10.1007/s11695-018-3216-x

46. Marin JJ, Macias RI, Briz O, Banales JM, Monte MJ. Bile acids in physiology, pathology and pharmacology. *Curr Drug Metab* (2015) 17(1):4–29. doi: 10.2174/1389200216666151103115454

47. Li T, Chiang JY. Bile acid signaling in metabolic disease and drug therapy. *Pharmacol Rev* (2014) 66(4):948–83. doi: 10.1124/pr.113.008201

48. Ryan KK, Tremaroli V, Clemmensen C, Kovatcheva-Datchary P, Myronovych A, Karns R, et al. FXR is a molecular target for the effects of vertical sleeve gastrectomy. *Nature* (2014) 509(7499):183–+. doi: 10.1038/nature13135

49. Kong X, Tu Y, Li B, Zhang L, Feng L, Wang L, et al. Roux-en-Y gastric bypass enhances insulin secretion in type 2 diabetes *via* FXR-mediated TRPA1 expression. *Mol Metab* (2019) 29:1–11. doi: 10.1016/j.molmet.2019.08.009

50. Li K, Zou J, Li S, Guo J, Shi W, Wang B, et al. Miao z et al: Farnesoid X receptor contributes to body weight-independent improvements in glycemic control after roux-en-Y gastric bypass surgery in diet-induced obese mice. *Mol Metab* (2020) 37:100980. doi: 10.1016/j.molmet.2020.100980

51. Ding L, Zhang E, Yang Q, Jin L, Sousa KM, Dong B, et al. Vertical sleeve gastrectomy confers metabolic improvements by reducing intestinal bile acids and lipid absorption in mice. *Proc Natl Acad Sci USA* (2021) 118(6). doi: 10.1073/pnas.2019388118

52. Bozadjieva N, Heppner KM, Seeley RJ. Targeting FXR and FGF19 to treat metabolic diseases-lessons learned from bariatric surgery. *Diabetes* (2018) 67 (9):1720–8. doi: 10.2337/dbi17-0007

53. McGavigan AK, Garibay D, Henseler ZM, Chen J, Bettaieb A, Haj FG, et al. TGR5 contributes to glucoregulatory improvements after vertical sleeve gastrectomy in mice. *Gut* (2017) 66(2):226–34. doi: 10.1136/gutjnl-2015-309871

54. Hao Z, Leigh Townsend R, Mumphrey MB, Gettys TW, Yu S, Münzberg H, et al. Roux-en-Y gastric bypass surgery-induced weight loss and metabolic improvements are similar in TGR5-deficient and wildtype mice. *Obes Surg* (2018) 28(10):3227–36. doi: 10.1007/s11695-018-3297-6

55. Whitman WB, Coleman DC, Wiebe WJ. Prokaryotes: The unseen majority. *Proc Natl Acad Sci* (1998) 95(12):6578–83. doi: 10.1073/pnas.95.12.6578

56. Fan Y, Pedersen O. Gut microbiota in human metabolic health and disease. *Nat Rev Microbiol* (2021) 19(1):55–71. doi: 10.1038/s41579-020-0433-9

57. Jandhyala SM, Talukdar R, Subramanyam C, Vuyyuru H, Sasikala M, Nageshwar Reddy D. Role of the normal gut microbiota. *World J Gastroenterol* (2015) 21(29):8787–803. doi: 10.3748/wjg.v21.i29.8787

58. Anand S, Mande SS. Diet, microbiota and gut-lung connection. *Front Microbiol* (2018) 9:2147. doi: 10.3389/fmicb.2018.02147

59. Tang WHW, Li DY, Hazen SL. Dietary metabolism, the gut microbiome, and heart failure. *Nat Rev Cardiol* (2019) 16(3):137–54. doi: 10.1038/s41569-018-0108-7

60. Methiwala HN, Vaidya B, Addanki VK, Bishnoi M, Sharma SS, Kondepudi KK. Gut microbiota in mental health and depression: role of pre/pro/synbiotics in their modulation. *Food Funct* (2021) 12:4284–314. doi: 10.1039/D0FO02855J

61. Mahmoudi E, Mozhgani S-H, Sharifinejad N. The role of mycobiota-genotype association in inflammatory bowel diseases: a narrative review. *Gut Pathog* (2021) 13(1):31. doi: 10.1186/s13099-021-00426-4

62. Maldonado-Arriaga B, Sandoval-Jiménez S, Rodríguez-Silverio J, Lizeth Alcaráz-Estrada S, Cortés-Espinosa T, Pérez-Cabeza de Vaca R, et al. Gut dysbiosis and clinical phases of pancolitis in patients with ulcerative colitis. *Microbiologyopen* (2021) 10(2):e1181. doi: 10.1002/mbo3.1181

63. Pokusaeva K, Johnson C, Luk B, Uribe G, Fu Y, Oezguen N, et al. GABA-producing bifidobacterium dentium modulates visceral sensitivity in the intestine. *Neurogastroenterol Motil* (2017) 29(1). doi: 10.1111/nmo.12904

64. Lin B, Wang Y, Zhang P, Yuan Y, Zhang Y, Chen G. Gut microbiota regulates neuropathic pain: potential mechanisms and therapeutic strategy. *J Headache Pain* (2020) 21(1):103–3. doi: 10.1186/s10194-020-01170-x

65. Allaband C, McDonald D, Vázquez-Baeza Y, Minich JJ, Tripathi A, Brenner DA, et al. Microbiome 101: Studying, analyzing, and interpreting gut microbiome data for clinicians. *Clin Gastroenterol Hepatol* (2019) 17(2):218–30. doi: 10.1016/j.cgh.2018.09.017

66. Ley RE, Bäckhed F, Turnbaugh P, Lozupone CA, Knight RD, Gordon JI. Obesity alters gut microbial ecology. *Proc Natl Acad Sci USA* (2005) 102(31):11070. doi: 10.1073/pnas.0504978102

67. Ley RE, Turnbaugh PJ, Klein S, Gordon JI. Human gut microbes associated with obesity. *Nature* (2006) 444(7122):1022–3. doi: 10.1038/4441022a

68. Turnbaugh PJ, Ley RE, Mahowald MA, Magrini V, Mardis ER, Gordon JI. An obesity-associated gut microbiome with increased capacity for energy harvest. *Nature* (2006) 444(7122):1027–31. doi: 10.1038/nature05414

69. Schwiertz A, Taras D, Schäfer K, Beijer S, Bos NA, Donus C, et al. Microbiota and SCFA in lean and overweight healthy subjects. *Obes (Silver Spring Md)* (2010) 18(1):190–5. doi: 10.1038/oby.2009.167

70. Walters WA, Xu Z, Knight R. Meta-analyses of human gut microbes associated with obesity and IBD. *FEBS Lett* (2014) 588(22):4223–33. doi: 10.1016/j.febslet.2014.09.039

71. Zheng F, Wang Z, Stanton C, Ross RP, Zhao J, Zhang H, et al. Lactobacillus rhamnosus FJSYC4-1 and lactobacillus reuteri FGSZY33L6 alleviate metabolic syndrome *via* gut microbiota regulation. *Food Funct* (2021) 12(9):3919–30. doi: 10.1039/D0FO02879G

72. Toshimitsu T, Gotou A, Sashihara T, Furuichi K, Hachimura S, Shioya N, et al. Ingesting yogurt containing lactobacillus plantarum OLL2712 reduces abdominal fat accumulation and chronic inflammation in overweight adults in a randomized placebo-controlled trial. *Curr Dev Nutr* (2021) 5(2):nzab006. doi: 10.1093/cdn/nzab006

73. Wang K, Liao M, Zhou N, Bao L, Ma K, Zheng Z, et al. Wang J Et al: Parabacteroides distasonis alleviates obesity and metabolic dysfunctions *via* production of succinate and secondary bile acids. *Cell Rep* (2019) 26(1):222–35.e225. doi: 10.1016/j.celrep.2018.12.028

74. Plovier H, Everard A, Druart C, Depommier C, Van Hul M, Geurts L, et al. Lichtenstein L et al: A purified membrane protein from akkermansia muciniphila or the pasteurized bacterium improves metabolism in obese and diabetic mice. *Nat Med* (2017) 23(1):107–13. doi: 10.1038/nm.4236

75. Depommier C, Everard A, Druart C, Plovier H, Van Hul M, Vieira-Silva S, et al. Delzenne NM et al: Supplementation with akkermansia muciniphila in overweight and obese human volunteers: a proof-of-concept exploratory study. *Nat Med* (2019) 25(7):1096–103. doi: 10.1038/s41591-019-0495-2

76. Winston JA, Theriot CM. Diversification of host bile acids by members of the gut microbiota. *Gut Microbes* (2020) 11(2):158–71. doi: 10.1080/19490976.2019.1674124

77. Long SL, Gahan CGM, Joyce SA. Interactions between gut bacteria and bile in health and disease. *Mol Aspects Med* (2017) 56:54–65. doi: 10.1016/j.mam.2017.06.002

78. Sayin SI, Wahlstrom A, Felin J, Jantti S, Marschall HU, Bamberg K, et al. Gut microbiota regulates bile acid metabolism by reducing the levels of tauro-beta-muricholic acid, a naturally occurring FXR antagonist. *Cell Metab* (2013) 17 (2):225–35. doi: 10.1016/j.cmet.2013.01.003

79. Mistry RH, Verkade HJ, Tietge UJF. Reverse cholesterol transport is increased in germ-free mice–brief report. *Arteriosclerosis Thrombosis Vasc Biol* (2017) 37(3):419–22. doi: 10.1161/ATVBAHA.116.308306

80. Sannasiddappa TH, Lund PA, Clarke SR. *In vitro* antibacterial activity of unconjugated and conjugated bile salts on staphylococcus aureus. *Front Microbiol* (2017) 8:1581–1. doi: 10.3389/fmicb.2017.01581

81. Winston JA, Rivera A, Cai J, Patterson AD, Theriot CM. Secondary bile acid ursodeoxycholic acid alters weight, the gut microbiota, and the bile acid pool in conventional mice. *PLoS One* (2021) 16(2):e0246161. doi: 10.1371/journal.pone.0246161

82. Islam KBMS, Fukiya S, Hagio M, Fujii N, Ishizuka S, Ooka T, et al. Bile acid is a host factor that regulates the composition of the cecal microbiota in rats. *Gastroenterology* (2011) 141(5):1773–81. doi: 10.1053/j.gastro.2011.07.046

83. Zhang H, DiBaise JK, Zuccolo A, Kudrna D, Braidotti M, Yu Y, et al. Rittmann BE et al: Human gut microbiota in obesity and after gastric bypass. *Proc Natl Acad Sci* (2009) 106(7):2365–70. doi: 10.1073/pnas.0812600106

84. Damms-Machado A, Mitra S, Schollenberger AE, Kramer KM, Meile T, Königsrainer A, et al. Effects of surgical and dietary weight loss therapy for obesity on gut microbiota composition and nutrient absorption. *BioMed Res Int* (2015) 2015:806248. doi: 10.1155/2015/806248

85. Gutiérrez-Repiso C, Molina-Vega M, Bernal-López MR, Garrido-Sánchez L, García-Almeida JM, Sajoux I, et al. Different weight loss intervention approaches reveal a lack of a common pattern of gut microbiota changes. *J Pers Med* (2021) 11 (2):109. doi: 10.3390/jpm11020109

86. Ilhan ZE, DiBaise JK, Isern NG, Hoyt DW, Marcus AK, Kang DW, et al. Distinctive microbiomes and metabolites linked with weight loss after gastric bypass, but not gastric banding. *Isme J* (2017) 11(9):2047–58. doi: 10.1038/ismej.2017.71

87. Chen G, Zhuang J, Cui Q, Jiang S, Tao W, Chen W, et al. Liu f et al: Two bariatric surgical procedures differentially alter the intestinal microbiota in obesity patients. *Obes Surg* (2020) 30(6):2345–61. doi: 10.1007/s11695-020-04494-4

88. Liou AP, Paziuk M, Luevano JMJr., Machineni S, Turnbaugh PJ, Kaplan LM. Conserved shifts in the gut microbiota due to gastric bypass reduce host weight and adiposity. *Sci Transl Med* (2013) 5(178):178ra141. doi: 10.1126/scitranslmed.3005687

89. de Groot P, Scheithauer T, Bakker GJ, Prodan A, Levin E, Khan MT, et al. De brauw m et al: Donor metabolic characteristics drive effects of faecal microbiota transplantation on recipient insulin sensitivity, energy expenditure and intestinal transit time. *Gut* (2020) 69(3):502–12. doi: 10.1136/gutjnl-2019-318320

90. Everard A, Belzer C, Geurts L, Ouwerkerk JP, Druart C, Bindels LB, et al. Delzenne NM et al: Cross-talk between akkermansia muciniphila and intestinal epithelium controls diet-induced obesity. *Proc Natl Acad Sci* (2013) 110(22):9066–71. doi: 10.1073/pnas.1219451110

91. Dao MC, Belda E, Prifti E, Everard A, Kayser BD, Bouillot JL, et al. Ehrlich SD et al: Akkermansia muciniphila abundance is lower in severe obesity, but its increased level after bariatric surgery is not associated with metabolic health improvement. *Am J Physiol Endocrinol Metab* (2019) 317(3):E446–e459. doi: 10.1152/ajpendo.00140.2019

92. Liu Y, Yang K, Jia Y, Shi J, Tong Z, Fang D, et al. Gut microbiome alterations in high-fat-diet-fed mice are associated with antibiotic tolerance. *Nat Microbiol* (2021) 6:874–84. doi: 10.1038/s41564-021-00912-0

93. Wasilewska N, Lebensztejn DM. Non-alcoholic fatty liver disease and lipotoxicity. *Clin Exp Hepatol* (2021) 7(1):1–6. doi: 10.5114/ceh.2021.104441

94. Wang Y, Wang G, Bai J, Zhao N, Wang Q, Zhou R, et al. Role of indole-3-Acetic acid in NAFLD amelioration after sleeve gastrectomy. *Obes Surg* (2021) 31:3040–52. doi: 10.1007/s11695-021-05321-0

95. Shen N, Caixàs A, Ahlers M, Patel K, Gao Z, Dutia R, et al. Longitudinal changes of microbiome composition and microbial metabolomics after surgical weight loss in individuals with obesity. *Surg Obes related Dis* (2019) 15(8):1367–73. doi: 10.1016/j.soard.2019.05.038

96. Velazquez-Villegas LA, Perino A, Lemos V, Zietak M, Nomura M, Pols TWH, et al. TGR5 signalling promotes mitochondrial fission and beige remodelling of white adipose tissue. *Nat Commun* (2018) 9(1):245. doi: 10.1038/s41467-017-02068-0

97. Maruyama T, Miyamoto Y, Nakamura T, Tamai Y, Okada H, Sugiyama E, et al. Identification of membrane-type receptor for bile acids (M-BAR). *Biochem Biophys Res Commun* (2002) 298(5):714–9. doi: 10.1016/S0006-291X(02)02550-0

98. Li M, Wang S, Li Y, Zhao M, Kuang J, Liang D, et al. Ma X et al: Gut microbiota-bile acid crosstalk contributes to the rebound weight gain after calorie restriction in mice. *Nat Commun* (2022) 13(1):2060. doi: 10.1038/s41467-022-29589-7

99. Cummings NE, Williams EM, Kasza I, Konon EN, Schaid MD, Schmidt BA, et al. Apelo SIA et al: Restoration of metabolic health by decreased consumption of branched-chain amino acids. *J Physiol-London* (2018) 596(4):623–45. doi: 10.1113/JP275075

100. Cheng Y, Meng QS, Wang CX, Li HK, Huang ZY, Chen SH, et al. Leucine deprivation decreases fat mass by stimulation of lipolysis in white adipose tissue and upregulation of uncoupling protein 1 (UCP1) in brown adipose tissue. *Diabetes* (2010) 59(1):17–25. doi: 10.2337/db09-0929

101. Du Y, Meng Q, Zhang Q, Guo F. Isoleucine or valine deprivation stimulates fat loss *via* increasing energy expenditure and regulating lipid metabolism in WAT. *Amino Acids* (2012) 43(2):725–34. doi: 10.1007/s00726-011-1123-8

102. Bozadjieva Kramer N, Evers SS, Shin JH, Silverwood S, Wang Y, Burant CF, et al. The role of elevated branched-chain amino acids in the effects of vertical sleeve gastrectomy to reduce weight and improve glucose regulation. *Cell Rep* (2020) 33(2):108239. doi: 10.1101/2020.06.01.128157

103. Jocken JWE, Gonzalez Hernandez MA, Hoebers NTH, van der Beek CM, Essers YPG, Blaak EE, et al. Short-chain fatty acids differentially affect intracellular lipolysis in a human white adipocyte model. *Front Endocrinol* (2017) 8:372. doi: 10.3389/fendo.2017.00372

104. Farup PG, Valeur J. Changes in faecal short-chain fatty acids after weight-loss interventions in subjects with morbid obesity. *Nutrients* (2020) 12(3):802. doi: 10.3390/nu12030802

105. Wang M, Li L, Chen Y, Lian G, Wang J, Zhang J, et al. Role of gut microbiome and microbial metabolites in alleviating insulin resistance after bariatric surgery. *Obes Surg* (2021) 31(1):327–36. doi: 10.1007/s11695-020-04974-7

106. Hubal MJ, Nadler EP, Ferrante SC, Barberio MD, Suh JH, Wang J, et al. Circulating adipocyte-derived exosomal MicroRNAs associated with decreased insulin resistance after gastric bypass. *Obesity* (2017) 25(1):102–10. doi: 10.1002/oby.21709

107. Huang Z, Xu A. Adipose extracellular vesicles in intercellular and inter-organ crosstalk in metabolic health and diseases. *Front Immunol* (2021) 12:608680. doi: 10.3389/fimmu.2021.608680

108. Chaudhari SN, Harris DA, Aliakbarian H, Luo JN, Henke MT, Subramaniam R, et al. Bariatric surgery reveals a gut-restricted TGR5 agonist with anti-diabetic effects. *Nat Chem Biol* (2021) 17(1):20–9. doi: 10.1038/s41589-020-0604-z

109. Xue H, Huang L, Tu J, Ding L, Huang W. Bile acids and metabolic surgery. *Liver Res* (2021) 5:164–70. doi: 10.1016/j.livres.2021.05.001

Frontiers in Endocrinology

Explores the endocrine system to find new therapies for key health issues

The second most-cited endocrinology and metabolism journal, which advances our understanding of the endocrine system. It uncovers new therapies for prevalent health issues such as obesity, diabetes, reproduction, and aging.

Discover the latest Research Topics

See more →

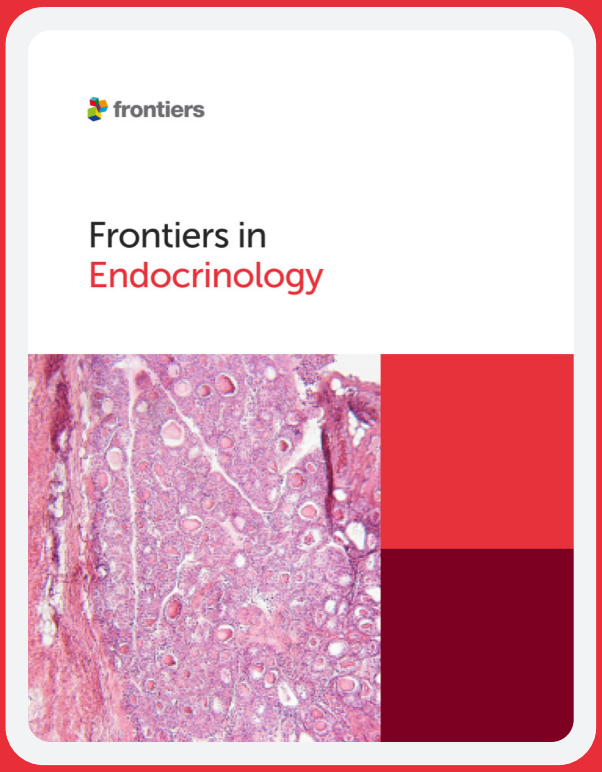

Frontiers

Avenue du Tribunal-Fédéral 34
1005 Lausanne, Switzerland
frontiersin.org

Contact us

+41 (0)21 510 17 00
frontiersin.org/about/contact